NASA CR - 152, 391
V.3

NASA CR-152391

NASA-CR-152391-VOL-3

19810014499

ANALYSIS OF WIND TUNNEL TEST RESULTS FOR A 9.39-PER CENT SCALE MODEL OF A VSTOL FIGHTER/ATTACK AIRCRAFT

VOLUME III - EFFECTS OF CONFIGURATION VARIATIONS FROM BASELINE E205 CONFIGURATION ON AERODYNAMIC CHARACTERISTICS

DR. J. R. LUMMUS
G. T. JOYCE
C. D. O'MALLEY

Prepared under Contract NAS2-10344
by
General Dynamics
Fort Worth Division
for
Ames Research Center

NATIONAL AERONAUTICS AND SPACE ADMINISTRATION

1. Report No.	2. Government Accession No.	3. Recipient's Catalog No.
NASA CR-152391		

4. Title and Subtitle
Analysis of Wind Tunnel Test Results for a 9.39-percent Scale Model of a VSTOL Fighter/Attack Aircraft

5. Report Date
October, 1980

6. Performing Organization Code

7. Author(s)
Dr. J.R.Lummus G. T. Joyce, C. D. O'Malley

8. Performing Organization Report No.

9. Performing Organization Name and Address
General Dynamics/Fort Worth Division
P. O. Box 748
Fort Worth, Texas 76101

10. Work Unit No.

11. Contract or Grant No.
NAS2-10344

12. Sponsoring Agency Name and Address
NASA, AMES Research Center,
Moffett Field, Ca 94035

13. Type of Report and Period Covered
Contractor Final Report
Sept. 10, 1970-Nov. 11, 1980

14. Sponsoring Agency Code

15. Supplementary Notes
AMES Research Center Technical Monitor W. P. Nelms
(415) 965-5880

16. Abstract

The results of a series of NASA AMES wind tunnel tests of a General Dynamics vectored-engine-over wing, Navy VSTOL fighter/attack configuration have been analyzed to (1) assess prediction method capabilities, (2) evaluate geometry variations such as multiple canard longitudinal locations and strake shapes, and (3) evaluate the effects of configuration changes associated with varying the propulsive lift system from a jet-diffuser ejector to a Remote Augmentation Lift System (RALS). Configuration modification and additional testing and analysis are recommended to adequately evaluate the configuration potential.

This document is presented in four volumes - Volume I - Study Overview, Volume II - Evaluation of Prediction Methodologies, Volume III - Effects of Configuration Variations from Baseline E205 Configuration on Aerodynamic Characteristics, and Volume IV - RALS R104 Aerodynamic Characteristics and Comparisons with E205 Configuration Aerodynamic Characteristics.

17. Key Words (Suggested by Author(s))	18. Distribution Statement
CANARD, STRAKE, AERODYNAMIC PREDICTION METHODS	

19. Security Classif. (of this report)	20. Security Classif. (of this page)	21. No. of Pages	22. Price*
UNCLASSIFIED	UNCLASSIFIED		

*For sale by the National Technical Information Service, Springfield, Virginia 22161

N81-23032#

VOLUME III - EFFECTS OF CONFIGURATION VARIATIONS FROM BASELINE E205 CONFIGURATION ON AERODYNAMIC CHARACTERISTICS

TABLE OF CONTENTS

LIST OF FIGURES

LIST OF FIGURES (CONT'D.)

LIST OF FIGURES (CONT'D.)

LIST OF FIGURES (CONT'D.)

LIST OF FIGURES (CONT'D.)

LIST OF FIGURES (CONT'D.)

LIST OF FIGURES (CONT'D.)

LIST OF FIGURES (CONT'D.)

LIST OF FIGURES (CONT'D.)

LIST OF FIGURES (CONT'D.)

LIST OF FIGURES (CONT'D.)

LIST OF FIGURES (CONT'D.)

LIST OF FIGURES (CONT'D.)

LIST OF FIGURES (CONT'D.)

LIST OF FIGURES (CONT'D.)

LIST OF FIGURES (CONT'D.)

FIGURE — PAGE

LIST OF FIGURES (CONT'D.)

FIGURE		PAGE

LIST OF FIGURES (CONT'D.)

LIST OF TABLES

LIST OF SYMBOLS

a. English Symbols

A	axial force, lb (N)
a.c.	aerodynamic center, %$\bar{c}$
AR	aspect ratio
b	span, in. (m)
$\bar{c}$, MAC	mean aerodynamic chord, in. (m)
C_A	axial force coefficient
$C_{A_{ejector}}$	axial force coefficient due to ejector
C_D	drag coefficient
$C_{D_{AERO}}$	aero-only drag coefficient (no thrust increments included)
$C_{D_{min}}$	minimum drag coefficient
C_{D_E}	equivalent drag coefficient
$C_{D_{RAM}}$	ram-drag coefficient (engine inlet)
C_{D_t}	total drag coefficient
C_L	lift coefficient
$C_{L_{buffet}}$	buffet-onset lift coefficient
C_{L_E}	equivalent lift coefficient
$C_{L_{max}}$	maximum lift coefficient
$C_{L_{aero}}$	aero-only lift coefficient (no thrust increments included)
C_{L_t}	total lift coefficient
C_l	rolling moment coefficient

C_{l_β}	rolling moment derivative due to sideslip, 1/deg
C_{m_E}	equivalent pitching moment coefficient
$C_{m_{x_{\bar{c}}}}$	pitching moment coefficient about x percent $\bar{c}$
C_{m_o}	zero lift pitching moment coefficient
C_{m_t}	total pitching moment coefficient
C_N	normal force coefficient
C_n	yawing moment coefficient
C_{n_β}	yawing moment derivative due to sideslip, 1/deg
C_T	thrust coefficient, $\frac{T}{aS_{REF}}$
C_Y	side force coefficient
C_{Y_β}	side force derivative due to sideslip, 1/deg
CMU, C	ideal thrust coefficient, $\dot{w}\, Vj/gqS_{REF}$
D	drag, lb(N)
e	span efficiency factor
ESF	engine scale factor, $\frac{T}{T_{ESF\,=\,1.0}}$
IGE	in ground effect
L	lift, lb(N)
L_Γ	lift due to supercirculation, lb(N)
l	rolling moment, ft lb (Nm)
M	Mach number
m	pitching moment, ft lb(Nm)
NPR	nozzle pressure ratio, $\frac{\text{Total Pressure}}{P}$

LIST OF SYMBOLS (Continued)

N	normal force, lb(kg)
n	yawing moment, ft lb (Nm)
OGE	out of ground effect
P	freestream static pressure, lb/ft^2 $(\frac{N}{m^2})$
P_o	freestream total pressure, lb/ft^2, $(\frac{N}{m^2})$
q	freestream dynamic pressure, lb/ft^2 $(\frac{N}{m^2})$
S_C	canard exposed area, ft^2 (m^2)
S_{ref}	reference area, ft^2(m^2) (usually equal to S_W)
STOL	short takeoff or landing
S_W	area of trapezoidal wing extended to centerline, ft^2(m^2)
S_{V_T}	exposed area of vertical tail, ft^2(m^2)
T	thrust, lb(N)
V_∞	freestream velocity, ft/sec, knots (m/sec)
V_j	jet velocity based on isentropic expansion from nozzle camber total pressure to freestream static pressure, ft/sec (m/sec)
VSTOL	vertical or short takeoff or landing
VTOL	vertical takeoff or landing
VEO-Wing	vectored engine over wing
$\dot{w}$	weight flow, lb/sec (kg/sec)
X_{cp}	action point of circulation lift relative to leading edge of MAC

LIST OF SYMBOLS (Continued)

b. Greek Symbols

α alpha	angle of attack, deg
β, beta	angle of sideslip, deg
Γ	supercirculation
γ	flight path angle, deg
δ_C, δ_i	canard deflection (positive, leading-edge up), deg
δ_{TE}, δ_F	VEO-Wing nozzle and outboard flaperon deflection, deg; except for aileron action the flaperons and VEO-Wing nozzle flaps always deflect together.
θ	pitch attitude angle, deg
θ_J	jet thrust deflection out of VEO-Wing nozzles when deflected, $_{TE}$, deg
Λ_{LE}	leading-edge sweep angle, deg
λ	taper ratio, $\frac{\text{tip chord}}{\text{root chord}}$
ϕ	ejector measured thrust/isentropic supply thrust (where isentropic supply thrust is the thrust which would be obtained from supplied air at the nozzle exit of pressures and flow rates expanded at isentropically to ambient pressure)

LIST OF SYMBOLS (Continued)

c. Model Symbols

B_1	VSTOL ejector configuration E-205 basic fuselage with fuselage strake that blends the fuselage to the inboard section to the wing.
B_2	VSTOL RALS configuration R-104 basic fuselage
C_1	All moveable nacelle-mounted horizontal canard of VSTOL ejector configuration E-205 in the mid-location
C_2	Horizontal canard in VSTOL E-205 or RALS R104 fwd-location
C_3	Horizontal canard in VSTOL E-205 or RALS R104 aft-location
N	VSTOL ejector configuration E-205 or RALS R104 VEO-wing nacelle
S_1	Baseline strake on E205 configuration
S_2	High sweep strake on E205 configuration
S_3	Low sweep strake on E205 configuration
V	All moveable vertical tail of VSTOL ejector configuration E-205 or RALS R104
W_1	VSTOL ejector configuration E-205 wing with linear elements between SS 96.496 and SS 223.695
W_2	VSTOL RALS configuration R-104 wing with linear elements between SS 87.231 and SS 214.430

SUMMARY

This volume presents the aerodynamic characteristics of the components of the baseline E205 configuration; geometry variations from the baseline E205 configuration are also presented including a matrix of canard longitudinal locations and strake shapes.

The component build-up for the E205 configuration is instructive in illustrating the canard/wing interaction although the magnitudes of the interaction would probably be different if the early wing stall experienced had been avoided by using the available wing leading edge flaps.

The investigation of the canard location/strake-shape matrix indicated there are major "first order" effects for varying canard location or strake shape; however, the influence of the strake shape on canard effectiveness and the effect of the canard location on the changes produced by the strake shape are "second order" for this type of configuration.

1.0 COMPONENT BUILDUP FOR BASELINE E205 CONFIGURATION

The aerodynamic characteristics of various combinations of the components of the E205 baseline configuration were investigated by performing a series of model component-buildup runs at various Mach numbers. The effects investigated include the lift, drag, and pitching moment characteristics of the (1) wing alone (canard removed), (2) wing in presence of canard at various deflections, (3) vertical tail, (4) canard alone (wing removed), (5) canard in presence of wing (plus interference on wing), and (6) the baseline body-nacelle-strake. All figures and tables are placed at the end of the text.

Figures 1-1 through 1-11 present the C_L vs α, C_L vs C_D, and C_L vs C_M curves that illustrate the effects of building up the complete E205 baseline configuration by adding various configuration components (such as the wing, canard at $\delta_c = 0^o$, and vertical tail) to the baseline fuselage + strake + nacelle. The effects of these various components are presented for Mach numbers from .2 to 2.0 where available (all of the component-effects are not available at each Mach number). The effects of varying canard longitudinal location are also included. These figures form the basis for the following discussions and for developing the lift, drag, and pitching moment increments due to the various configuration components (and combinations of components); these increments illustrate the magnitude of the

effects of the individual configuration components as well as the mutual interference of these components. Figures 1-12 through 1-20 were developed from the data illustrated in Figures 1-1 through 1-11 and illustrate the variation of increments due to the configuration components (and combinations of components) with angle of attack and Mach number. Additional data has been used to develop the increments due to the canard (relative to canard off) at various canard deflections. (A comparison of the E205 and R104 component-buildup characteristics is presented in Volume IV and reiterates many of the observations in this section).

The increments in lift, drag and pitching moment due to the vertical tail vary little with angle of attack and Mach number.

The "wing-alone" lift, drag, and pitching moment increments (in the presence of the body-nacelle-strake) indicate that the wing exhibits the expected characteristics in the linear α-region; however, wing stall beings at approximately $\alpha = 8^{\circ}$ at all Mach numbers. This is a profound effect because it carries over to adversely affect the remaining aerodynamic coefficients. The early stall of the wing is the result of failing to employ the available wing leading-edge flaps on the model; these flaps were not used because test time limitation precluded an optimization of the leading edge flap. Had these been employed and optimized, the wing performance and canard/wing interaction would be substantially improved.

The addition of the canard (at each canard location tested) complicates the characteristic aerodynamic picture. Figure 1-12 compares the incremental effects of the isolated wing-alone to that of the wing in the presence of the baseline-location canard at several deflection angles; the mutual interference of the canard on the wing and the wing on the canard can be deduced from this figure. The upwash, ϵ , at the baseline canard location was developed in and out of the presence of the wing for M = .2 as shown in Figure 1-21. The variation in upwash with angle of attack was determined by plotting C_m vs α for the cases of canard on (at a given δ_c) and canard-off. The intersection of the two curves yields the angle of attack for which no moment exists on the canard at that S according to the equation $\epsilon = \alpha + \delta_c$. The bias of 2.5 degrees in the upwash due to the wing acting on the canard (Figure 1-21) increases the loading on the canard because the wing increases the effective angle of attack and the magnitude of the velocity vector on the canard. The downwash due to the canard acting on the wing decreases the loading on the wing (which is carrying more of the total airplane lift than the canard) resulting in a negative interference effect of the

canard on the wing. This can be seen in Figure 1-12 as a decrease in slope of the wing lift coefficient with respect to angle of attack in the presence of the canard (at zero deflection). The aerodynamic center (ac) also shifts forward because of the positive interference of the wing on the canard and the negative influence of the canard on the wing as reflected in Figure 1-12. As the deflection of the canard is decreased (to -20^{o}), its load is decreased which in turn, decreases its negative interference on the wing because the downwash on the wing is decreased thus increasing the lift on the wing. This explanation of the canard/wing interaction holds at all Mach numbers while the wing-canard is operating in the linear range. After approximately $8\text{-}10^{o}$ airplane angle of attack, the interaction story becomes more obscure. With the use of the wing leading-edge flaps, this deterioration could be delayed to higher angles of attack at all Mach numbers.

The addition of the canard acts in the same manner as a leading-edge device to maintain the wing effectiveness.

The "canard alone" increments are developed for the E205 configuration at M = .2, 1.6, 1.8 and 2.0. The lift slope of the isolated canard is predictable in the linear angle of attack range. The isolated canard begins to lose effectiveness near $8\text{-}10^{o}$ fuselage angle of attack at all Mach numbers.

Figure 1-21 shows the M = .2 upwash field at the canard (deduced from the experimental data) due to the baseline body-nacelle-strake combination (wing-off) compared to the upwash at the canard with the wing on. With the wing removed, the gradient of upwash with angle of attack is approximately one near zero angle of attack. The wing biases the upwash at the canard by about 2.5 degrees but does little to the upwash gradient until the wing begins to lose effectiveness. Because of the higher upwash induced by the wing at the canard, the local effective angle of attack and dynamic pressure are higher at the canard with the wing on (subsonically and transonically) resulting in higher loading on the canard than with the wing off. However, a separate balance would be required to isolate the canard load in the presence of the wing so the increments between canard off and on in the presence of the wing presented in Figures 1-12 through 1-20 also include the lift loss on the wing caused by the canard. Canard loads in and out of the presence of the wing are not possible with the experimental data.

Supersonically the wing induces little effect on the canard. Figure 1-22 compares the untrimmed minimum drag variation with Mach number for various combinations of components. It is noteworthy that the wing supersonic drag increment (including the wing-body interference) is a major contributor to the total supersonic drag.

2.0 EFFECTS OF ALTERNATE LONGITUDINAL CANARD LOCATIONS WITH BASELINE CONFIGURATION STRAKE S_1

The aerodynamic characteristics of the baseline E205 configuration wind tunnel model and its components have been described in Volume II and the preceding section of this volume. One of the primary goals of this research is to investigate the effects of geometry variations from the baseline configuration. The effects of varying the canard longitudinal location on both the longitudinal and lateral-directional aerodynamics of the baseline E205 wind tunnel model (with baseline strake S_1) are presented in this section. (In the next section, the effects of varying the strake shape with the baseline and other canard locations are investigated.

2.1 Effects on Untrimmed Lift, Drag and Pitching Moment

The objectives of varying canard longitudinal location with the baseline strake S_1 (in this section) and in combination with various strake shapes (in Section 3.0) are to determine the effects on (1) canard control power, (2) canard/wing interference, (3) static balance and ac (as a design consideration), (4) optimum canard location, and (5) the lateral-directional characteristics.

Table 2-1 presents a catalog of the lift, drag, and pitching moment curves illustrating the effects of canard longitudinal location with the baseline strake for Mach numbers ranging from .2 to 2.0, with varying canard deflections and trailing-edge flap deflections (Figures 2-1 to 2-18 and 2-33 to 2-35).

Table 2-2 catalogs the plots of the increments in lift, drag, and pitching moment due to the canard plus wing interference at various canard longitudinal locations relative to the canard-off case (Figures 2-19 to 2-31). These increments were developed from the curves described in Table 2-1.

<u>Canard Control Power</u>

The plots cataloged above indicate that at M = .2 for all δ_C's tested, the baseline canard location, C_1, (which is the mid position) produces the highest <u>net</u> airplane lift (increased canard lift and decreased wing lift) but has less actual control power (pitching moment increment) than the forward position, C_2, but more than the aft location, C_3, because of the larger canard moment arm to the c.g. While the forward and aft canard locations produce about the same lift increments for a given α and δ_C, the drag increment of the forward canard is less, especially at high α's. The absolute value of the ratio of the change in a.c. produced by the canard (at a given location) to the geometric tail

Table 2-1: CATALOG OF LONGITUDINAL CANARD LOCATION PLOTS WITH BASELINE STRAKE

M	CANARD LOCATION/STRAKE	$\delta_{TE} = 0°$ δ_C	$\delta_{TE} = 0°$ FIGURE NO	$\delta_{TE} = 10°$ δ_C	$\delta_{TE} = 10°$ FIGURE NO	$\delta_{TE} = 25°$ δ_C	$\delta_{TE} = 25°$ FIGURE NO
.2	C1S1	V	2-1	V	2-32	V	2-33
.2	C2S1	V	2-2			-20	2-35
.2	C3S1	V	2-3				
.2	C1S1, C2S1, C3S1	0	2-4, 1-1				
.4	C1S1	V	2-5			0	2-34
.6	C1S1	V	2-6				
.6	C2S1	V	2-9				
.6	C3S1	V	2-12				
.6	C1S1, C2S1, C3S1	0	1-6				
.9	C1S1	V	2-7				
.9	C2S1	V	2-10				
.9	C3S1	V	2-13				
.9	C1S1, C2S1, C3S1	0	1-7				
1.2	C1S1	V	2-8				
1.2	C2S1	V	2-11				
1.2	C3S1	V	2-14				
1.2	C1S1, C2S1, C3S1	0	1-8				
1.6	C1S1	V	2-15	V	2-36		
1.6	C2S1	V	---				
1.6	C3S1	V	---				
1.6	C1S1, C2S1, C3S1	0	2-16				
2.0	C1S1	V	2-17	V	2-37		
2.0	C2S1	V	---				
2.0	C3S1	V	---				
2.0	C1S1, C2S1, C3S1	0	2-18				

V : VARIES

Table 2-2 CATALOG OF LONGITUDINAL CANARD LOCATION PLOTS: LIFT, DRAG AND PITCHING INCREMENTS (CANARD ON-CANARD OFF IN PRESENCE OF WING)

M	CANARD LOCATION/STRAKE	δ_{TE}	δ_C	FIGURE NO
.2	C1S1, C2S1, C3S1	0	+10	2-19
.2	C1S1, C2S1, C3S1	0	0	2-20
.2	C1S1, C2S1, C3S1	0	-10	2-21
.4	C1S1, C2S1, C3S1	0	0	2-22
.6	C1S1, C2S1, C3S1	0	+10	2-23
.6	C1S1, C2S1, C3S1	0	0	2-24
.6	C1S1, C2S1, C3S1	0	-10	2-25
.9	C1S1, C2S1, C3S1	0	+10	2-26
.9	C1S1, C2S1, C3S1	0	0	2-27
.9	C1S1, C3S1, C3S1	0	-10	2-28
1.2	C1S1, C2S1, C3S1	0	+10	2-29
1.2	C1S1, C2S1, C3S1	0	0	2-30
1.2	C1S1, C2S1, C3S1	0	-10	2-31

arm, $l_T/\bar{c}$, is approximately constant for the three longitudinal canard locations. As speed is increased these trends basically continue to hold although there are some slight variations at the transonic Mach numbers with some δ_C's. There is virtually no effect of the canard location on the variation of canard control-power-gradient-with-canard-deflection ($\Delta C_M/\delta_C$).

Canard/Wing Interference

When the canard is shifted from the aft to the forward position the a.c. of the total configuration is shifted forward and a more nose-up moment is produced but with less net airplane lift and a corresponding reduction in drag. Shifting the canard location forward also results in increased effective configuration camber which in turn produces a change in C_{M_0}, $C_{D_{MIN}}$, and C_L @ $C_{D_{MIN}}$. One of the reasons for these changes with canard location are the variations in the mutual interference between the canard and wing. As stated throughout this report, at all speeds, the canard produces a downwash, or reduction in the effective angle of attack of the portion of the wing inboard of the canard tip as well as a reduction in the magnitude of the local wing velocity vectors. An upwash or increased effective angle of attack as well as an increase in magnitude of the local velocity vector is induced on the portion of the wing outboard of the canard tip. The wing, however, only influences the canard flowfield at subsonic and transonic speeds where it induces an upwash on the canard and an increase in the local velocity at the canard. The result of this mutual interference is an increased loading on the canard and a decreased loading on the wing. The design objective is of course to obtain the most favorable interference by placing the canard in a position relative to the wing to achieve the best possible trimmed lift curve and drag polars. The effects of canard location on the trimmed characteristics are discussed in Section 2.3 but the untrimmed data presented in this section does indicate that, at the subsonic Mach numbers, the wing does influence the canard substantially and that the highest net lift is achieved with the canard in the mid position. As supersonic speeds are approached, the wing interference on the canard is diminished and the canard behavior is primarily influenced by its own induced, local angle of attack and that of the body-nacelle-strake. At M = 1.2 the forward and mid canard locations produce higher net loadings than the aft position indicating that opening the "gap" between the canard and wing may also avoid the detrimental effects of the canard trailing-edge shock being imposed on the wing (or the wing leading-edge shock imposing on the canard).

The limited amount of canard effectiveness data obtained with wing trailing-edge flap deflections are not adequate to deduce differences produced by canard location with the flaps deflected. These data are used, however, to develop

optimum trimmed characteristics using combinations of canard and trailing-edge flaps. They also provide an excellent data base for future design efforts, especially the low speed data covering the full ninety-degree angle of attack range which will be invaluable for VTOL transition studies.

2.2 Effects on Aerodynamic Center

The variation of aerodynamic center (a.c.) as a function of canard location is presented in Figure 2-38. The predicted curve from Volume II is presented for the baseline (mid) canard location also. Subsonically, the a.c. can be predicted rather well using the Woodward procedure. Supersonically, the test a.c. is approximately 5-percent forward of the predicted a.c. The shift in a.c. with canard is 7.5-percent forward with the forward shifted canard and 5.5-percent aft with the aft shift. It is evident from this that there is more canard-wing interference at the aft (overlapped) location. At the supersonic speeds, the a.c. shift due to canard is reduced considerably. At Mach = 2.0, there is no shift for the forward located canard and only a 2-percent shift aft for the aft located canard.

2.3 Effects on Trimmed Lift on Drag

The effects of varying longitudinal canard location (with the baseline strake) on the power-off, canard-trimmed lift curves and drag polars for the E205 configuration at M = .6, .9, and 1.2 are shown in Figure 2-39, 2-40, and 2-41 respectively. The α-range for trim is limited by the range of δ_C's tested. The low speed (M = .2) trimmed data was not developed because for this configuration, the power-off characteristics are of little interest because the configuration relies on power effects and ejector thrust to trim over a reasonable angle-of-attack range. The supersonic trimmed data for trimming with the forward and aft canard locations was not developed because only zero-degrees canard deflection was tested for those configurations; however, the M = 1.6 and 2.0 trimmed polars were developed (Figure 2-42).

At M = .6, (Figure 2-39), the aft canard, C_3, has a higher trimmed C_{L_0} than with C_1 or C_2 but there is a substantial minimum trimmed drag penalty relative to the mid and forward canard locations. The trimmed drag polar obtained using the forward canard, C_2, provides the lowest trimmed drag for a given C_L at M = .6. These same trends are exhibited at M = .9 (Figure 2-40). However, supersonically, at M = 1.2 (Figure 2-41) the mid-canard trimmed polar is so much better than with the fore or aft canard locations that if any supersonic maneuvering is required, the mid-canard location would be selected. The mid-canard location would also be selected because of its

superior lateral-directional characteristics across the Mach number range as demonstrated in Section 2.4.

2.4 Effects on Lateral-Directional Characteristics

The lateral-directional characteristics of Configuration E205 at low speed (M = .2) are indicated in Figures 2-43 through 2-47. Figure 2-43 contains the lateral-directional aerodynamic characteristics of the basic wing-body (BSNW), the wing-body-vertical (BSNWV) and the wing-body-vertical plus canard (BSNWCV) configurations. The wing-body directional stability increases with angle of attack until at 20 degrees it is almost stable. The wing-body-vertical also shows increasing directional stability with angle of attack. The vertical tail effectiveness decreases only slightly with increasing angle of attack over this range of α's. The addition of the canard changes this condition markedly. Initially, the addition of the canard is slightly destabilizing for both vertical tail-on and off. At approximately the angle of attack where the basic wing begins to lose effectiveness, the canard begins to influence the vertical tail adversely so that at $\alpha = 22°$, the vertical tail contribution to stability is almost zero. Although the data was not obtained to verify it, this is probably caused by an adverse change in sidewash characteristics due to the addition of the canard as noted in the transonic data. This is true for the aft and nominal longitudinal canard positions (C3 and C1). The forward-canard (C2) influence on the vertical tail is even more pronounced as shown in Figure 2-46. Although vertical-tail-off data was not obtained with the forward canard, it is presumed that, since the wing-body-vertical data did not change significantly from that of the forward-canard-location case, C1, the changes due to C2 must be due to an adverse change in sidewash due to the location of C2 relative to that of C1 or C3.

Canard location lateral-directional characteristics were not obtained at M = .6 but that of the baseline configuration is indicated in Figure 2-48. The trends are about the same as seen at M = .2. Aileron effectiveness is presented in Figure 2-49 for M = .6 and exhibits the same characteristics as those of the wing; that is, the aileron effectiveness deteriorates as the wing (and flap) effectiveness decreases.

The baseline wing-body-canard configuration of E205 (i.e., vertical tail off) at transonic speed has a different trend with angle of attack than that displayed from the low speed test. The trend at Mach 0.9 indicates the body-wing canard is becoming more unstable with angle of attack. This is contrary to the trend exhibited from the low speed test. Testing was only accomplished to 12 degrees angle of attack so this trend may reverse at the higher angles of attack.

The effect of canard location for Mach = 0.9 and 1.2 is shown in Figures 2-50 through 2-54. This shows the addition of the canard to be slightly unfavorable in directional stability at low angles of attack as was the result from the low speed test. At larger angles of attack, the entire configuration is directionally unstable but the addition of the canard is not degrading. The forward canard is more destabilizing for all angles of attack than the mid canard; the aft canard is slightly stabilizing at the high angle of attack tested. At Mach = 1.2, the effect of canard location at low angles of attack is insignificant. At the larger angles of attack, moving the canard in either direction from the mid location is destabilizing. Supersonically, the effect of the canard changes again. At Mach = 1.6 (Figures 2-55, 2-57, 2-59, 2-61), the aft canard is slightly more stable than either the mid or forward canard. At higher angles of attack, i.e., 6 degrees or higher, the mid canard is the most destabilizing of the three locations. At Mach = 2.0 (Figures 2-56, 2-58, 2-60, 2-62), the forward canard location is more stable at low angles of attack while with increasing angles of attack it becomes more destabilizing than the others. The aft location (C3) generally is more stable at the larger angles of attack tested.

The directional control effectiveness of the all moving vertical tail is presented in Figures 2-63 through 2-68. The control effectiveness holds up well with angle of attack. The derivative slopes change little with control deflection indicating the surface is operating in the linear region.

3.0 EFFECT OF STRAKE SHAPE WITH ALTERNATE CANARD LOCATIONS

In the preceding section, the effects of varying the canard longitudinal location on the canard effectiveness, the static stability and balance (a.c.) and the lateral-directional characteristics with the baseline E205 configuration were considered. In this section, the effects of varying the longitudinal canard locations with three different strakes (including the baseline strake) are examined to determine the relative importance of the mutual interactions of the canard location and strake shape on the overall airplane design. (See Volume I, Section 3.4, for a description of canard locations and strake shapes as well as sketches in Figures 3-68 through 3-76.) The "first order" effects of the geometry variations on the untrimmed lift, drag, pitching moment, the aerodynamic center, the trimmed lift and drag, and the lateral-directional characteristics were examined.

3.1 Untrimmed Lift, Drag and Pitching Moment

Table 3-1 summarizes the lift, drag, and pitching moment curves developed to illustrate the effects of the matrix of canard longitudinal location and strake shape variations across the whole Mach number test range. Three types of comparison plots have been developed: (1) strake variations with a constant canard location and deflection, (2) canard location variation with a constant strake shape and canard deflection, and (3) varying canard deflection with constant canard location and strake shape. Table 3-2 summarizes the plots of lift, drag, and pitching moment increments due to varying strake shape (relative to the baseline strake) at each canard location and deflection.

"First order" changes are observed for changing strake shape at a given canard location or changing canard location with a given strake shape. In general, reducing the strake area across the Mach number range from S1 to S2 to S3 at a given canard location and deflection tends to produce a slight reduction in $C_{L\alpha}$ and lift loss near $C_{L_{max}}$, with a reduction in α-BREAK (departure from linear characteristics); the most significant effect of reducing strake area (and changing shape) is a marked aft shift in aerodynamic center for a more positive stability level. The primary effect of the strake shape is seen at high α's near $C_{L_{max}}$. <u>The strake shape can definitely be used to tailor the shape of the pitching moment curve near stall and even produce a stable break at $C_{L_{max}}$</u>. Reducing the strake area also produces small changes in drag, especially at high α's but the drag trends with strake shape are not as clearly defined as the lift and moment. Obviously, the real test of the optimum strake shape for a given canard location is determined from the trimmed lift and drag as discussed in Section 3.3.

Table 3-1 . CATALOG OF CANARD LOCATION/STRAKE VARIATION PLOTS INCLUDING THE EFFECTS OF CANARD DEFLECTION

M	CANARD LOCATION/STRAKE	δ_C	FIGURE NO	REMARKS
.2	C1S1, C1S2, C1S3	0	3-1/3-2	A
.2	C2S1, C2S2, C2S3	0	3-3/3-4	
.2	C3S1, C3S2, C3S3	0	3-5/3-6	
.2	C1S1, C2S1, C3S1	0	2-4	B
.2	C1S2, C2S2, C3S2	0	3-7/3-8	
.2	C1S3, C2S3, C3S3	0	3-9/3-10	
.4	C1S1, C2S1, C3S1	0	---	B
.4	C1S2, C2S2, C3S2	0	3-11	
.4	C1S3, C3S3, C3S3	0	3-12	
.6	C1S1, C1S2, C1S3	+10	3-13	A
.6	C1S1, C1S3, C1S2	0	3-14	
.6	C1S1, C1S2, C1S3	-10	3-15	
.6	C2S1, C2S2, C2S3	10	3-16	A
.6	C2S1, C2S2, C2S3	0	3-17	
.6	C2S1, C3S2, C2S3	-10	3-18	
.6	C3S1, C3S2, C3S3	10	3-19	A
.6	C3S1, C3S2, C3S3	0	3-20	
.6	C3S1, C3S2, C3S3	-10	3-21	
.6	C1S1	V	2-6	C
.6	C2S1	V	2-9	
.6	C3S1	V	2-12	
.6	C1S2	V	3-22	C
.6	C2S2	V	3-23	
.6	C3S2	V	3-24	
.6	C1S3	V	3-25	C
.6	C2S3	V	3-26	
.6	C3S2	V	3-27	
.9	C1S1, C1S2, C1S3	10	3-28	A
.9	C1S1, C1S2, C1S3	0	3-29	
.9	C1S1, C1S2, C1S3	-10	3-30	
.9	C2S1, C2S2, C2S3	10	3-31	A
.9	C2S1, C2S2, C2S3	0	3-32	
.9	C2S1, C2S2, C2S3	-10	3-33	
.9	C3S1, C3S3, C3S3	10	3-34	A
.9	C3S1, C3S3, C3S3	0	3-35	
.9	C3S1, C3S3, C3S3	-10	3-36	
.9	C1S1	V	2-7	C
.9	C2S1	V	2-10	
.9	C3S1	V	2-13	
.9	C1S2	V	3-37	C
.9	C2S2	V	3-38	
.9	C3S2	V	3-39	
.9	C1S3	V	3-40	C
.9	C2S3	V	3-41	
.9	C2S3	V	3-42	

Table 3-1 CATALOG OF CANARD LOCATION/STRAKE VARIATION PLOTS INCLUDING THE EFFECTS OF CANARD DEFLECTION (CONT'D)

M	CANARD LOCATION/STRAKE	δ_C	FIGURE NO	REMARKS
1.2	C1S1, C1S3, C1S3	10	3-43	A
1.2	C1S1, C1S2	0	3-44	
1.2	C1S1, C1S3, C1S3	-10	3-45	
1.2	C2S1, C2S2, C2S3	10	3-46	A
1.2	C2S1, C2S2, C2S3	0	3-47	
1.2	C2S1, C2S2, C2S3	-10	3-48	
1.2	C3S1, C3S2, C3S3	10	3-49	A
1.2	C3S1, C3S2, C3S3	0	3-50	
1.2	C3S1, C3S2, C3S2	-10	3-51	
1.2	C1S1	V	2-8	C
1.2	C2S1	V	2-11	
1.2	C3S1	V	2-14	
1.2	C1S2	V	3-52	C
1.2	C2S2	V	3-53	
1.2	C3S2	V	3-54	
1.2	C1S3	V	3-55	C
1.2	C2S3	V	3-56	
1.2	C3S3	V	3-57	
1.6	C1S1, C1S3, C1S3	0	3-58	A
1.6	C2S1, C2S2, C2S3	0	3-59	
1.6	C3S1, C3S2, C3S3	0	3-60	
1.6	C1S1, C2S1, C3S1	0	2-16	B
	C1S2, C2S2, C3S2	0	3-61	
	C1S3, C2S3, C3S3	0	3-62	
2.0	C1S1, C1S2, C1S3	0	3-63	A
	C2S1, C2S2, C2S3	0	3-64	
	C3S1, C3S2, C3S3	0	3-65	
2.0	C1S1, C2S1, C3S1	0	2-18	B
	C1S2, C2S2, C3S2	0	3-66	
	C1S3, C2S3, C3S3	0	3-67	

NOTES:

A = CONSTANT CANARD LOCATION, VARY STRAKE, δ_C = CONSTANT

B = VARY CANARD LOCATION, CONSTANT STRAKE, δ_C = CONSTANT

C = CONSTANT CANARD LOCATION, CONSTANT STRAKE, δ_C = VARIES

LOW α-RANGE/HIGH α-RANGE FIG NO'S WERE APPLICABLE

"Second order" changes were observed for the effects of canard location on the changes produced by varying strake shape or the effects of varying strake shape on the canard effectiveness at different canard locations.

Table 3-2 provides a catalog of the plots of transonic lift, drag, and pitching moment increments due to changing strake shape (relative to the baseline strake) as a function of angle of attack, canard location, and canard deflection (Figures 3-68 to 3-76). These plots indicate that the canard location and deflection has little effect on the increments due to a particular strake. As an indicator of this, Table 3-3 is provided which shows a comparison of the pitching moment increment due to changing strake shape at each canard location. The comparison is shown for $M = .6$, $\delta_C = 10°$ and α's of 10° and 20° and demonstrates that the changes in moment due to the strake-change are not affected appreciably by canard location. This trend holds for other Mach numbers, angles of attack, and canard deflections.

Table 3-4 indicates that the moment increment due to changing canard location from the baseline location is virtually unaffected by the strake shape for Mach number = .6 and $\alpha = +10°$. This trend holds for other Mach numbers and α's.

In summary, the primary consideration at the preliminary design stage should be canard location and strake shape and not the interaction between the canard and strake because these interactions produce second order effects compared to the canard location and strake shape.

3.2 Effect on Aerodynamic Center

The change in aerodynamic center with strake configuration is presented for the three strakes tested in Figure 3-77. The a.c. is shifted aft as the strake area and sweep are varied from the baseline to S2 and S3. These changes are on the order of 3 to 4 percent at Mach = 0.6 and 1.2. The variation is less at Mach = 0.9. Strakes 2 and 3, though different in sweep and area, have little impact on aerodynamic center variation. The primary effect of the strake shape can be seen in the incremental effects that are presented in Section 3.1. There, it can be seen that there is a very small variation in C_{M_α} at small angles of attack (i.e., aerodynamic center). As the wing becomes less efficient near eight degrees angle of attack, the forebody strake-canard contributes more to pitching moment. The changes in incremental lift or drag are small until angles-of-attack of 18-20 degrees is reached. After the wing begins to lose effectiveness, the local pitching-moment-slope changes as a function of the strake configuration.

Table 3-2 CATALOG OF PLOTS OF LIFT, DRAG, AND PITCHING MOMENT INCREMENTS DUE TO CHANGING FROM THE BASELINE STRAKE SHAPE (AT δ_C = CONSTANT) AT VARIOUS CANARD LOCATIONS

M	CANARD LOCATION/STRAKE	FIGURE NO
.6	C1	3-68
	C2	3-69
	C3	3-70
.9	C1	3-71
	C2	3-72
	C3	3-73
1.2	C1	3-74
	C2	3-75
	C3	3-76

Table 3-3: EFFECT OF CANARD LOCATION ON PITCHING MOMENT INCREMENT DUE TO CHANGING STRAKE SHAPE (RELATIVE TO BASELINE STRAKE, S1)

M = .6
δ_C = 10°

α	STRAKE INCREMENT	ΔCM AT CANARD LOCATION:		
		C1	C2	C3
10°	S1-S2	+.135	+.120	.10
20°	S1-S3	+.10	+.07	+.07

Table 3-4: EFFECT OF STRAKE SHAPE ON INCREMENT IN CANARD MOMENT DUE TO CHANGING CANARD LOCATION FROM BASELINE, C1

M = .6, δ_C = +10°, α = +10°

STRAKE	CM DUE TO CHANGING CANARD LOCATION FROM BASELINE	
	C1-C2	C1-C3
S1	-.065	+.090
S2	-.034	+.106
S3	-.052	+.088

3.3 Effect on Trimmed Lift and Drag

Figures 3-78 through 3-86 summarize the effects of varying strake shape at each longitudinal canard location on the trimmed, power-off lift curves and drag polars obtained by trimming with the canard only (no trailing-edge flap deflection) at M = .6, .9, and 1.2.

With the canard in the baseline location, C1, reducing the strake area from S1 to S2 and S3 tends to improve the trimmed lift curves and drag polars at α's > α-BREAK for the baseline strake at M = .6 (Figure 3-78). At M = .9 (Figure 3-81), changing strake shape produces almost no changes in the trimmed lift, an improved polar shape but increased minimum drag penalties from S1 to S3. At M = 1.2 (Figure 3-84), reducing the strake area from S1 to S2 and S3 produces substantial increases in trimmed C_{L_0} and $C_{D_{MIN}}$ but the lift slope and polar shape are identical.

With the canard in the forward location, C2, the same trends are exhibited with strake-area reduction that were noted above for the baseline canard location at M = .6 and .9 (Figure 3-79 and 3-82). At M = 1.2 (Figure 3-85), the trimmed C_{L_0} is reduced, the C_{L_α} is increased, the polar shape is improved but with an accompanying minimum drag penalty.

At the aft canard location, C3, the trimmed C_{L_α} is increased with no change in C_{L_0} as the strake is varied from S1 to S3 at M = .6; there is a very small increase in minimum drag but with a substantially improved polar shape at the higher α's (Figure 3-80). The same trends observed above were noted at M = .9 (Figure 3-83); however, at M = 1.2 (Figure 3-86) reducing the strake from S1 to S2 has little effect on trimmed lift or drag but S3 produces a very substantial increased minimum drag and reduced polar shape.

Figures 3-87, through 3-92 provide a comparison of the trimmed lift curves and drag polars for a given strake shape and varying canard locations on the same page.

All of the above comparisons yield the following general conclusions: (1) Strake effects on the trimmed lift curves and drag polars become more pronounced with increasing angles of attack and speed. The increment in minimum trimmed drag at M = .6 is approximately 30 counts for changing from S1 to S2 and 15 counts for S1 to S3. At Mach 1.2 the differences are 56 and 82 counts respectively. (2) <u>The location and strake-shape combination exhibiting the best overall choice of trimmed lift curves and drag polars from M = .6 to 1.2 is the baseline canard location C1 and baseline strake shape, S1</u>. (Although the S2 strake provides

a better trimmed drag polar at M = .6 with all canard locations, the advantage of C1S1 at the higher Mach numbers outweighs the advantage at M = .6 for C1S2.)

3.4 Effects on Lateral Directional Characteristics

At low speed, M = .2, the effects of varying strake shape on the lateral-directional characteristics are shown in Figure 3-93. There are small changes in the dihedral effect, $C_{\ell\beta}$ due to changing strake shape. The principal effect is in the directional stability parameter, $C_{n\beta}$. Slight improvements are noticed by changing strake shape from S1 to S2 or S3 at low angles of attack but as angles of attack are increased past 8-10 degrees (where the wing loses effectiveness) the directional stability deteriorates rapidly changing from srakes S1 to S2 to S3. Changing from strake S1 to S2 and S3 produces a rapidly decreasing level of directional stability that is unstable with strake S3 at α's as low as 17° (Figure 3-93). It can be speculated from this plot, that as long as the wing is working, the vertical tail can work effectively. After the wing effectiveness is lost, the resulting flow at the vertical tail renders it ineffective also. To verify this, the vertical tail-off runs are required to examine the wing-body-strake effects at large angles of attack.

The transonic testing examined vertical tail-off with a strake variation (Figures 3-94 through 3-97). Transonically, the vertical tail rapidly loses effectiveness at the higher angle of attack tested. At Mach = 0.9 and 18 degrees angle of attack, the difference in vertical tail contribution to directional stability for the three strakes is:

$\Delta C_{n\beta}$ (S1) = 0.0018 $\qquad$ $\Delta C_{n\beta}$ (S2) = 0.0017
$\Delta C_{n\beta}$ (S3) = 0.008

These values of $\Delta C_{n\beta}$ indicate that strake S3 causes an interference that deteriorates the vertical tail contribution by a factor of 2. There are small changes in the lateral or sideforce derivatives, $C_{\ell\beta}$ and $C_{Y\beta}$, with strake configuration but these are second order effects compared to the effects of strake shape on $C_{n\beta}$.

The trends are essentially the same at Mach = 1.2. The vertical tail increment to $C_{n\beta}$ deteriorates more rapidly with angle of attack than for the subsonic case. <u>At low speeds, the overall best canard/strake configuration from the standpoint of lateral-directional characteristics is the baseline canard location C1 and baseline strake S1. At transonic Mach numbers, the limited amount of data precludes determining the best canard/strake combination for lateral-directional characteristics. The baseline canard/strake</u>

combination did however yield the best overall longitudinal trimmed configuration characteristics.

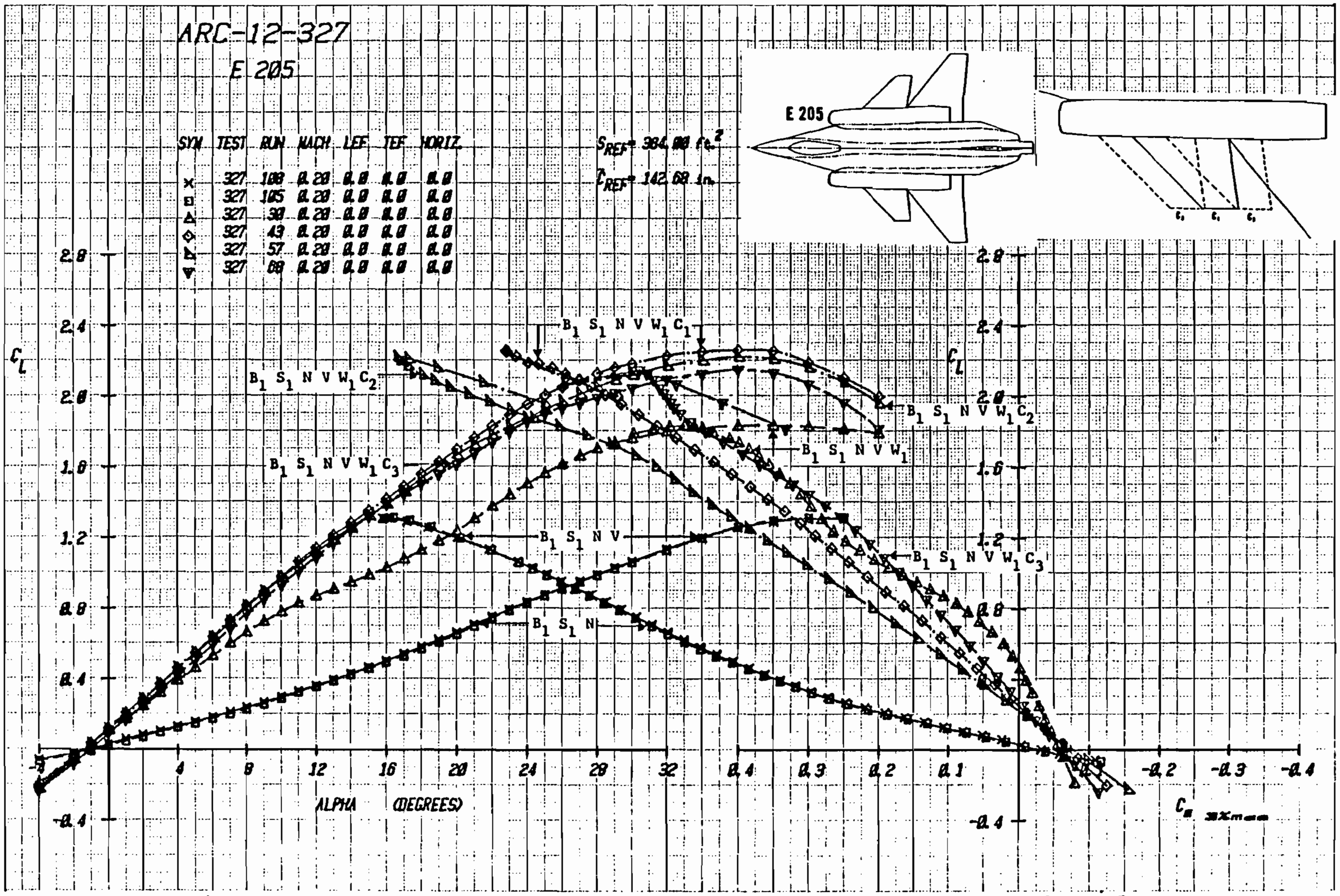

Figure 1-1a Effect of Component Buildup on Lift and Moment, Mach = .2

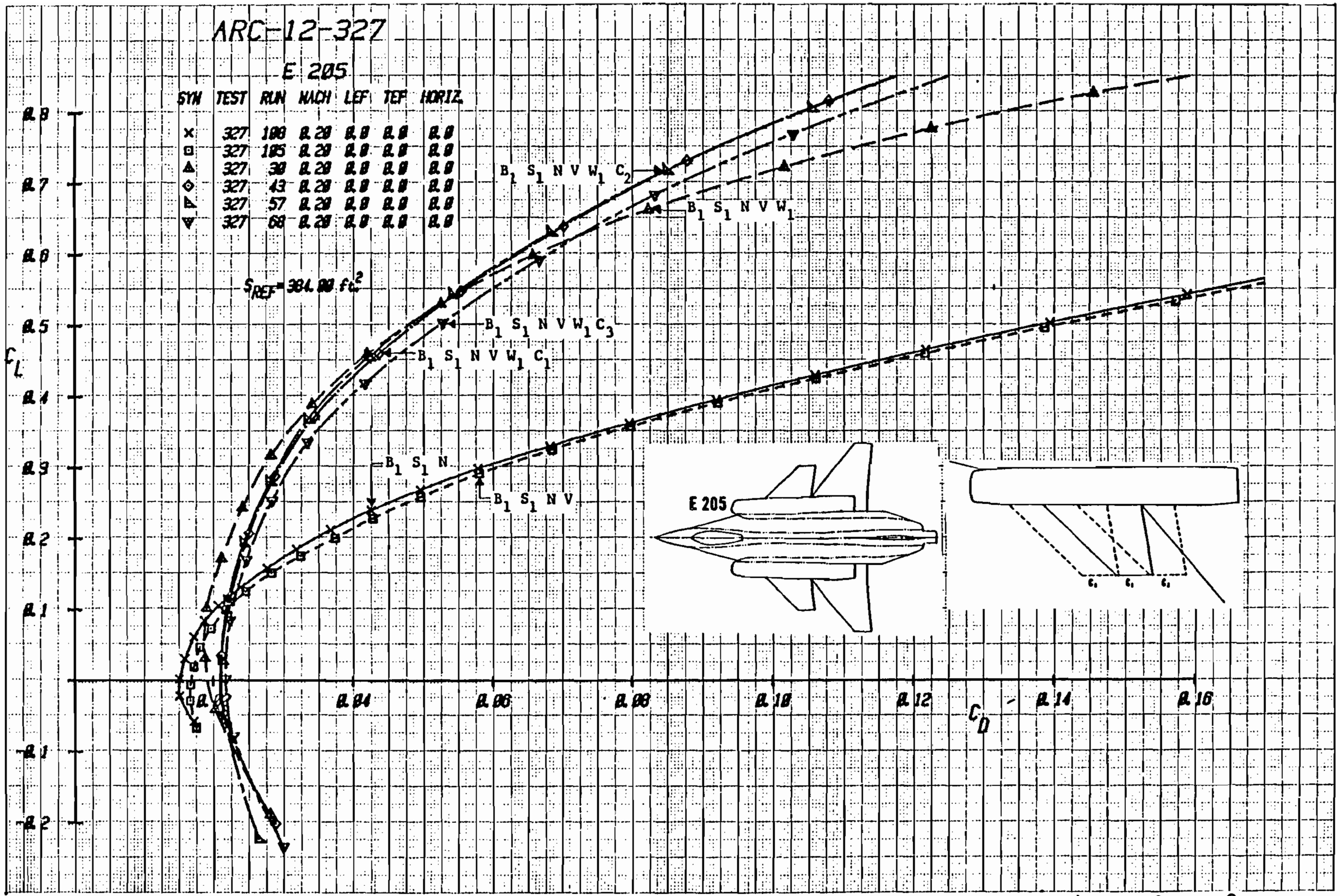

Figure 1-1b Effect of Component Buildup on Drag, (Expanded Drag Scale), Mach = .2

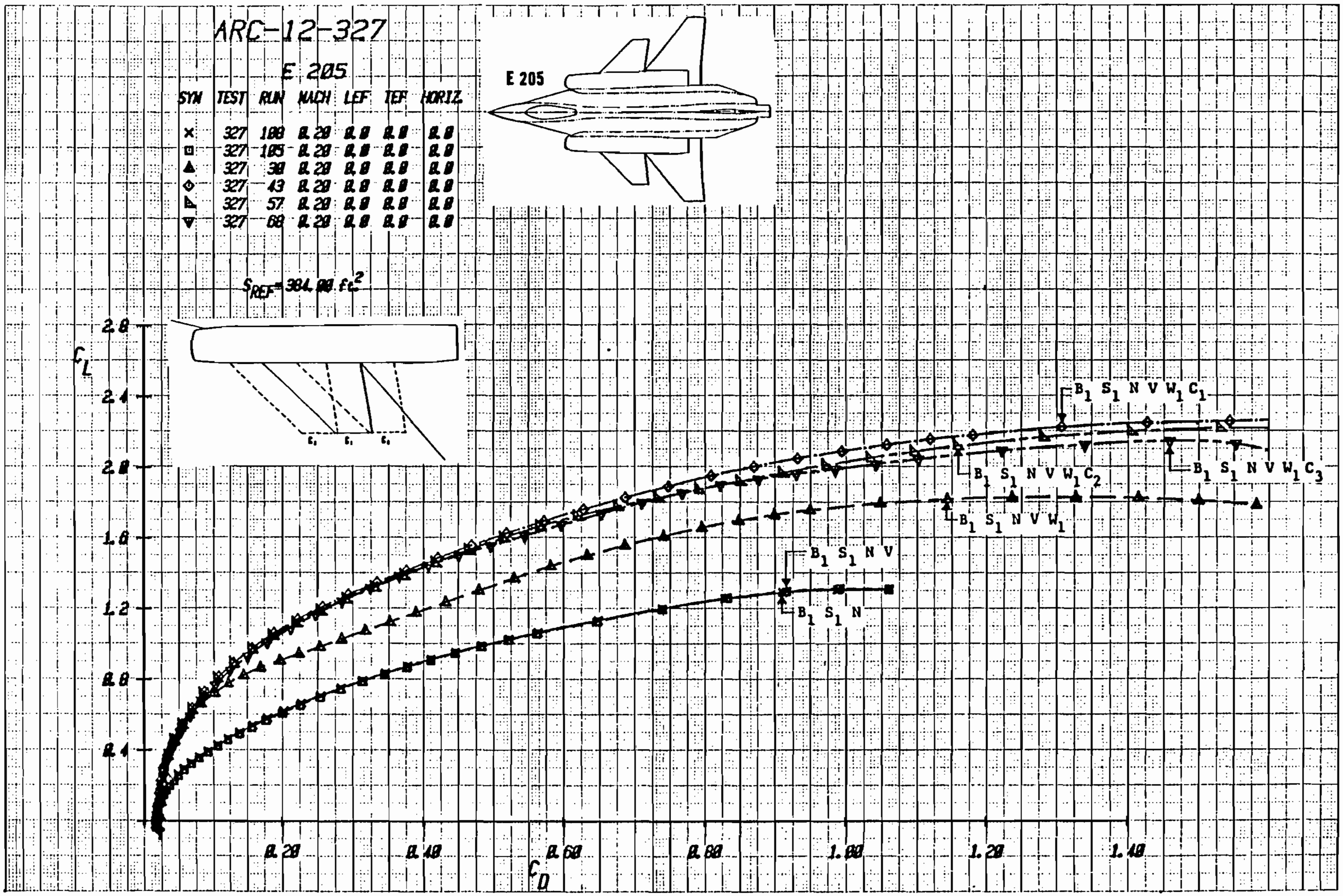

Figure 1-1c Effect of Component Buildup on Drag, Mach = .2

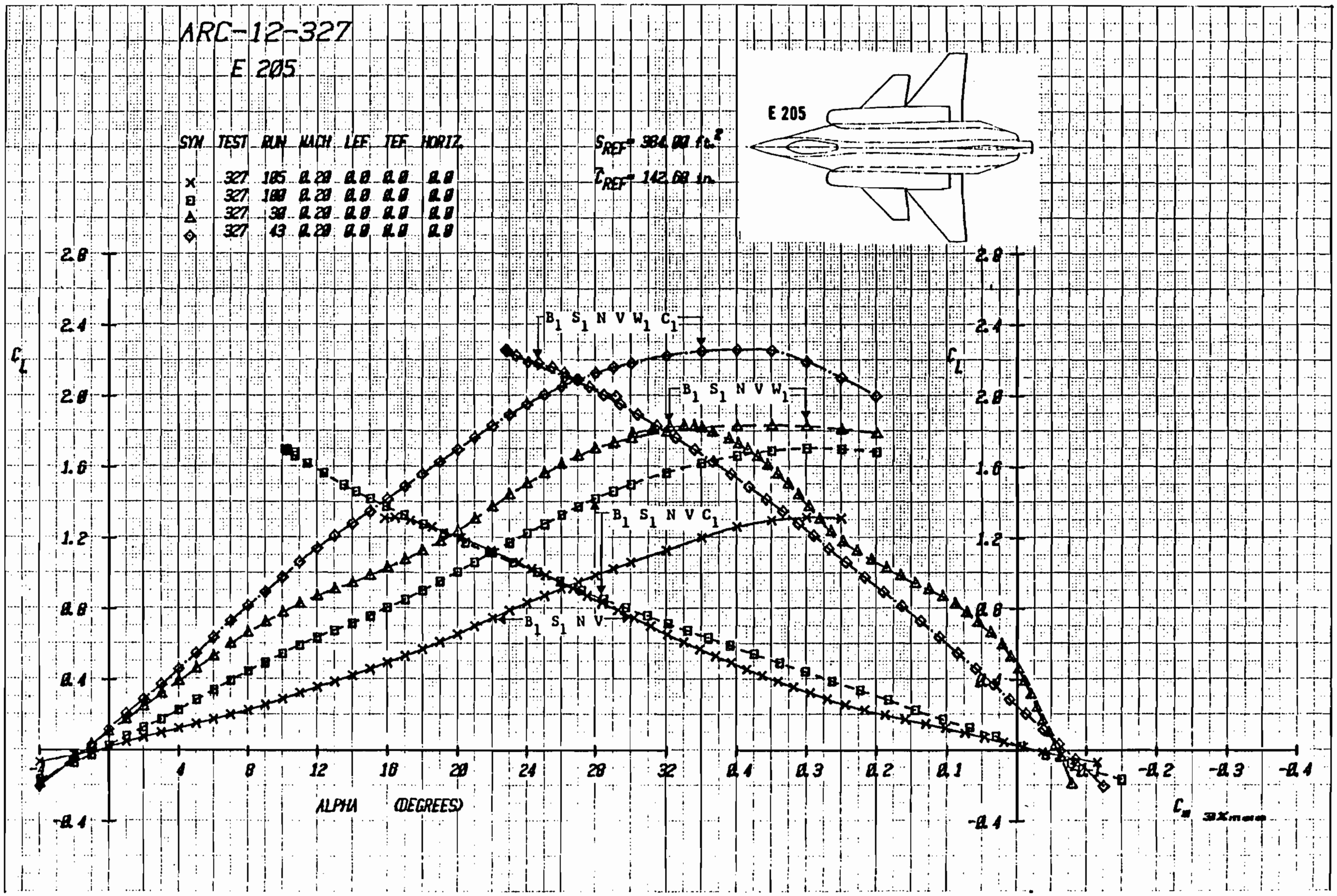

Figure 1-2a Lift and Moment Interference Data for E205 Configuration, $\delta_c = 0°$, Mach = .2

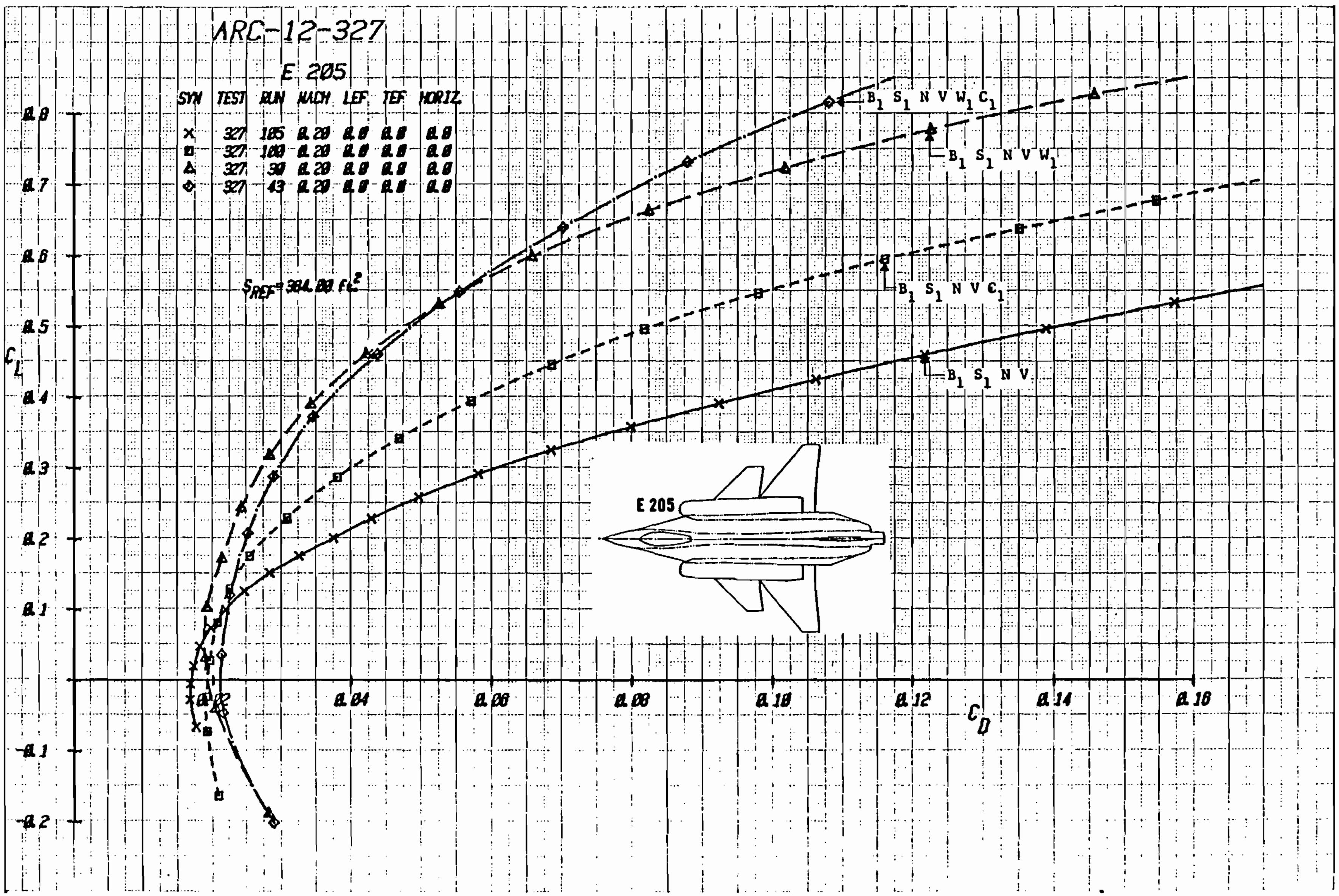

Figure 1-2b Drag Interference Data for E205 Configuration, δ_c = 0°, (Expanded Drag Scale), Mach = .2

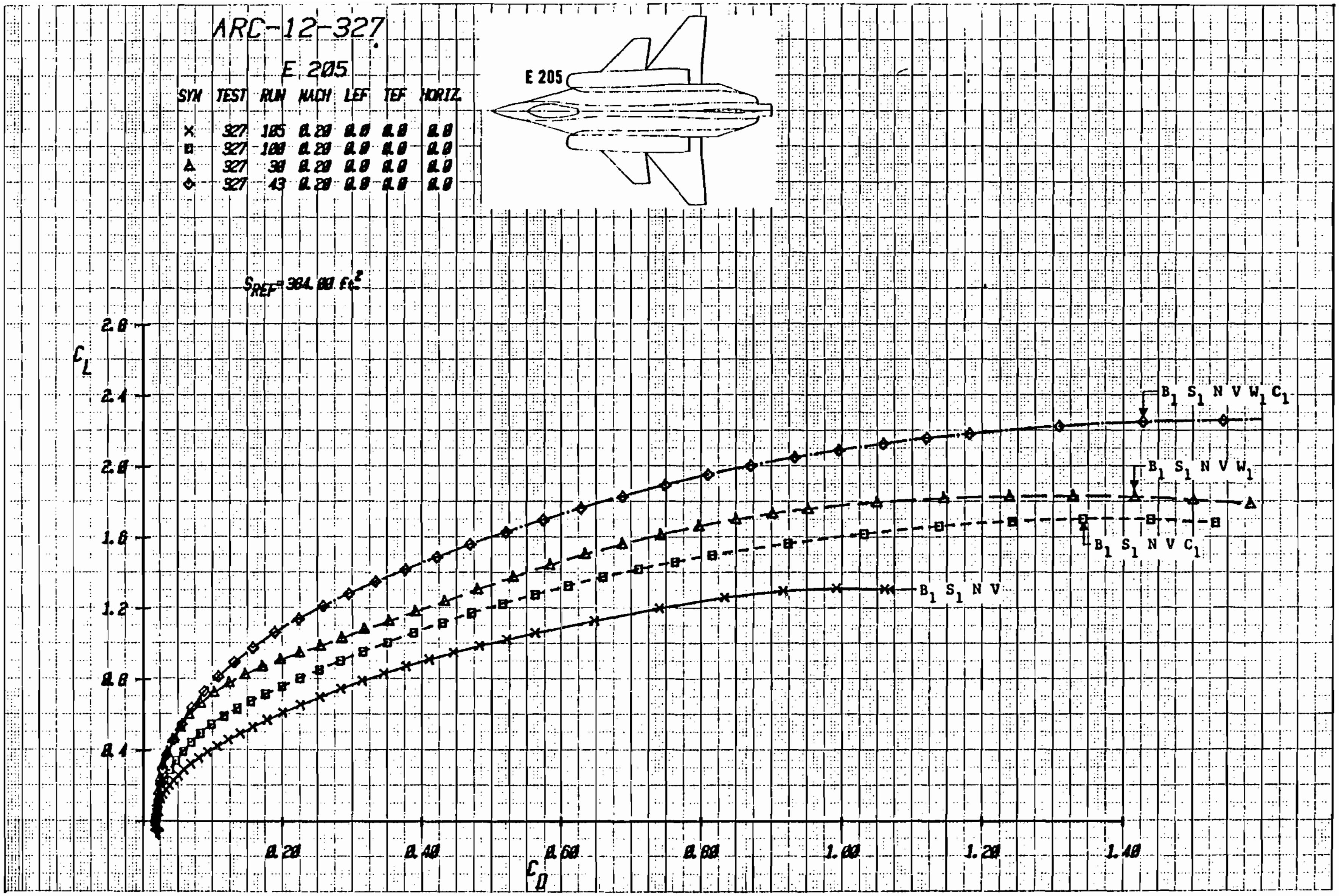

Figure1-2c Drag Interference Data for E205 Configuration, $\delta_c = 0°$, Mach = .2

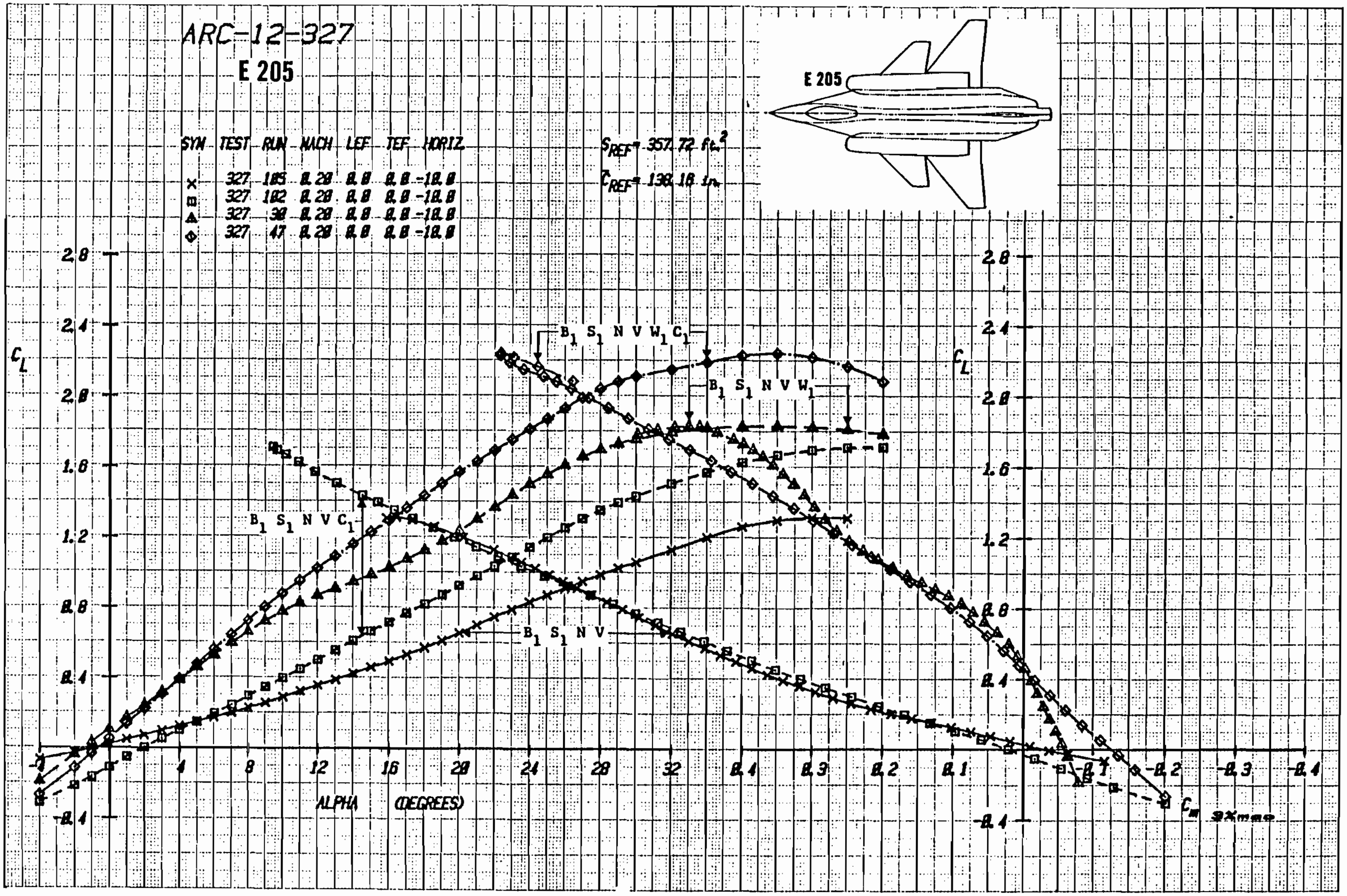

Figure1-3a Lift and Moment Inteference Data for E205 Configuration, δ_c = -10°, Mach = .2

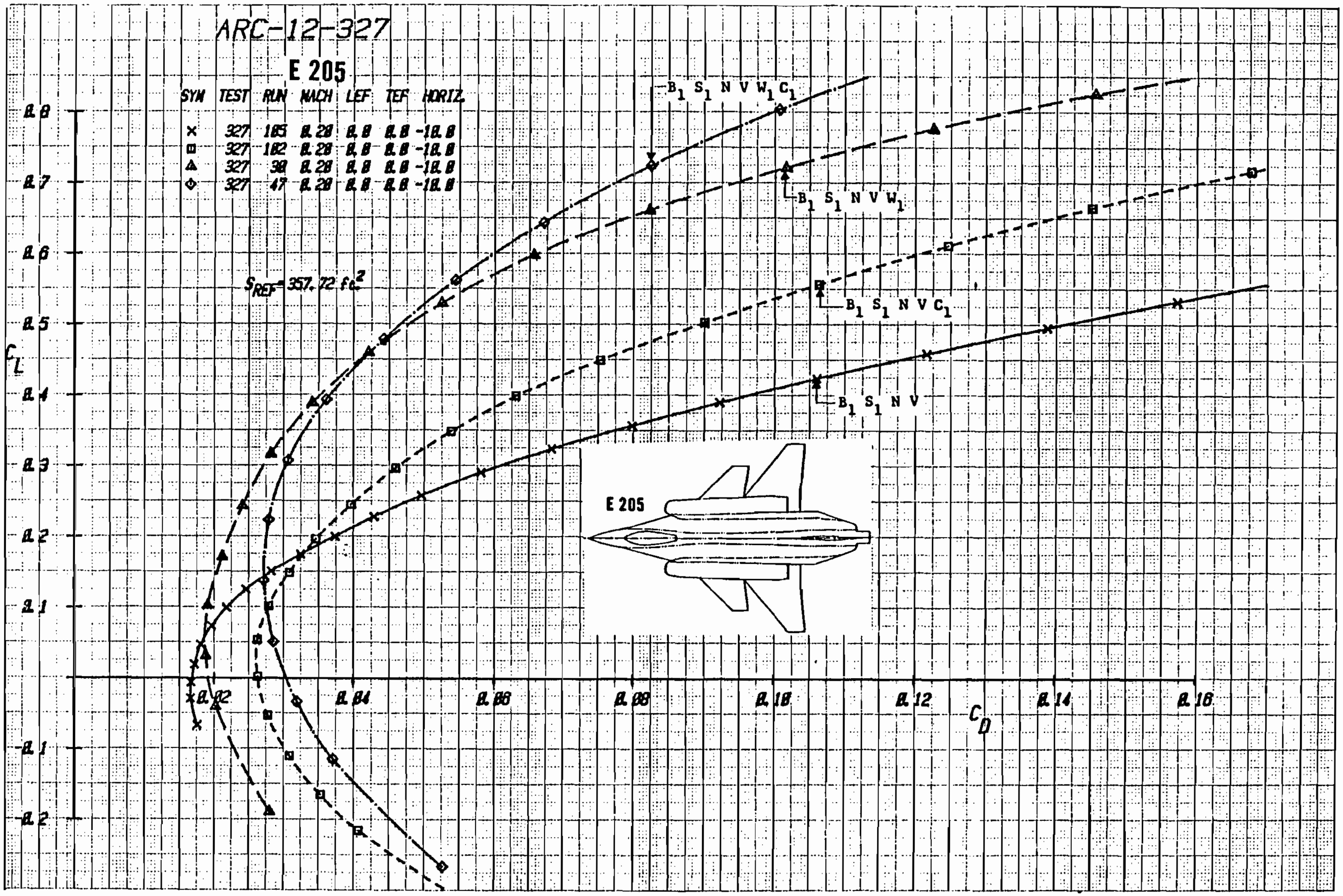

Figure 1-3b Drag Interference Data for E205 Configuration, δ_c = -10°, (Expanded Drag Scale), Mach = .2

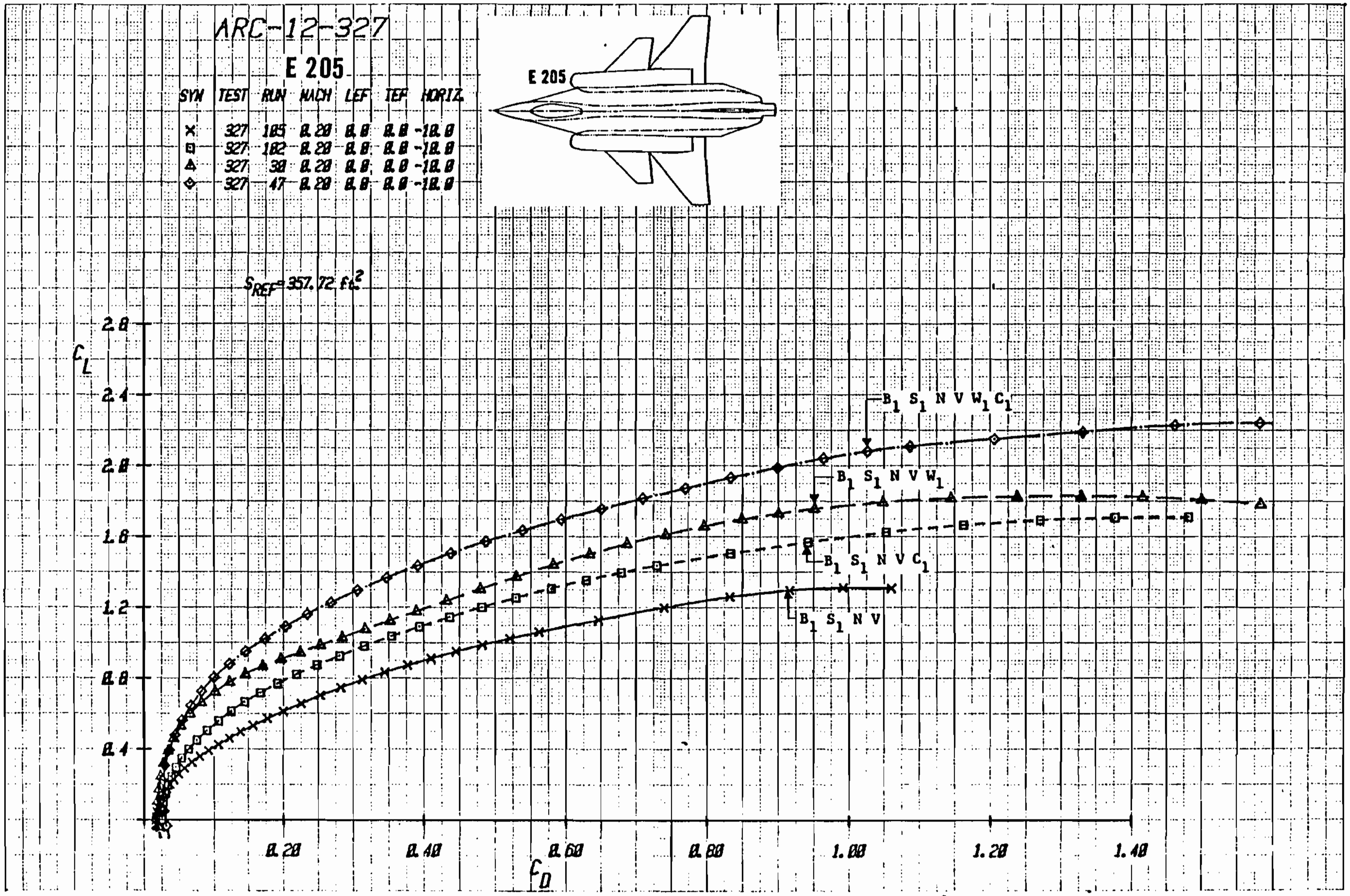

Figure 1-3c Drag Interference Data for E205 Configuration, δ_c = -10°, Mach = .2

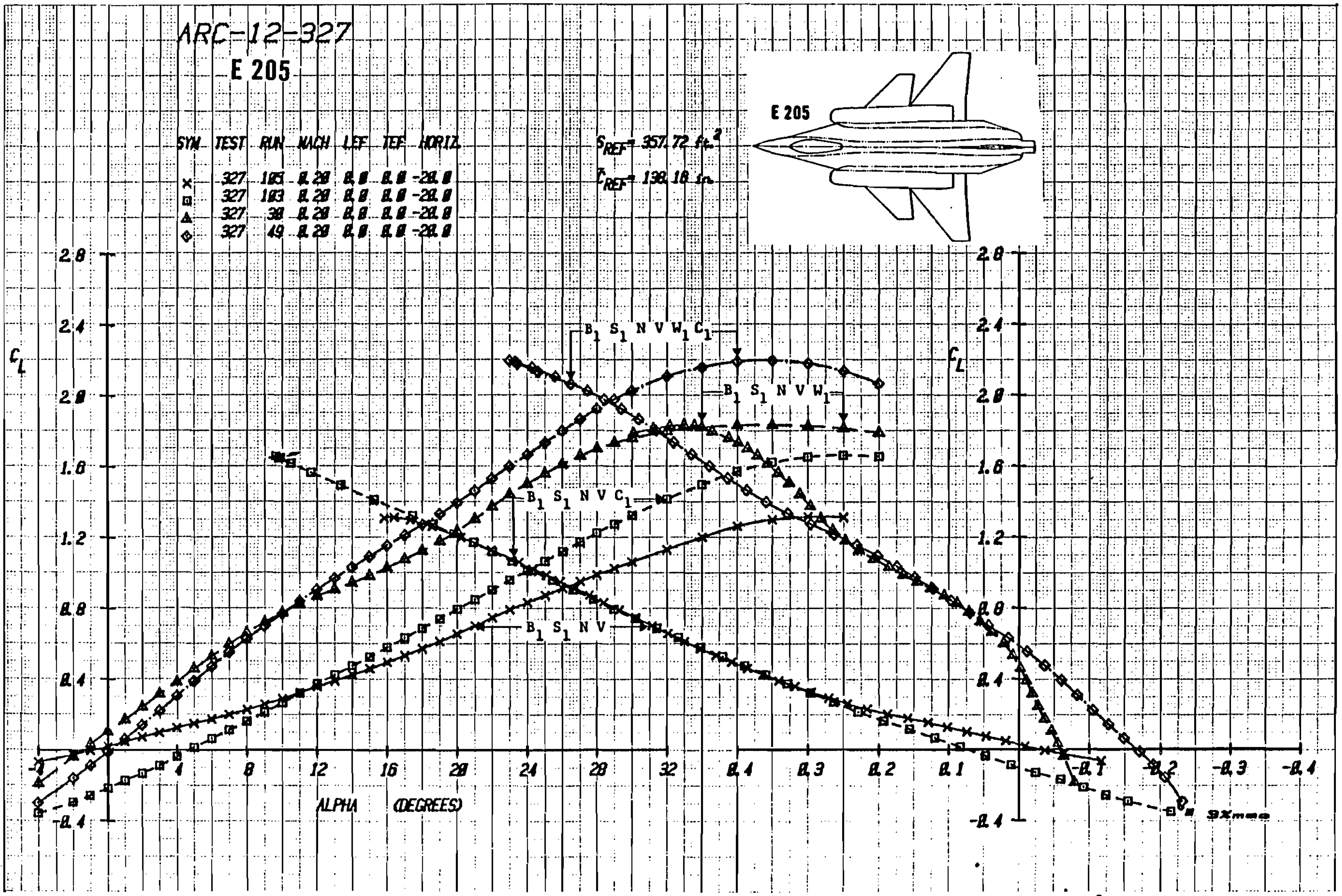

Figure1-4a Lift and Moment Interference Data For E205 Configuration, δ_c = -20°, Mach = .2

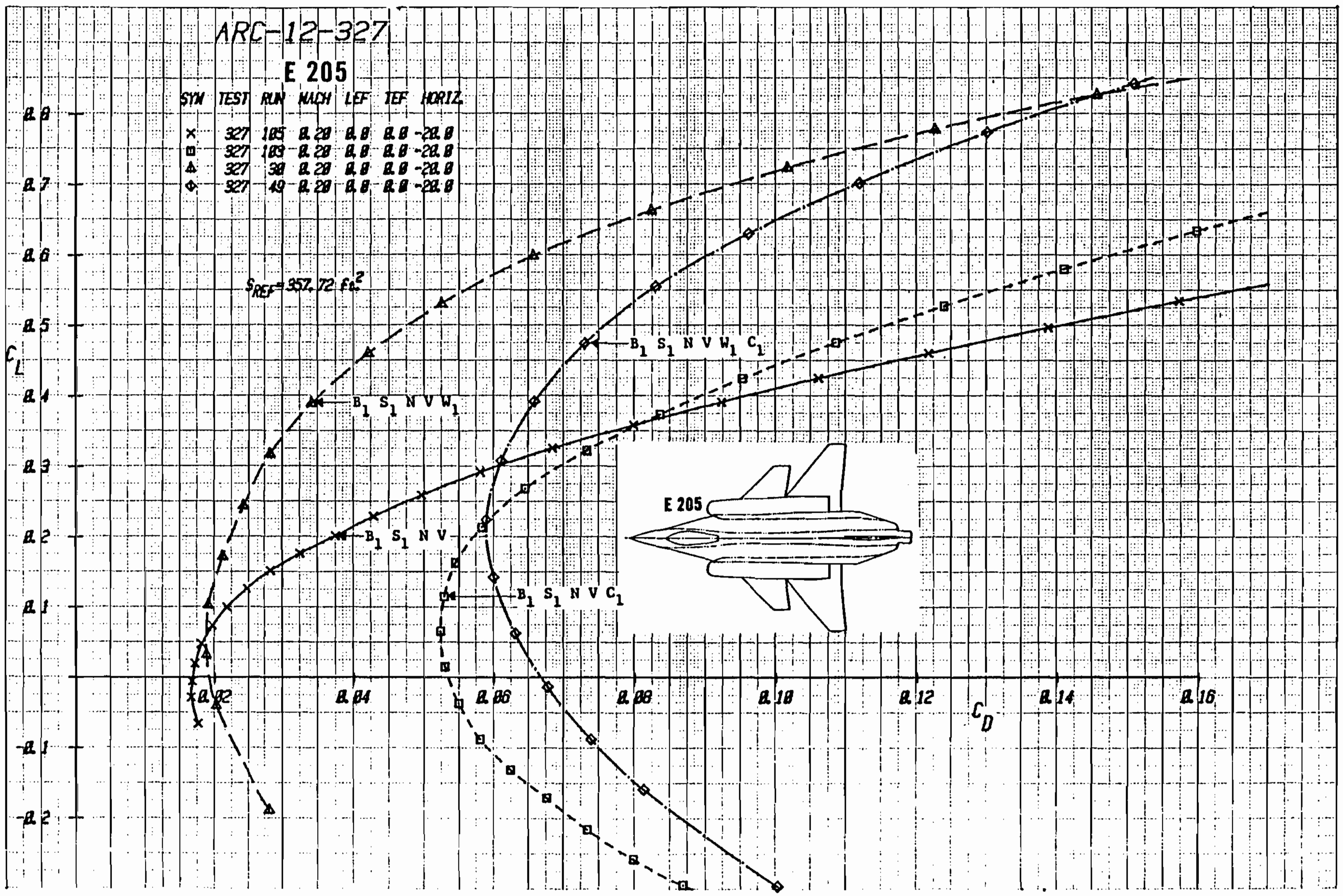

Figure 1-4b Drag Interference Data for E205 Configuration, $\delta_c = -20°$, (Expanded Drag Scale), Mach = .2

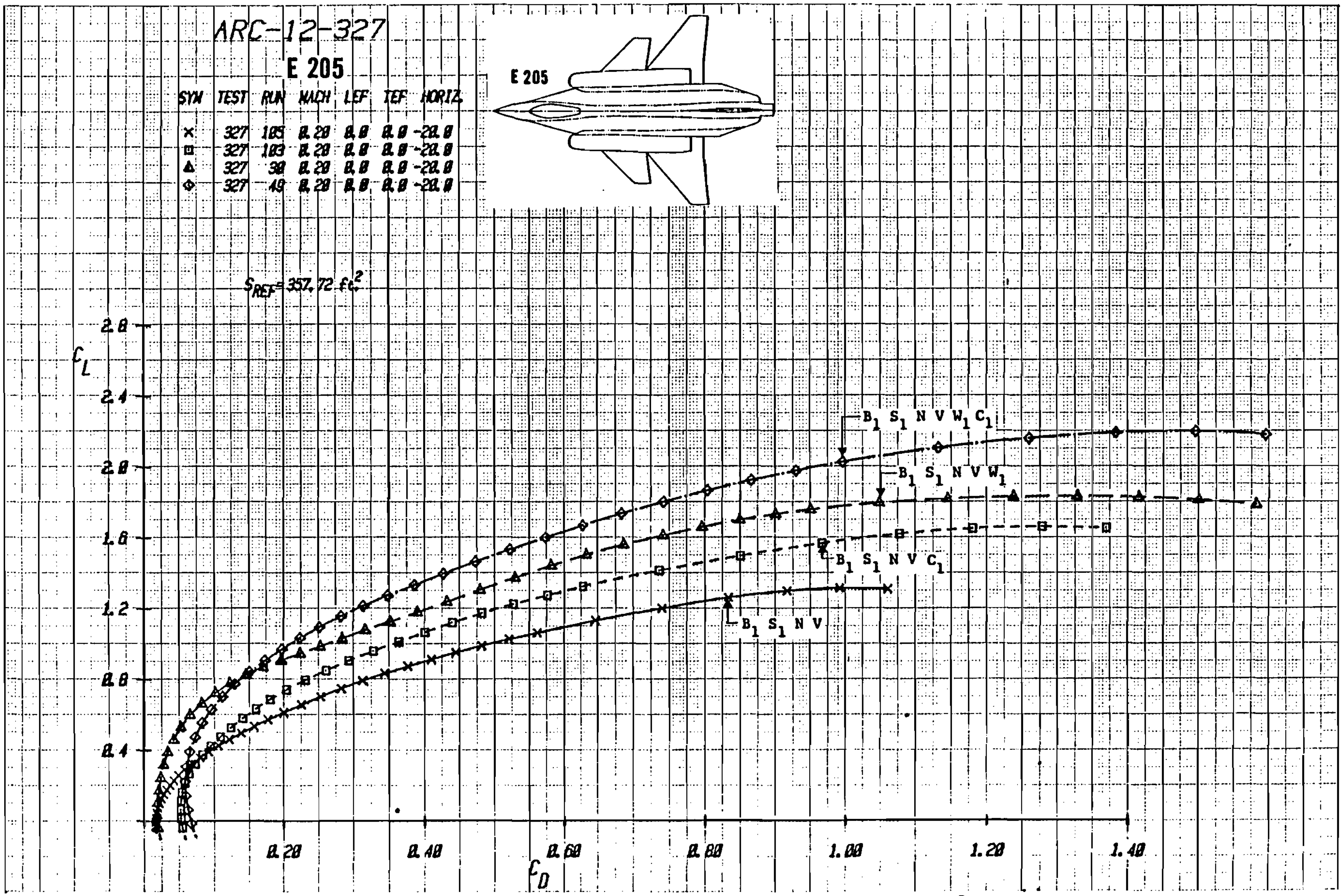

Figure 1-4c Drag Interference Data for E205 Configuration, δ_c = -20°, Mach = .2

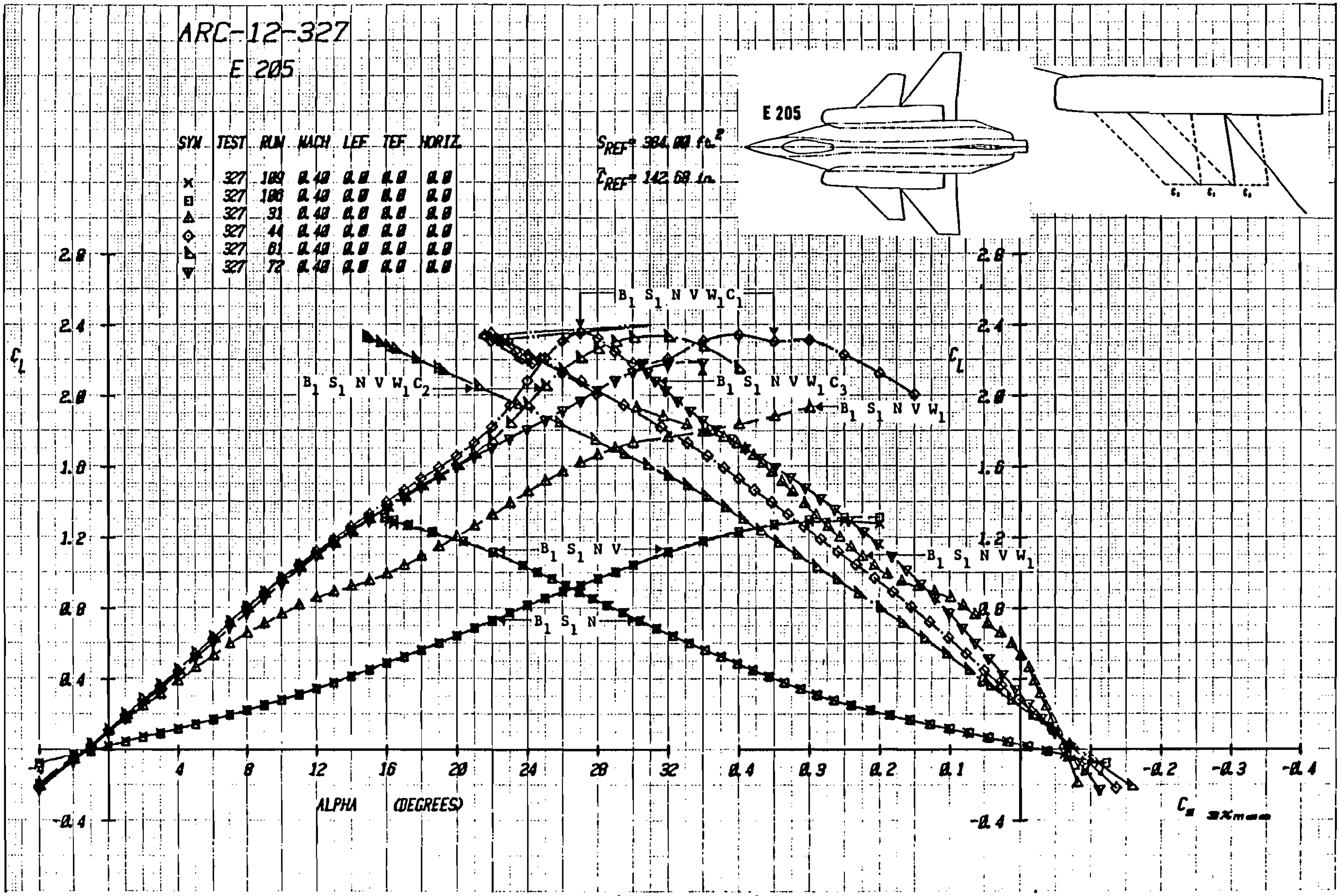

Figure1-5a Effect of Component Buildup on Lift and Moment, Mach = .4

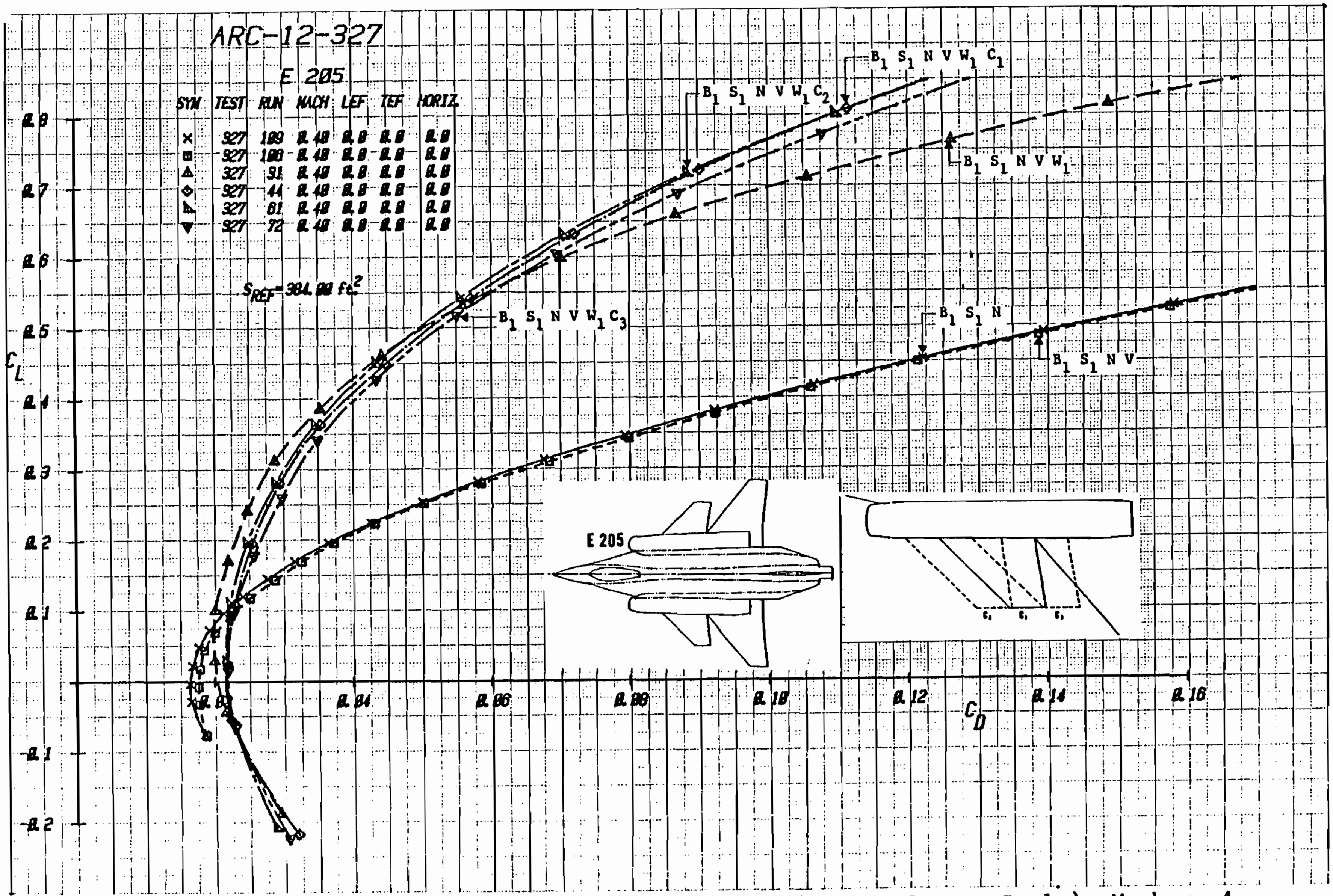

Figure 1-5b Effect of Component Buildup on Drag, (Expanded Drag Scale), Mach = .4

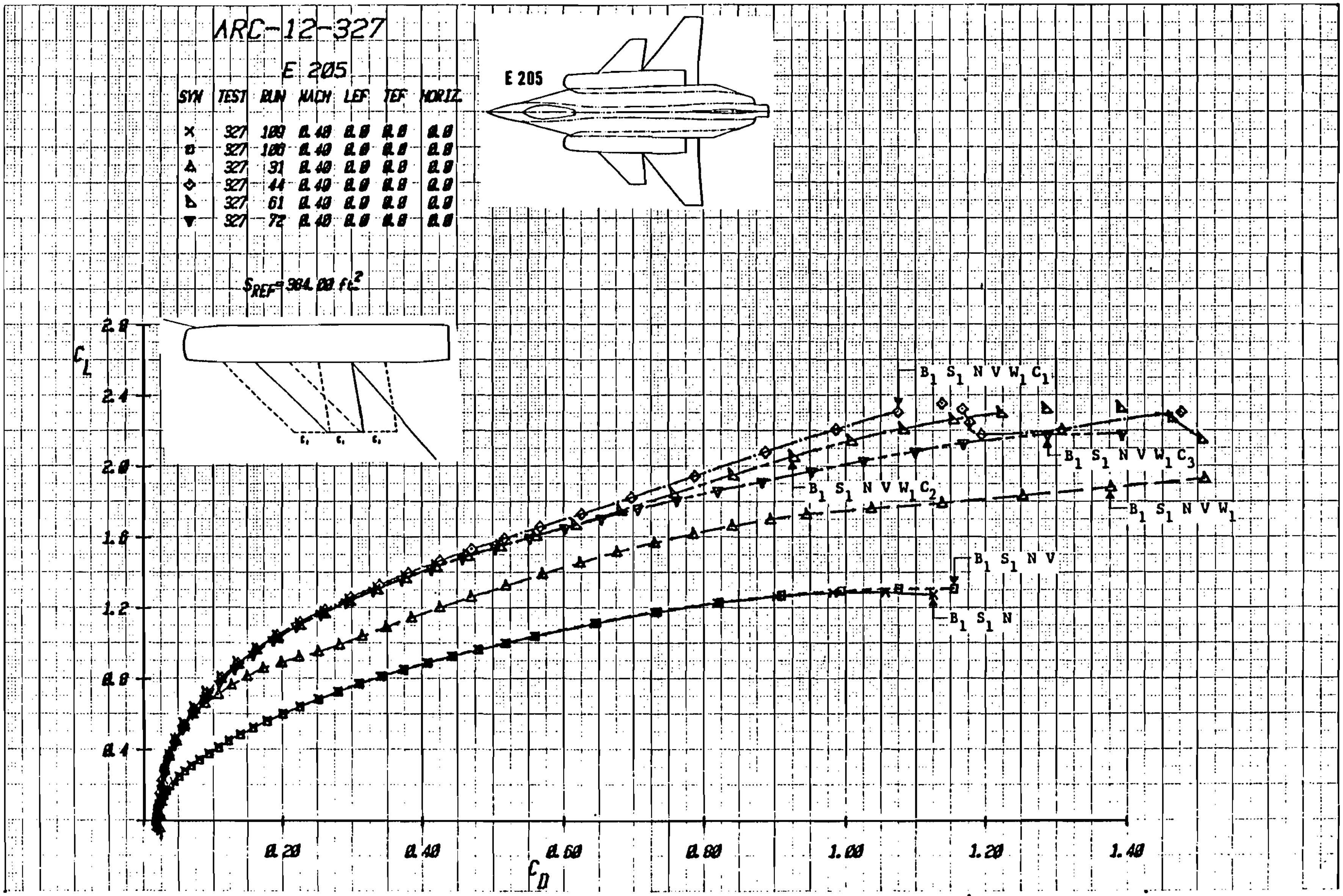

Figure 1-5c Effect of Component Buildup on Drag, Mach = .4

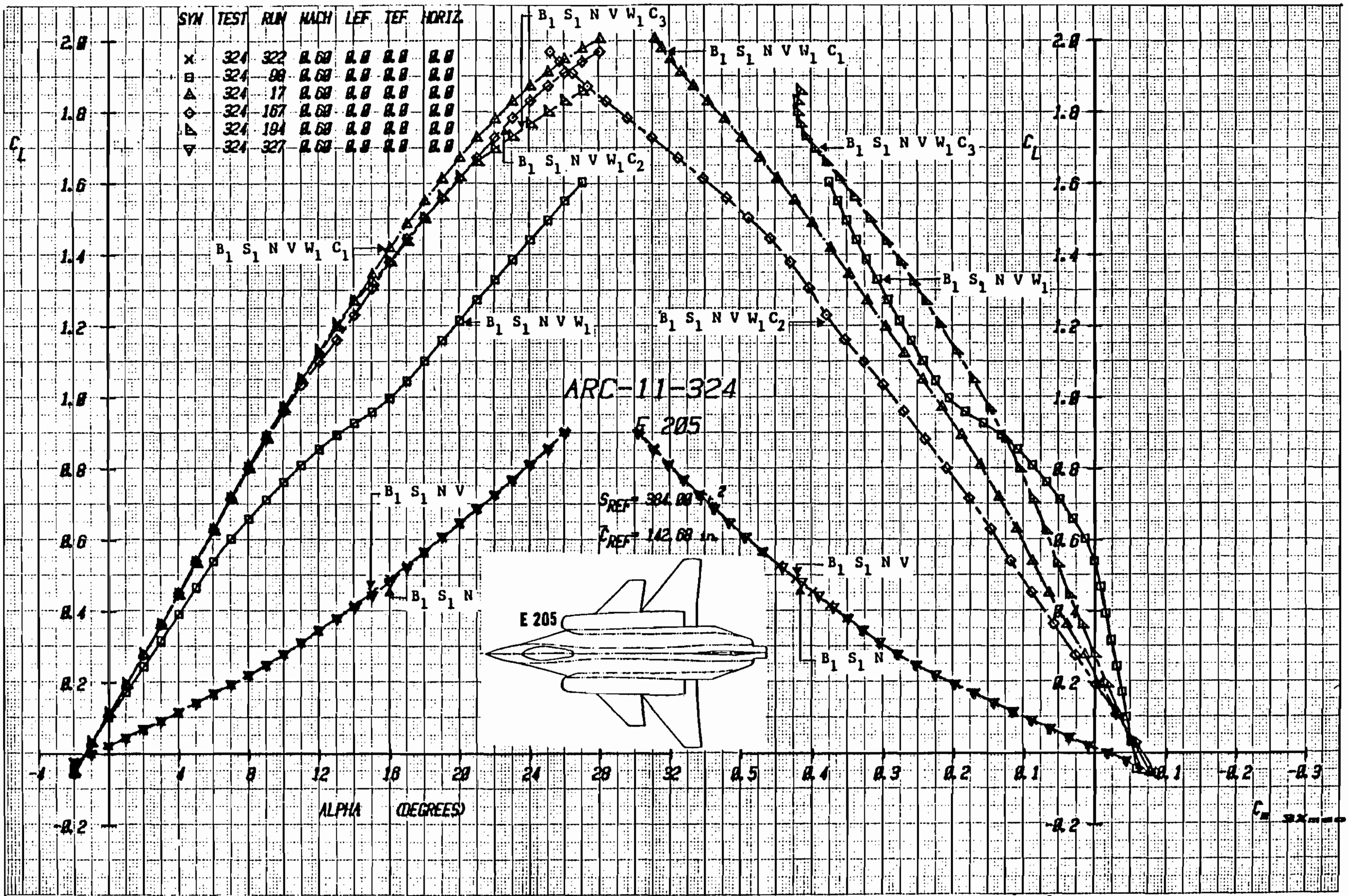

Figure 1-6a Effect of Component Buildup on Lift and Moment, Mach = .6

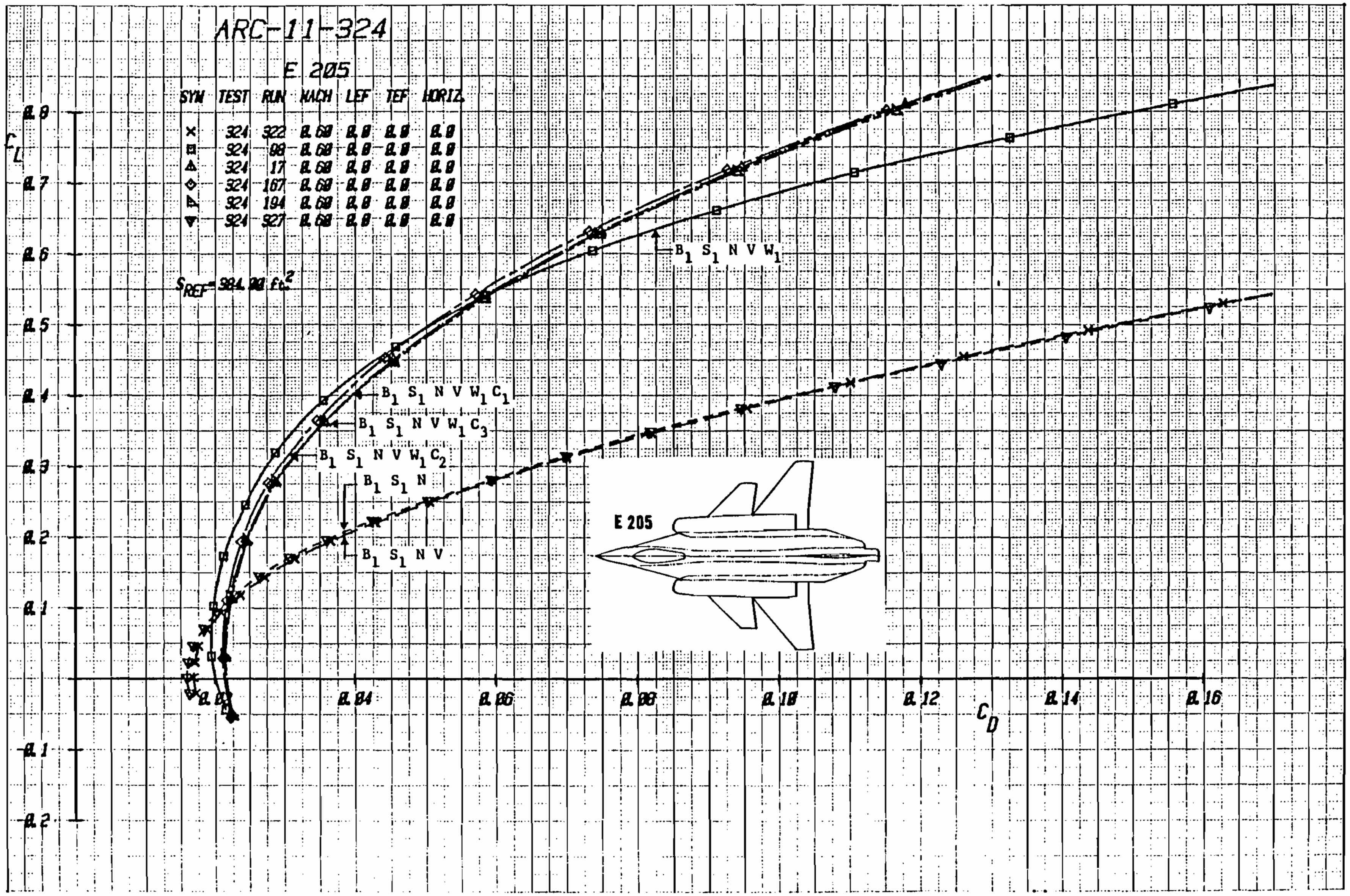

Figure1-6b Effect of Component Buildup on Drag, Mach = .6

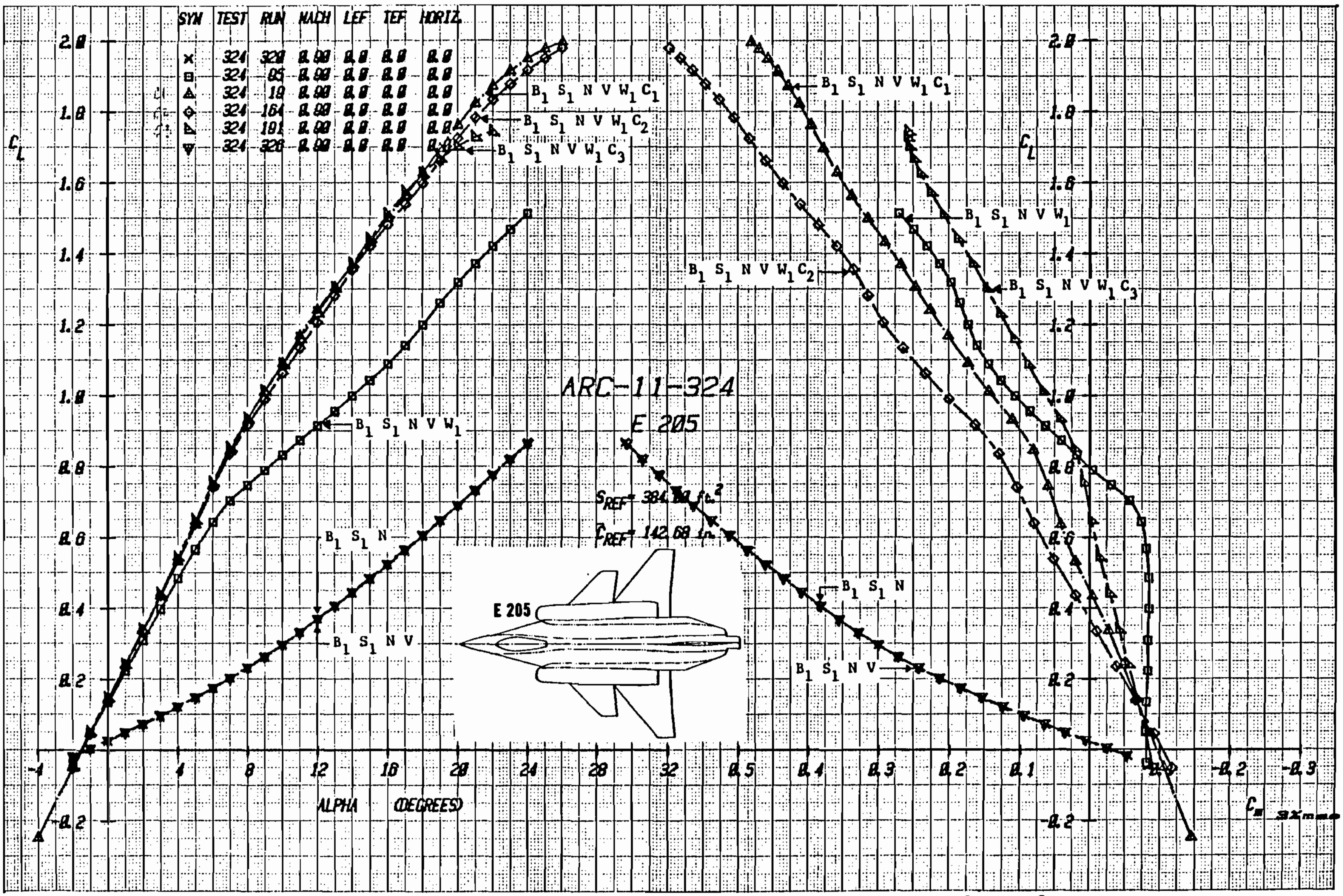

Figure 1-7a Effect of Component Buildup on Lift and Moment, Mach = .9

37

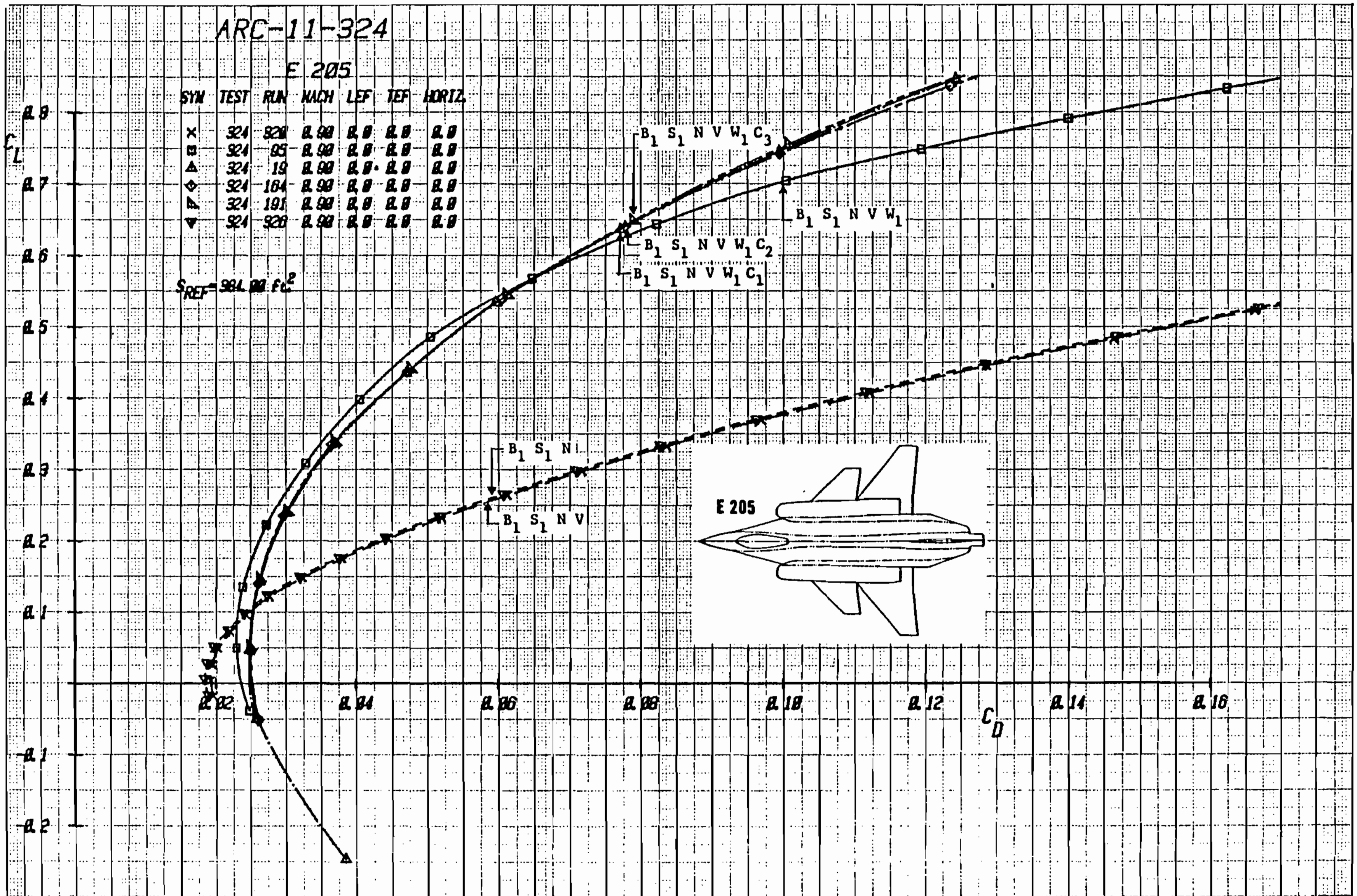

Figure 1-7b Effect of Component Buildup on Drag, Mach = .9

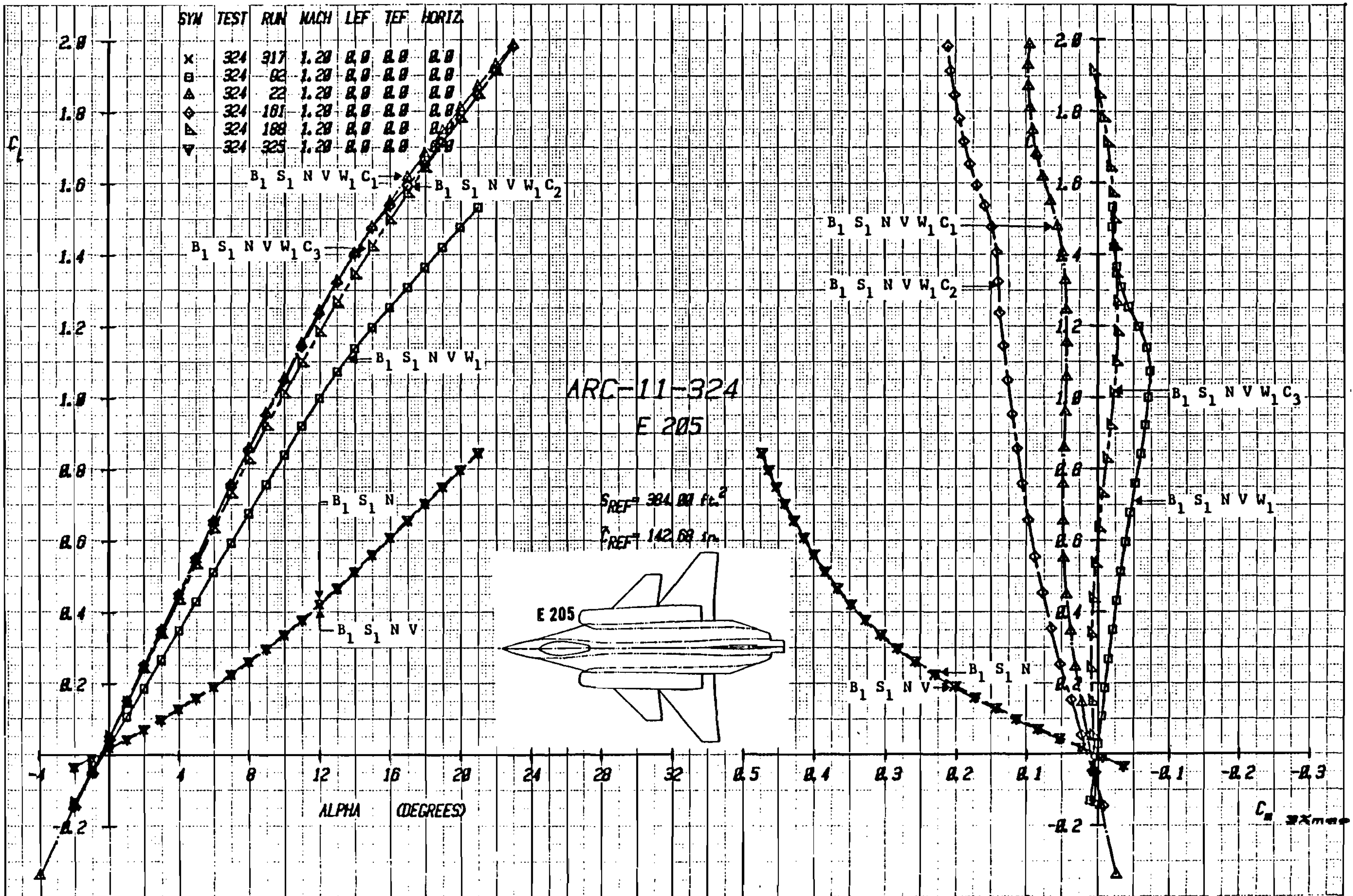

Figure 1-8a Effect of Component Buildup on Lift and Moment, Mach = 1.2

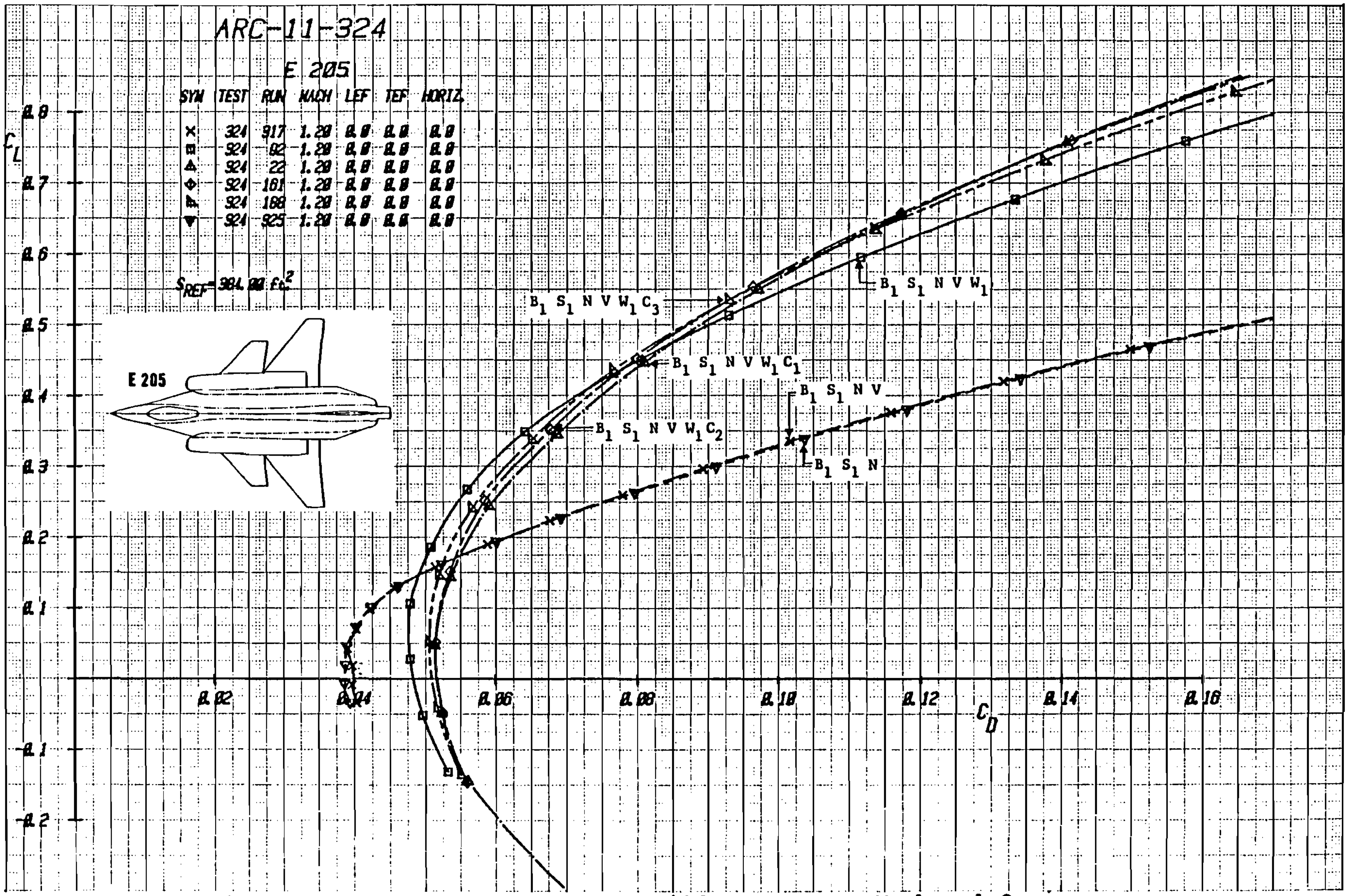

Figure 1-8b Effect of Component Buildup on Drag, Mach = 1.2

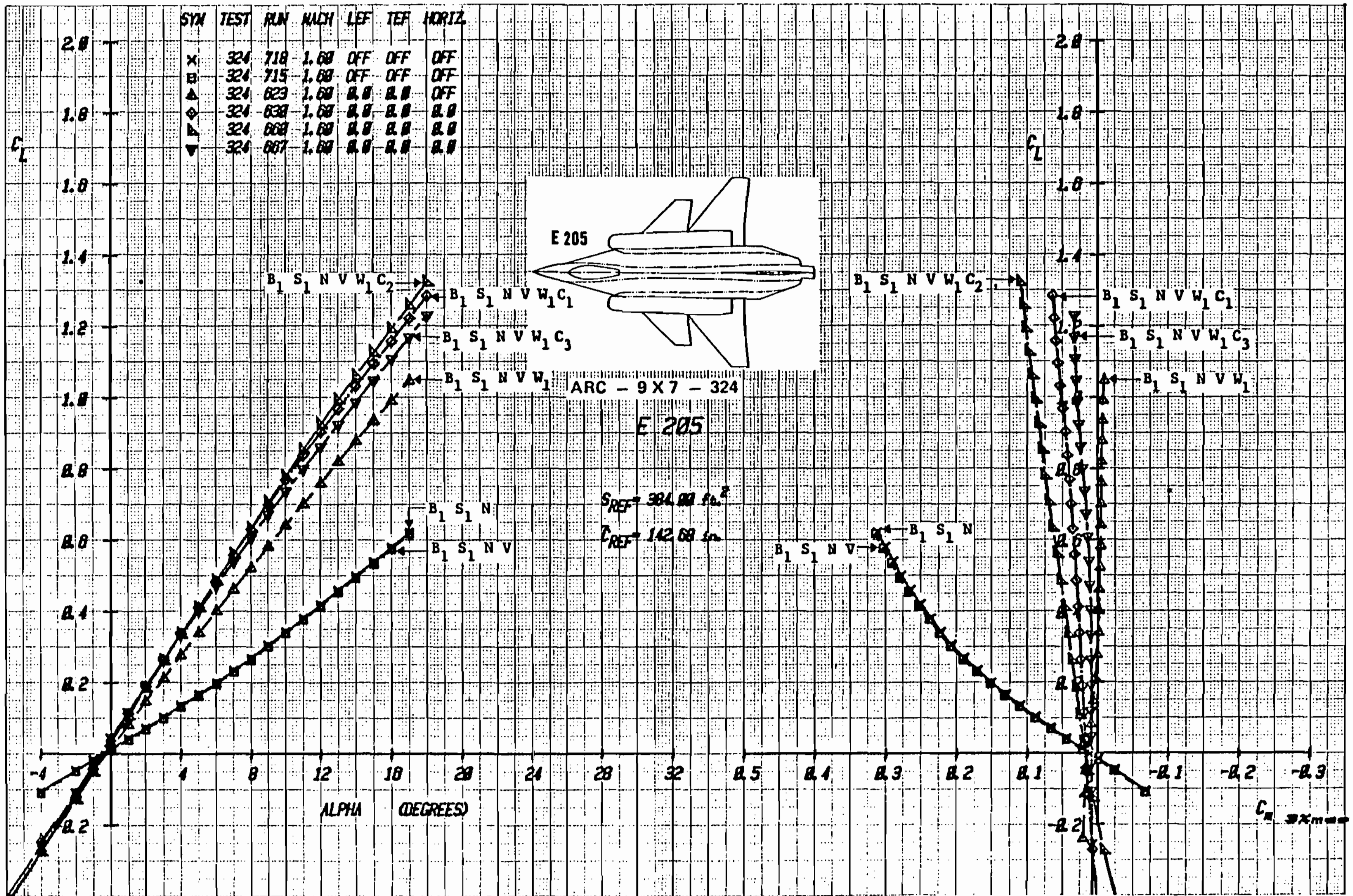

Figure 1-9a Effect of Component Buildup on Lift and Moment, Mach = 1.6

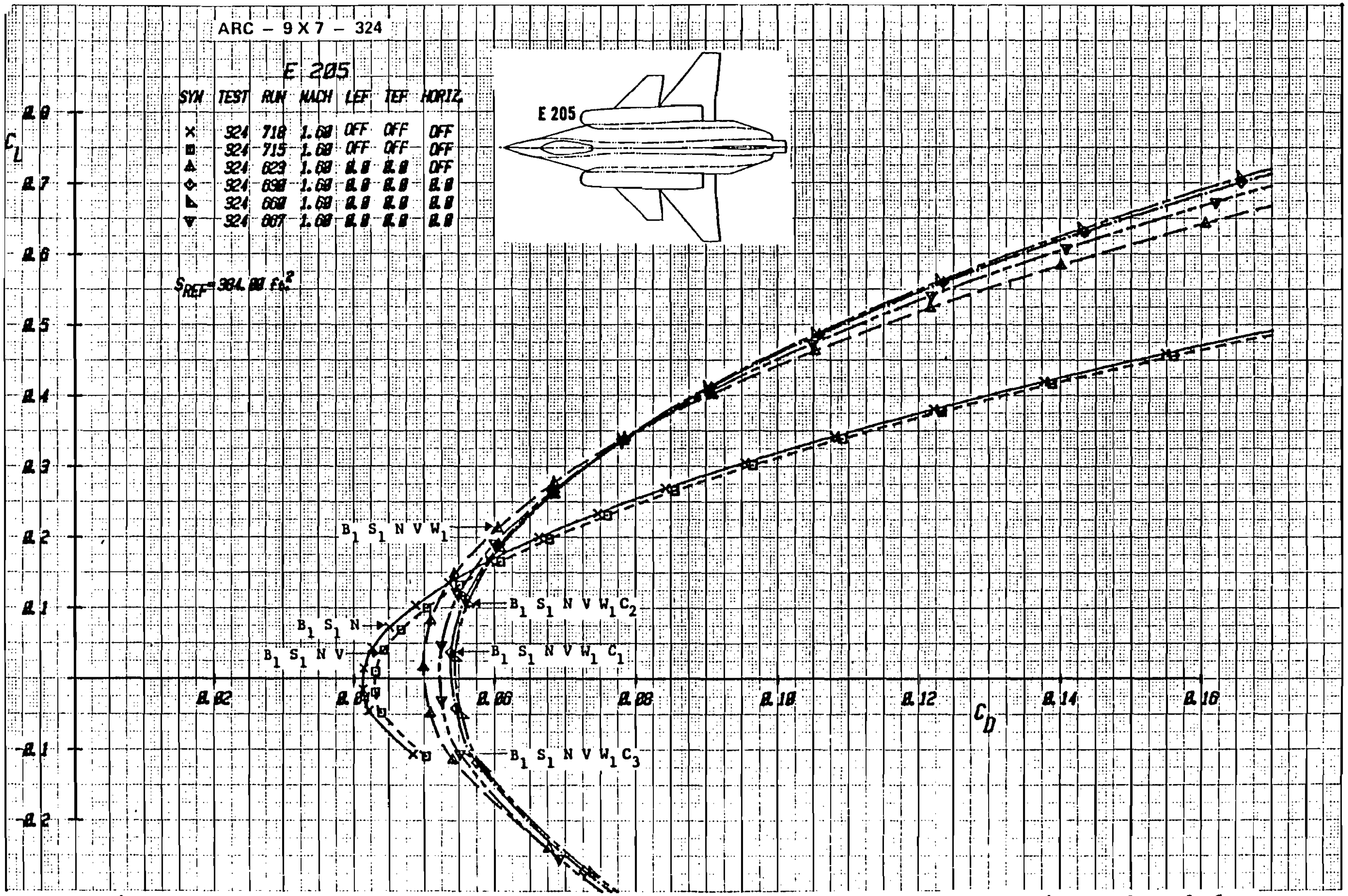

Figure 1-9b Effect of Component Buildup on Drag, (Expanded Drag Scale), Mach = 1.6

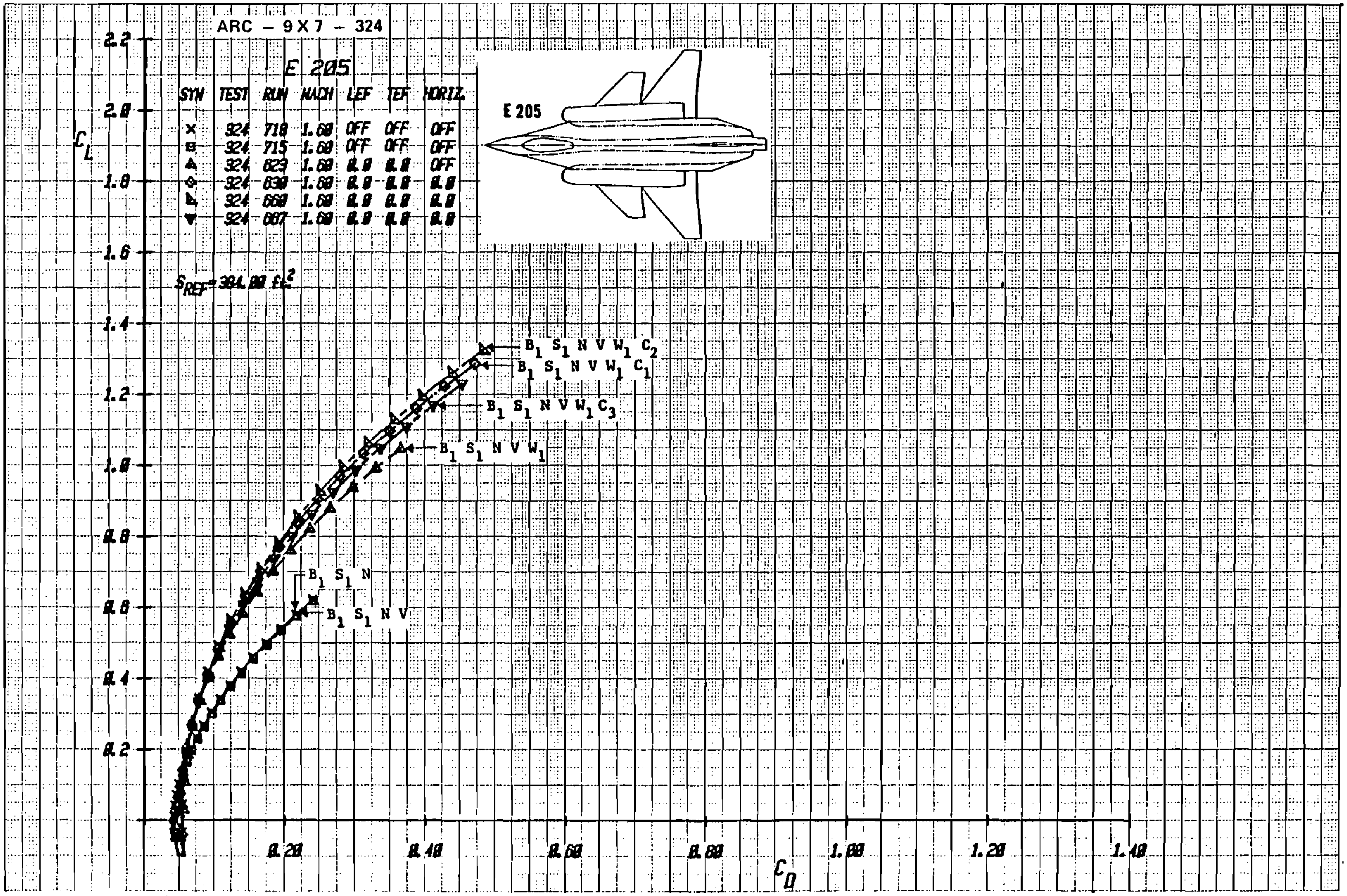

Figure 1-9c Effect of Component Buildup on Drag, Mach = 1.6

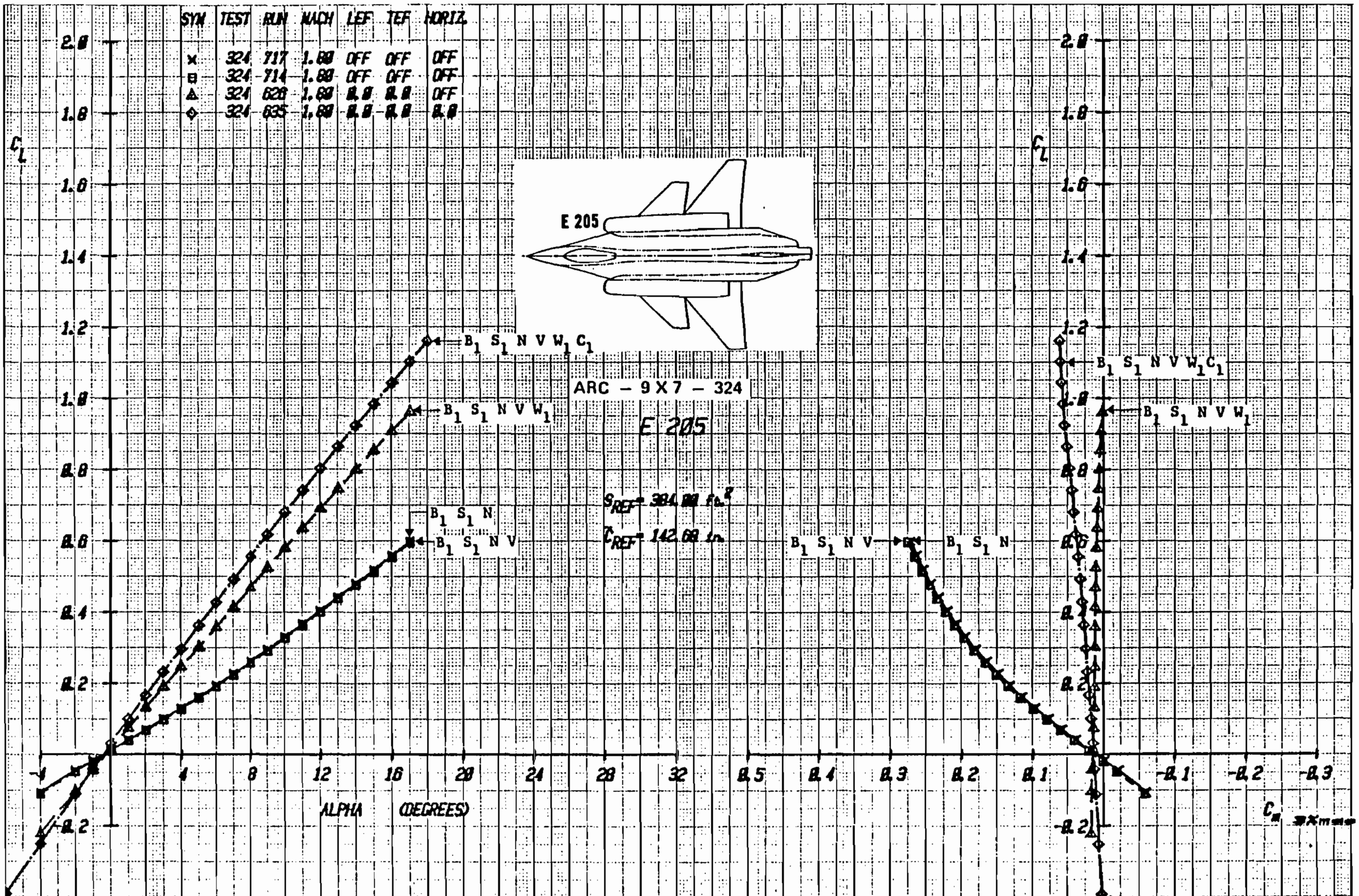

Figure1-10aEffect of Component Buildup on Lift and Moment, Mach = 1.8

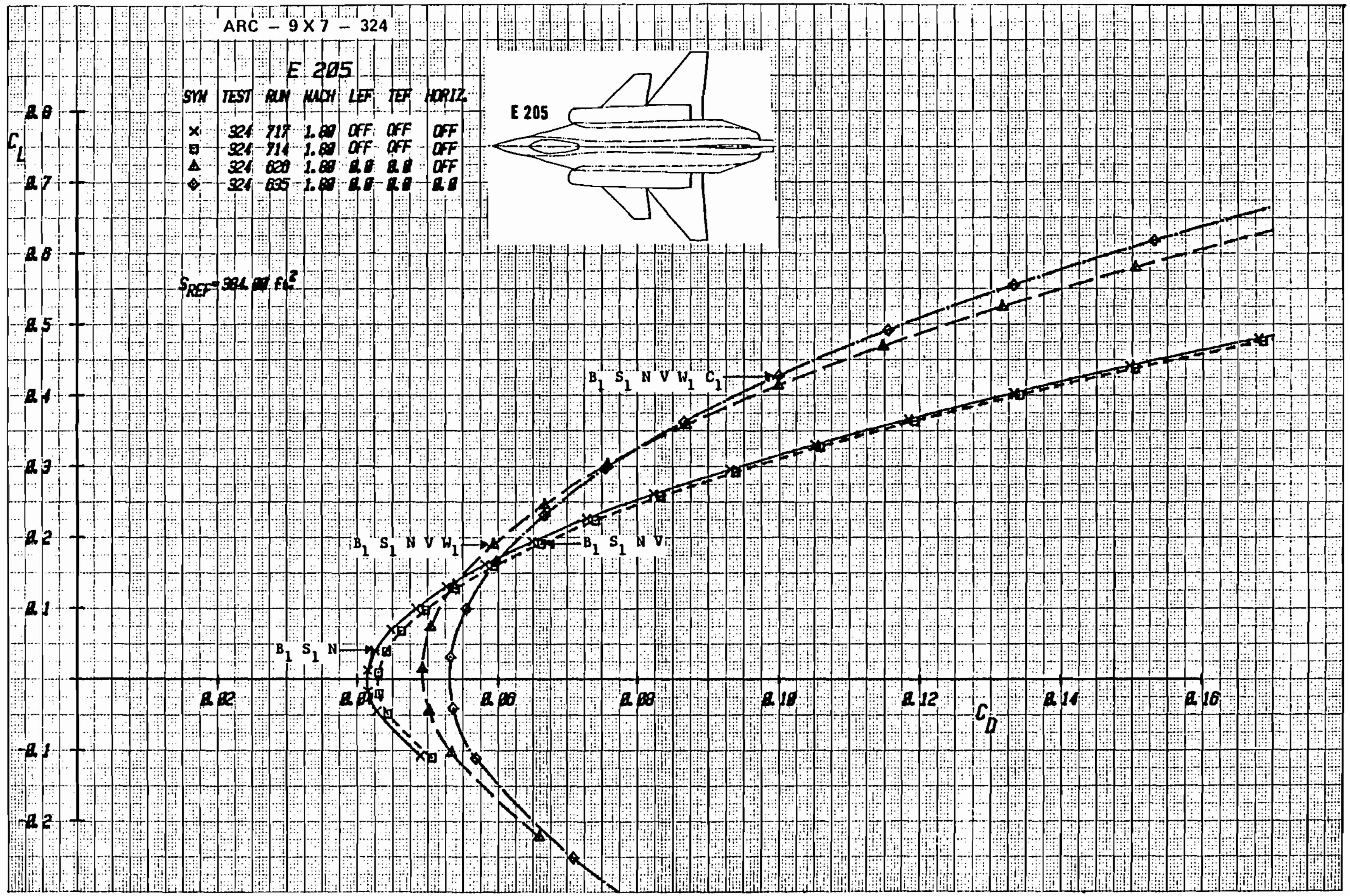

Figure1-10bEffect of Component Buildup on Drag, (Expanded Drag Scale), Mach = 1.8

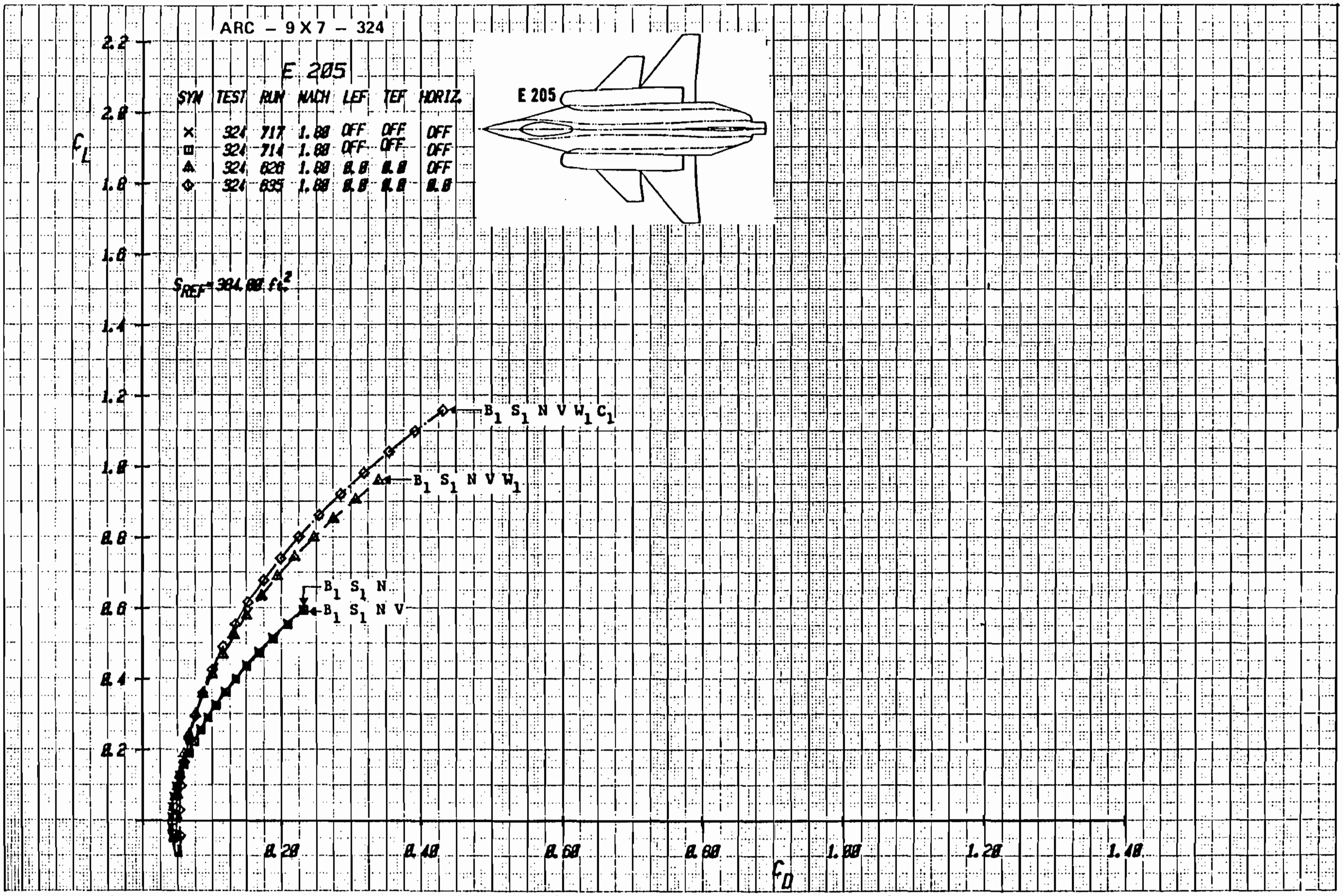

Figure1-10cEffect of Component Buildup on Drag, Mach = 1.8

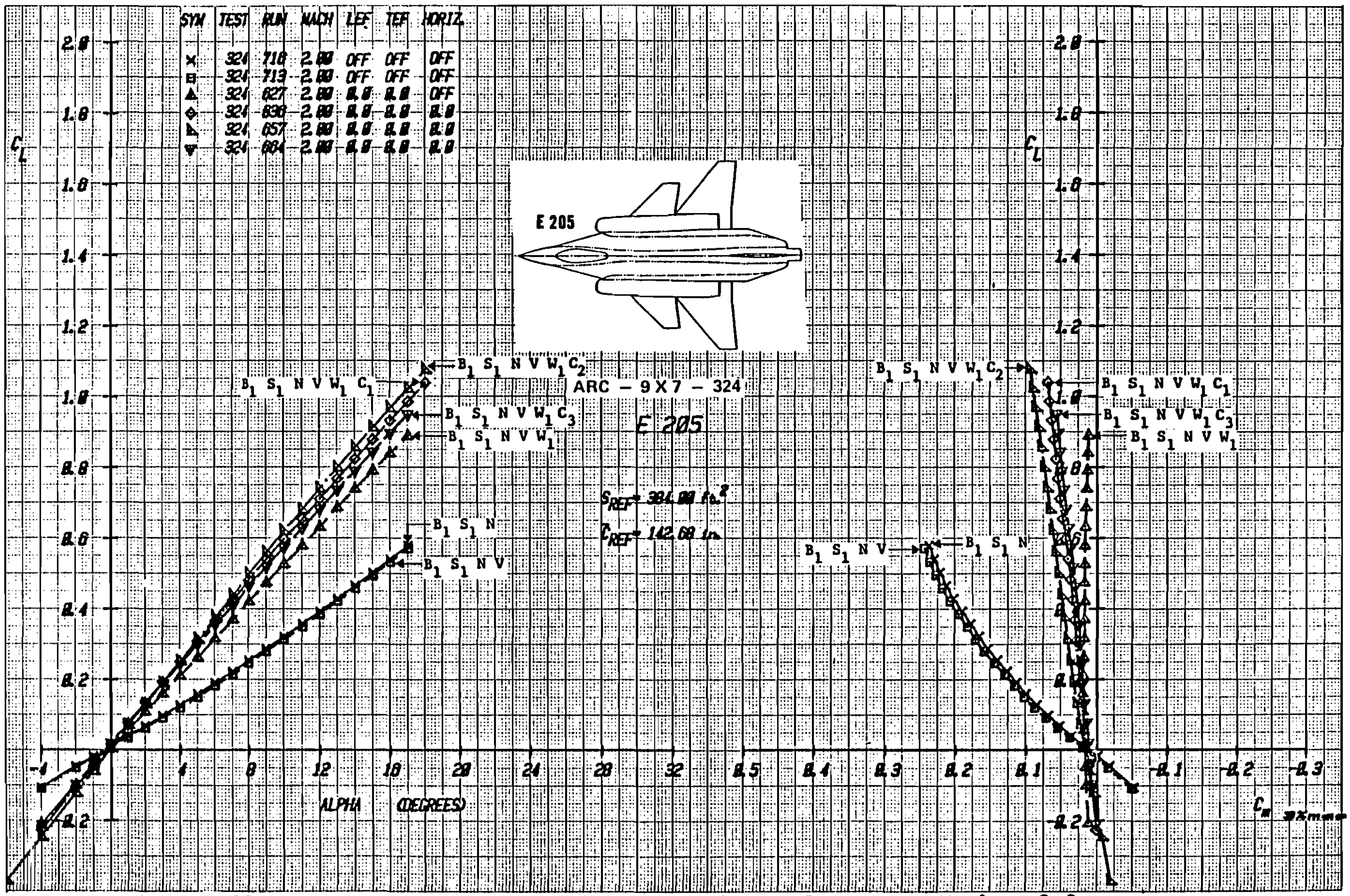

Figure1-11a Effect of Component Buildup on Lift and Moment, Mach = 2.0

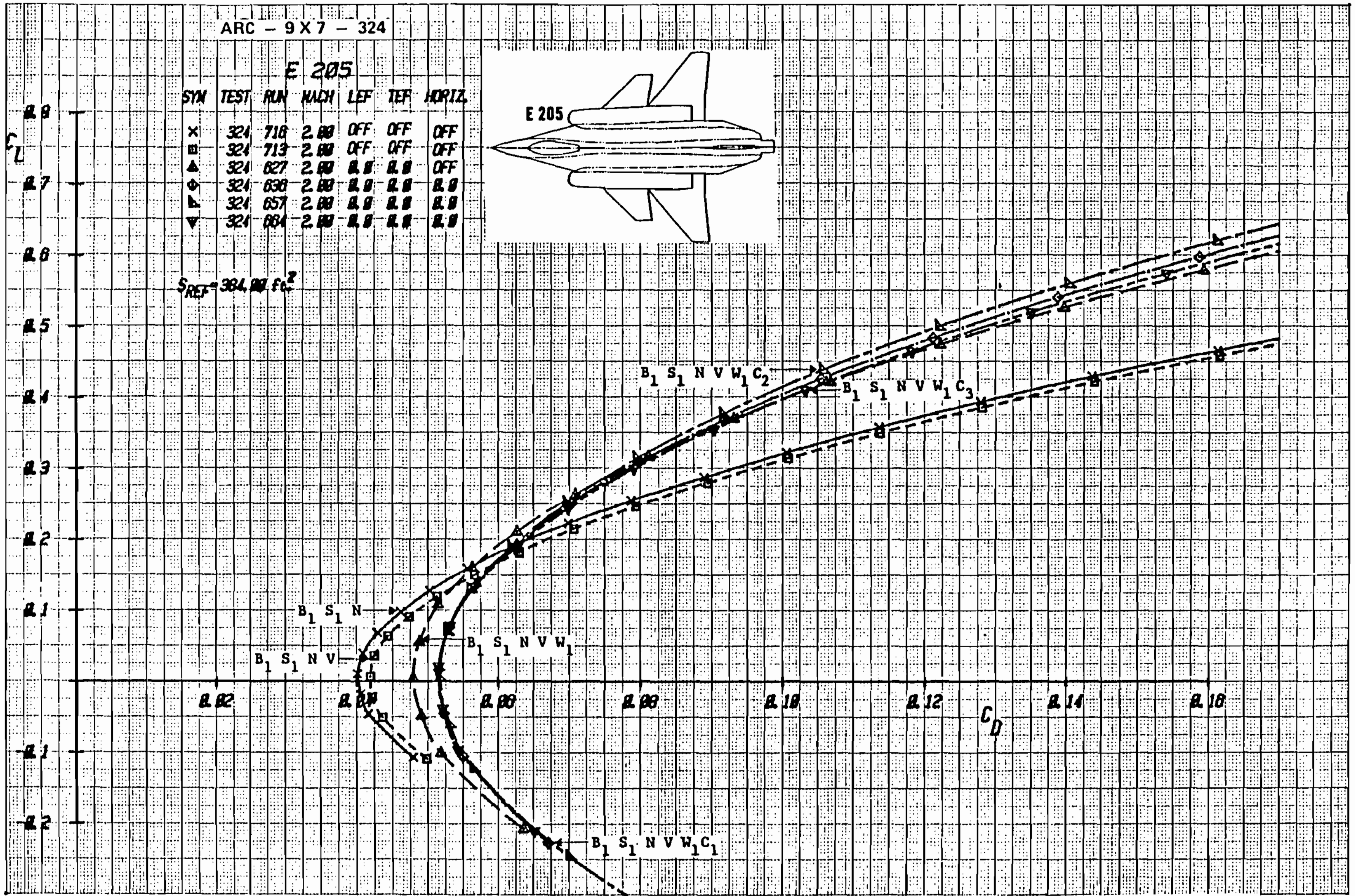

Figurel-11bEffect of Component Buildup on Drag, (Expanded Drag Scale), Mach = 2.0

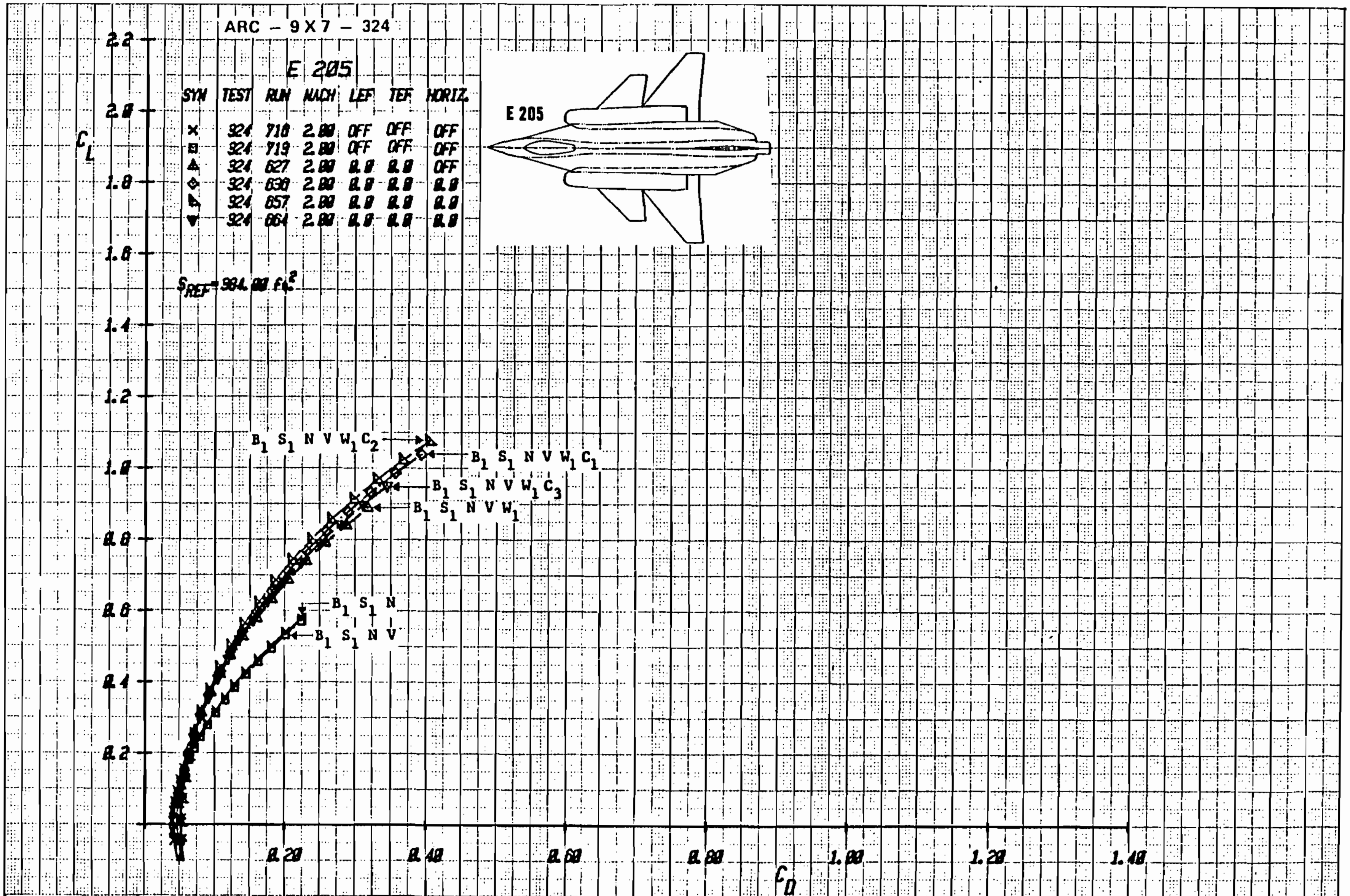

Figurel-llcEffect of Component Buildup on Drag, Mach = 2.0

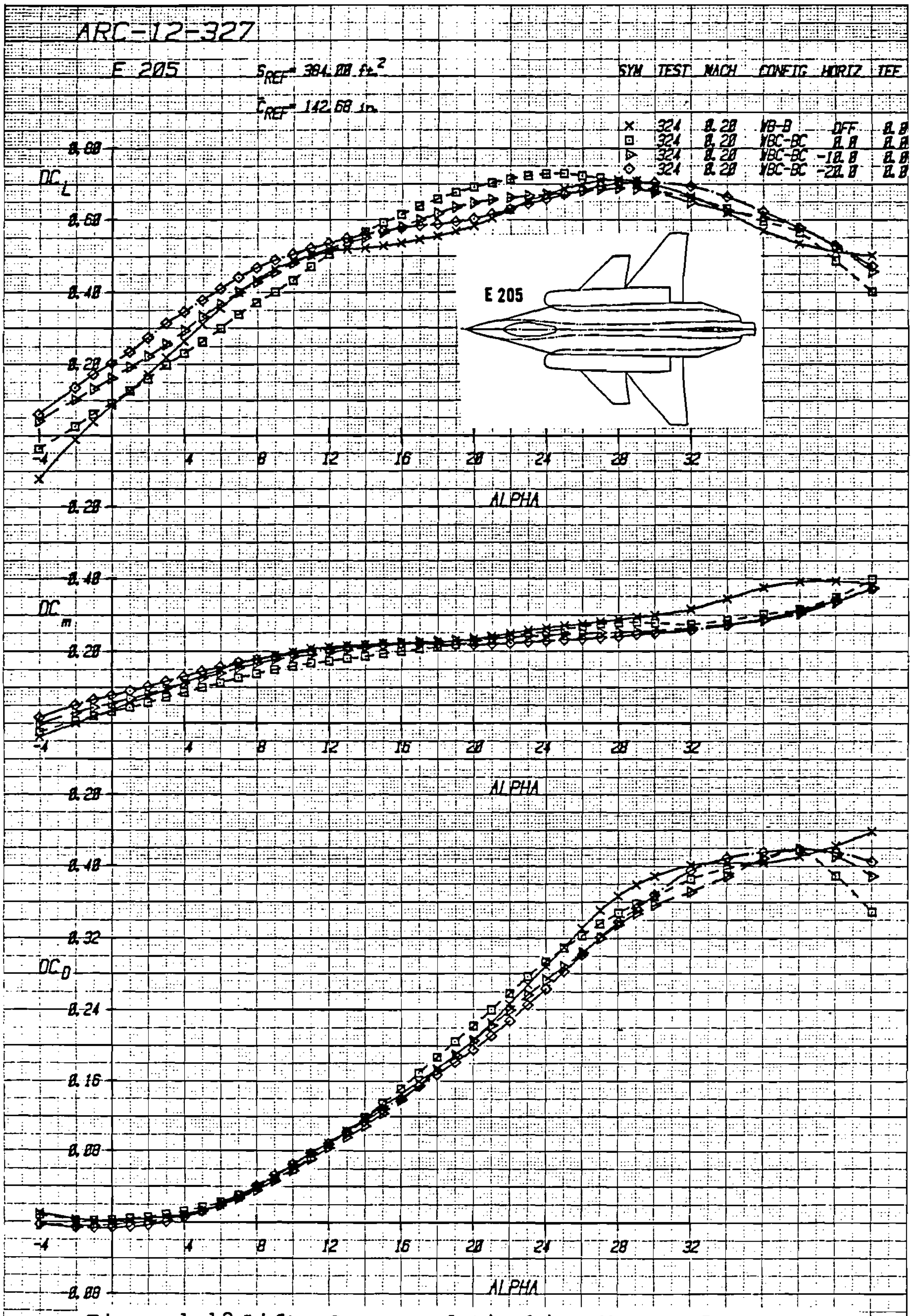

Figure 1-12 Lift, Drag, and Pitching Moment Increments for E205 Wing-Alone and Wing in Presence of Baseline Canard at Three Canard Deflections. = .2

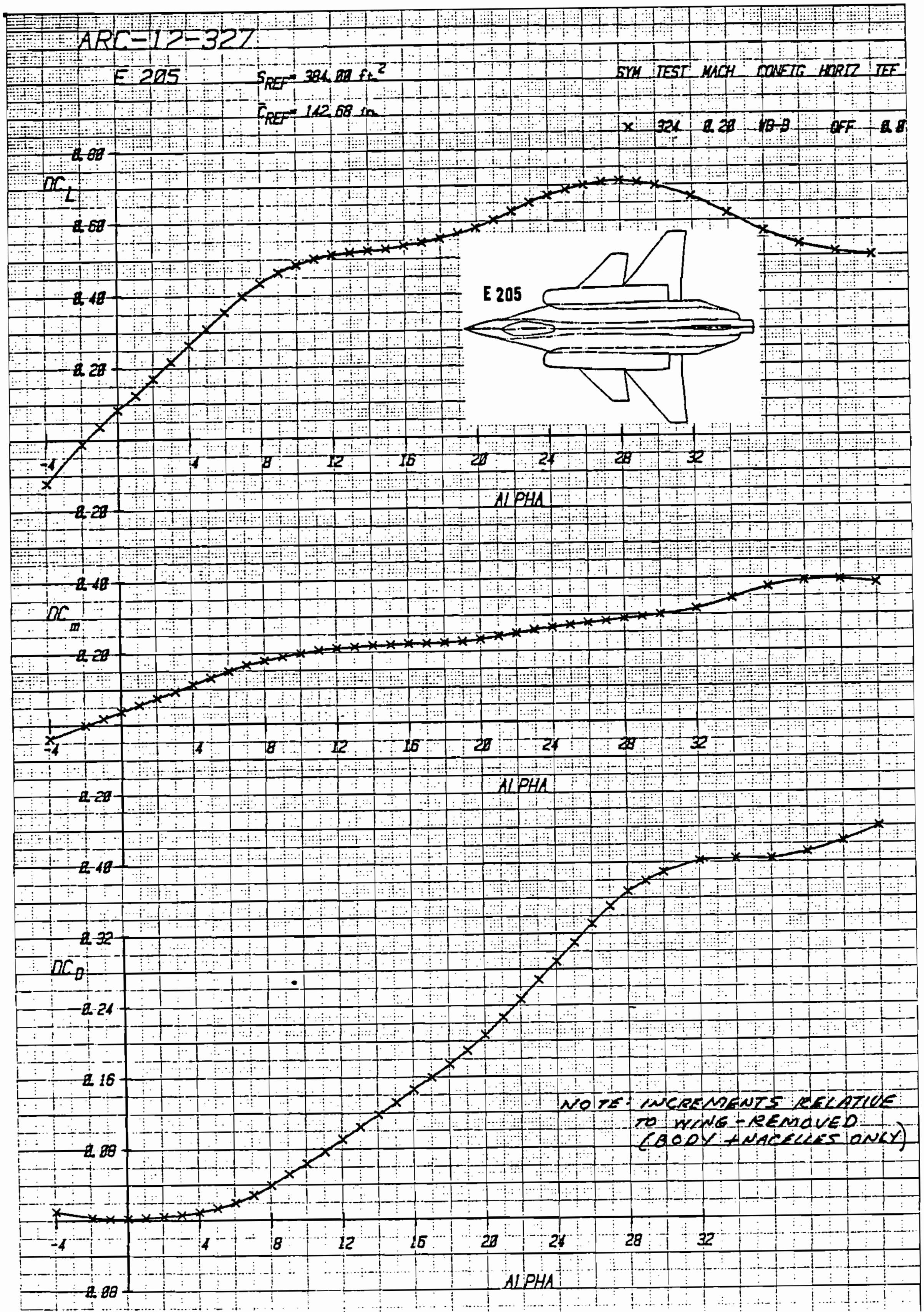

Figure 1-13 Lift, Drag, and Pitching Moment Increments for E205 Wing-Alone, M = .2

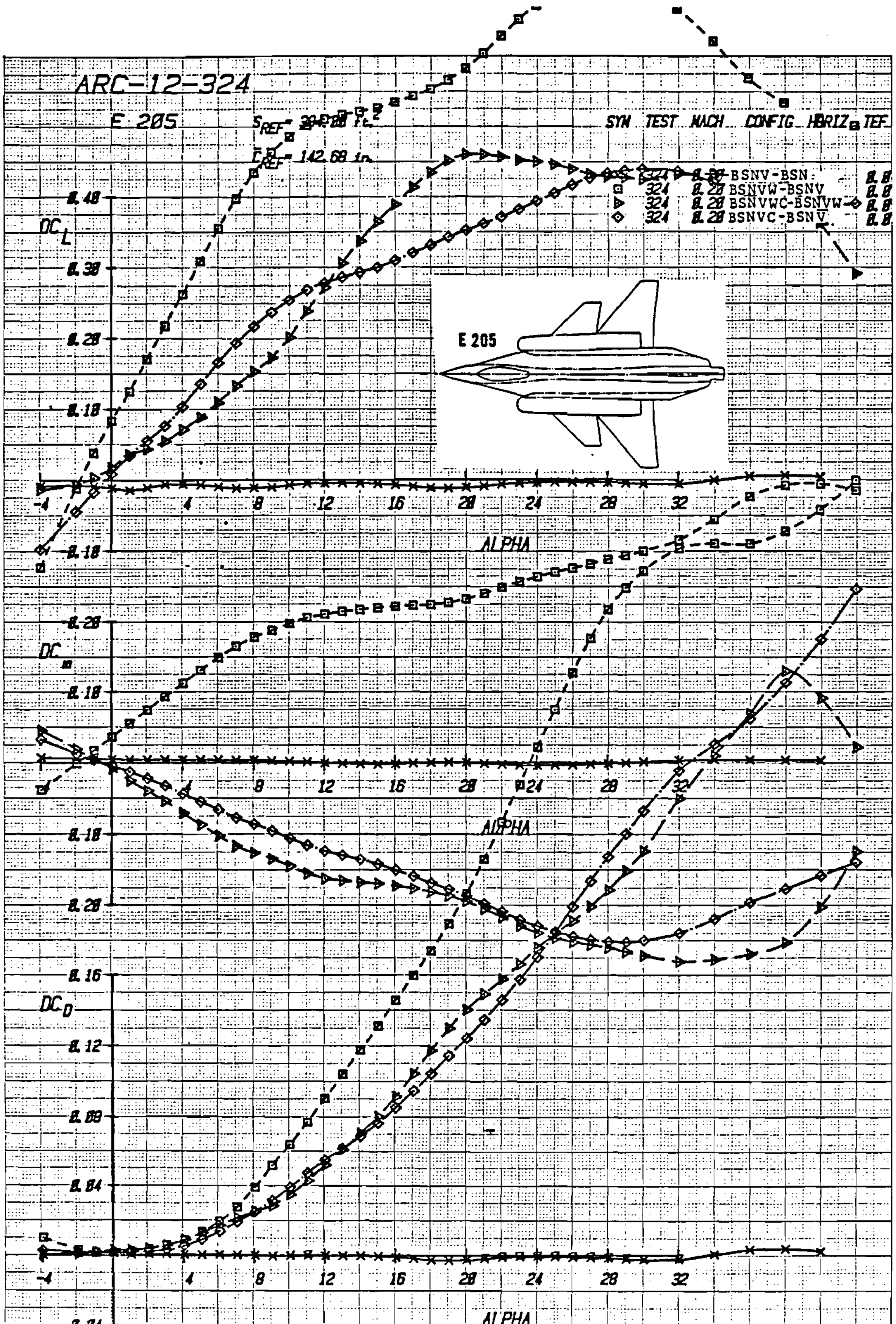

Figure 1-14 Lift, Drag, and Pitching Moment Increments for E205 Vertical Tail (with Canard Removed), Wing Alone, Canard + Wing Interference (δ_C = 0°), and Canard with Wing Removed, M = .2

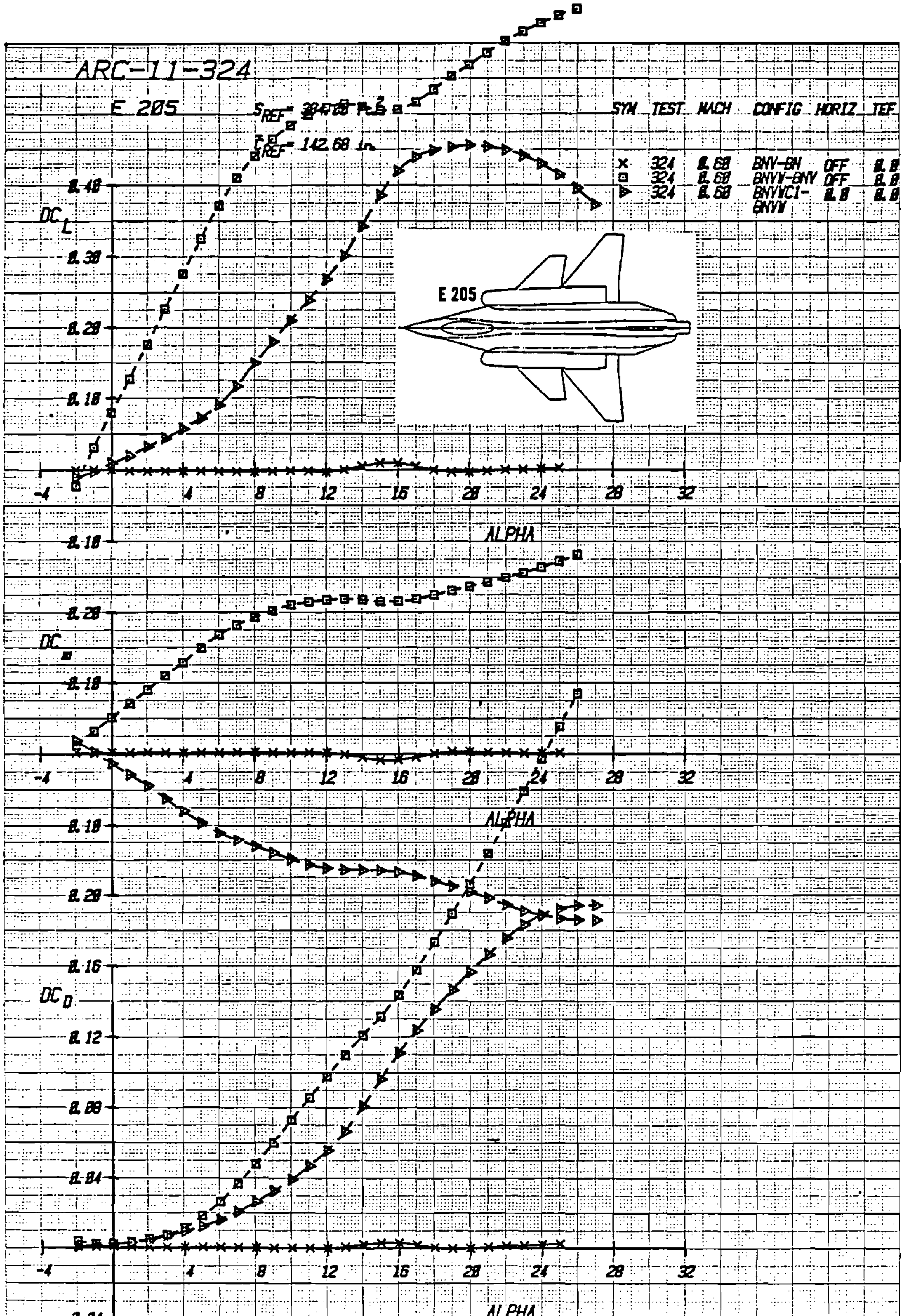

Figure 1-15 Lift, Drag, and Pitching Moment Increments for E205 Vertical Tail (Wing and Canard Removed), Wing (Canard Removed), and Canard + Wing Interference, M = .6

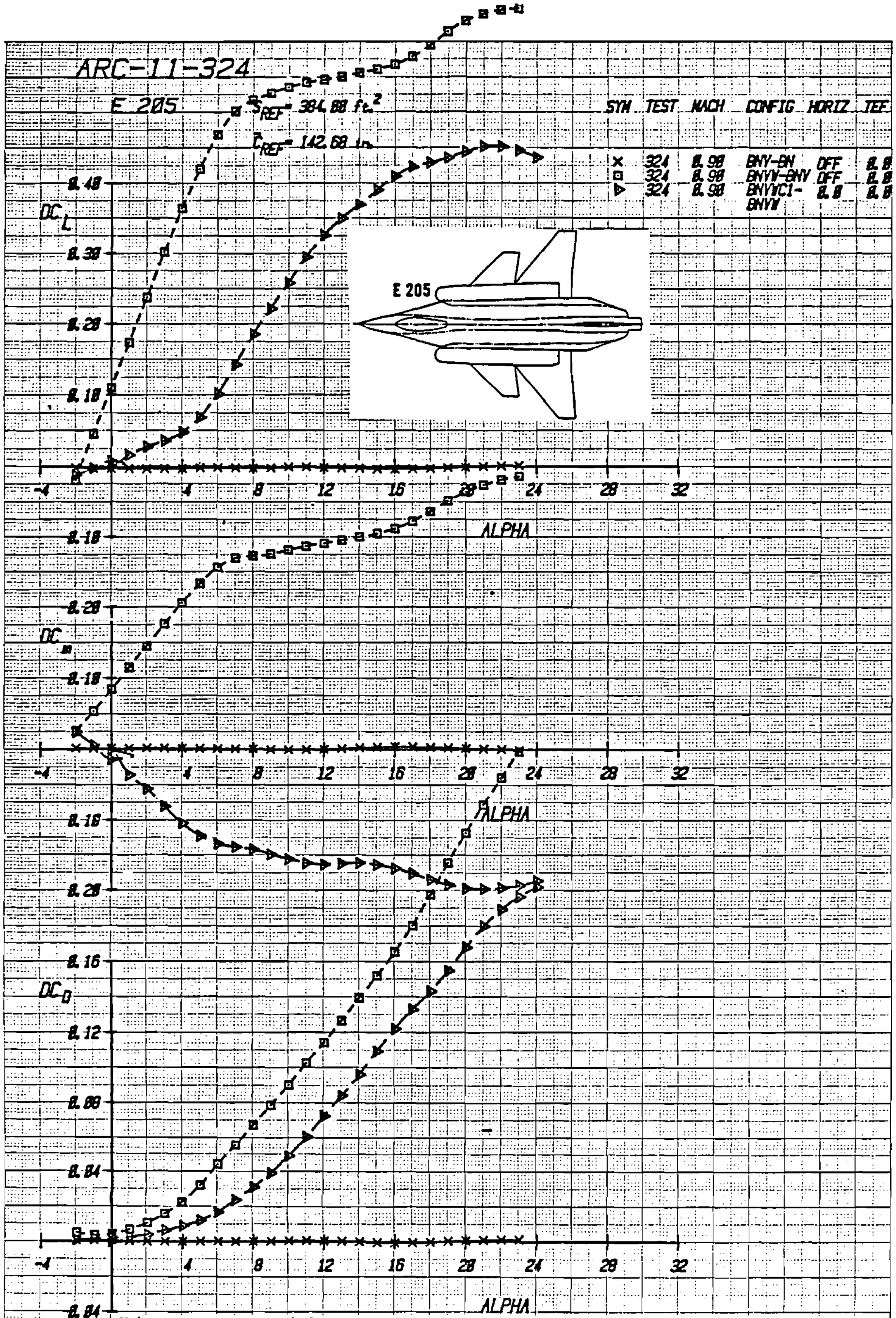

Figure 1-16 Lift, Drag, and Pitching Moment Increments for E205 Vertical Tail (Wing and Canard Removed), Wing (Canard Removed), and Canard + Wing Interference, M = .9

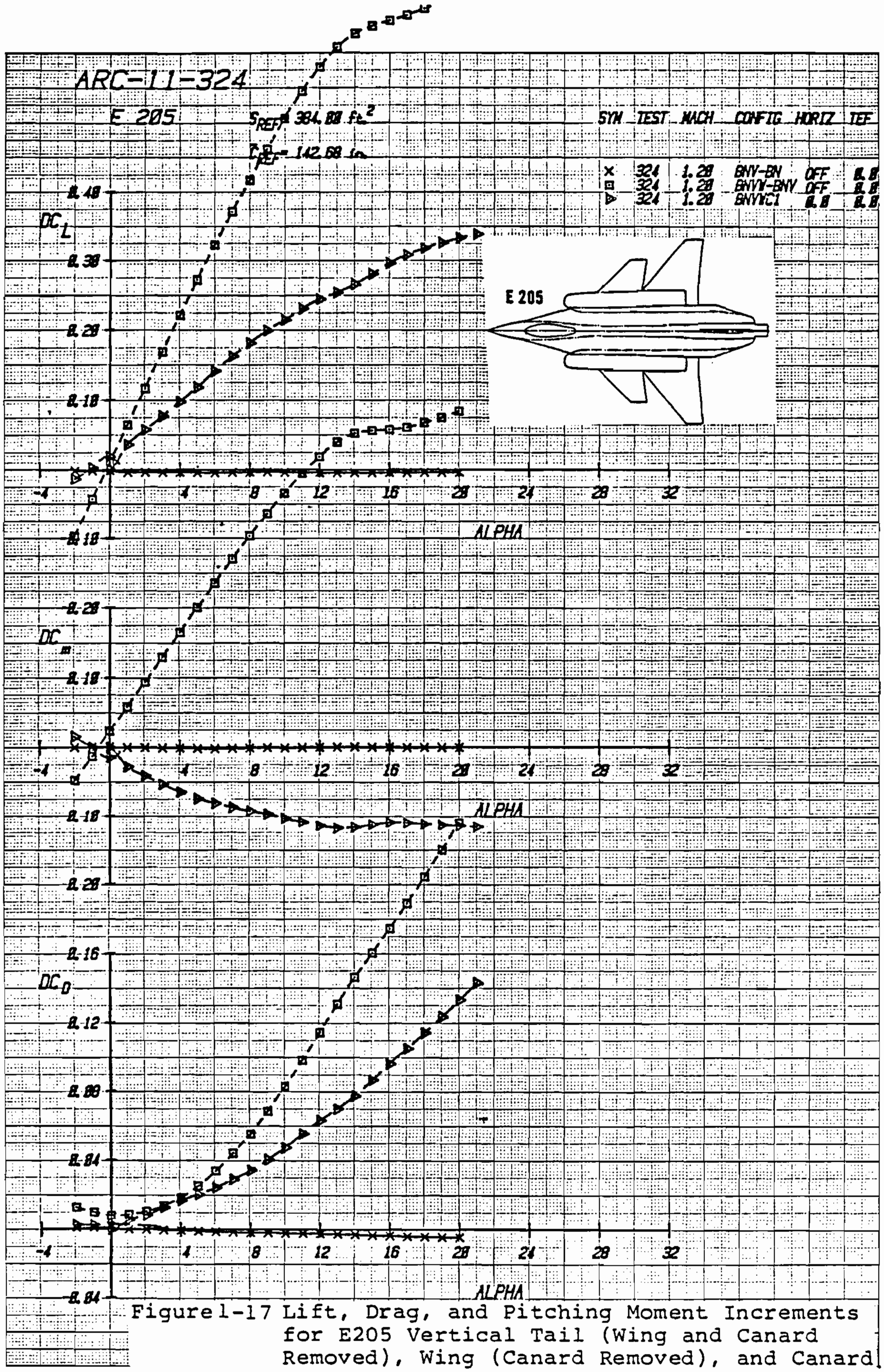

Figure 1-17 Lift, Drag, and Pitching Moment Increments for E205 Vertical Tail (Wing and Canard Removed), Wing (Canard Removed), and Canard + Wing Interference, M = 1.2

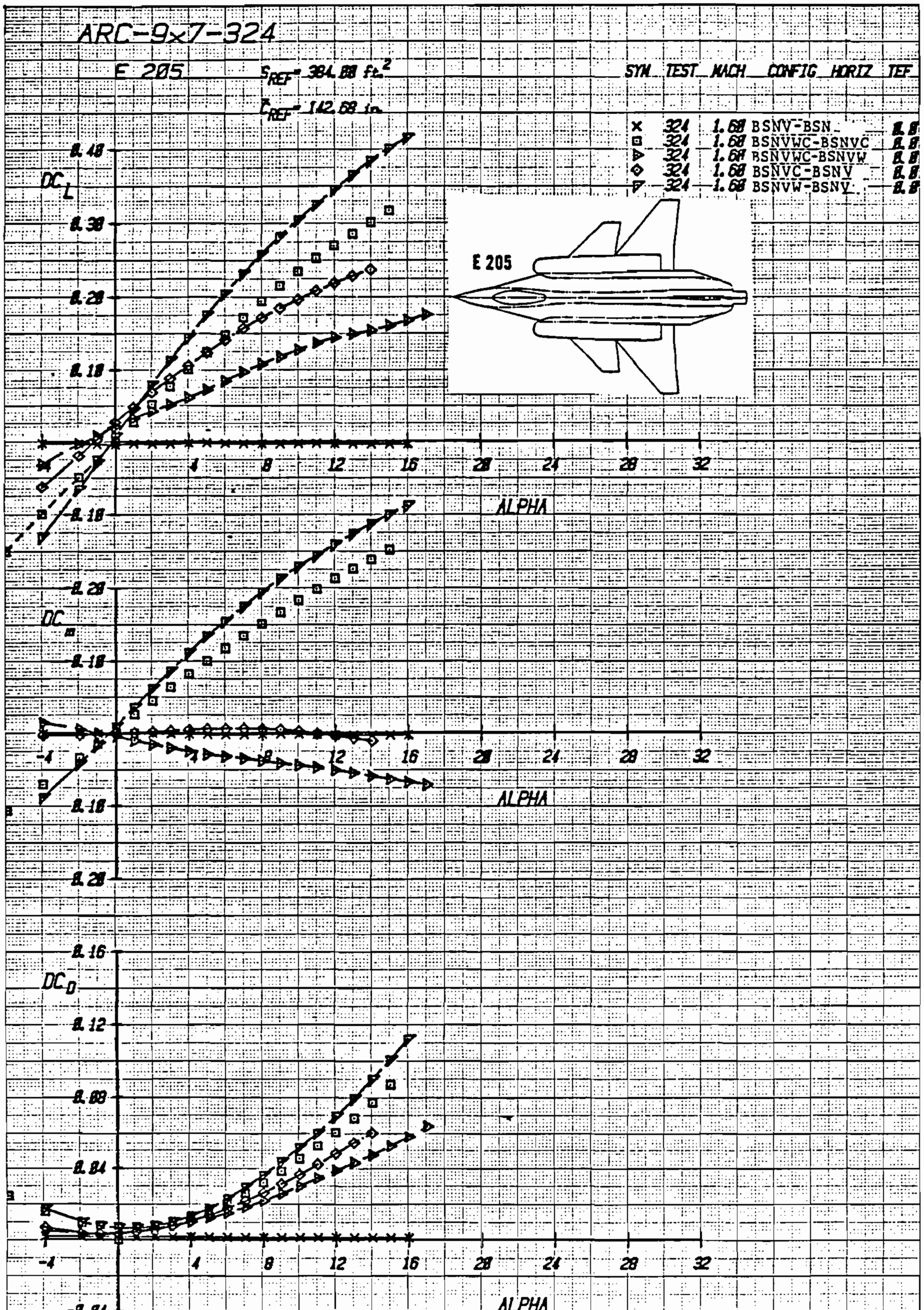

Figure 1-18 Lift, Drag, and Pitching Moment Increments for E205 Vertical Tail (Wing and Canard Removed), Wing (In Presence of Canard), Canard (In Presence of Wing), Canard (Wing Removed), Wing (Canard Removed), M = 1.6

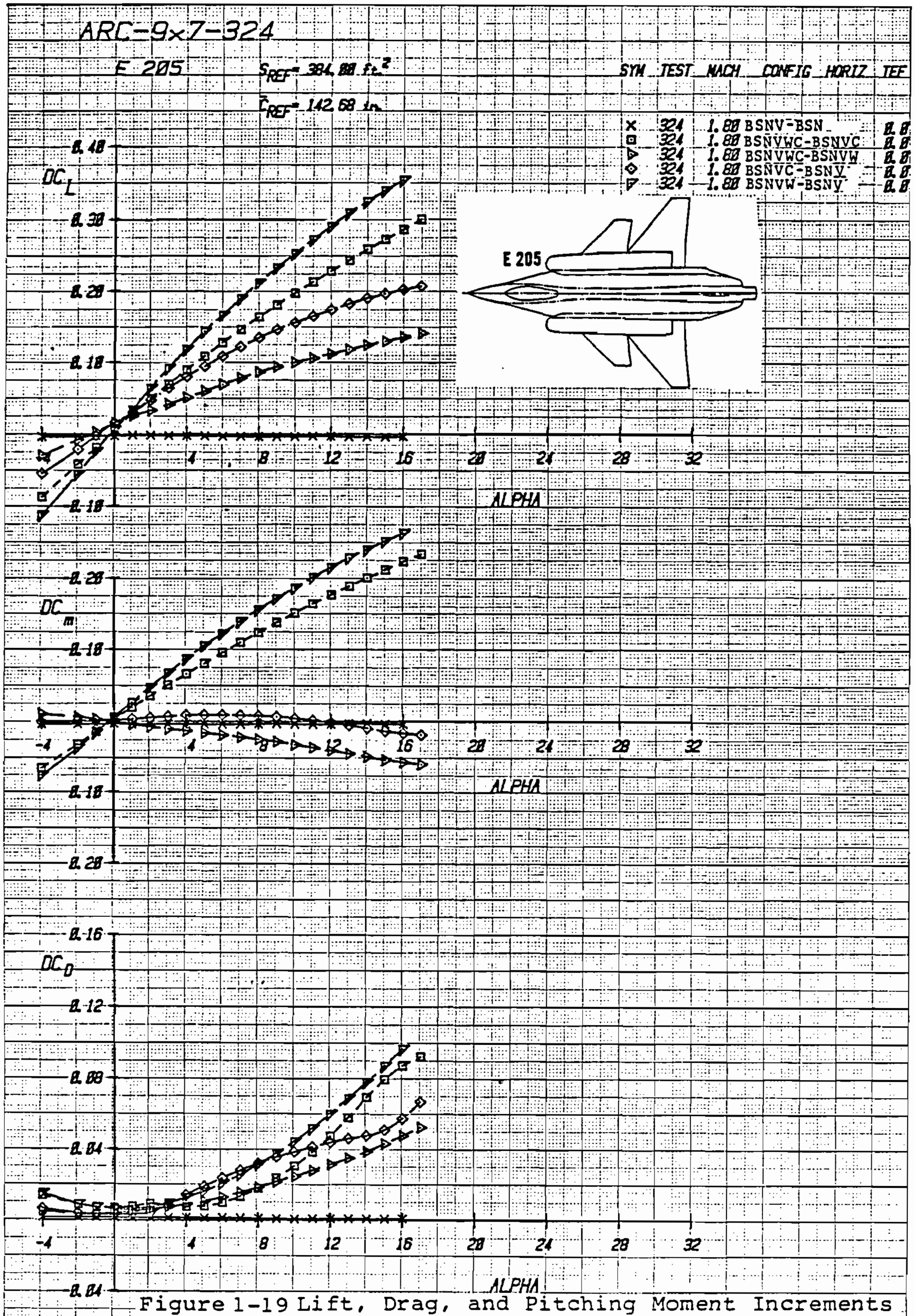

Figure 1-19 Lift, Drag, and Pitching Moment Increments for E205 Vertical Tail (Wing and Canard Removed), Wing (In Presence of Canard), Canard (In Presence of Wing), Canard (Wing Removed), Wing (Canard Removed), M = 1.8

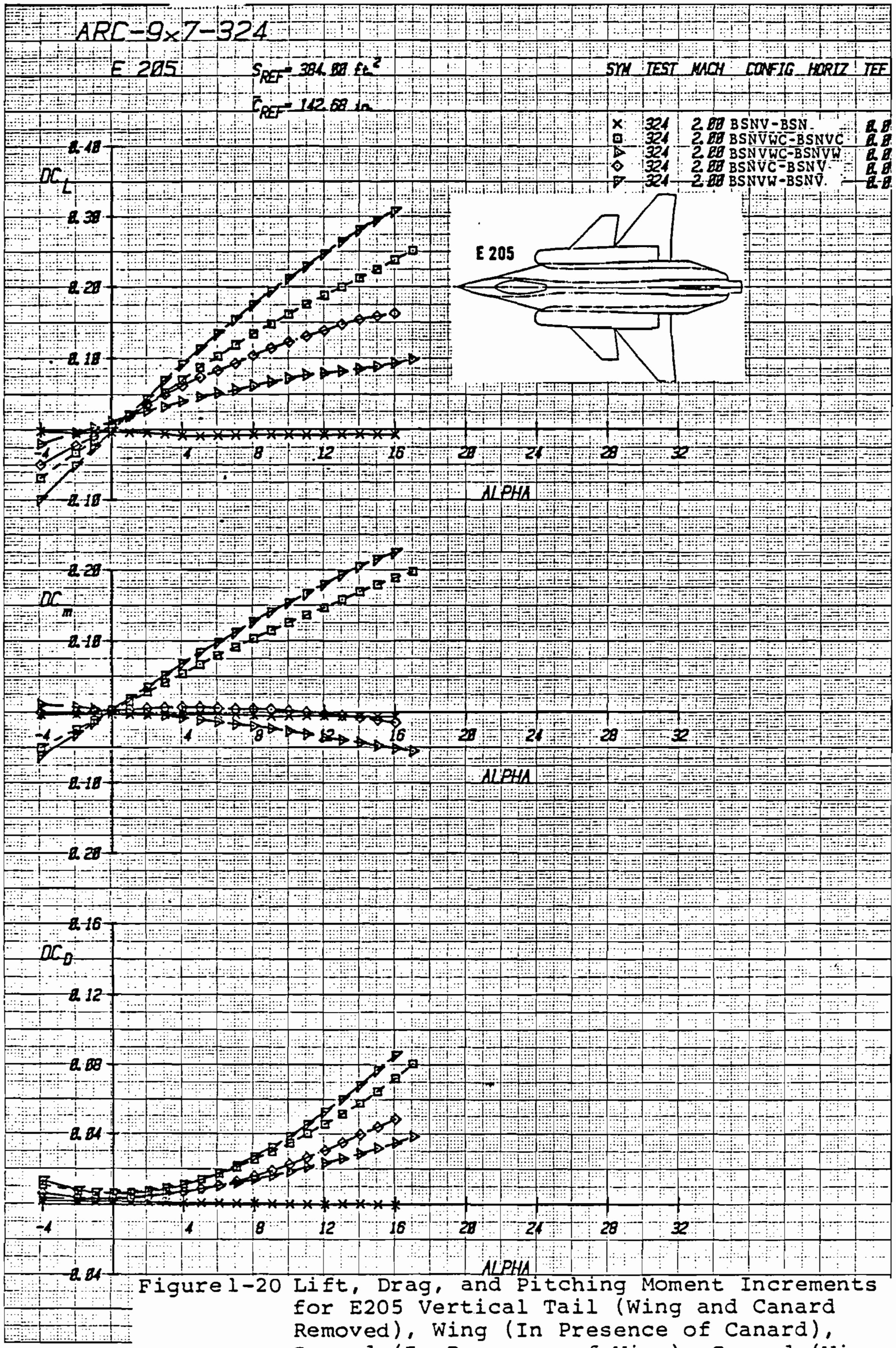

Figure 1-20 Lift, Drag, and Pitching Moment Increments for E205 Vertical Tail (Wing and Canard Removed), Wing (In Presence of Canard), Canard (In Presence of Wing), Canard (Wing Removed), Wing (Canard Removed), Mach = 2.0

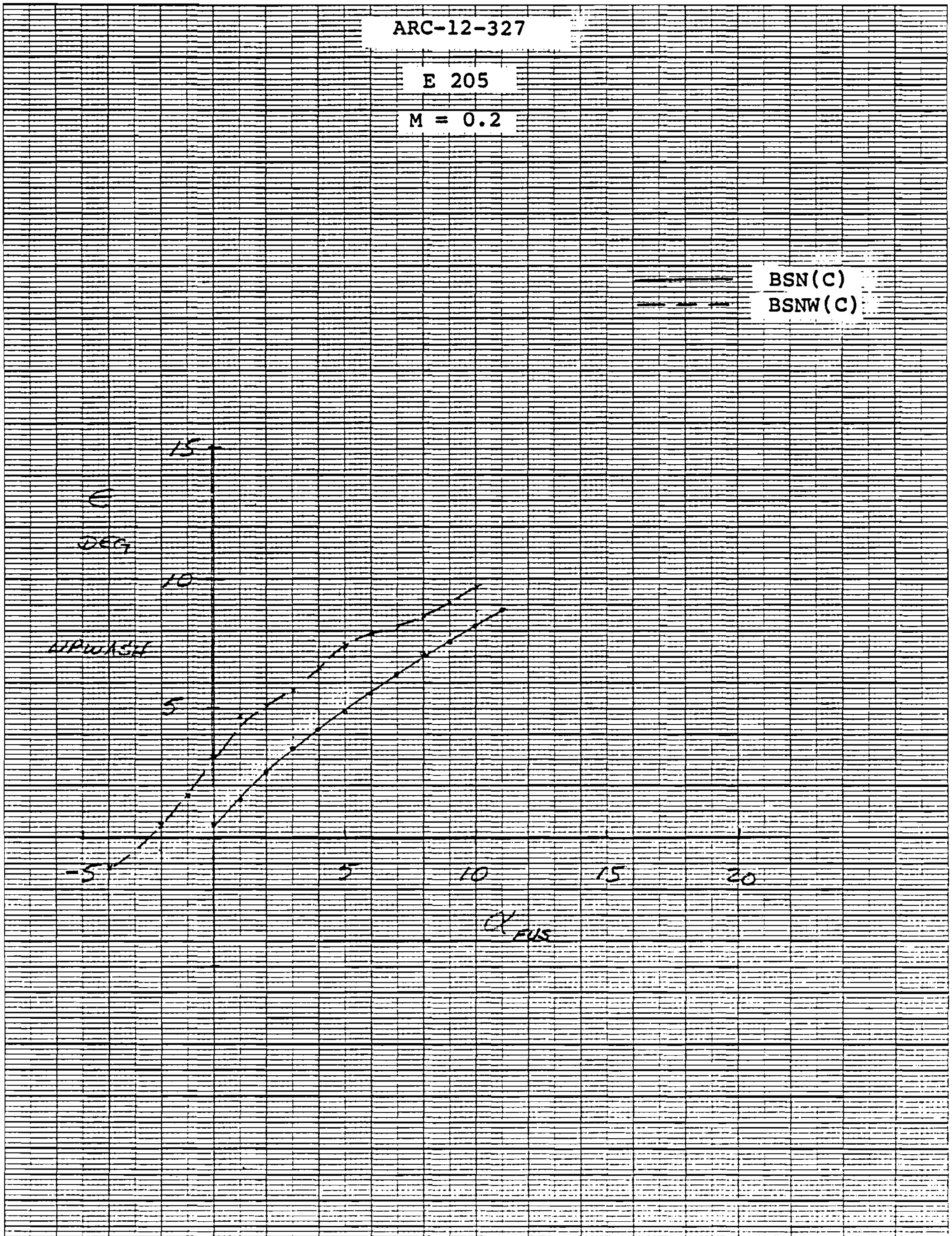

Figure 1-21 Upwash at the Canard vs. Fuselage Angle of Attack in and out of the Presence of the Wing

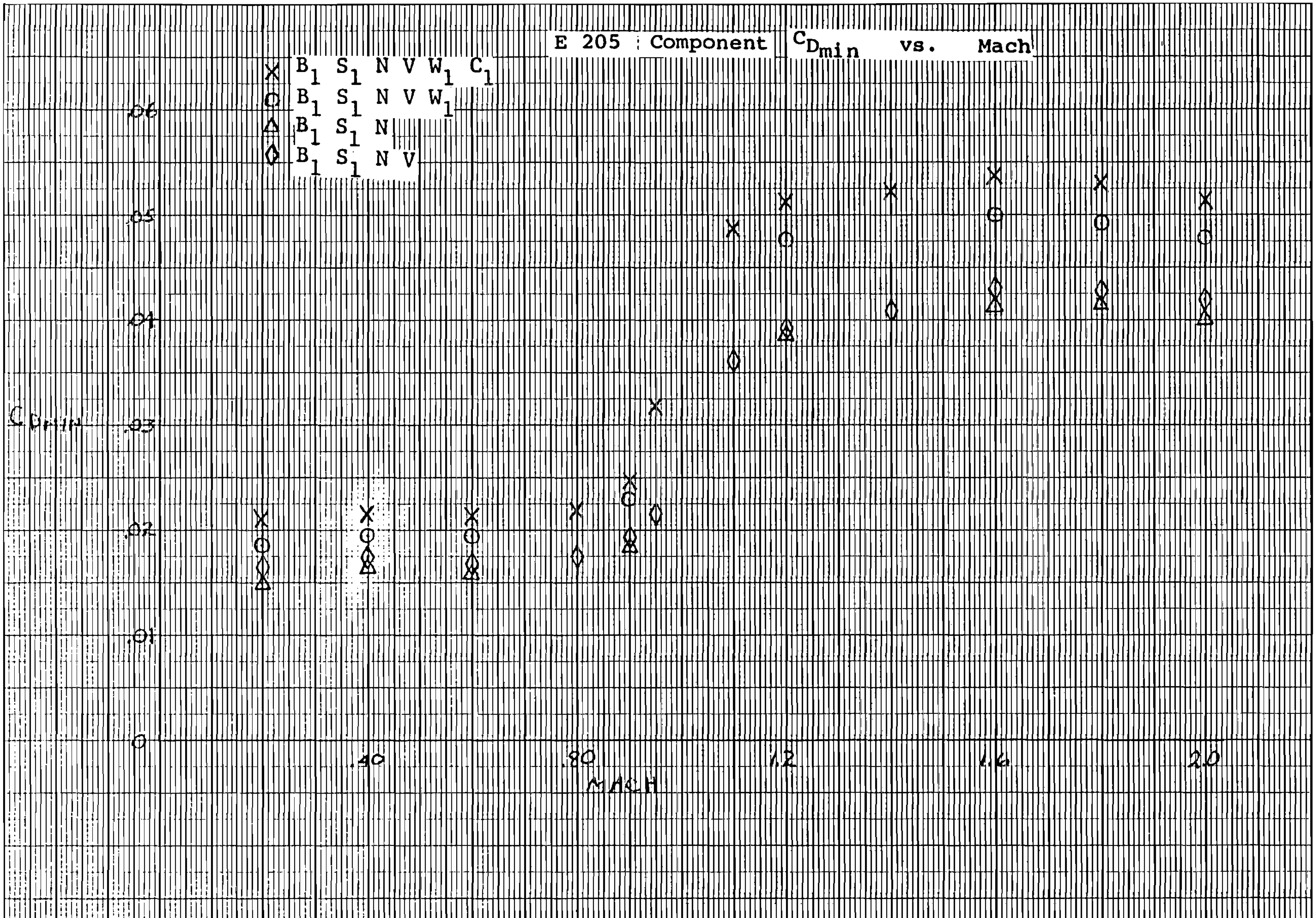

Figure 1-22 E205 Component $C_{D_{MIN}}$ vs. Mach No.

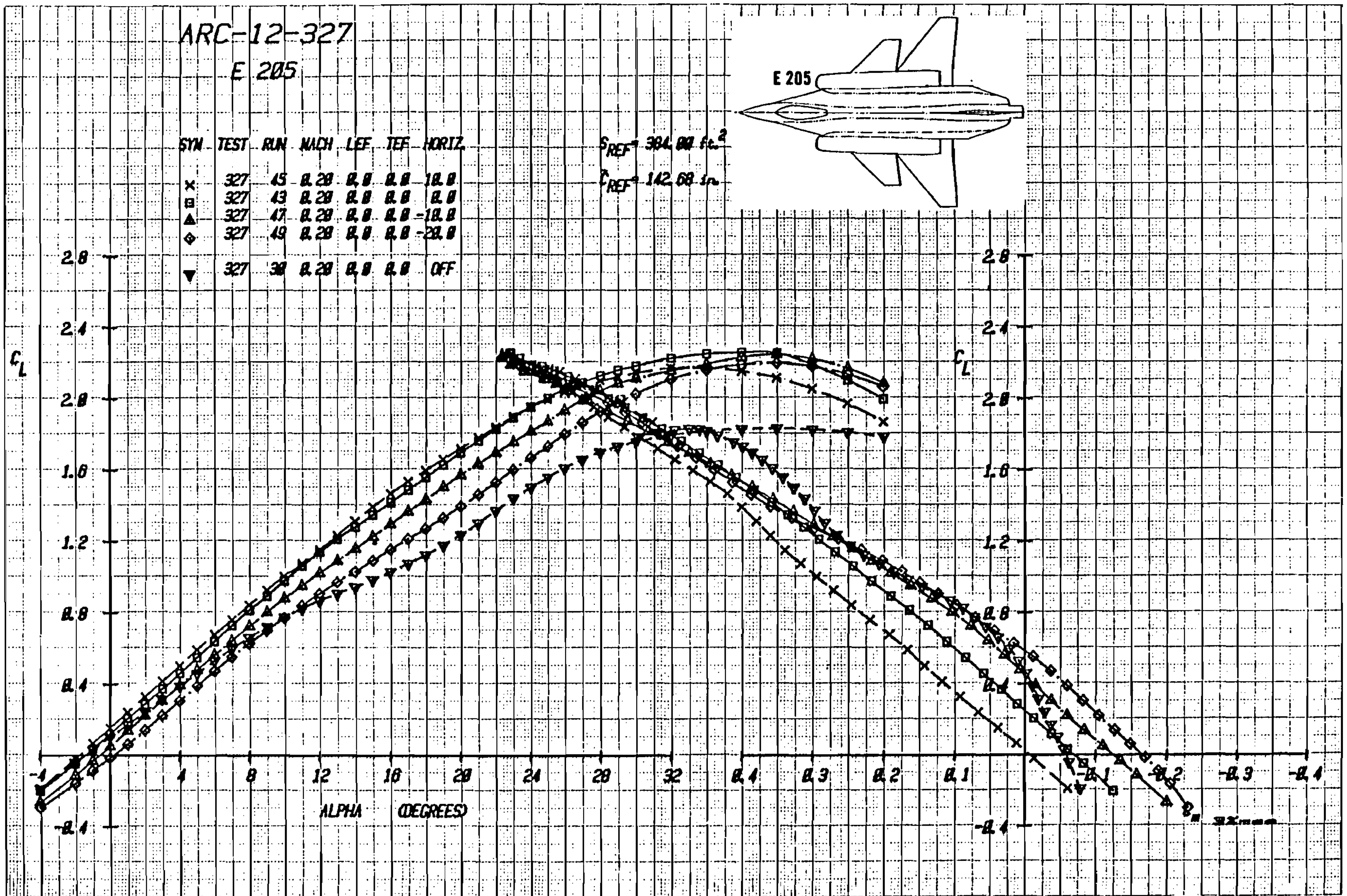

Figure 2-1a Effect of Canard Deflection on Lift and Moment with Wing Trailing-Edge Flap Undeflected, Mach = .2

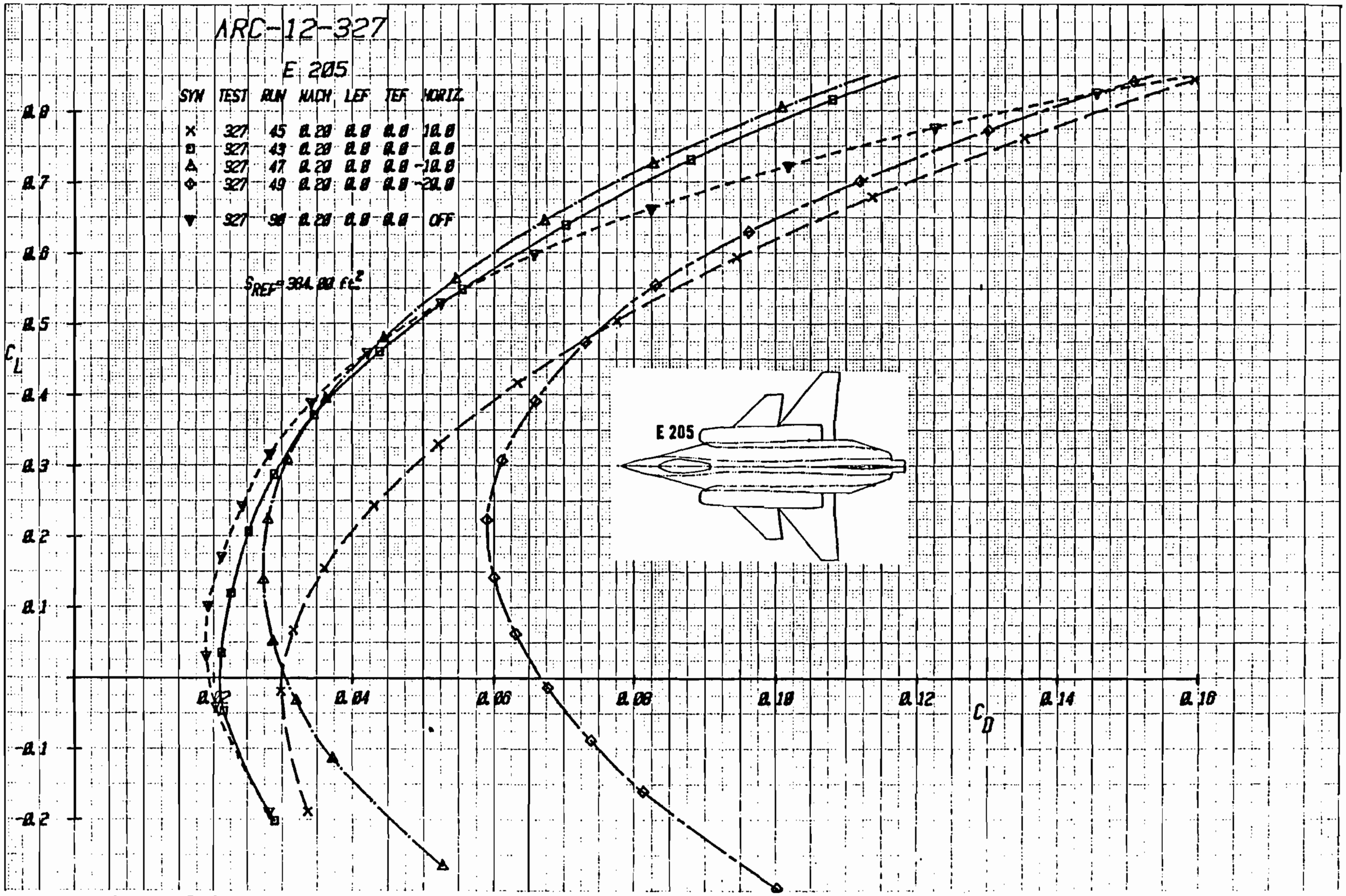

Figure 2-1b Effect of Canard Deflection on Drag with Wing Trailing-Edge Flap Undeflected, (Expanded Drag Scale), Mach = .2

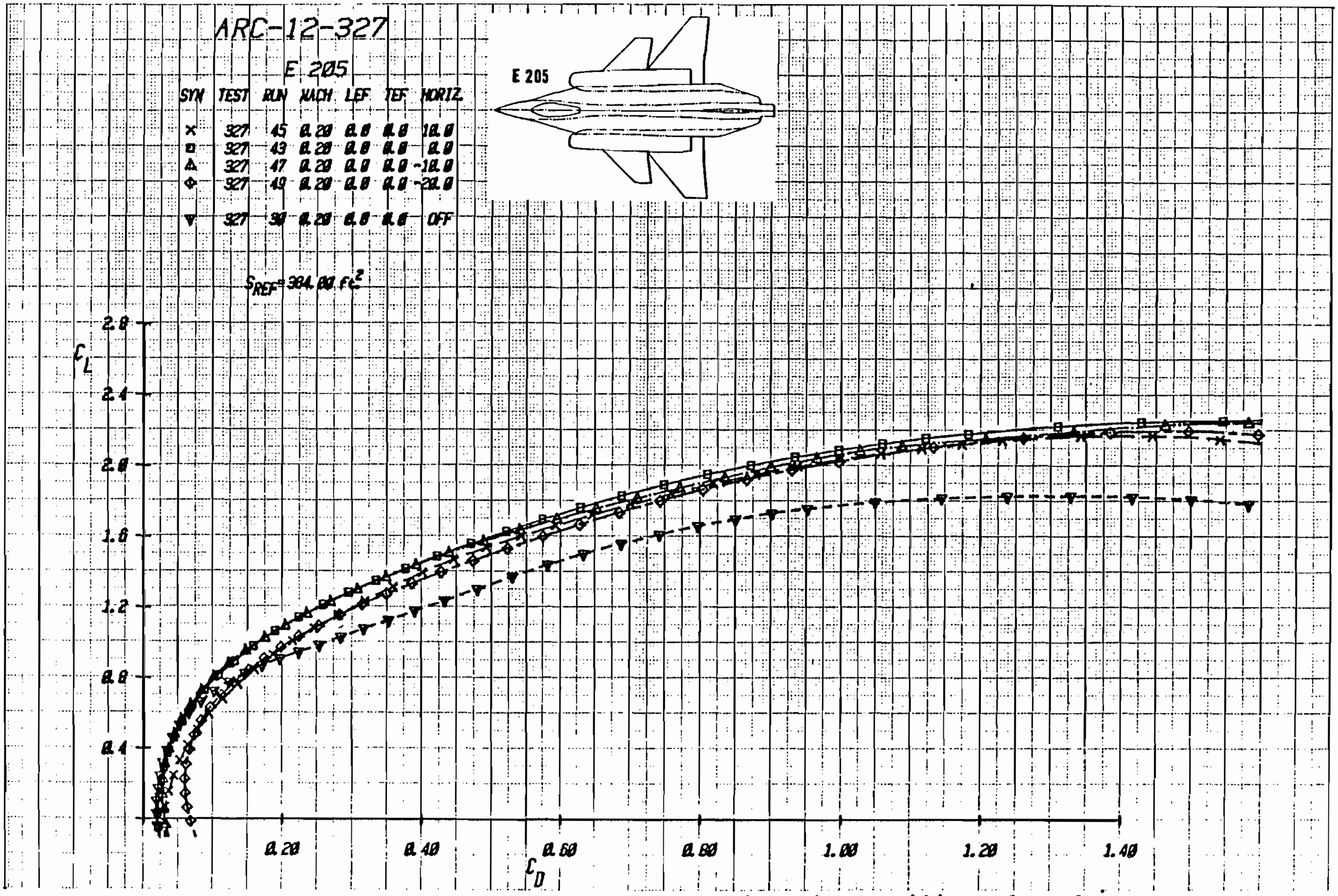

Figure 2-1c Effect of Canard Deflection on Drag with Wing Trailing-Edge Flap Undeflected, Mach = .2

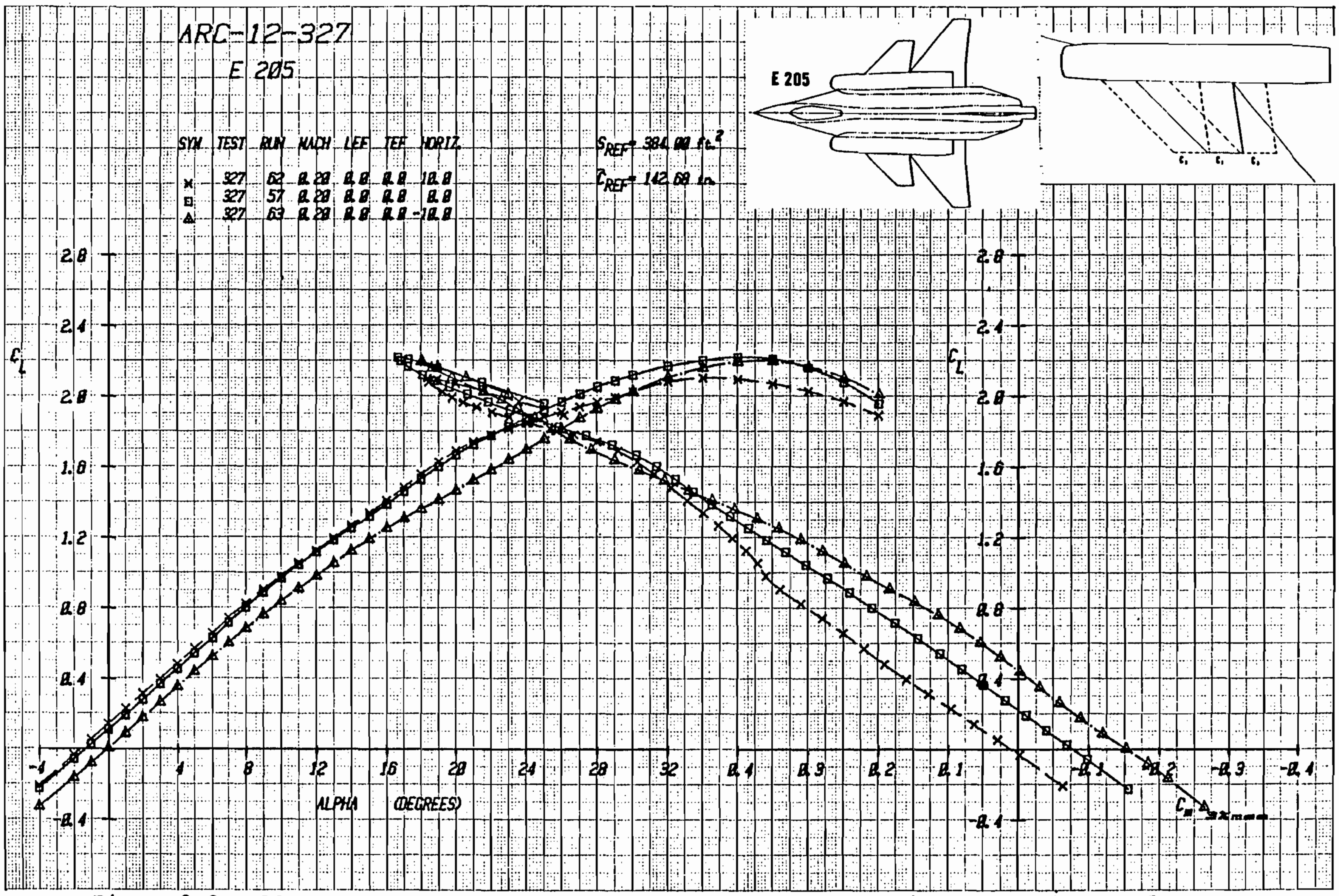

Figure 2-2a Effect of Canard Deflection on Lift and Moment with Forward Canard Longitudinal Location, C_2, and Baseline Strake, S_1, Mach = .2

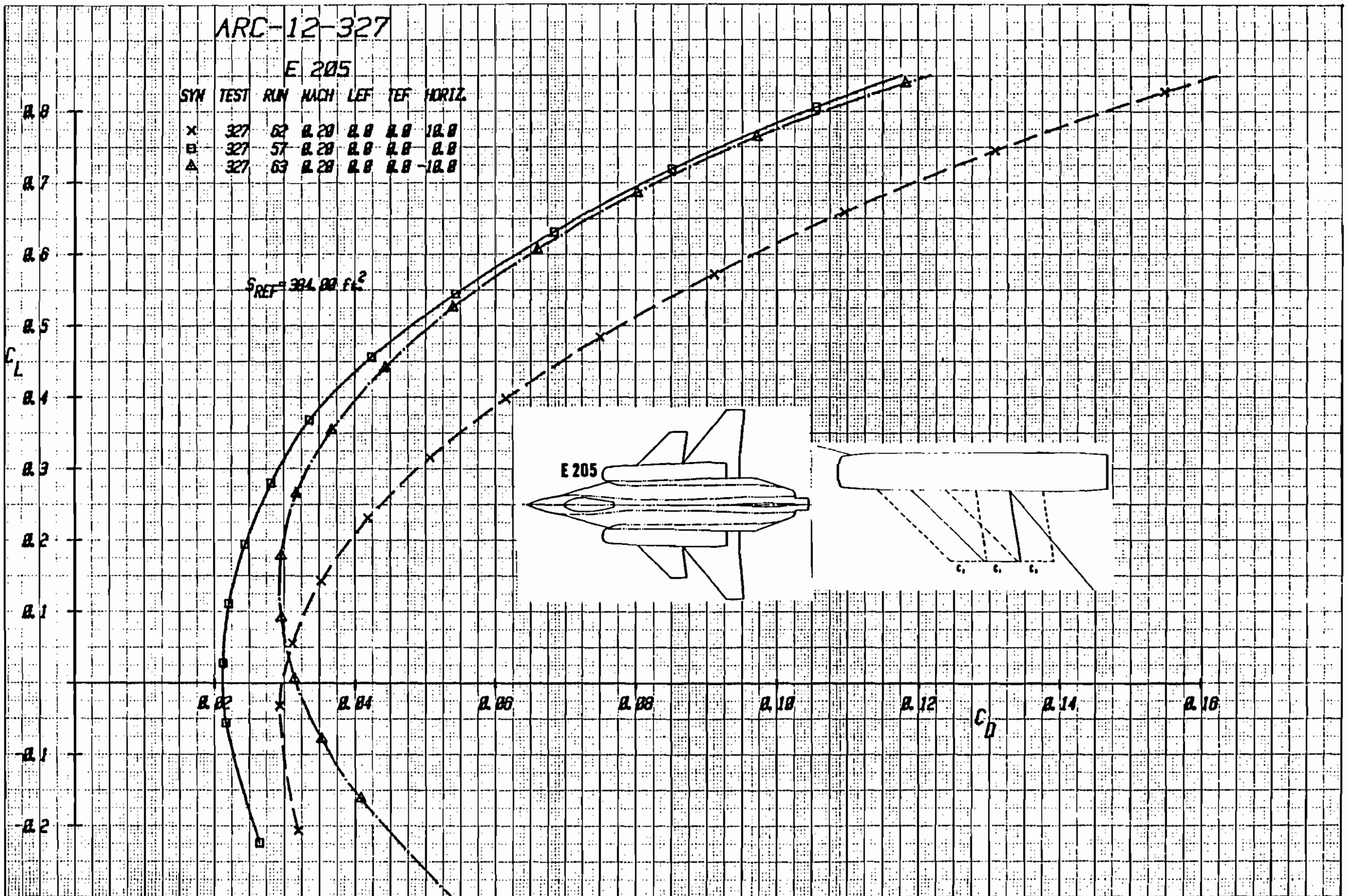

Figure 2-2b Effect of Canard Deflection on Drag with Forward Canard Longitudinal Location, C_2, and Baseline Strake, S_1, (Expanded Drag Scale), Mach = .2

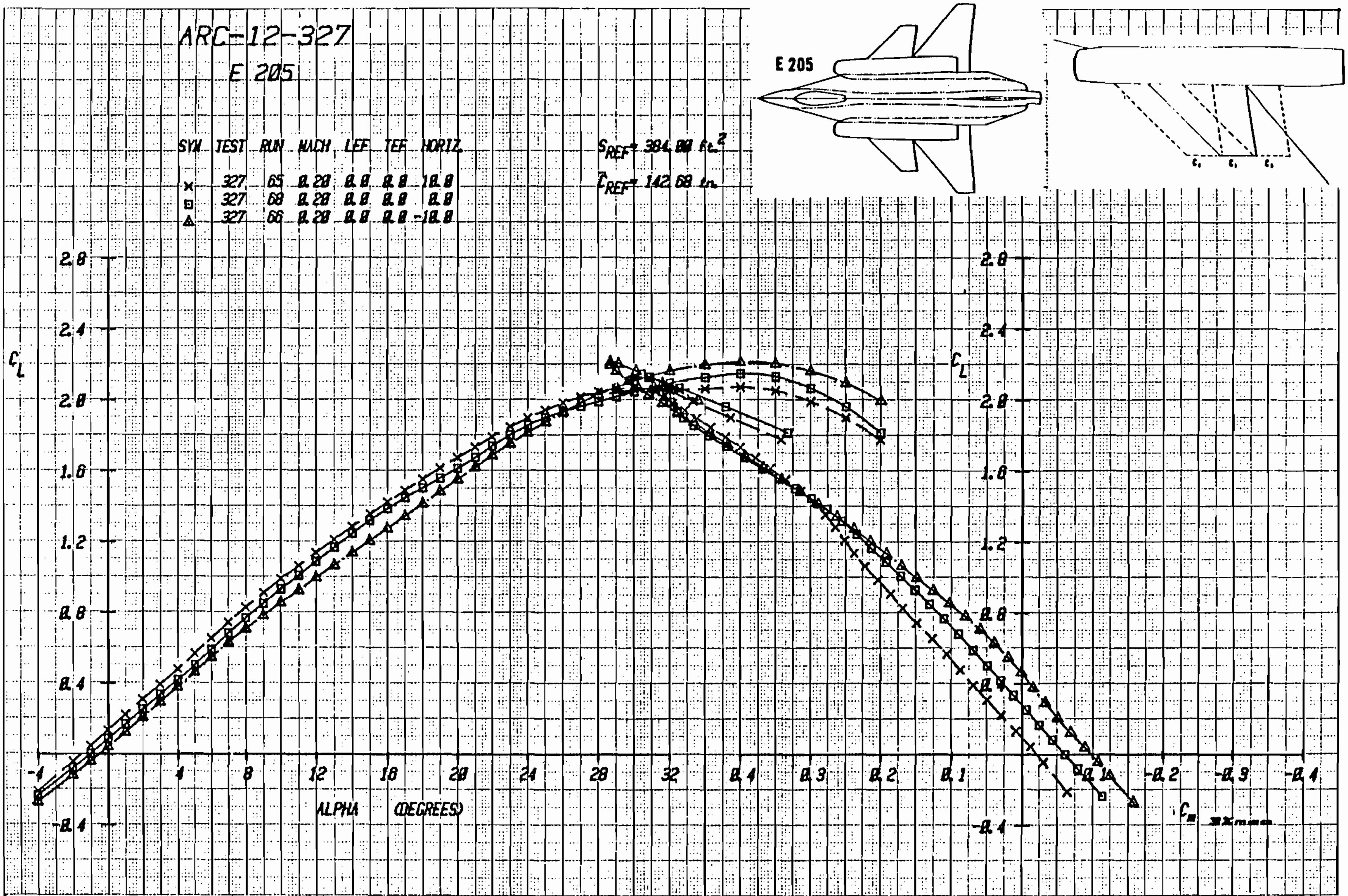

Figure 2-3a Effect of Canard Deflection on Lift and Moment with Aft Canard Longitudinal Location, C_3, and Baseline Strake, S_1, Mach = .2

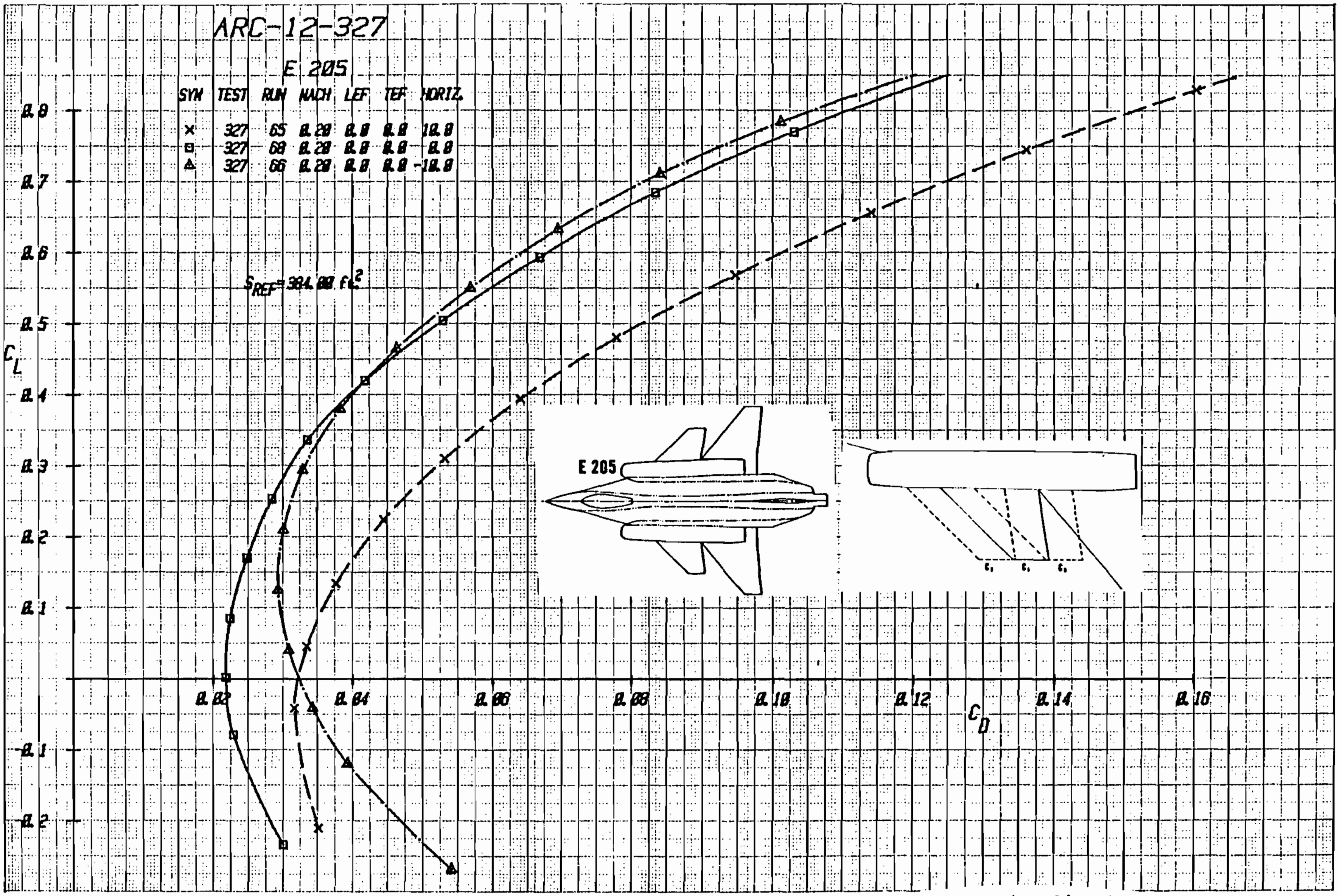

Figure 2-3b Effect of Canard Deflection on Drag with Aft Canard Longitudinal Location, C_3, and Baseline Strake, S_1, (Expanded Drag Scale), Mach = .2

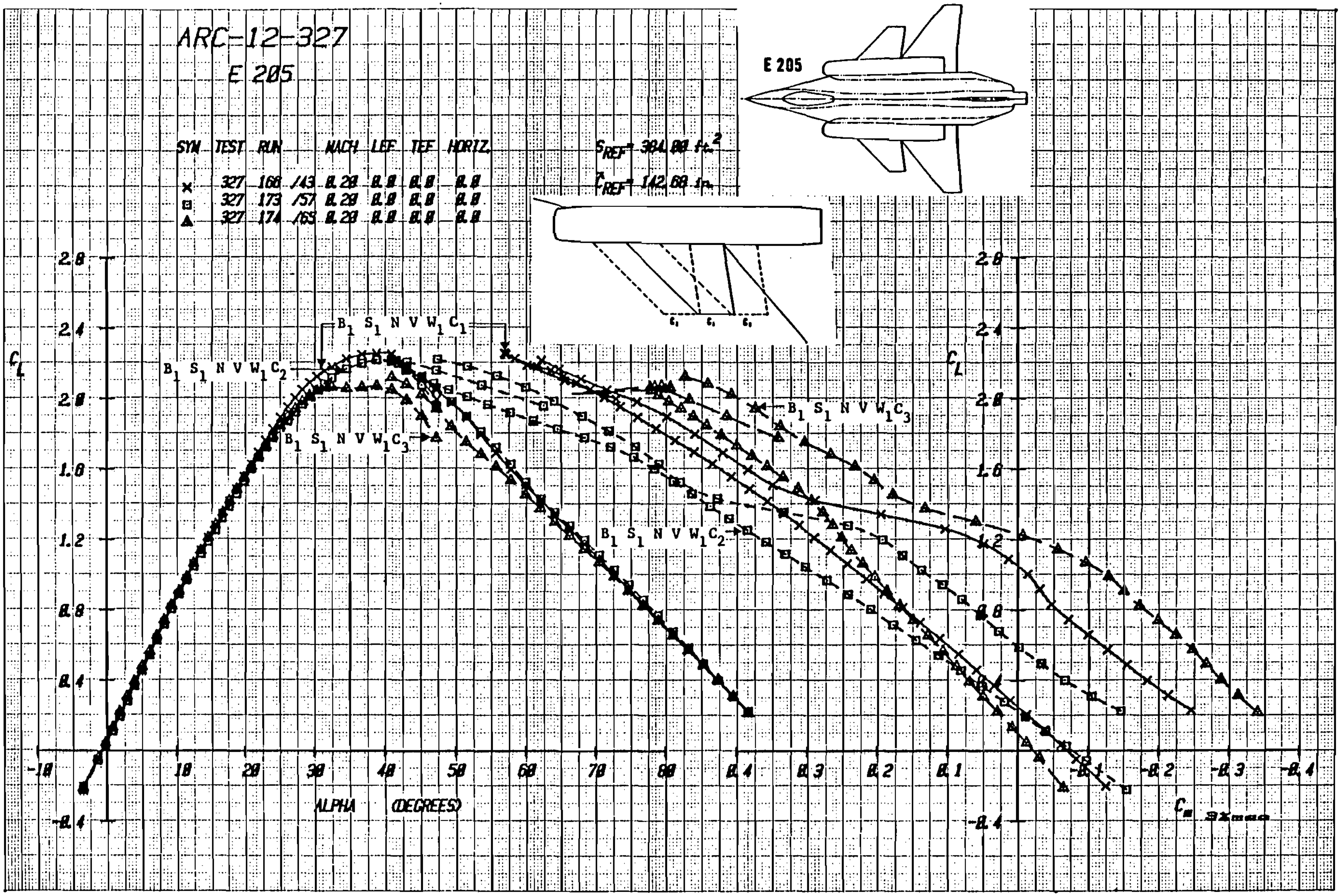

Figure 2-4a Effect of Canard Location with Baseline Strake, S_1, on E205 Lift and Pitching Moment (α = 0° to 90°), M = .2

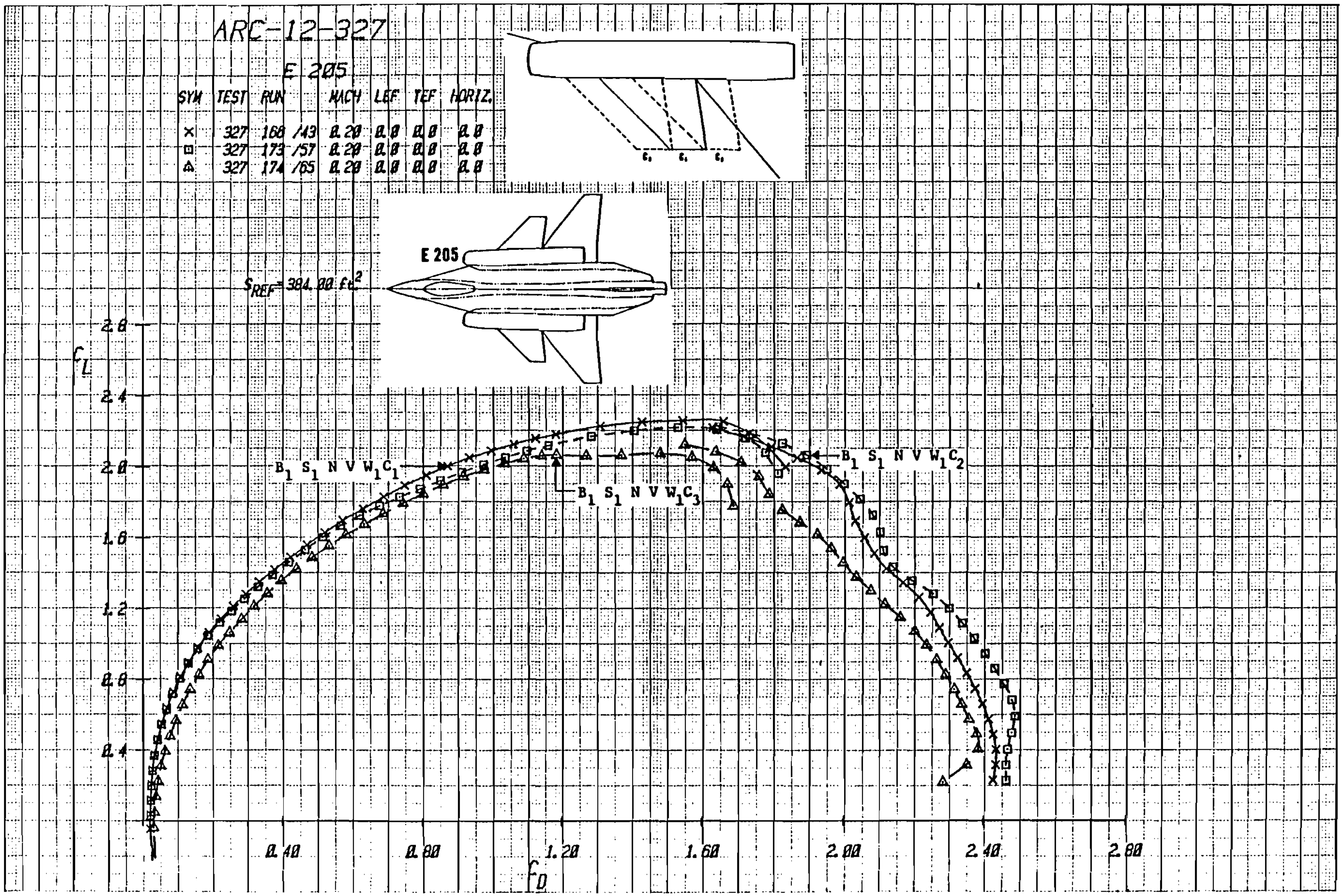

Figure 2-4b Effect of Canard Location with Baseline Strake, S_1, on E205 Drag (α = 0° to 90°), M = .2

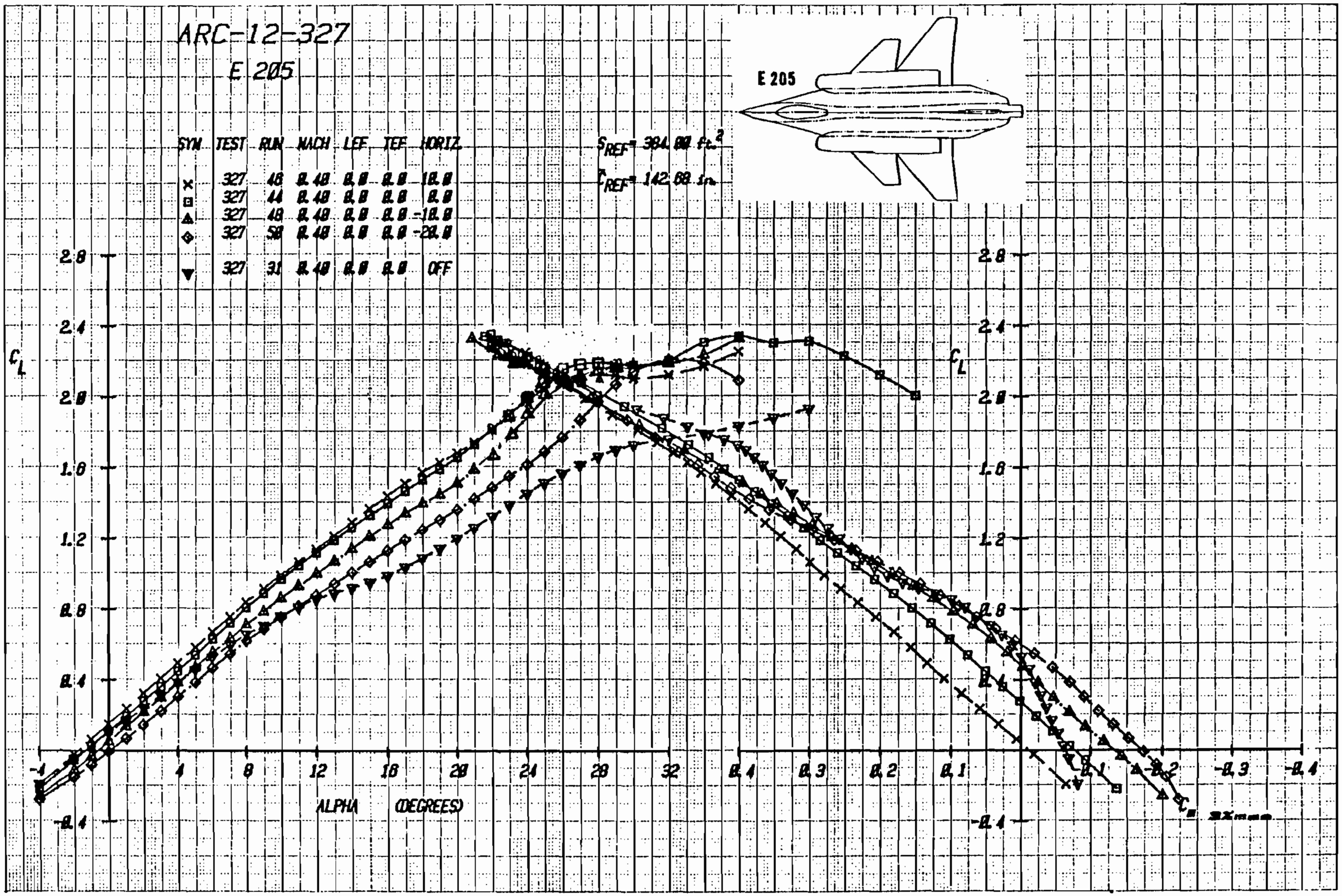

Figure 2-5a Effect of Canard Deflection on Lift and Moment with Wing Trailing-Edge Flap Undeflected, Mach = .4

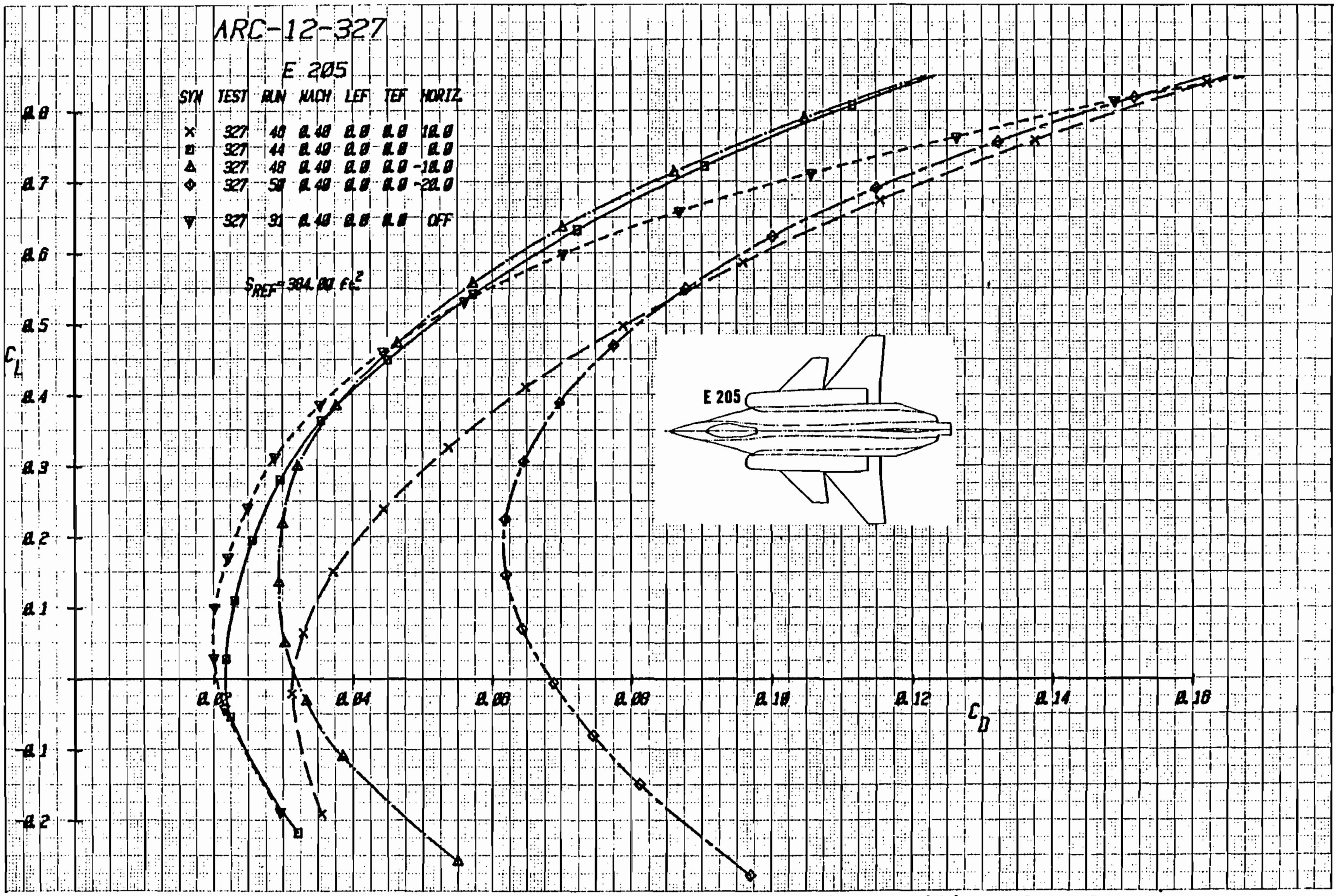

Figure 2-5b Effect of Canard Deflection on Drag with Wing Trailing-Edge Flap Undeflected, (Expanded Drag Scale), Mach = .4

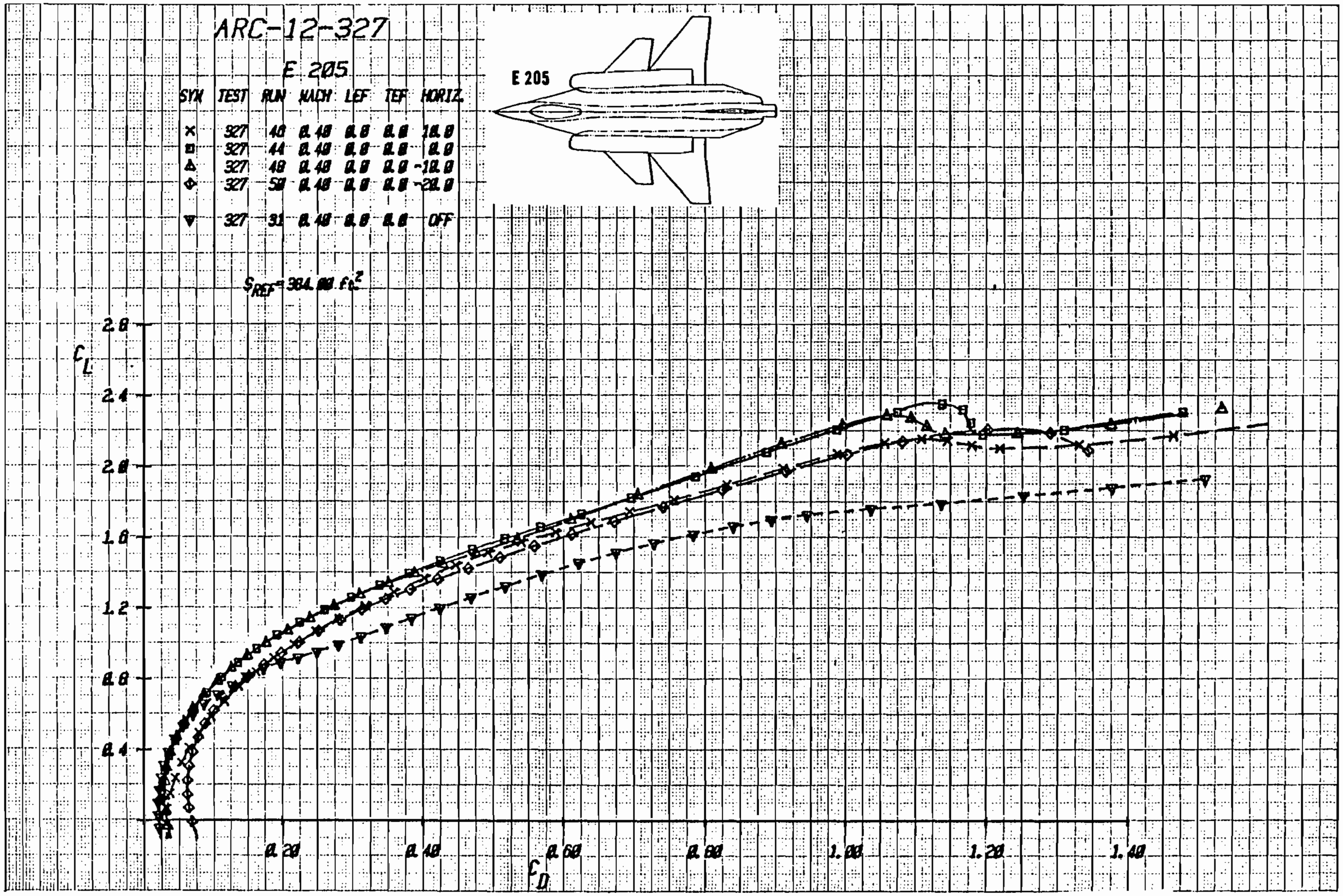

Figure 2-5c Effect of Canard Deflection on Drag with Wing Trailing-Edge Flap Undeflected, Mach = .4

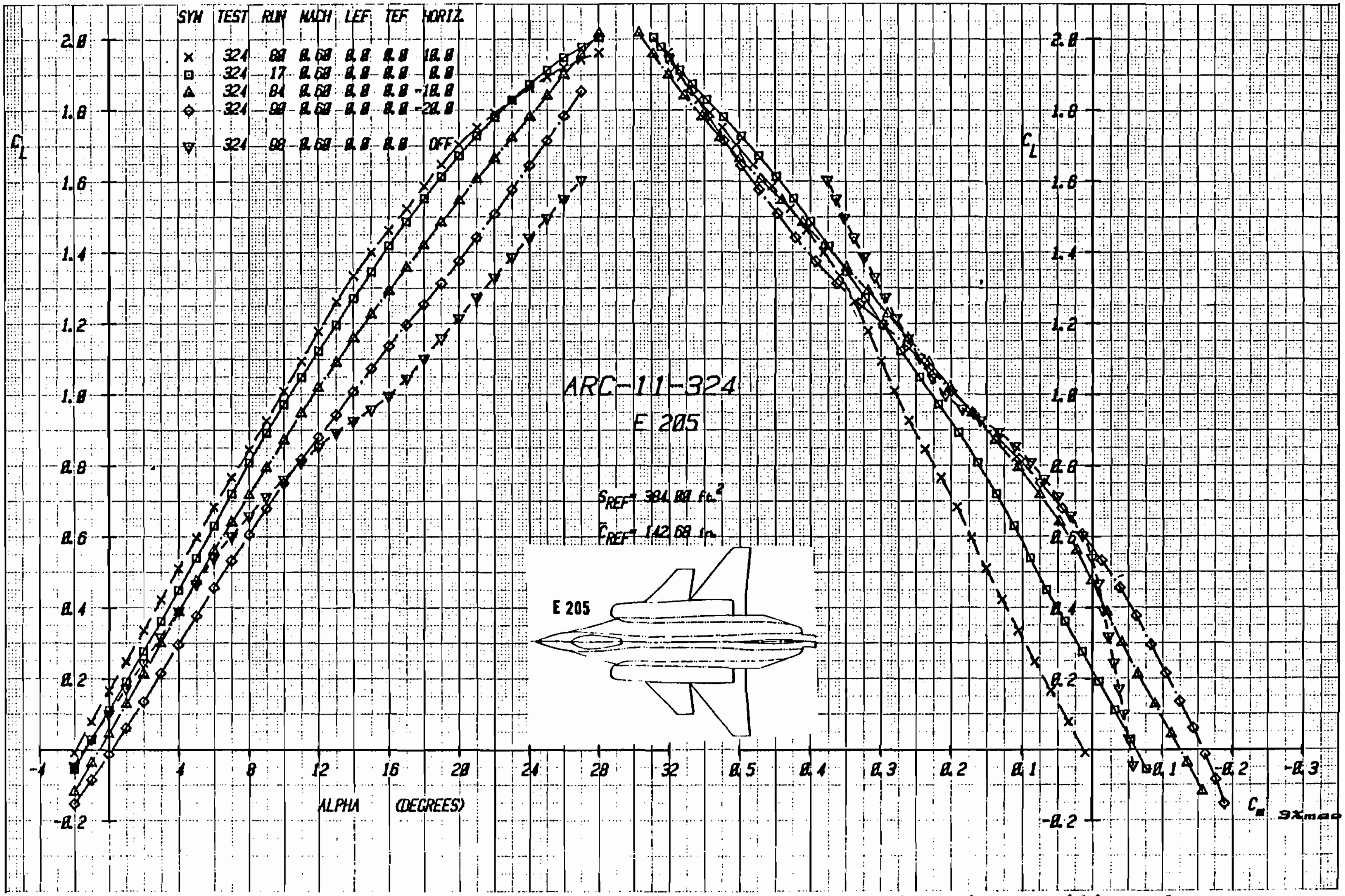

Figure 2-6a Effect of Canard Deflection on Lift and Moment With Wing Trailing-Edge Flap Undeflected, Mach = .6

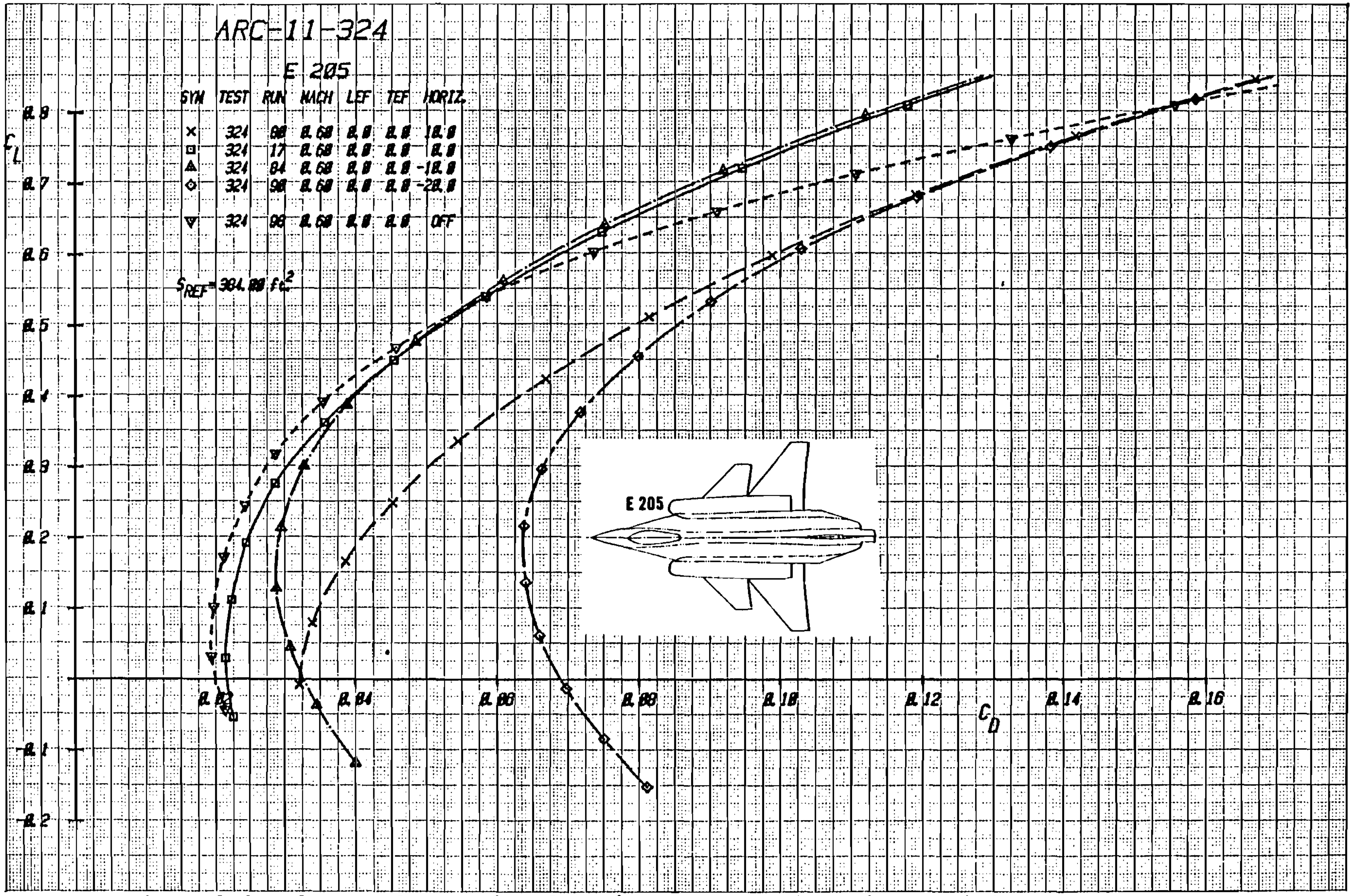

Figure 2-6b Effect of Canard Deflection on Drag with Wing Trailing-Edge Flap Undeflected, (Expanded Drag Scale), Mach = .6

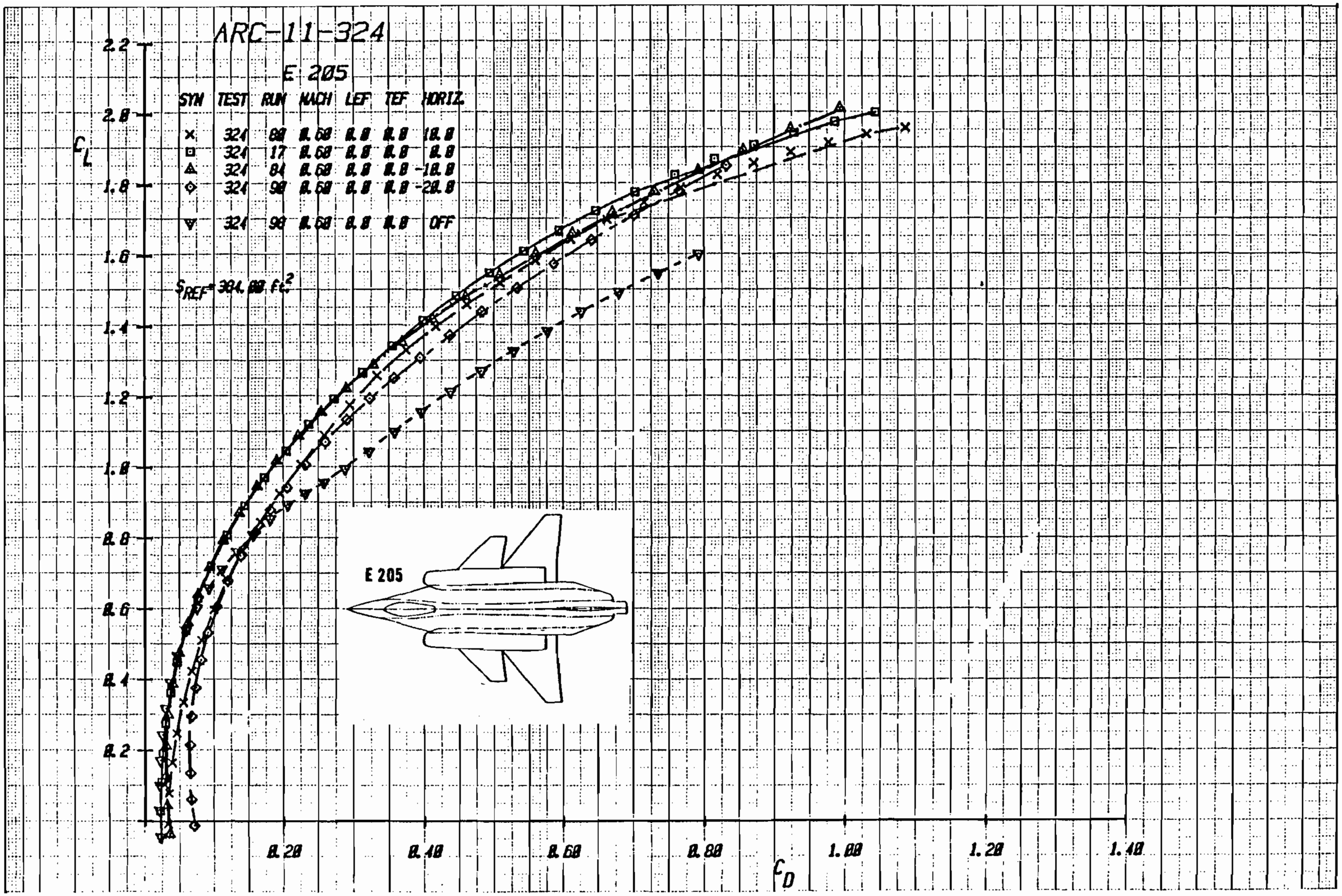

Figure 2-6c Effect of Canard Deflection on Drag With Wing Trailing-Edge Flap Undeflected, Mach = .6

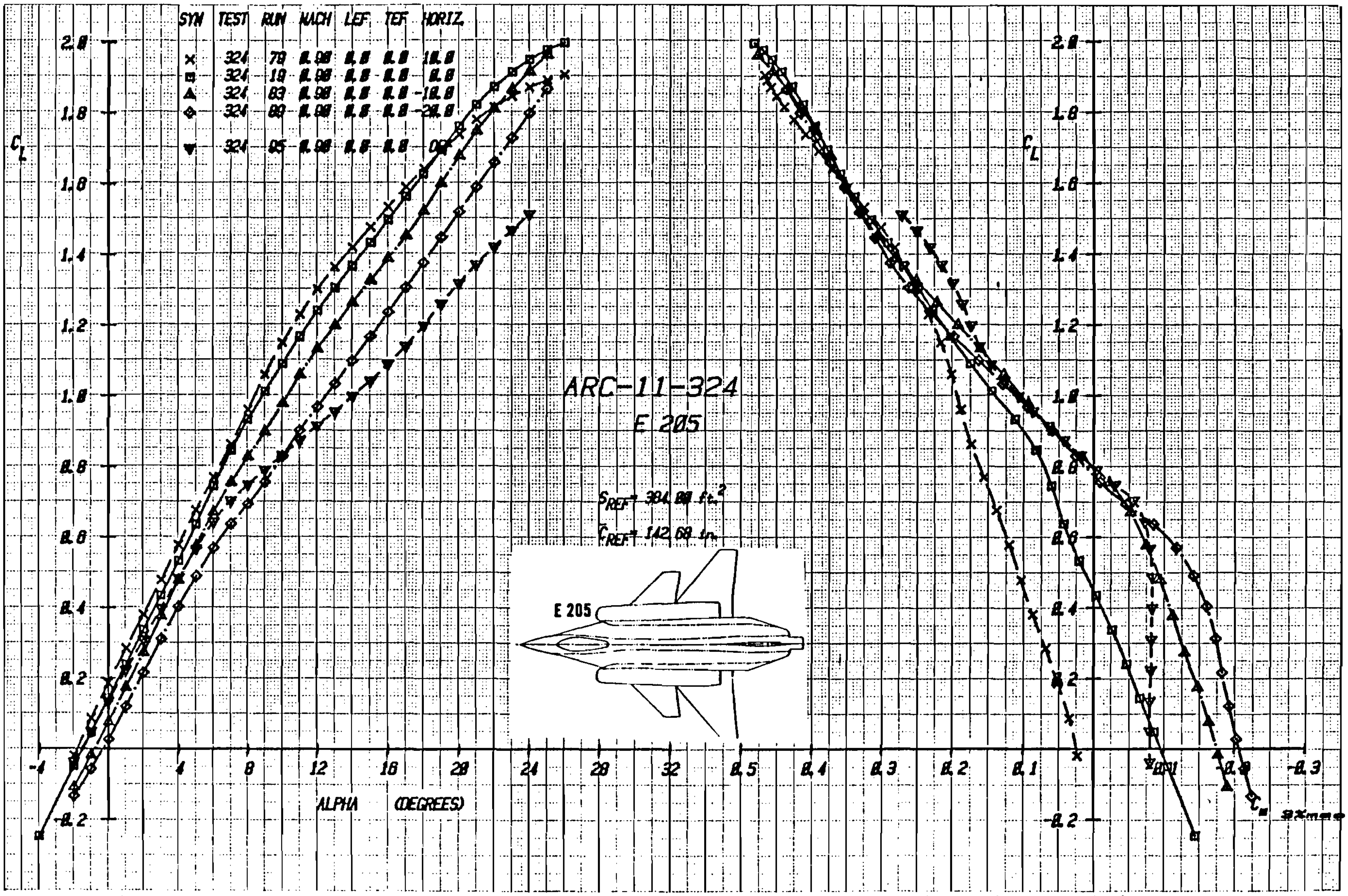

Figure 2-7a Effect of Canard Deflection on Lift and Moment With Wing Trailing-Edge Flap Undeflected, Mach = .9

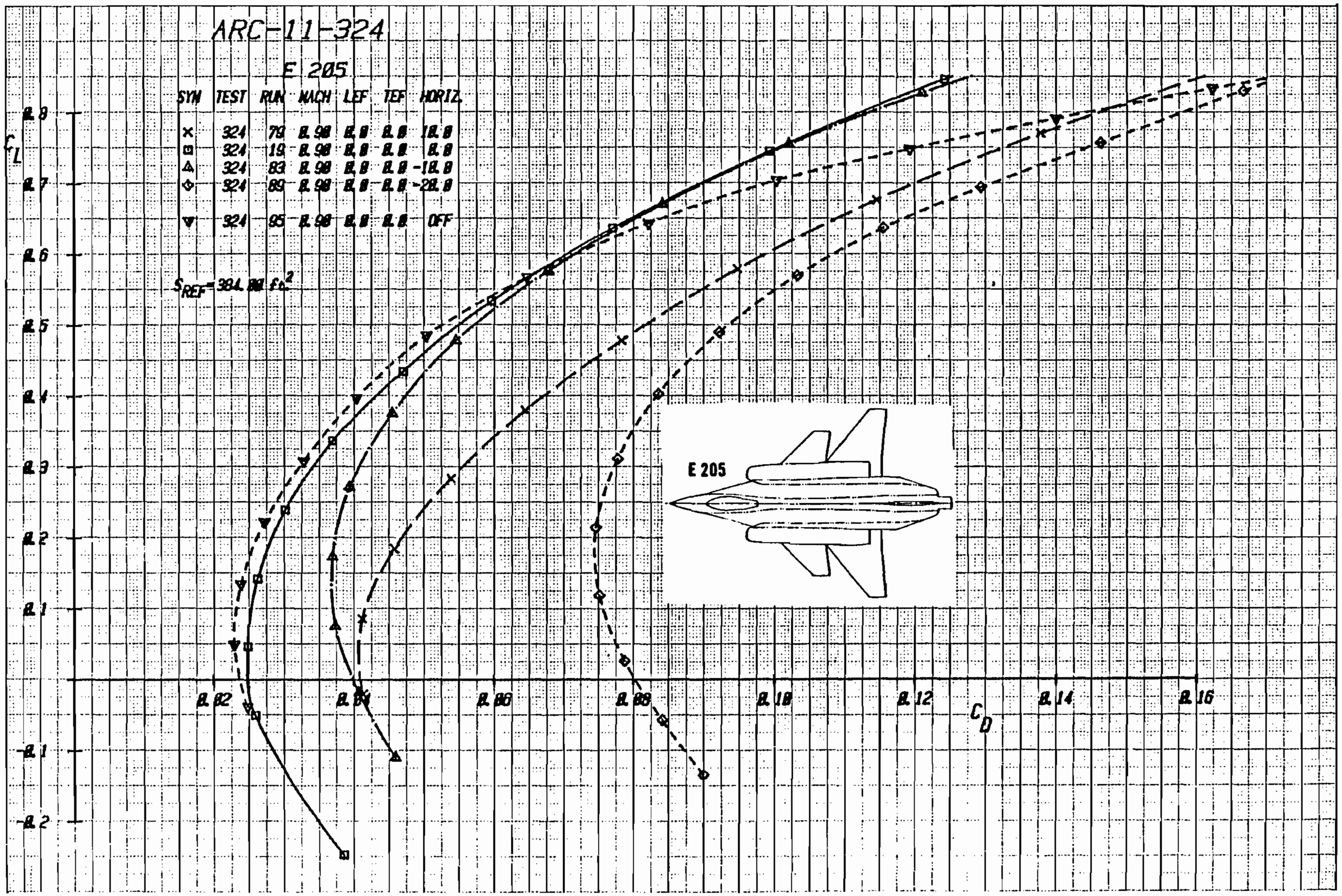

Figure 2-7b Effect of Canard Deflection on Drag with Wing Trailing-Edge Flap Undeflected, (Expanded Drag Scale), Mach = .9

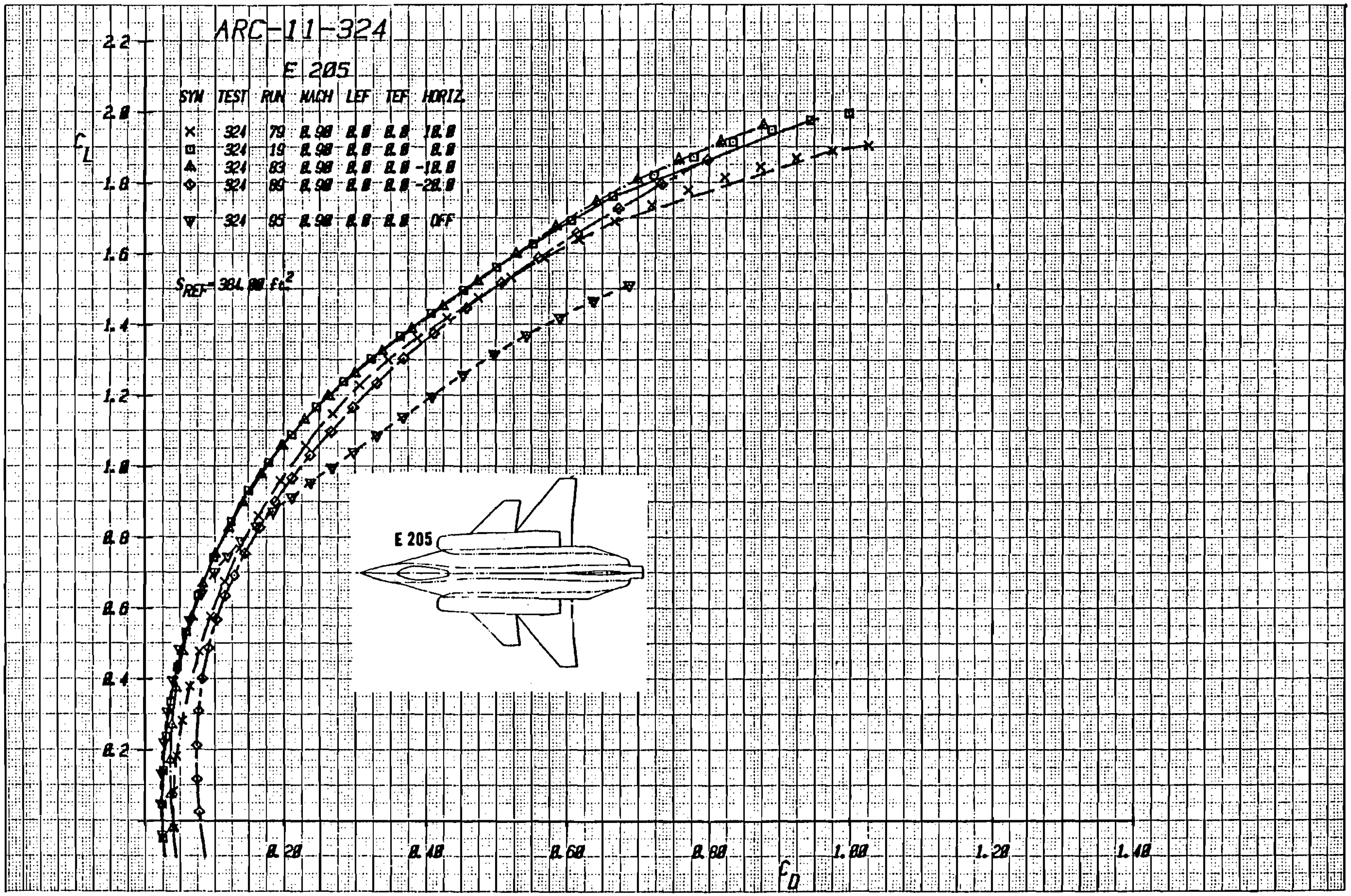

Figure 2-7c Effect of Canard Deflection on Drag With Wing Trailing-Edge Flap Undeflected, Mach = .9

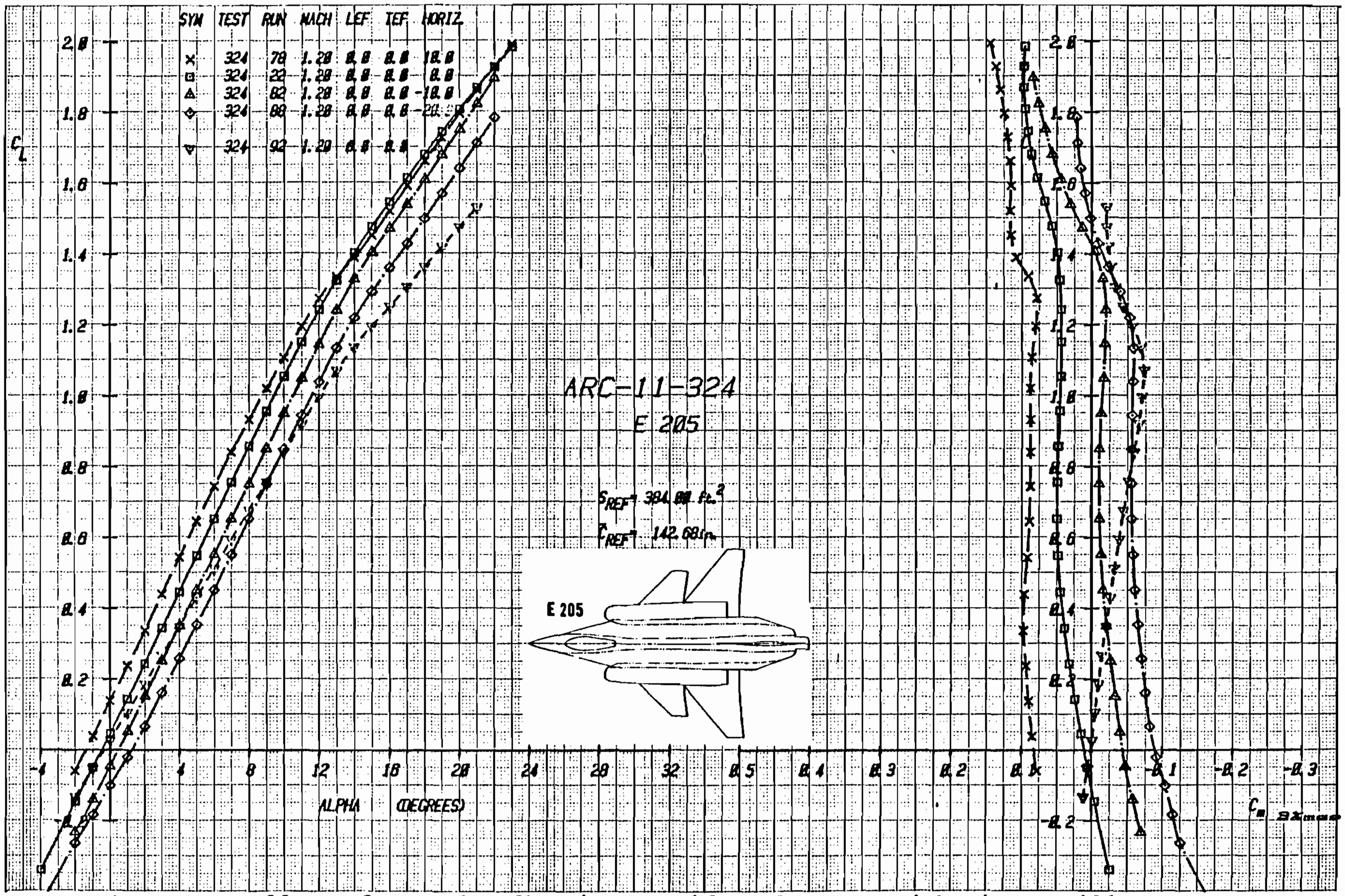

Figure 2-8a Effect of Canard Deflection on Lift and Moment With Wing Trailing-Edge Flap Undeflected, Mach = 1.2

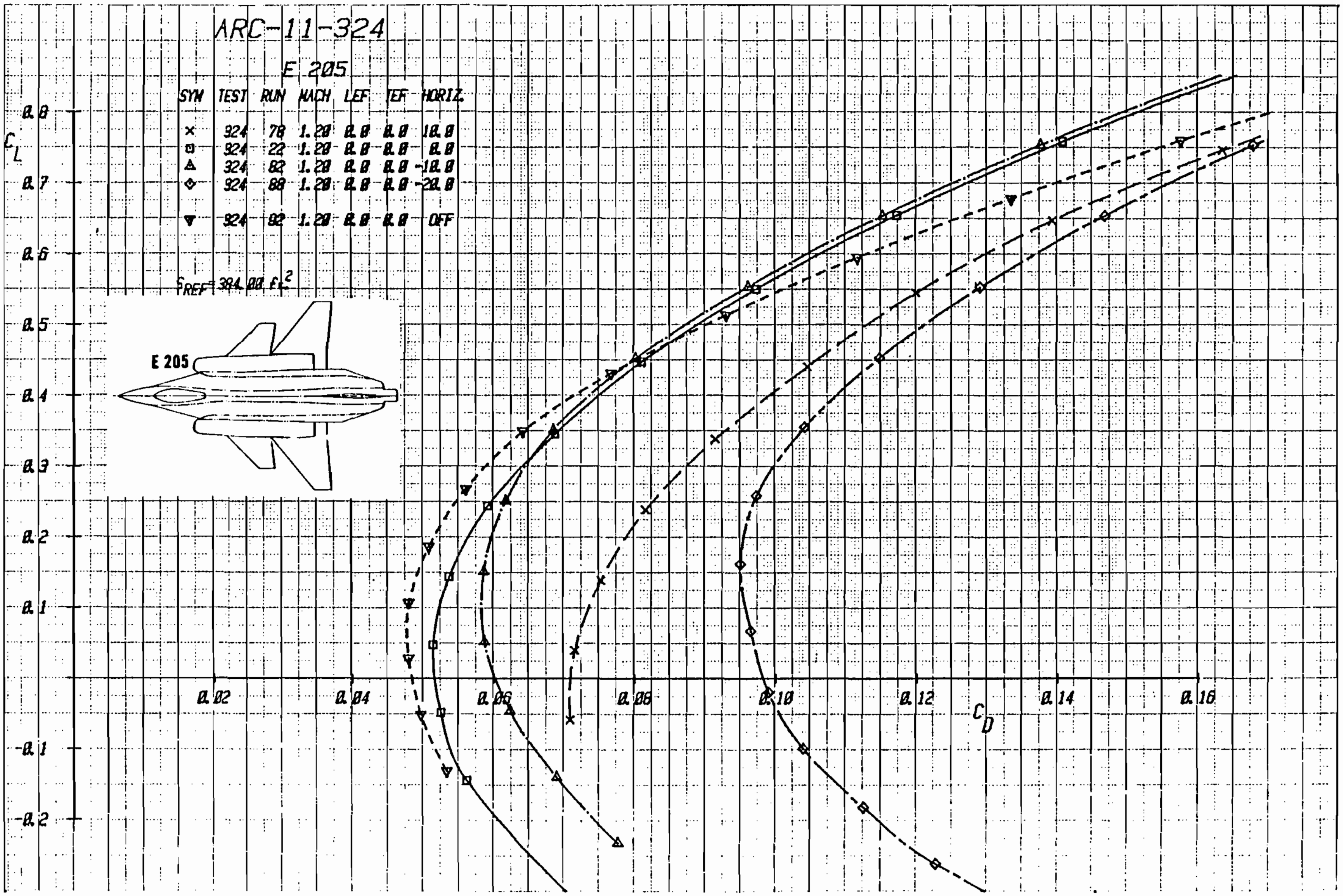

Figure 2-8b Effect of Canard Deflection on Drag With Wing Trailing-Edge Flap Undeflected, Mach = 1.2

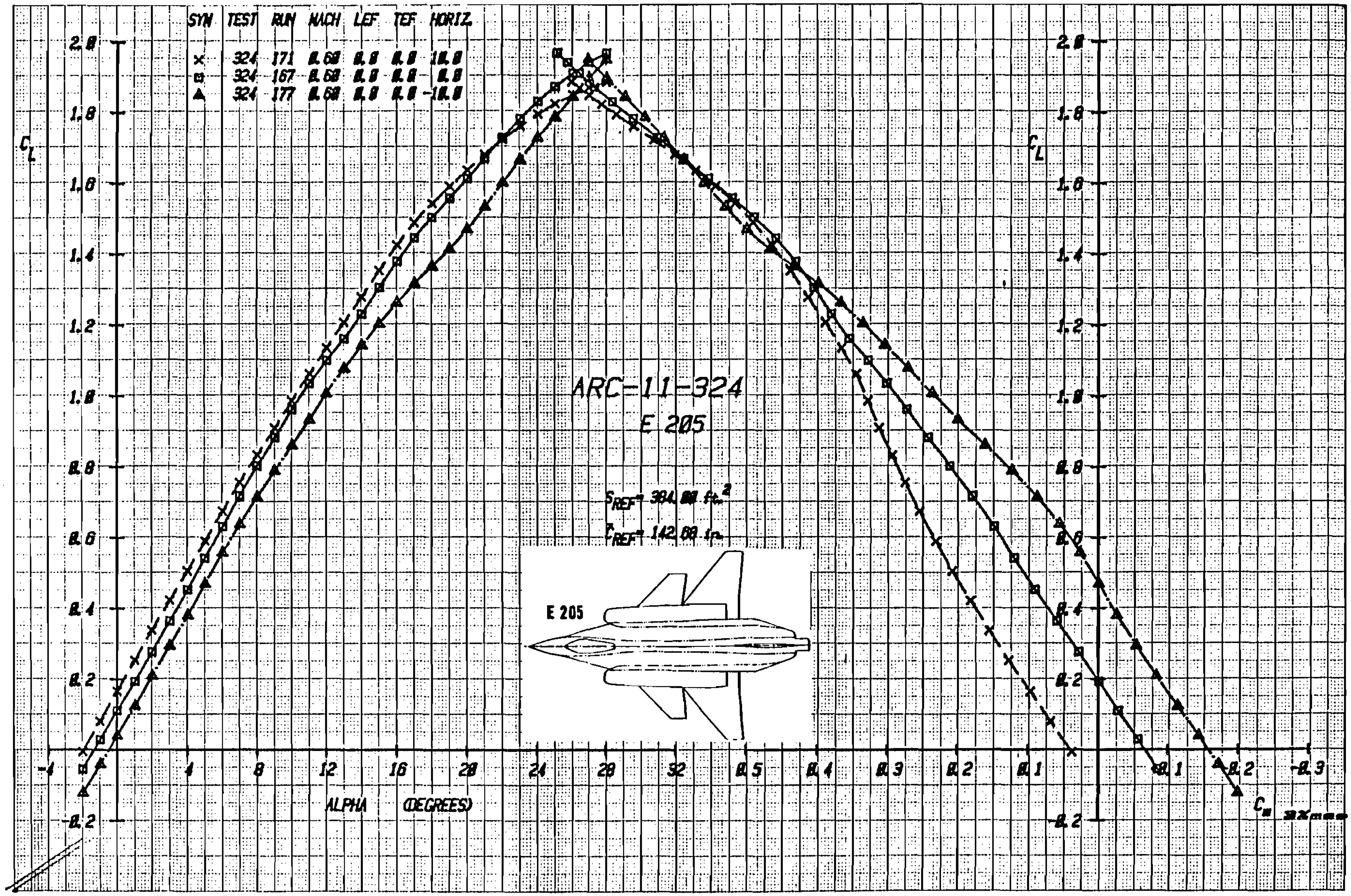

Figure 2-9a Effect of Canard Deflection on Lift and Moment With Forward Canard Longitudinal Location, C_2, and Baseline Strake, S_1, Mach = .6

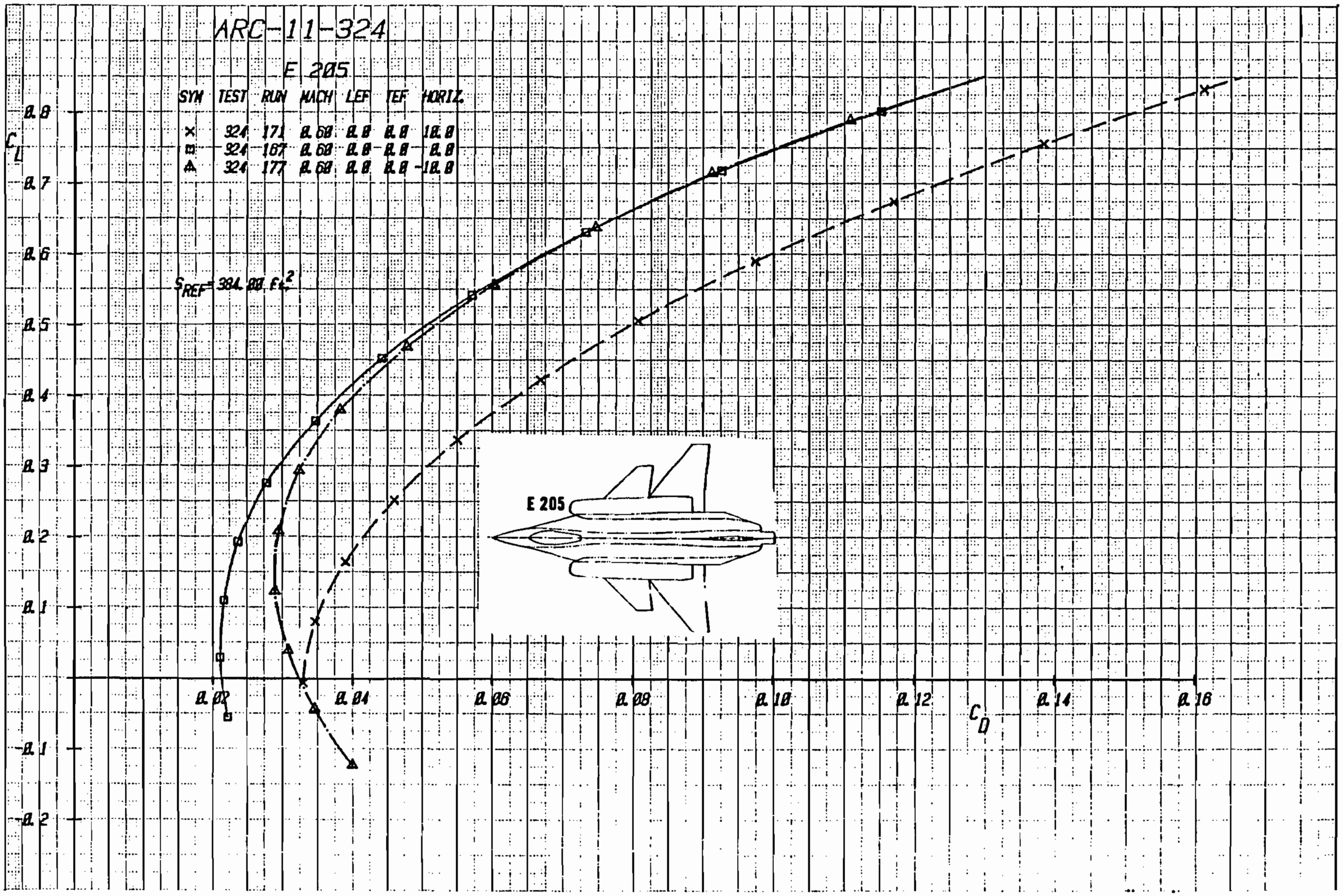

Figure 2-9b Effect of Canard Deflection on Drag With Forward Canard Longitudinal Location, C_2, and Baseline Strake, S_1, Mach = .6

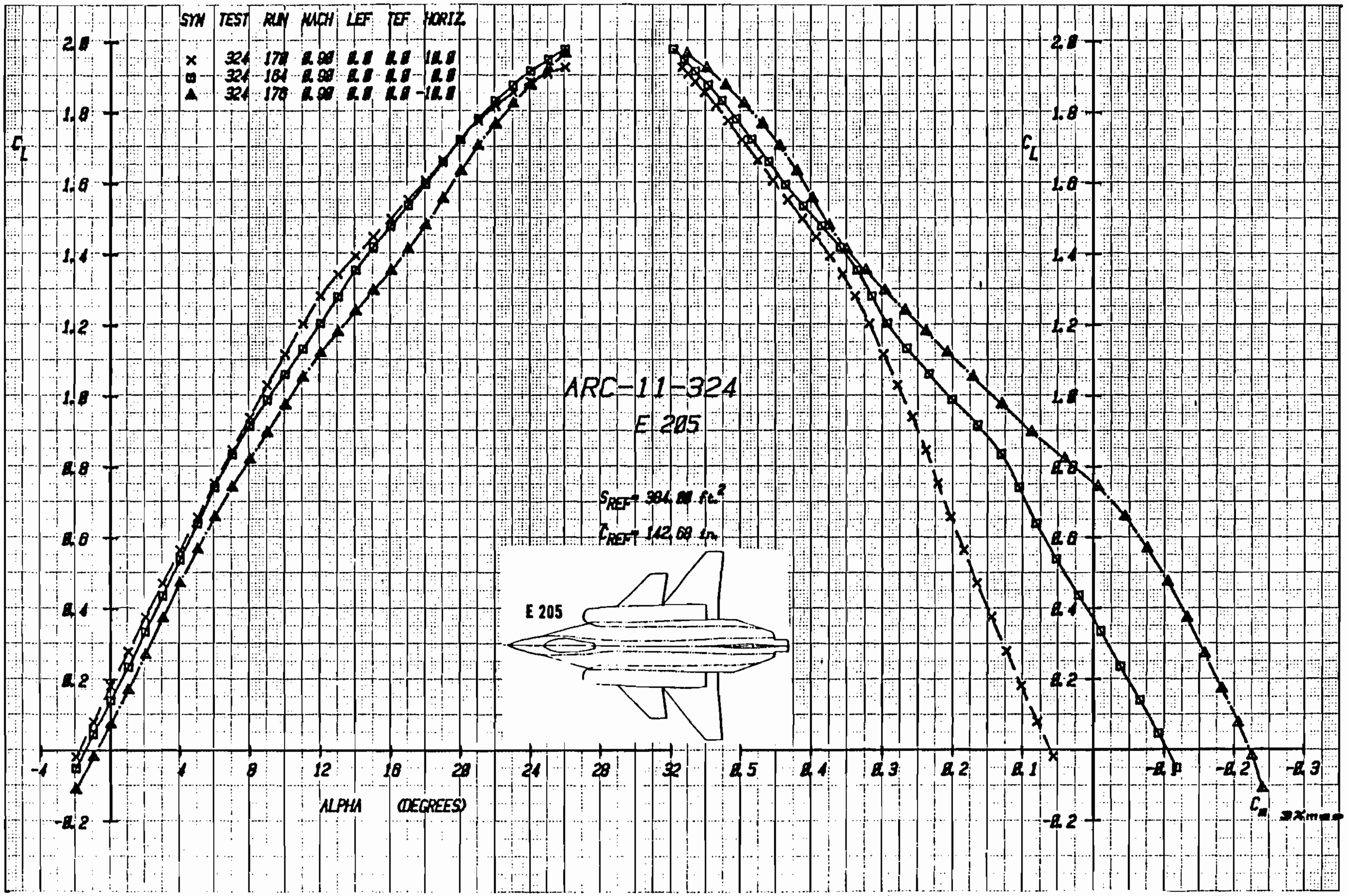

Figure2-10aEffect of Canard Deflection on Lift and Moment With Forward Canard Longitudinal Location, C_2, and Baseline Strake, S_1, Mach = .9

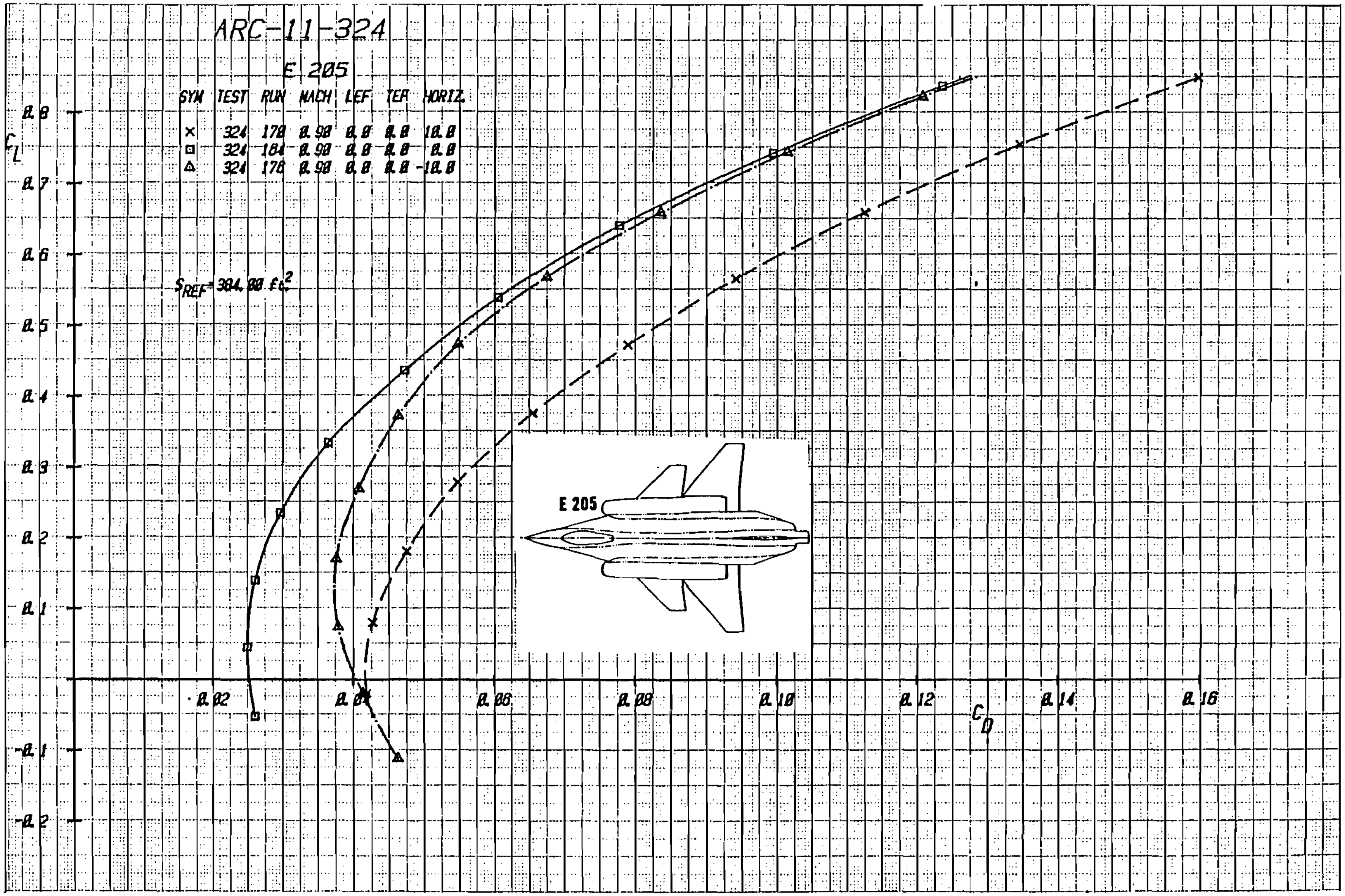

Figure 2-10b Effect of Canard Deflection on Drag With Forward Canard Longitudinal Location, C_2, and Baseline Strake, S_1, Mach = .9

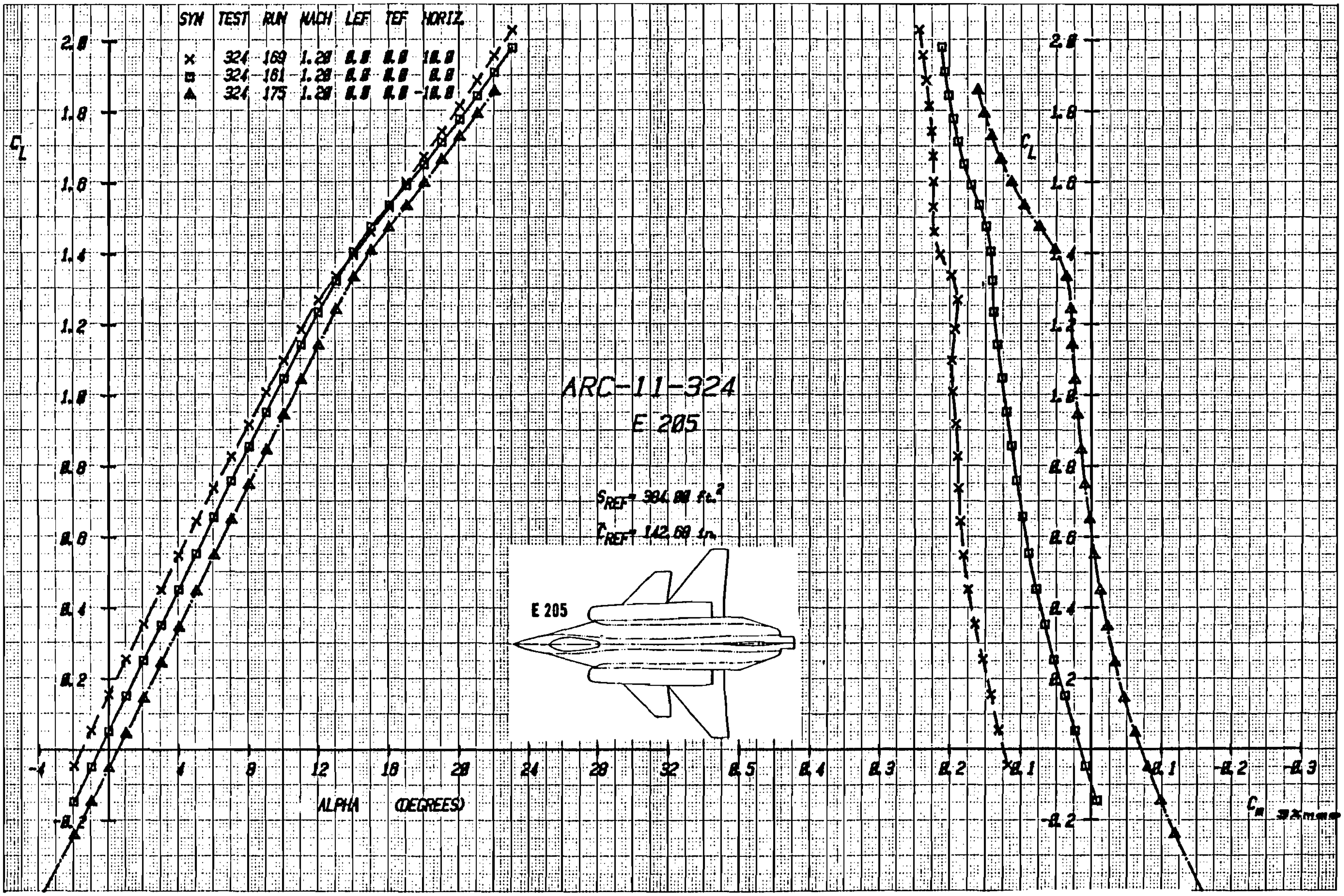

Figure 2-11a Effect of Canard Deflection on Lift and Moment With Forward Canard Longitudinal Location, C_2, and Baseline Strake, S_1, Mach = 1.2

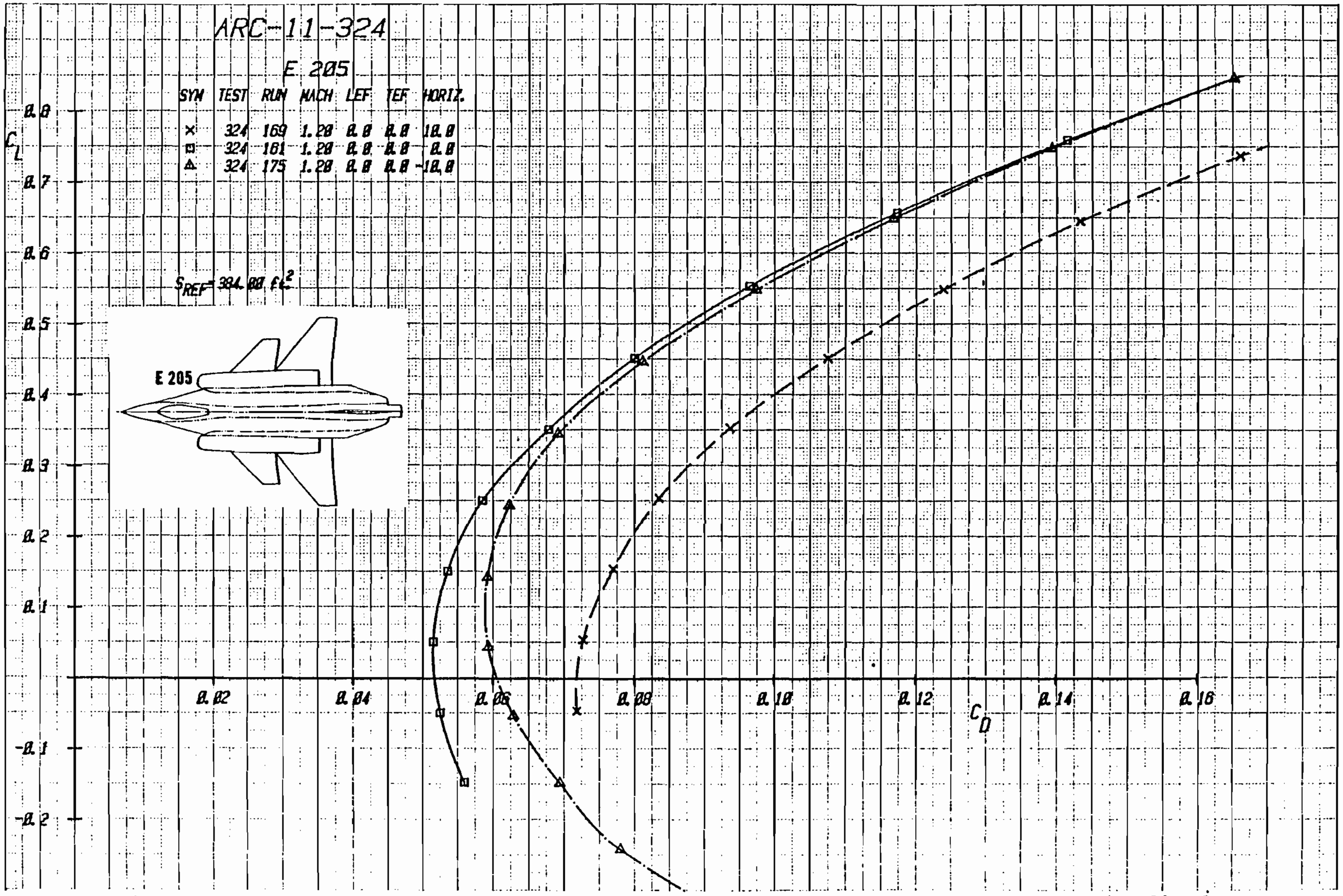

Figure2-11bEffect of Canard Deflection on Drag With Forward Canard Longitudinal Location, C_2, and Baseline Strake, S_1, Mach = 1.2

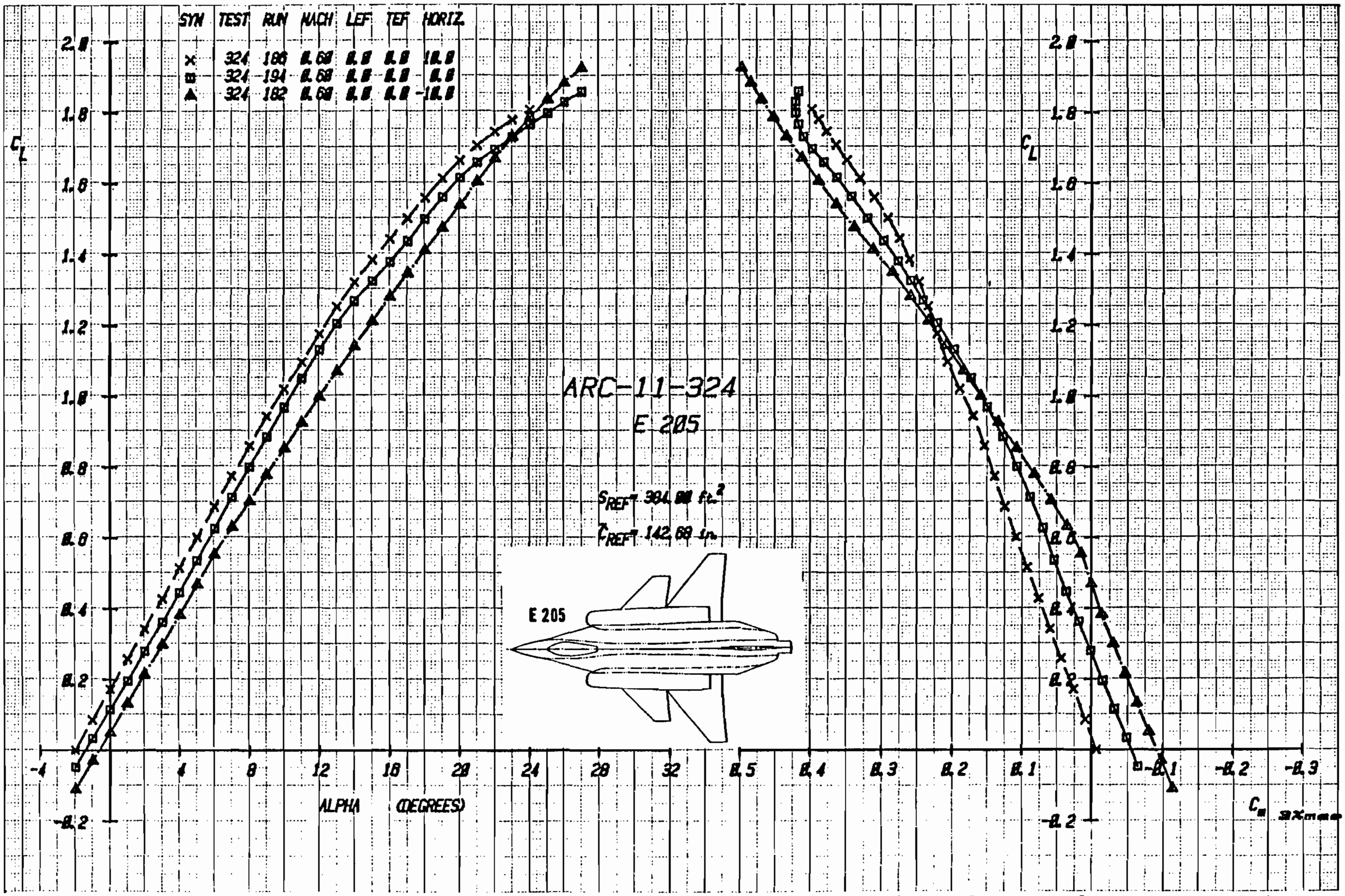

Figure2-12aEffect of Canard Deflection on Lift and Moment With Aft Canard Longitudinal Location C_3, and Baseline Strake, S_1, Mach = .6

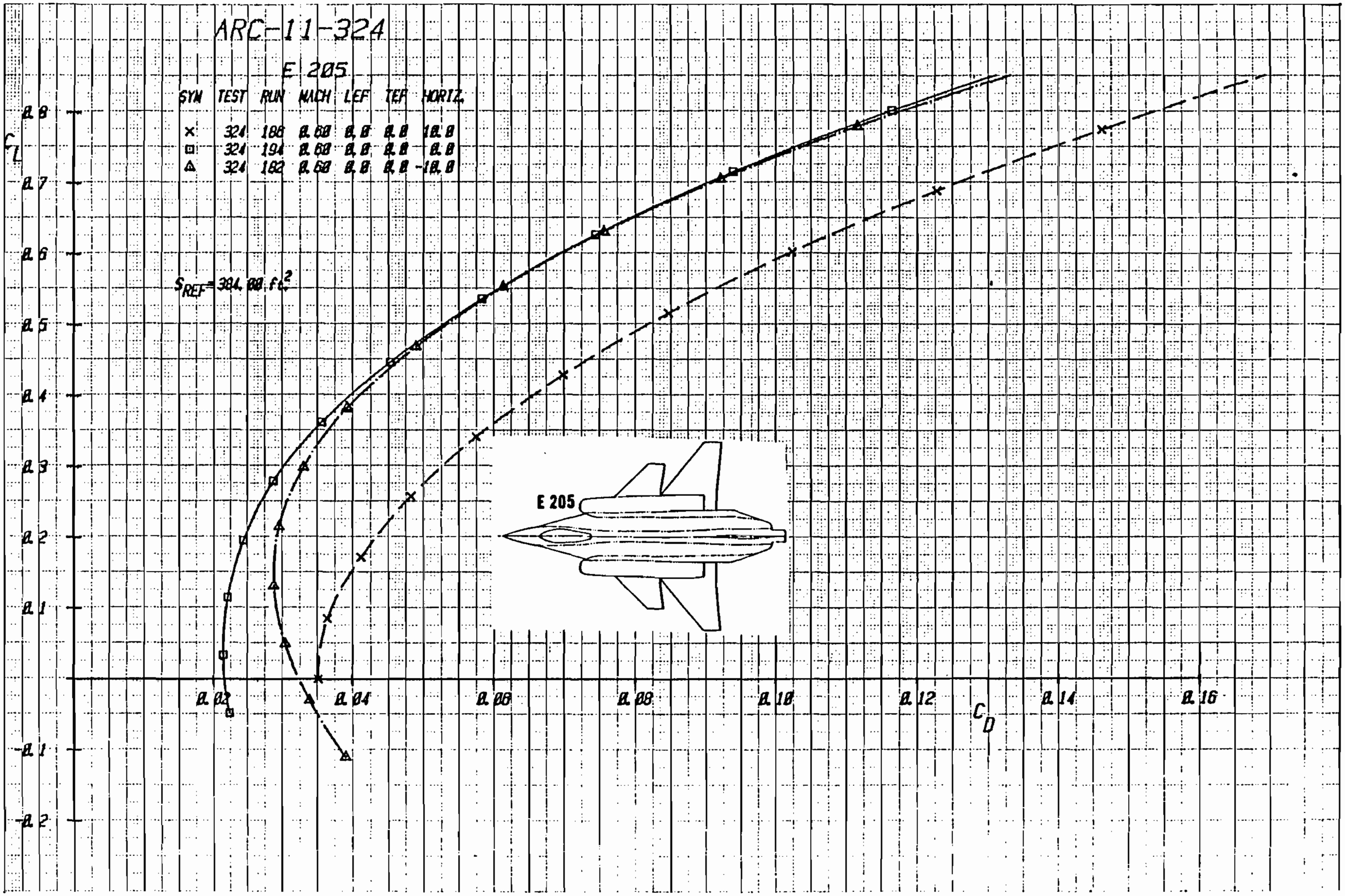

Figure2-12bEffect of Canard Deflection on Drag With Aft Canard Longitudinal Location, C_3, and Baseline Strake, S_1, Mach = .6

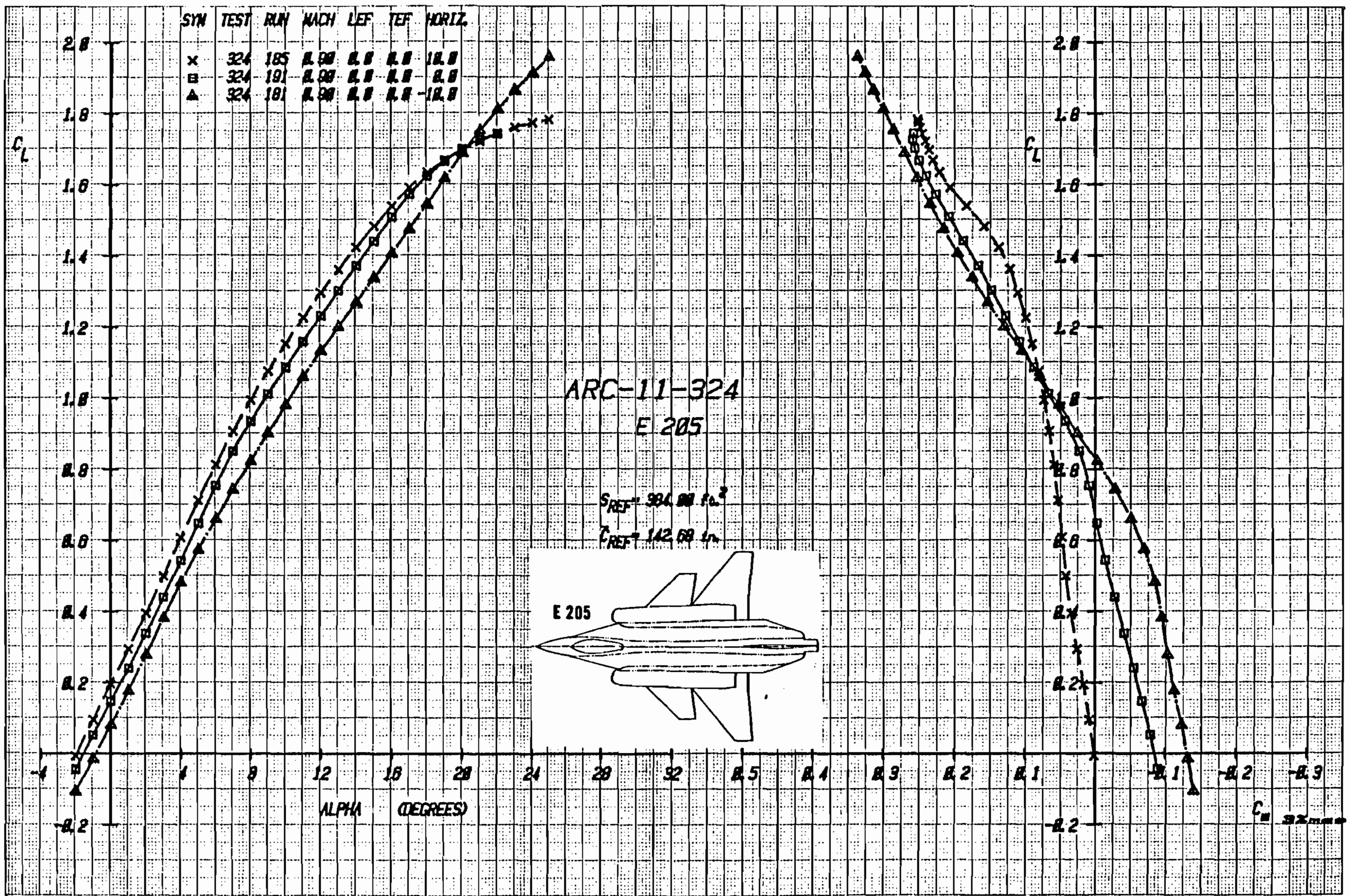

Figure2-13aEffect of Canard Deflection on Lift and Moment With Aft Canard Longitudinal Location, C_3, and Baseline Strake, S_1, Mach = .9

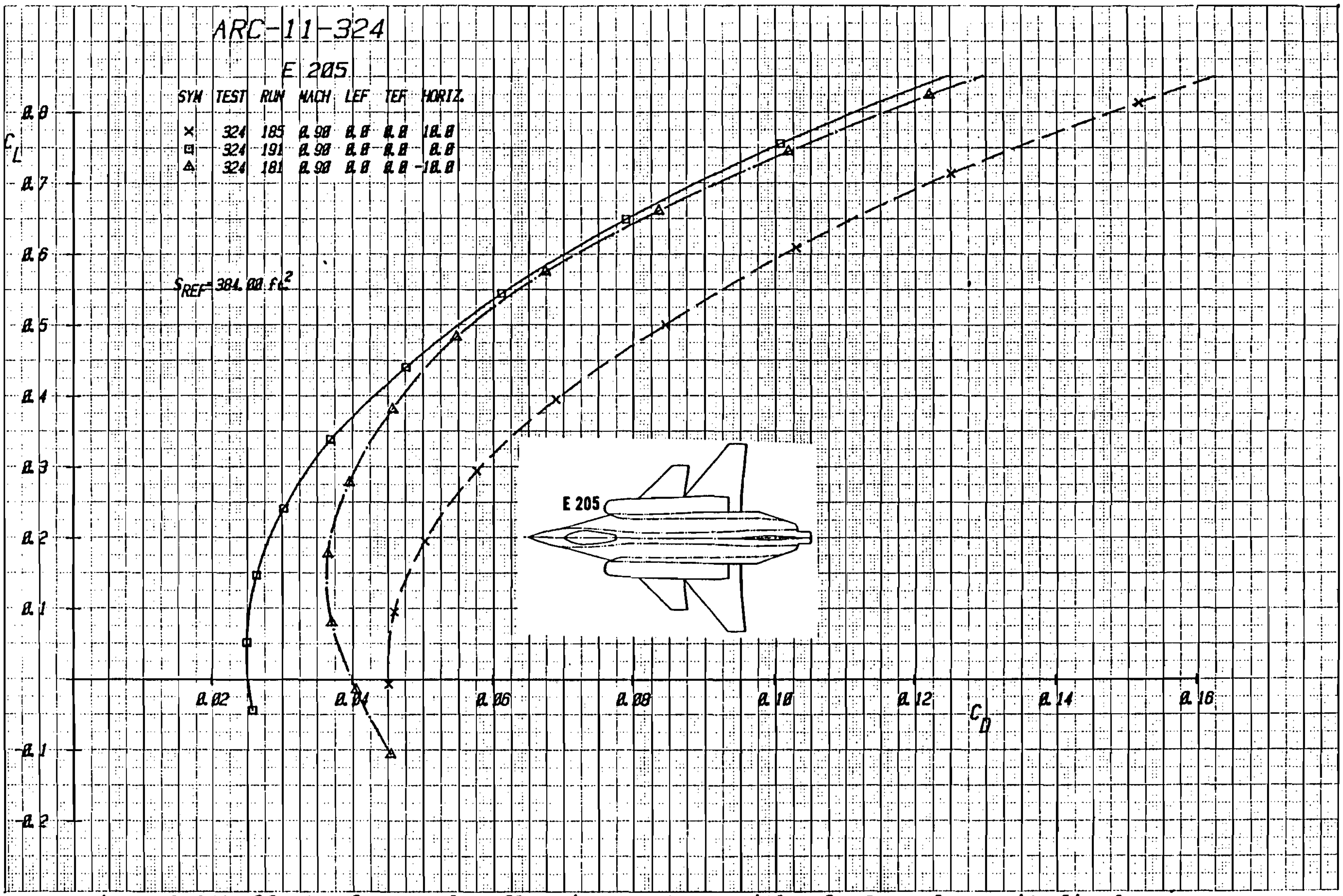

Figure2-13bEffect of Canard Deflection on Drag With Aft Canard Longitudinal Location, C_3, and Baseline Strake, S_1, Mach = .9

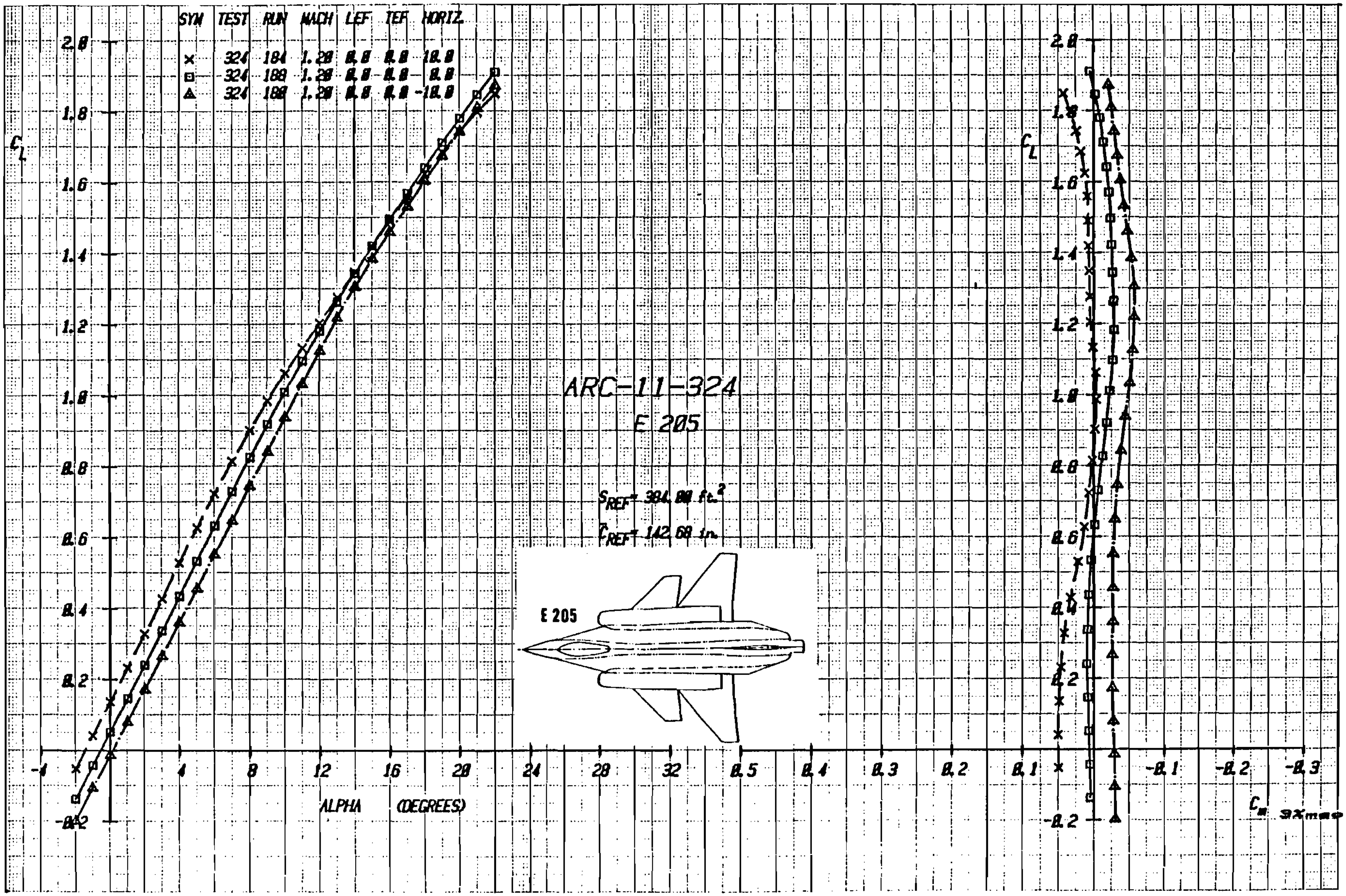

Figure2-14aEffect of Canard Deflection on Lift and Moment With Aft Canard Longitudinal Location, C_3, and Baseline Strake, S_1, Mach = 1.2

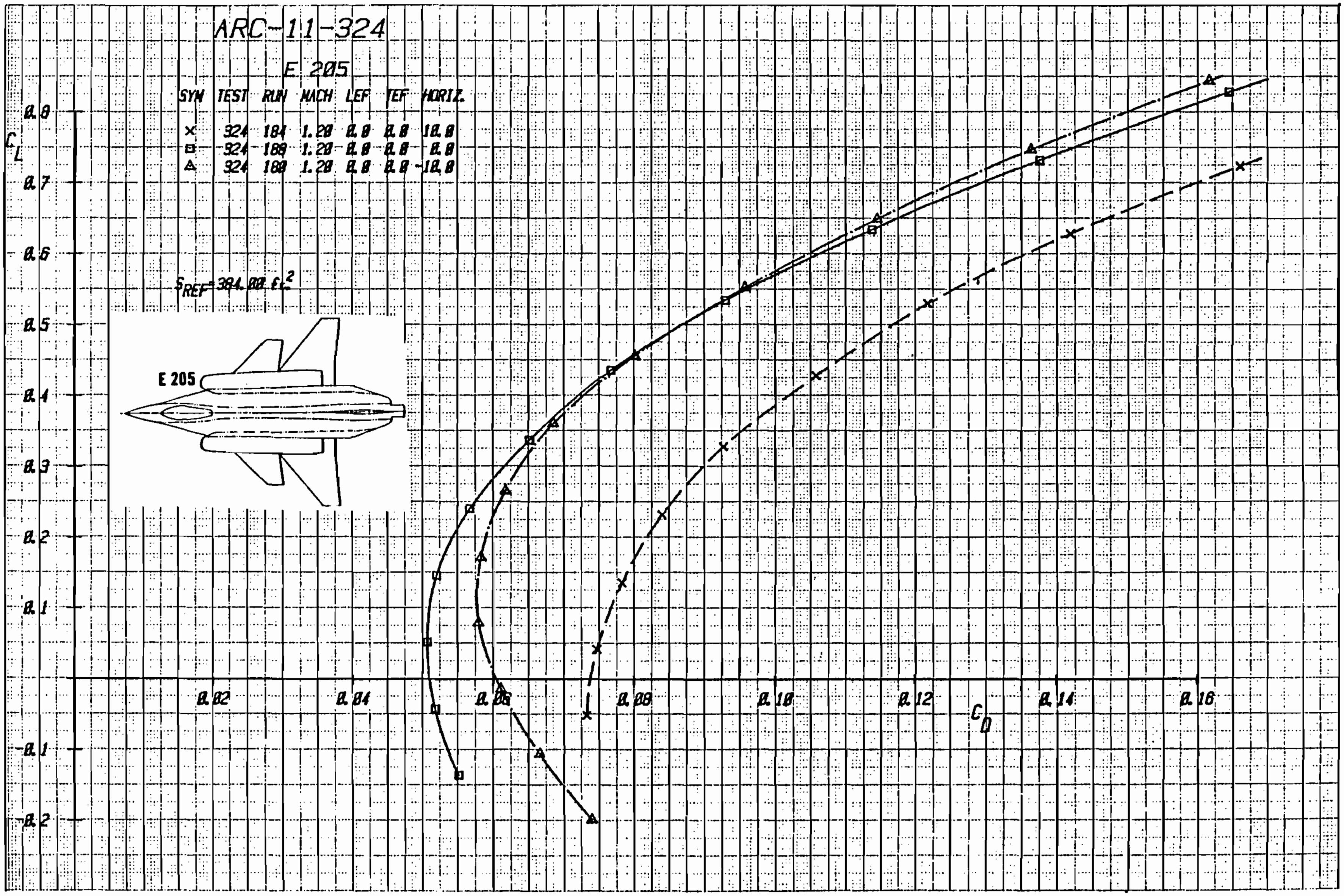

Figure2-14bEffect of Canard Deflection on Drag With Aft Canard Longitudinal Location, C_3, and Baseline Strake, S_1, Mach = 1.2

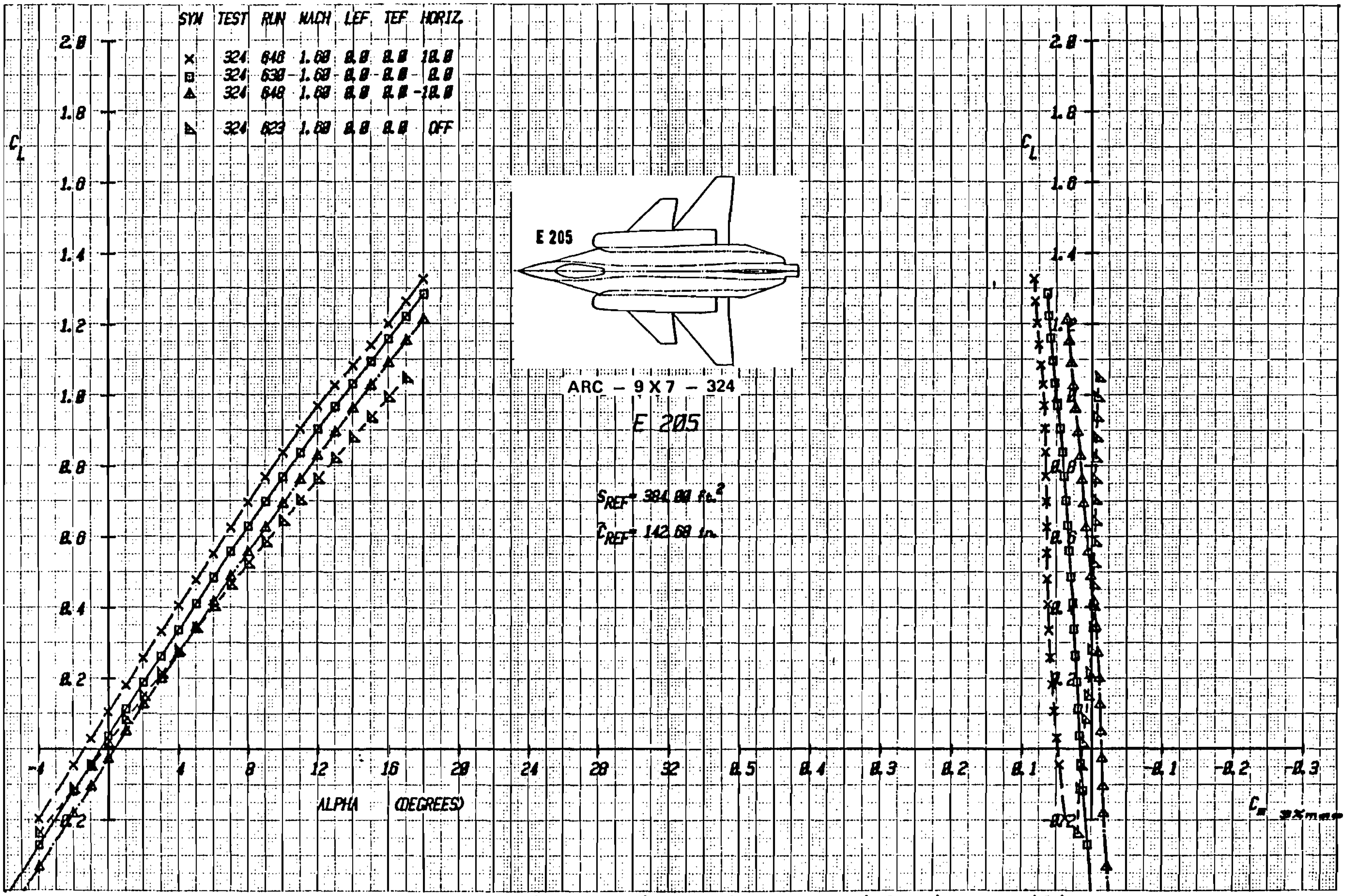

Figure2-15aEffect of Canard Deflection on Lift and Moment with Wing Trailing-Edge Flap Undeflected, Mach = 1.6

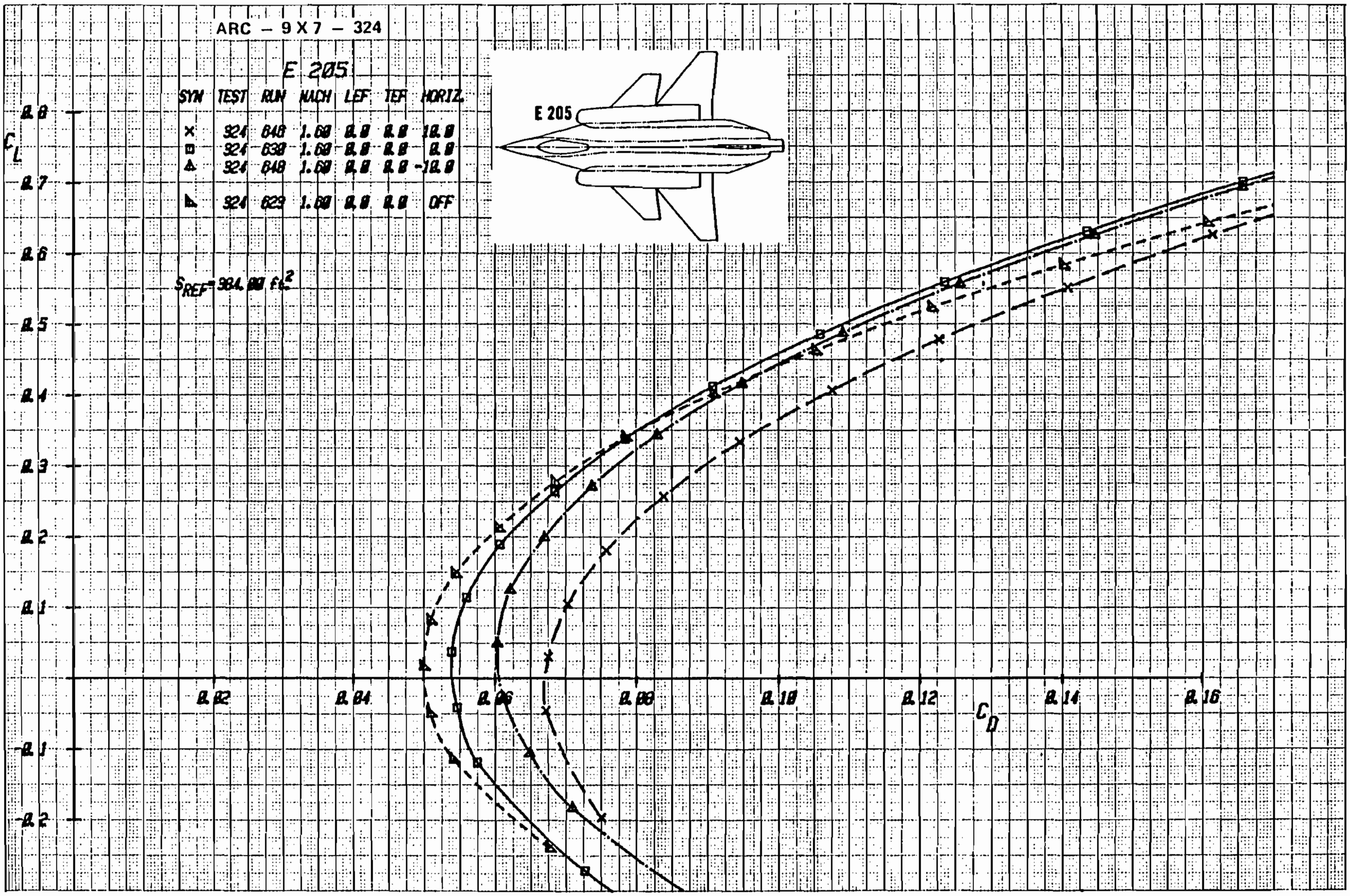

Figure2-15bEffect of Canard Deflection on Drag with Wing Trailing-Edge Flap Undeflected, (Expanded Drag Scale), Mach = 1.6

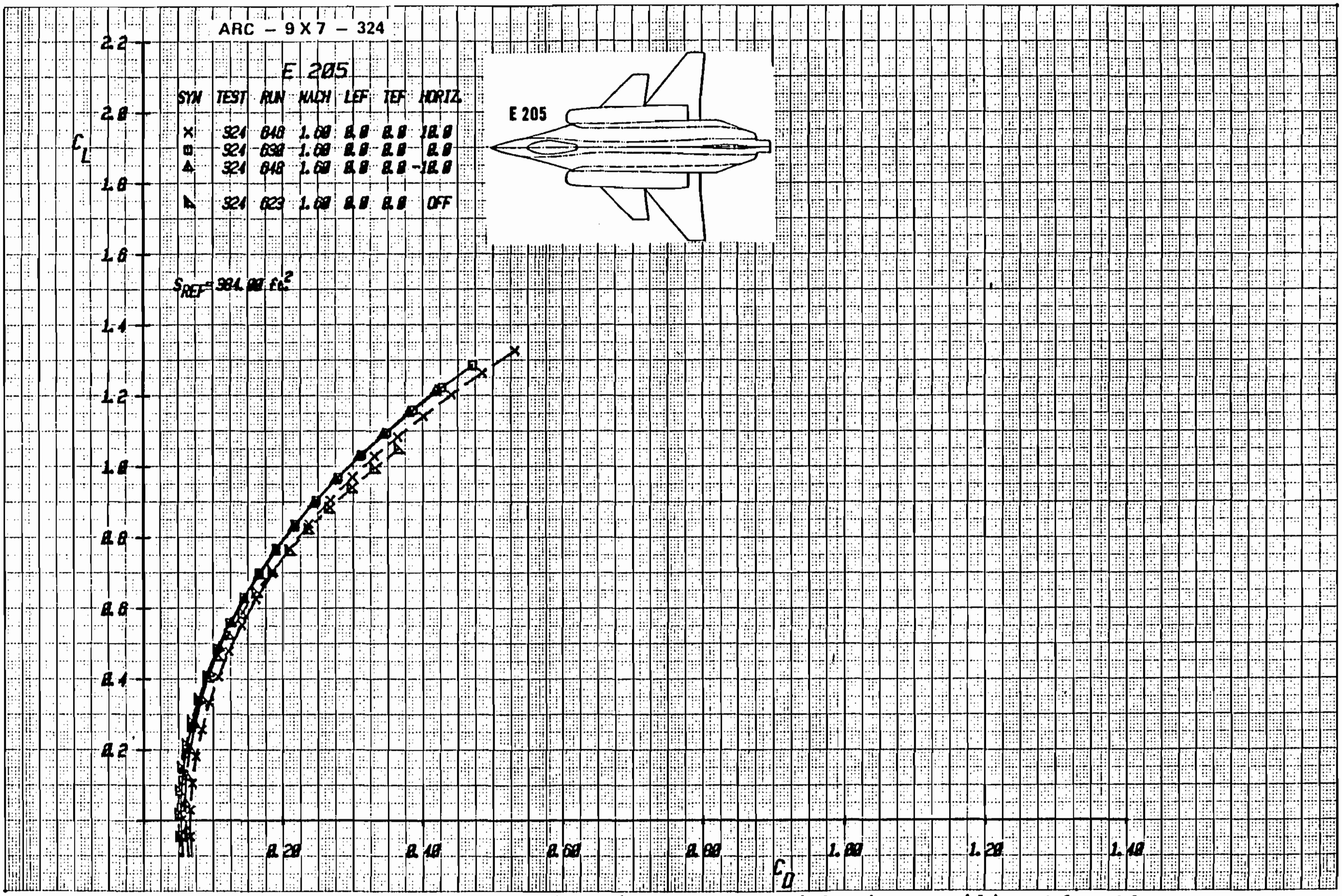

Figure2-15cEffect of Canard Deflection on Drag With Wing Trailing-Edge Flap Undeflected, Mach = 1.6

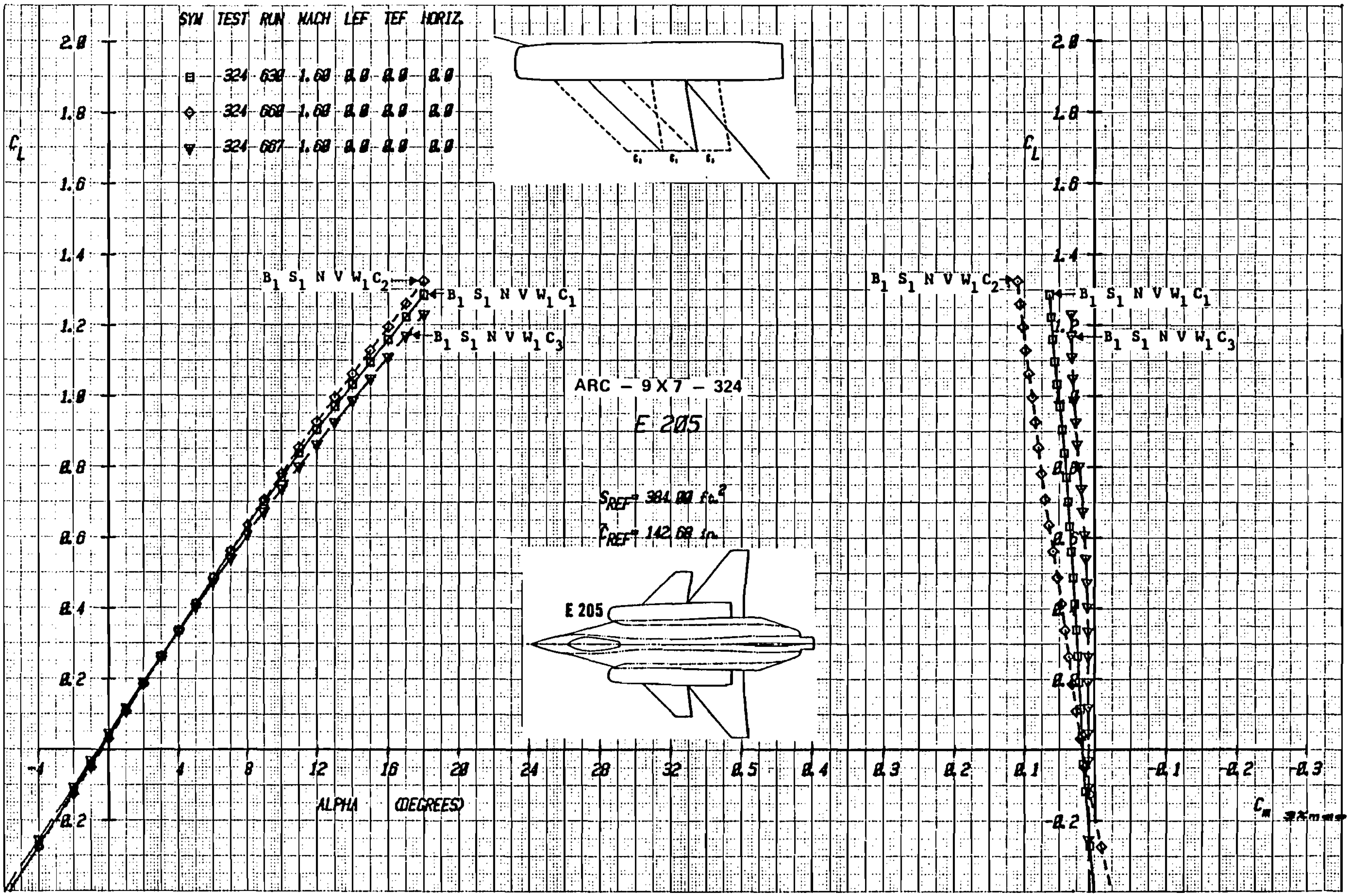

Figure2-16aEffect of Canard Longitudinal Location on Lift and Moment With Baseline Strake, Mach = 1.6

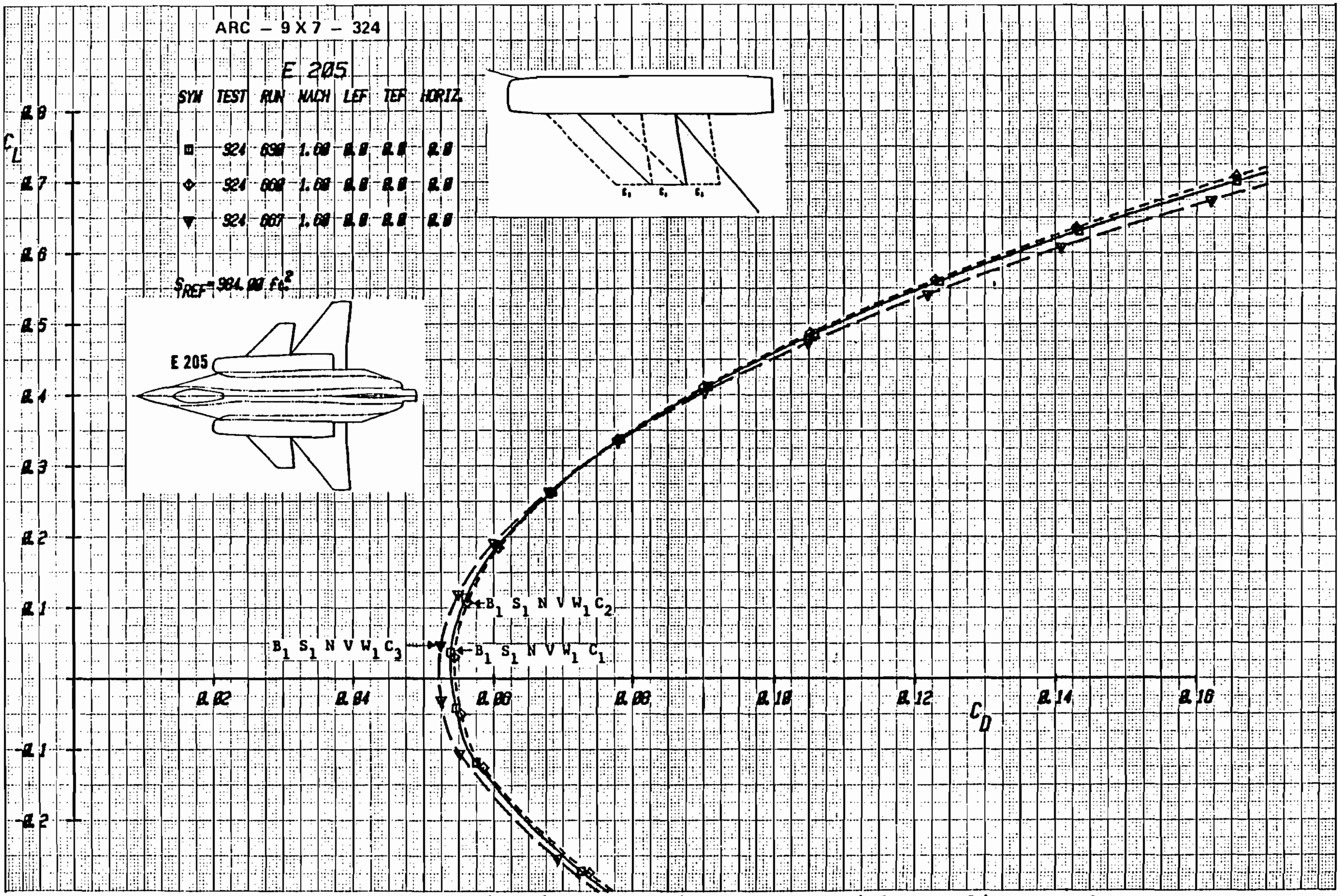

Figure2-16bEffect of Canard Longitudinal Location on Drag With Baseline Strake, (Expanded Drag Scale), Mach = 1.6

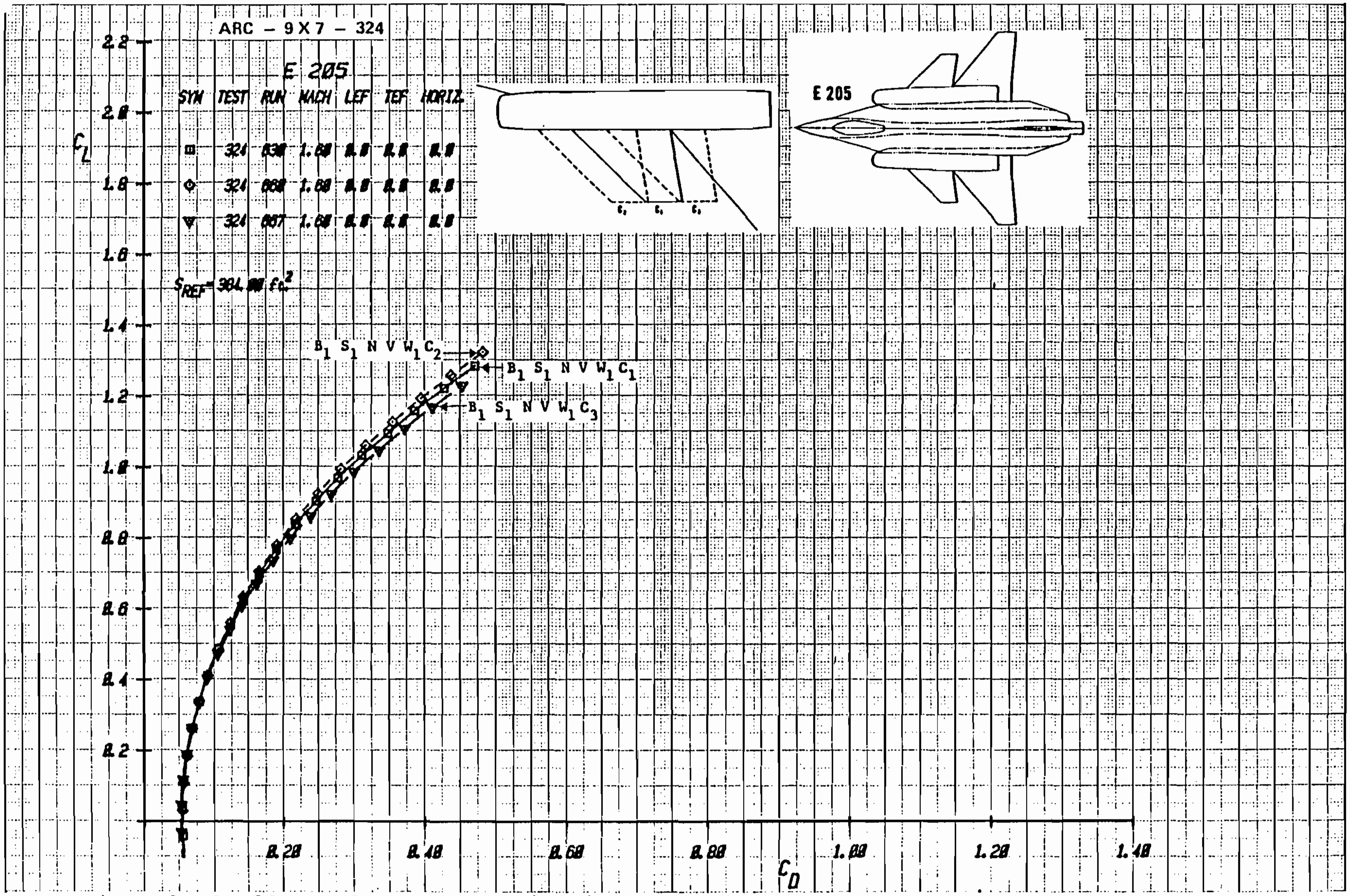

Figure2-16cEffect of Canard Longitudinal Location on Drag With Baseline Strake,
Mach = 1.6

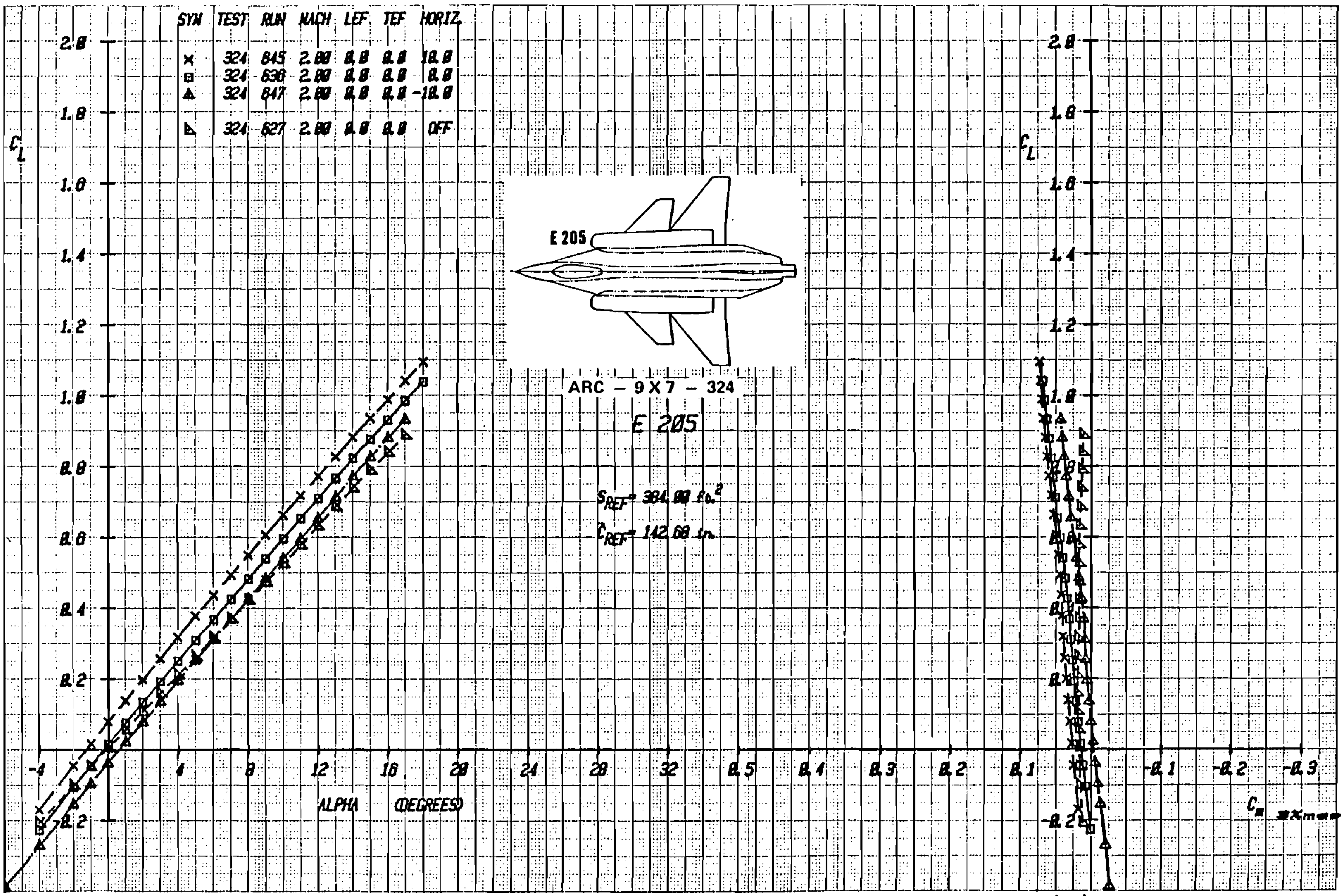

Figure2-17aEffect of Canard Deflection on Lift and Moment With Wing Trailing-Edge Flap Undeflected, Mach = 2.0

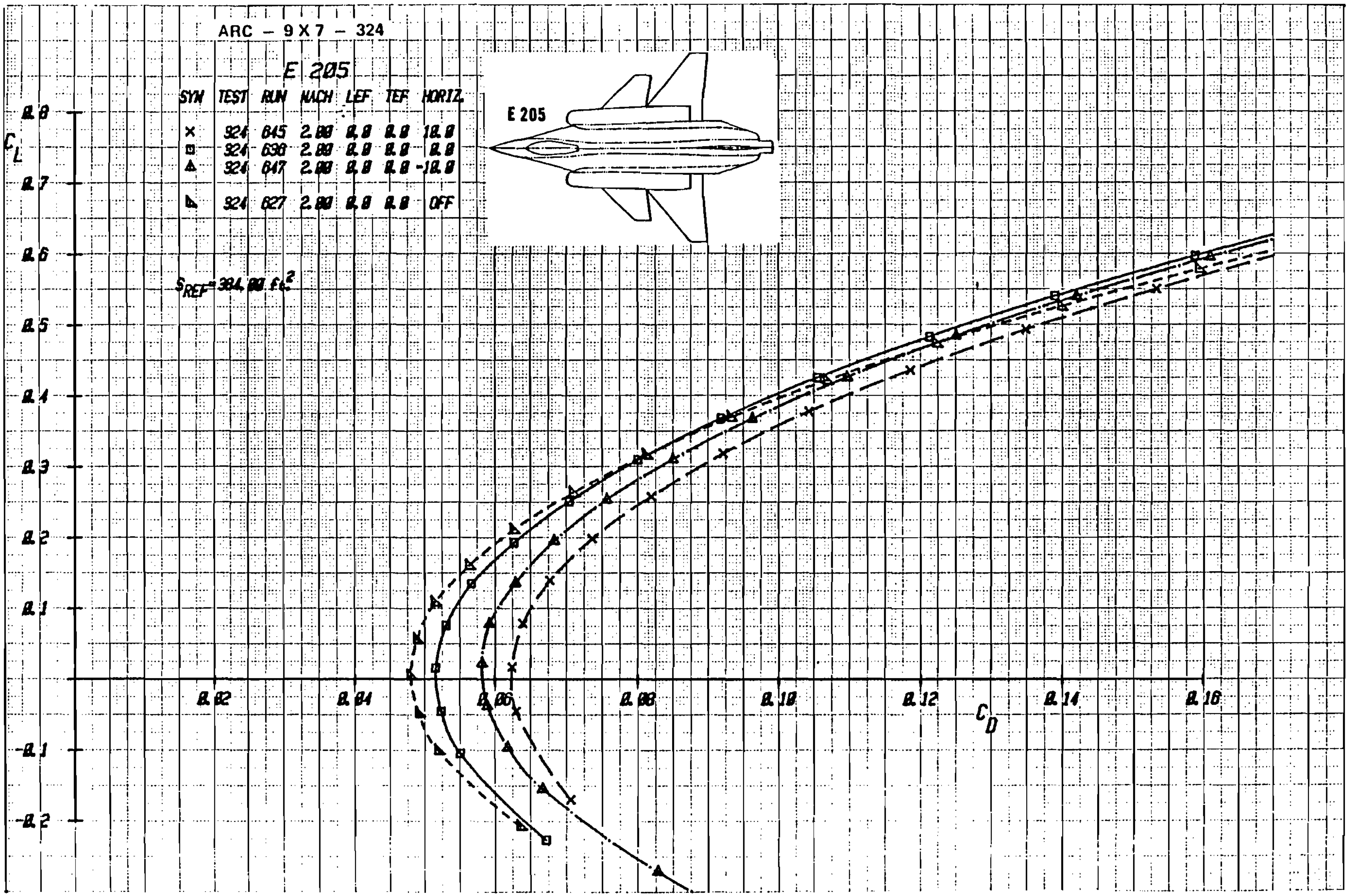

Figure2-17bEffect of Canard Deflection on Drag With Wing Trailing-Edge Flap Undeflected, (Expanded Drag Scale), Mach = 2.0

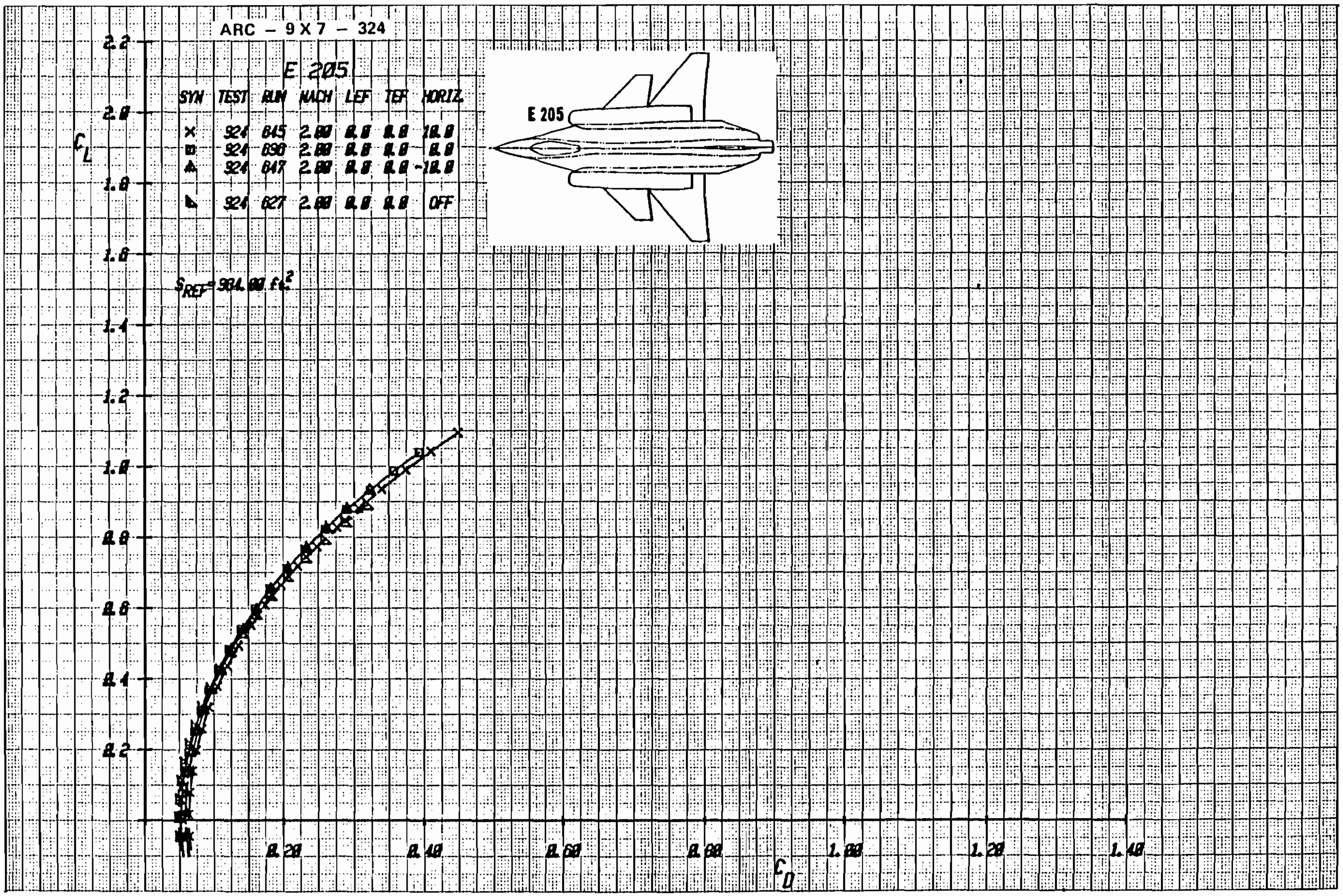

Figure2-17cEffect of Canard Deflection on Drag With Wing Trailing-Edge Flap Undeflected, Mach = 2.0

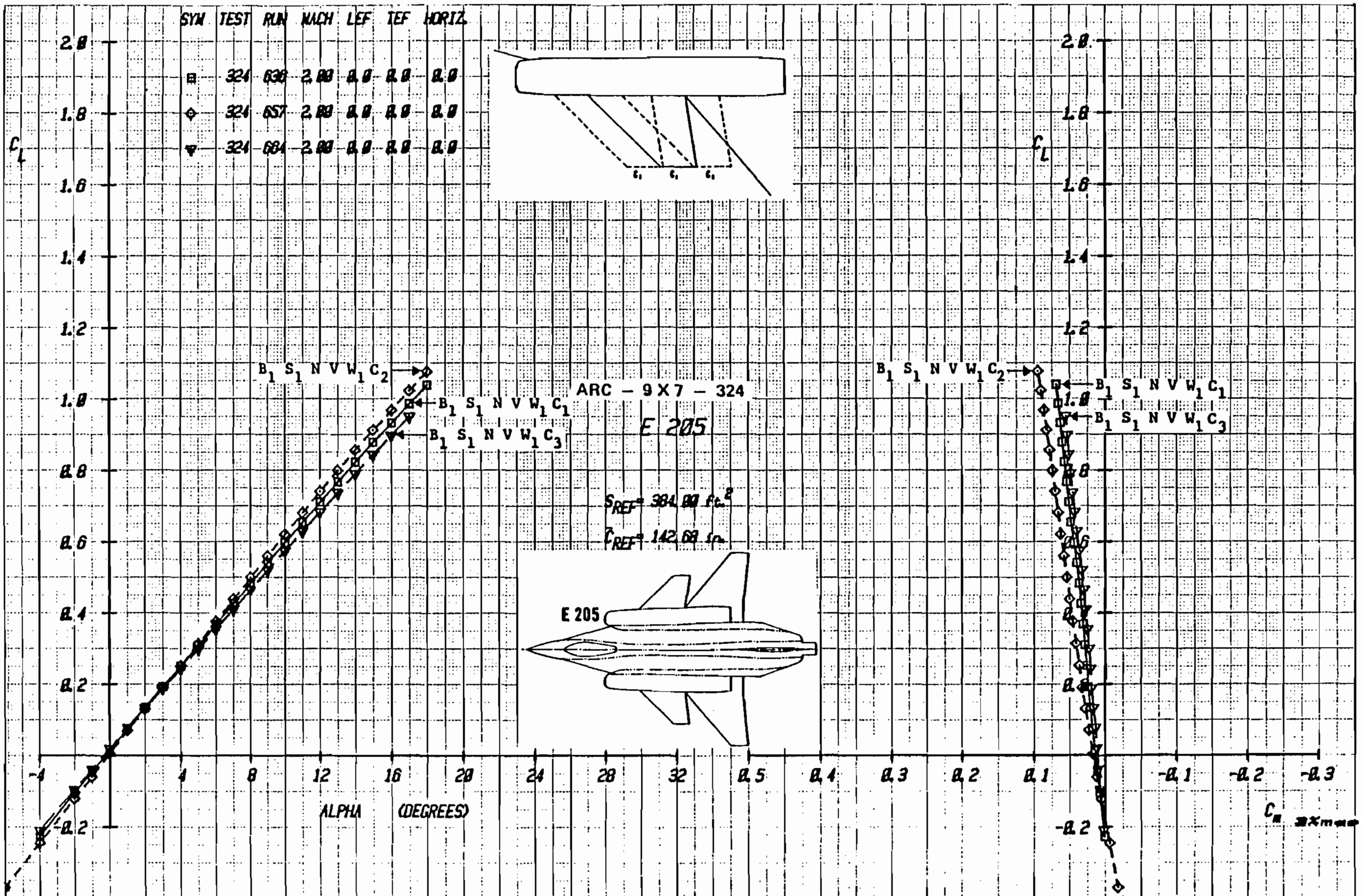

Figure2-18aEffect of Canard Longitudinal Location on Lift and Moment With Baseline Strake, Mach = 2.0

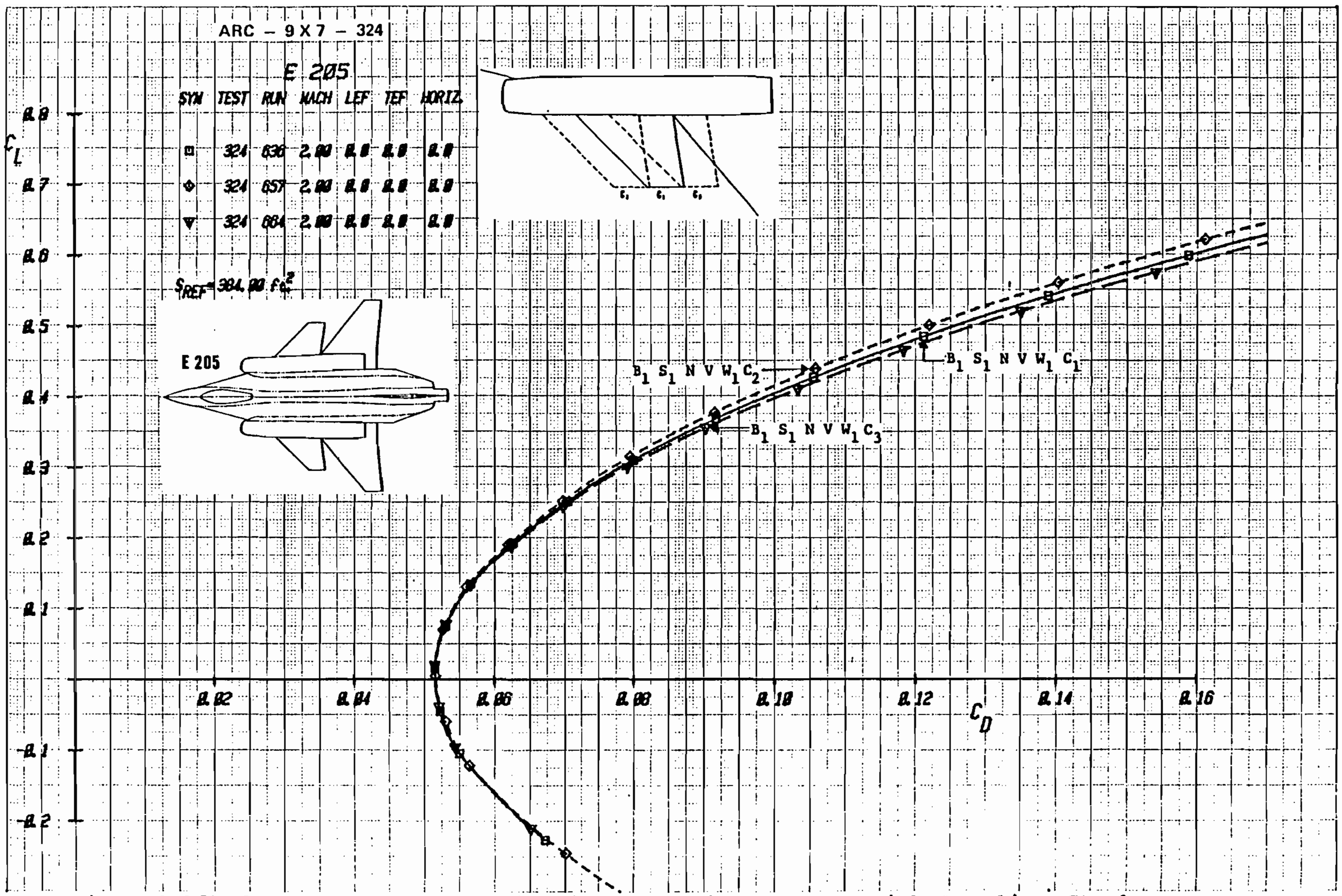

Figure2-18bEffect of Canard Longitudinal Location on Drag With Baseline Strake, (Expanded Drag Scale), Mach = 2.0

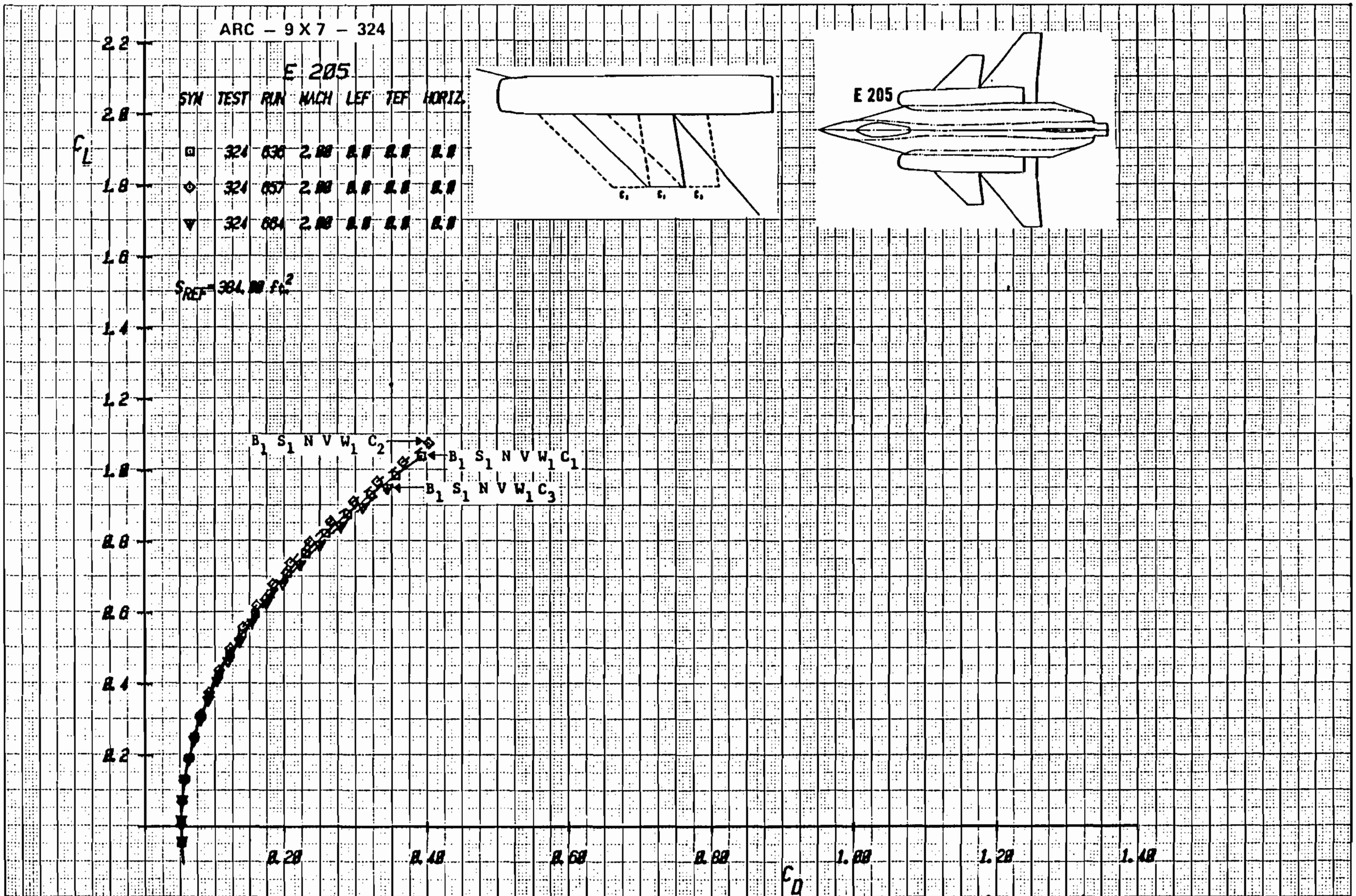

Figure2-18cEffect of Canard Longitudinal Location on Drag With Baseline Strake, Mach = 2.0

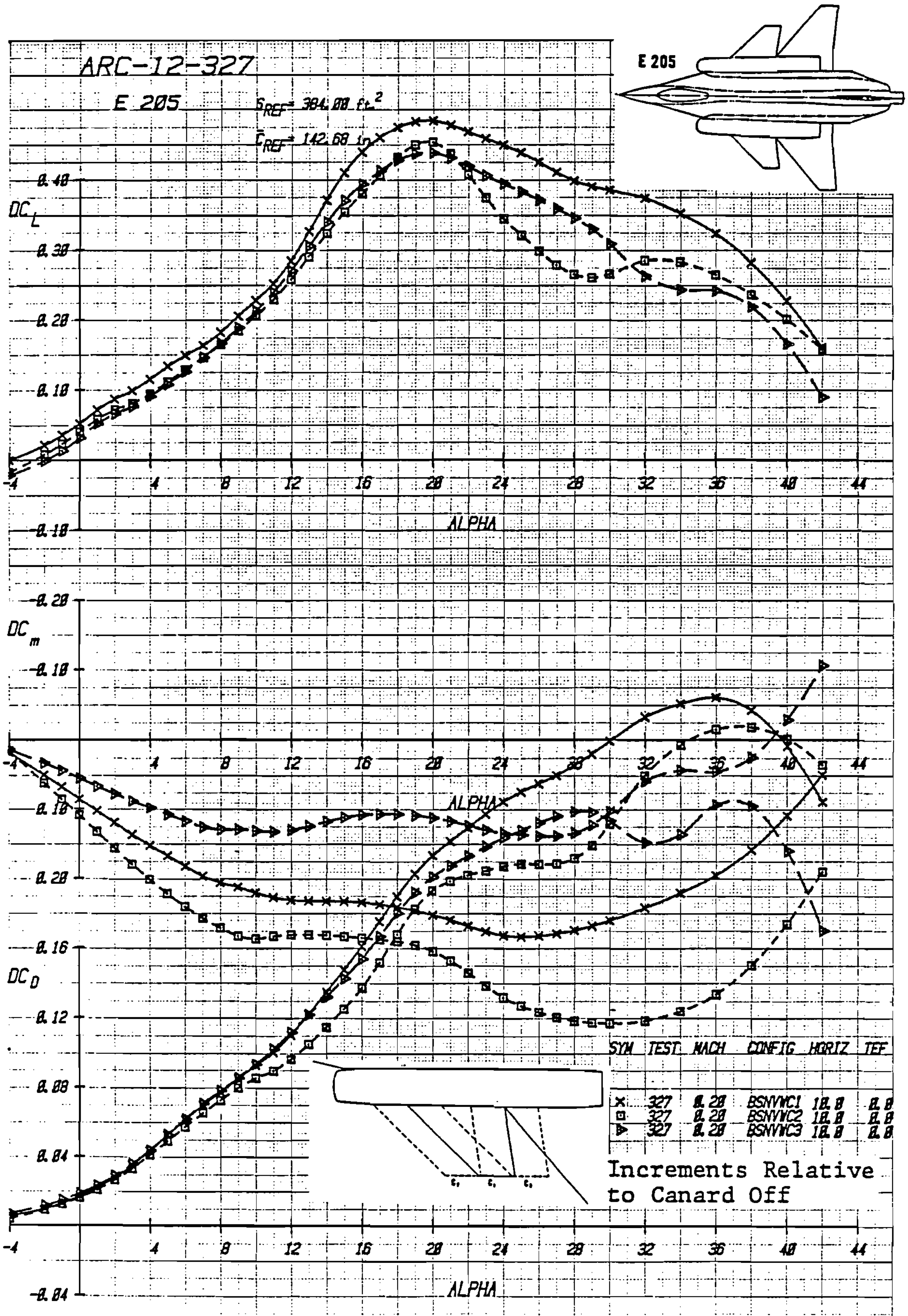

Figure 2-19 Incremental Effects of Canard Longitudinal Location on Canard Effectiveness at δi = +10°, Mach = .2

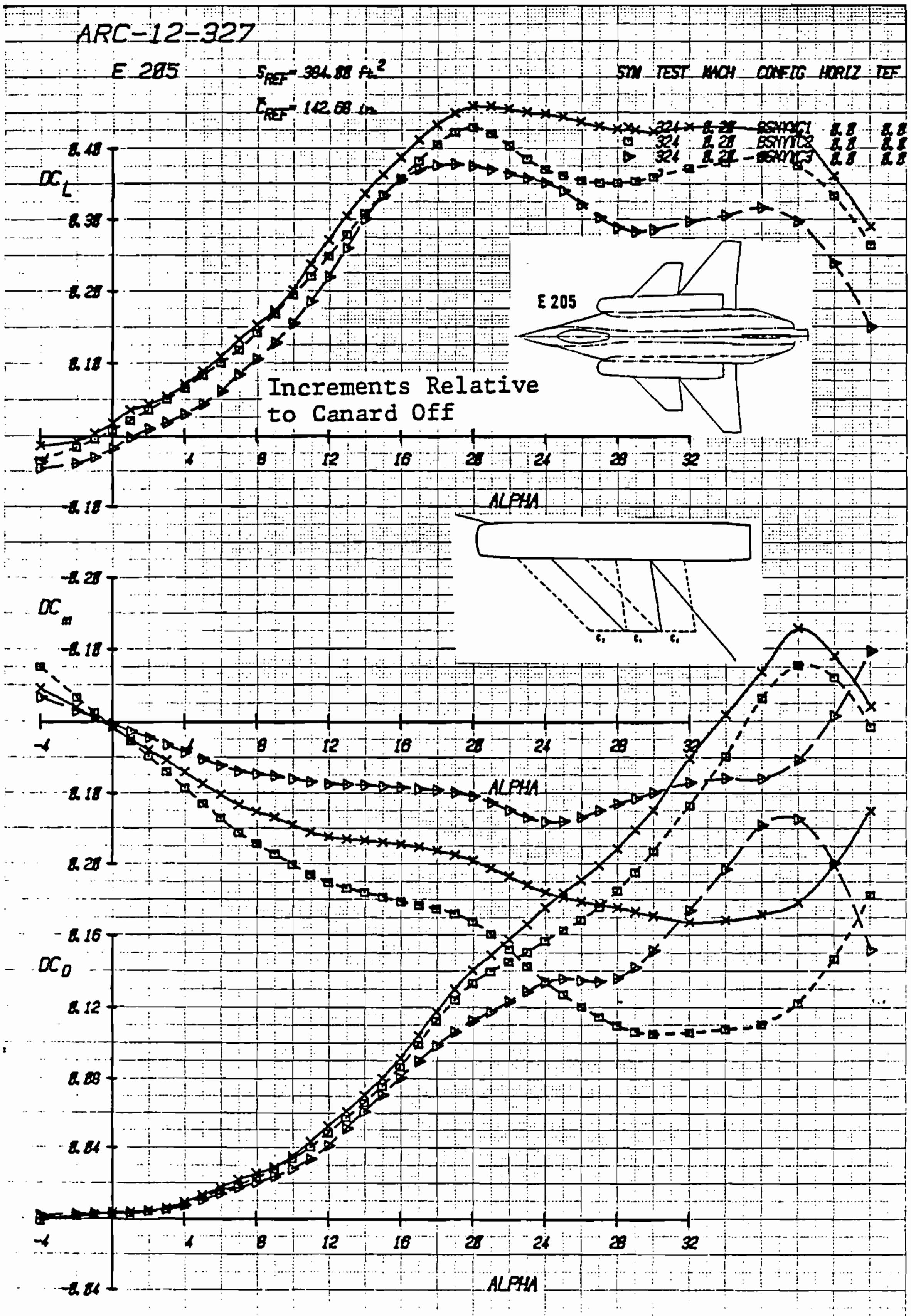

Figure 2-20 Incremental Effects of Canard Longitudinal Location on Canard Effectiveness at δi = 0°, Mach = .2

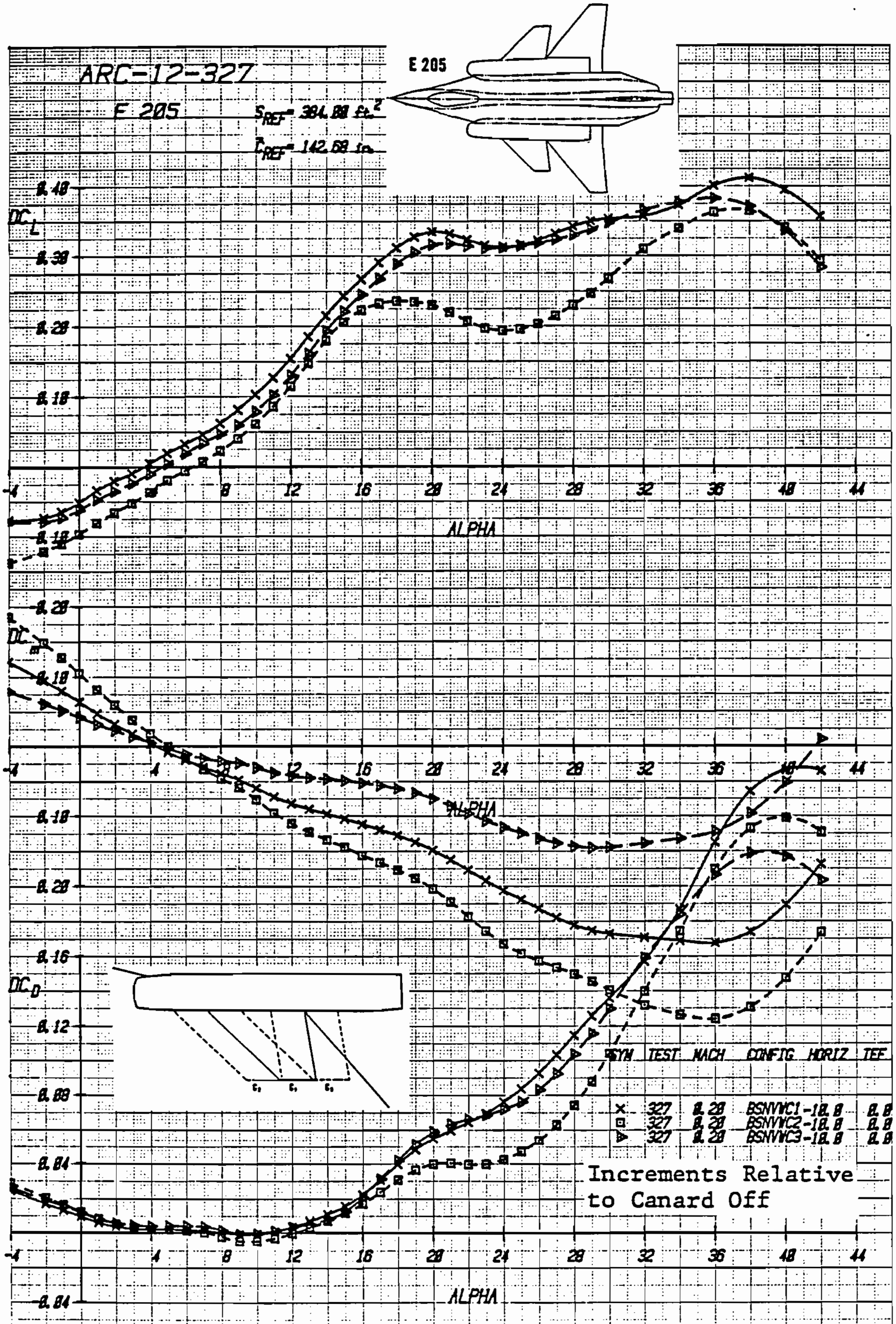

Figure 2-21 Incremental Effects of Canard Longitudinal Location on Canard Effectiveness at $\delta i = -10°$, Mach = .2

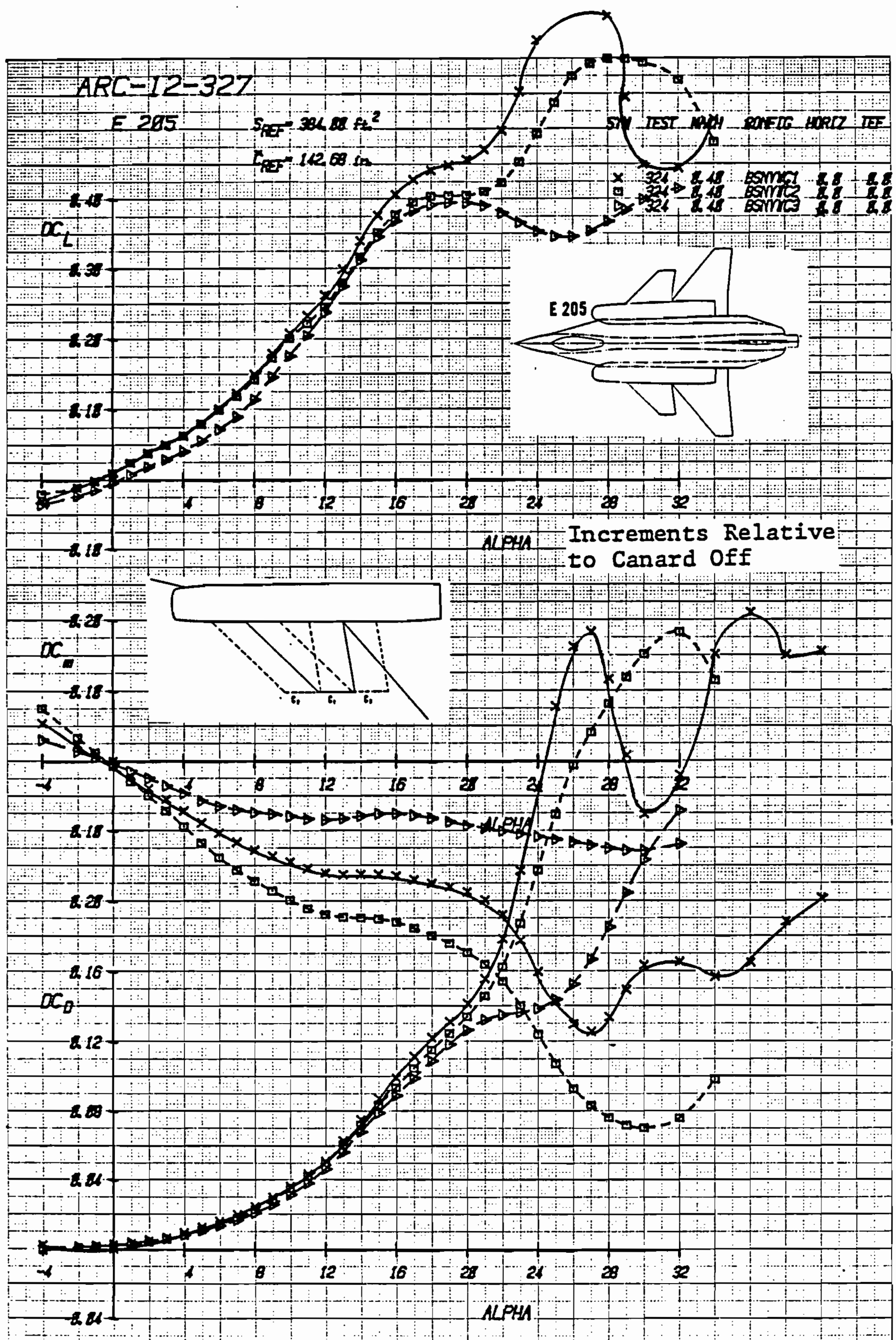

Figure 2-22 Incremental Effects of Canard Longitudinal Location on Canard Effectiveness at δi = 0°, Mach = .4

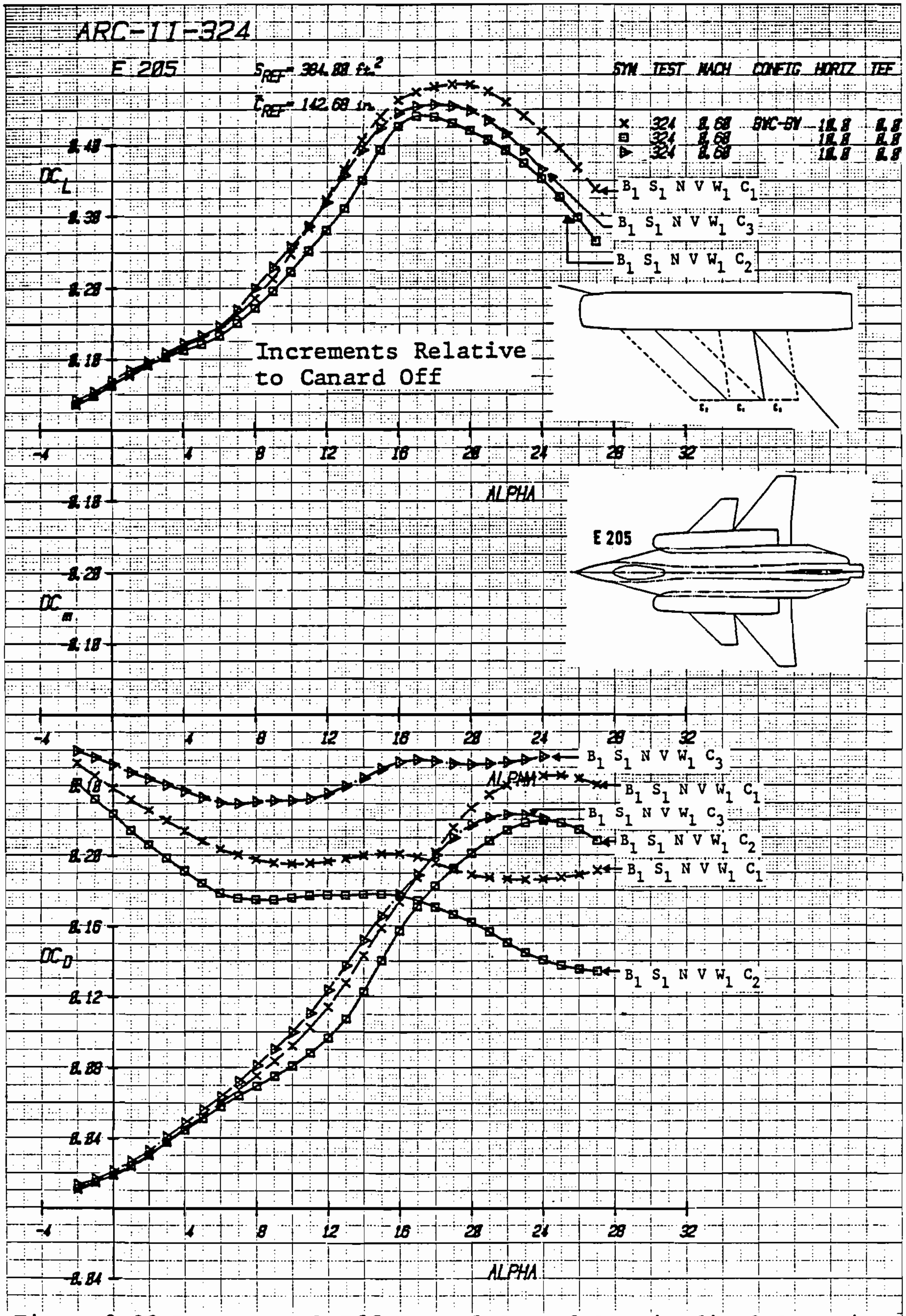

Figure 2-23 Incremental Effects of Canard Longitudinal Location on Canard Effectiveness at δ_i = 10°. Mach = .6

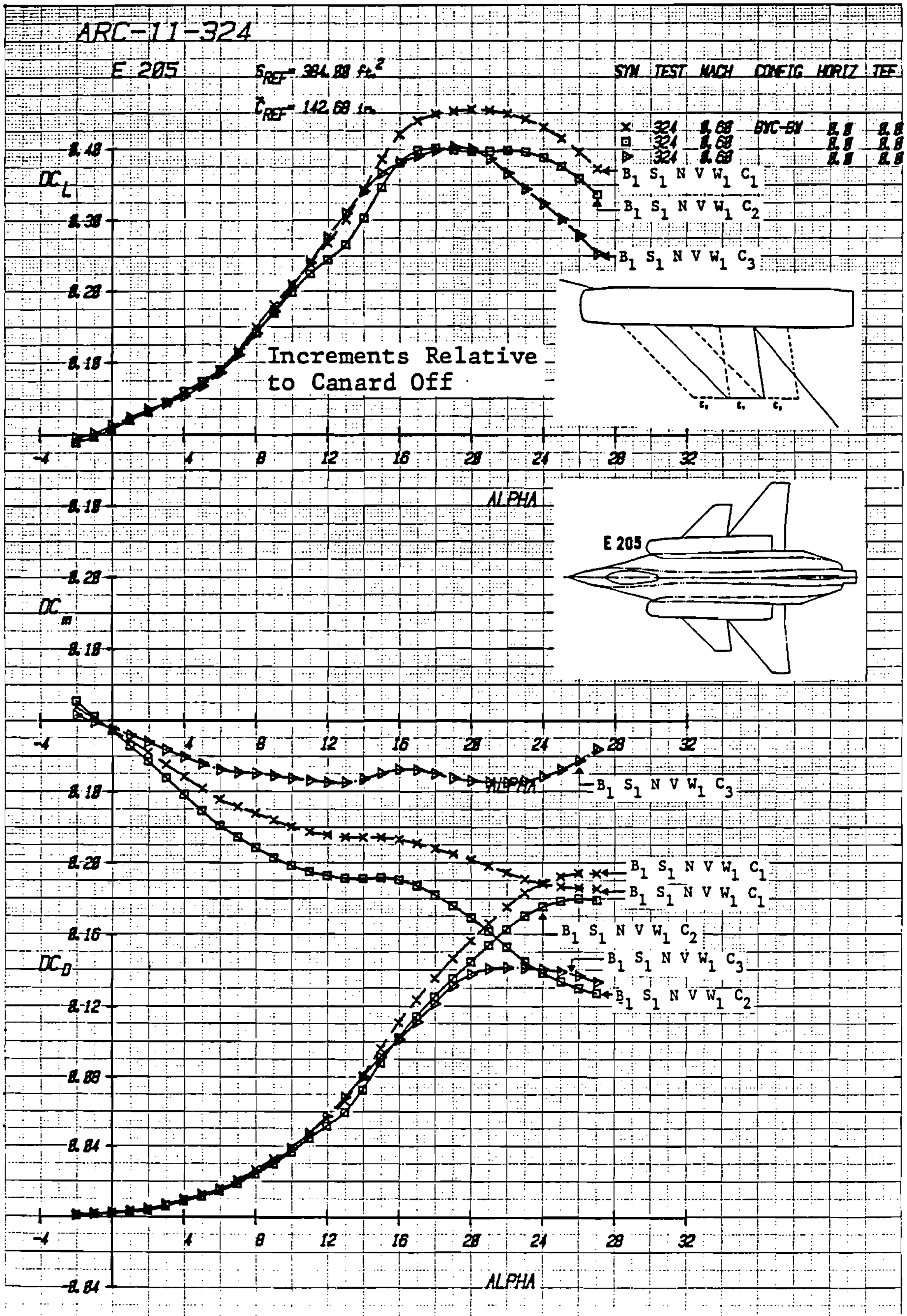

Figure 2-24 Incremental Effects of Canard Longitudinal Location on Canard Effectiveness at $\delta_i = 0°$, Mach = .6

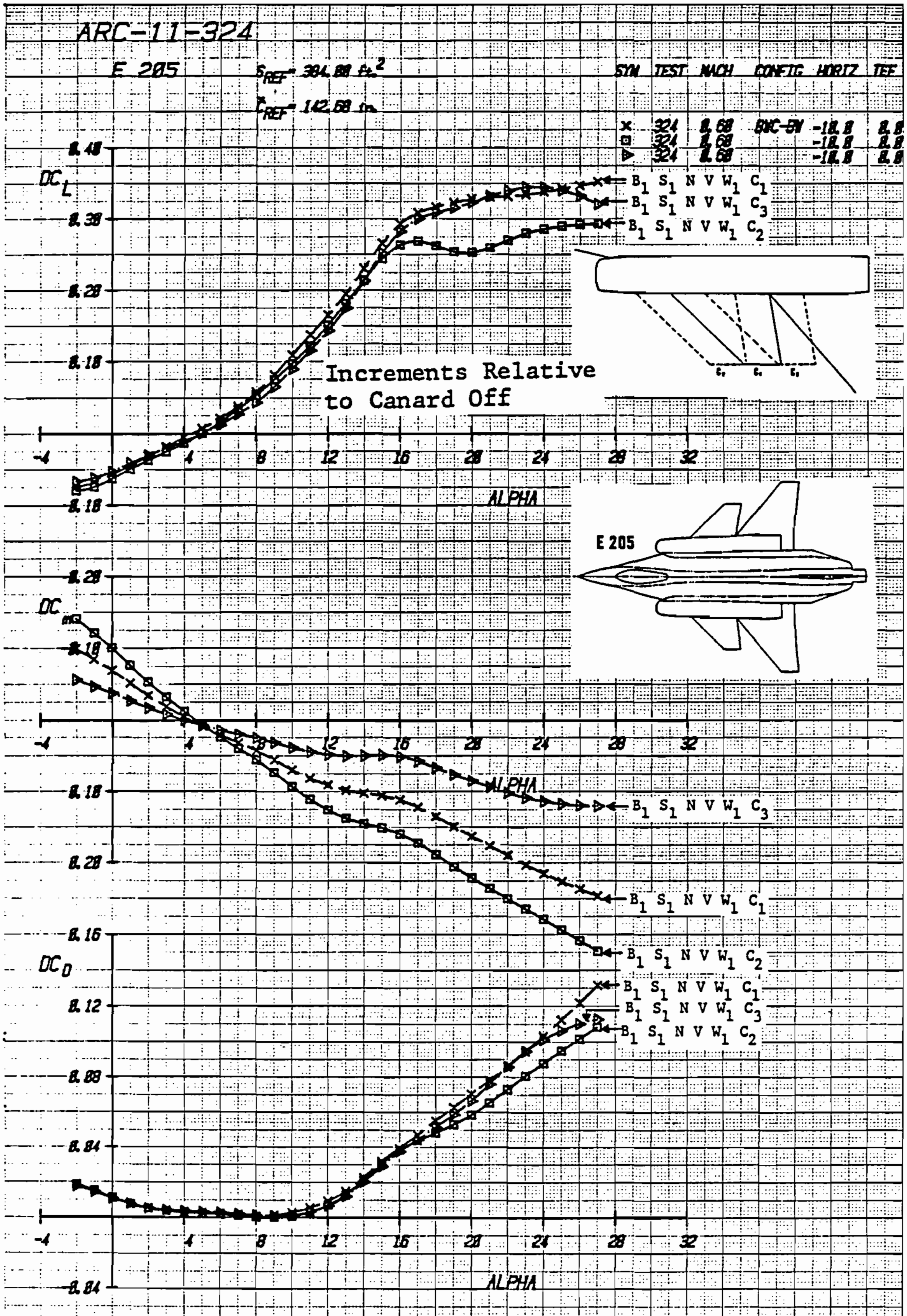

Figure 2-25 Incremental Effects of Canard Longitudinal Location on Canard Effectiveness at δ_i = -10°, Mach = .6

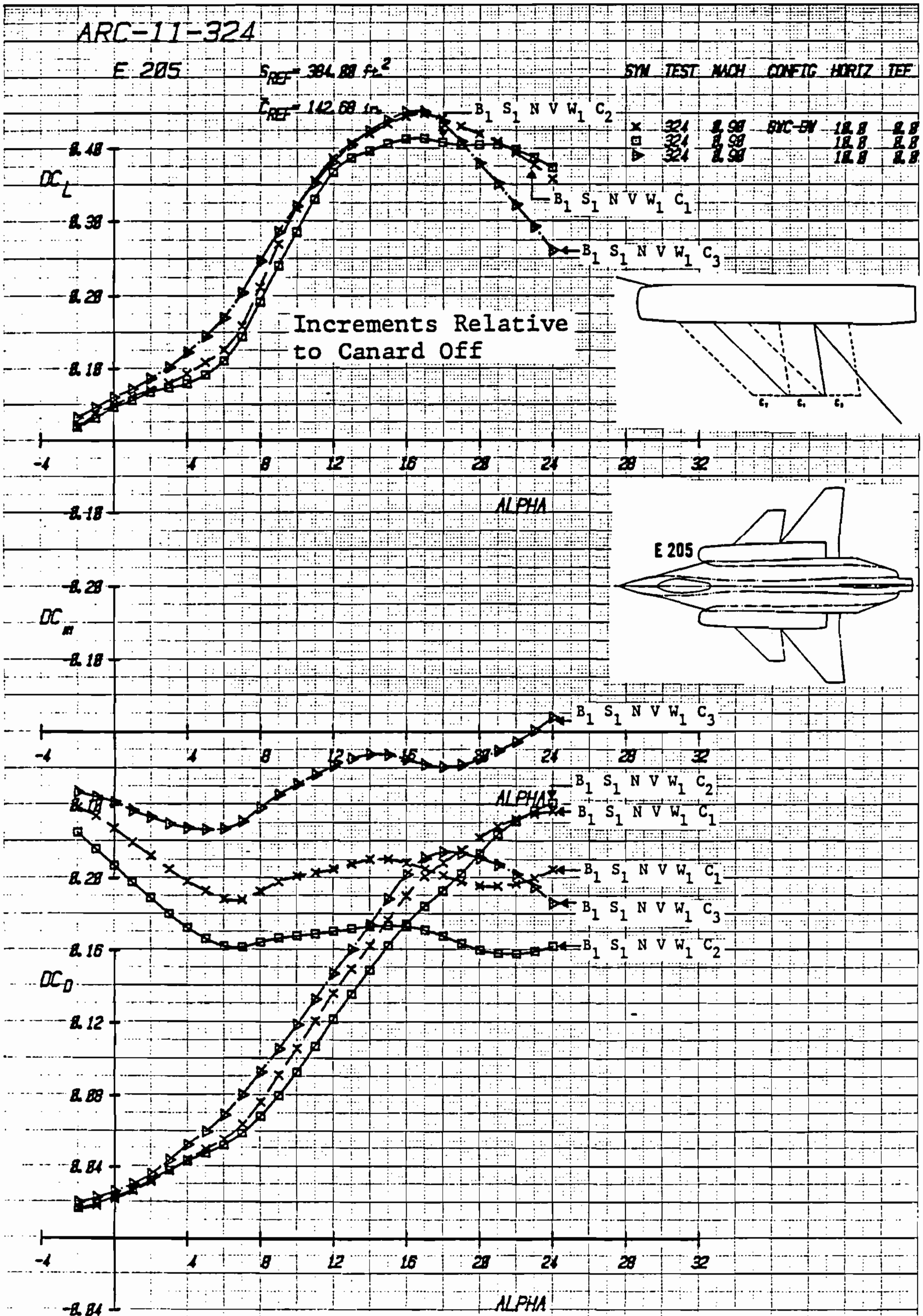

Figure 2-26 Incremental Effects of Canard Longitudinal Location on Canard Effectiveness at δ_i = 10°, Mach = .9

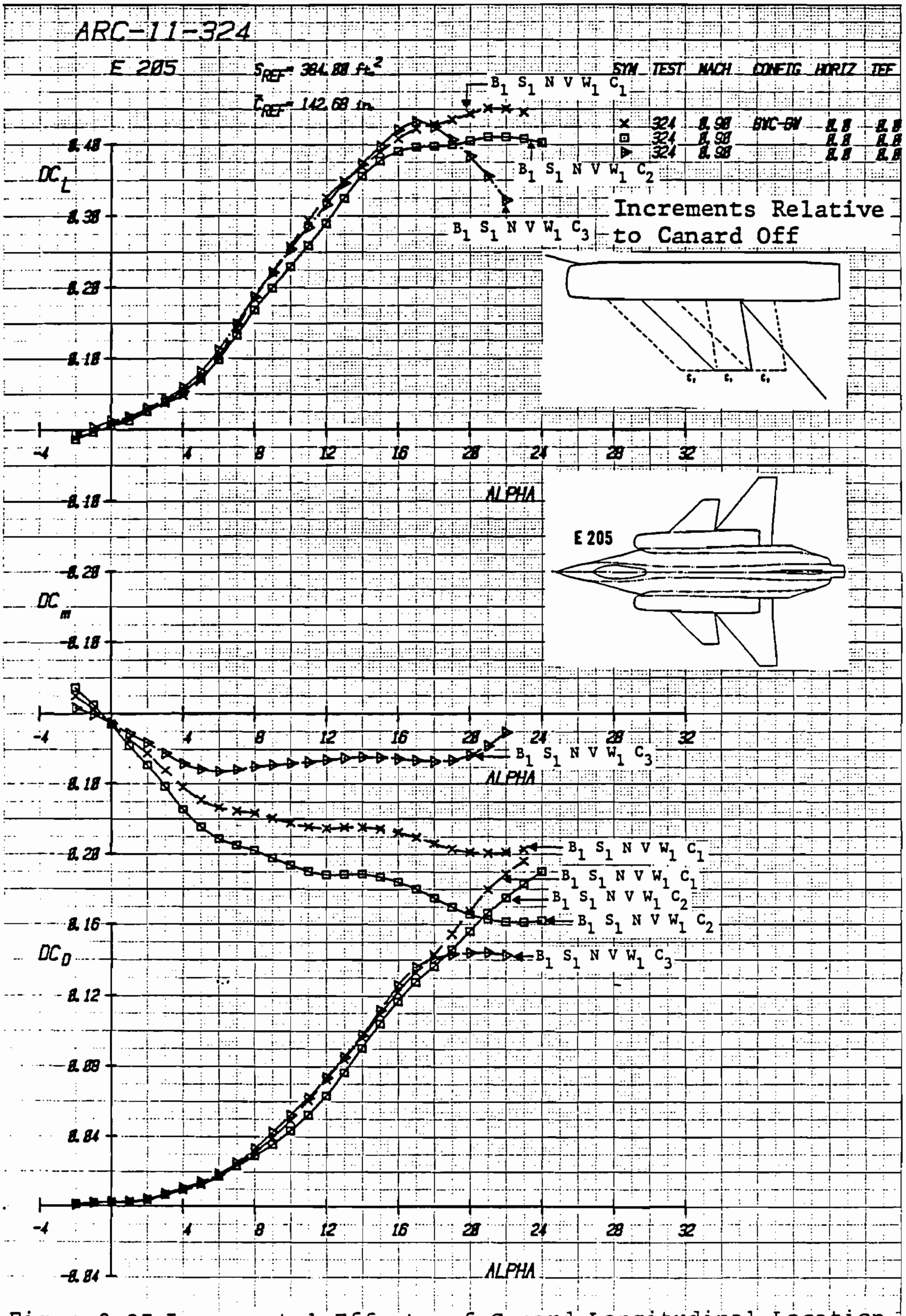

Figure 2-27 Incremental Effects of Canard Longitudinal Location on Canard Effectiveness at δ_i = 0°, Mach = .9

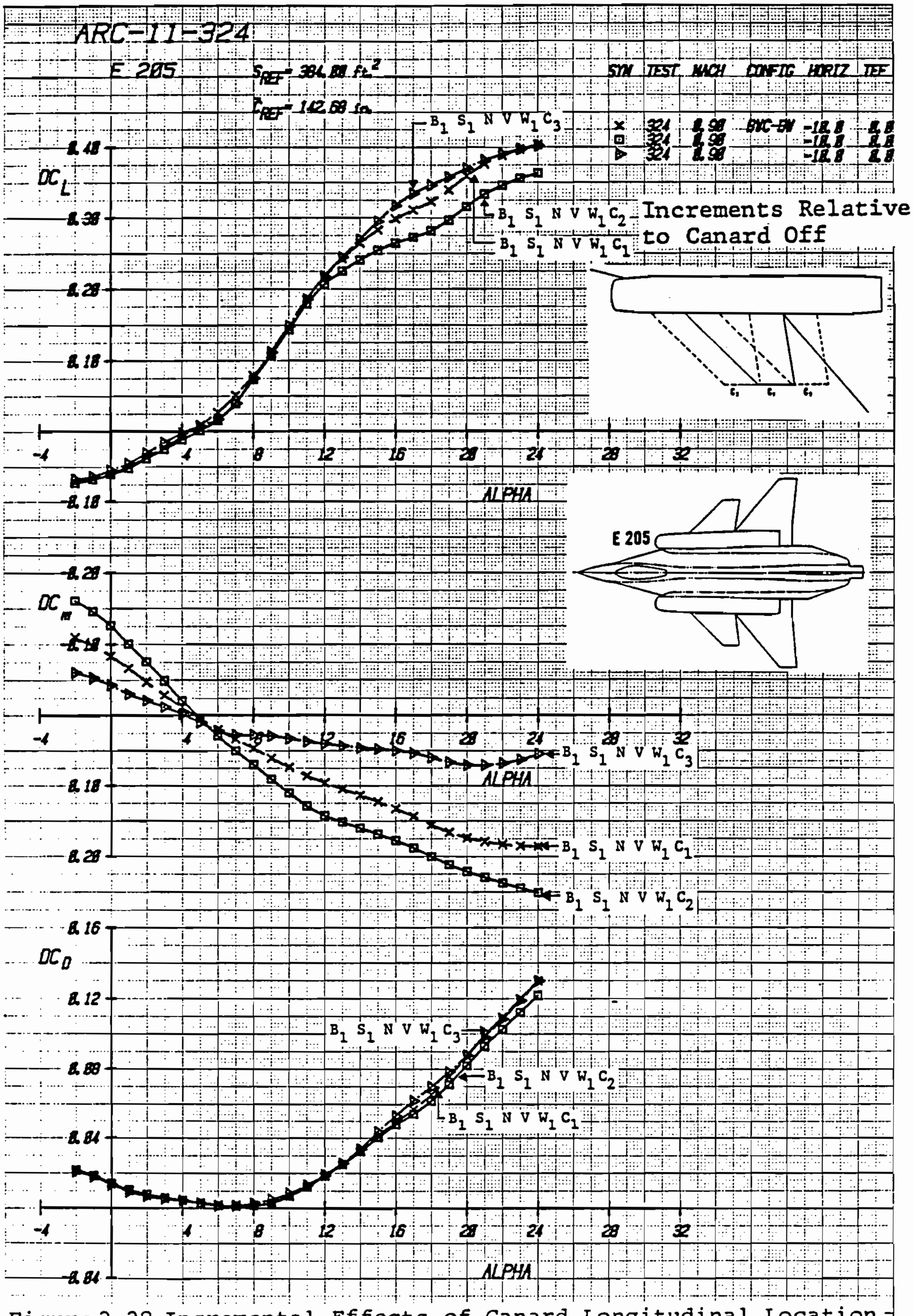

Figure 2-28 Incremental Effects of Canard Longitudinal Location on Canard Effectiveness at δ_i = -10°, Mach = .9

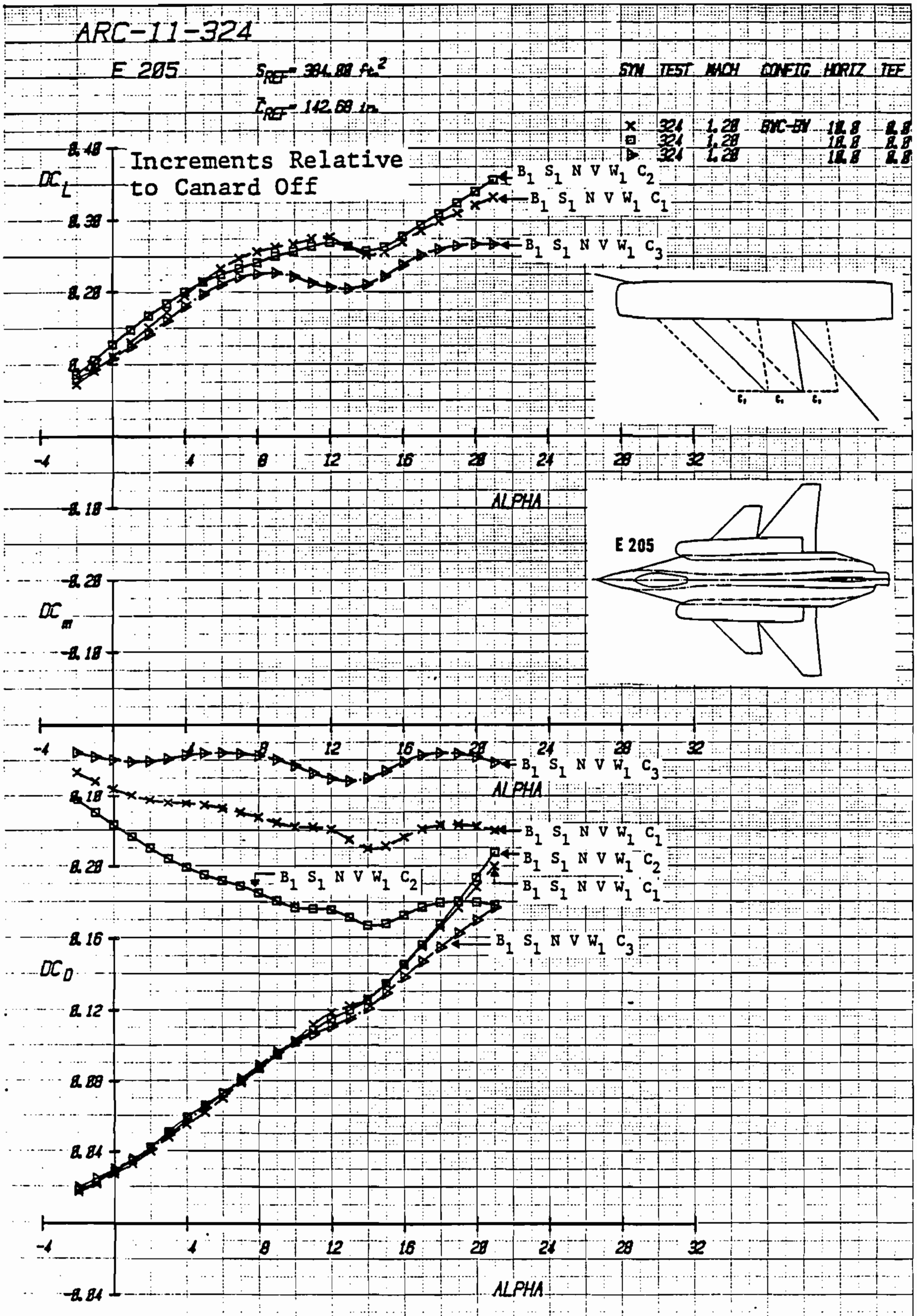

Figure 2-29 Incremental Effect of Canard Longitudinal Location on Canard Effectiveness at δ_i =10°, Mach = 1.2

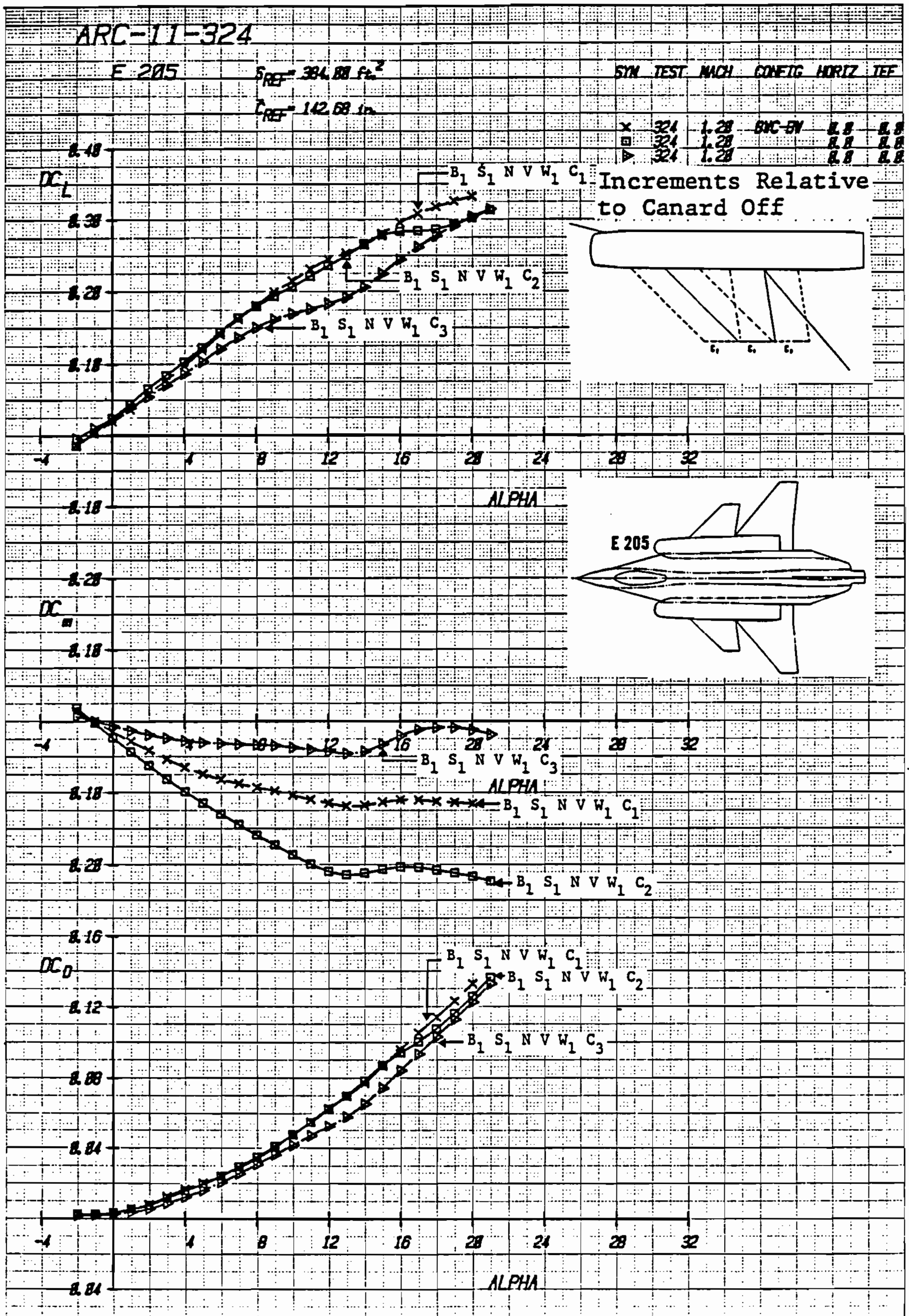

Figure 2-30 Incremental Effects of Canard Longitudinal Location on Canard Effectiveness at $\delta_i = 0°$, Mach = 1.2

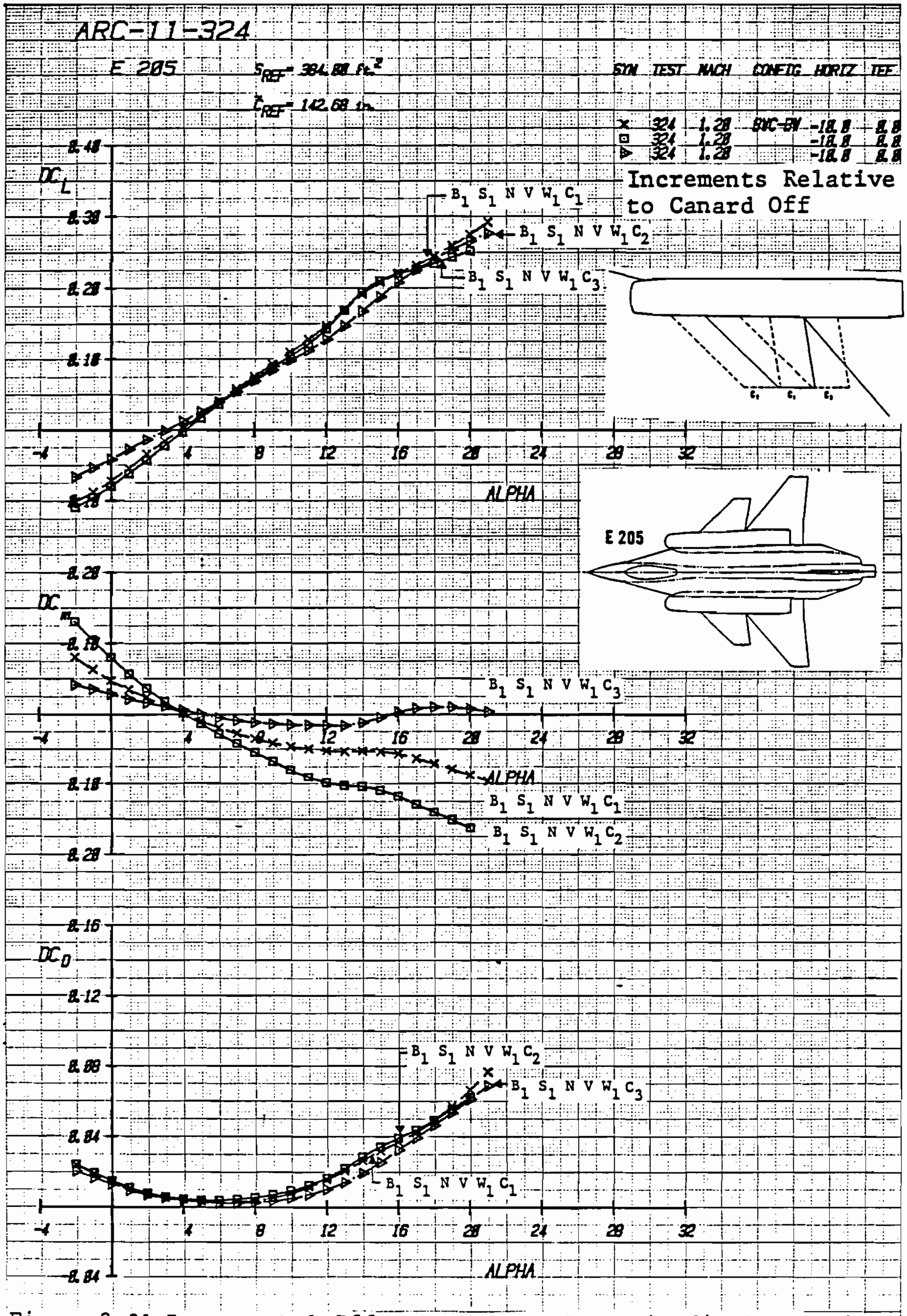

Figure 2-31 Incremental Effects of Canard Longitudinal Location on Canard Effectiveness at δ_i = -10°, Mach = 1.2

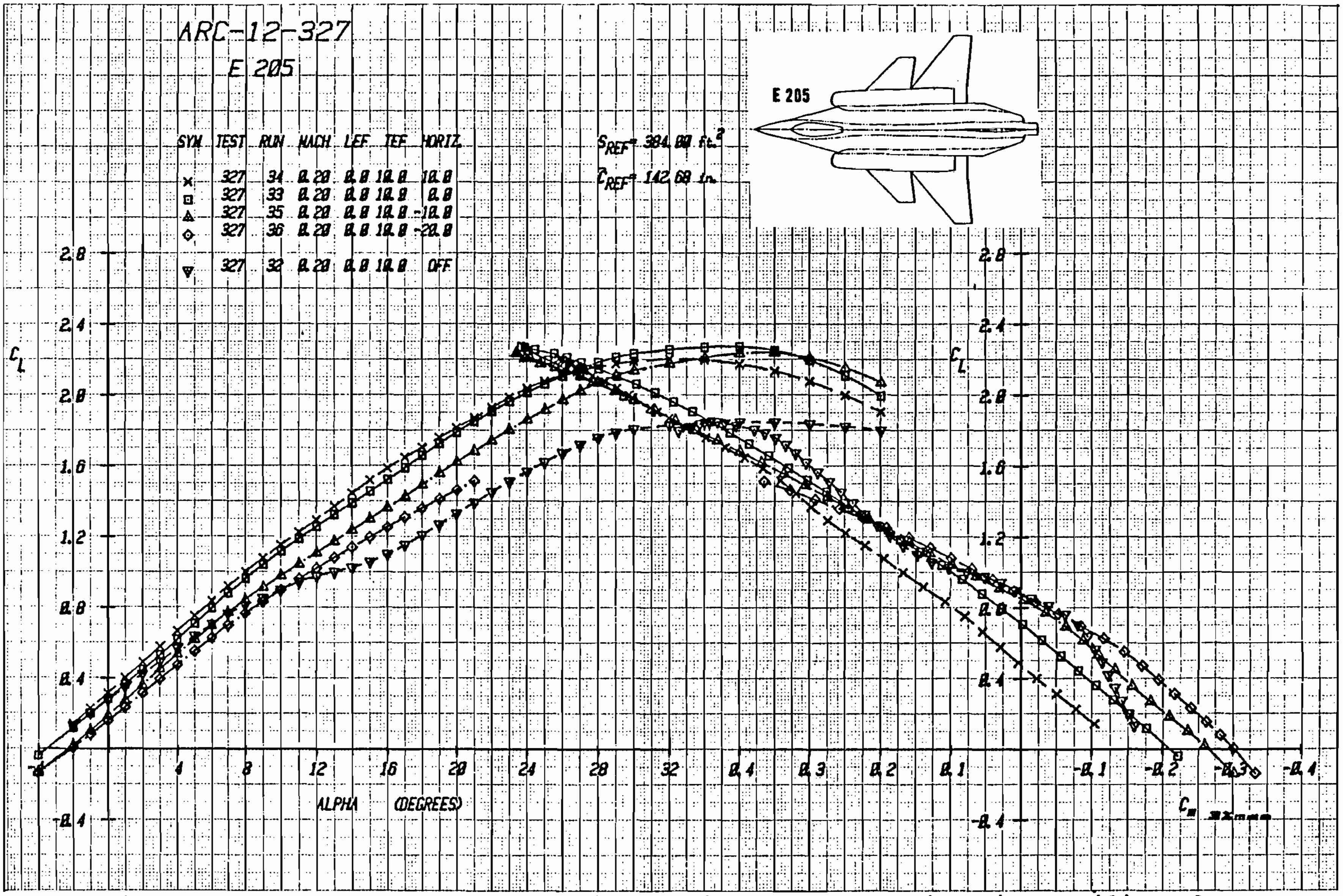

Figure2-32aEffect of Canard Deflection on Lift and Moment with Wing Trailing-Edge
Flap Deflected +10°, Mach = .2

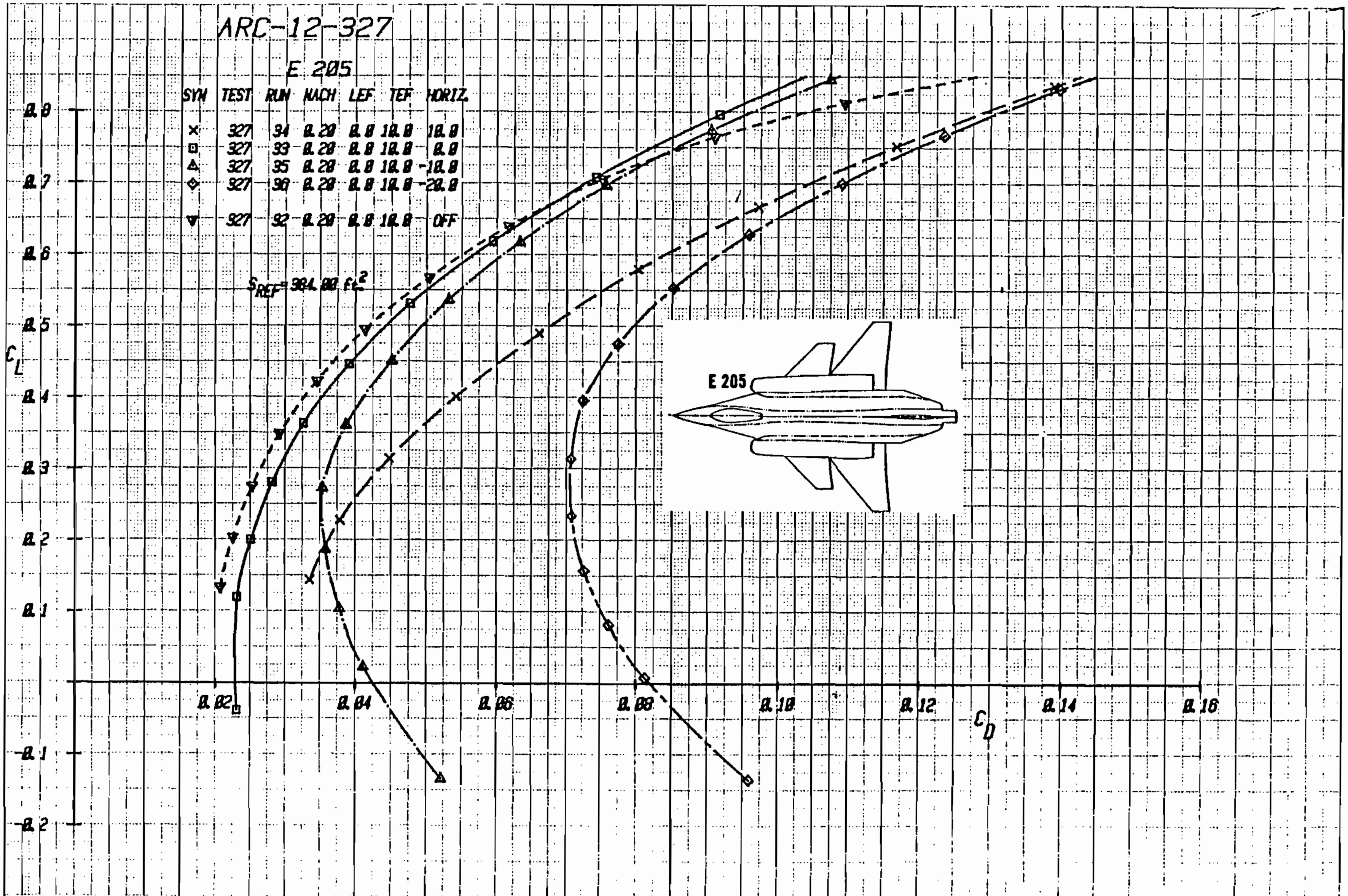

Figure2-32bEffect of Canard Deflection on Drag with Wing Trailing-Edge Flap Deflected +10°, (Expanded Drag Scale), Mach = .2

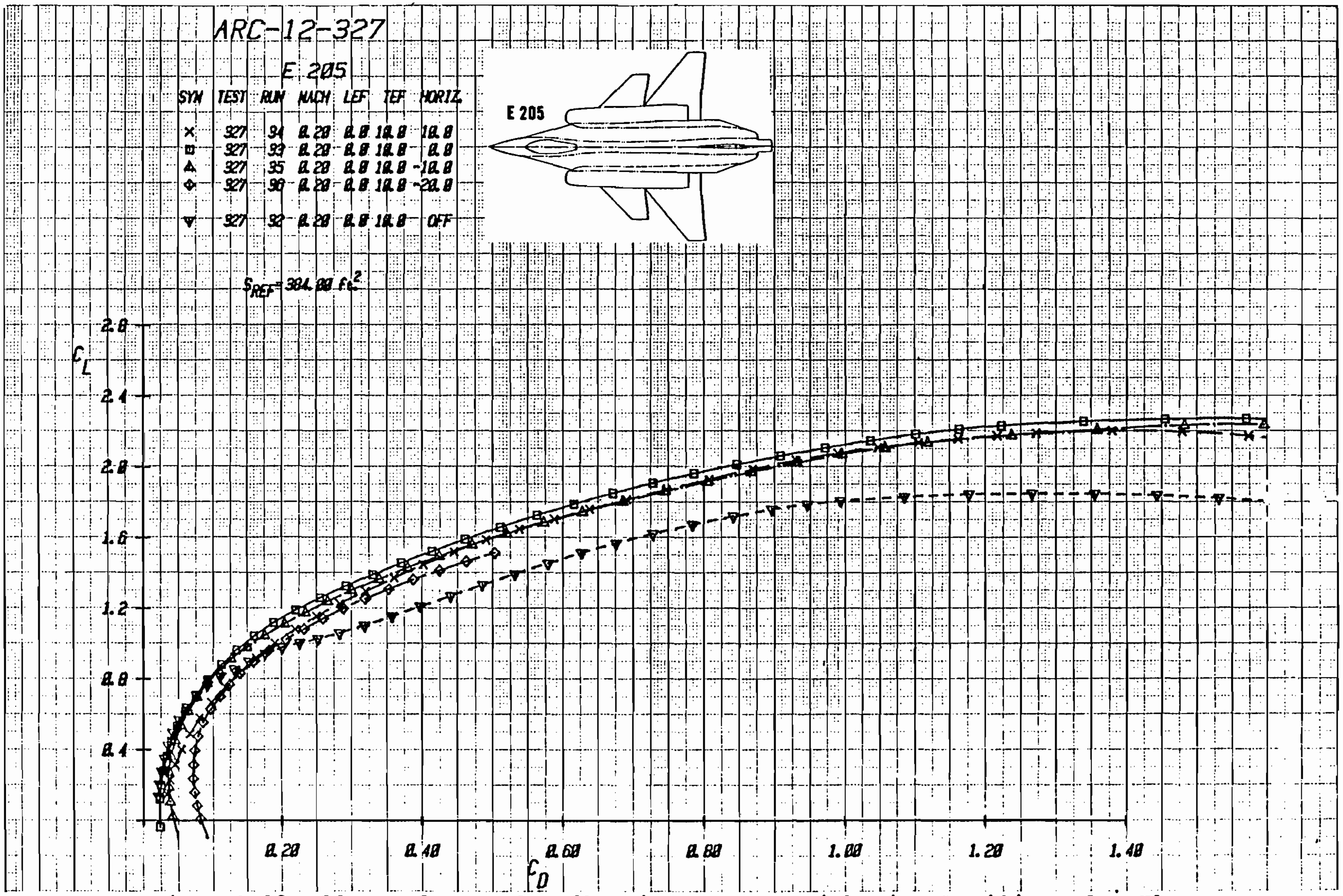

Figure2-32cEffect of Canard Deflection on Drag with Wing Trailing-Edge Flap Deflected +10°, Mach = .2

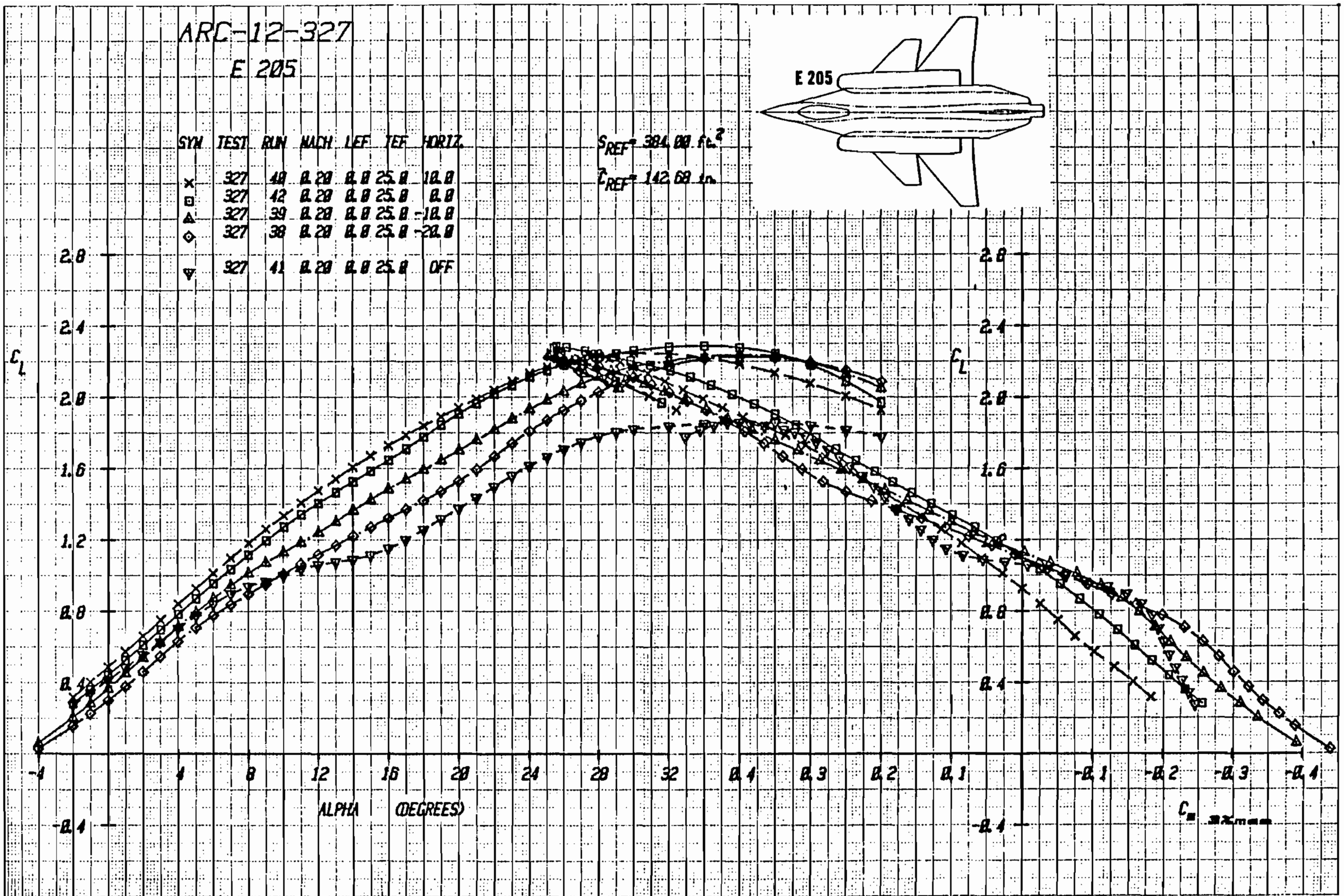

Figure2-33aEffect of Canard Deflection on Lift and Moment with Wing Trailing-Edge Flap Deflected +25°, Mach = .2

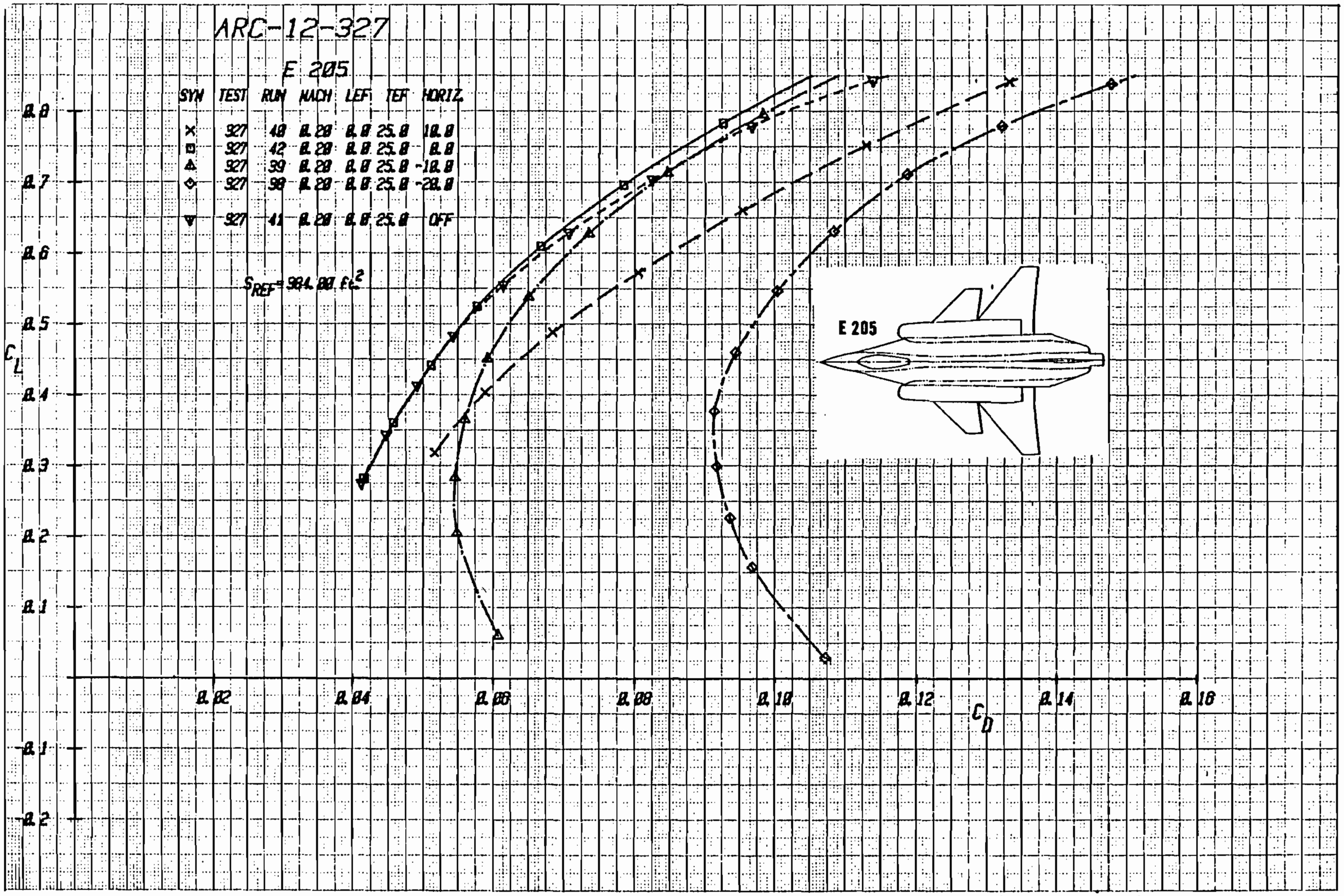

Figure2-33bEffect of Canard Deflection on Drag with Wing Trailing-Edge Flap Deflected +25°, (Expanded Drag Scale), Mach = .2

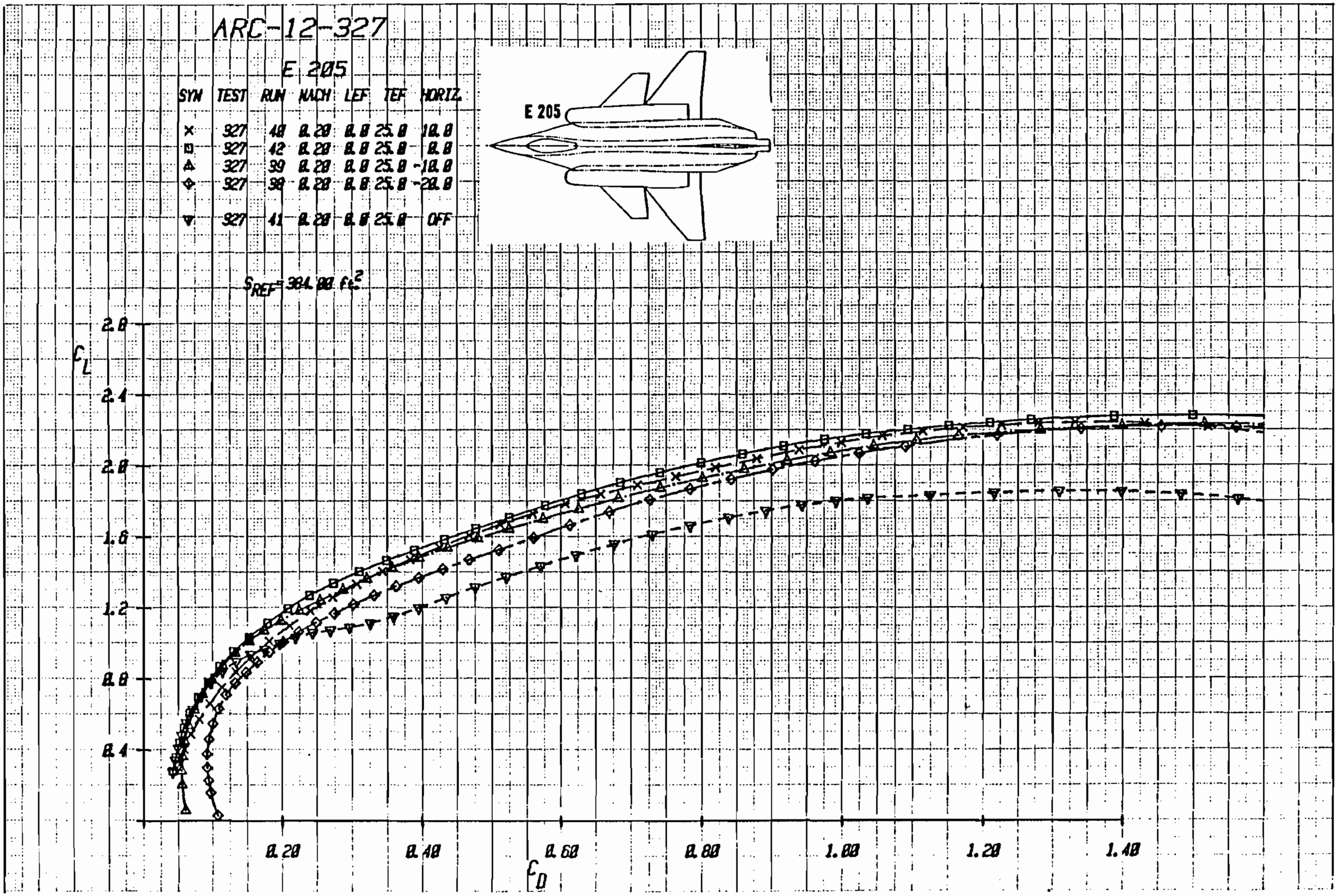

Figure2-33cEffect of Canard Deflection on Drag with Wing Trailing-Edge Flap Deflected +25°, Mach = .2

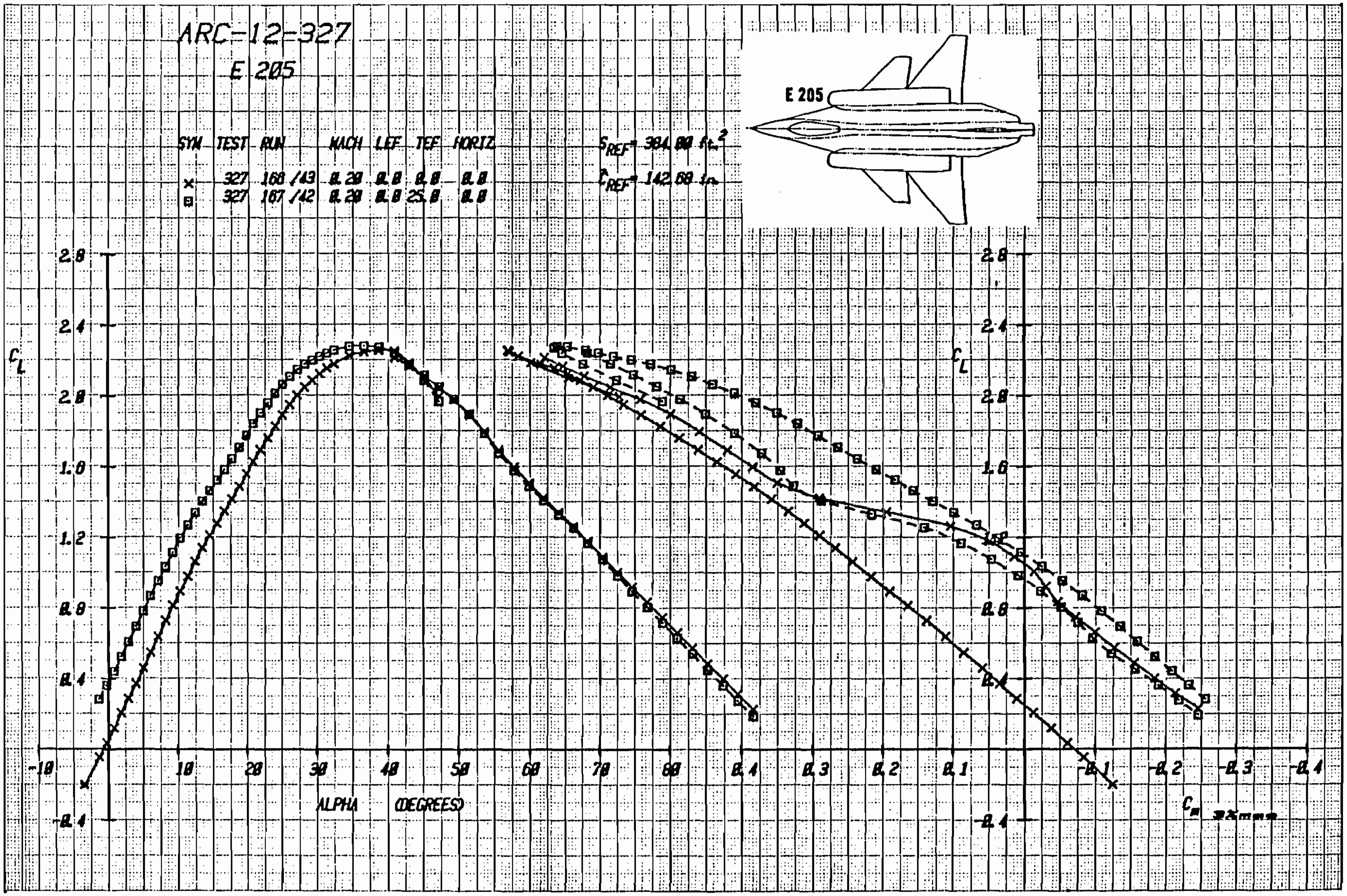

Figure2-34aEffect of Wing Trailing-Edge Flap Deflection on E205
Baseline Lift and Pitching Moment (α = 0° to 90°), M = .2 , δc = 0°

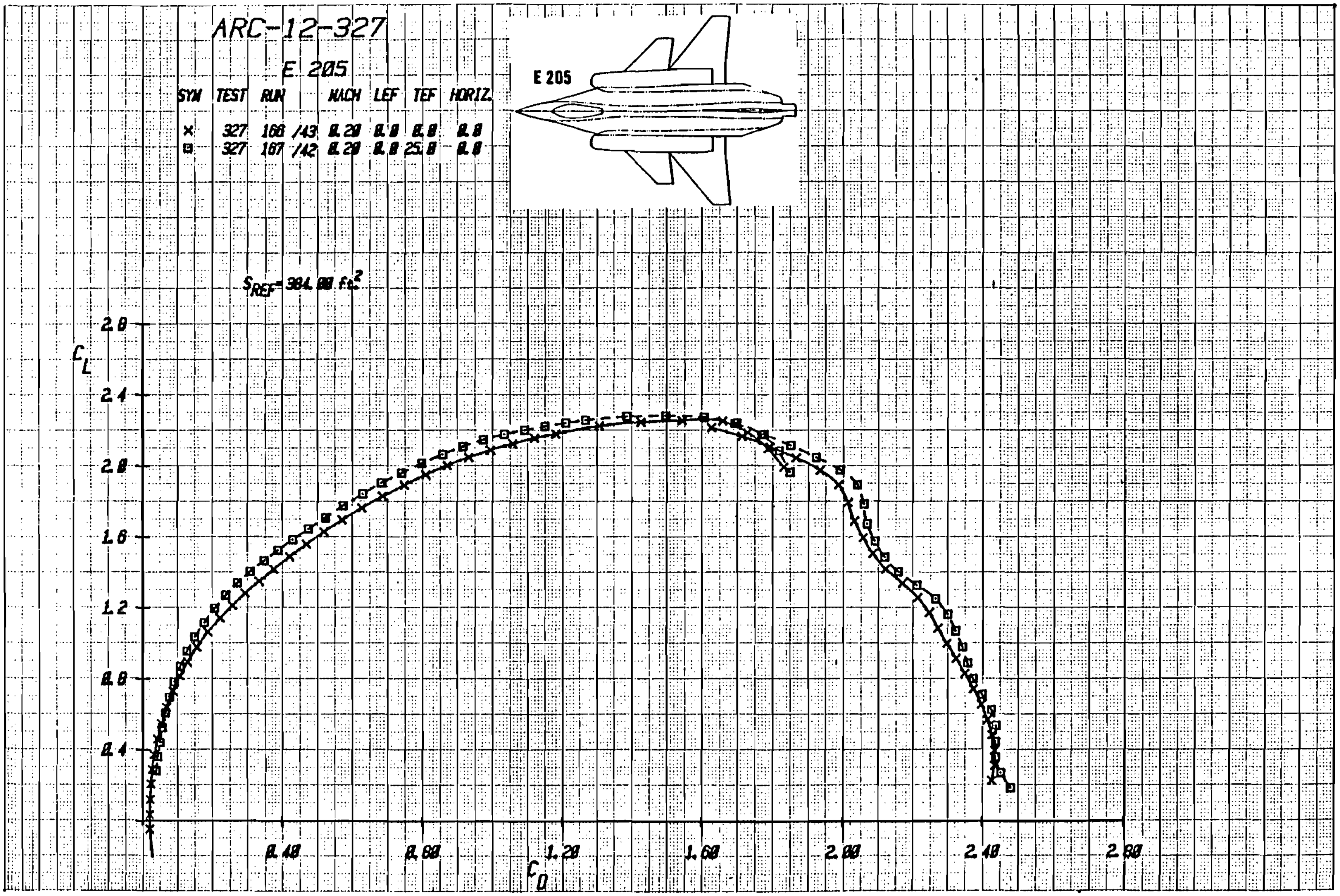

Figure2-34bEffect of Wing Trailing-Edge Flap Deflection on E205 Baseline Drag (α = 0° to 90°), M = .2, δc = 0°

125

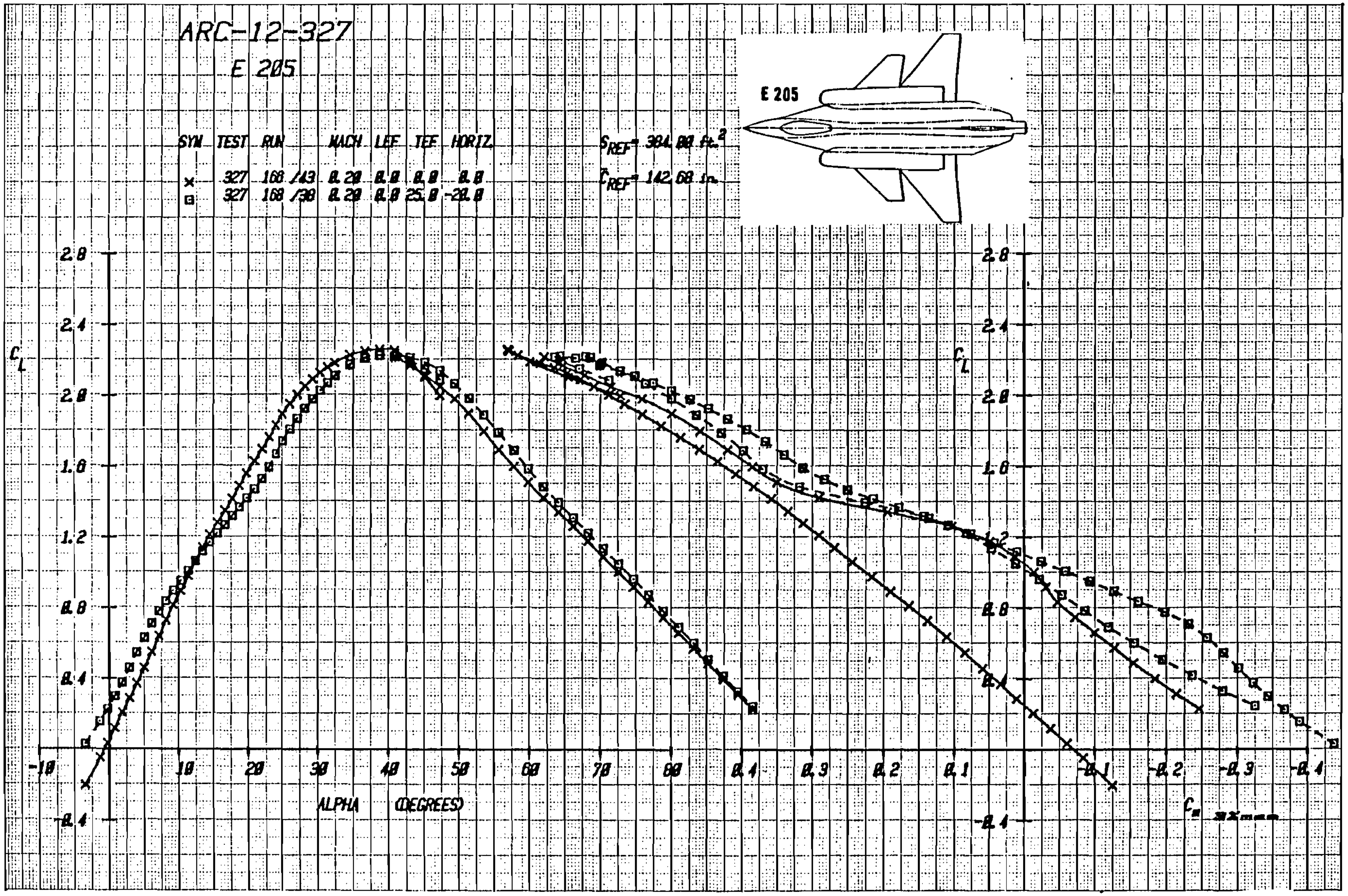

Figure2-35aEffect of Wing Trailing-Edge Flap Deflection on E205 Baseline Lift and Pitching Moment (α = 0° to 90°), M = .2, δc = 0°, -20°

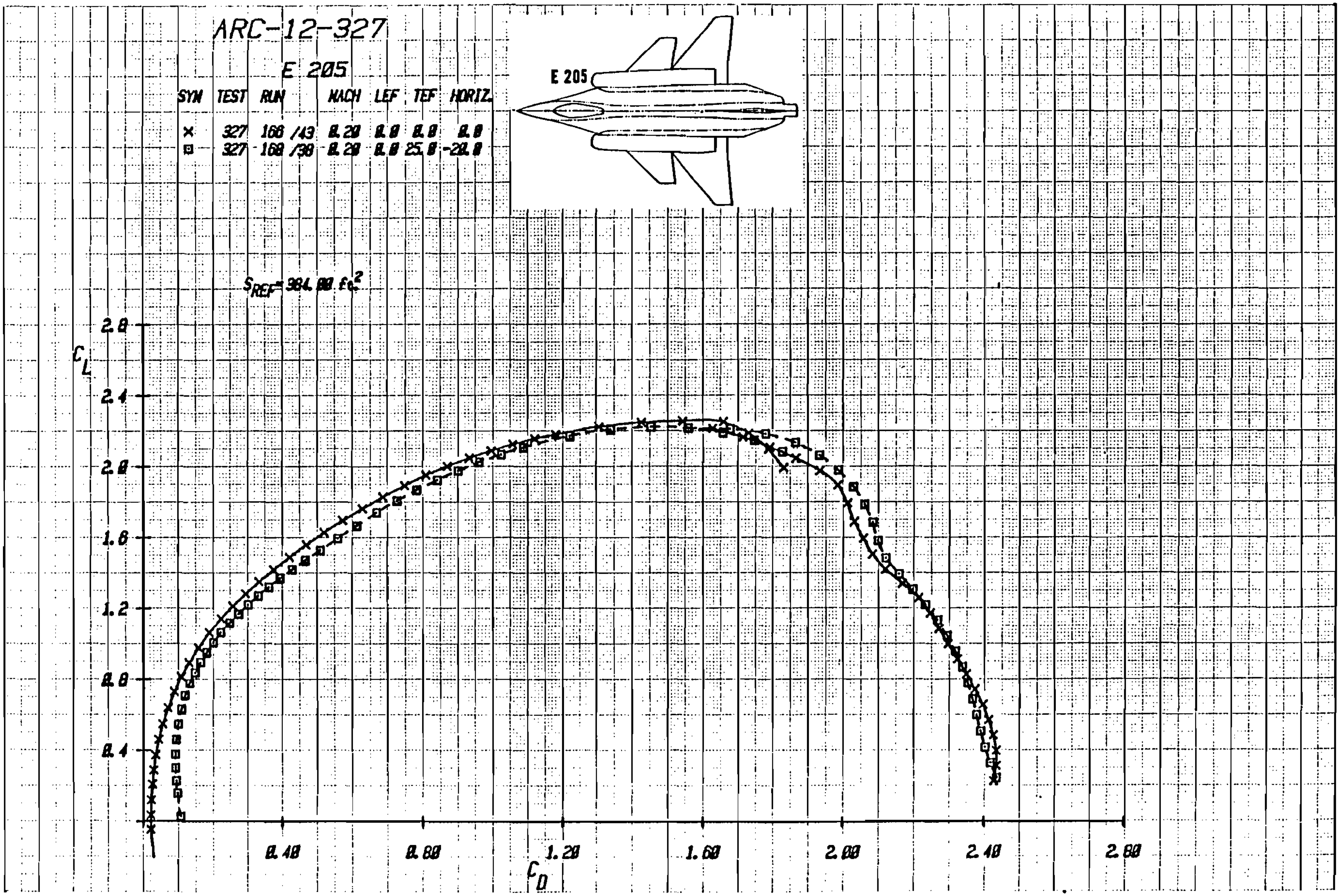

Figure2-35bEffect of Wing Trailing-Edge Flap Deflection on E205 Baseline Drag (α = 0° to 90°), M = .2, δc = 0°, -20°

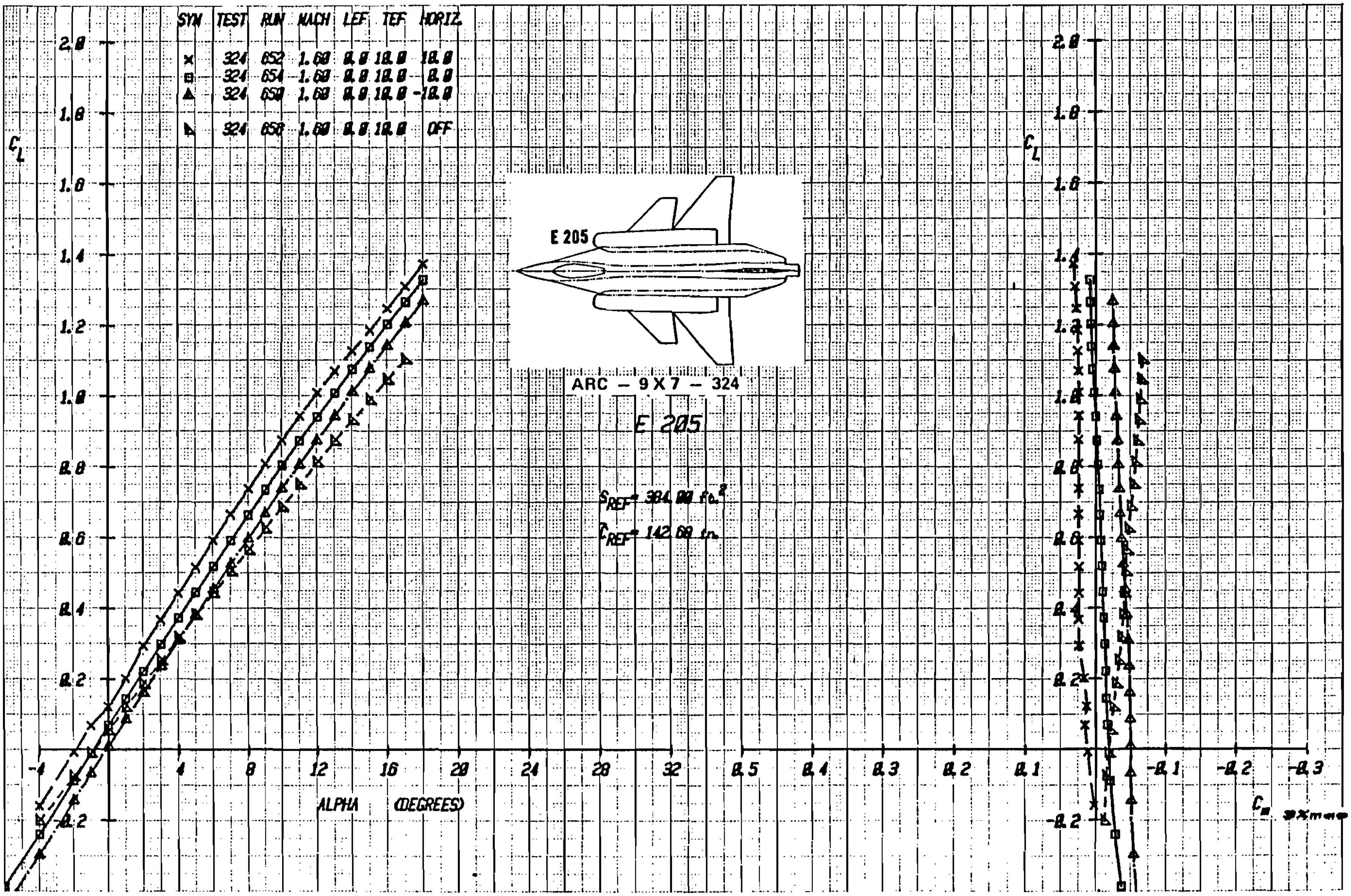

Figure2-36aEffect of Canard Deflection on Lift and Moment With Trailing-Edge Flap Deflected +10°, Mach = 1.6

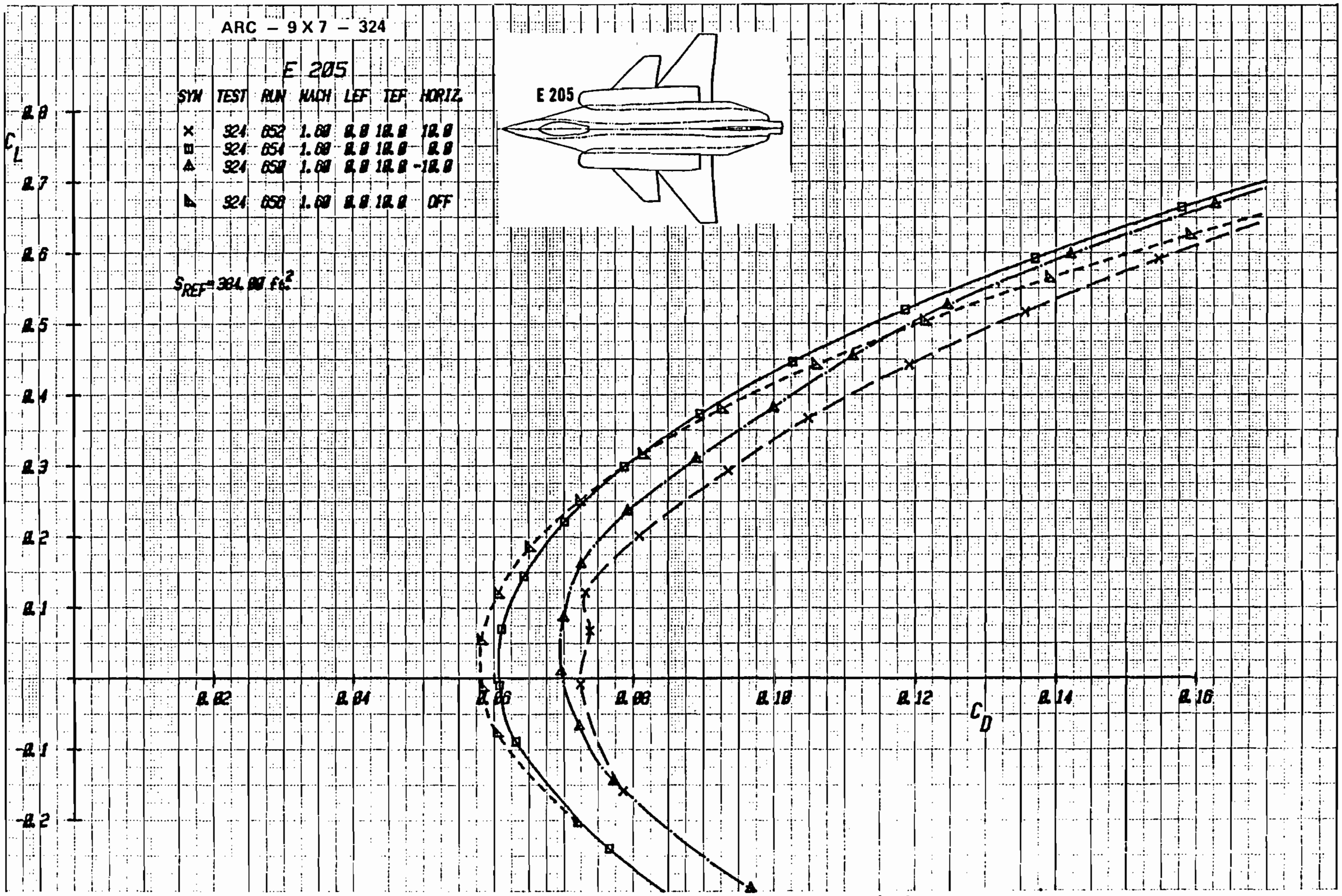

Figure2-36bEffect of Canard Deflection on Drag With Wing Trailing-Edge Flap Deflected +10°, (Expanded Drag Scale), Mach = 1.6

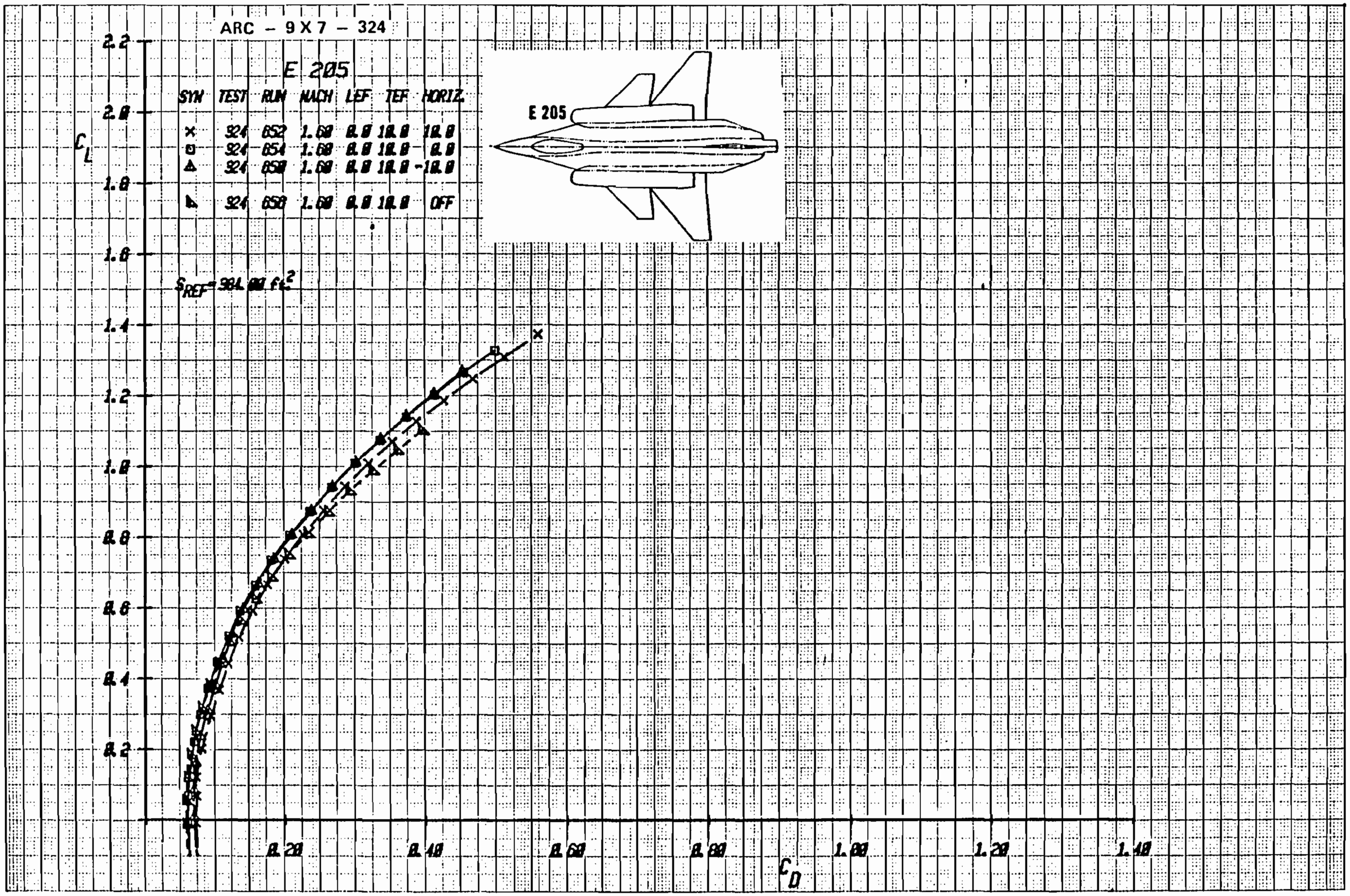

Figure2-36cEffect of Canard Deflection on Drag With Wing Trailing-Edge Flap Deflected +10°, Mach = 1.6

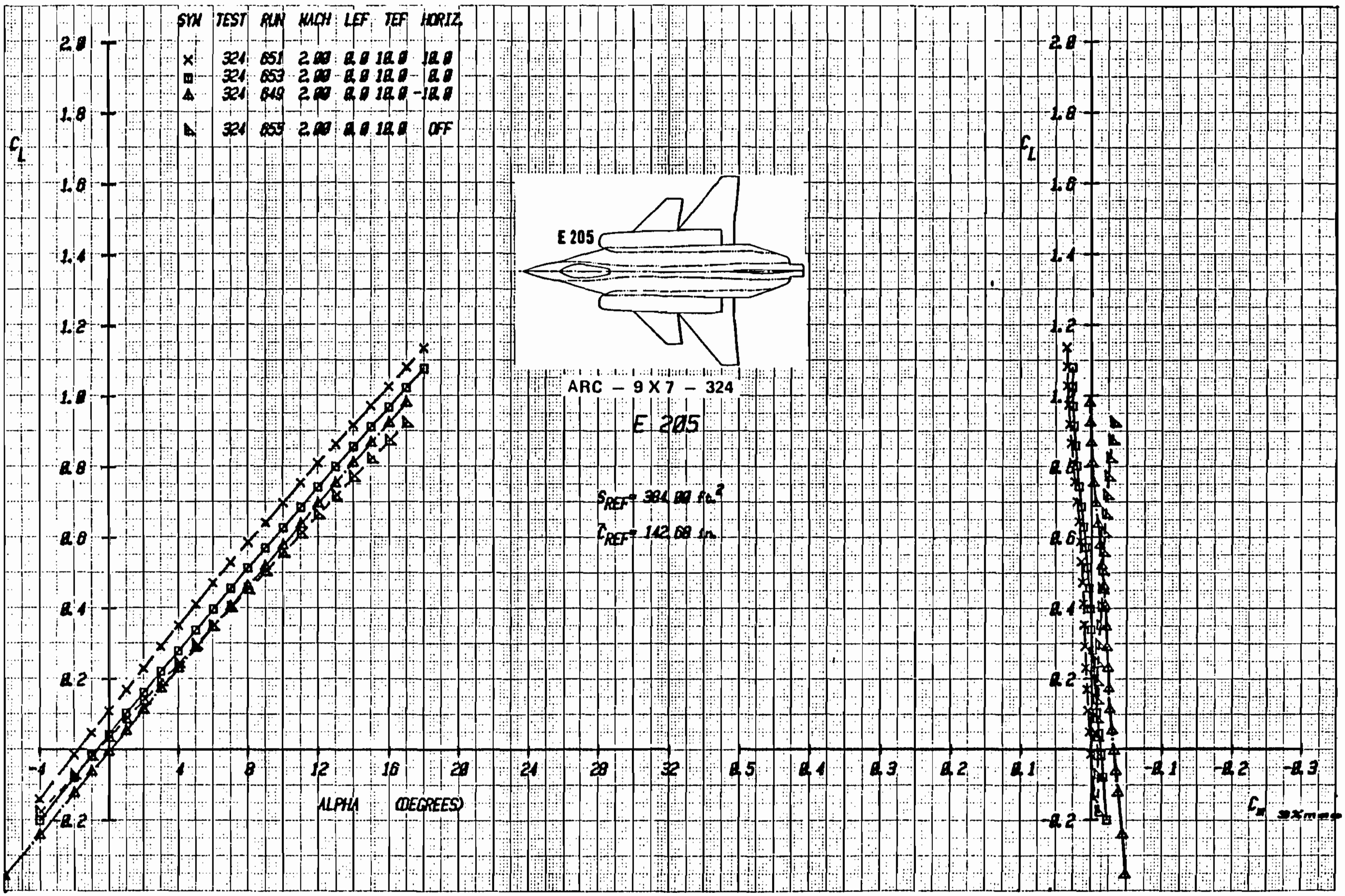

Figure2-37aEffect of Canard Deflection on Lift and Moment With Wing Trailing-Edge Flap Deflected +10°, Mach = 2.0

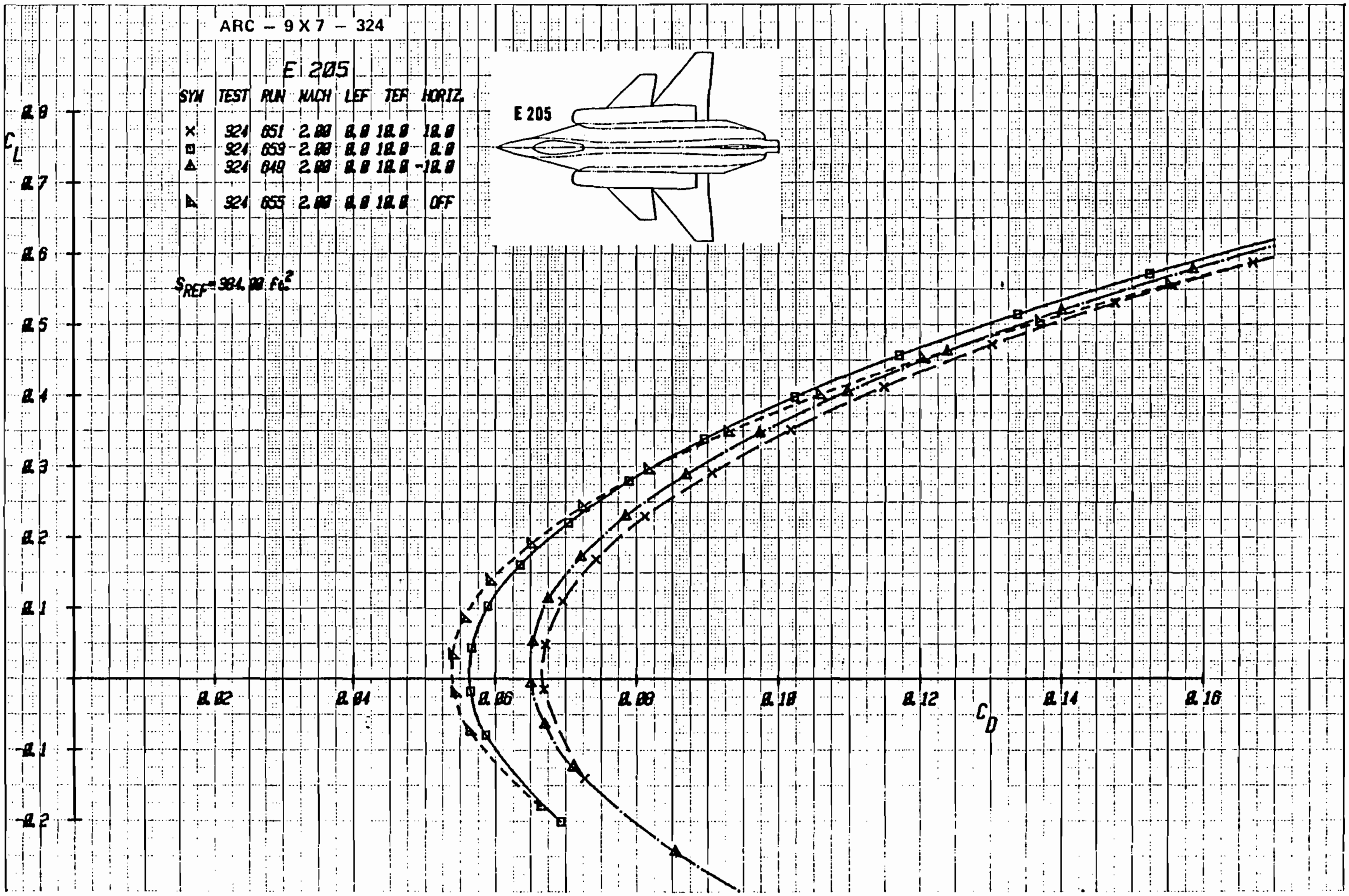

Figure2-37bEffect of Canard Deflection on Drag With Wing Trailing-Edge Flap Deflected +10°, (Expanded Drag Scale), Mach = 2.0

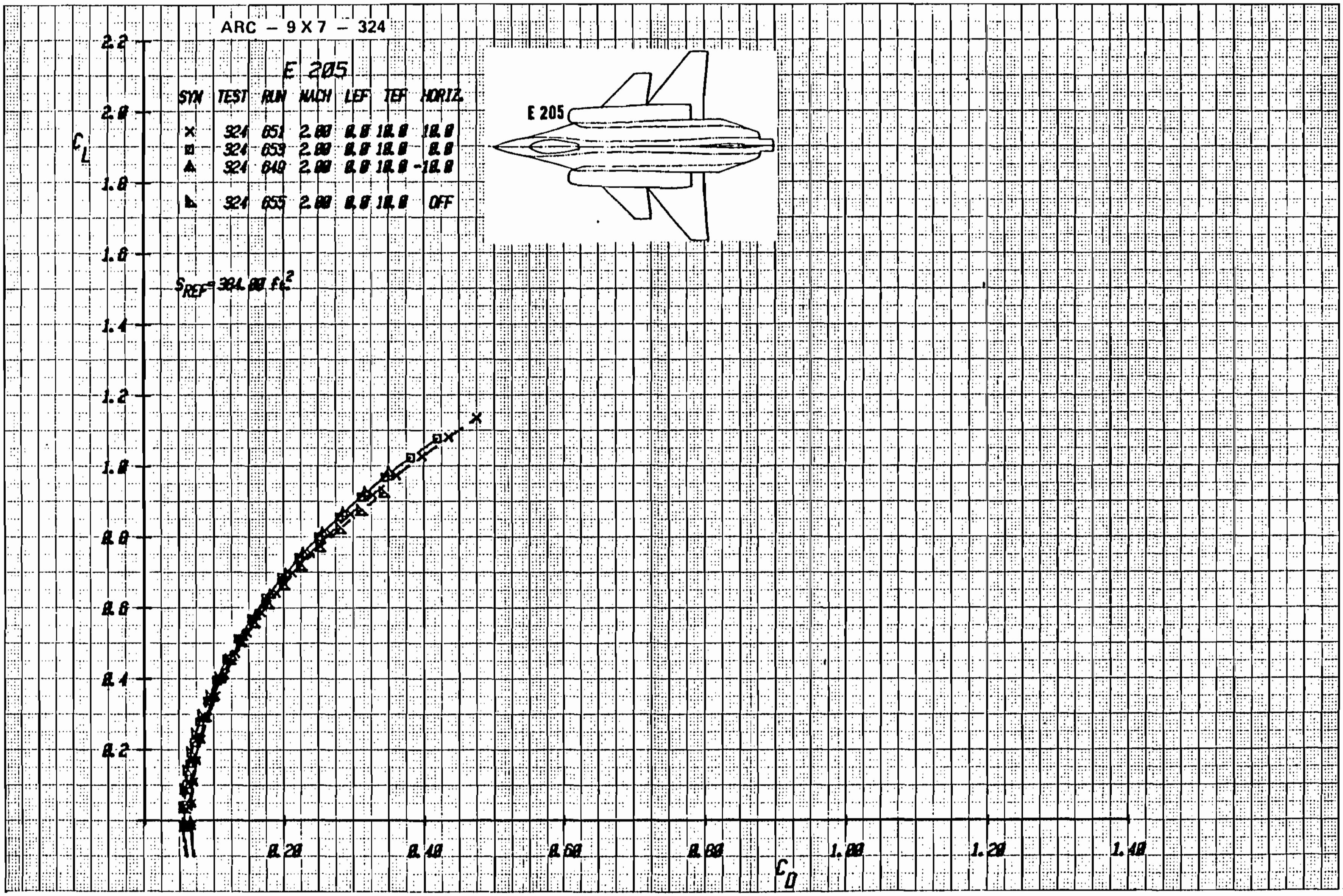

Figure2-37cEffect of Canard Deflection on Drag With Wing Trailing-Edge Flap Deflected +10°, Mach = 2.0

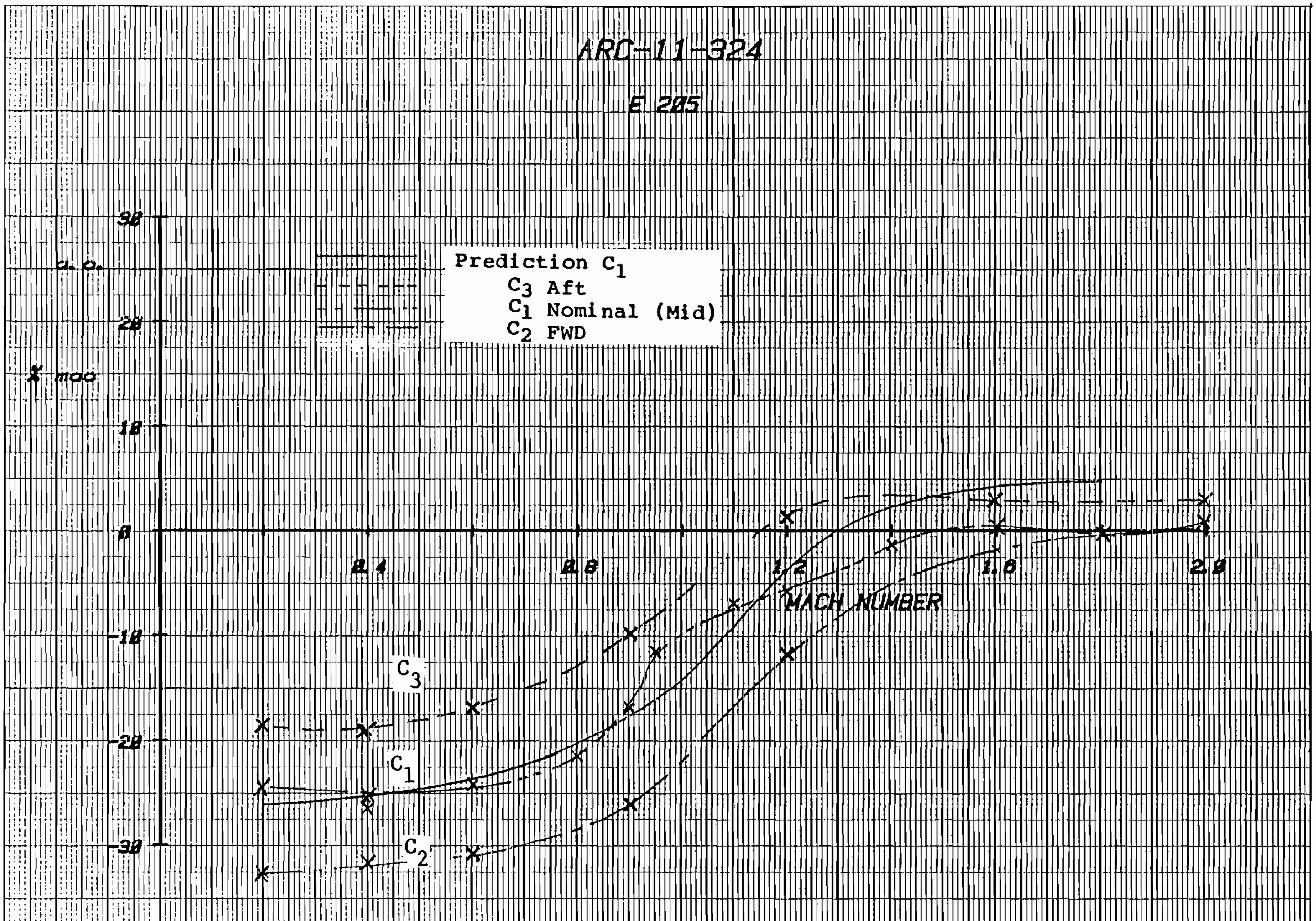

Figure 2-38 Effect of Canard Location on Aerodynamic Center

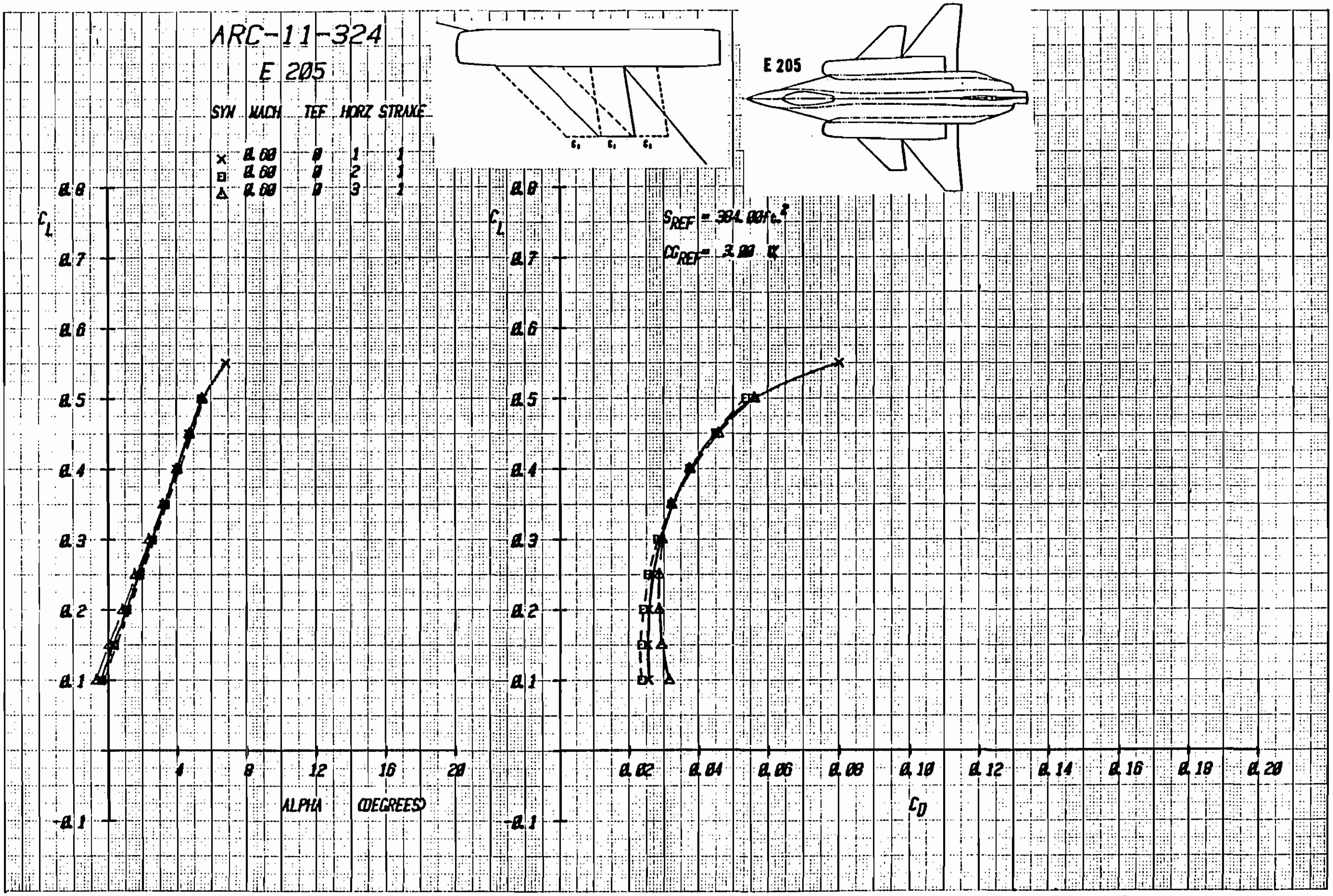

Figure 2-39 Effect of Canard Longitudinal Location on Trimmed Aerodynamics With Baseline Strake, Mach = .6

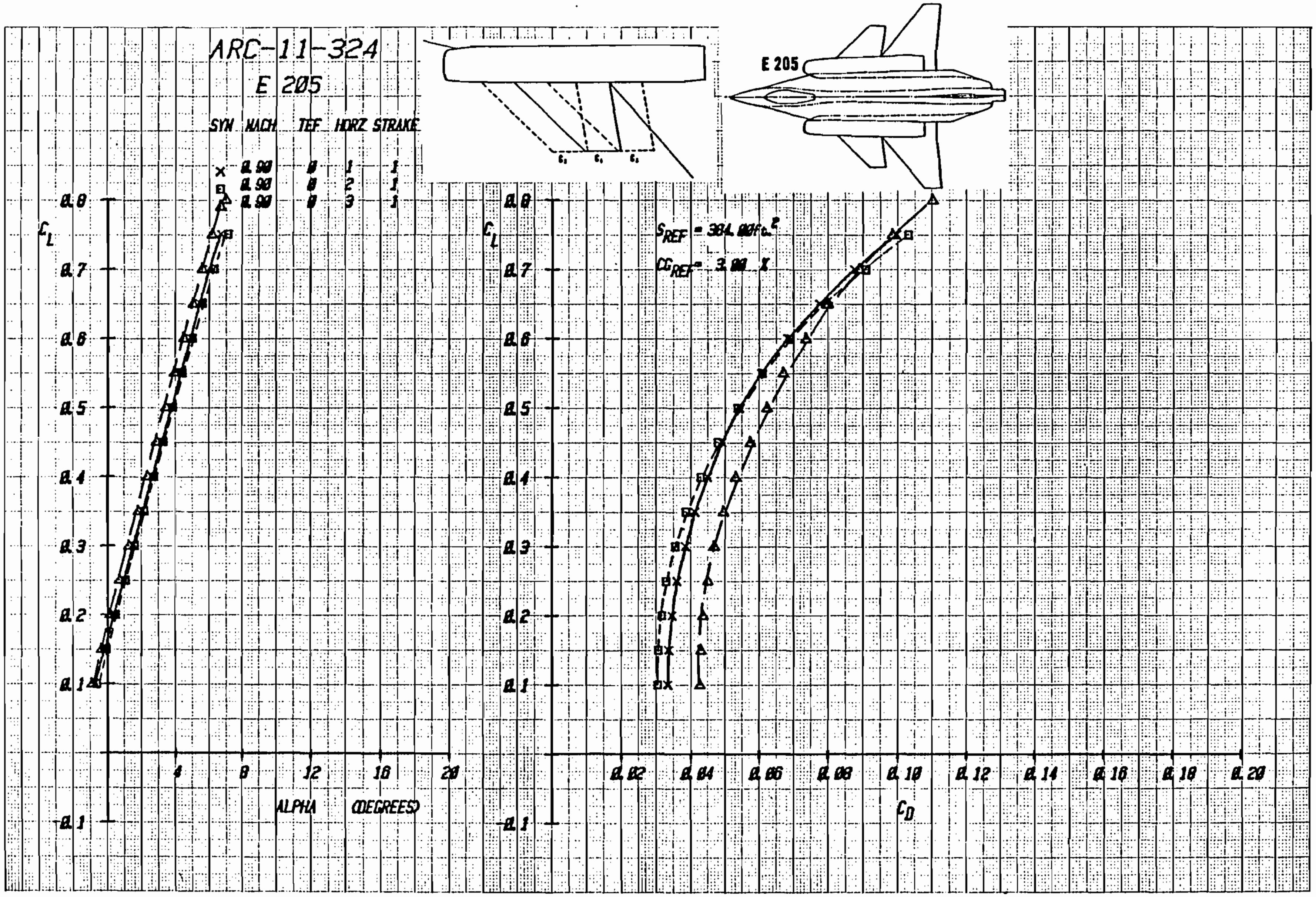

Figure 2-40 Effect of Canard Longitudinal Location on Trimmed Aerodynamics With Baseline Strake, Mach = .9

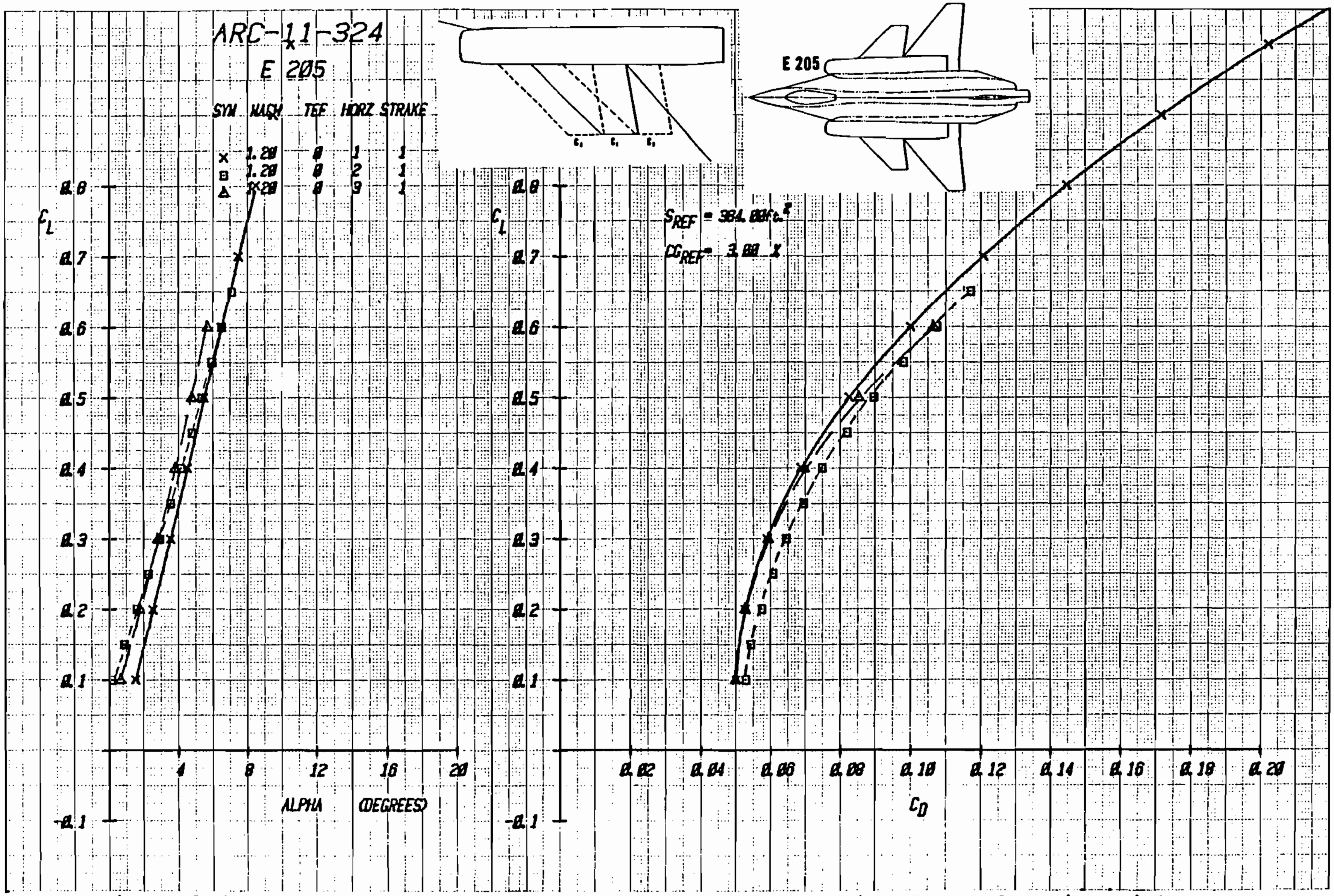

Figure 2-41 Effect of Canard Longitudinal Location on Trimmed Aerodynamics With Baseline Strake, Mach = 1.2

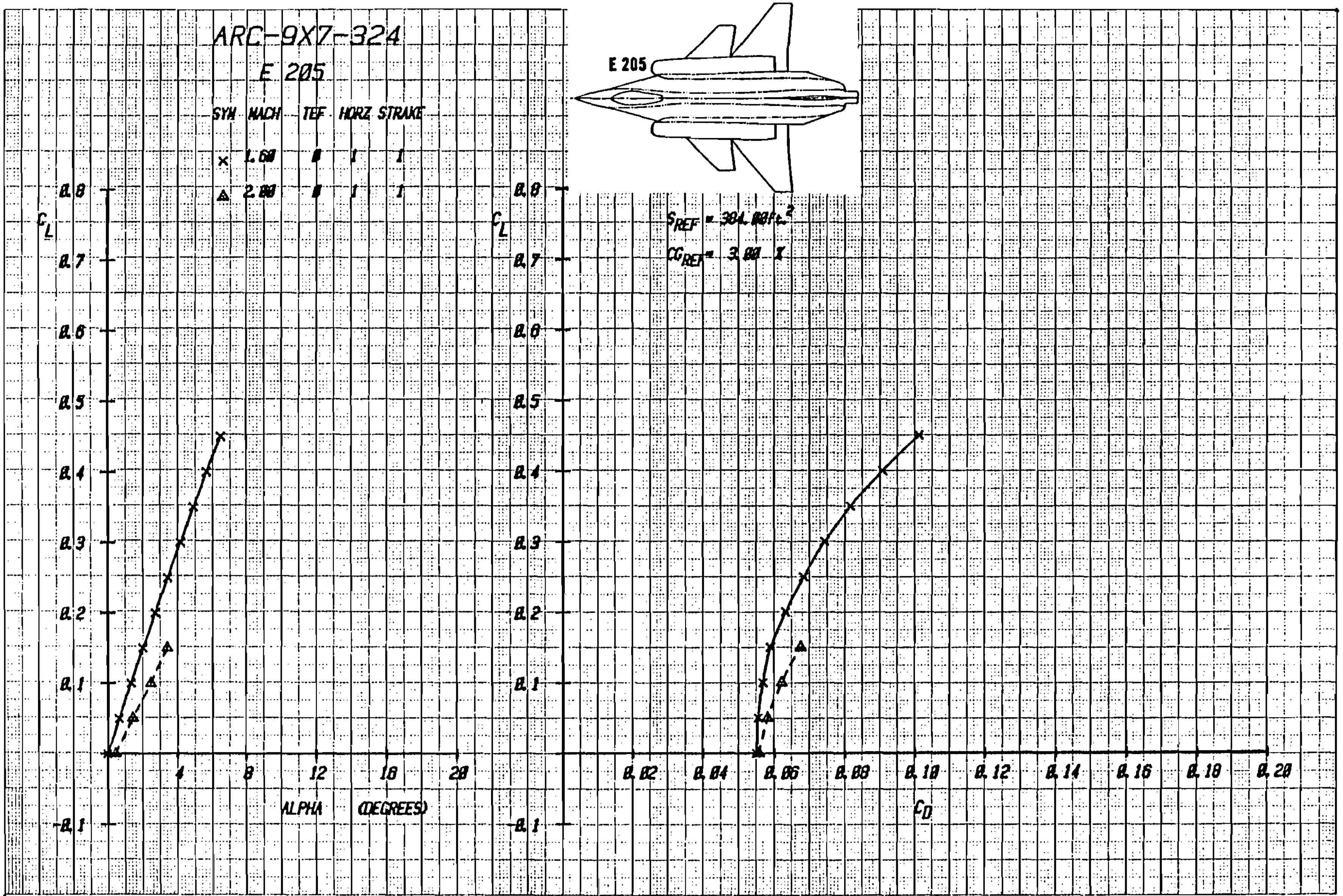

Figure 2-42 Trimmed Lift and Drag for Baseline E205 Configuration with Wing Trailing-Edge Flap Undeflected

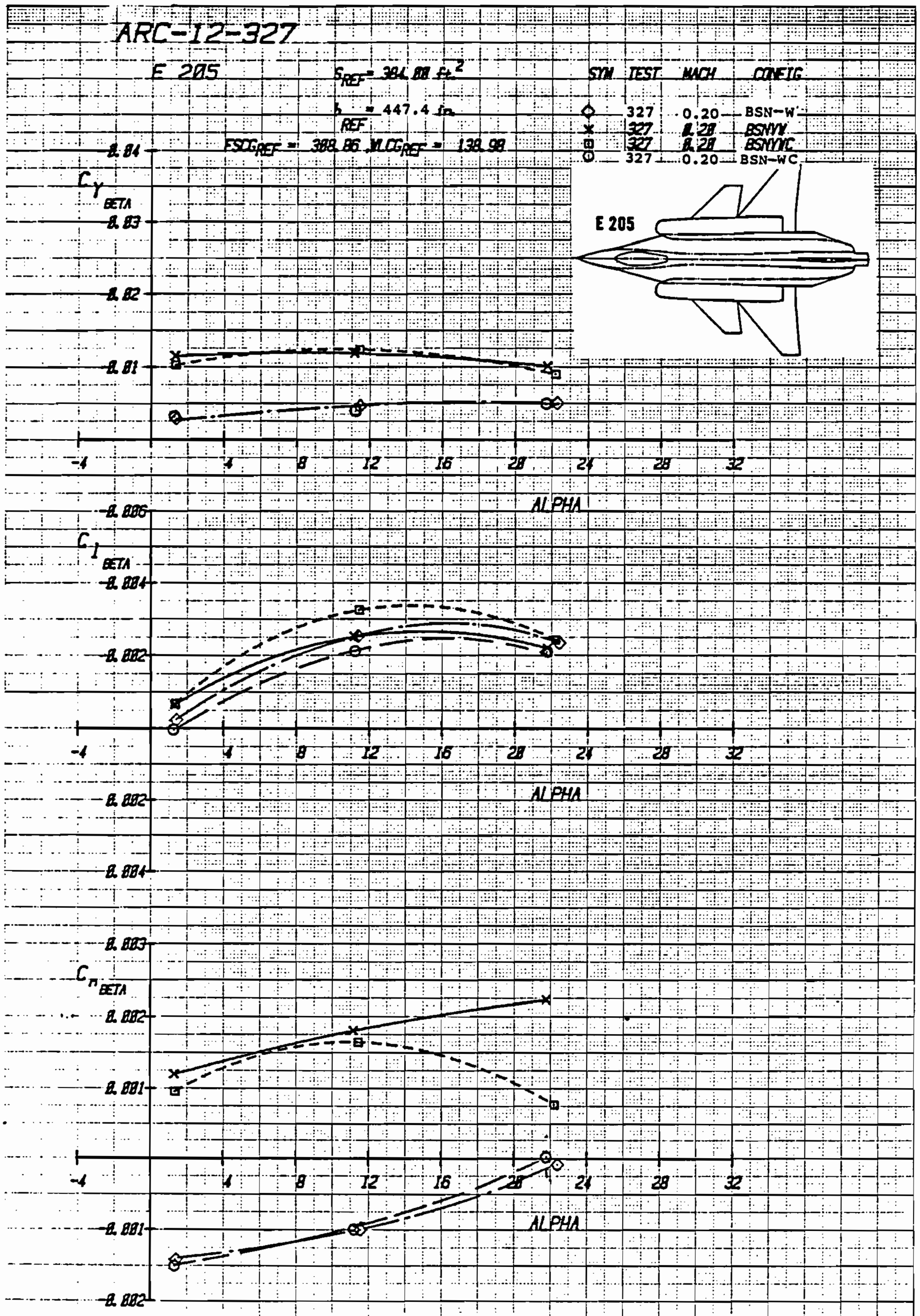

Figure 2-43 Vertical Tail Effectiveness for the E 205 Baseline Configuration, with Canard C_1, on and off, $\delta_{VT} = 0°$, Mach = .2

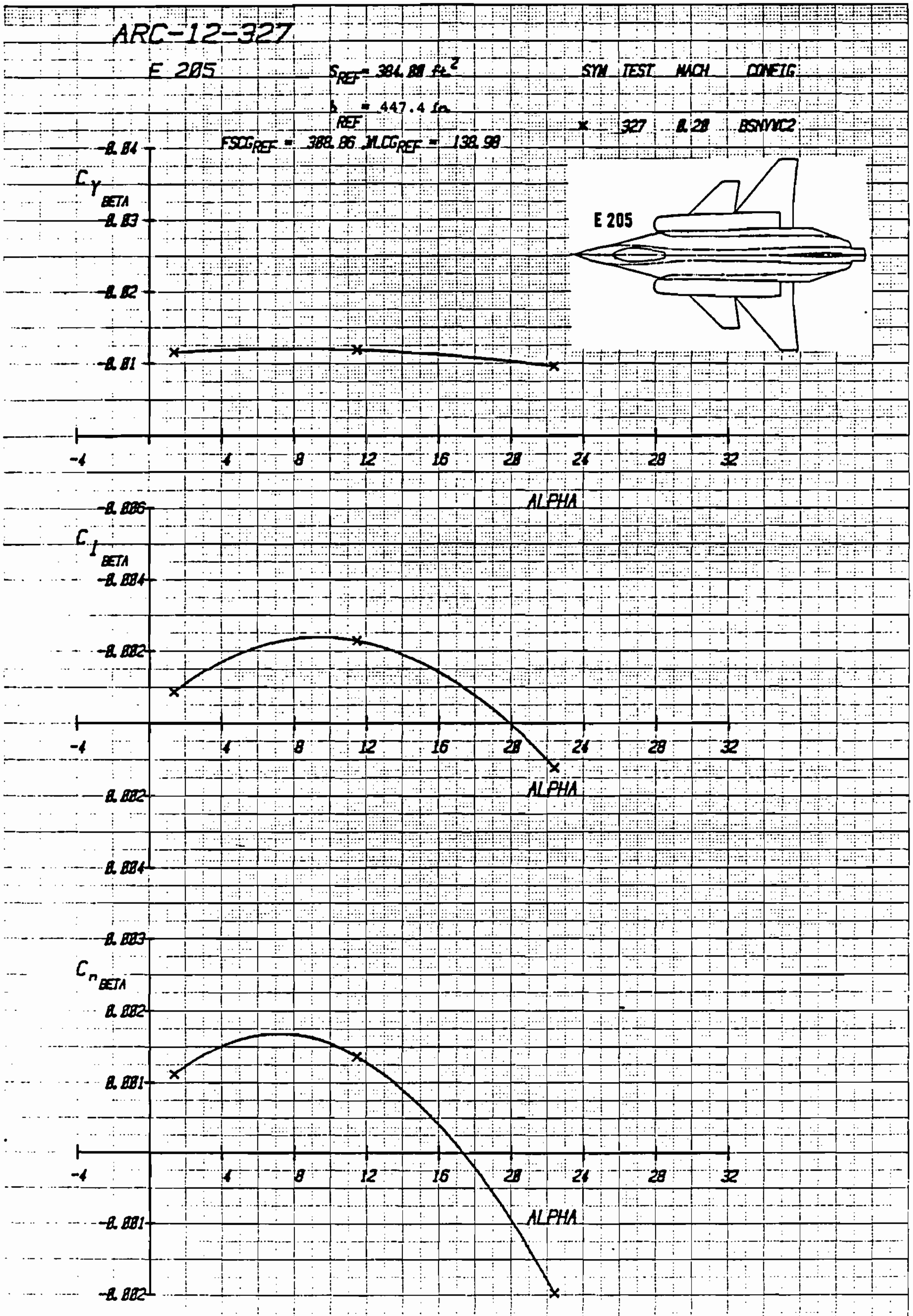

Figure 2-44 Vertical Tail Effectiveness for the E 205 Configuration, with Strake S_1, Canard C_2, $\delta_{VT} = 0°$, Mach = .2

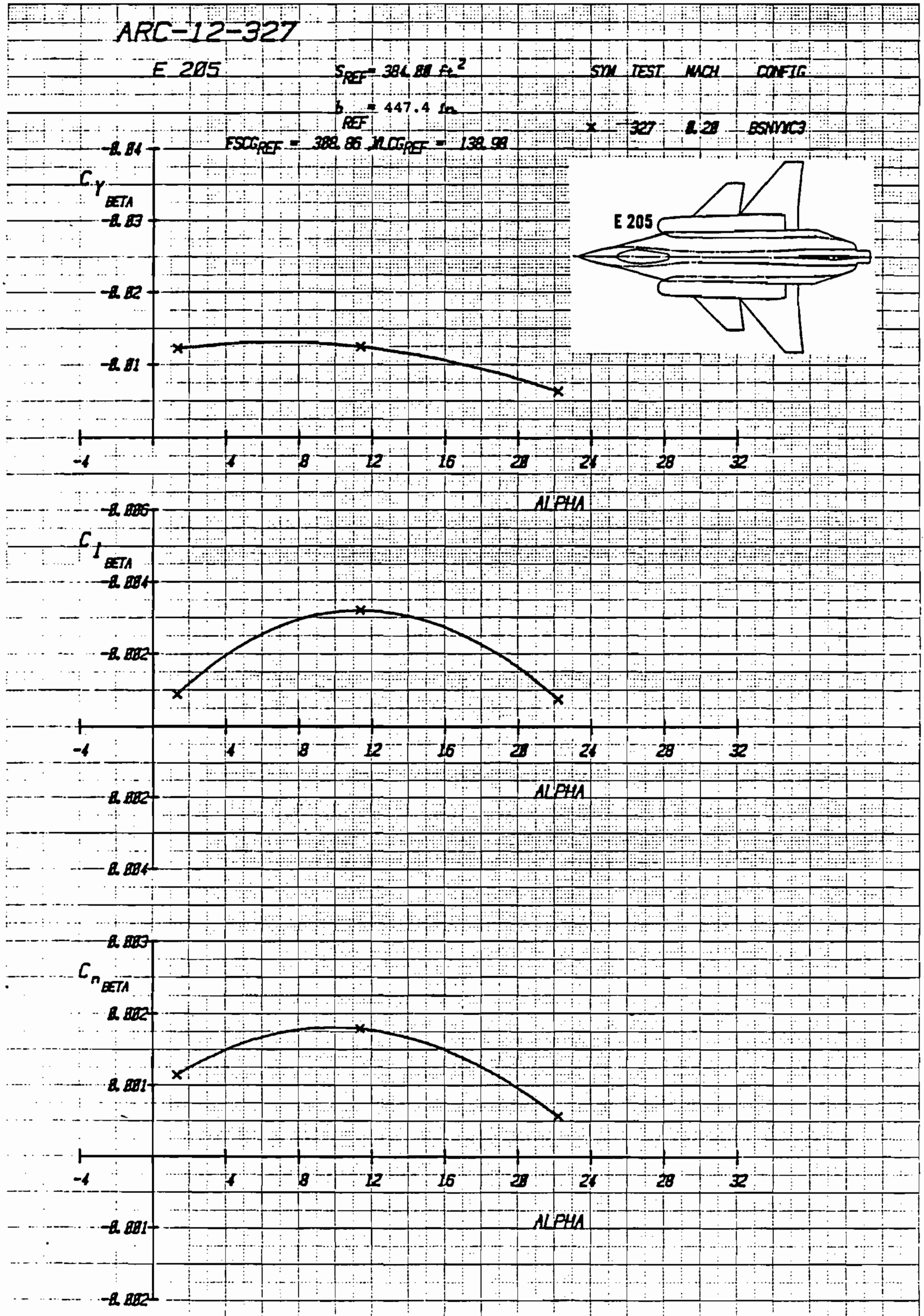

Figure 2-45 Vertical Tail Effectiveness for the E 205 Configuration, with Strake S_1, Canard C_3, δ_{VT} = 0°, Mach = .2

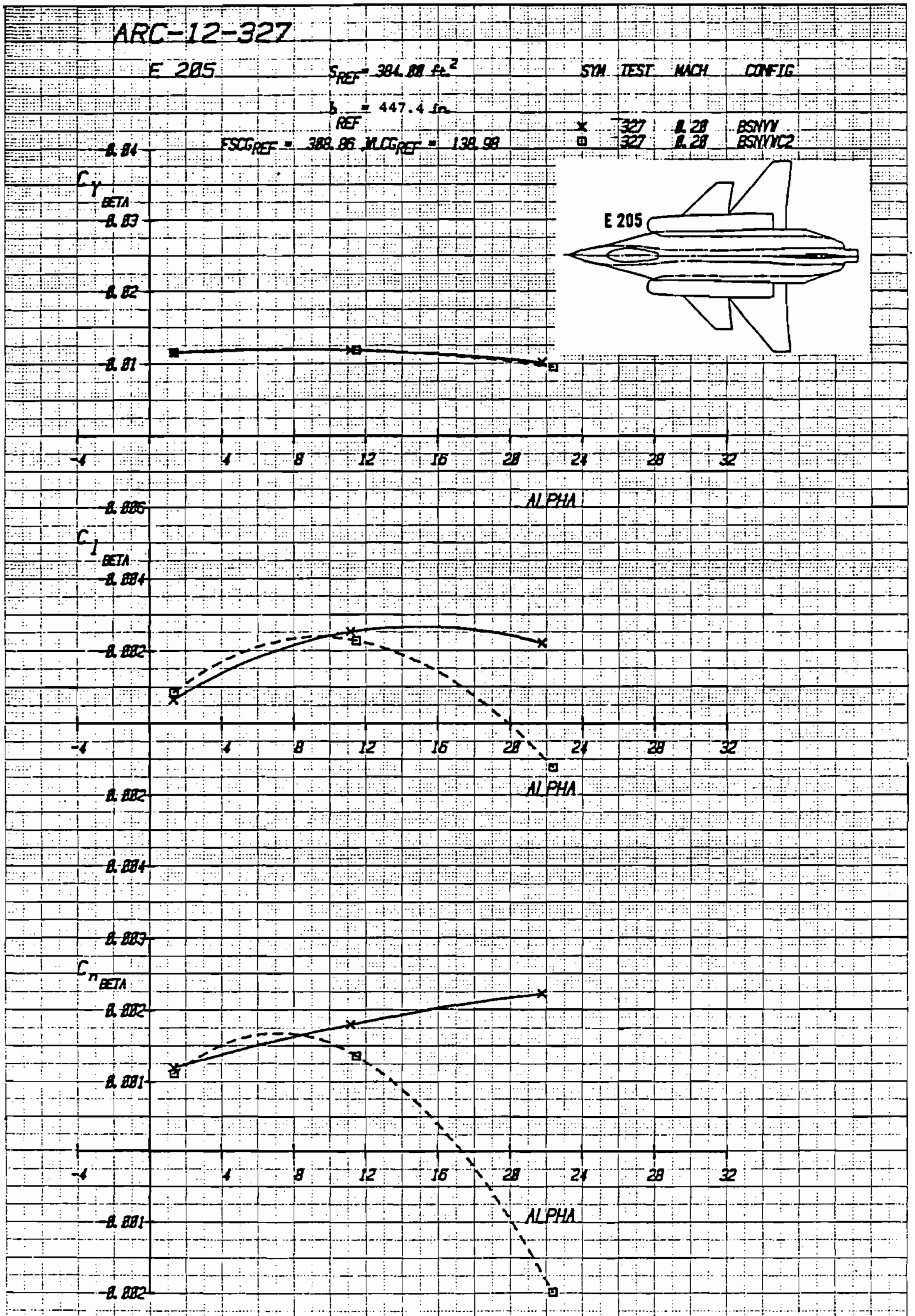

Figure 2-46 Vertical Tail Effectiveness for the E 205 Configuration, with Strake S_1, Canard C_2, on and off, $\delta_{VT} = 0°$, Mach = .2

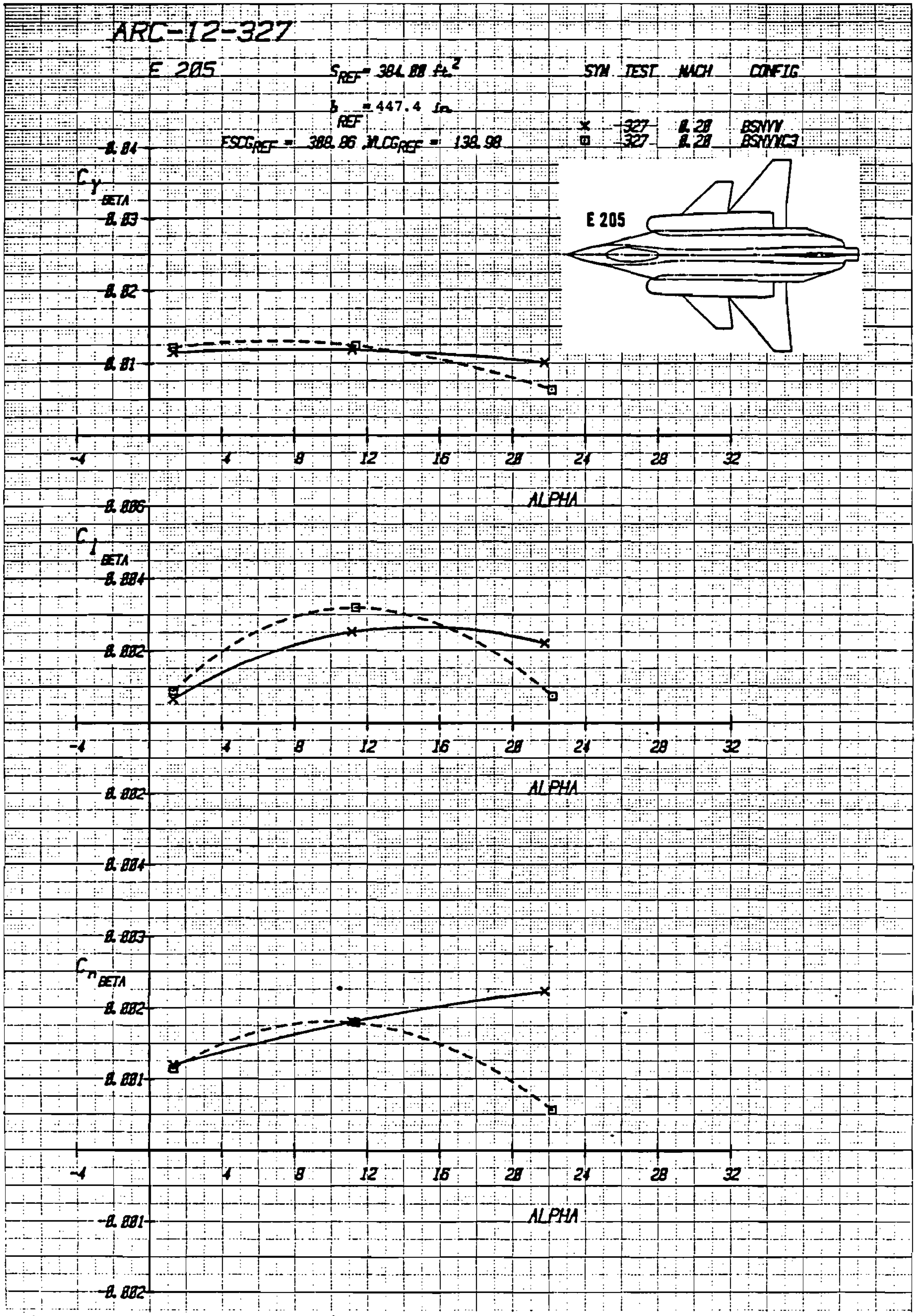

Figure 2-47 Vertical Tail Effectiveness for the E 205 Configuration, with Strake S_1, Canard C_3, on and off, $\delta_{VT} = 0°$, Mach = .2

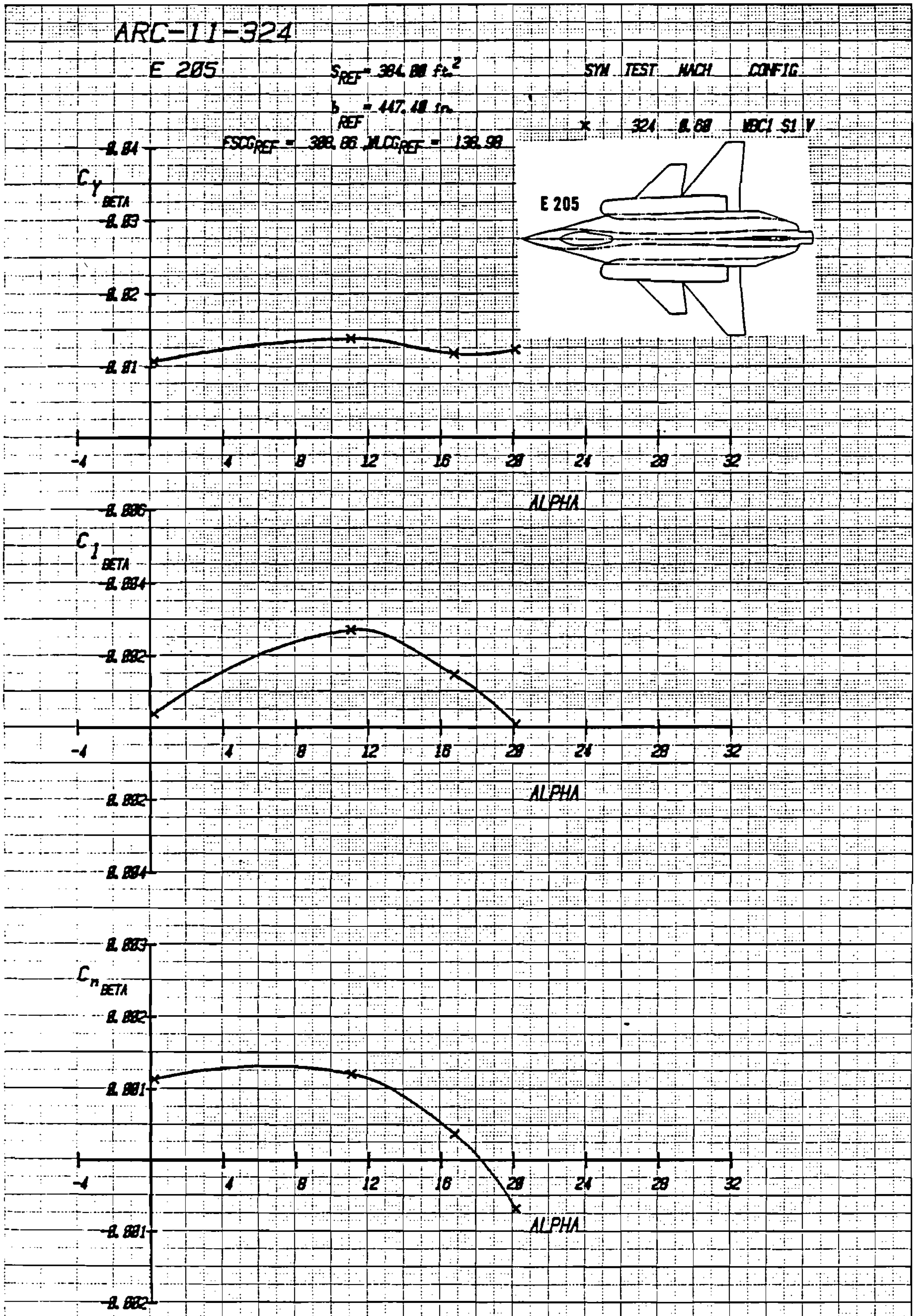

Figure 2-48 Lateral-Directional Characteristics for Baseline E205 Configuration, M = .6

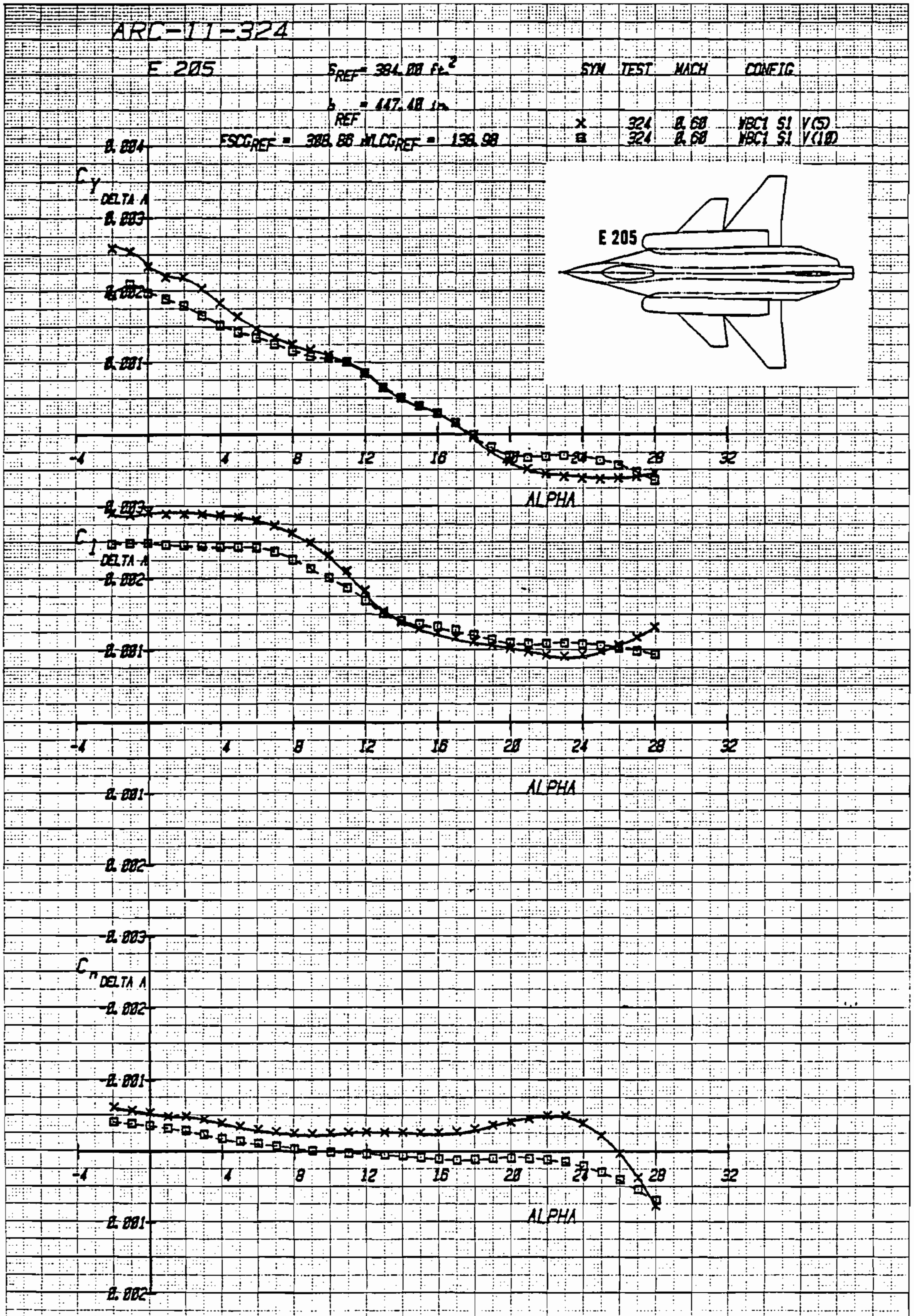

Figure 2-49 Aileron Effectiveness for Baseline E205 Configuration, Mach = .6

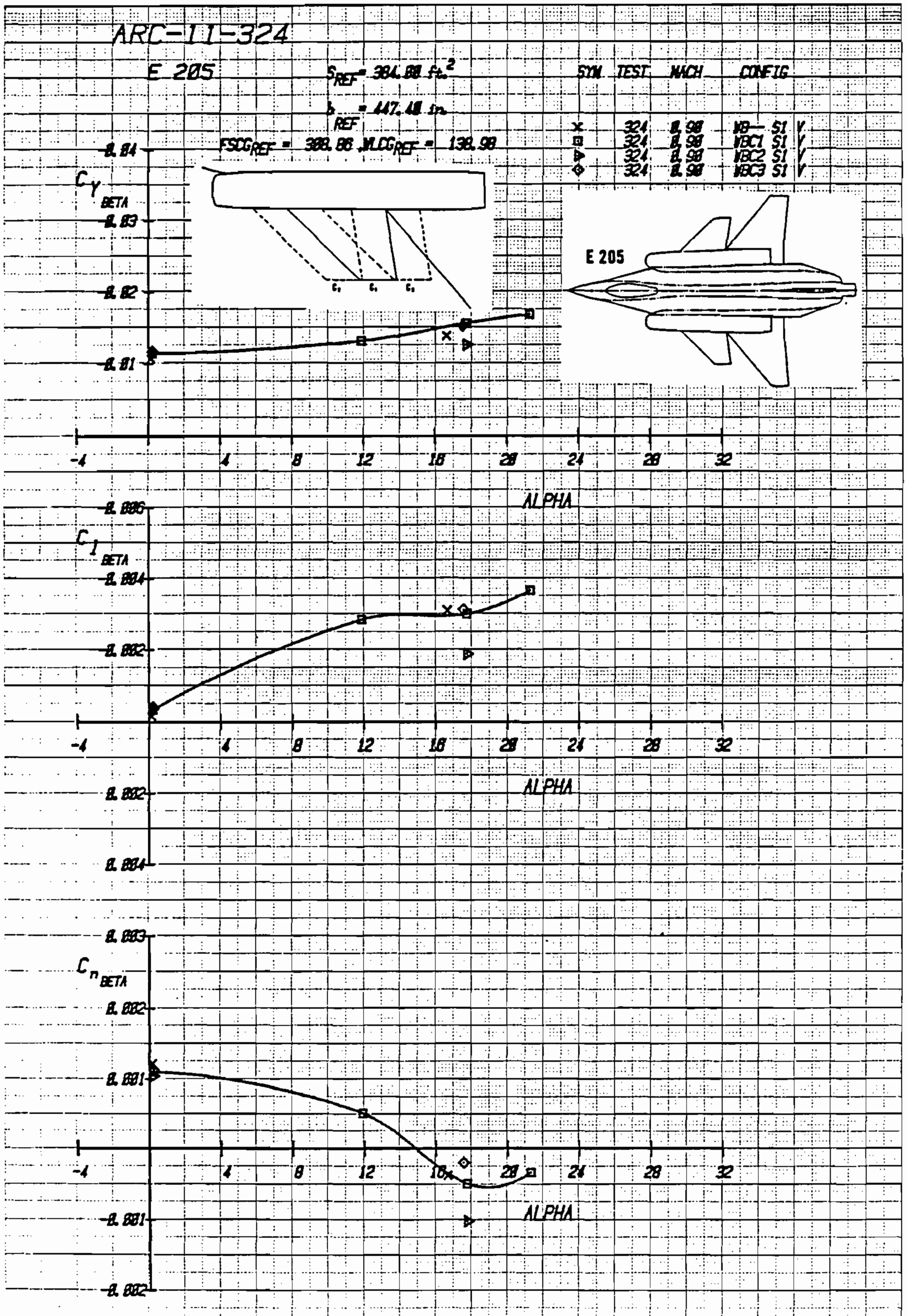

Figure 2-50 Effect of Canard Location on Vertical Tail Effectiveness, Mach = .9

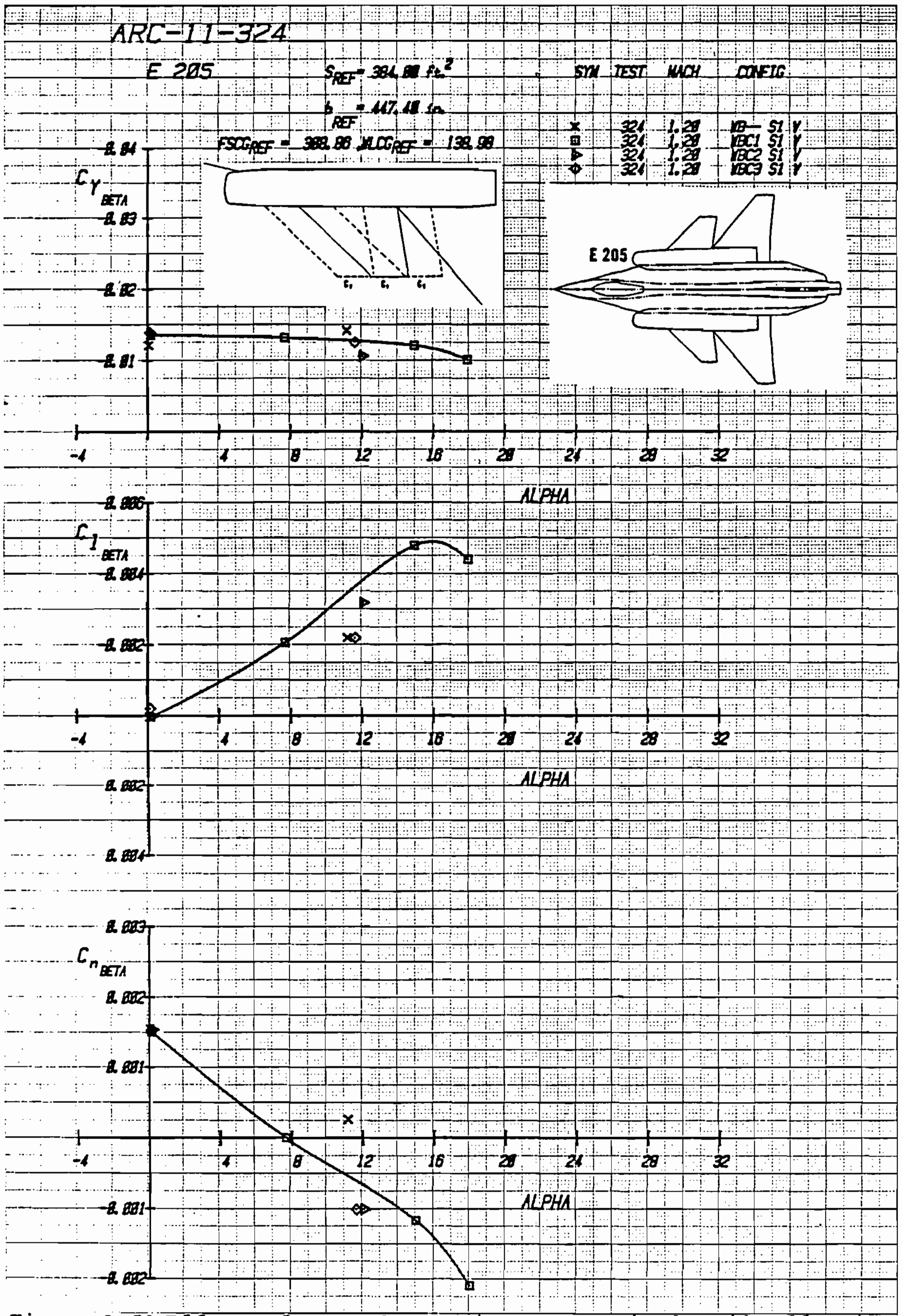

Figure 2-51 Effect of Canard Location on Vertical Tail Effectiveness, Mach = 1.2

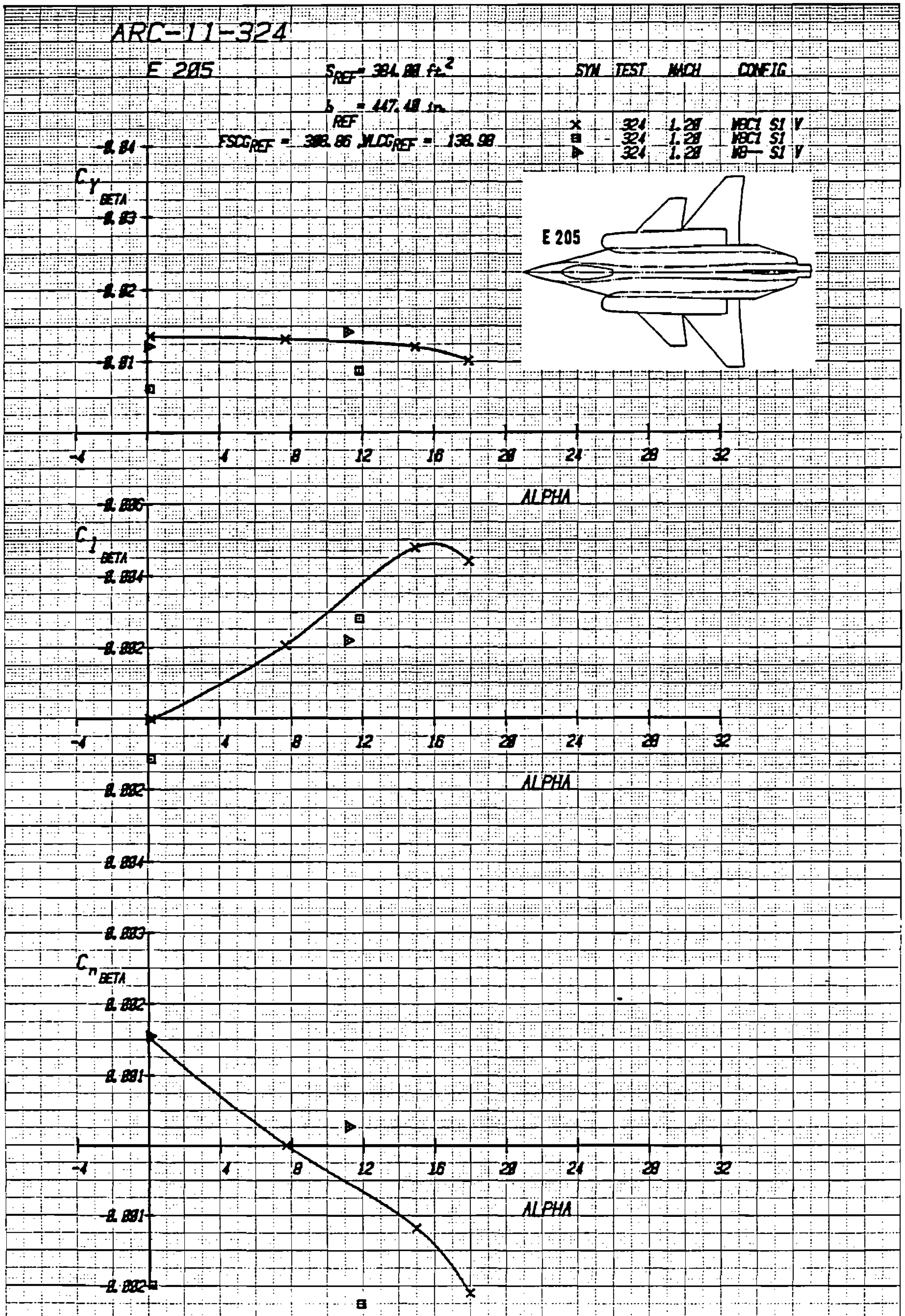

Figure 2-52 Vertical Tail Effectiveness for the E205 Baseline Configuration, with Canard C_1, Mach = 1.2

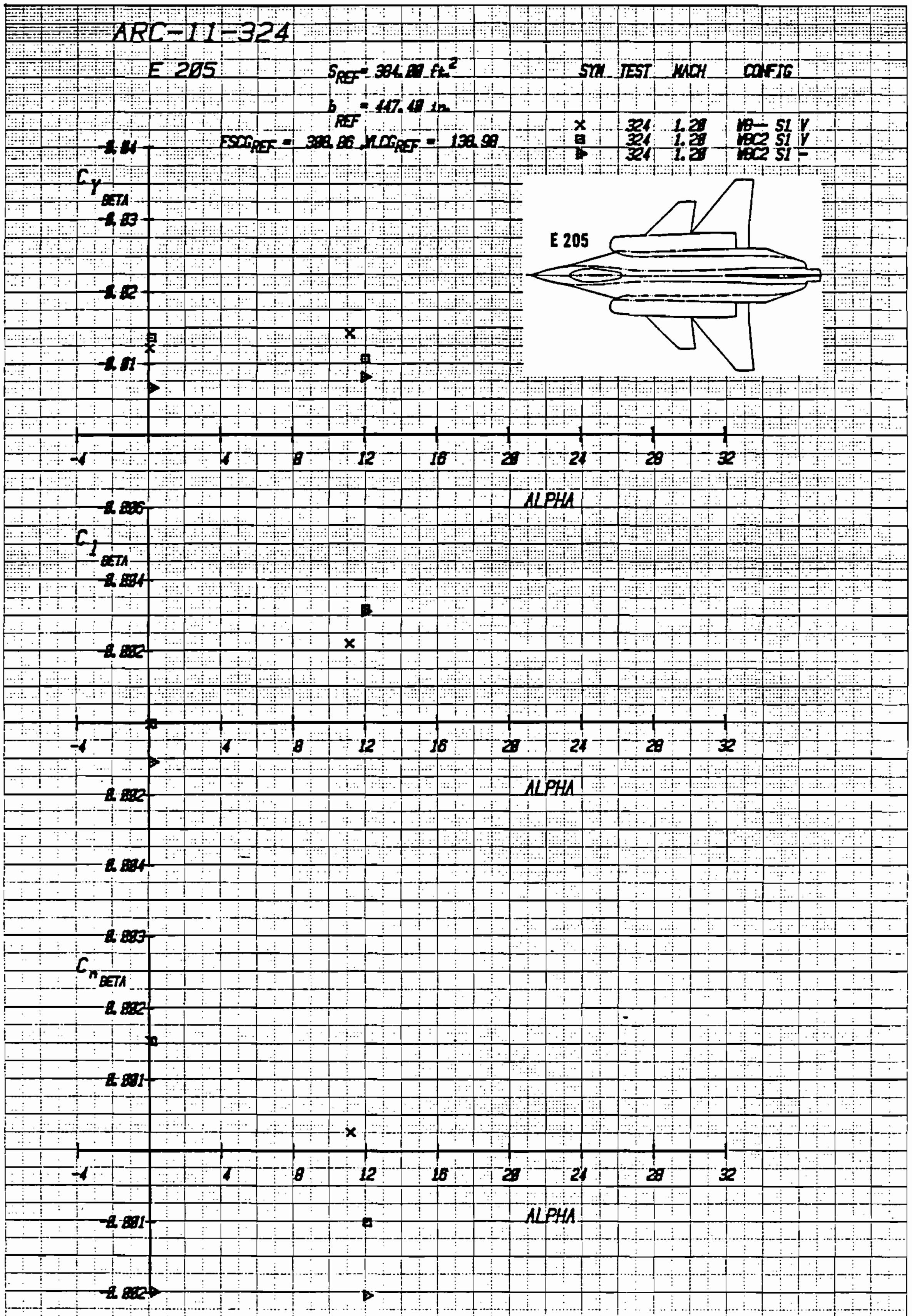

Figure 2-53 Vertical Tail Effectiveness for the E205 Configuration, with Strake S_1, Canard C_2, Mach = 1.2

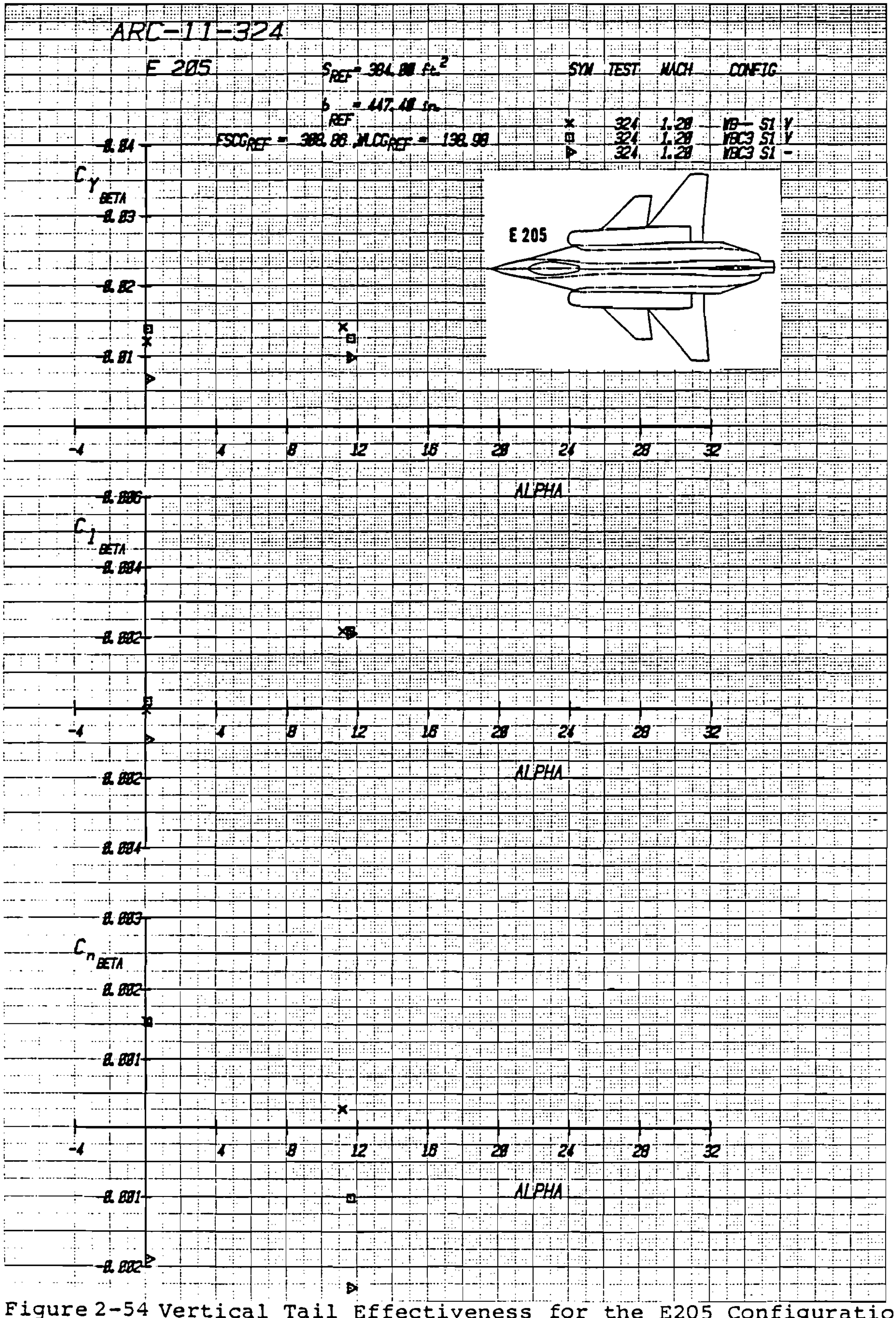

Figure 2-54 Vertical Tail Effectiveness for the E205 Configuration, with Strake S_1, Canard C_3, Mach = 1.2

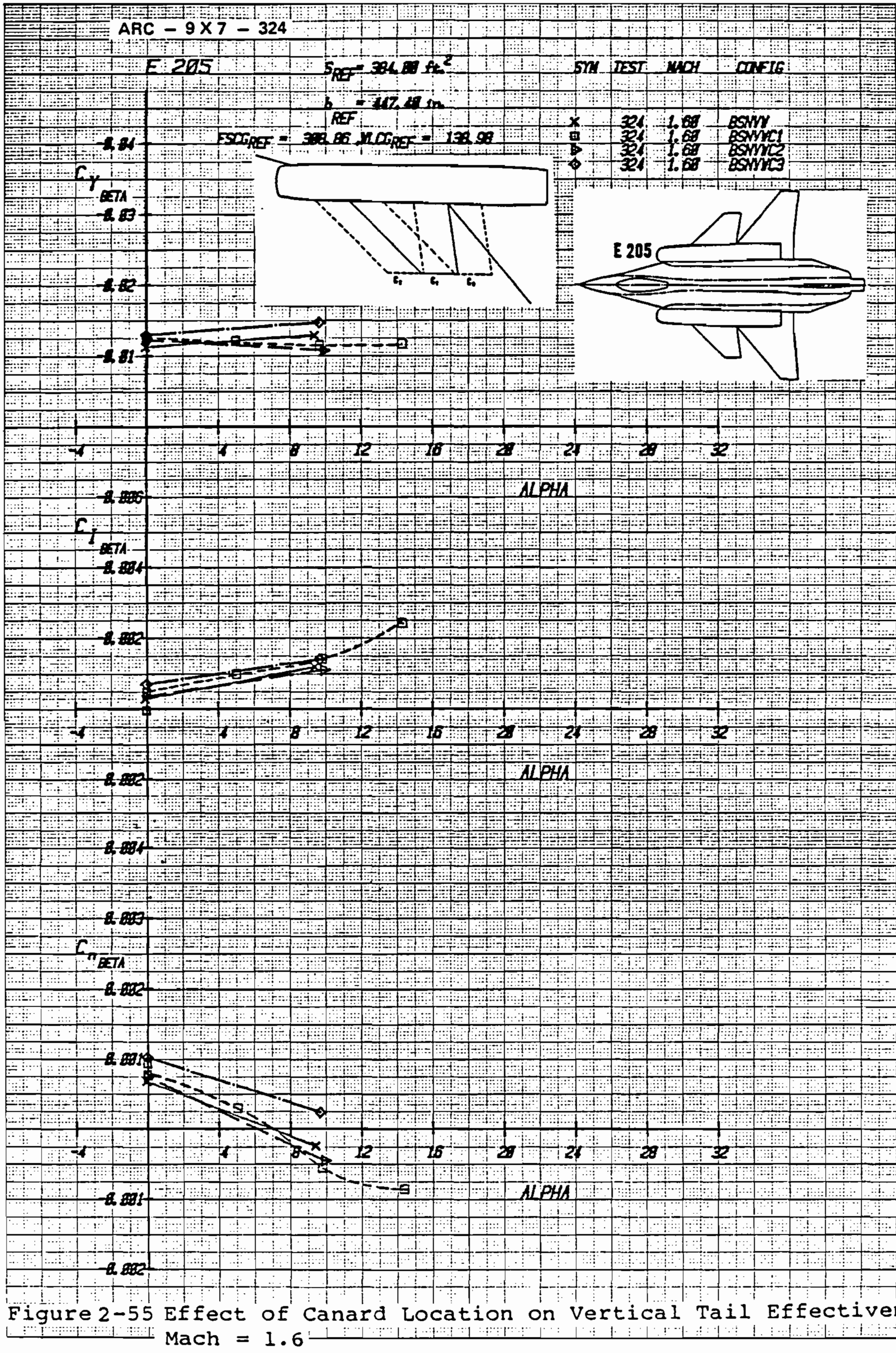

Figure 2-55 Effect of Canard Location on Vertical Tail Effectiveness, Mach = 1.6

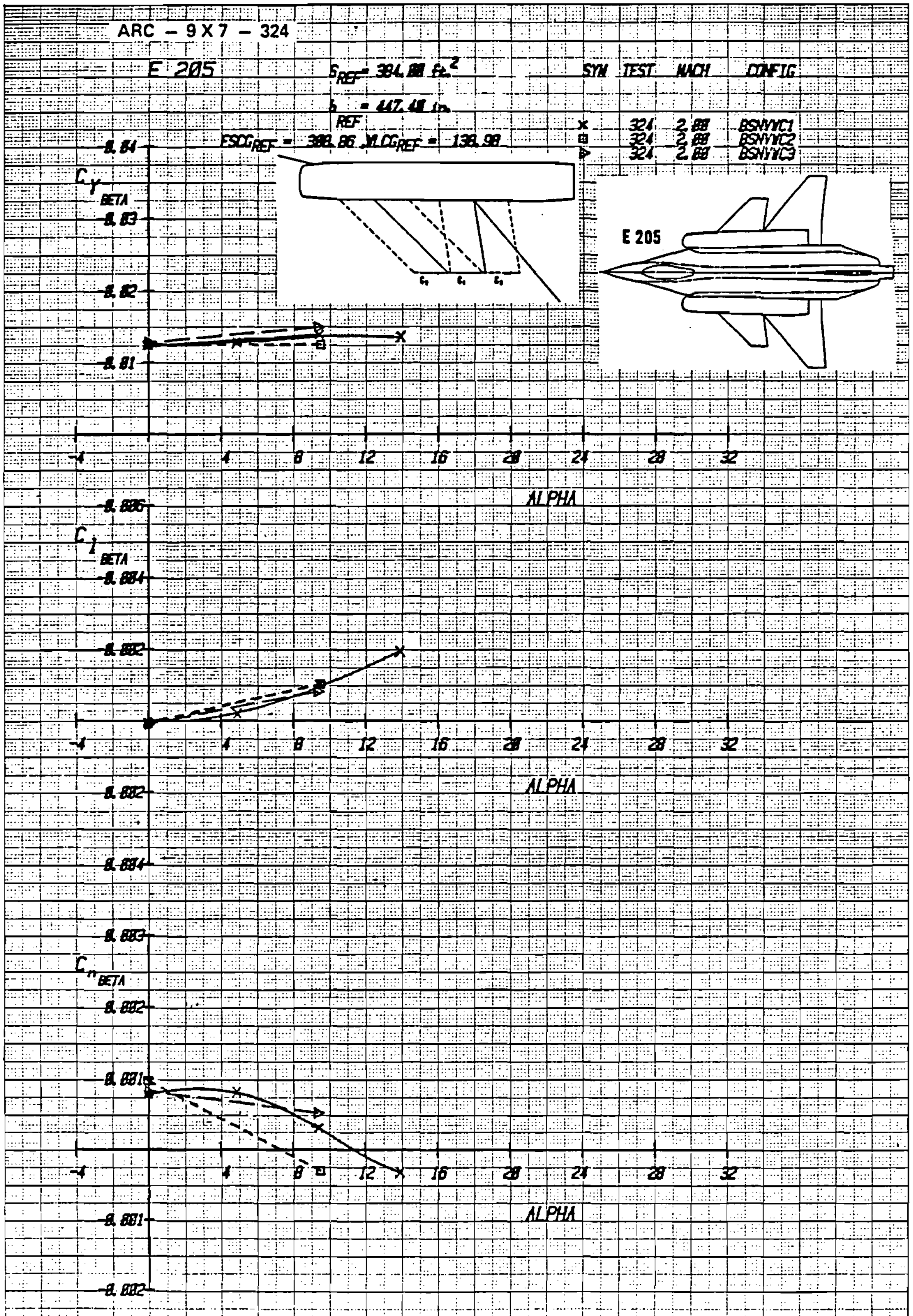

Figure 2-56 Effect of Canard Location on Vertical Tail Effectiveness, Mach = 2.0

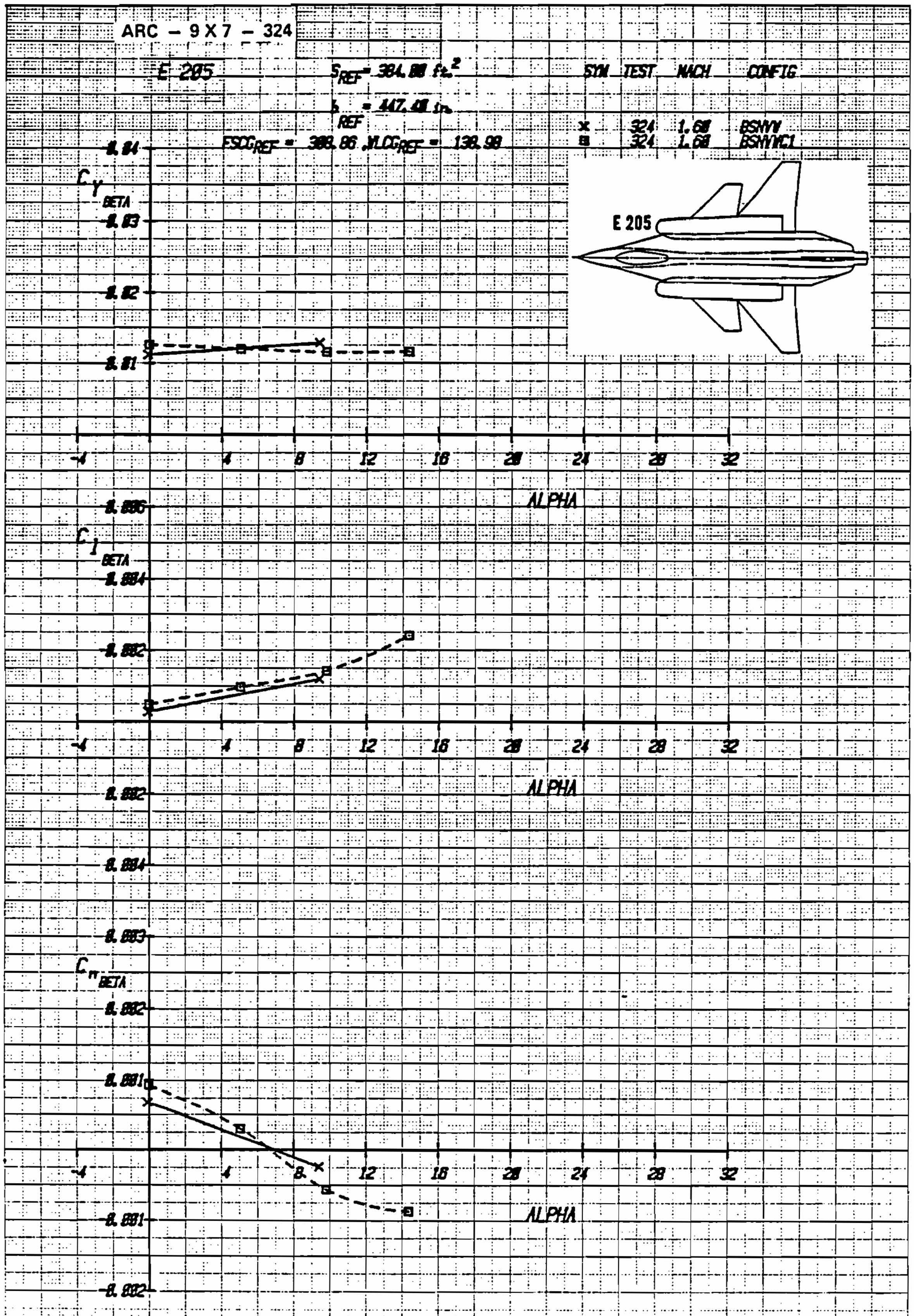

Figure 2-57 Vertical Tail Effectiveness for the E 205 Baseline Configuration with Canard C_1, on and Off, Mach = 1.6

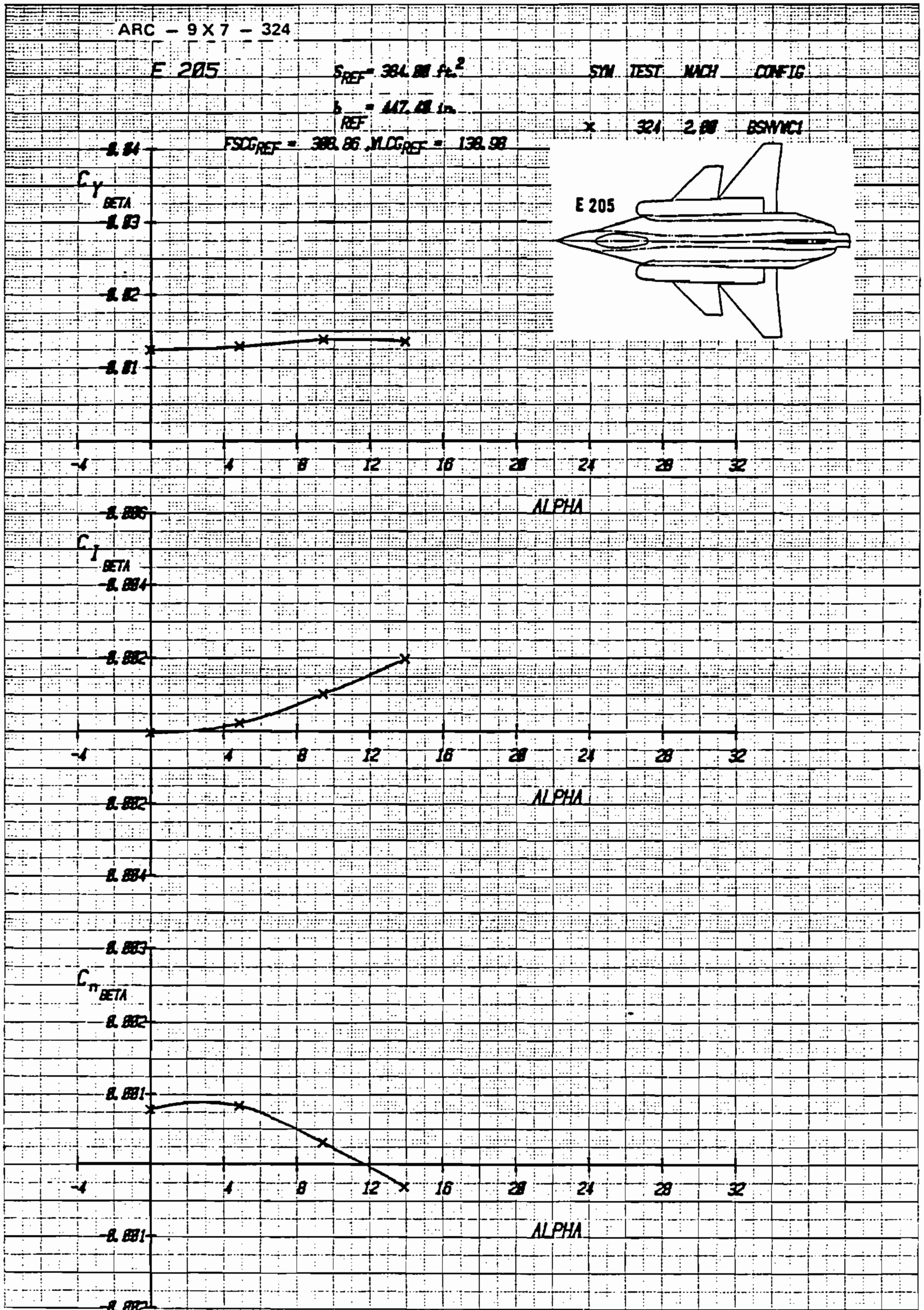

Figure 2-58 Vertical Tail Effectiveness for the E 205 Baseline Configuration with Canard C_1, Mach = 2.0

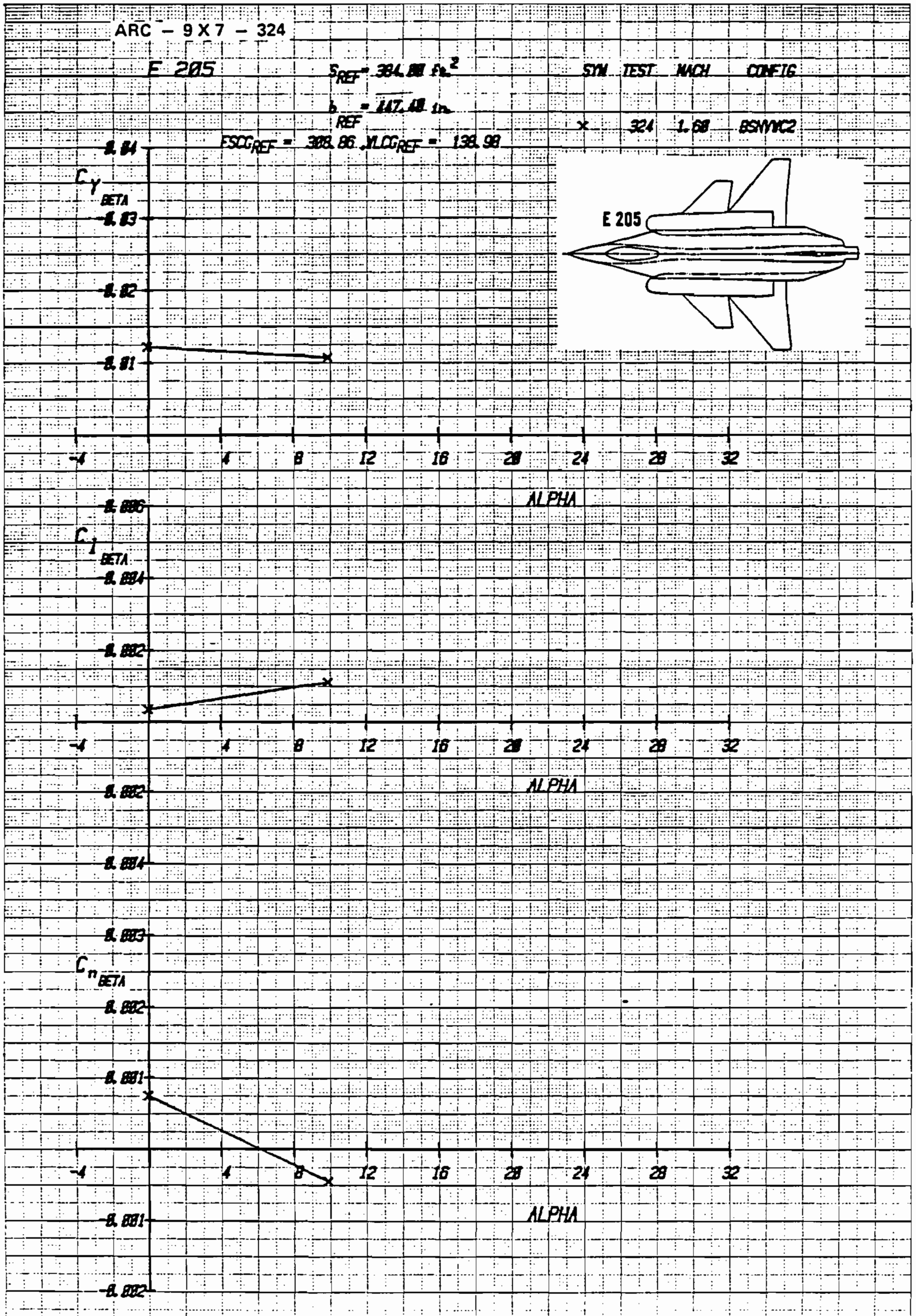

Figure 2-59 Vertical Tail Effectiveness for the E 205 Configuration, with Strake S_1, Canard C_2, Mach = 1.6

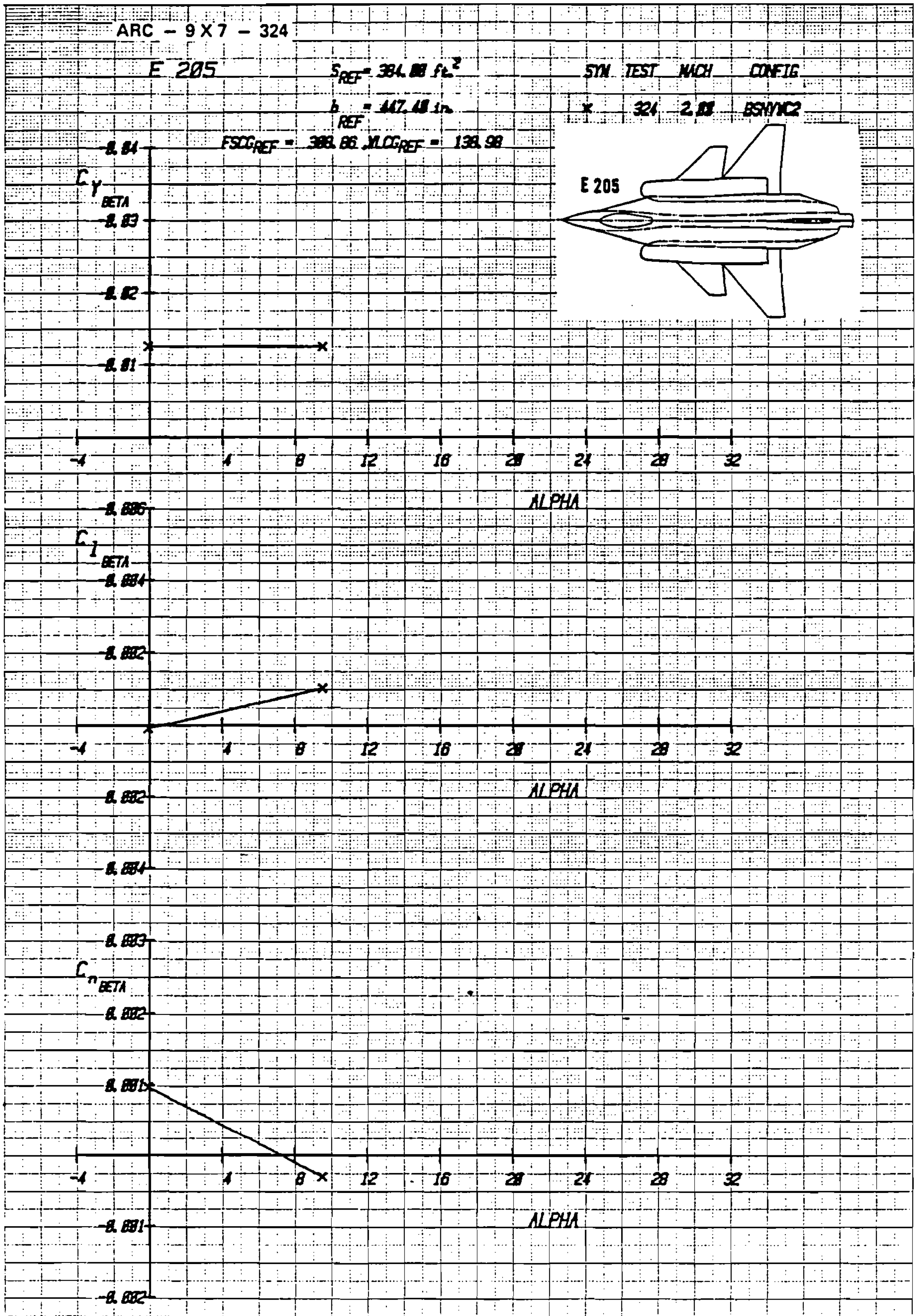

Figure 2-60 Vertical Tail Effectiveness for the E 205 Configuration with Strake S_1, Canard C_2, Mach = 2.0

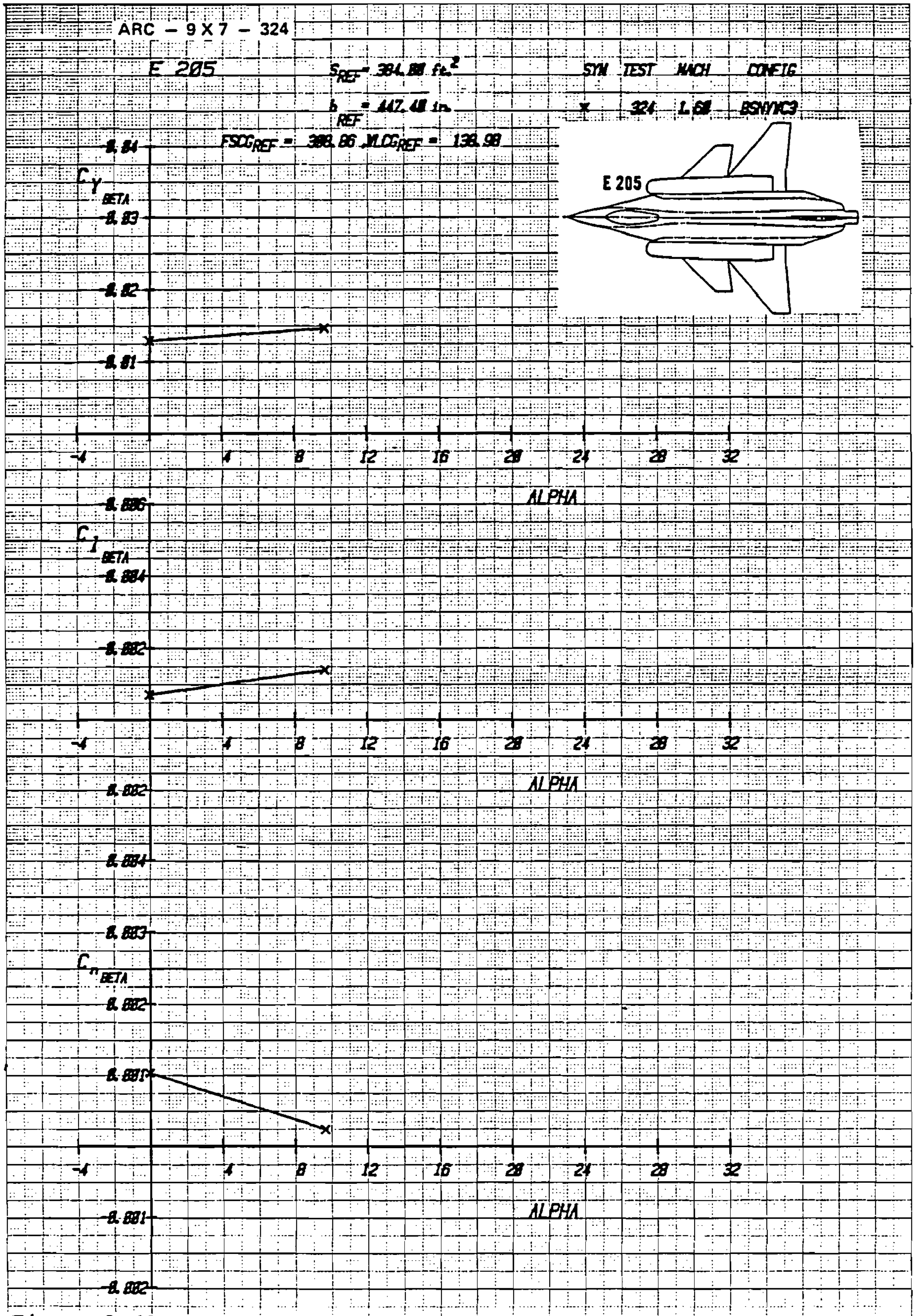

Figure 2-61 Vertical Tail Effectiveness for the E205 Configuration with Strake S_1, Canard C_3, Mach = 1.6

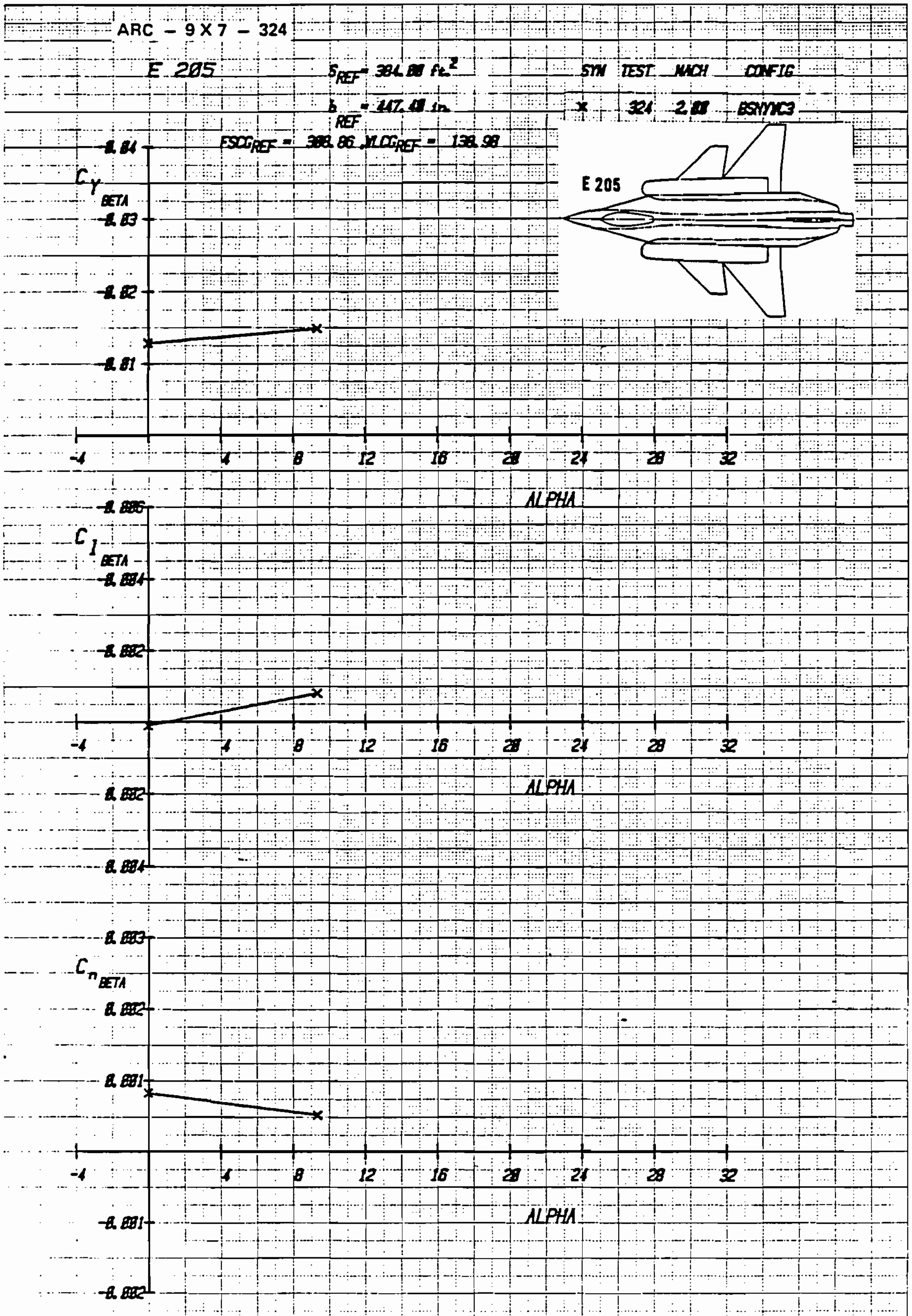

Figure 2-62 Vertical Tail Effectiveness for the E 205 Configuration with Strake S_1, Canard C_3, Mach = 2.0

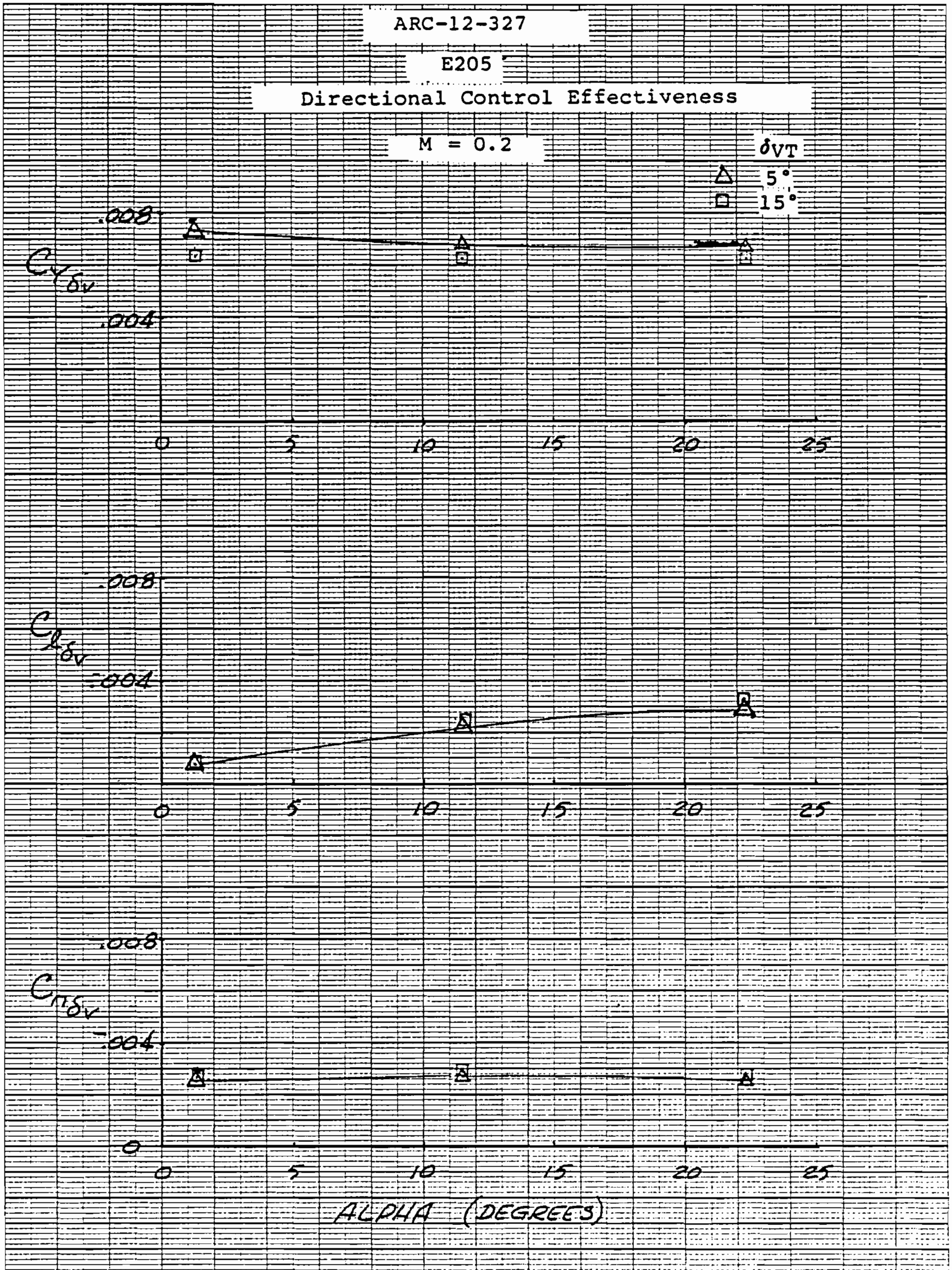

Figure 2-63 Directional Control Effectiveness of All Moving Vertical Tail, Mach = .2

E205
Vertical Tail Effectiveness

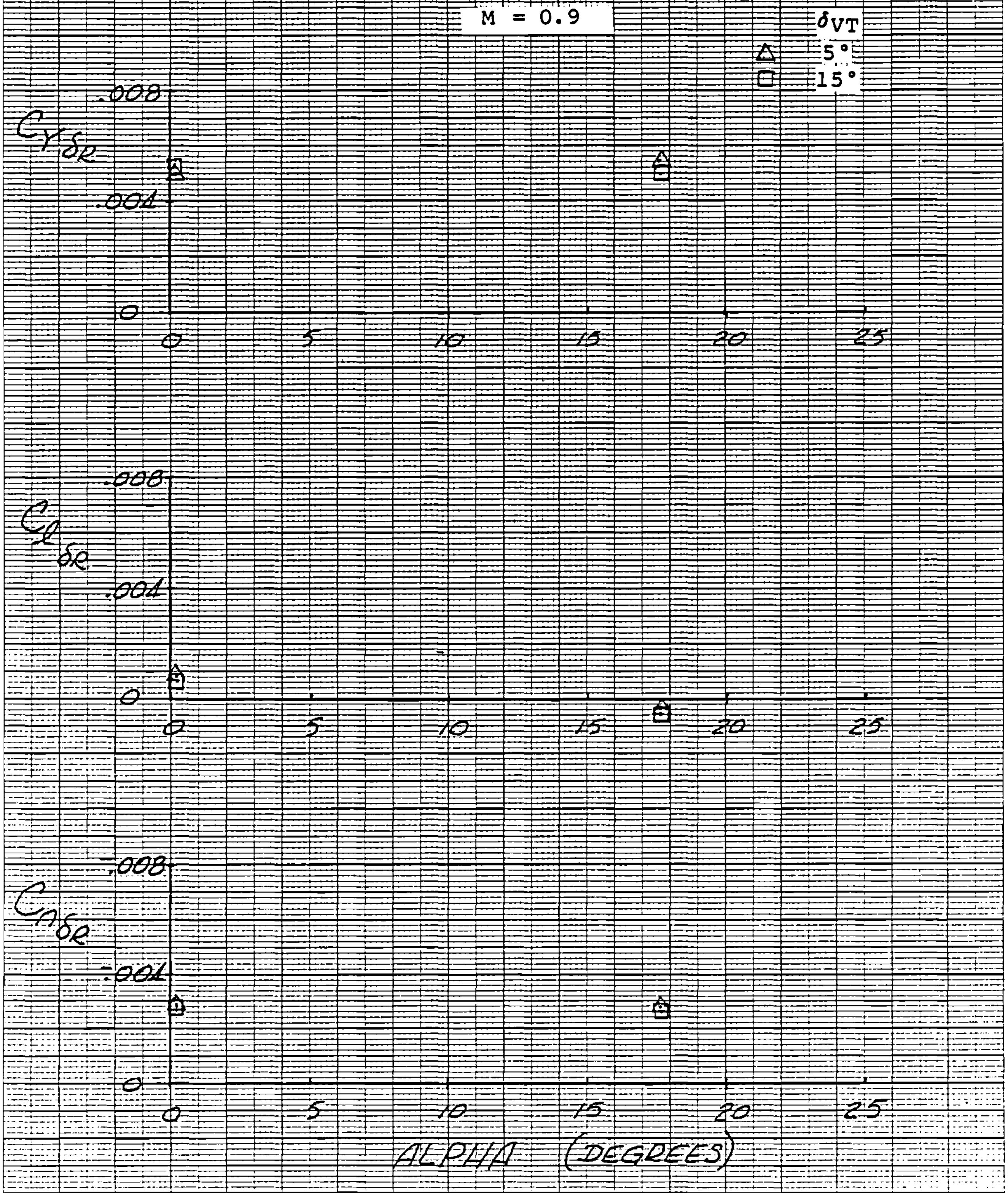

Figure 2-64 Effect of Vertical Tail Deflection, M = .9

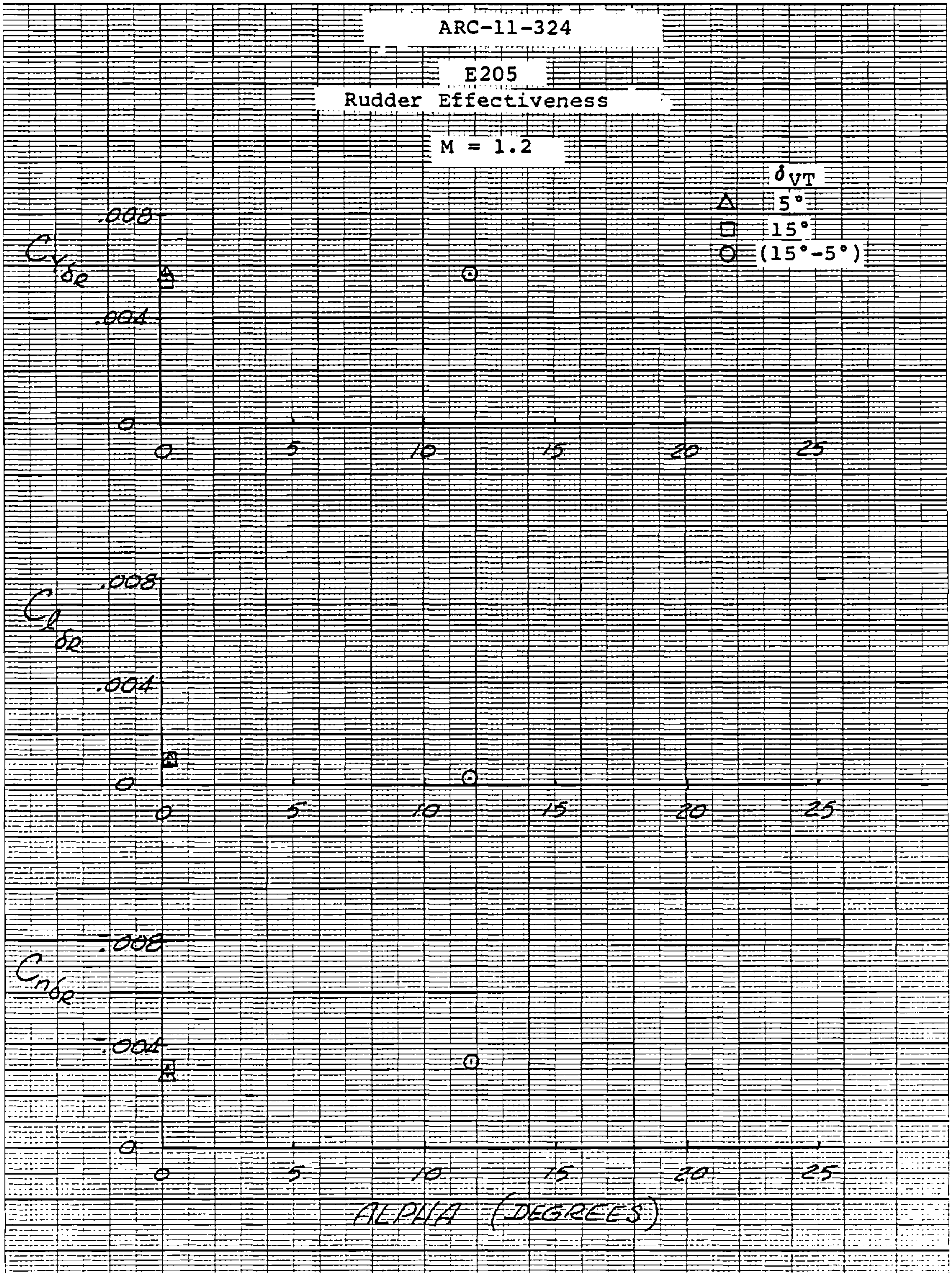

Figure 2-65 Effect of Vertical Tail Deflection, M = 1.2

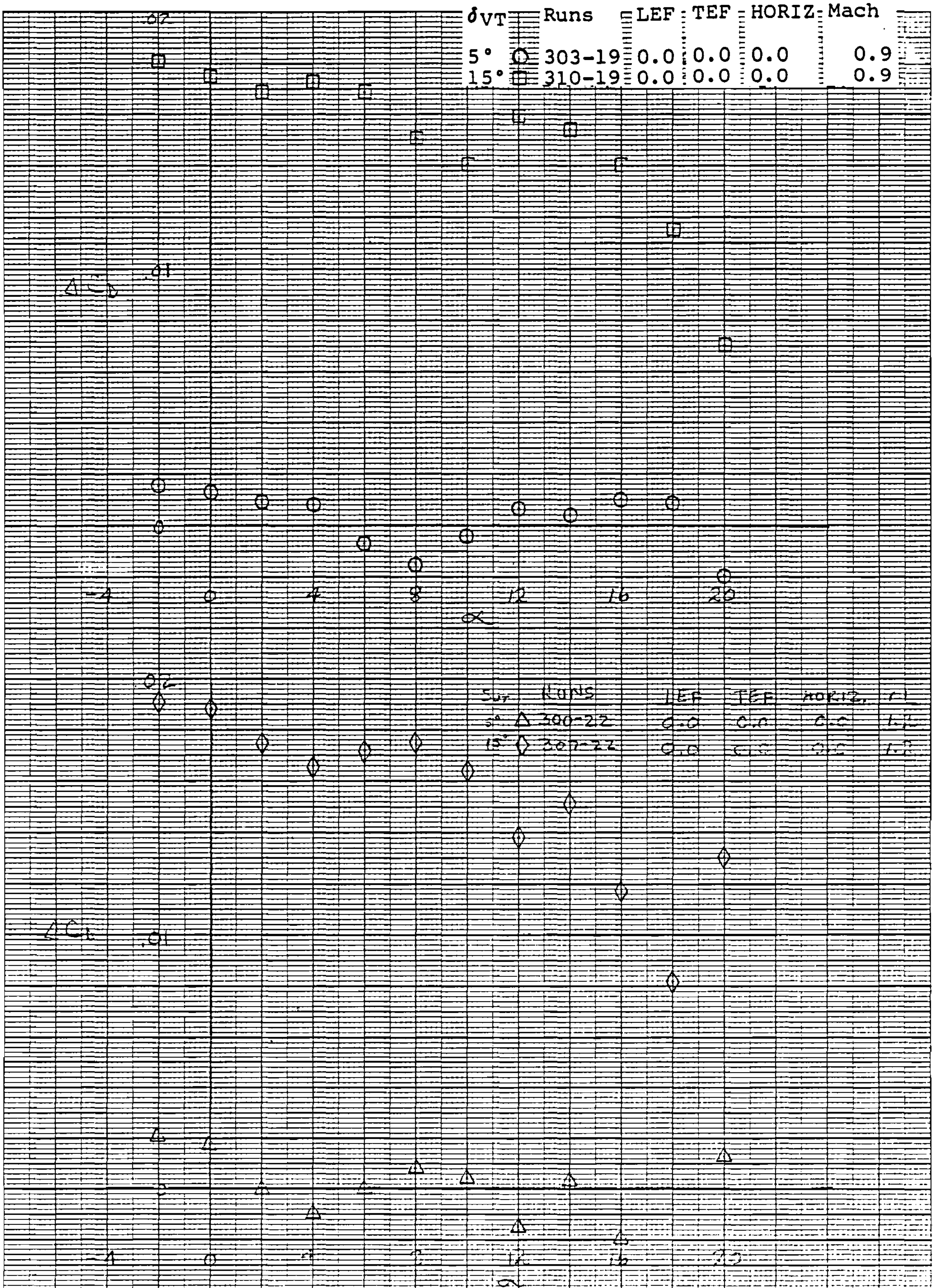

Figure 2-66 Incremental Effect of Vertical Tail Deflection on Drag, Mach = .9, Mach = 1.2

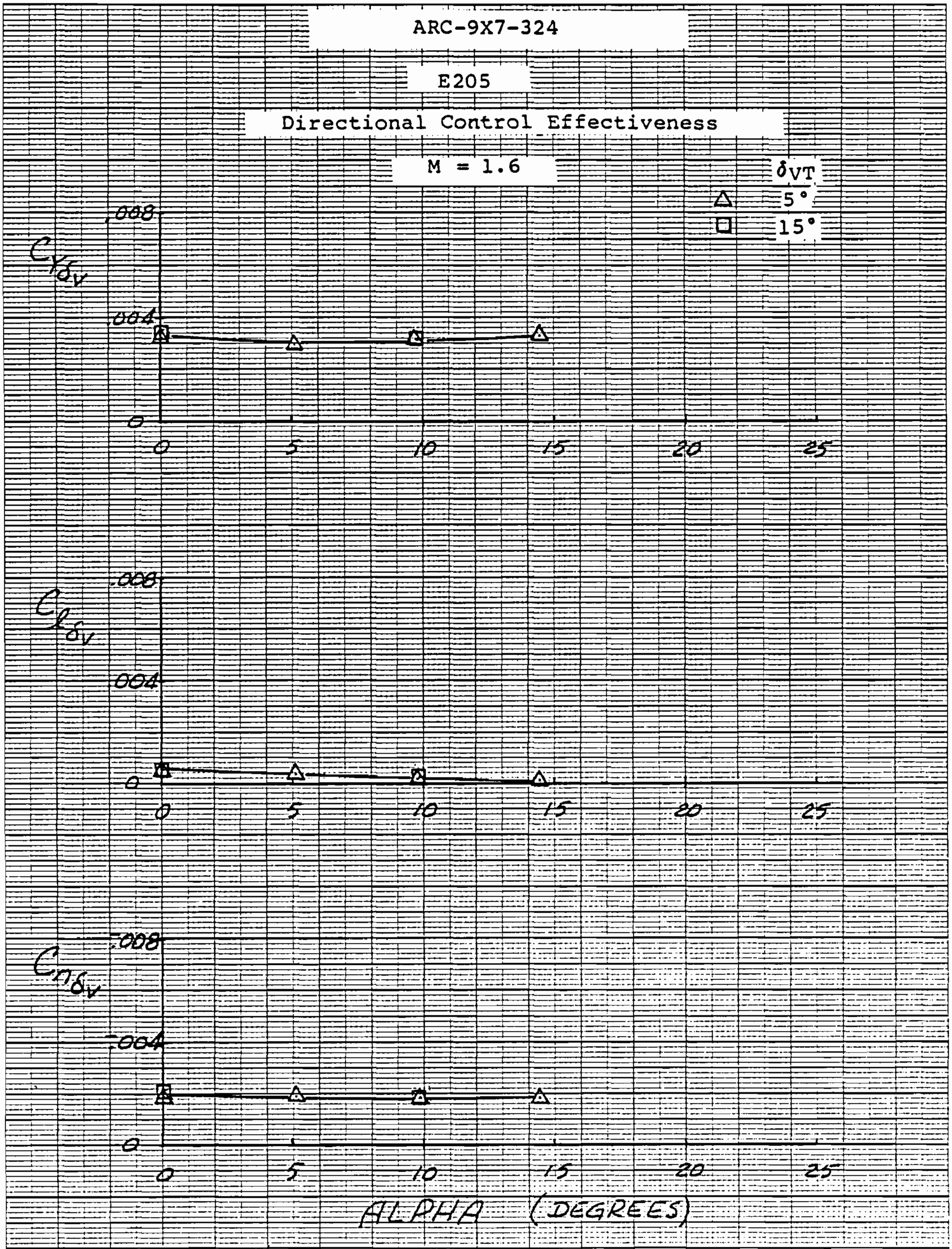

Figure 2-67 Vertical Tail Effectiveness for the E 205 Baseline Configuration, Mach = 1.6

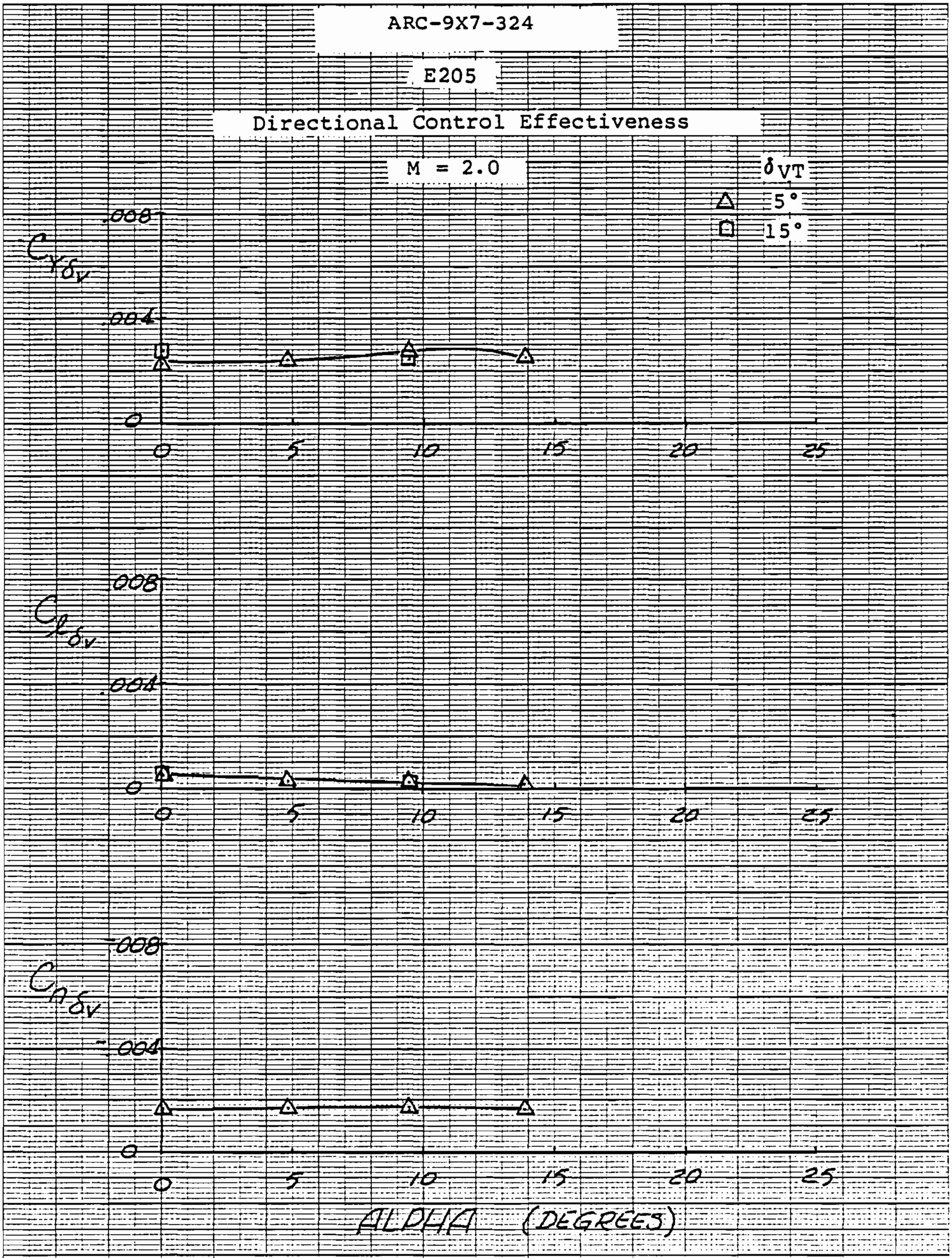

Figure 2-68 Vertical Tail Effectiveness for the E205 Baseline Configuration, Mach = 2.0

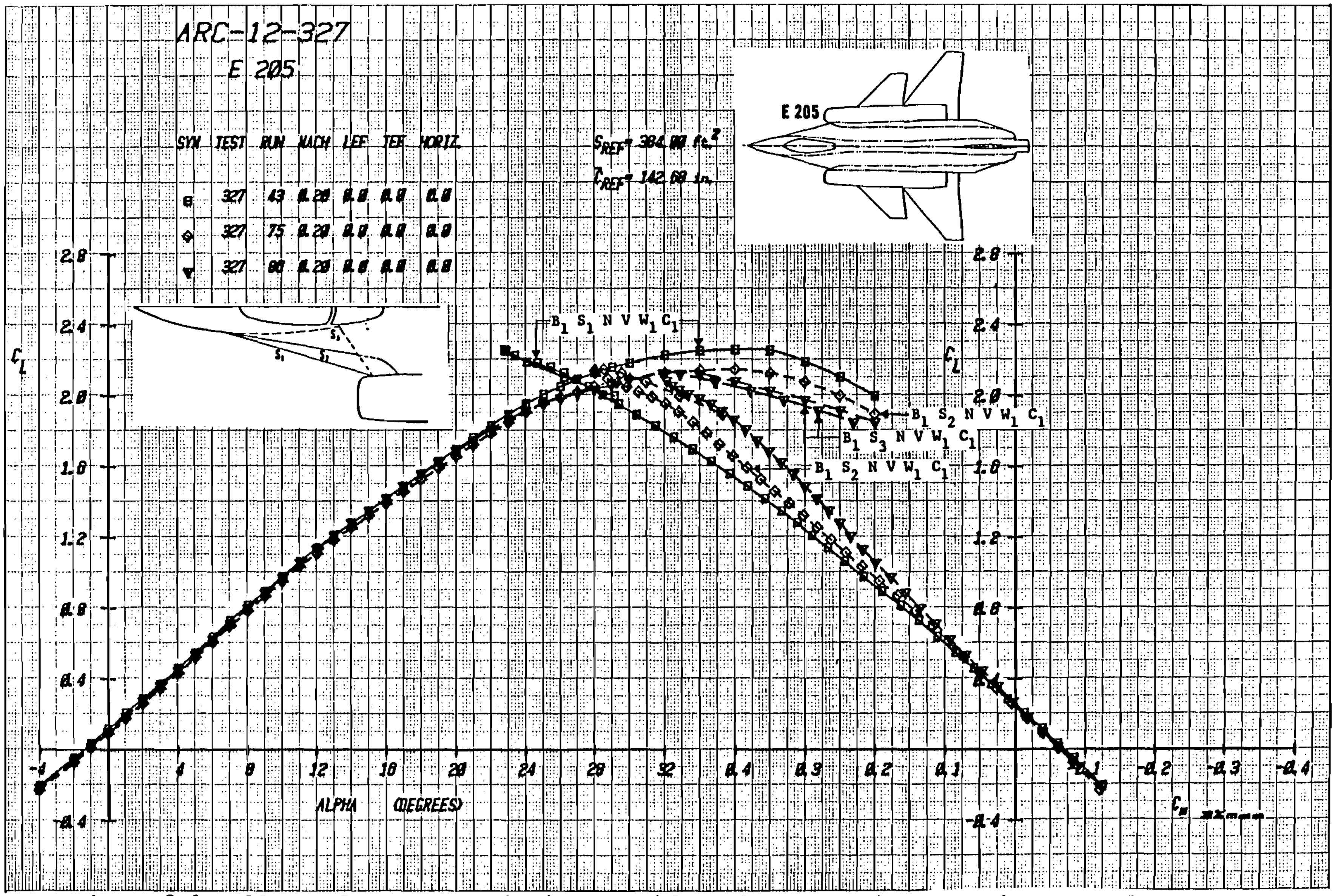

Figure 3-1a Effect of Strake Variation on Lift and Moment with Baseline Canard Longitudinal Location, C_1, and $\delta i = 0°$, Mach = .2

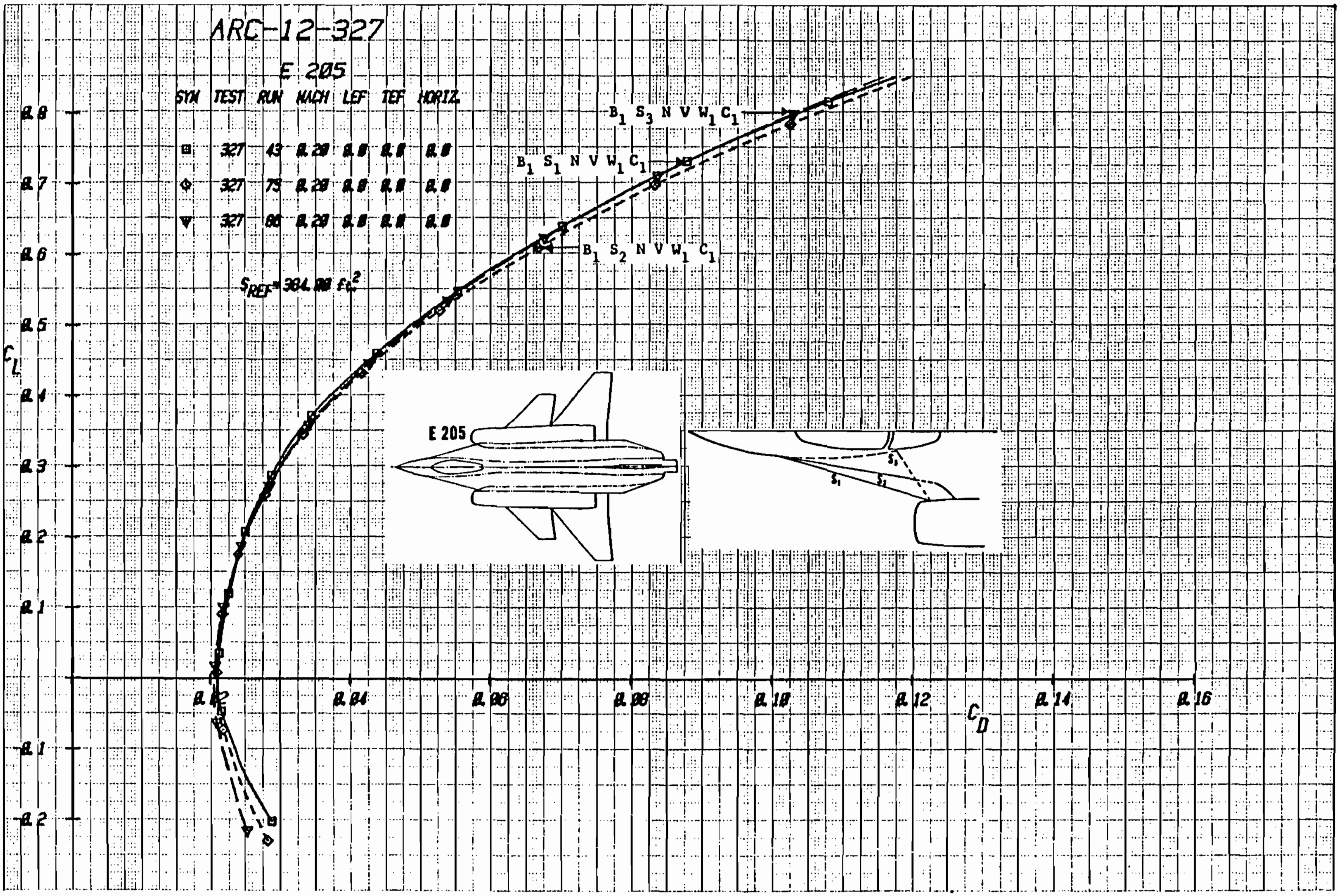

Figure 3-1b Effect of Strake Variation on Drag with Baseline Canard Longitudinal Location, C_1, and $\delta i = 0°$, (Expanded Drag Scale), Mach = .2

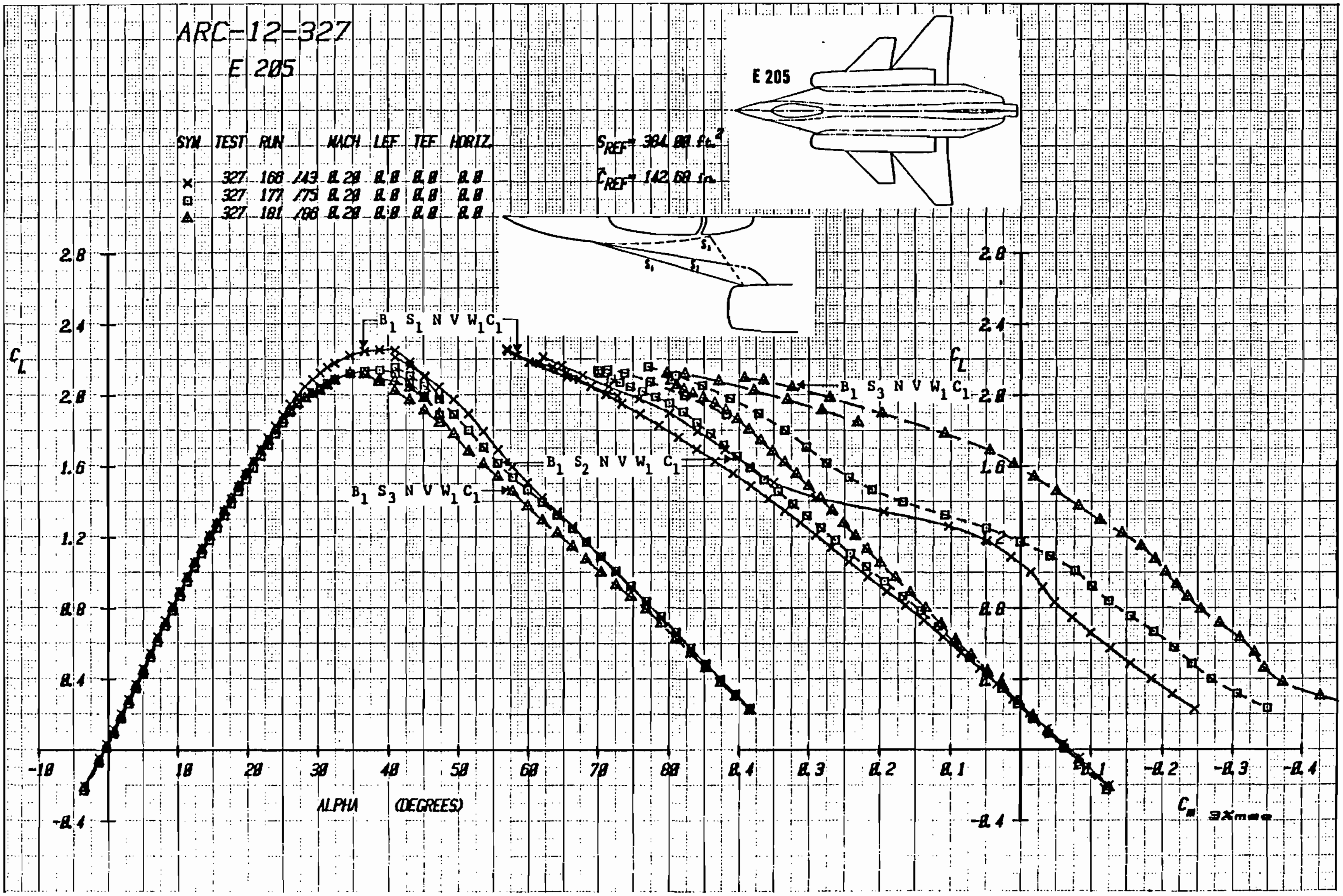

Figure 3-2a Effect of Strake Shape with Baseline Canard Location, C_1, on E205 Lift and Pitching Moment (α = 0° to 90°), δc = 0°, M = .2

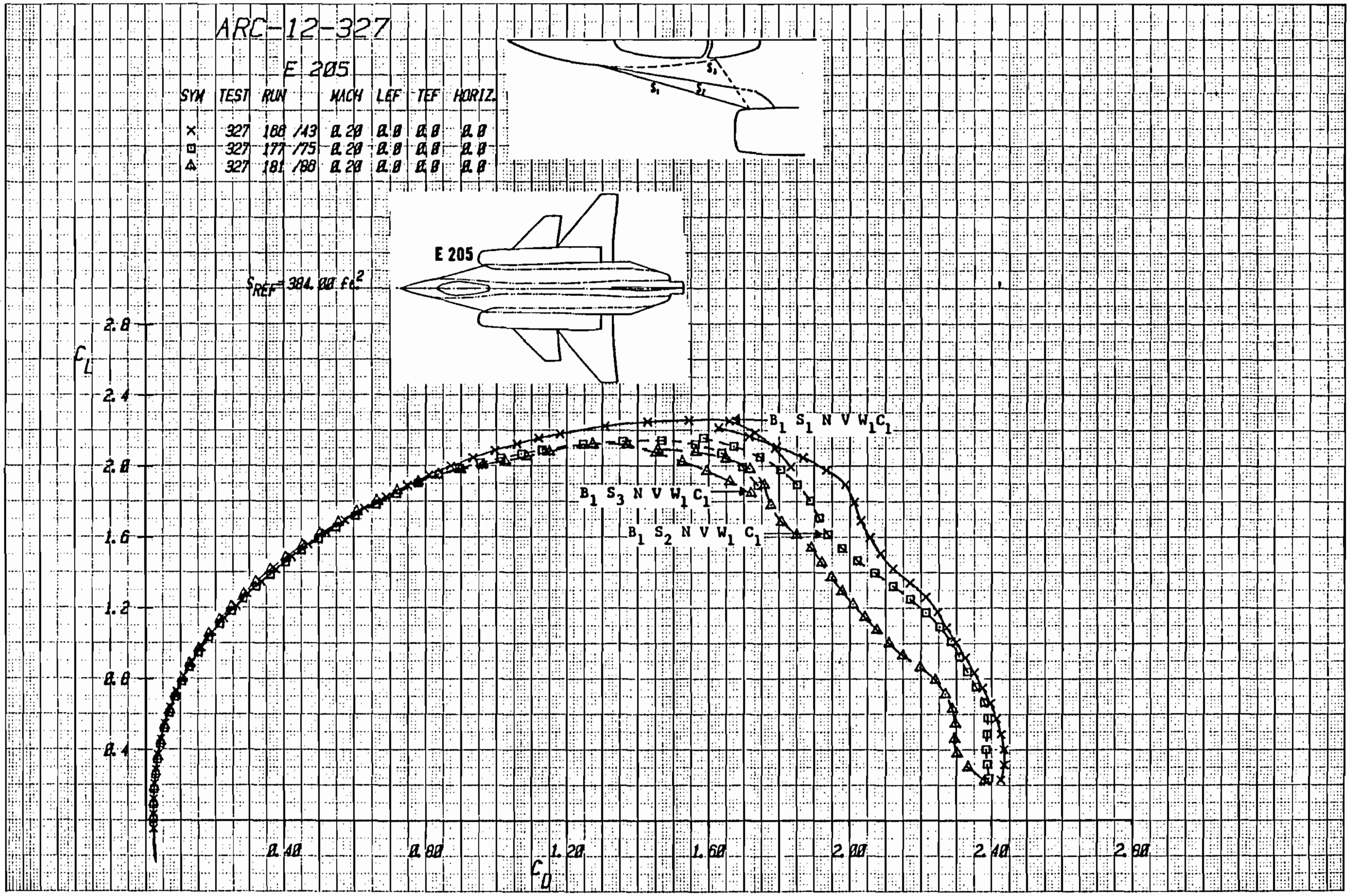

Figure 3-2b Effect of Strake Shape with Baseline Canard Location, C_1, on E205 Drag (α = 0° to 90°), δc = 0°, M = .2

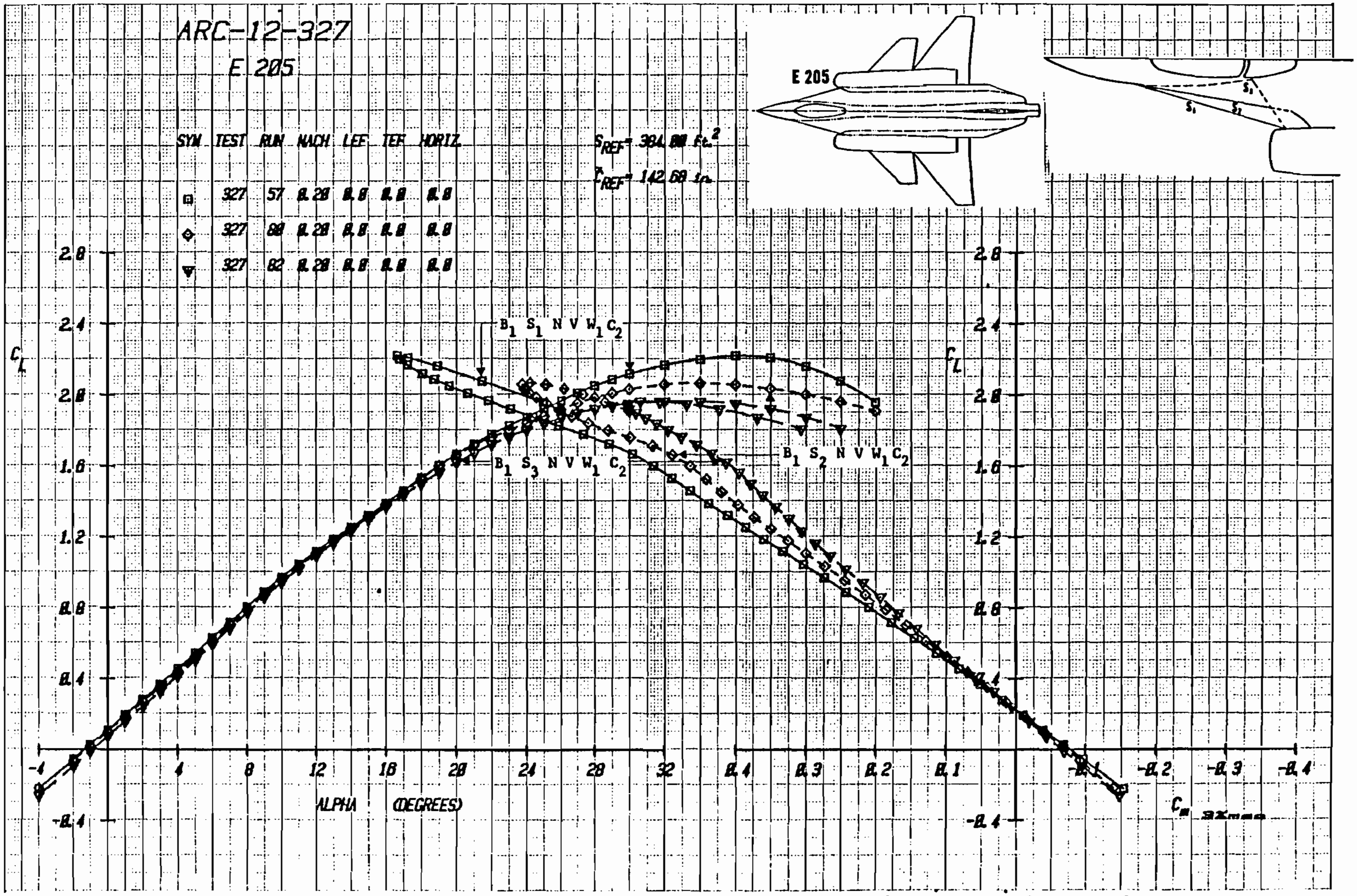

Figure 3-3a Effect of Strake Variation on Lift and Moment with Forward Canard Longitudinal Location, C_2, and $\delta i = 0°$, Mach = .2

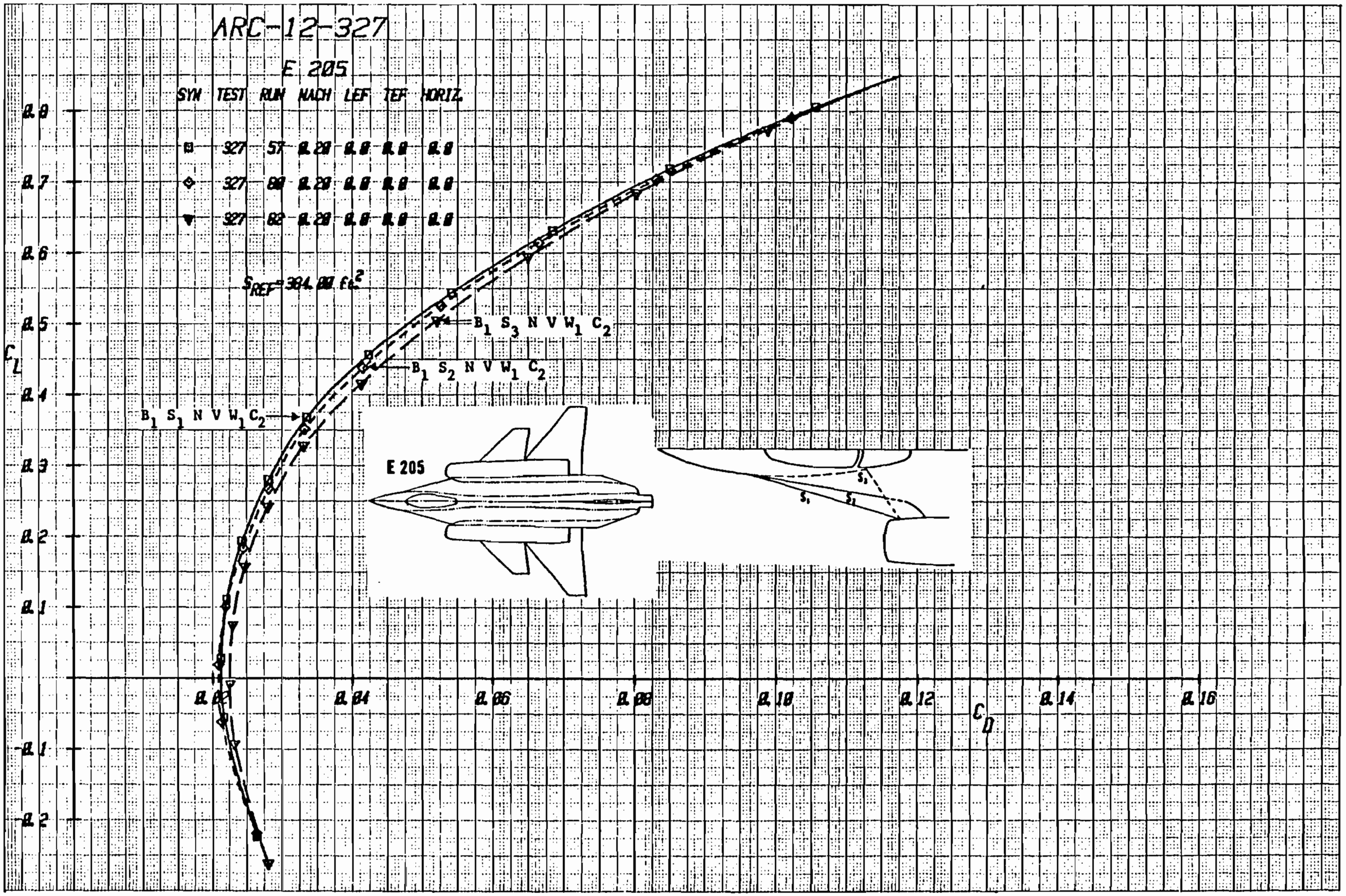

Figure 3-3b Effect of Strake Variation on Drag with Forward Canard Longitudinal Location, C_2, and δi = 0°, (Expanded Drag Scale), Mach = .2

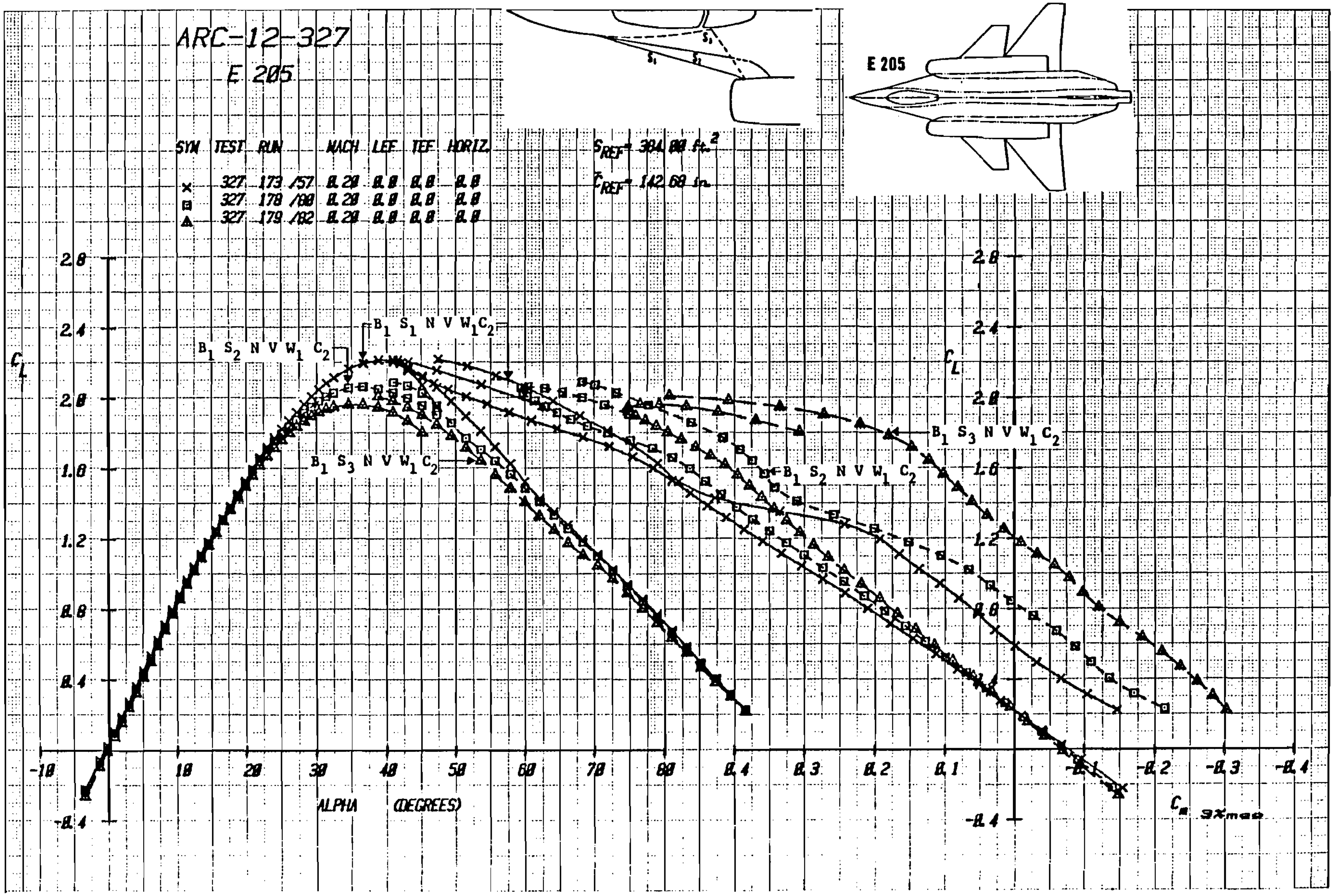

Figure 3-4a Effect of Strake Shape with Forward Canard Location on E205 Lift and Pitching Moment (α = 0° to 90°), δ_c = 0°, M = .2

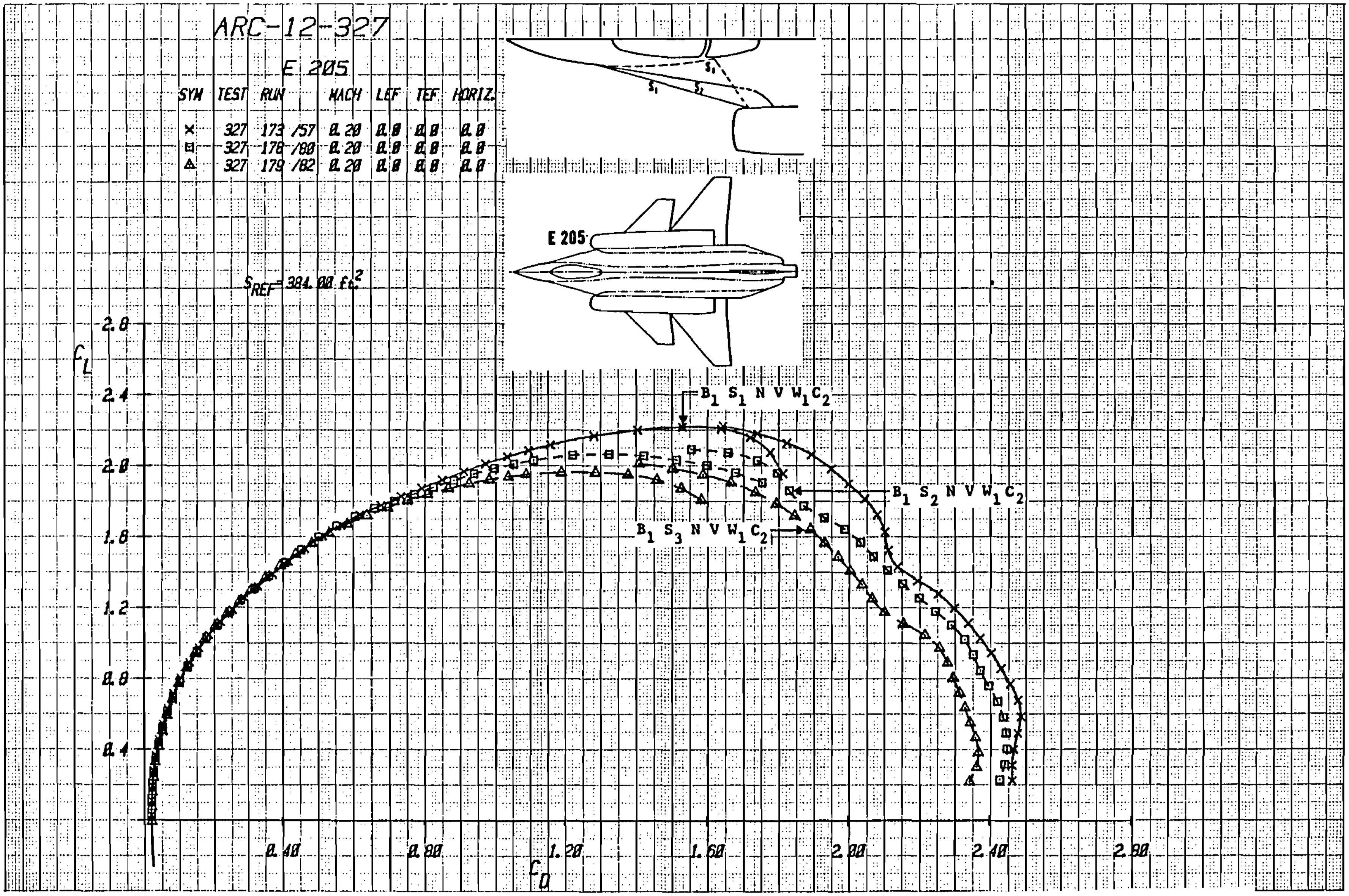

Figure 3-4b Effect of Strake Shape with Forward Canard Location on E205 Drag (α = 0° to 90°), δ_c = 0°, M = .2

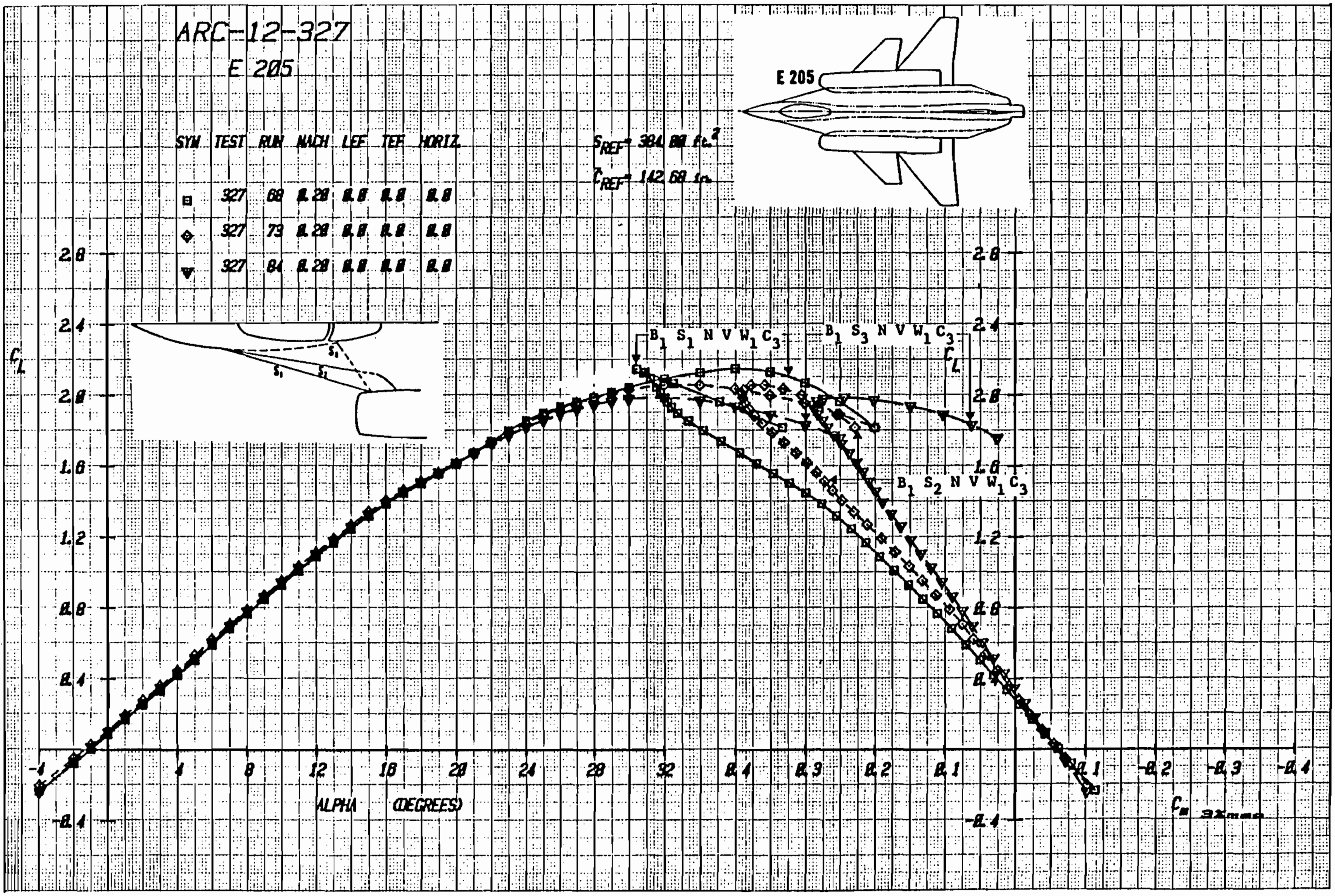

Figure 3-5a Effect of Strake Variation on Lift and Moment with Aft Canard Longitudinal Location, C_3, and $\delta i = 0°$, Mach = .2

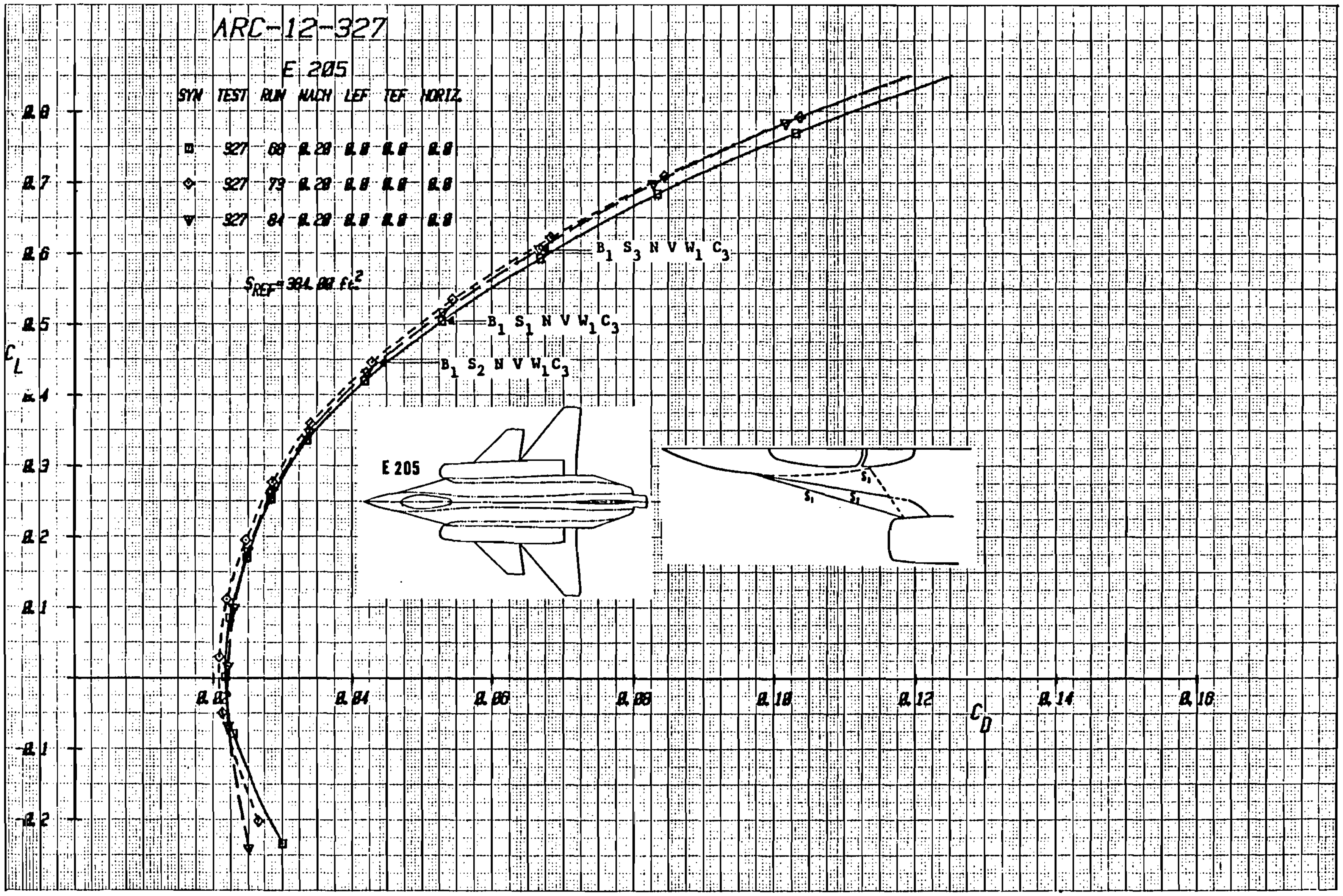

Figure 3-5b Effect of Strake Variation on Drag with Aft Canard Longitudinal Location, C_3, and $\delta i = 0°$, (Expanded Drag Scale), Mach = .2

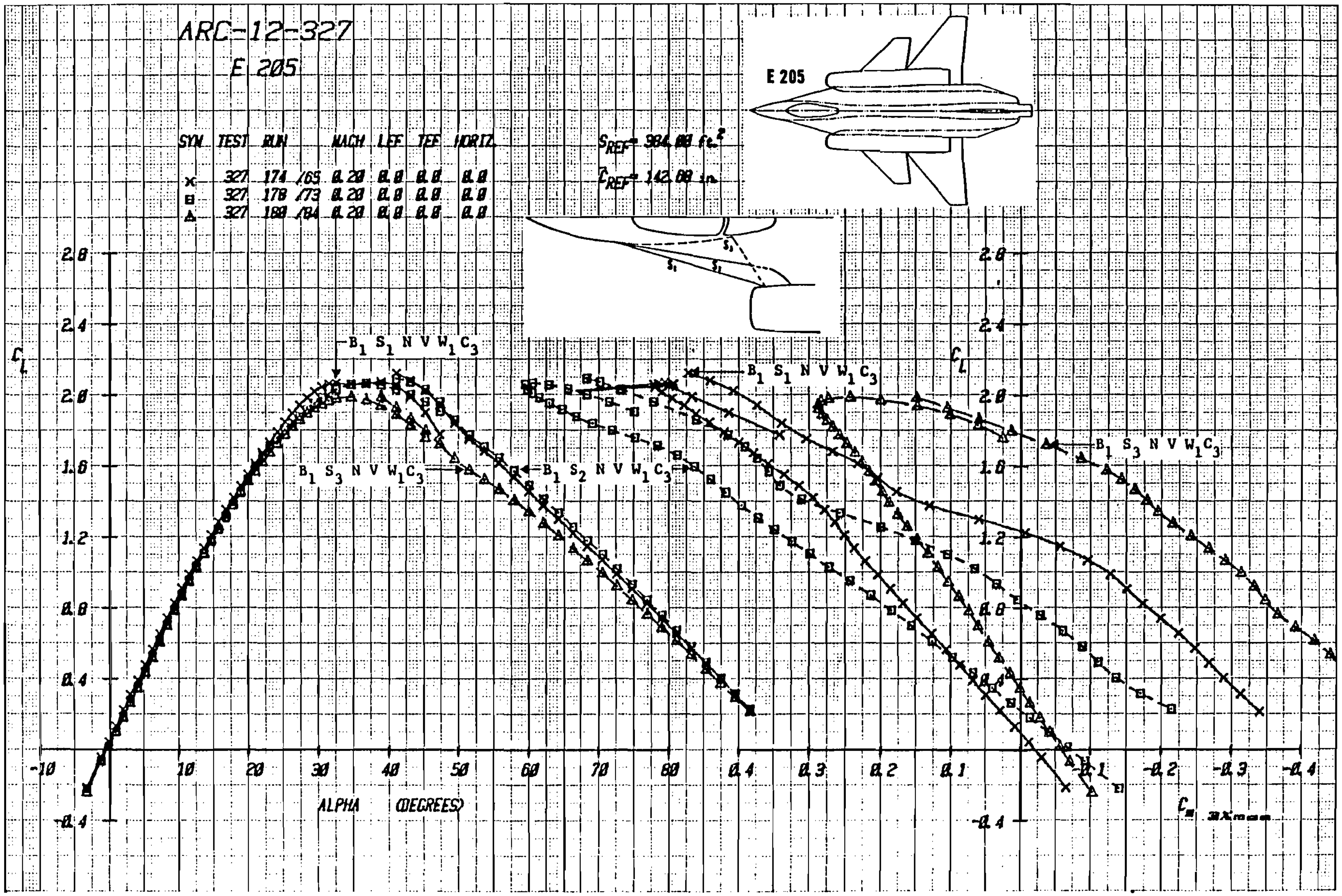

Figure 3-6a Effect of Strake Shape with Aft Canard Location, C_3, on E205 Lift and Pitching Moment (α = 0° to 90°), δ_c = 0°, M = .2

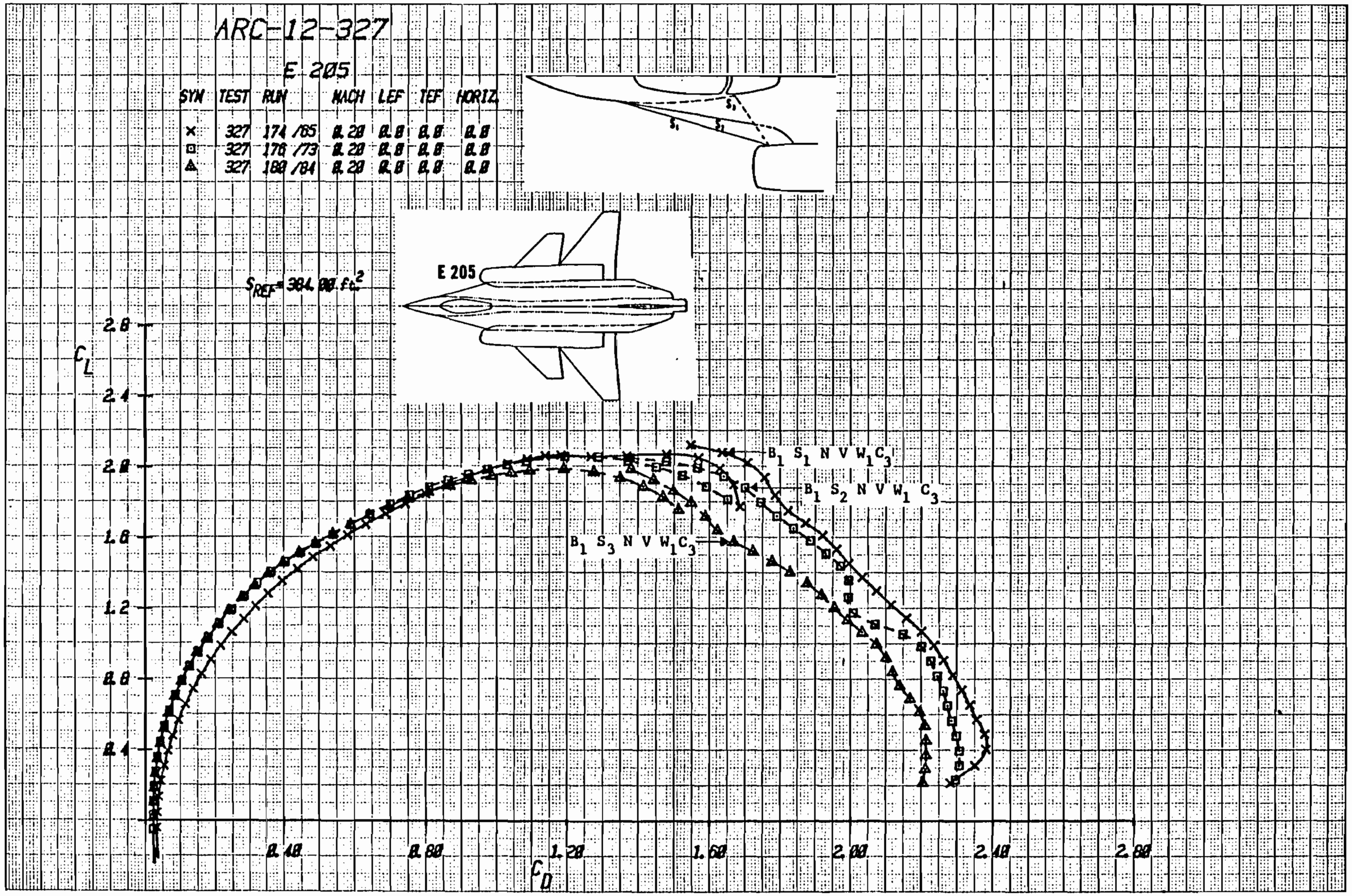

Figure 3-6b Effect of Strake Shape with Aft Canard Location, C_3, on E205 Drag (α = 0° to 90°), δc = 0°, M = .2

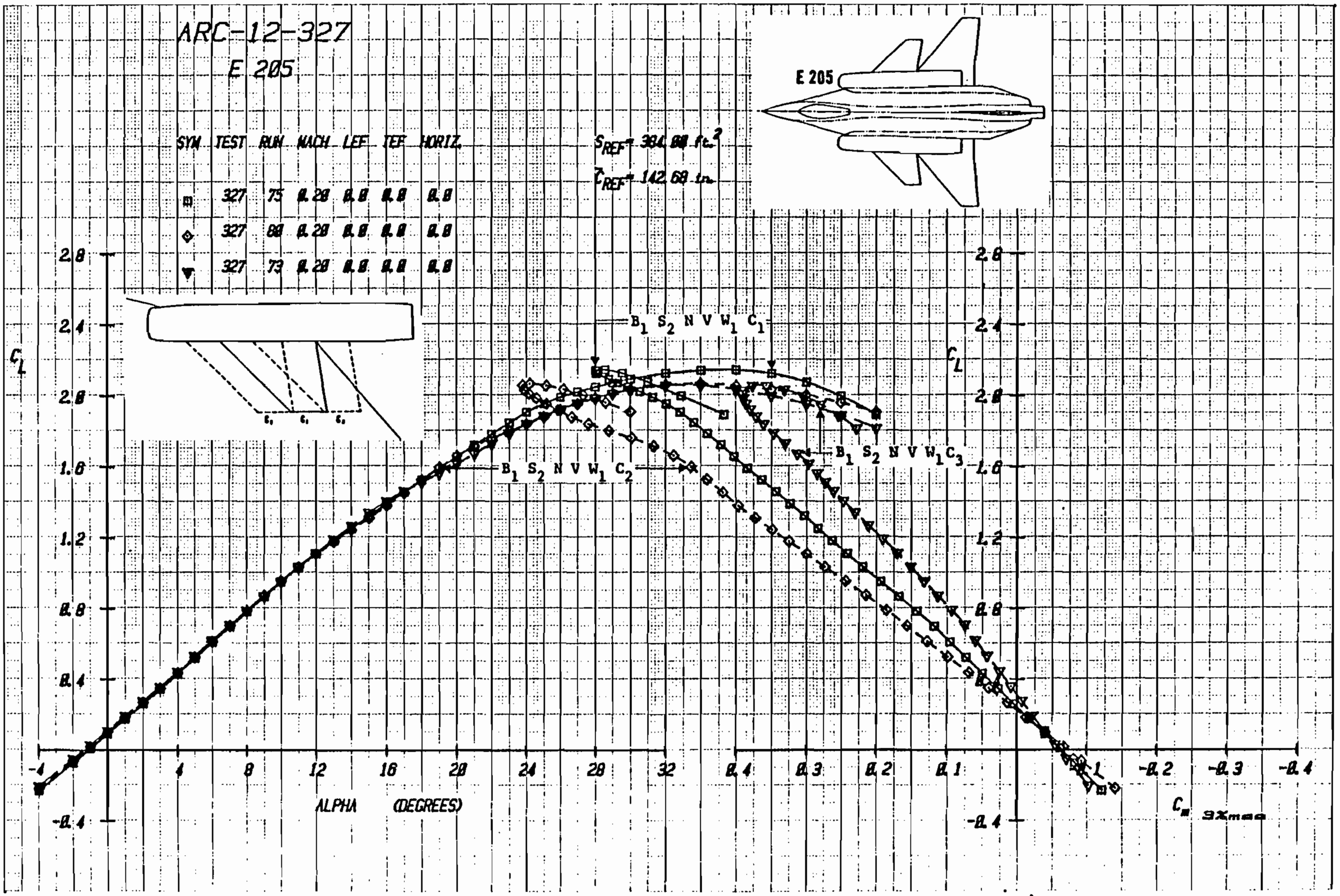

Figure 3-7a Effect of Canard Longitudinal Location on Lift and Moment with Strake S_2, Mach = .2

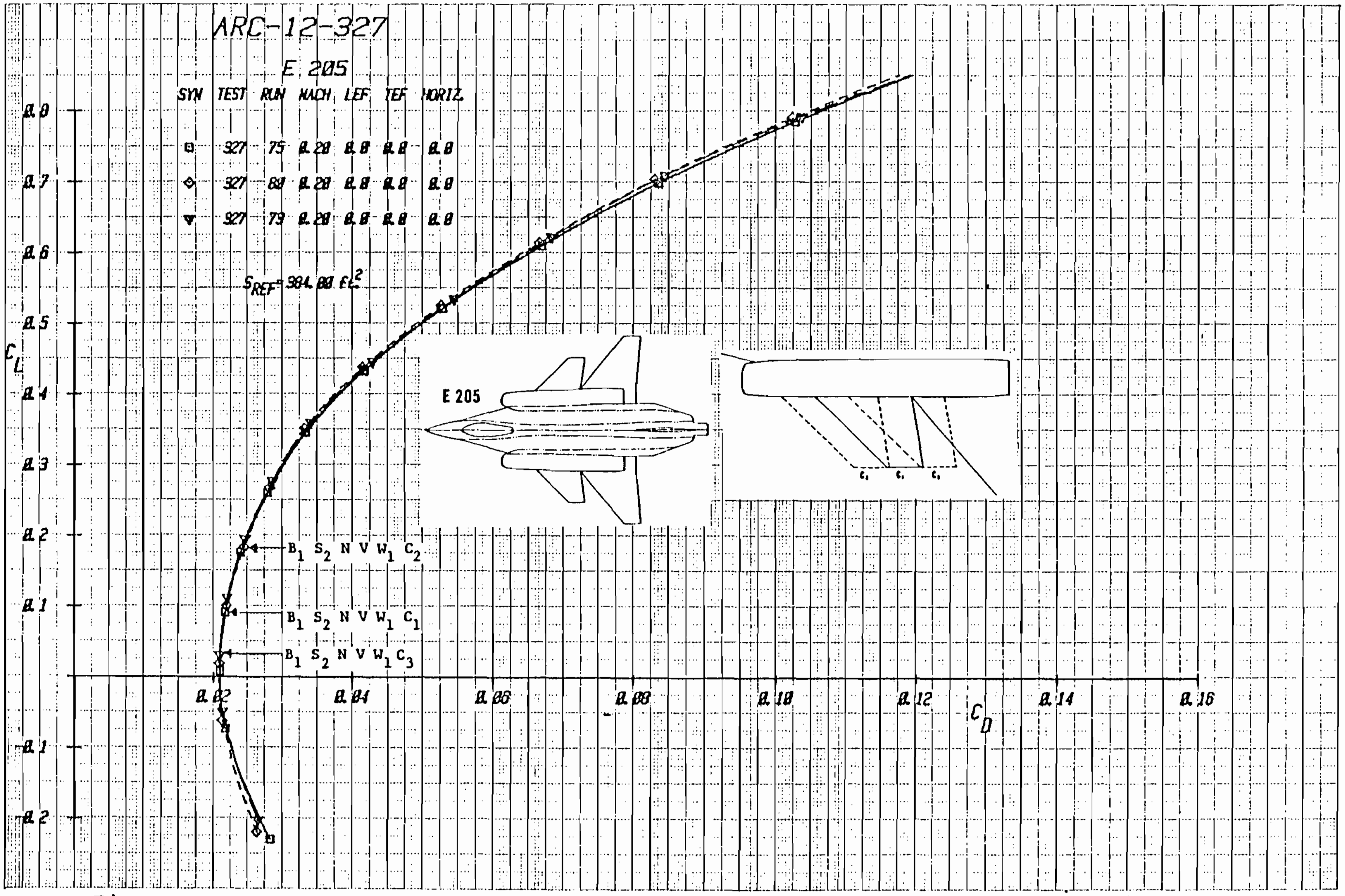

Figure 3-7b Effect of Canard Longitudinal Location on Drag with Strake S_2, (Expanded Drag Scale), Mach = .2

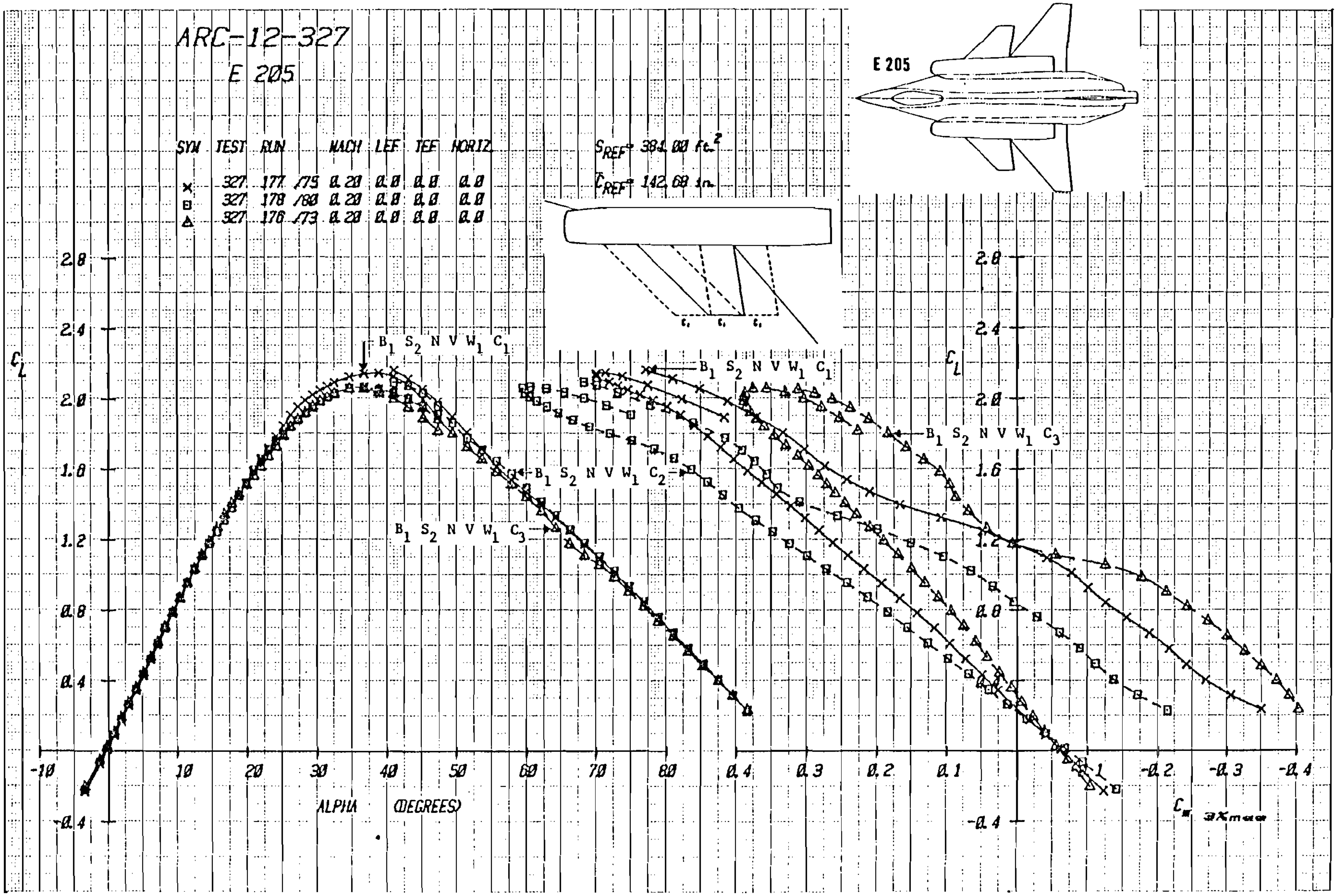

Figure 3-8a Effect of Canard Location with Strake S_2 on E205 Lift and Pitching Moment (α = 0° to 90°), δ_c = 0°, M = .2

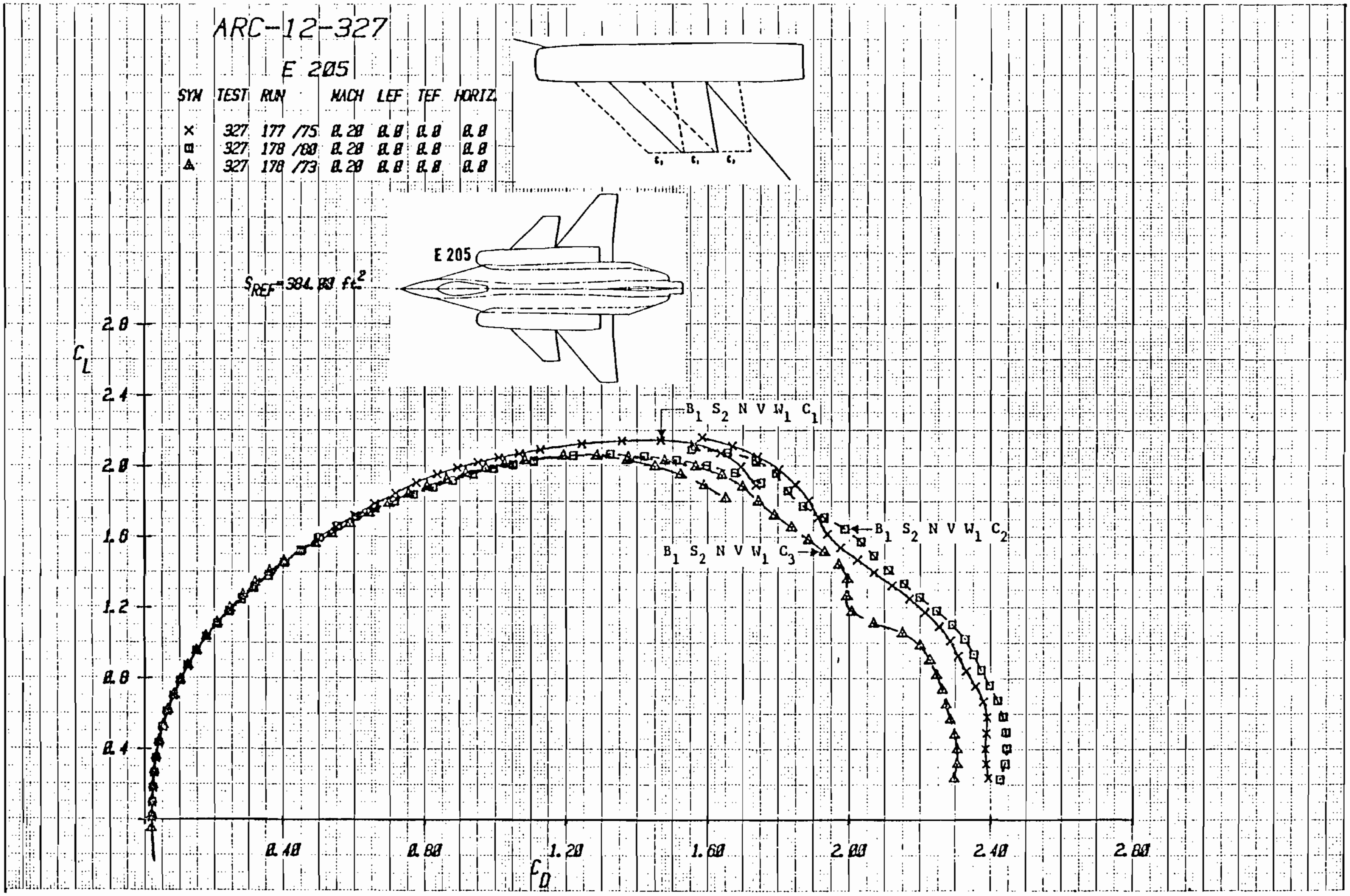

Figure 3-8b Effect of Canard Location with Strake S_2, on E205 Drag (α = 0° to 90°), δc = 0°, M = .2

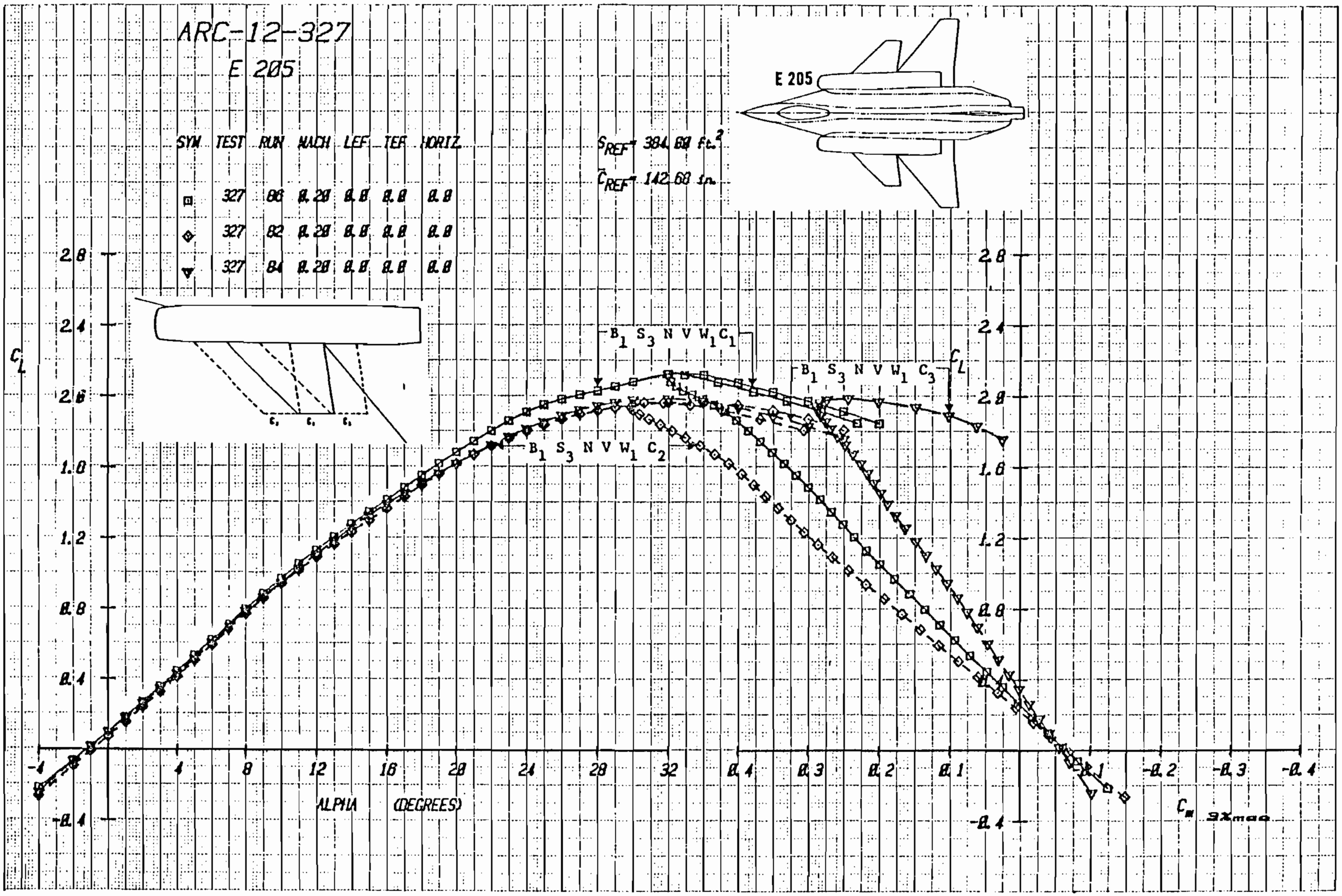

Figure 3-9a Effect of Canard Longitudinal Location on Lift and Moment with Strake S_3, Mach = .2

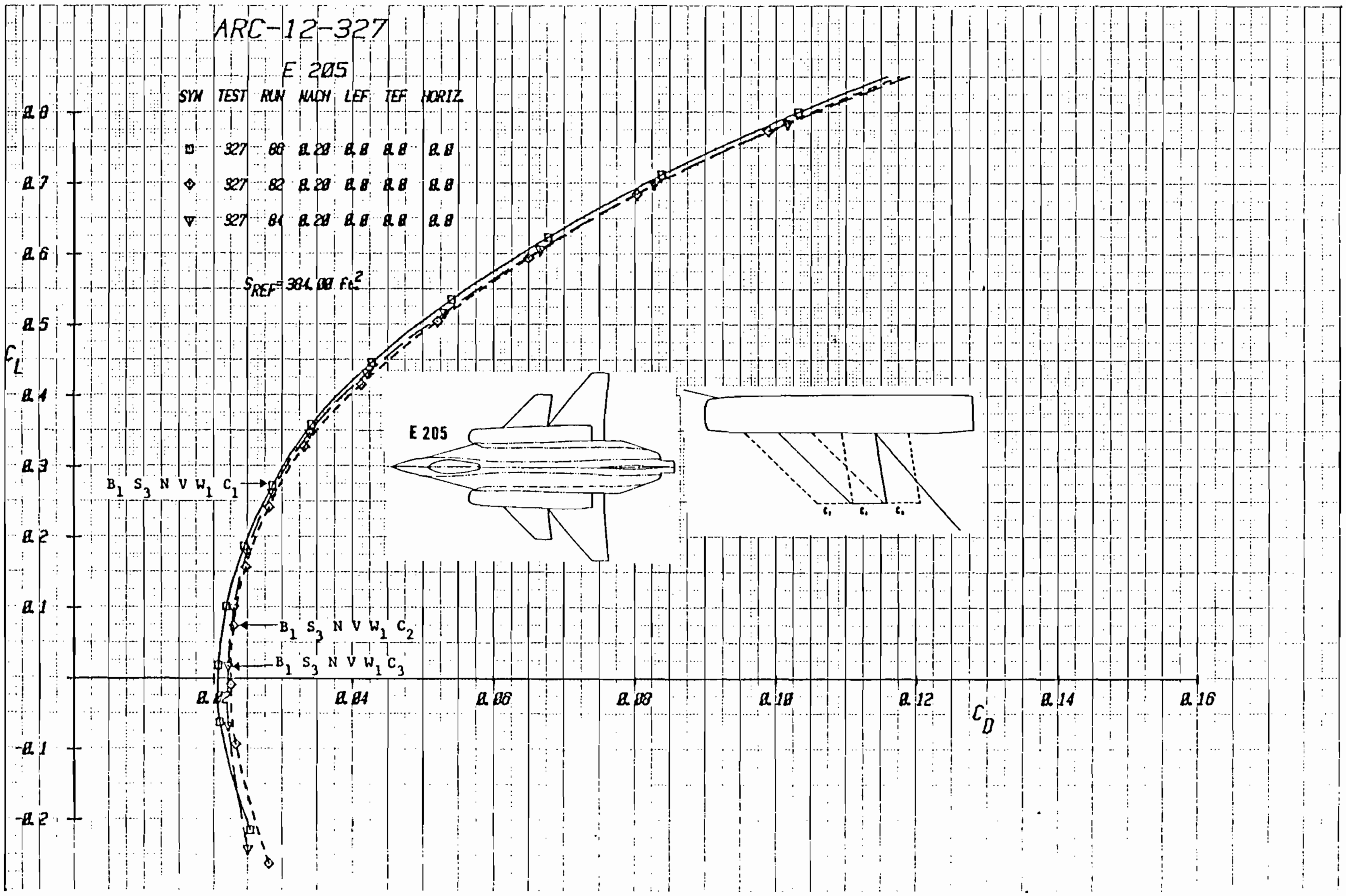

Figure 3-9b Effect of Canard Longitudinal Location on Drag with Strake S_3, (Expanded Drag Scale), Mach = .2

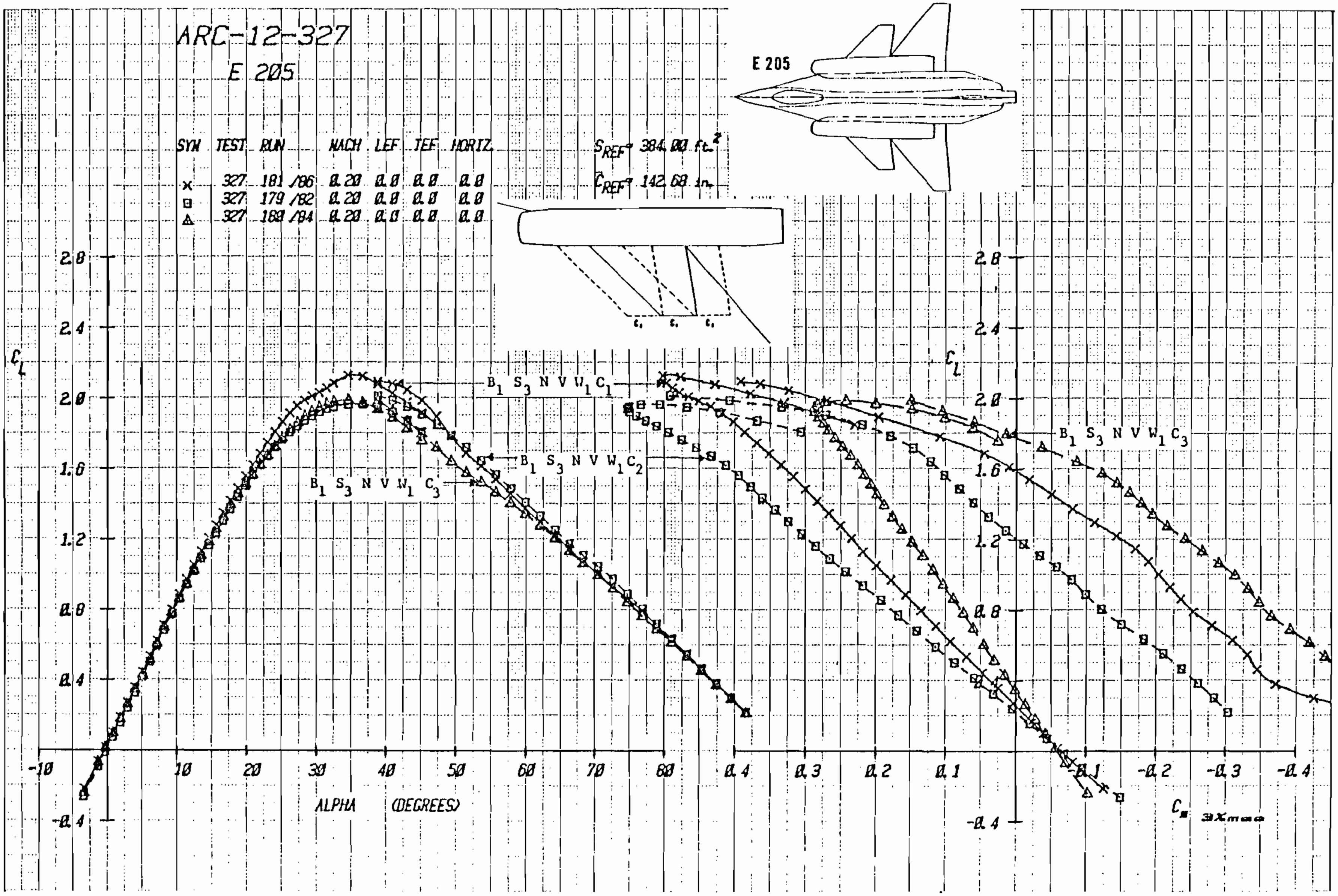

Figure3-10aEffect of Canard Location with Strake S_3, on E205 Lift and Pitching Moment (α = 0° to 90°), δc = 0°, M = .2

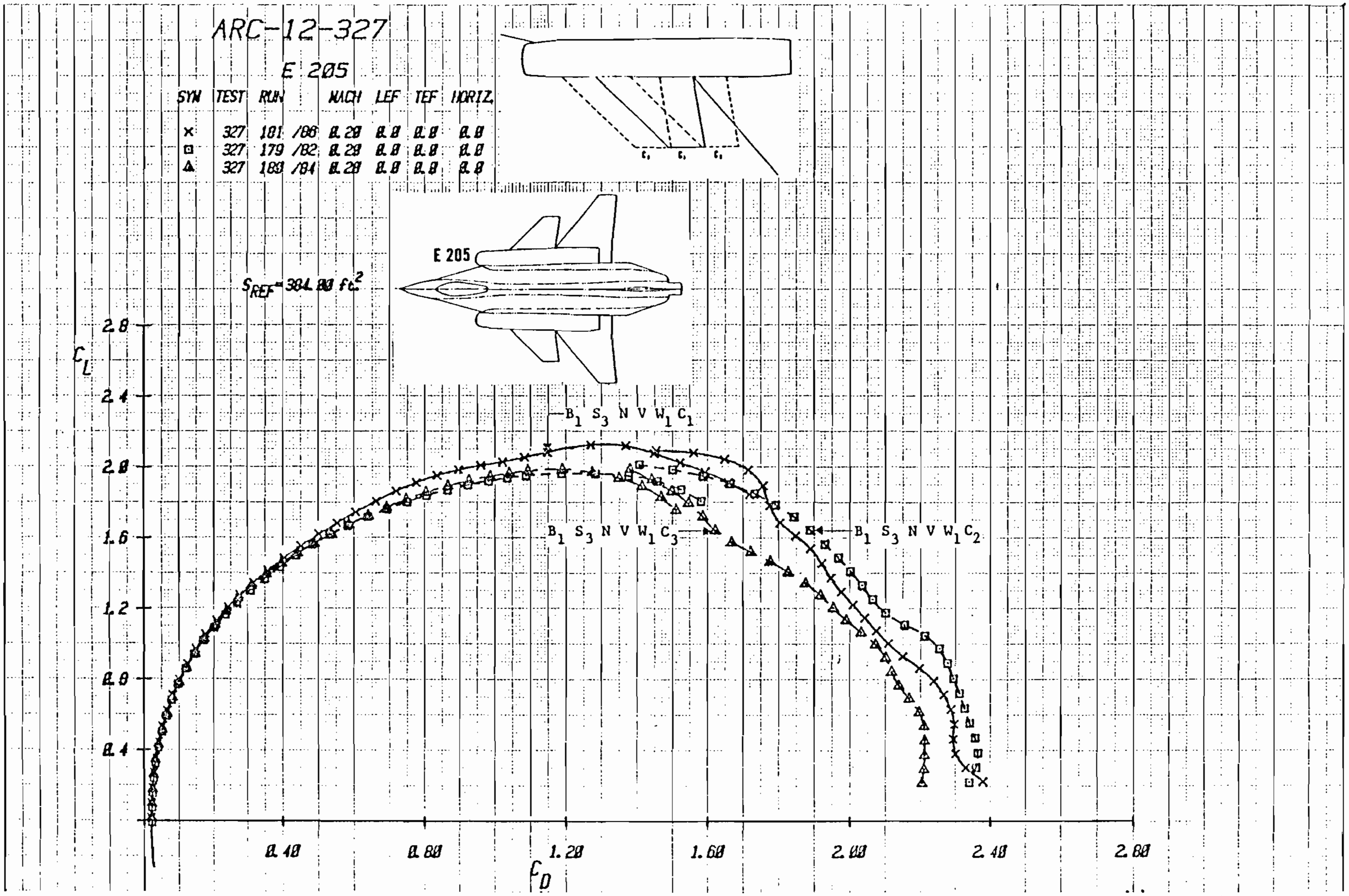

Figure3-10bEffect of Canard Location with Strake S_3 on E205 Drag (α = 0° to 90°), δc = 0°, M = .2

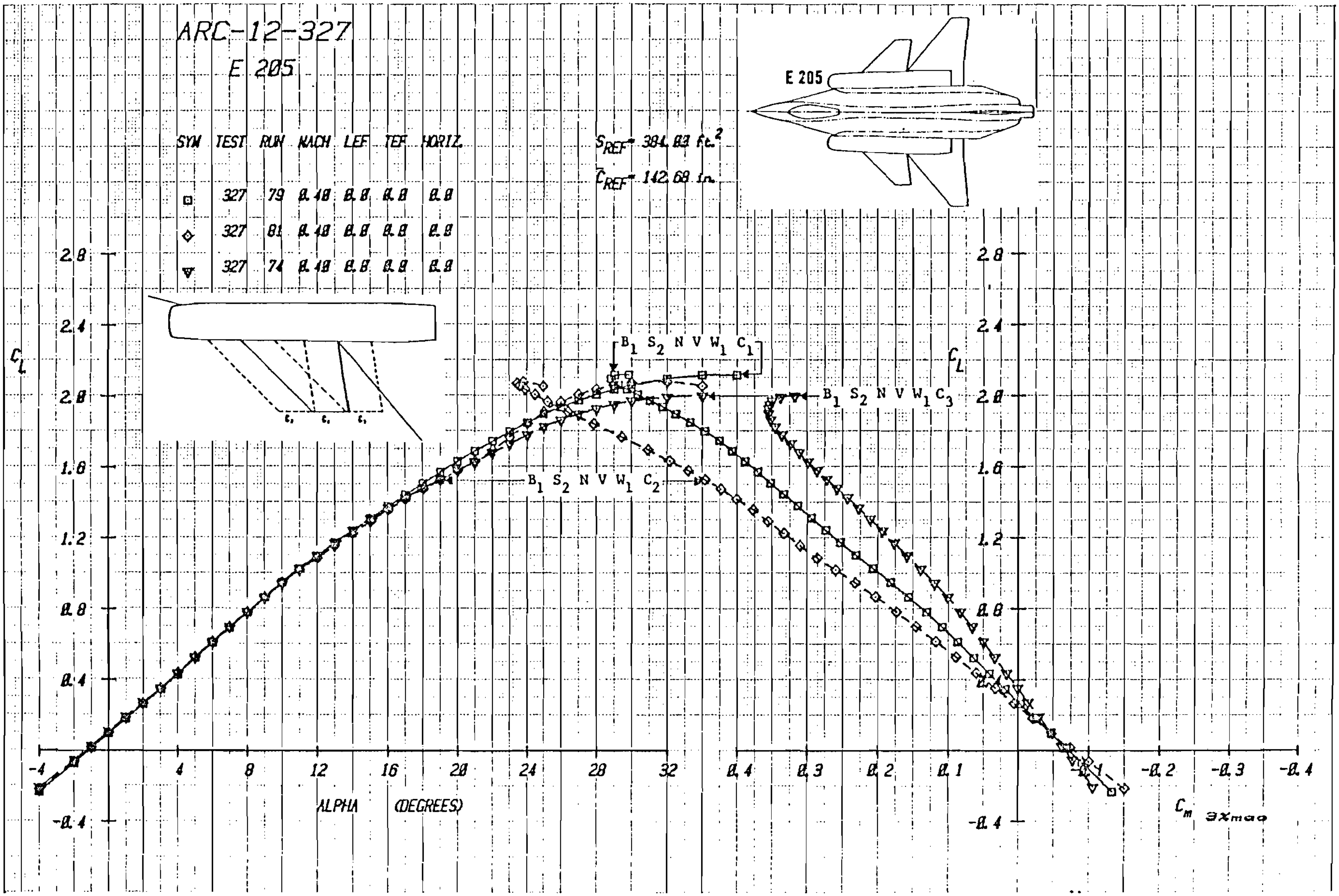

Figure3-11aEffect of Canard Longitudinal Location on Lift and Moment with Strake S_2, Mach = .4

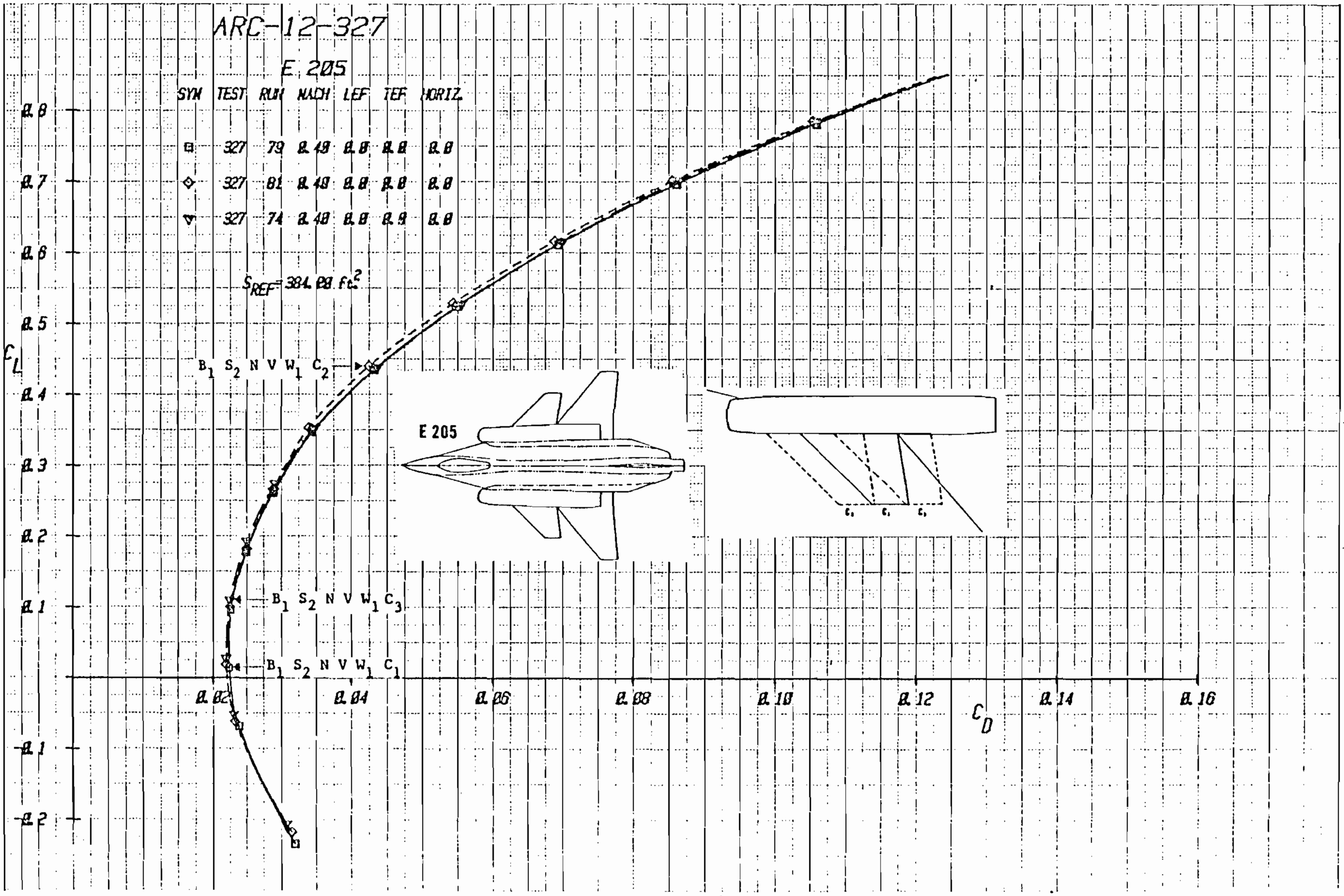

Figure3-11bEffect of Canard Longitudinal Location on Drag with Strake S_2, (Expanded Drag Scale), Mach = .4

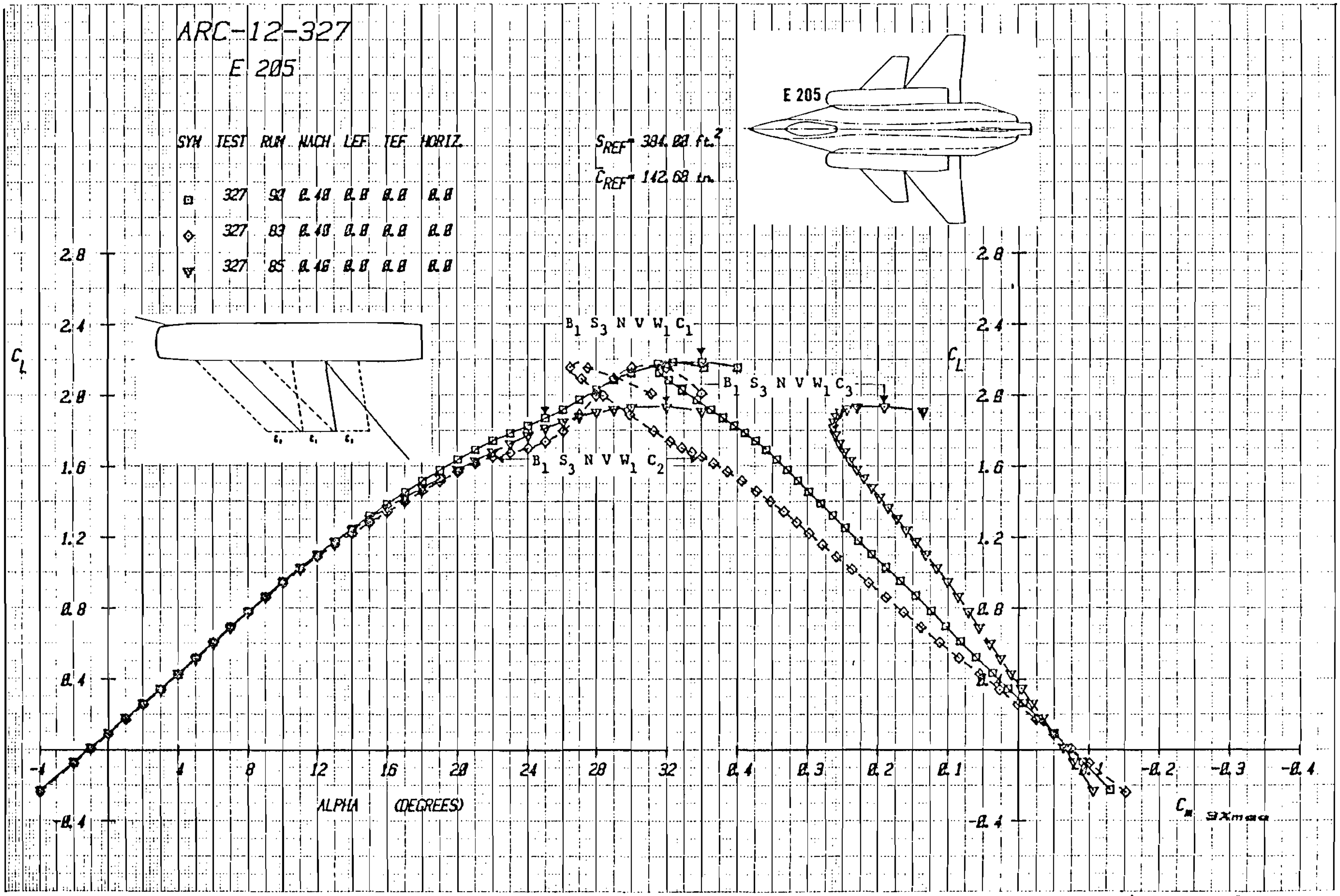

Figure3-12aEffect of Canard Longitudinal Location on Lift and Moment with Strake S_3, Mach = .4

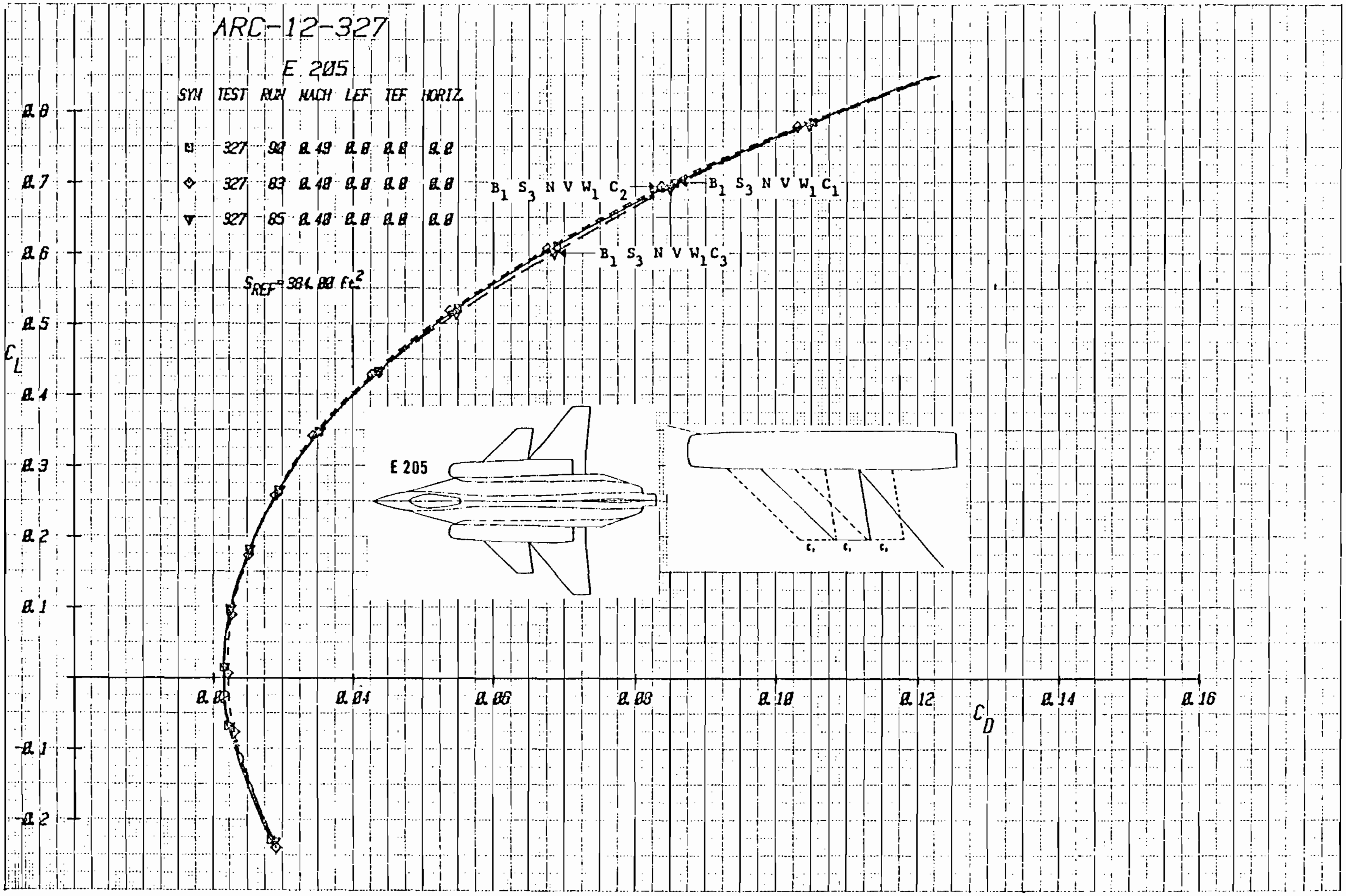

Figure3-12bEffect of Canard Longitudinal Location on Drag with Strake S_3, (Expanded Drag Scale), Mach = .4

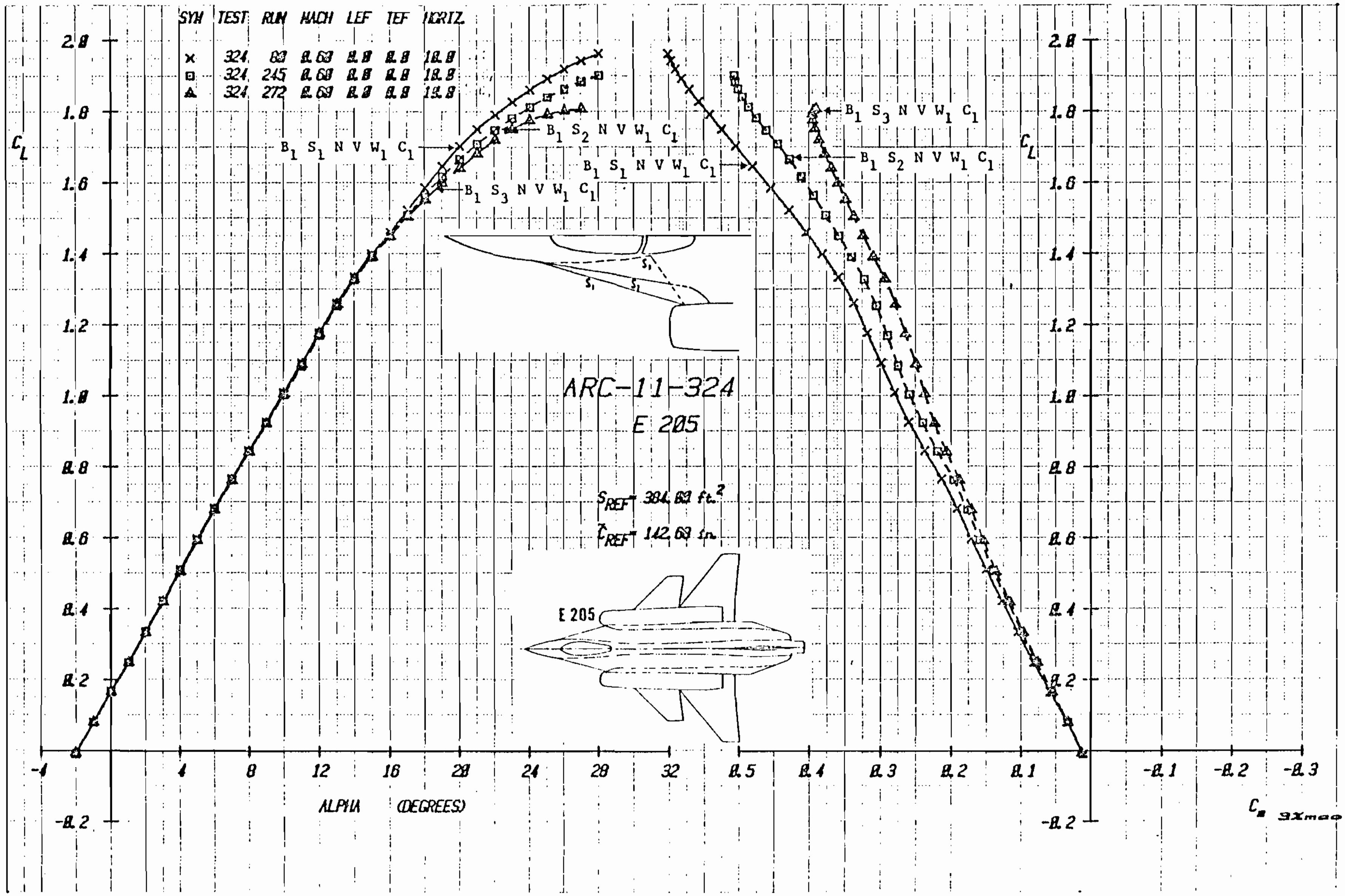

Figure3-13aEffect of Strake Shape on Lift and Moment with Canard C_1 Deflected +10°, Mach = .6

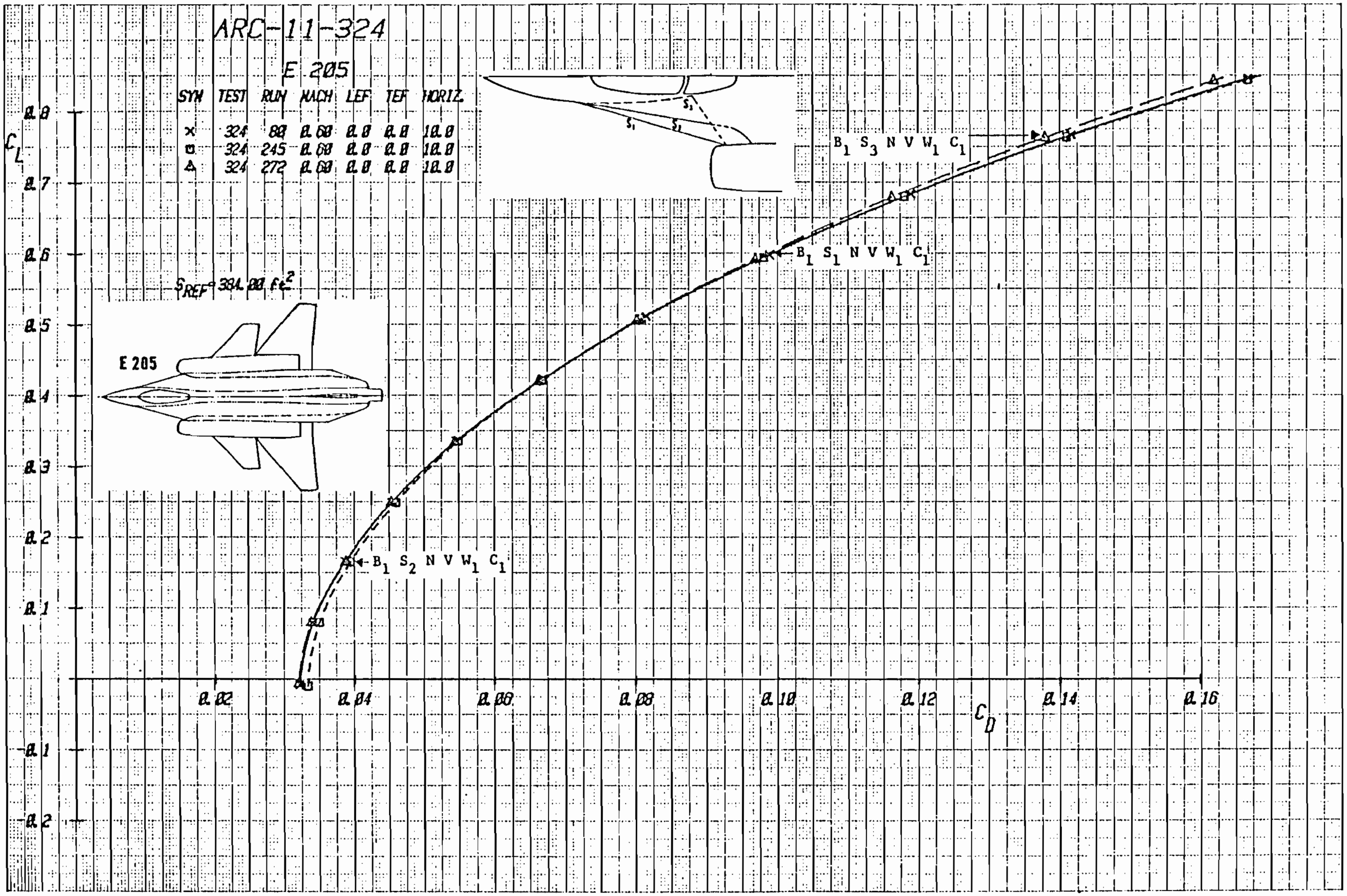

Figure3-13bEffect of Strake Shape on Drag with Canard C_1 Deflected + 10°, Mach = .6

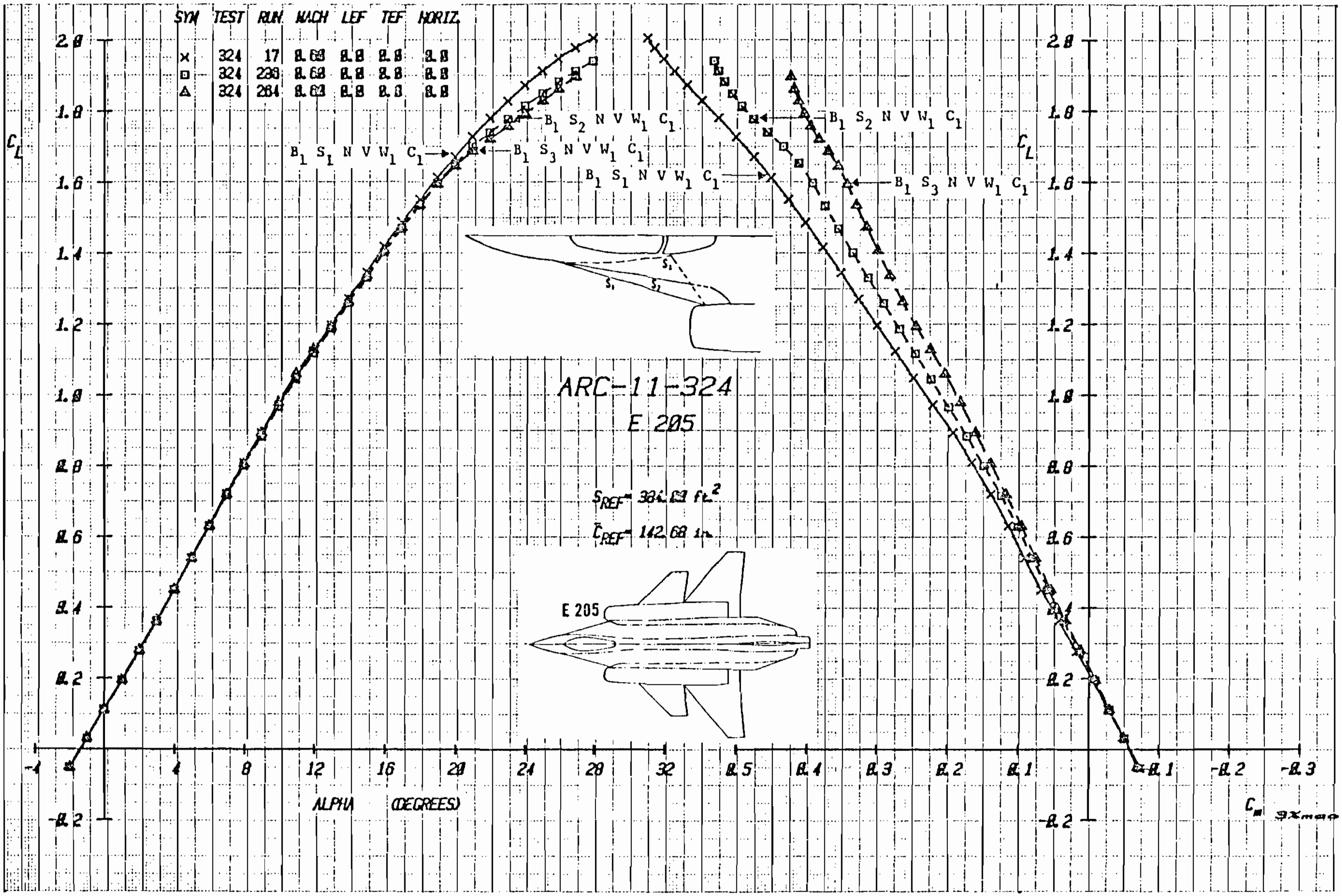

Figure3-14aEffect of Strake Shape on Lift and Moment with Canard C_1 Undeflected, Mach = .6

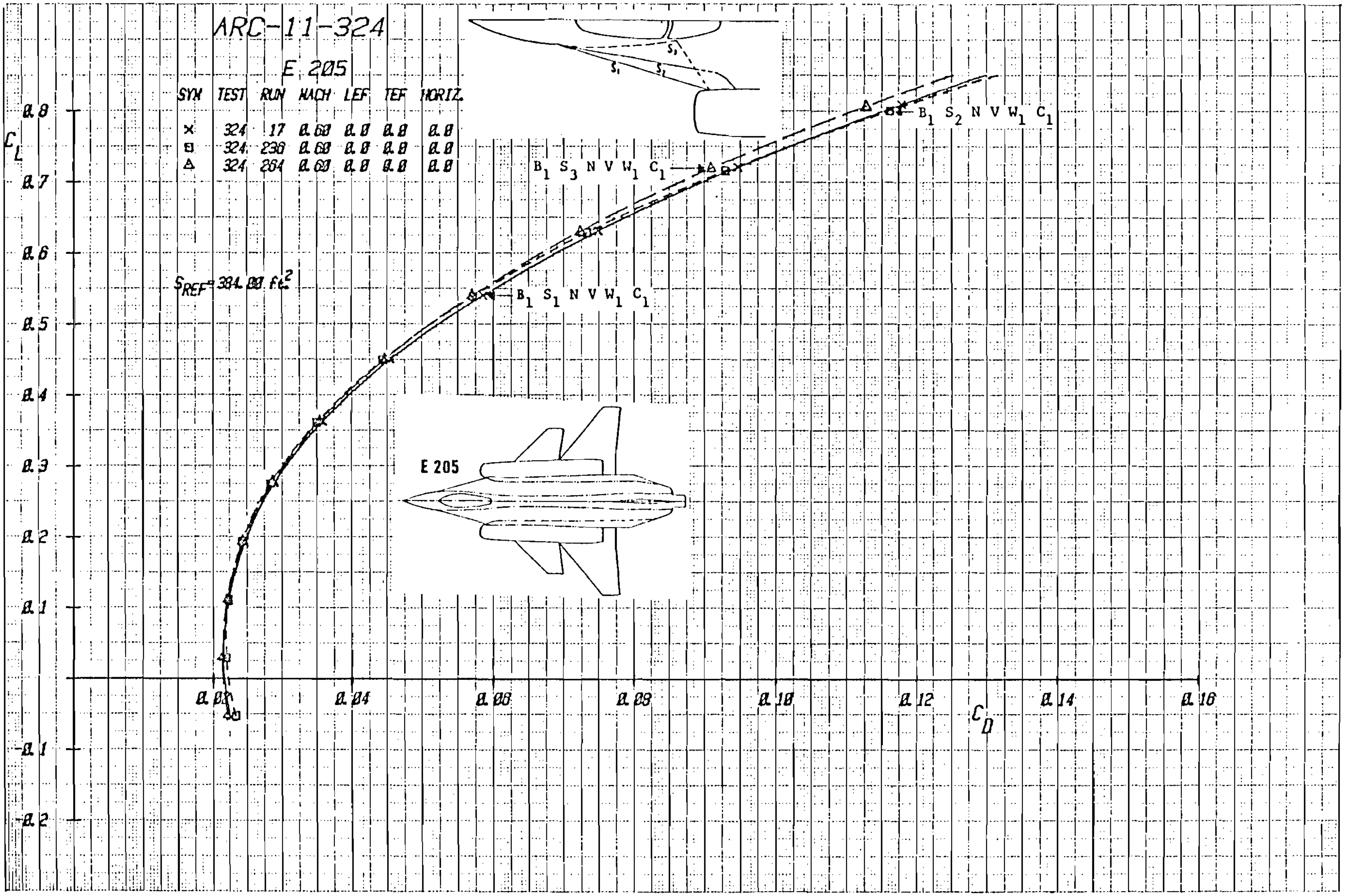

Figure3-14bEffect of Strake Shape on Drag with Canard C_1 Undeflected, Mach = .6

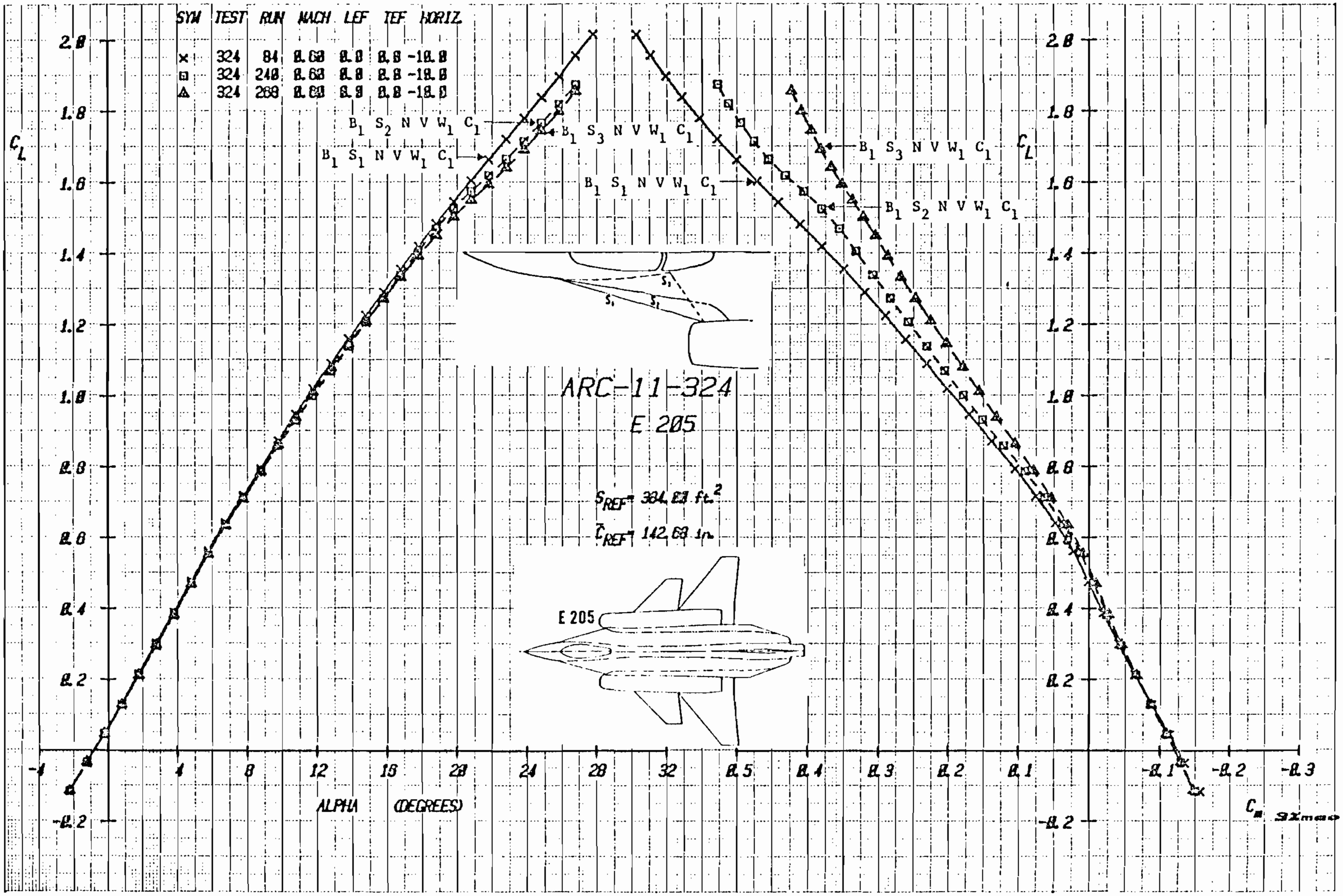

Figure3-15aEffect of Strake Shape on Lift and Moment with Canard C_1 Deflected -10°, Mach = .6

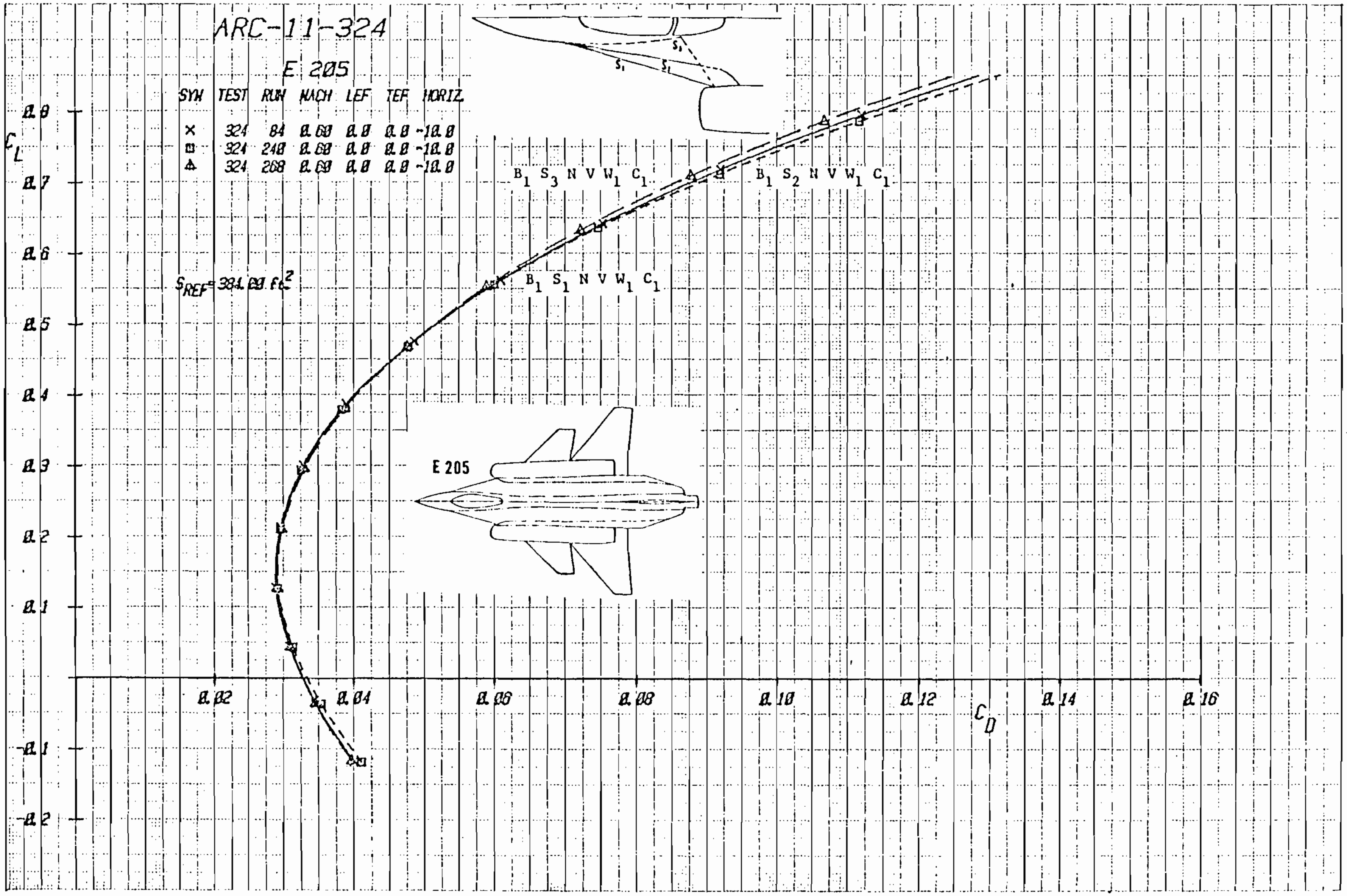

Figure3-15bEffect of Strake Shape on Drag with Canard C_1 Deflected -10°, Mach = .6

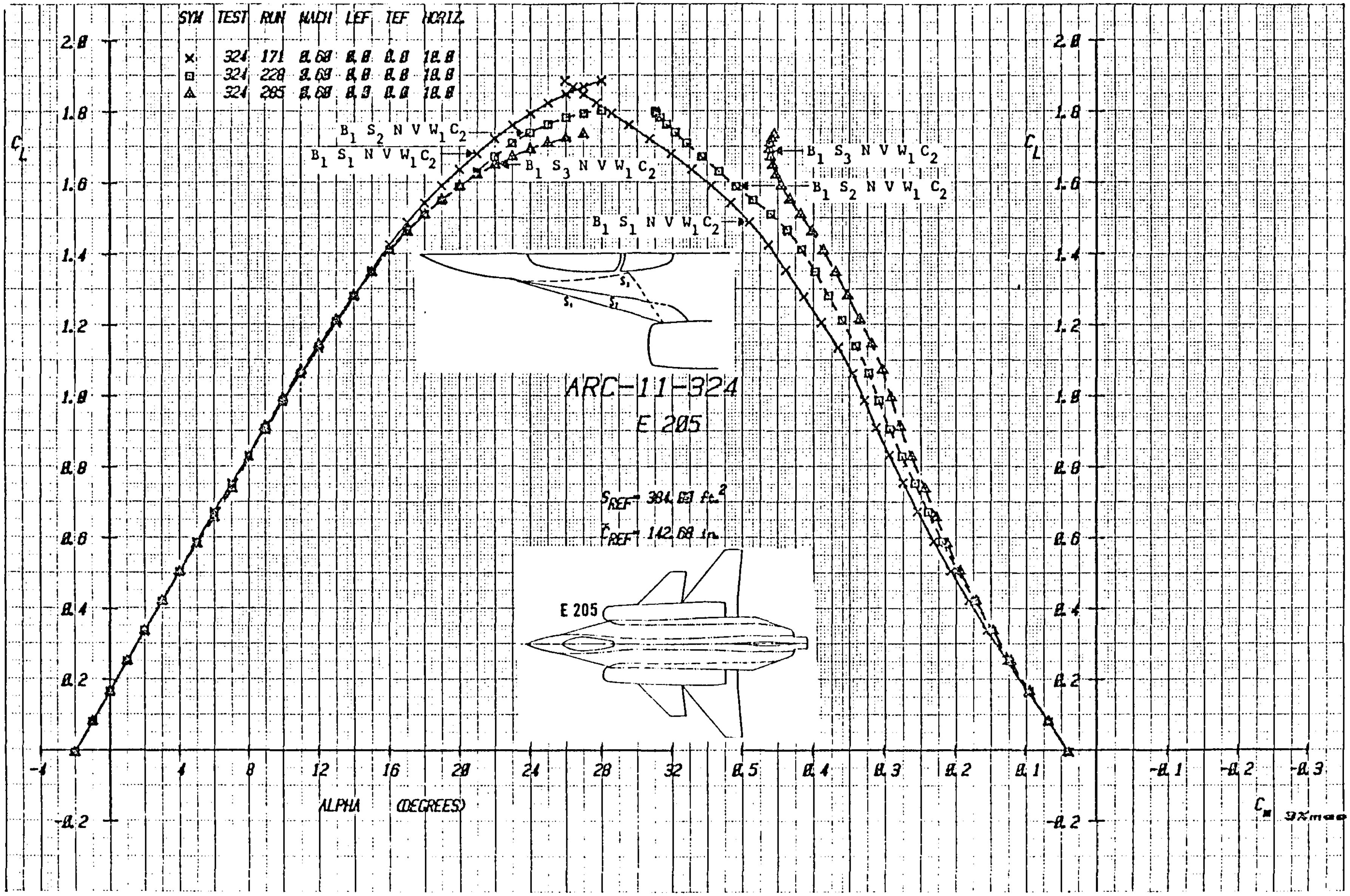

Figure3-16aEffect of Strake Shape on Lift and Moment with Canard C_2 Deflected +10°, Mach = .6

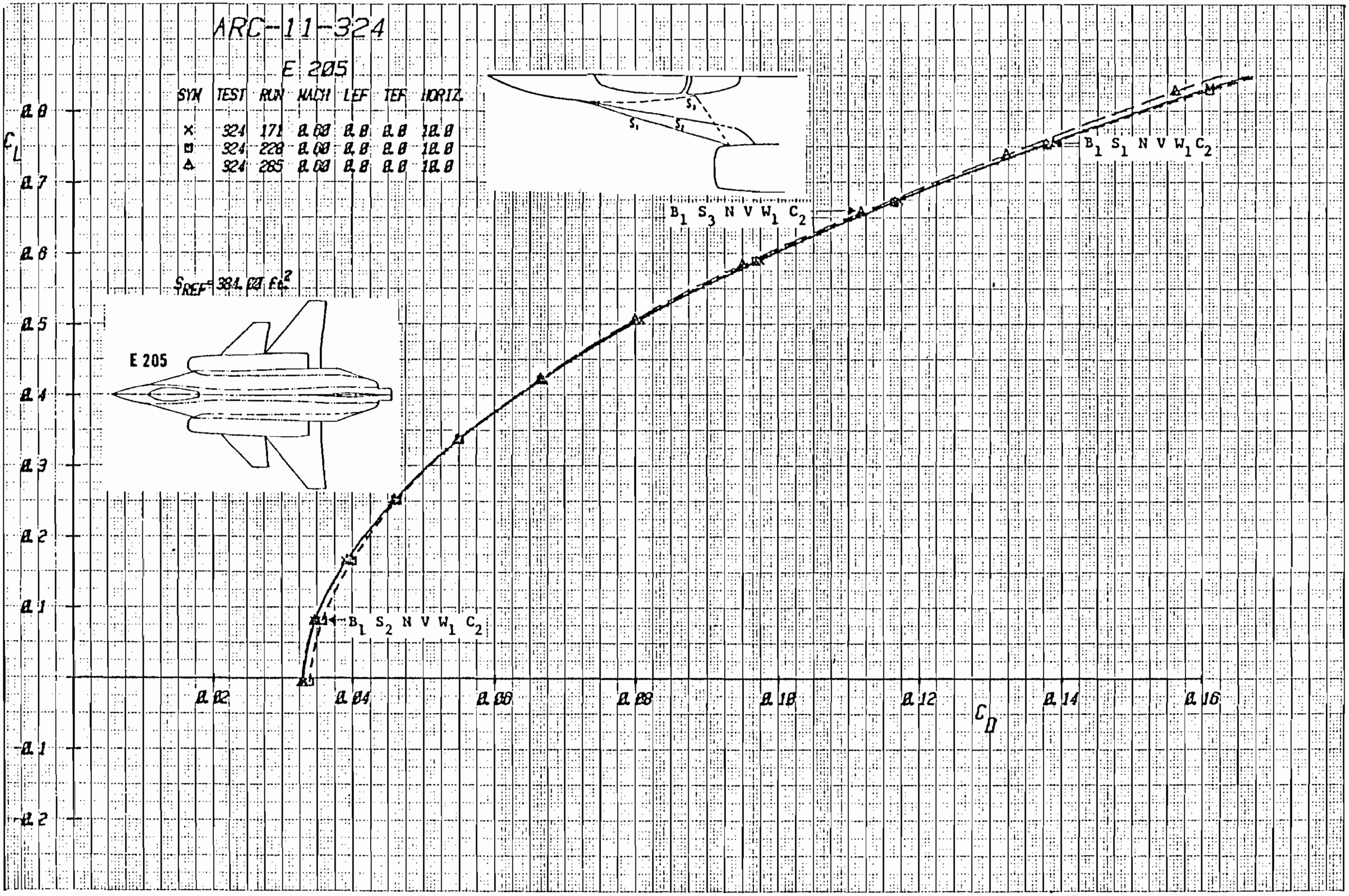

Figure3-16bEffect of Strake Shape on Drag with Canard C_2 Deflected +10°, Mach = .6

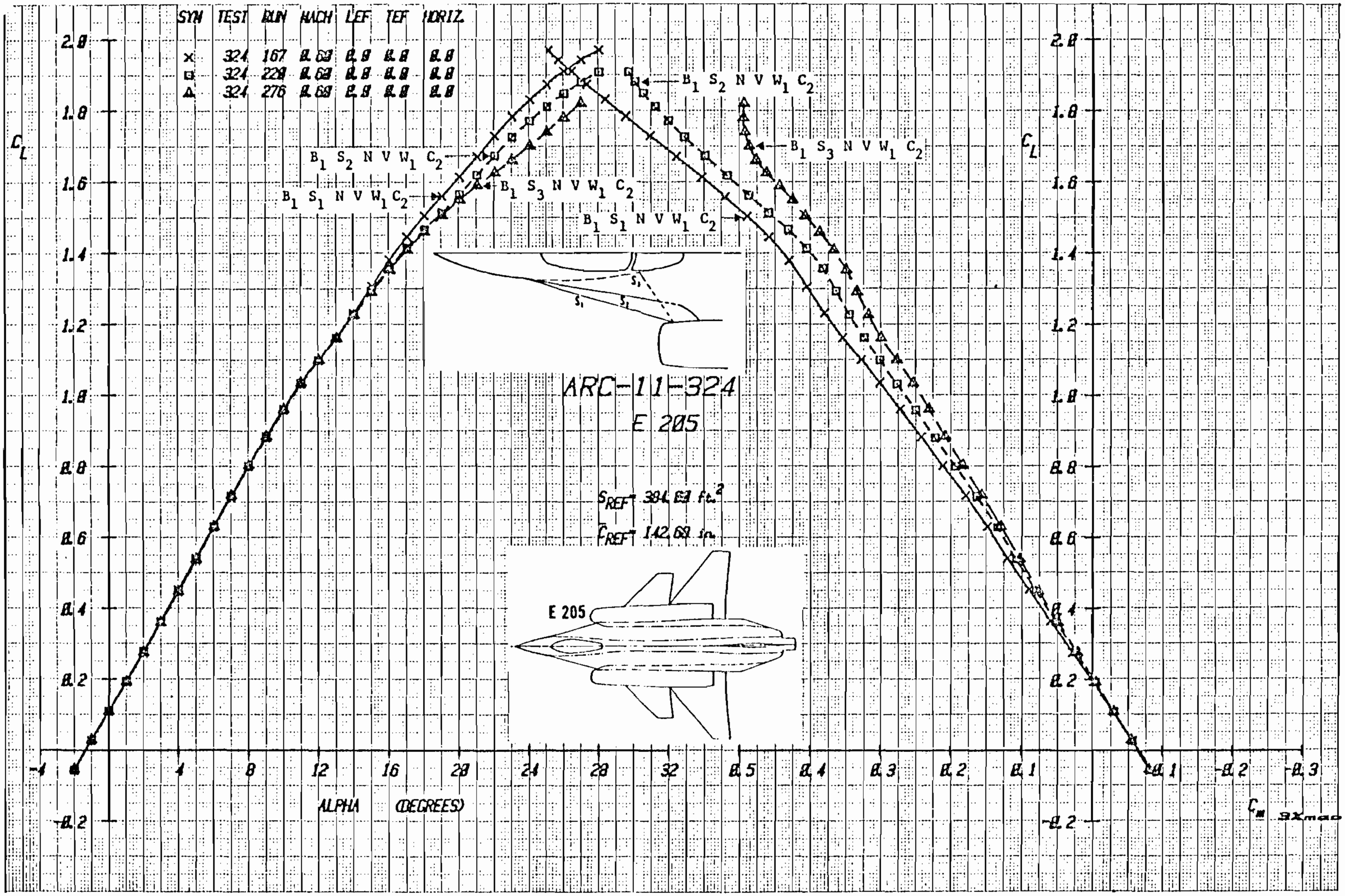

Figure3-17aEffect of Strake Shape on Lift and Moment with Canard C_2 Undeflected, Mach = .6

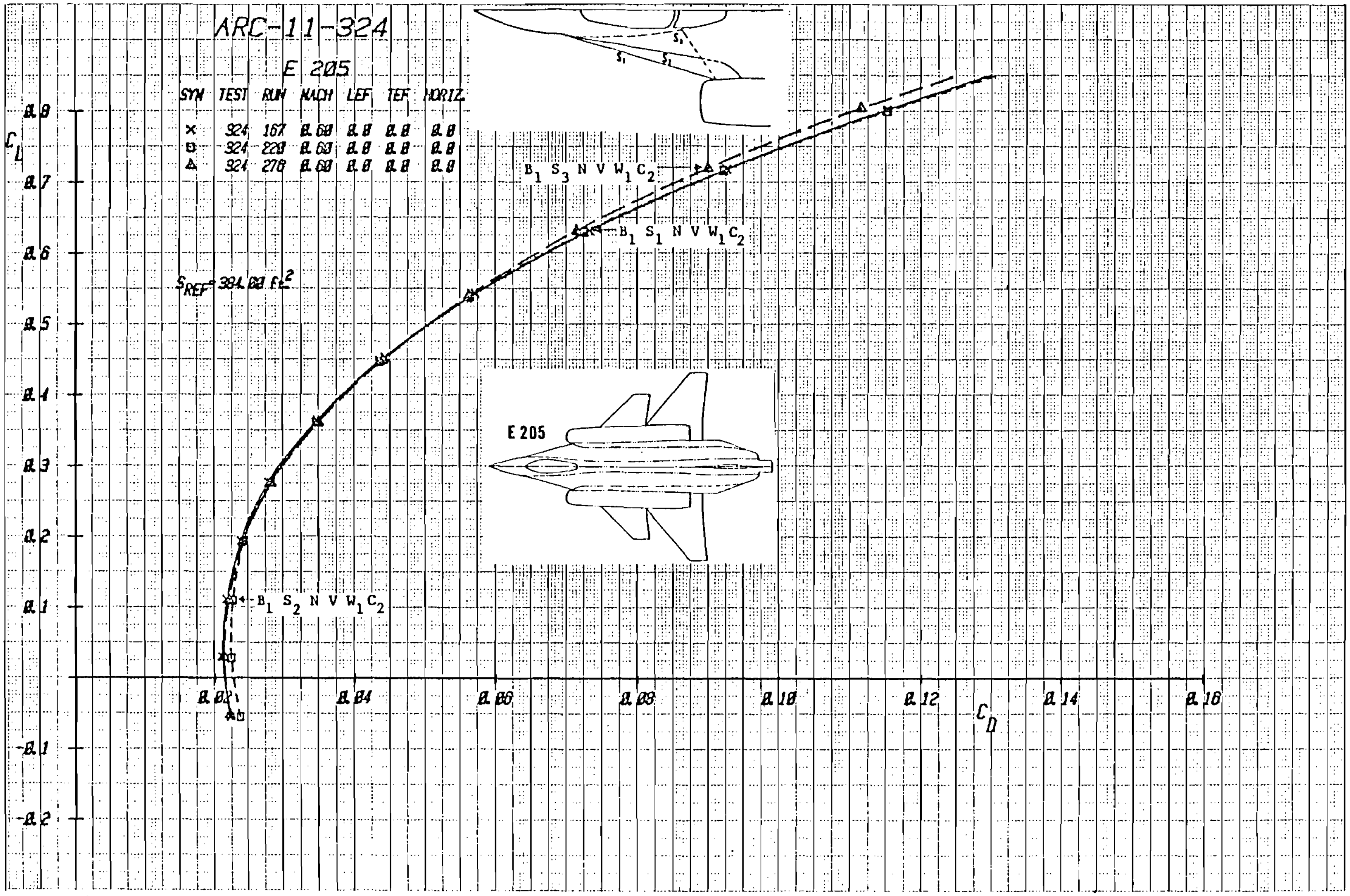

Figure3-17bEffect of Strake Shape on Drag with Canard C_2 Undeflected, Mach = .6

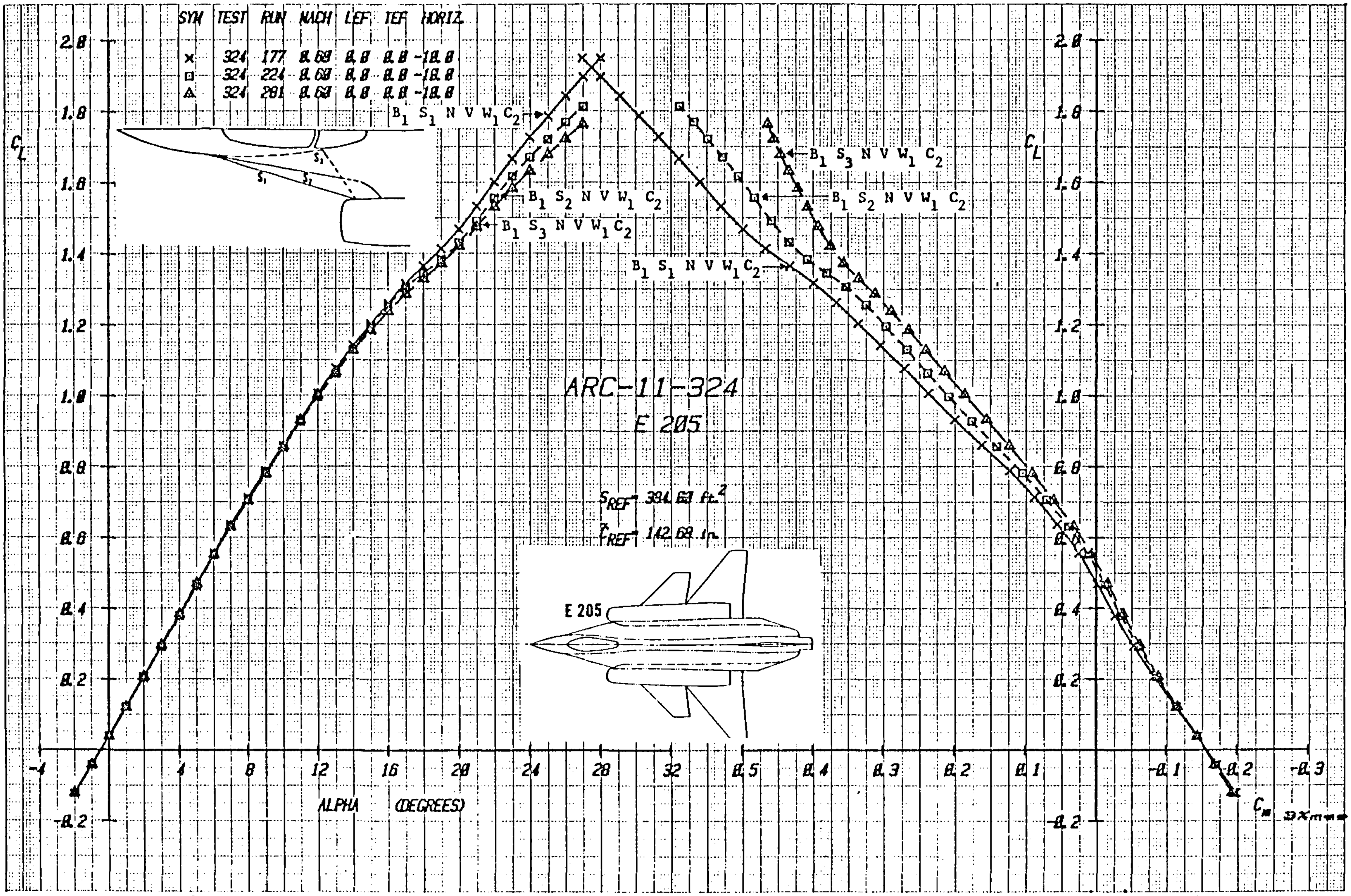

Figure3-18aEffect of Strake Shape on Lift and Moment with Canard C_2 Deflected -10°, Mach = .6

199

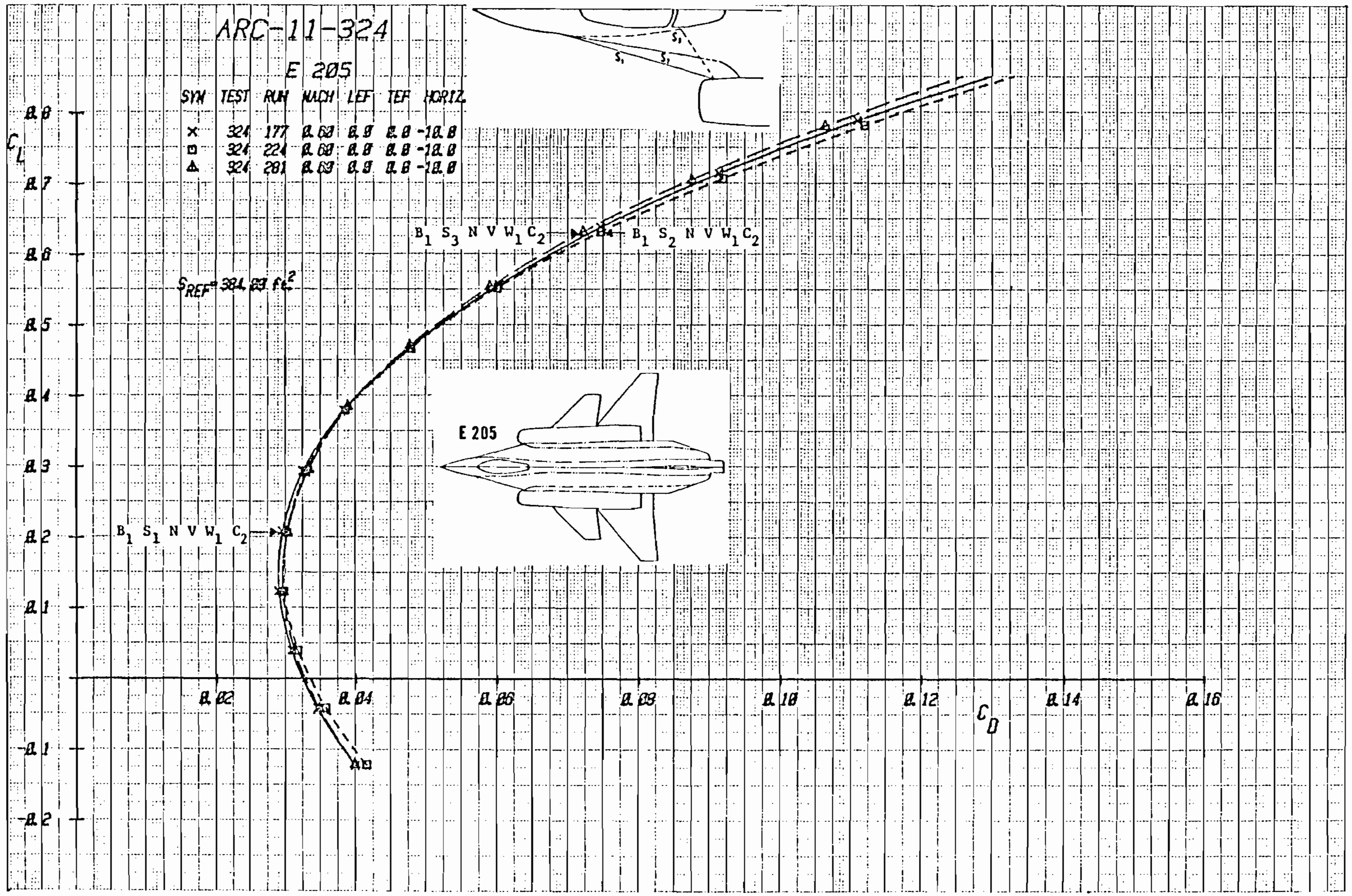

Figure3-18bEffect of Strake Shape on Drag with Canard C_2 Deflected -10°, Mach = .6

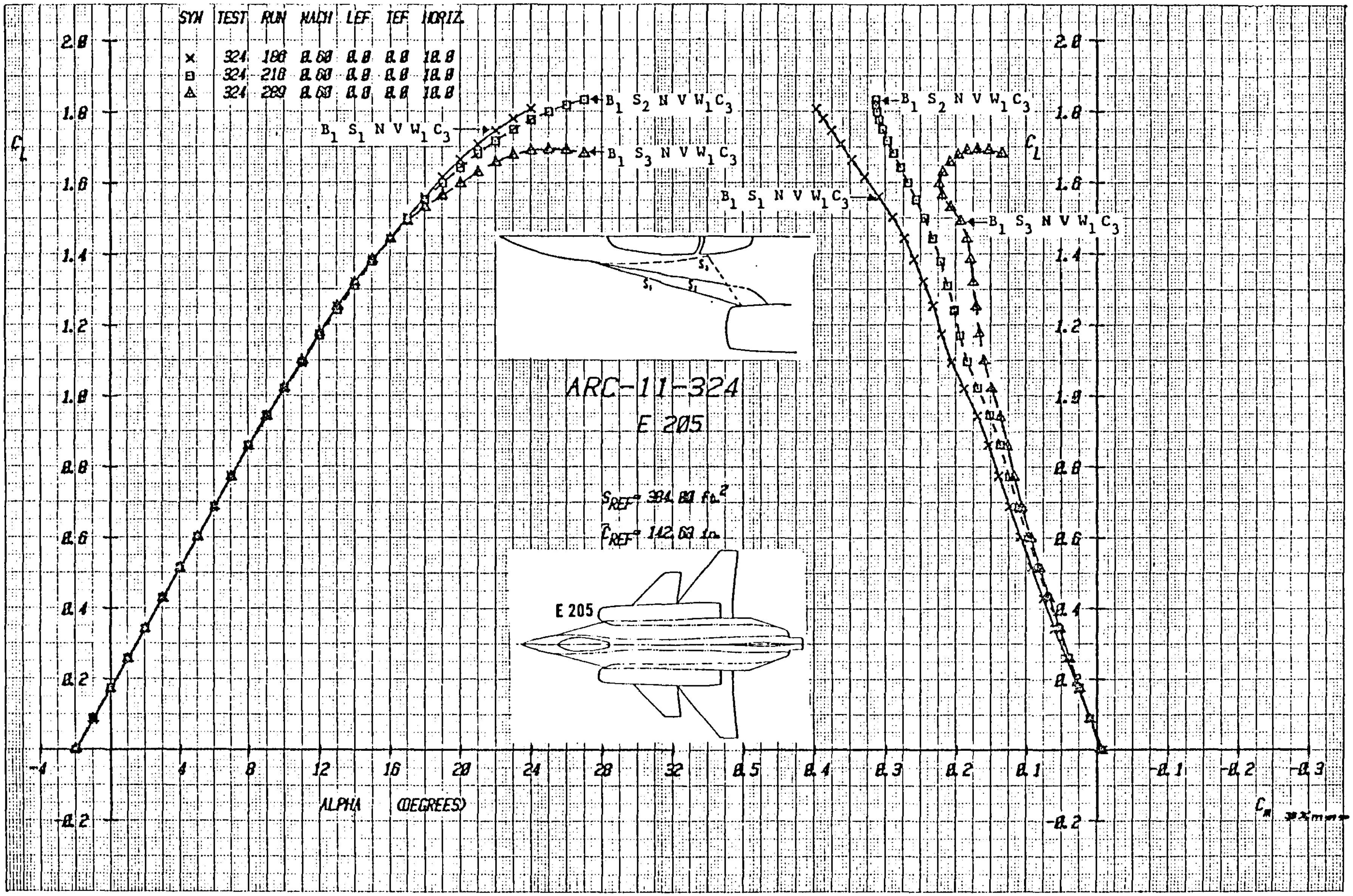

Figure3-19aEffect of Strake Shape on Lift and Moment with Canard C_3 Deflected +10°, Mach = .6

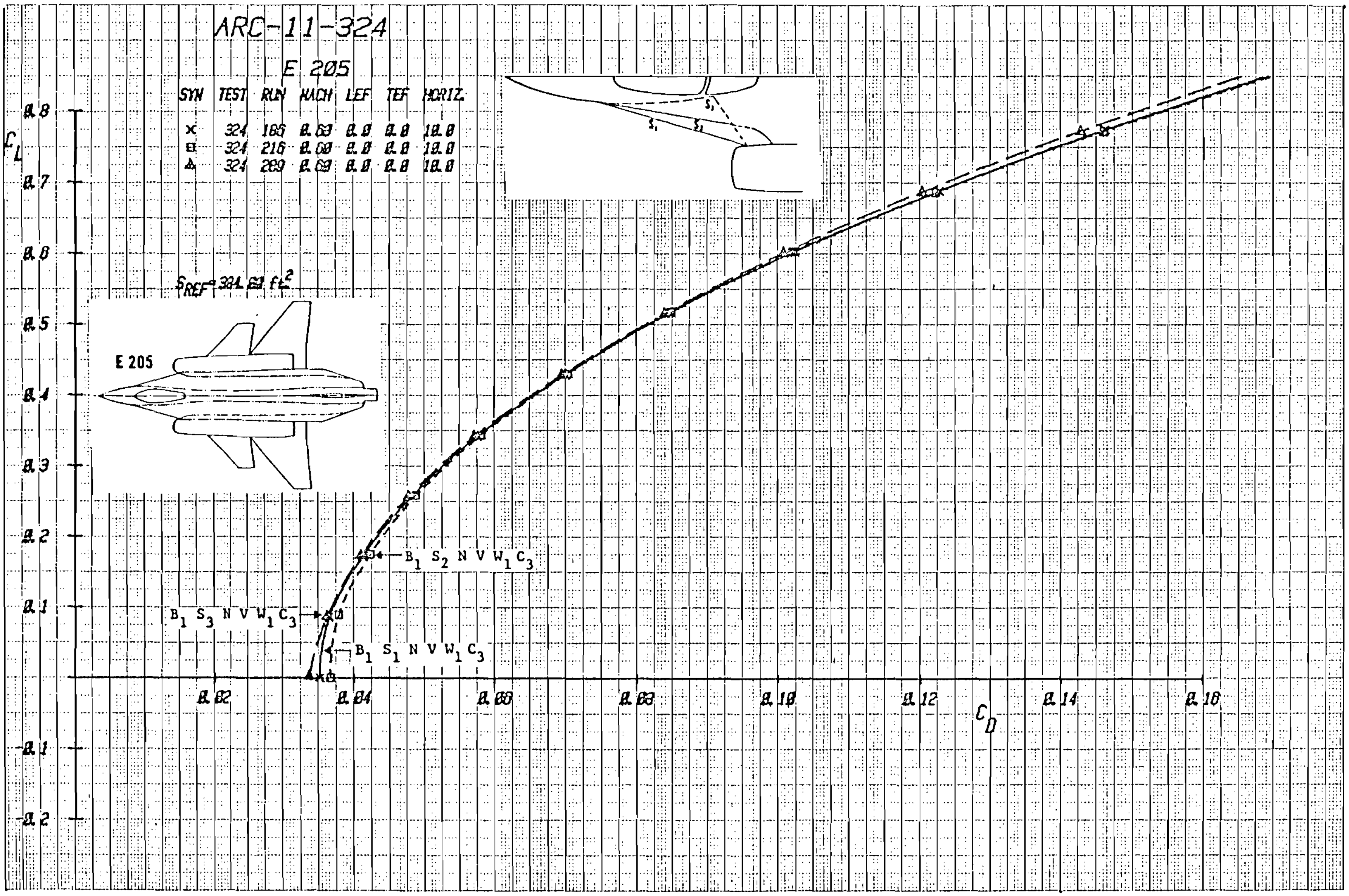

Figure3-19bEffect of Strake Shape on Drag with Canard C_3 Deflected +10°, Mach = .6

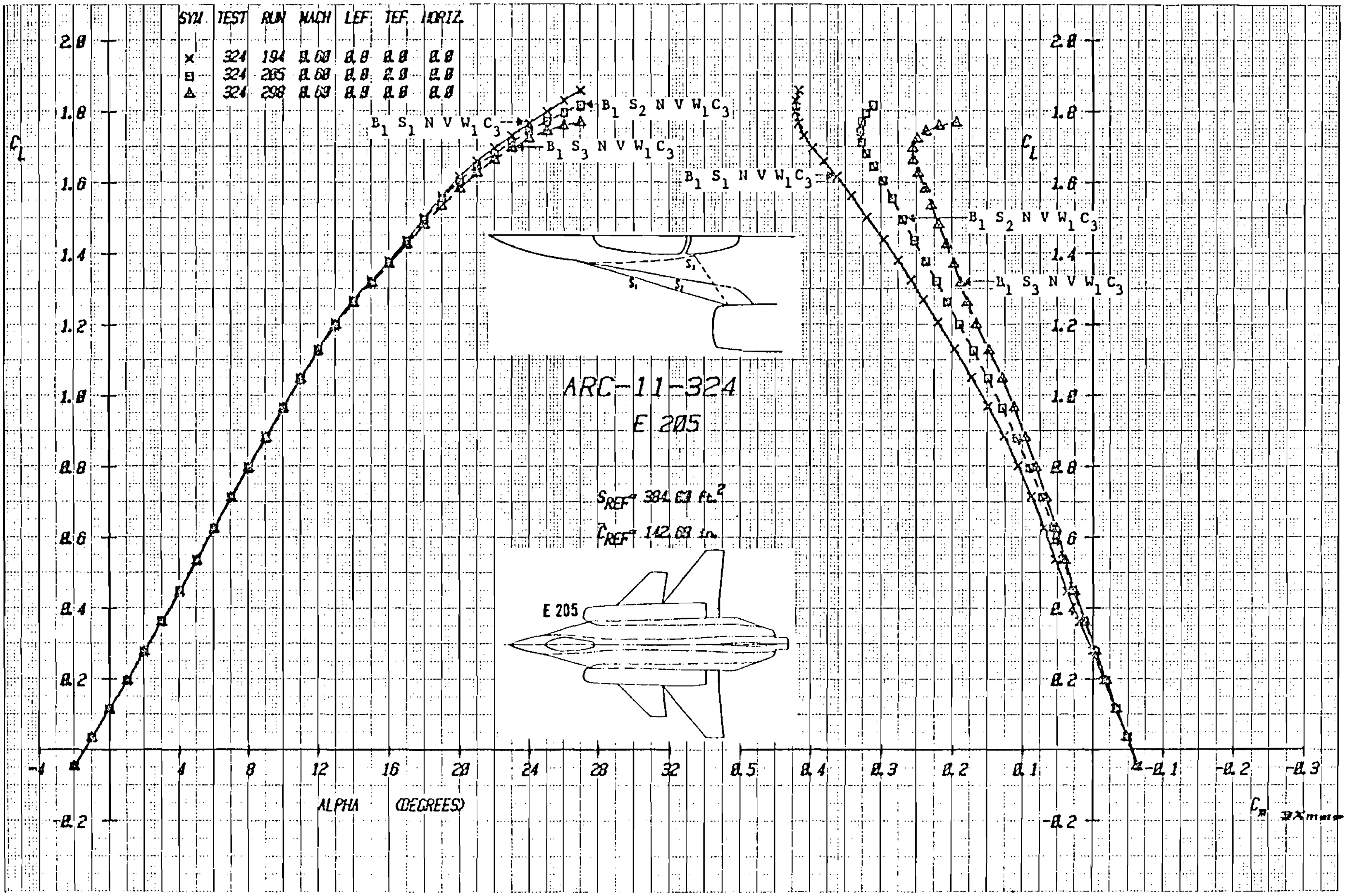

Figure3-20aEffect of Strake Shape on Lift and Moment with Canard C_3 Undeflected, Mach = .6

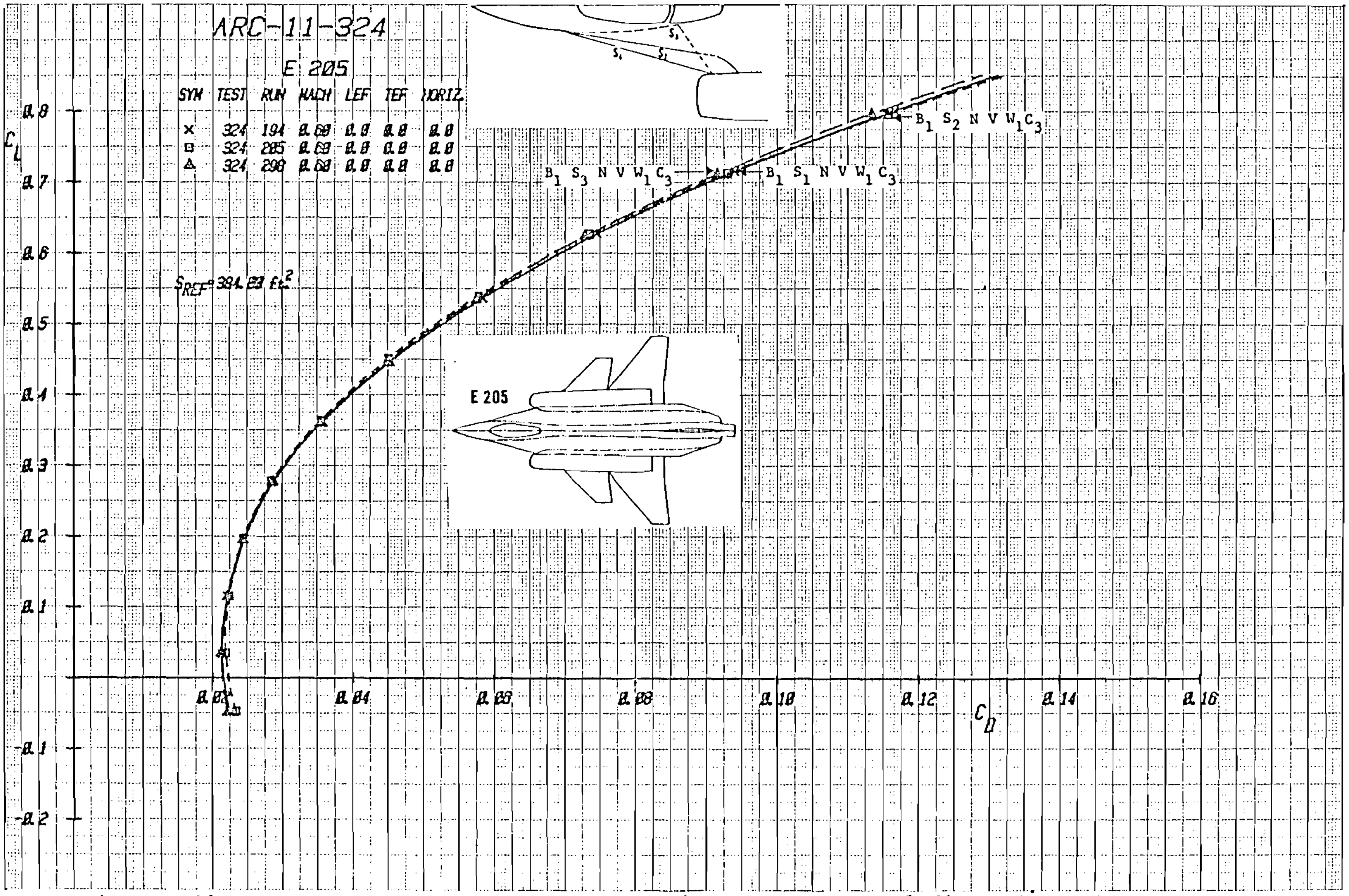

Figure3-20bEffect of Strake Shape on Drag with Canard C_3 Undeflected, Mach = .6

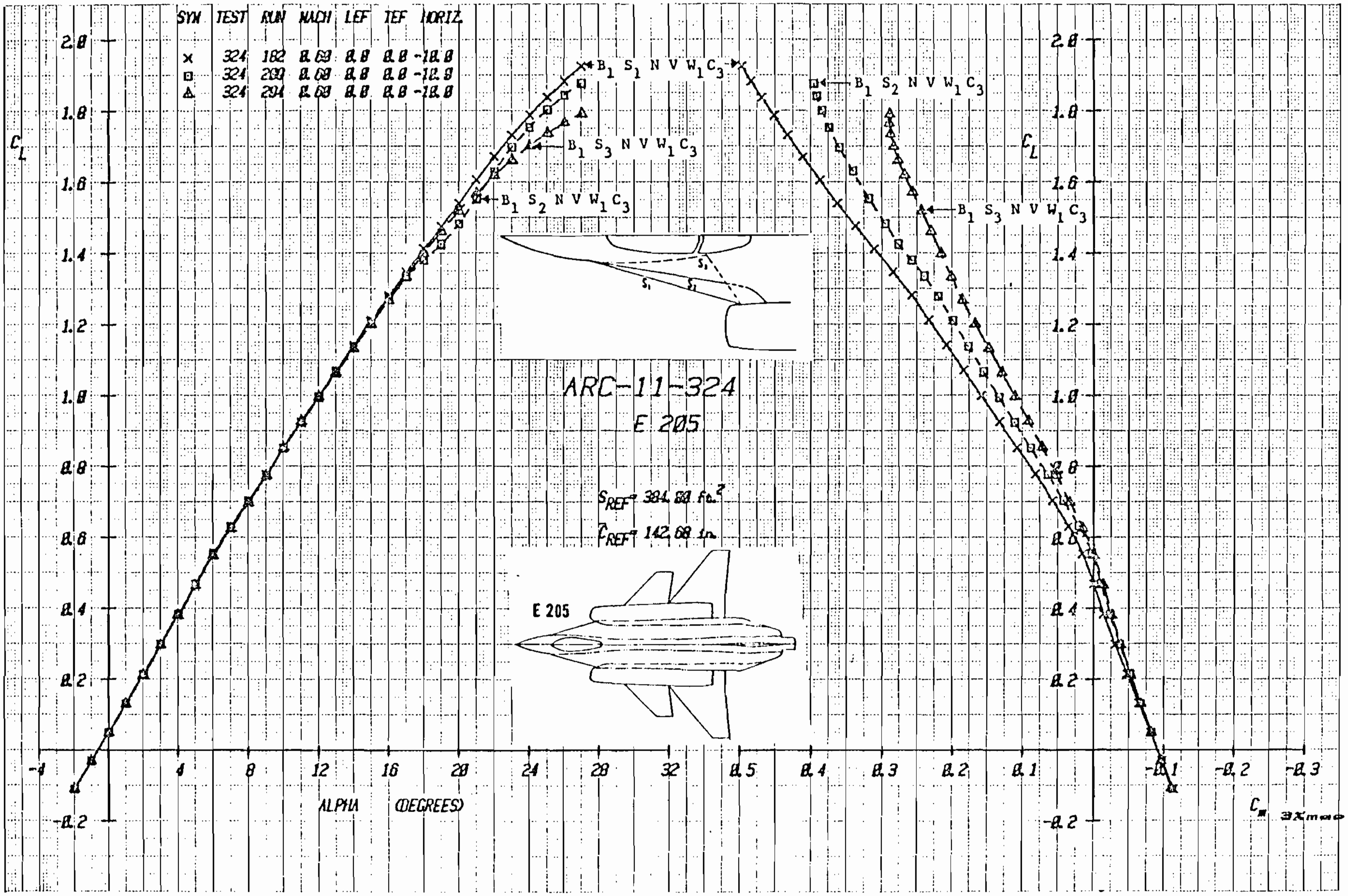

Figure3-21aEffect of Strake Shape on Lift and Moment with Canard C_3 Deflected -10°, Mach = .6

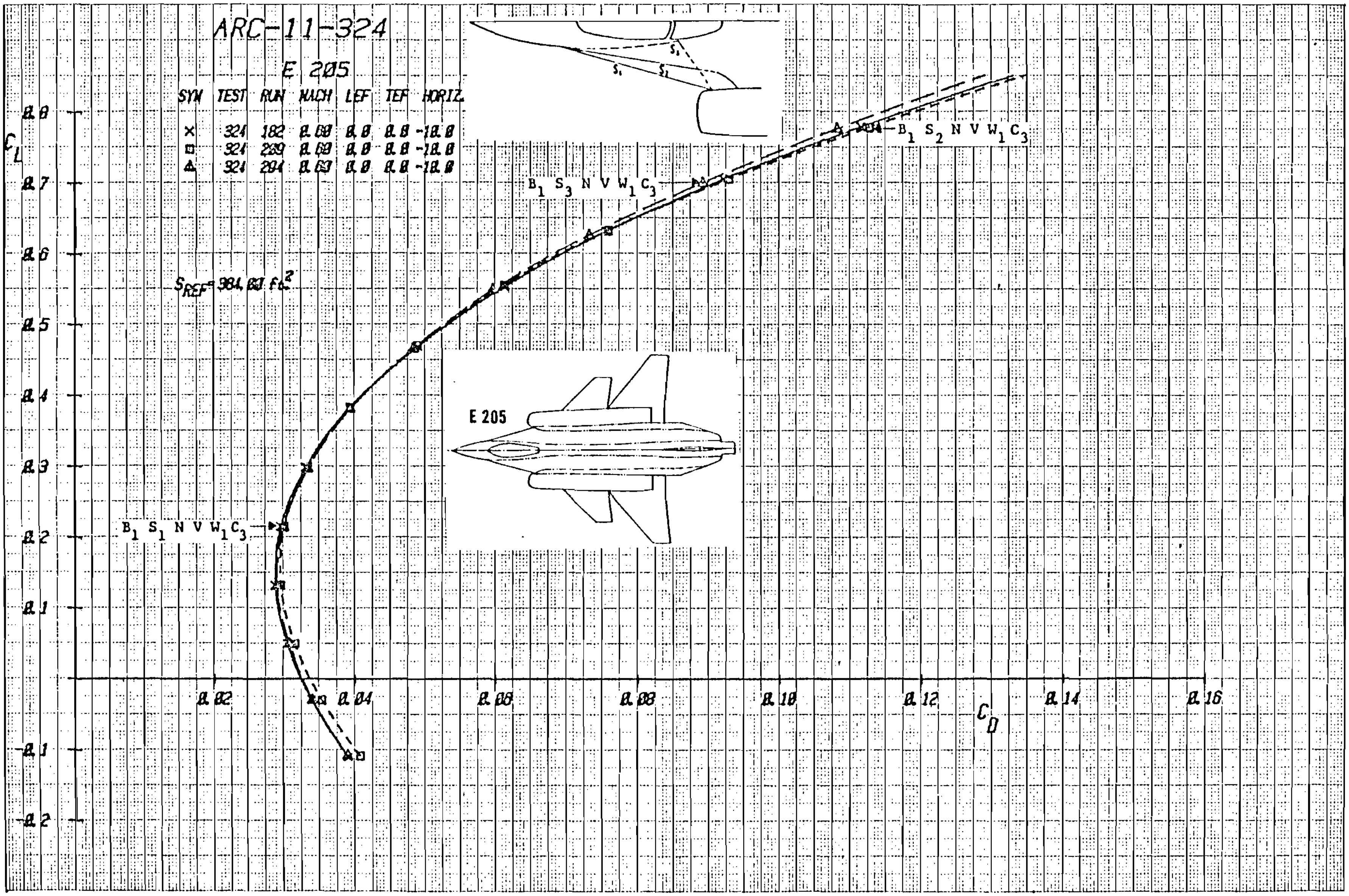

Figure3-21bEffect of Strake Shape on Drag with Canard C_3 Deflected -10°, Mach = .6

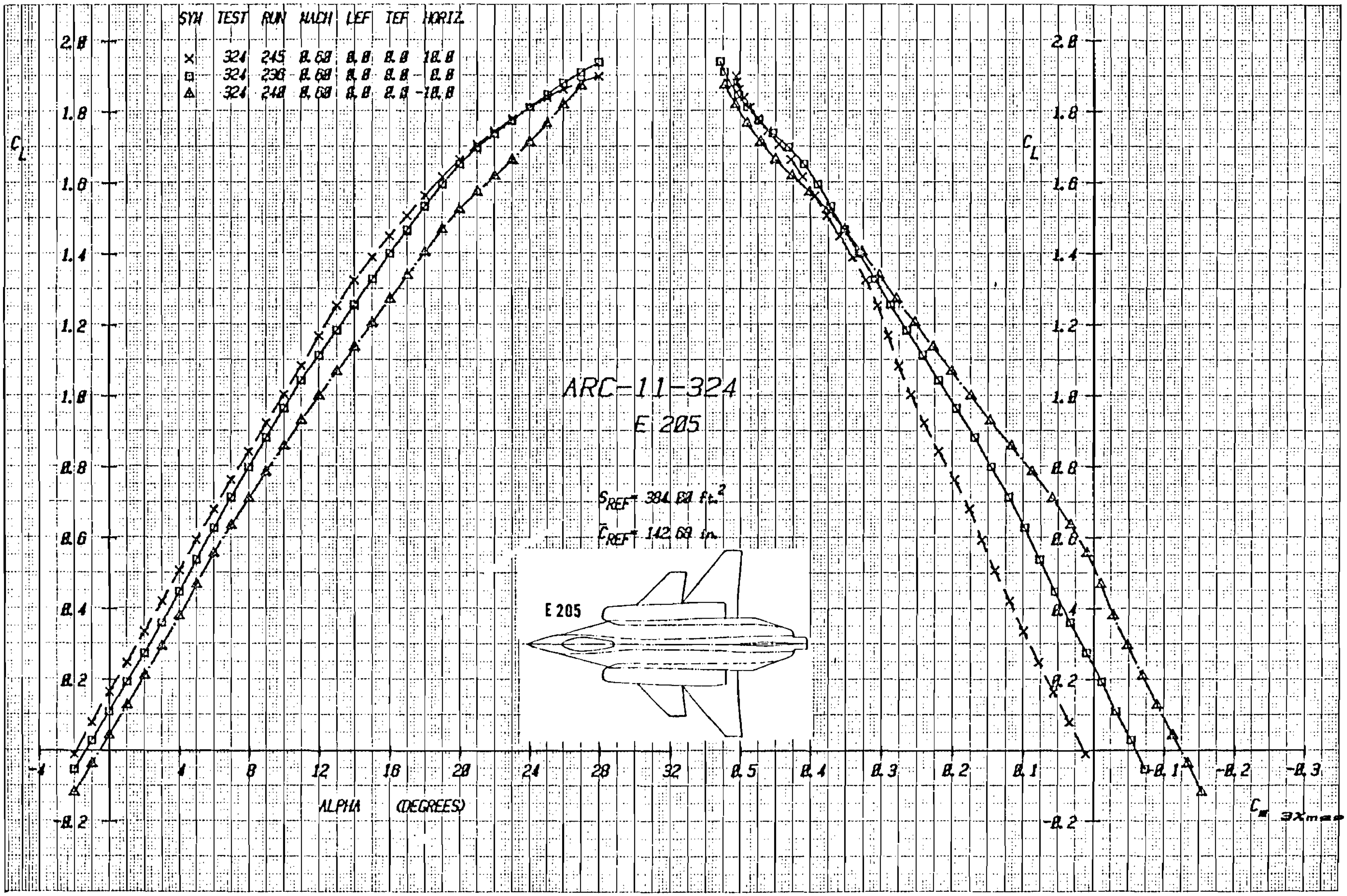

Figure3-22aEffect of Canard Deflection on Lift and Moment With Canard, C_1, and Strake S_2, Mach = .6

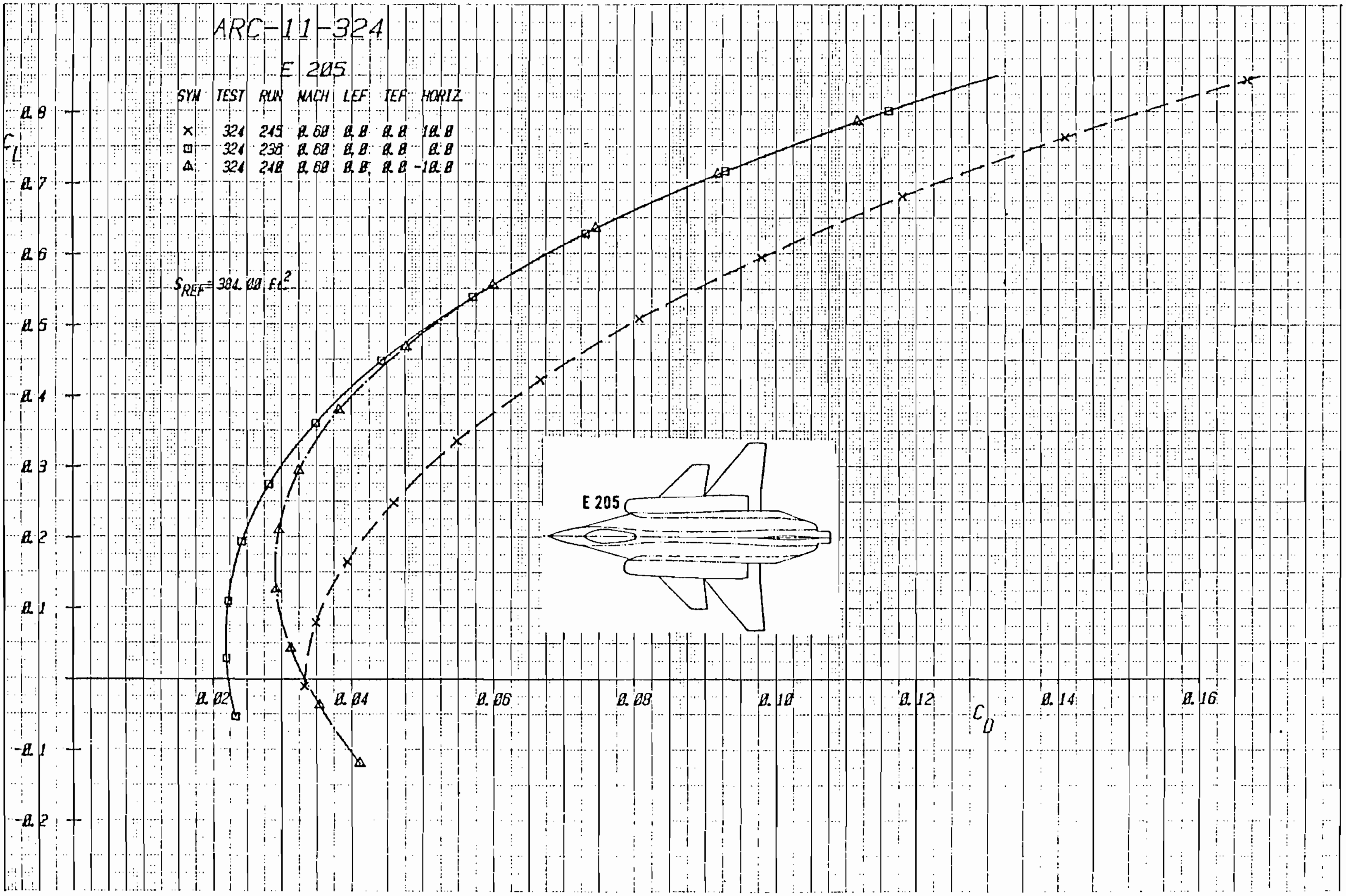

Figure3-22bEffect of Canard Deflection on Drag With Canard C_1, and Strake S_2, Mach = .6

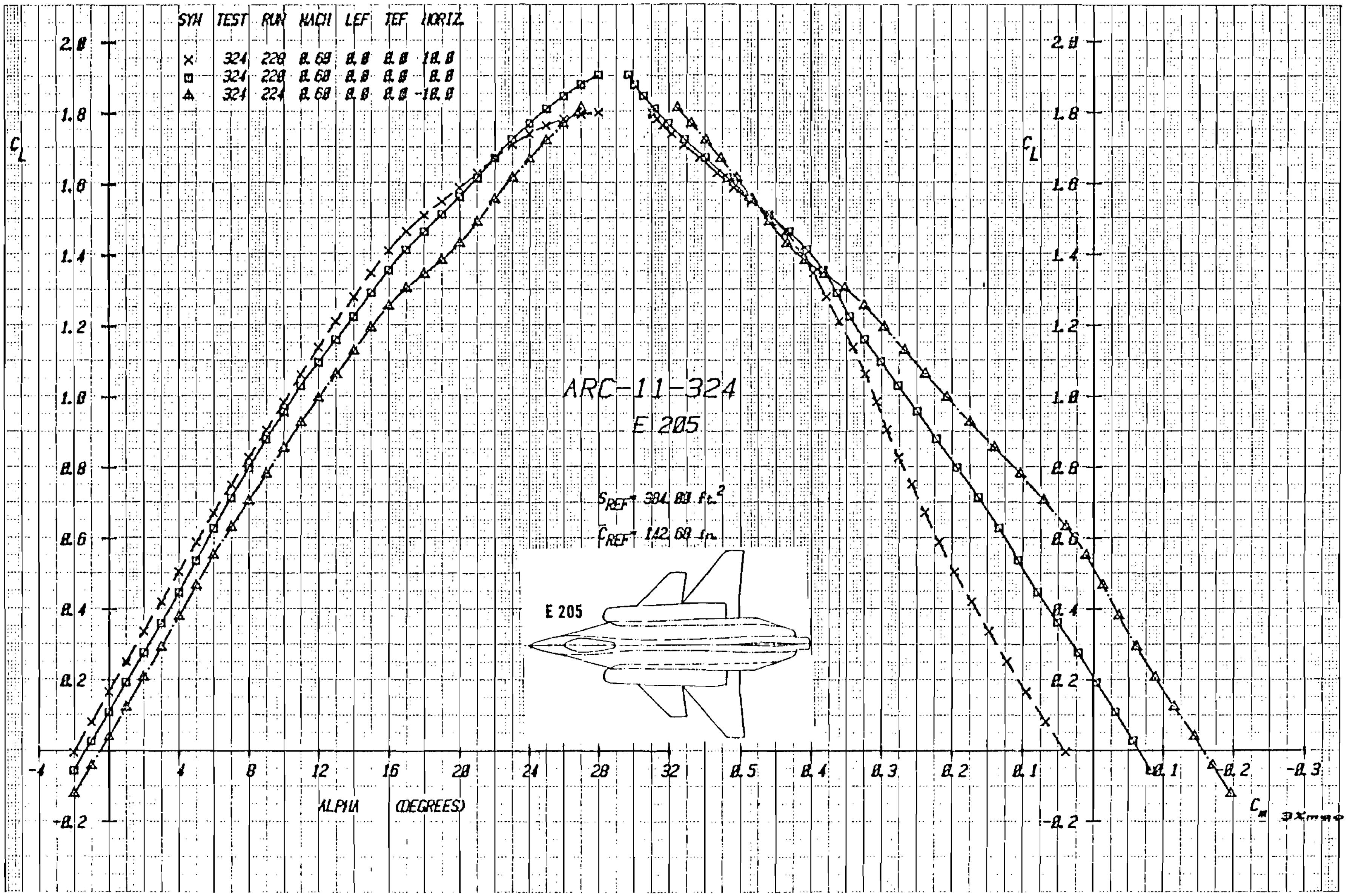

Figure3-23aEffect of Canard Deflection on Lift and Moment With Canard C_2, and Strake S_2, Mach = .6

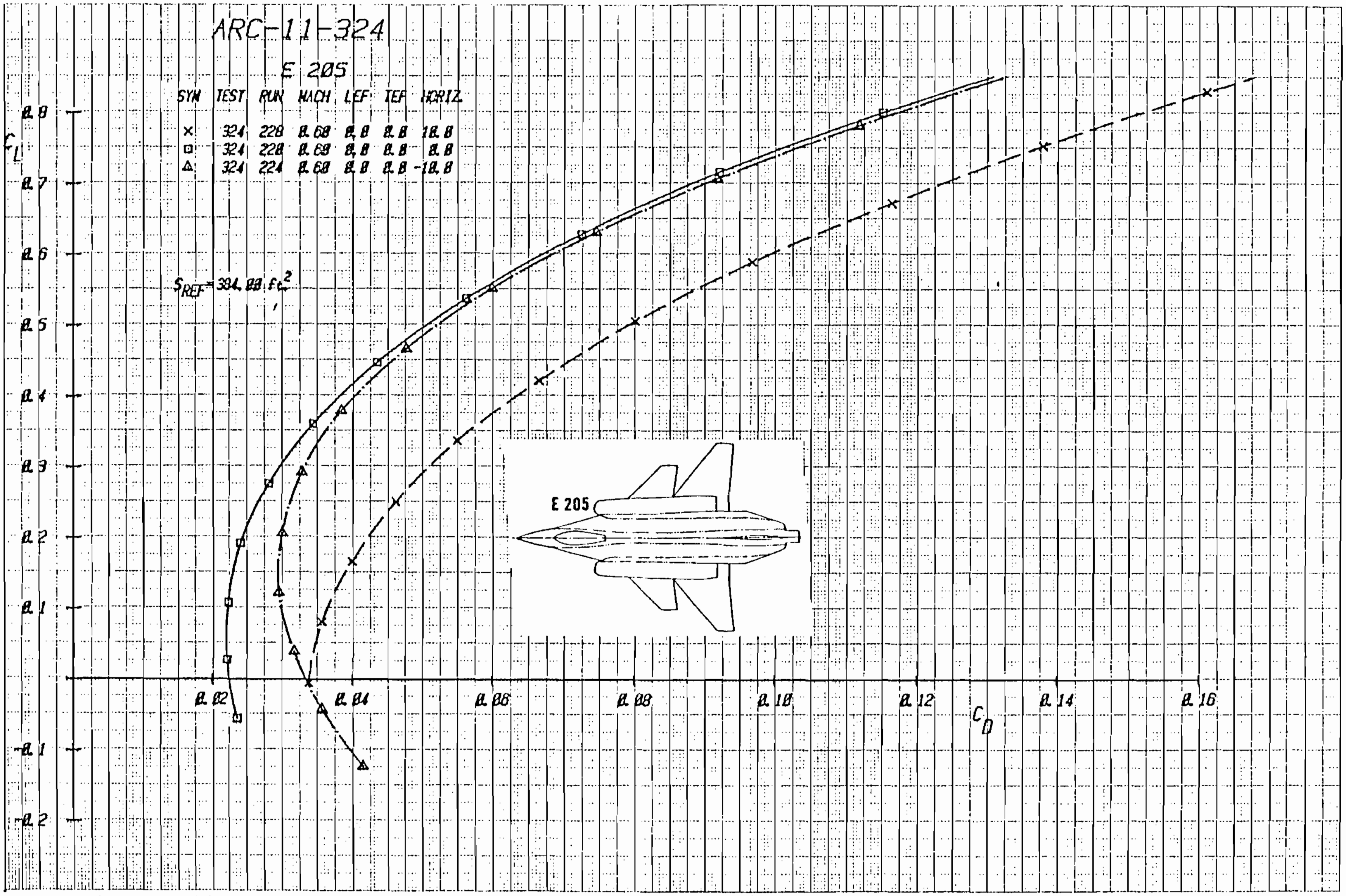

Figure3-23bEffect of Canard Deflection on Drag With Canard C_2, and Strake S_2, Mach = .6

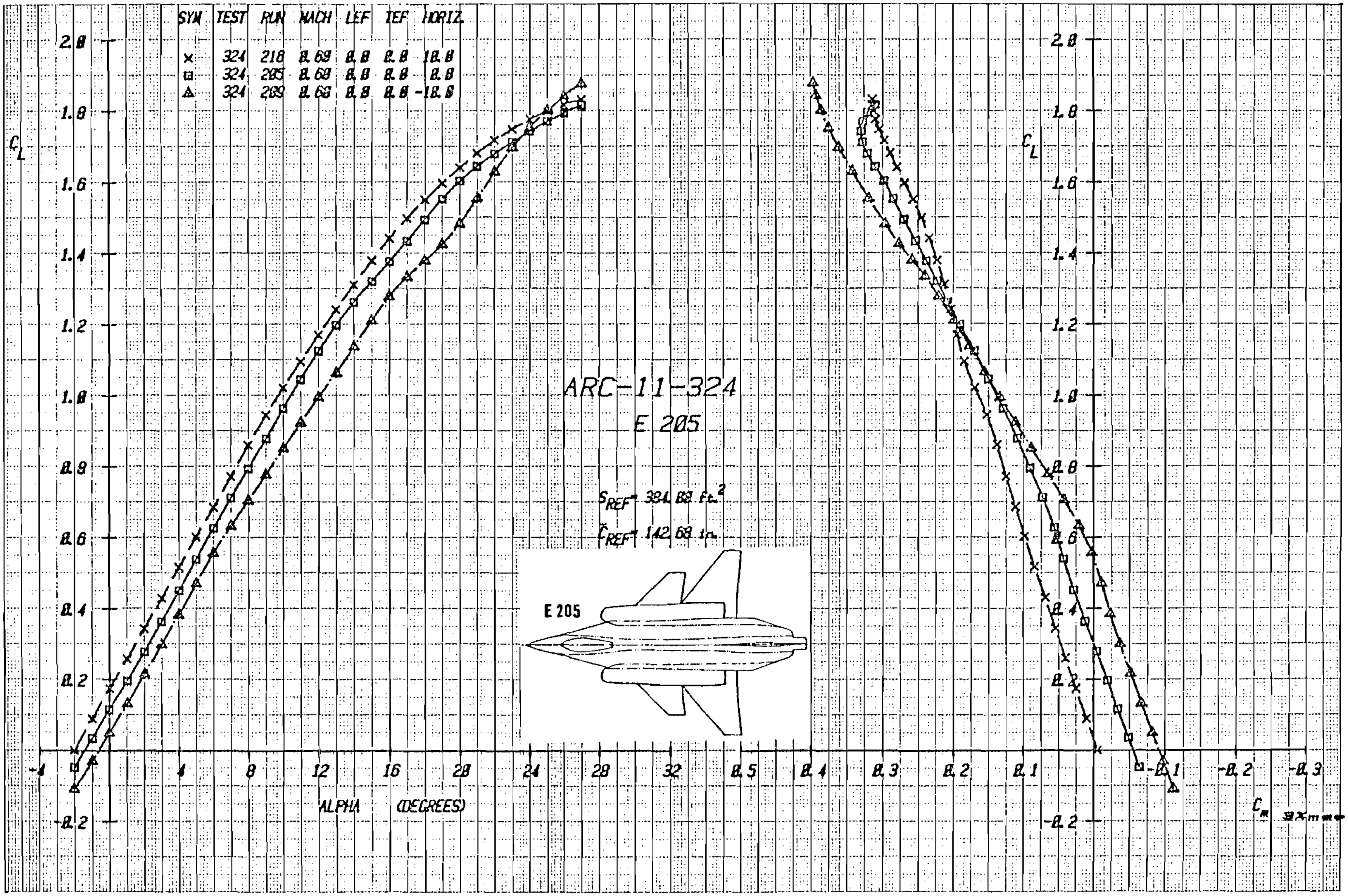

Figure 3-24a Effect of Canard Deflection on Lift and Moment With Canard, C_3, and Strake S_2, Mach = .6

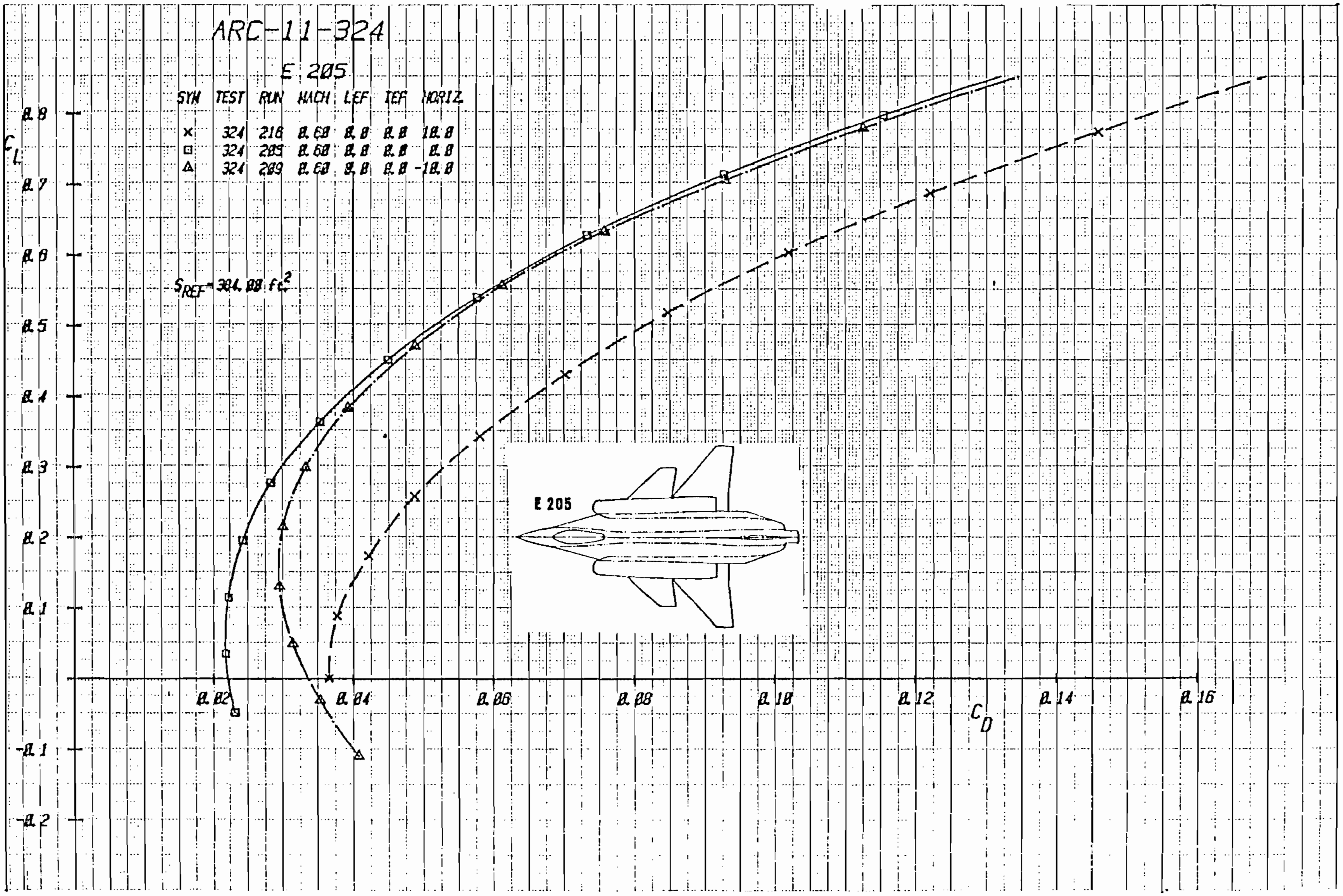

Figure3-24bEffect of Canard Deflection on Drag With Canard C_3, and Strake S_2, Mach = .6

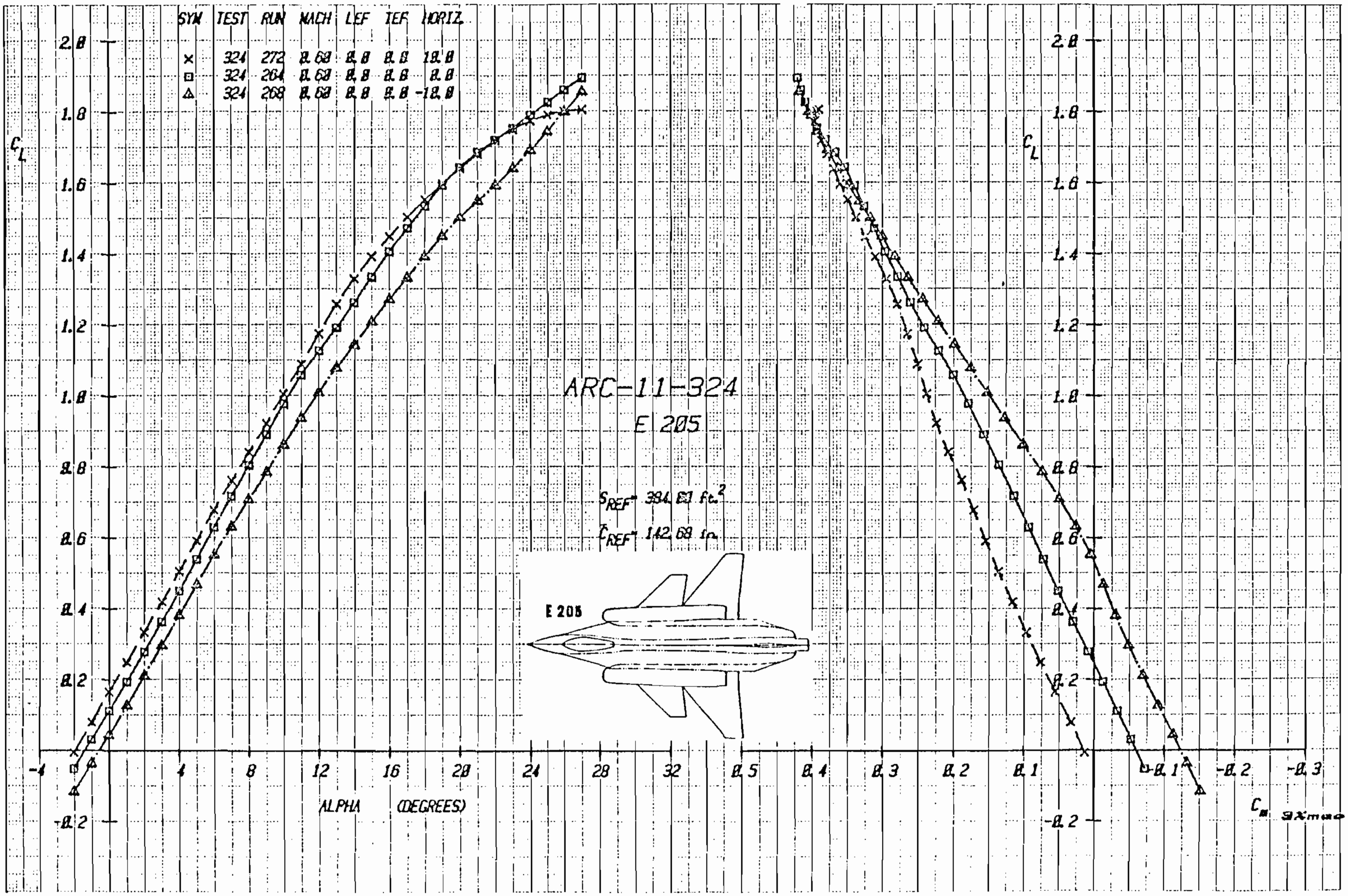

Figure3-25aEffect of Canard Deflection on Lift and Moment with Canard C_1, and Strake S_3, Mach = .6

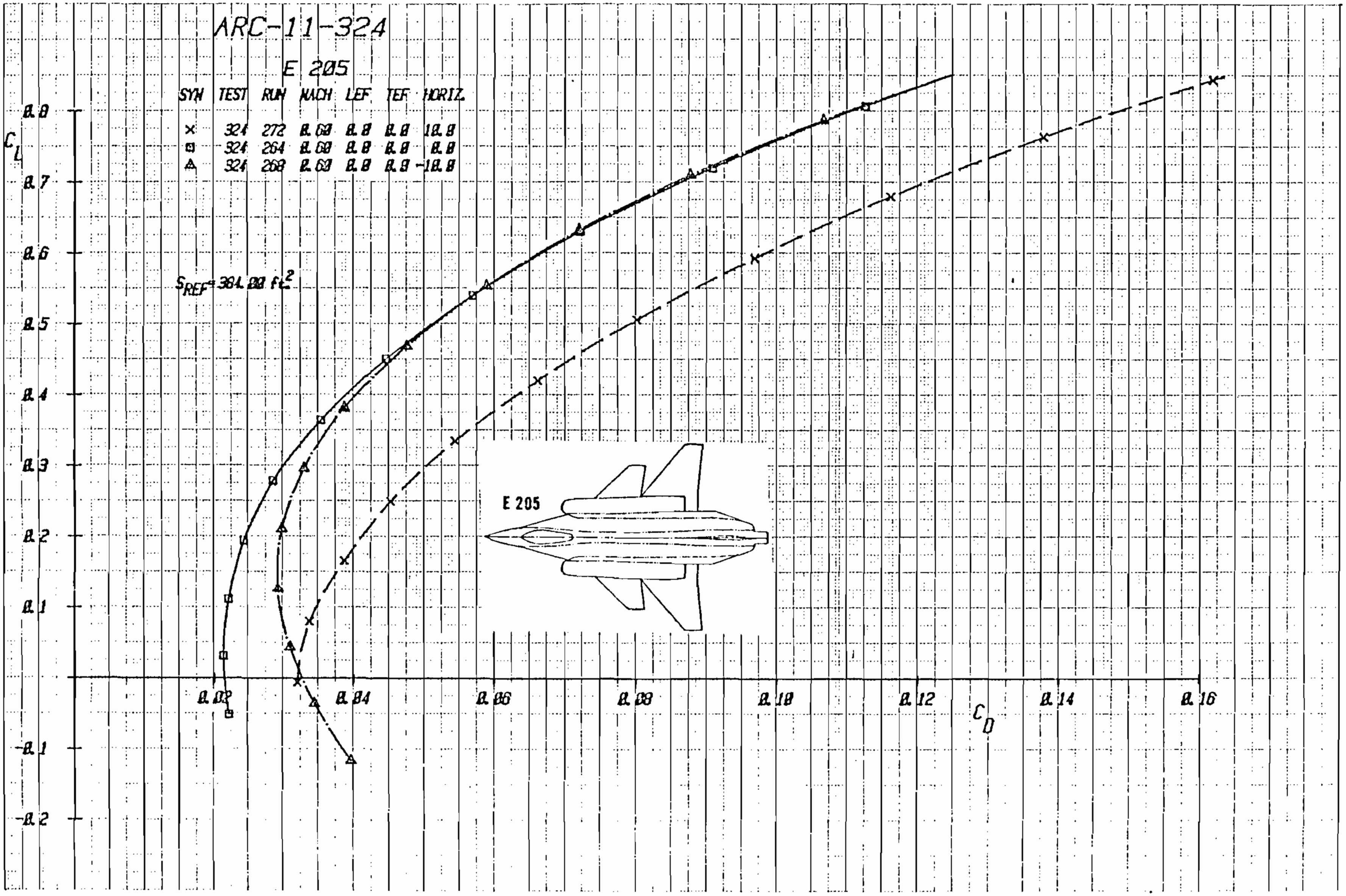

Figure3-25b Effect of Canard Deflection on Drag with Canard C_1, and Strake S_3, Mach = .6

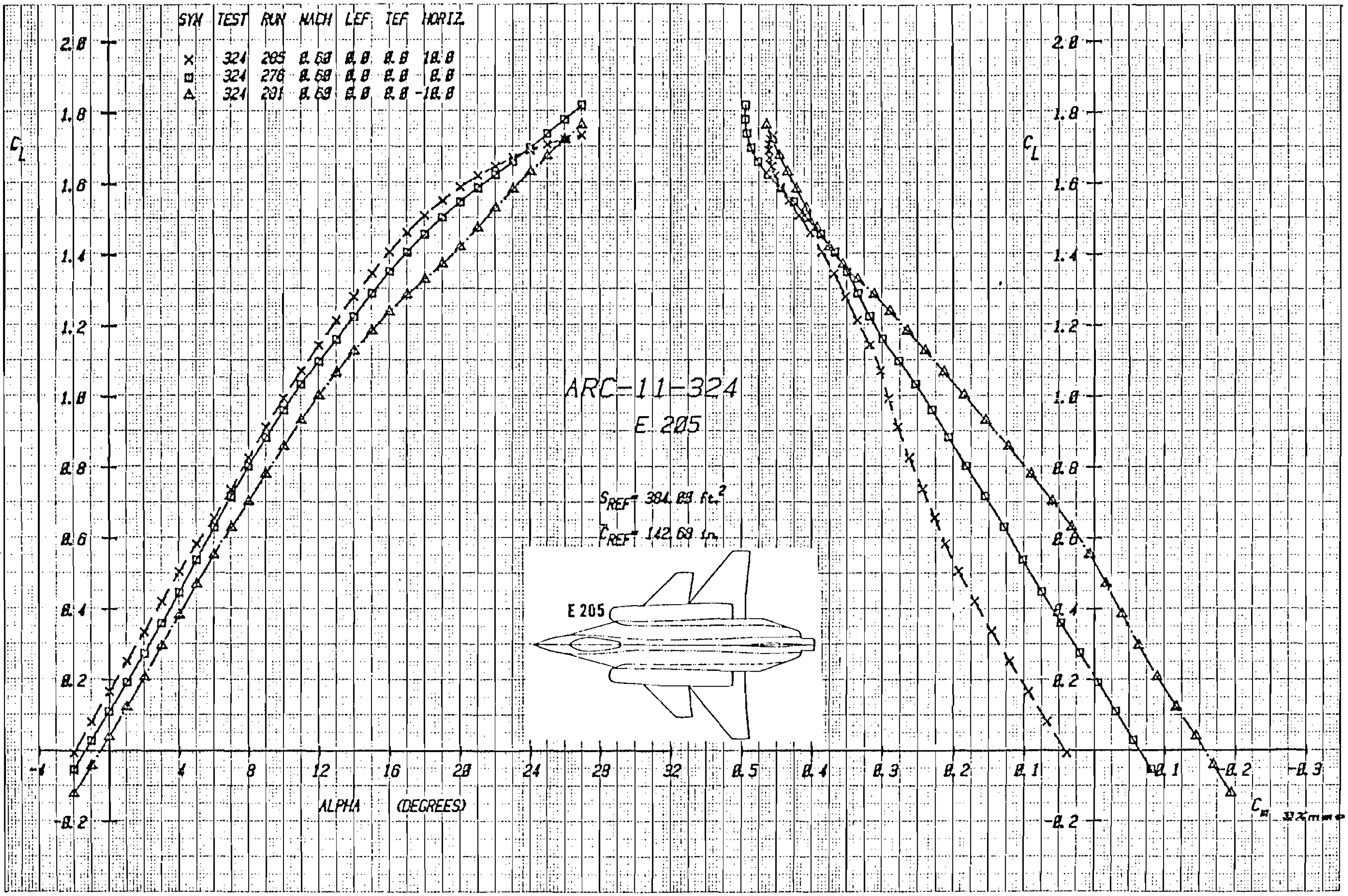

Figure3-26aEffect of Canard Deflection on Lift and Moment with Canard C_2, and Strake S_3, Mach = .6

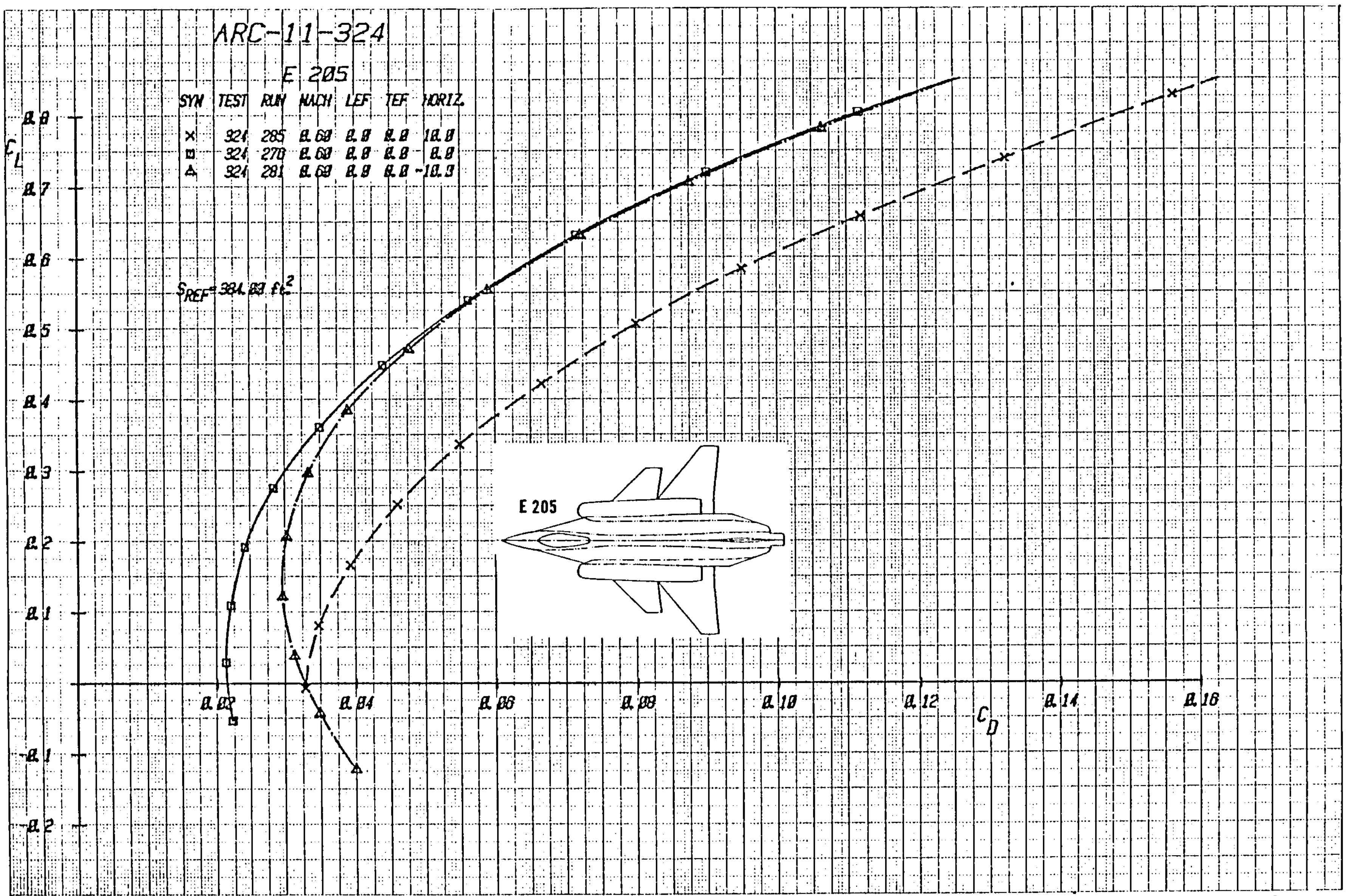

Figure3-26bEffect of Canard Deflection on Drag with Canard C_2, and Strake S_3, Mach = .6

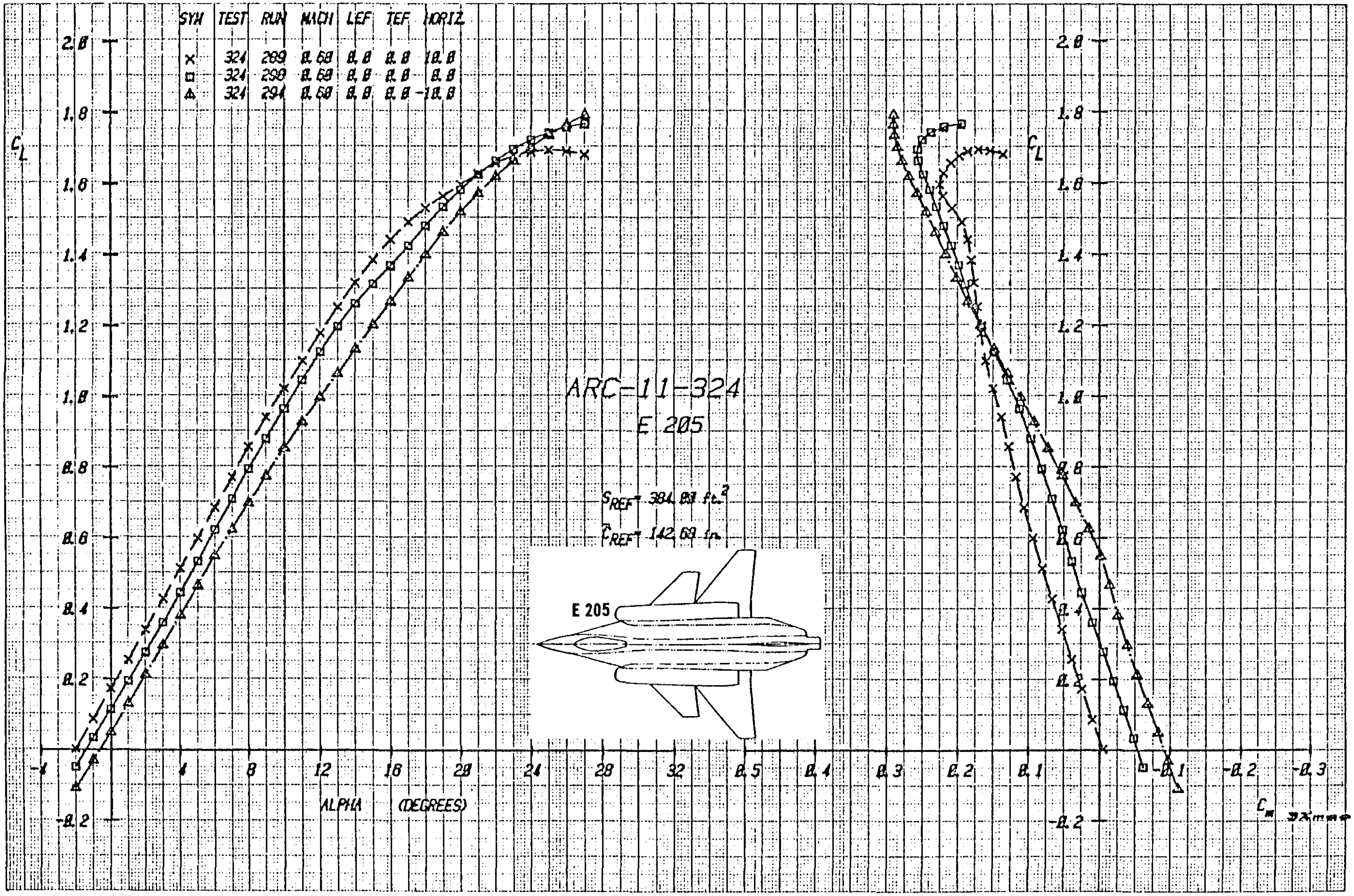

Figure3-27aEffect of Canard Deflection on Lift and Moment with Canard C_3, and Strake S_3, Mach = .6

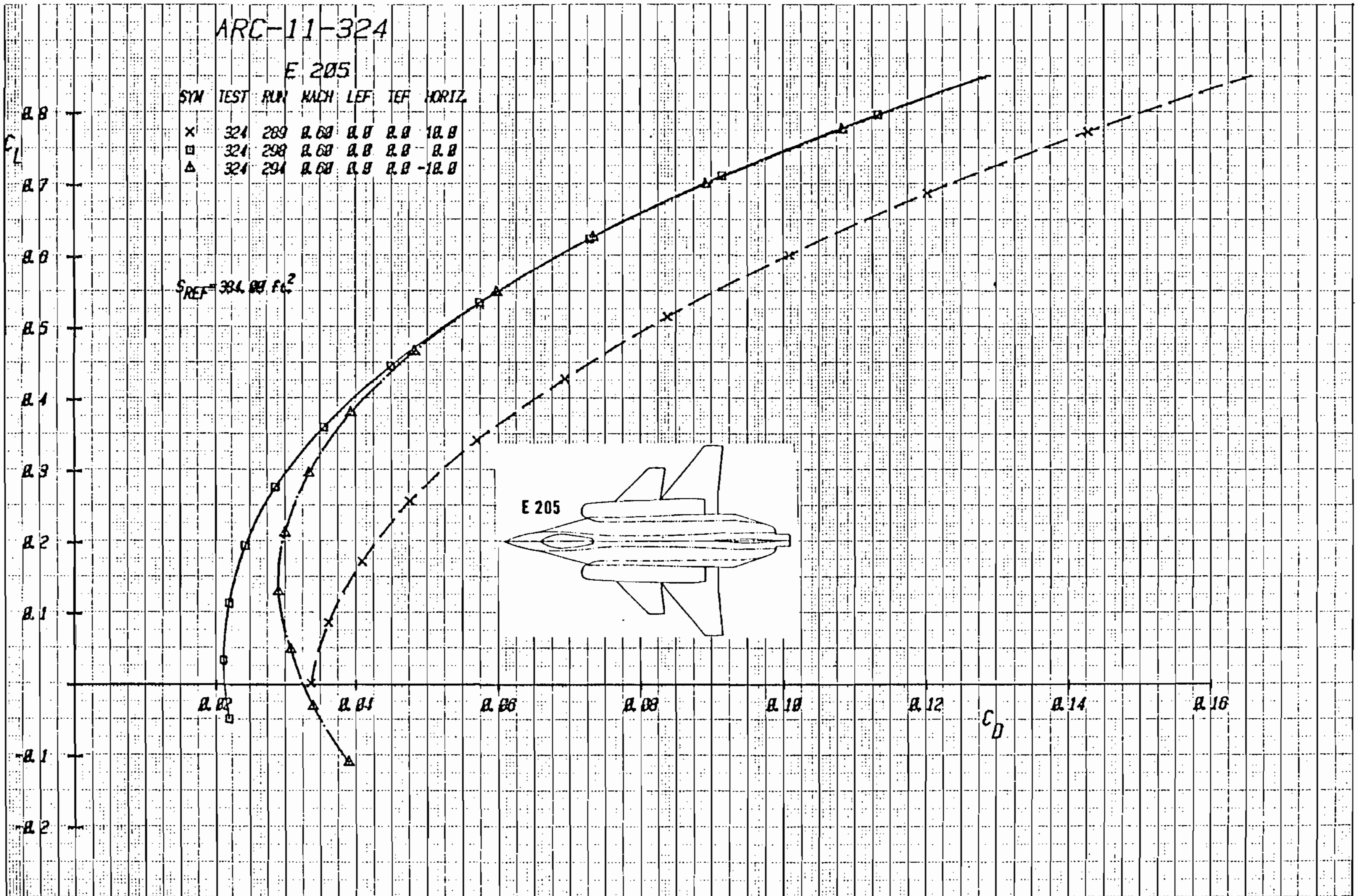

Figure3-27bEffect of Canard Deflection on Drag with Canard C_3, and Strake S_3, Mach = .6

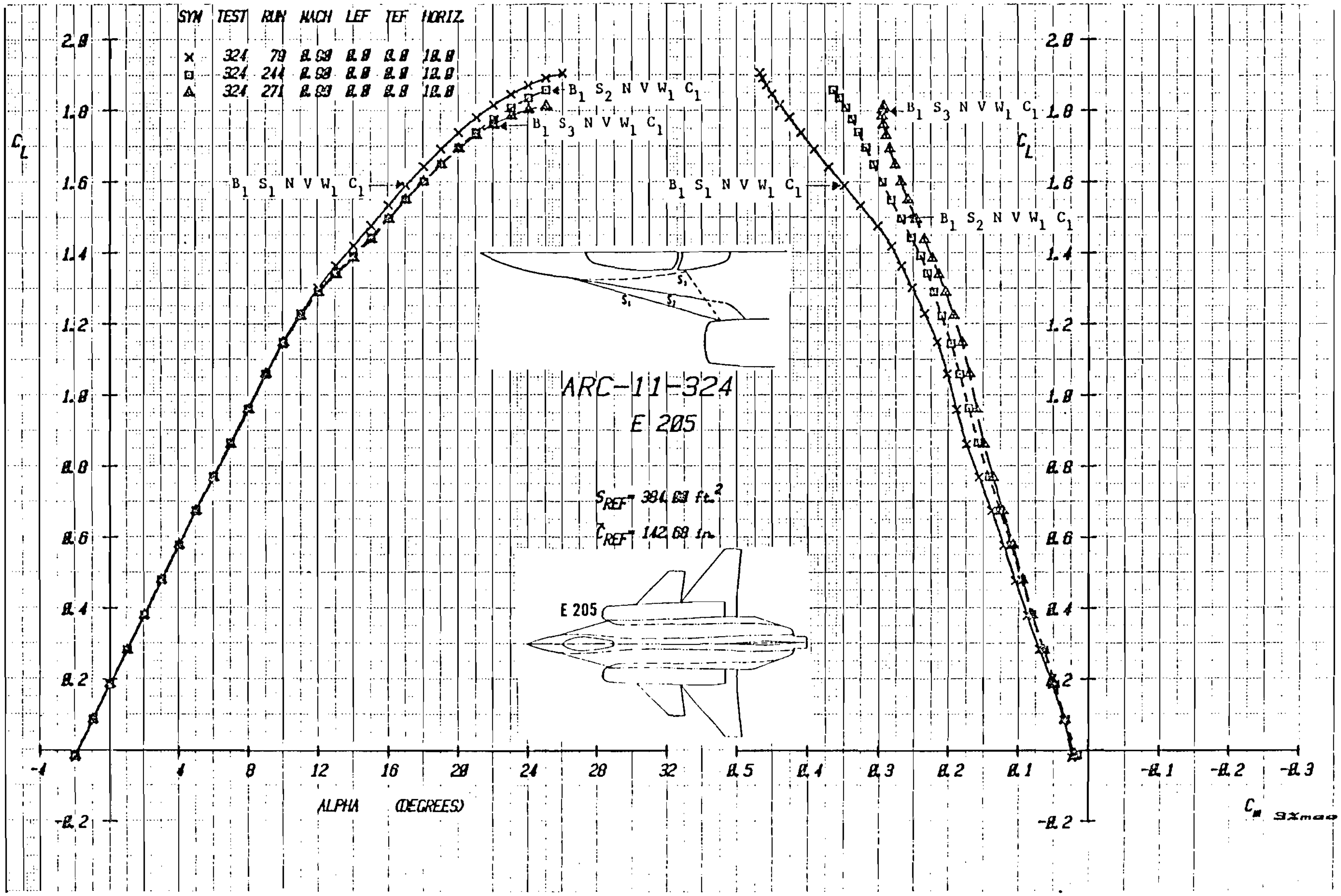

Figure 3-28a Effect of Strake Shape on Lift and Moment with Canard C_1 Deflected +10°, Mach = .9

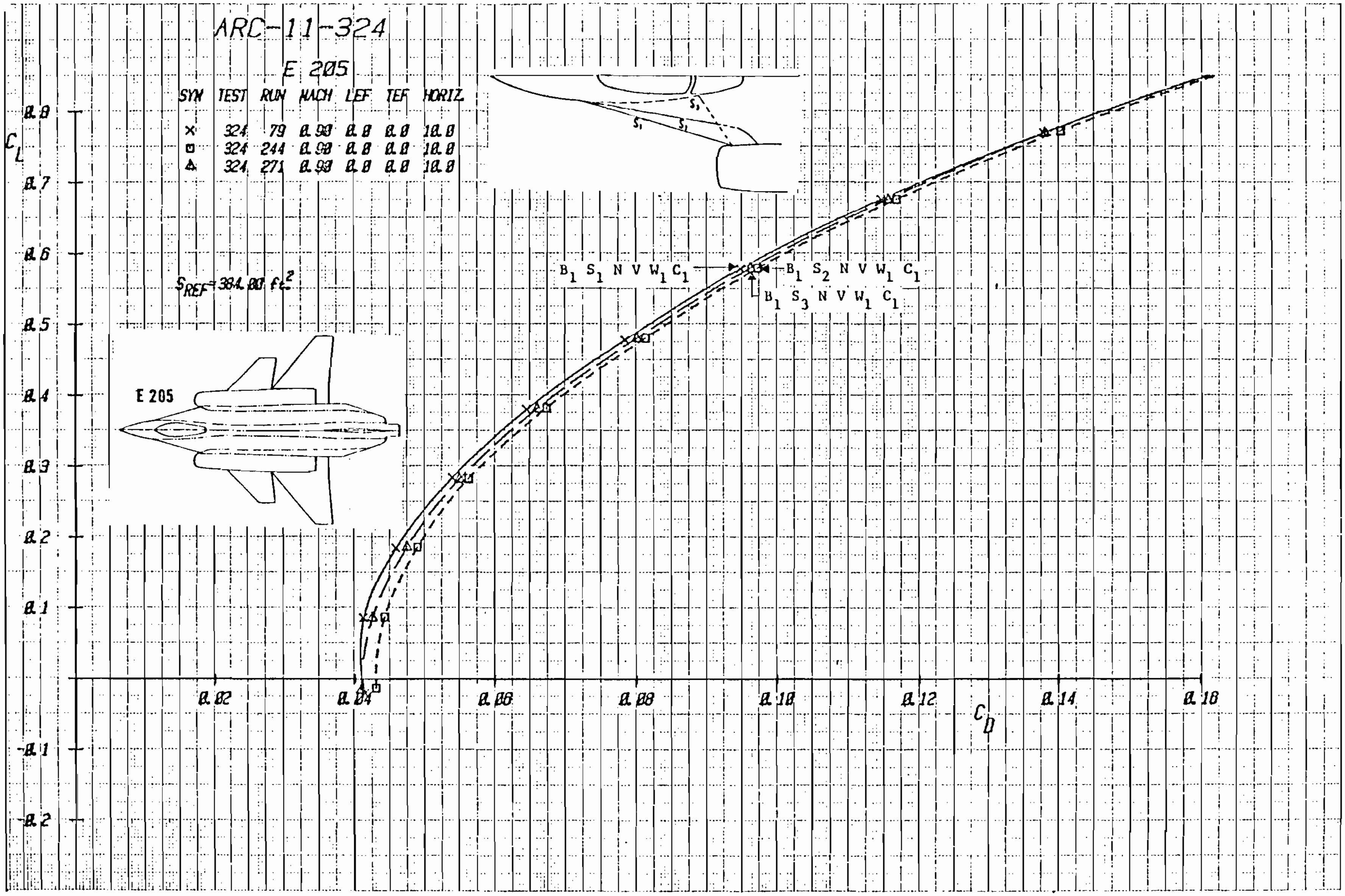

Figure3-28bEffect of Strake Shape on Drag with Canard C_1 Deflected +10°, Mach = .9

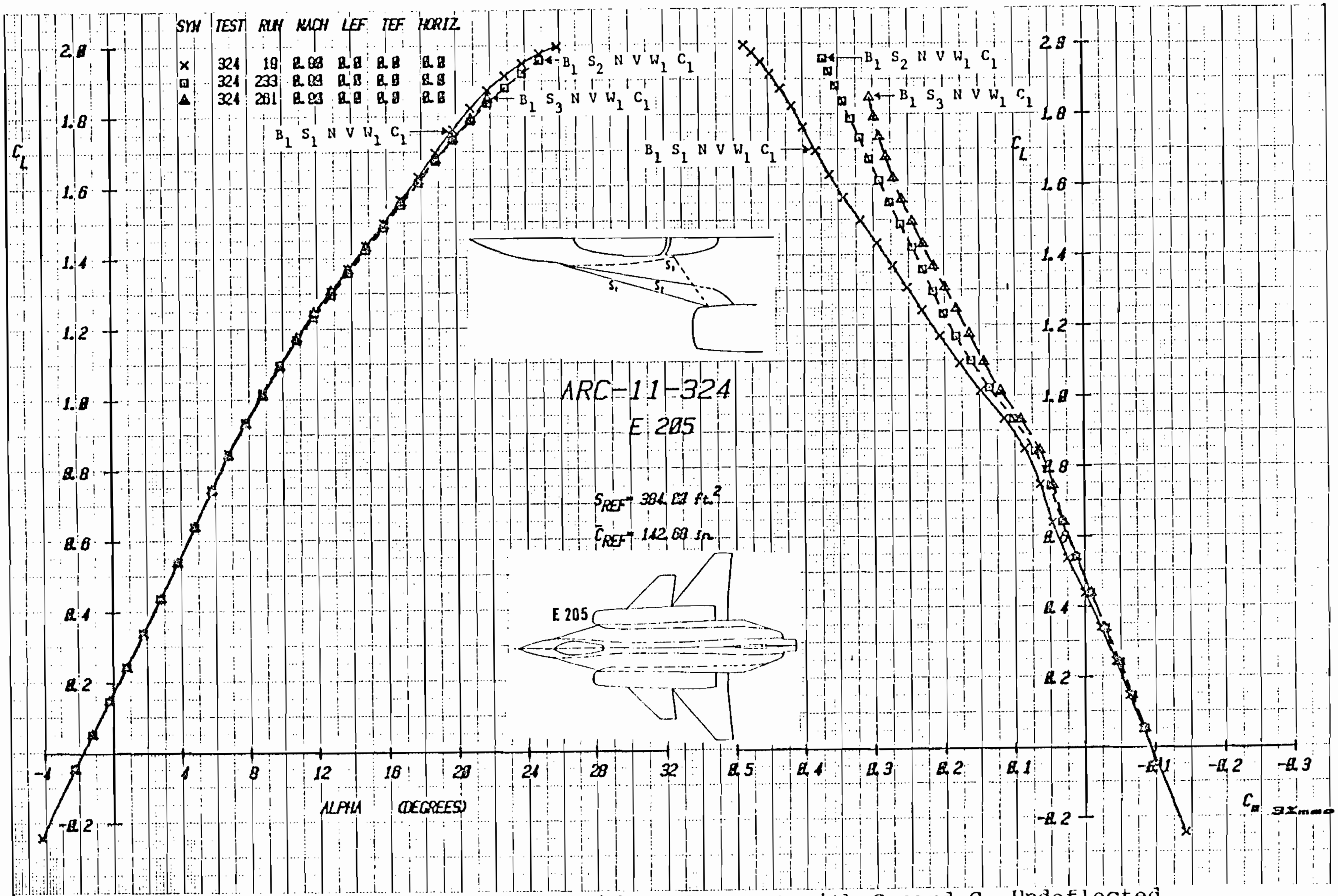

Figure3-29aEffect of Strake Shape on Lift and Moment with Canard C_1 Undeflected, Mach = .9

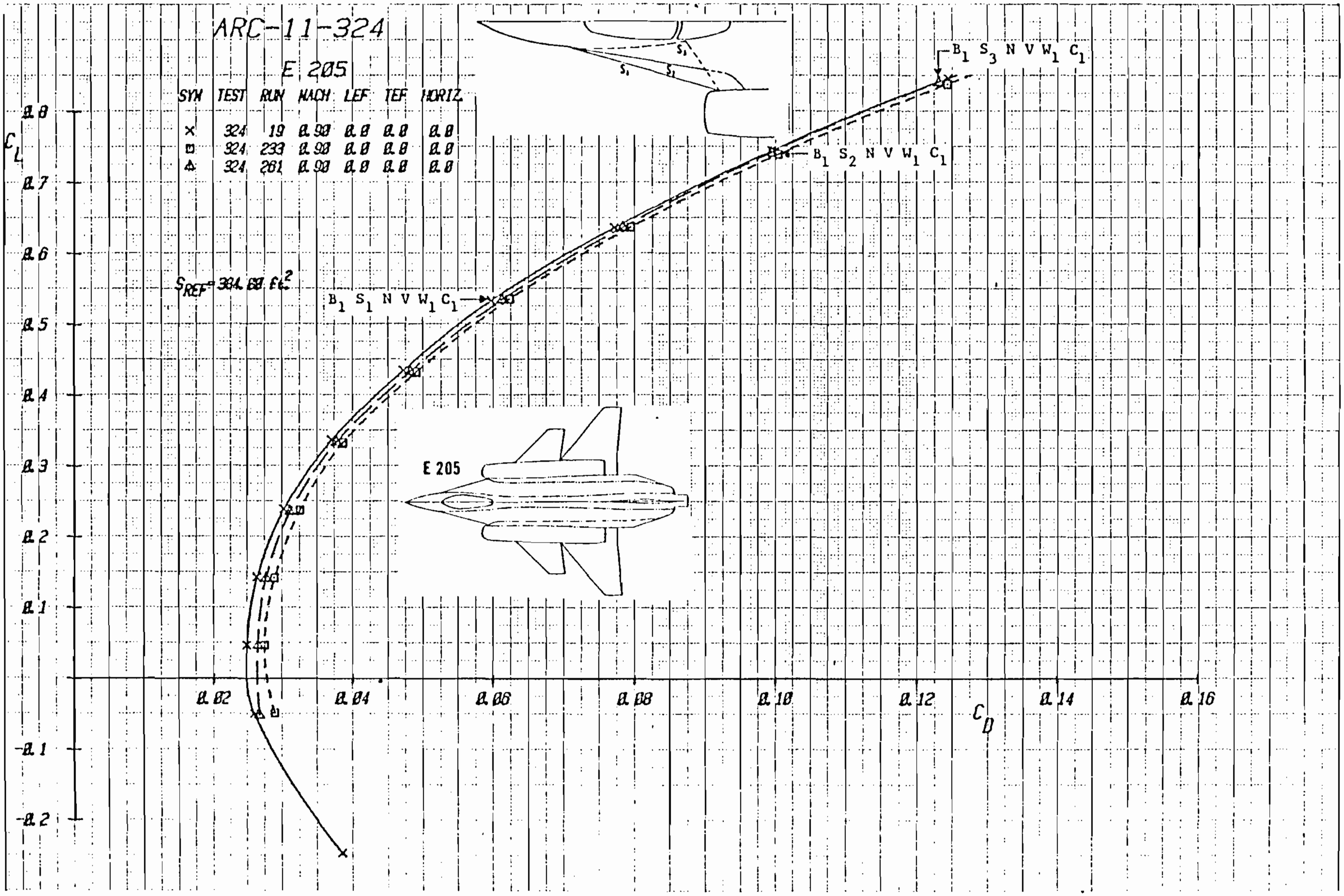

Figure3-29bEffect of Strake Shape on Drag with Canard C_1 Undeflected, Mach = .9

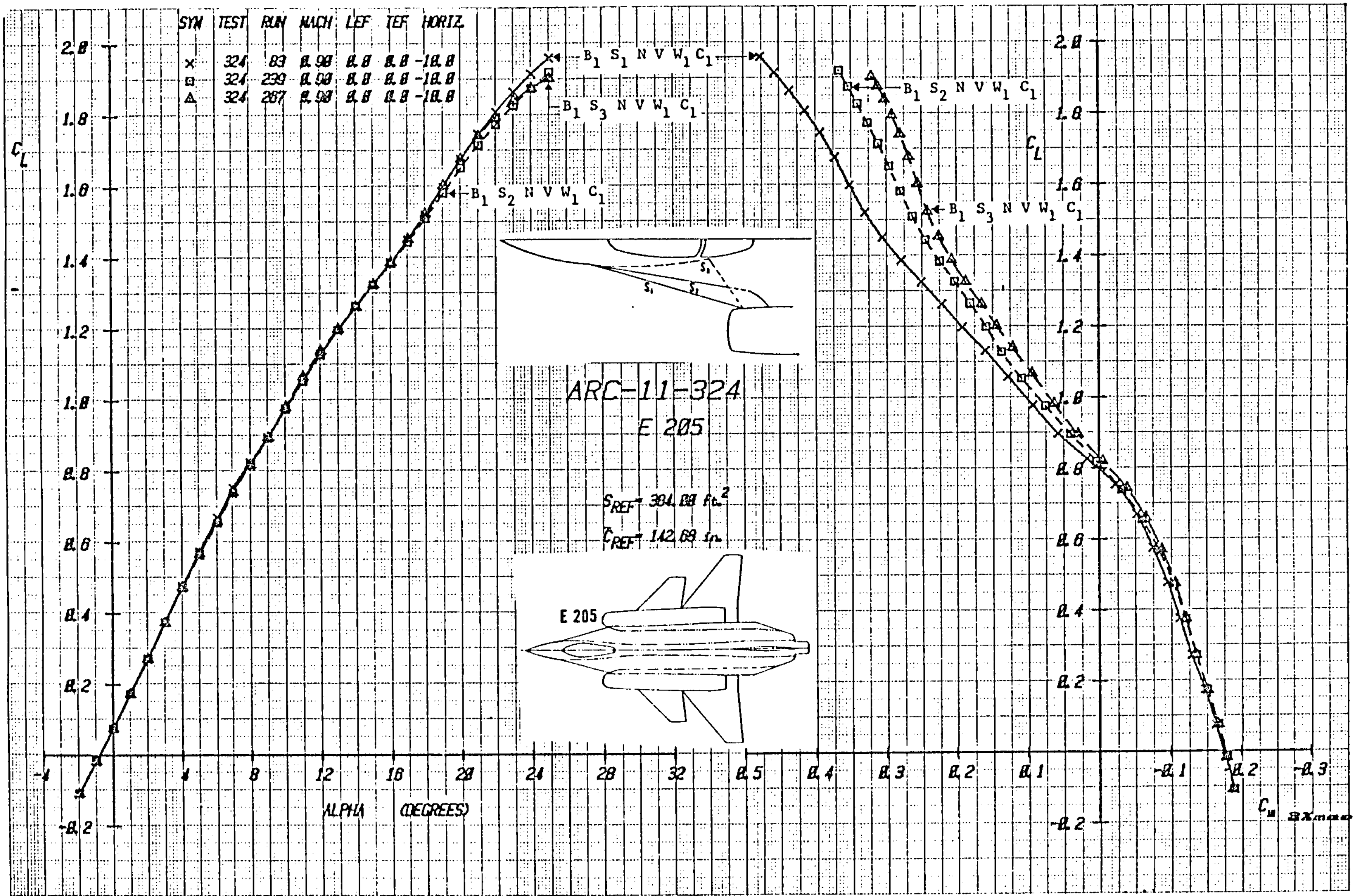

Figure 3-30a Effect of Strake Shape on Lift and Moment with Canard C_1 Deflected -10°, Mach = .9

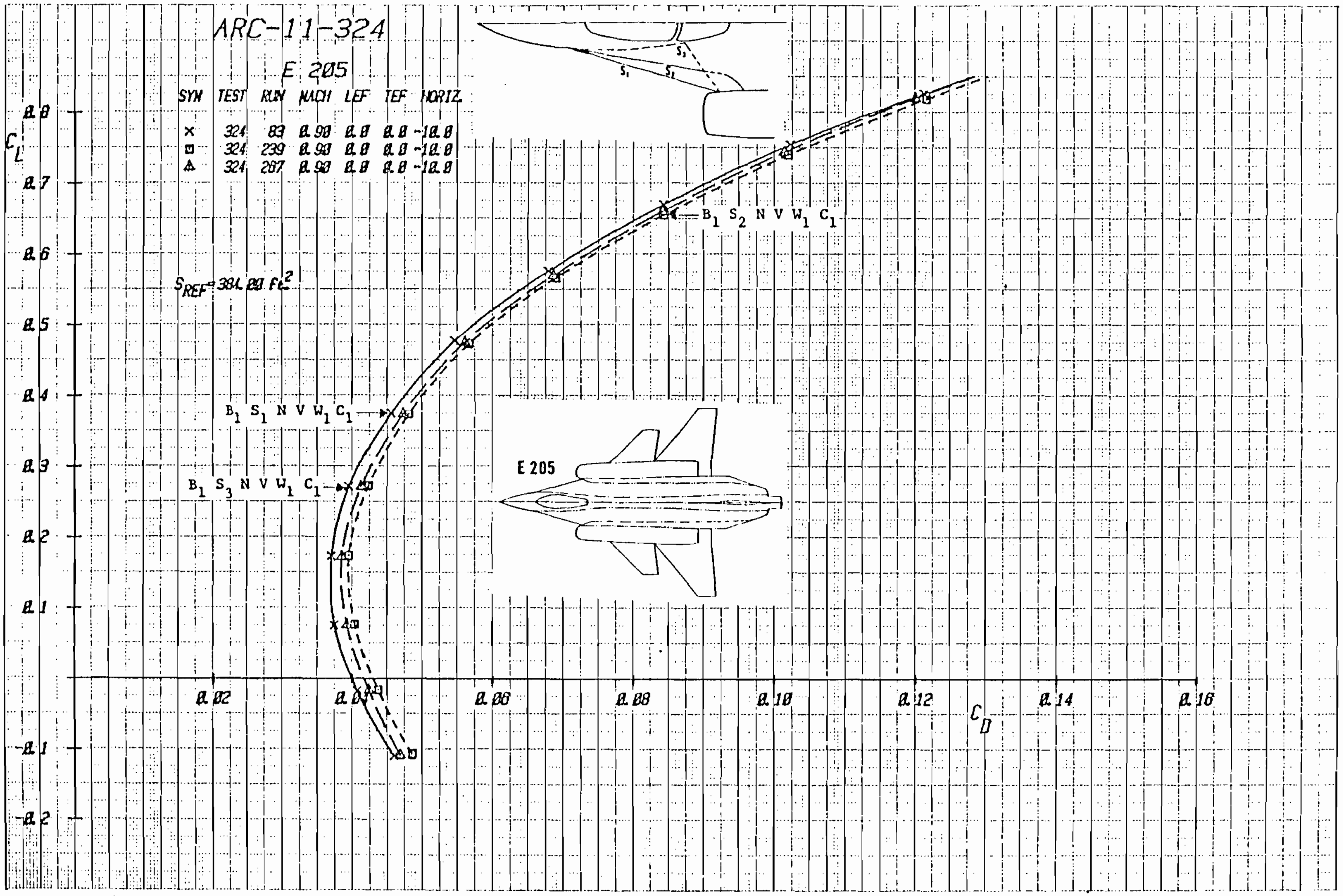

Figure3-30bEffect of Strake Shape on Drag with Canard C_1 Deflected -10°, Mach = .9

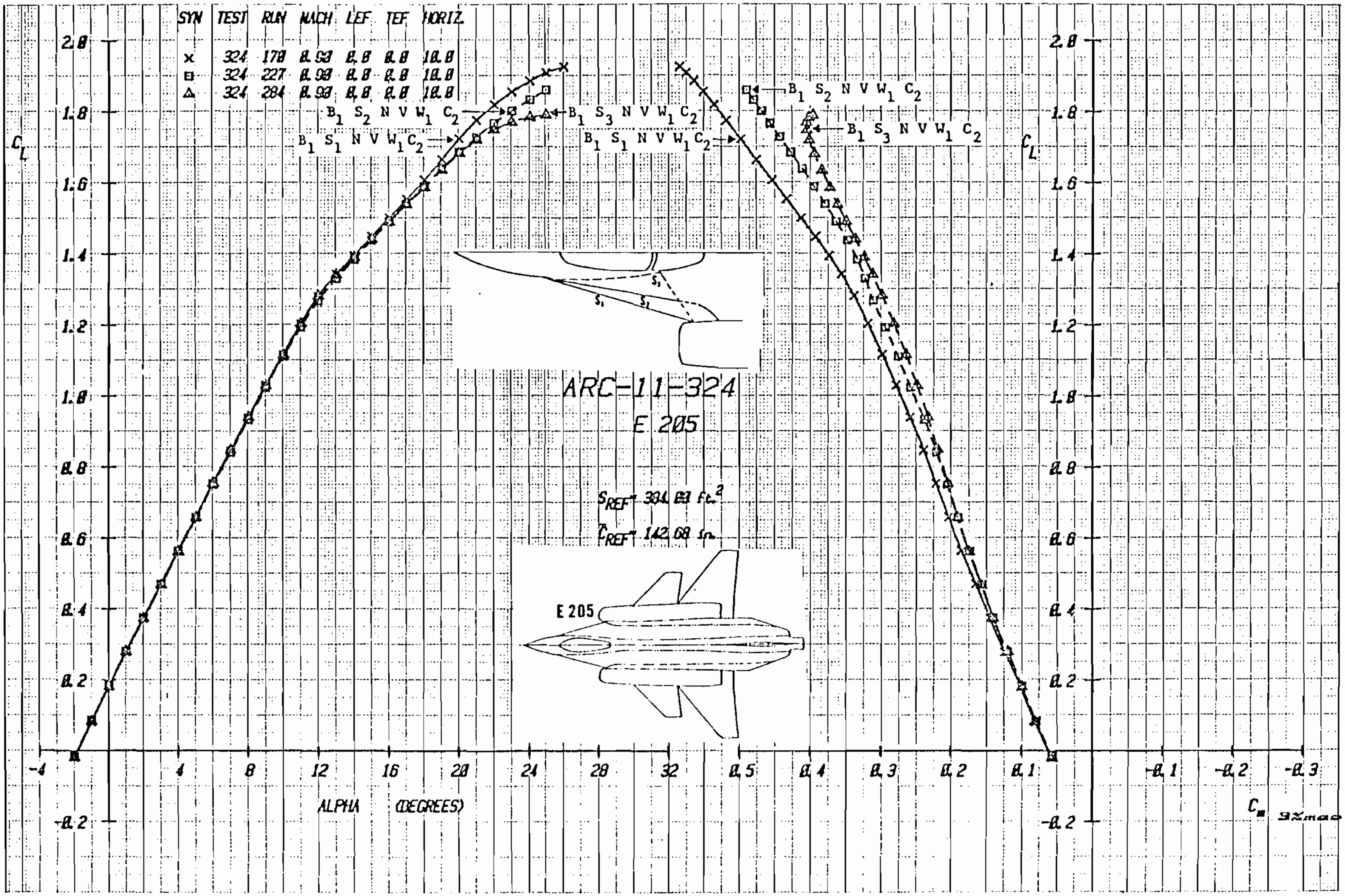

Figure3-31a Effect of Strake Shape on Lift and Moment with Canard C_2 Deflected +10°, Mach = .9

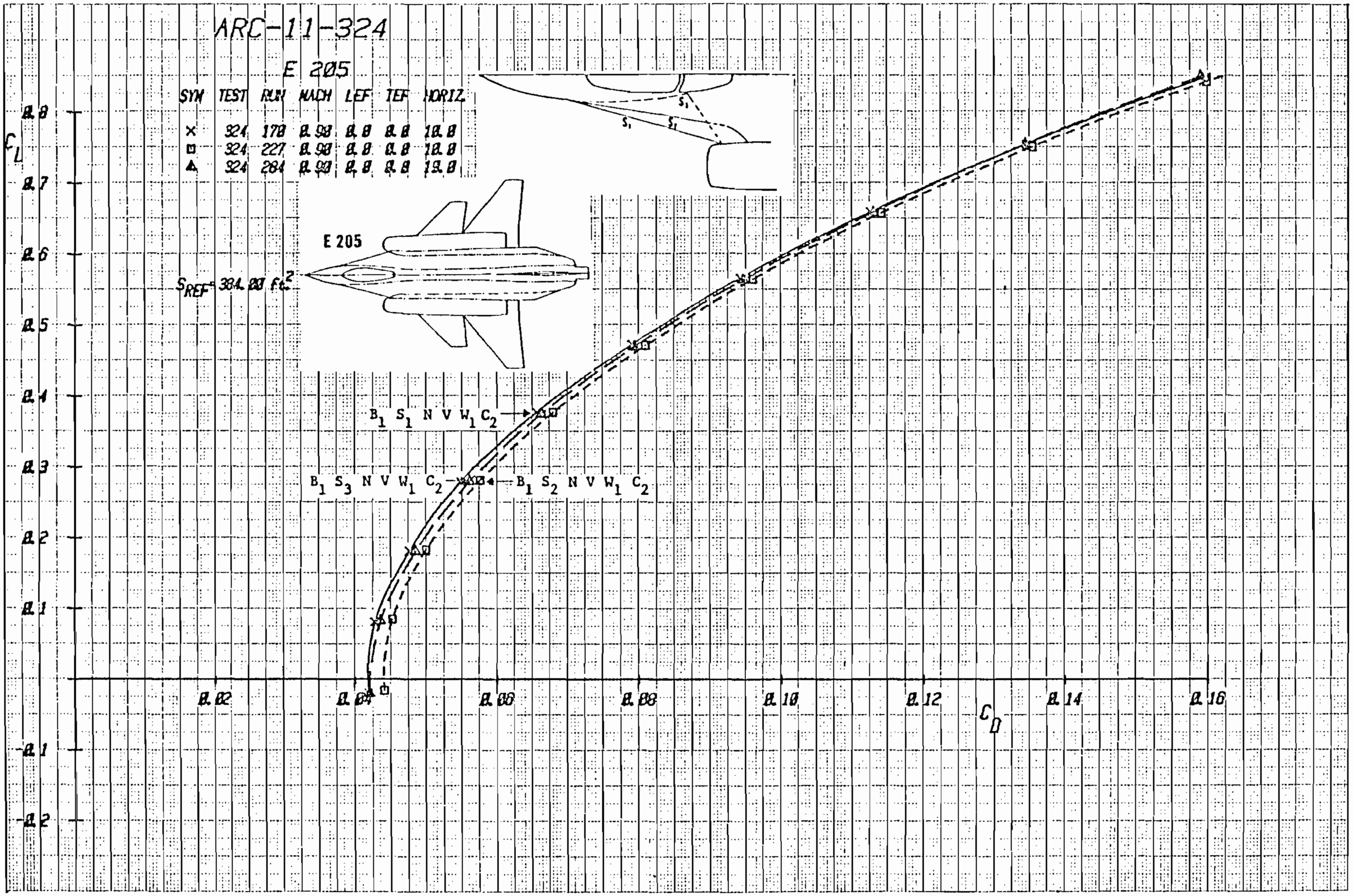

Figure3-31bEffect of Strake Shape on Drag with Canard C_2 Deflected +10°, Mach = .9

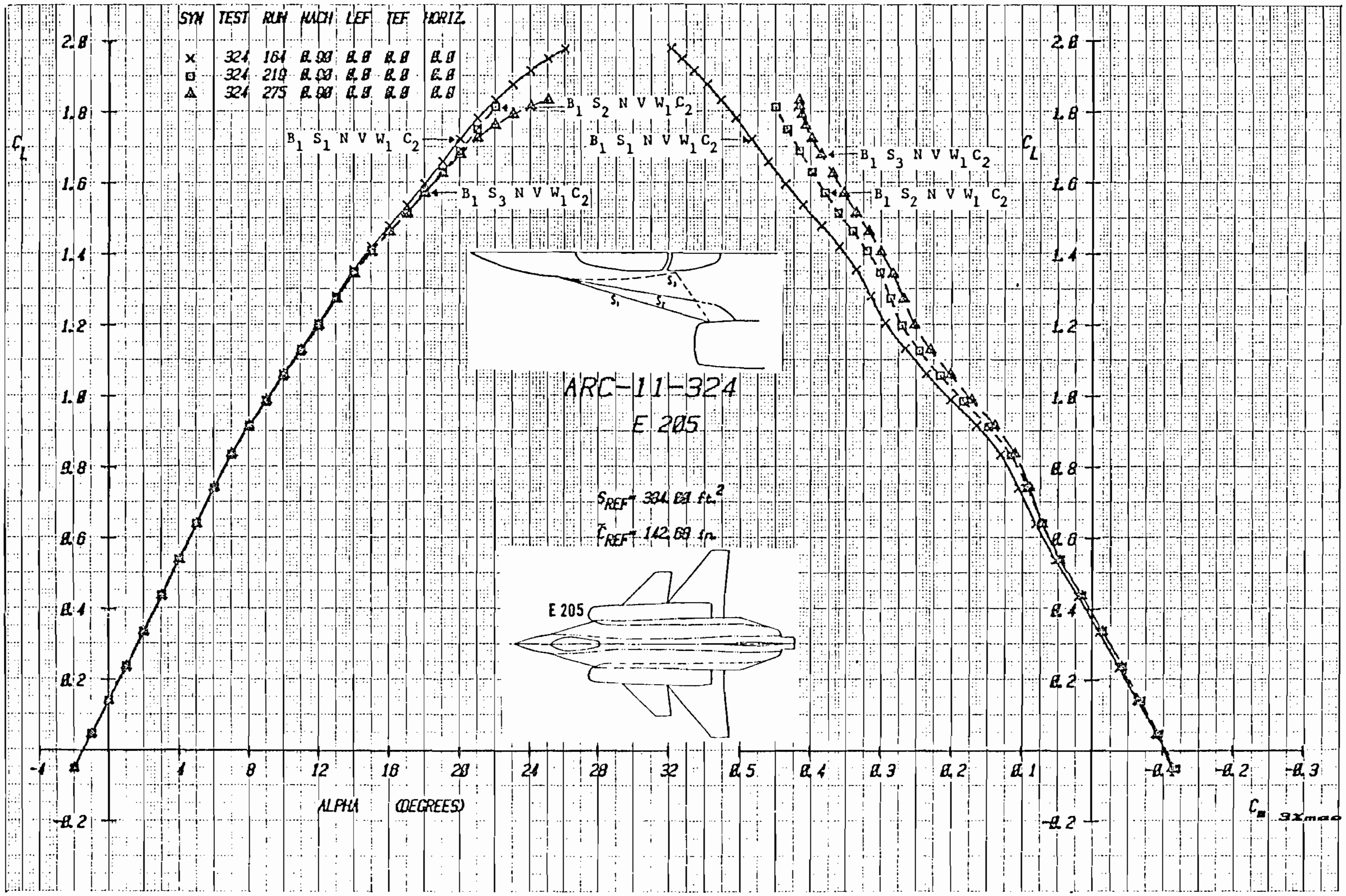

Figure3-32aEffect of Strake Shape on Lift and Moment with Canard C_2 Undeflected, Mach = .9

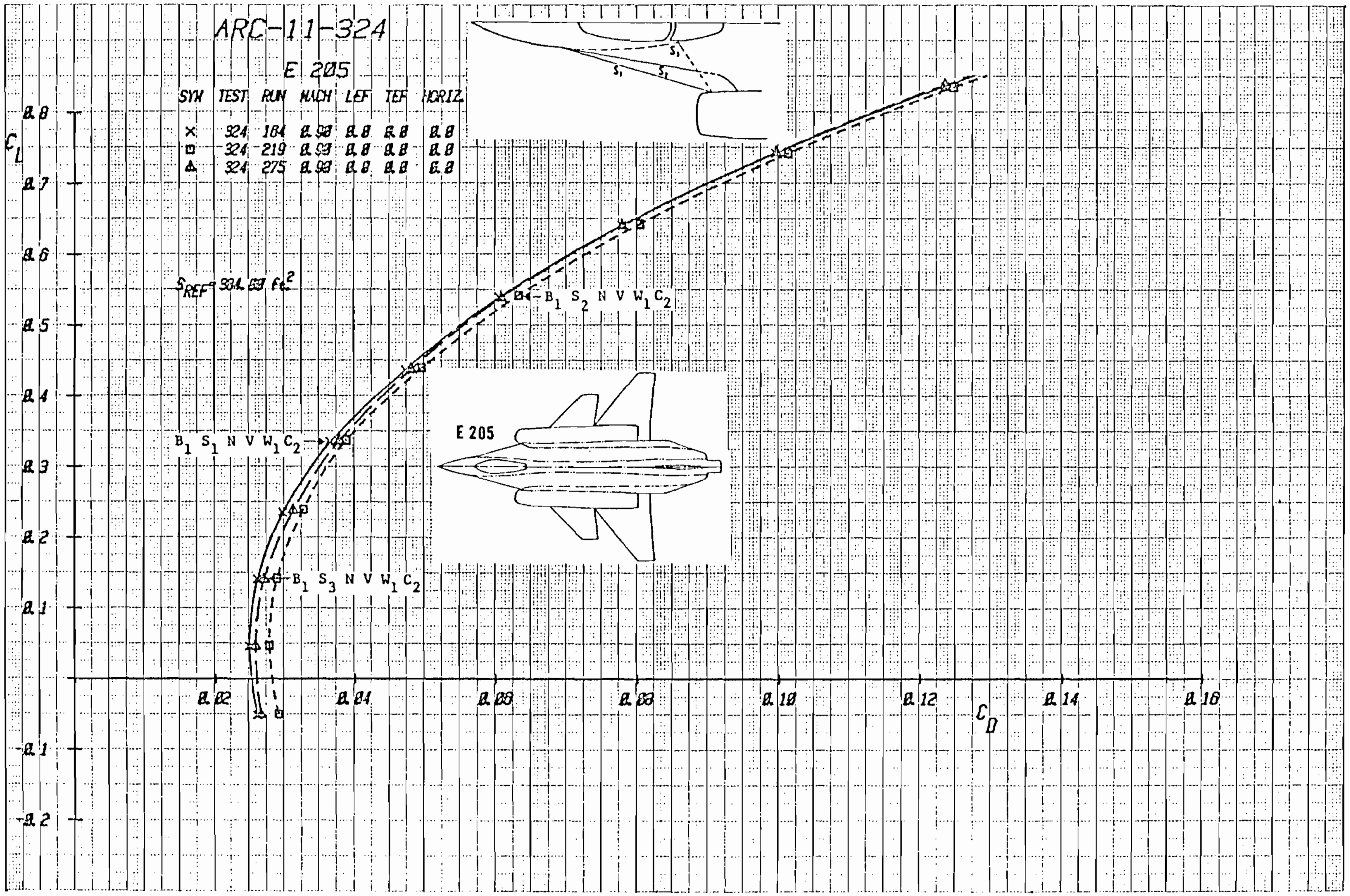

Figure3-32bEffect of Strake Shape on Drag with Canard C_2 Undeflected, Mach = .9

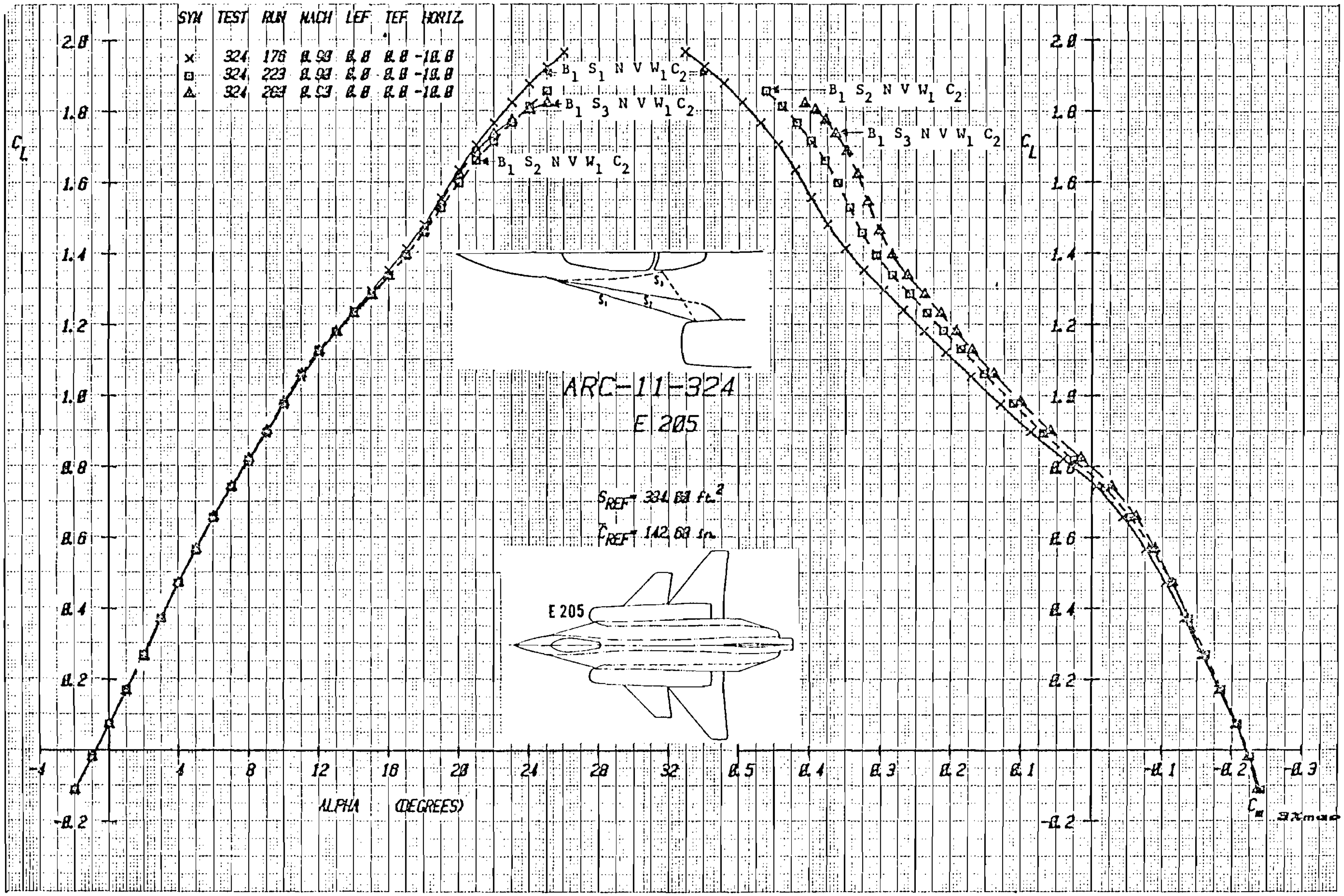

Figure3-33aEffect of Strake Shape on Lift and Moment with Canard C_2 Deflected -10°,
Mach = .9

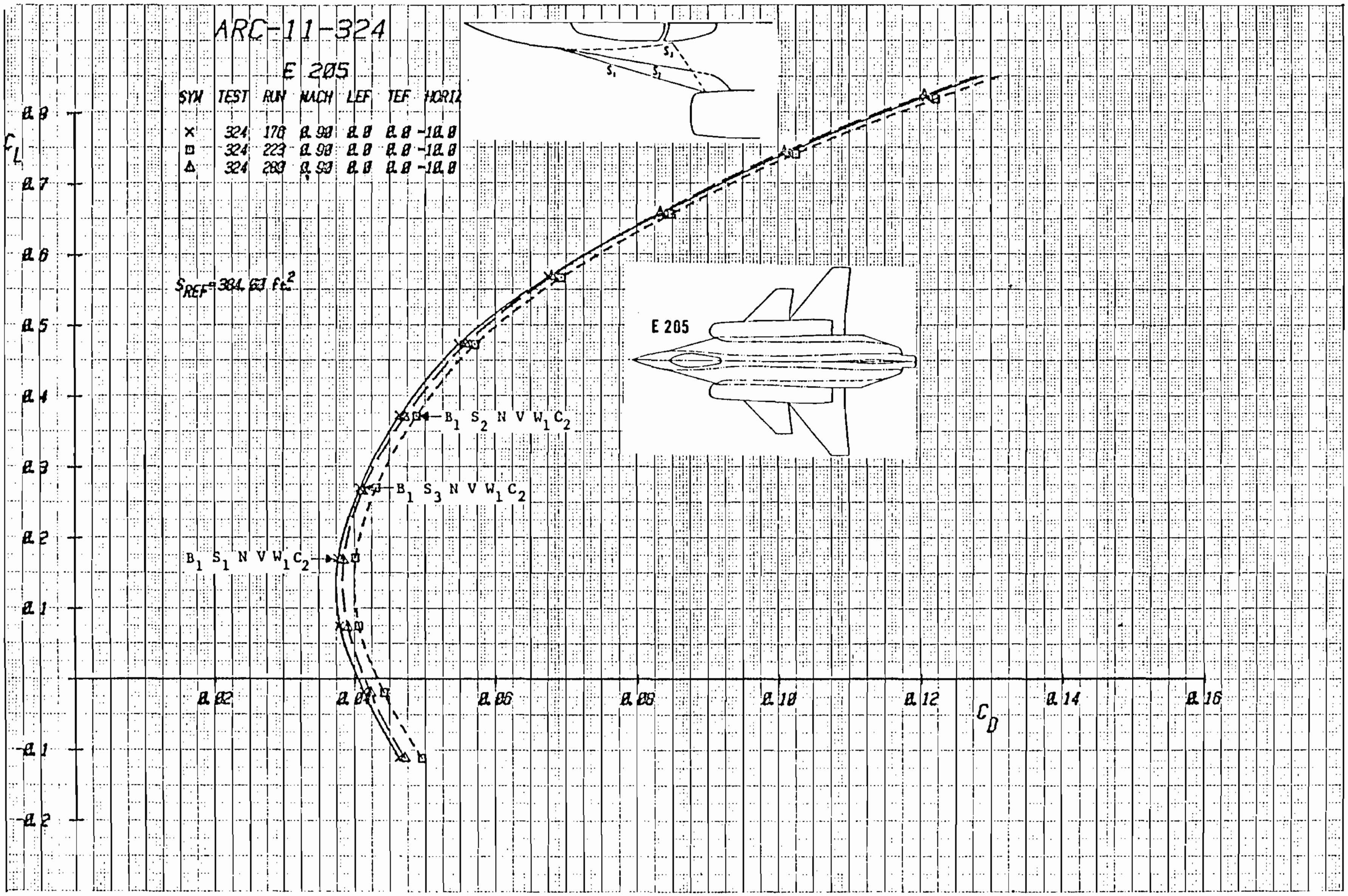

Figure3-33bEffect of Strake Shape on Drag with Canard C_2 Deflected -10°, Mach = .9

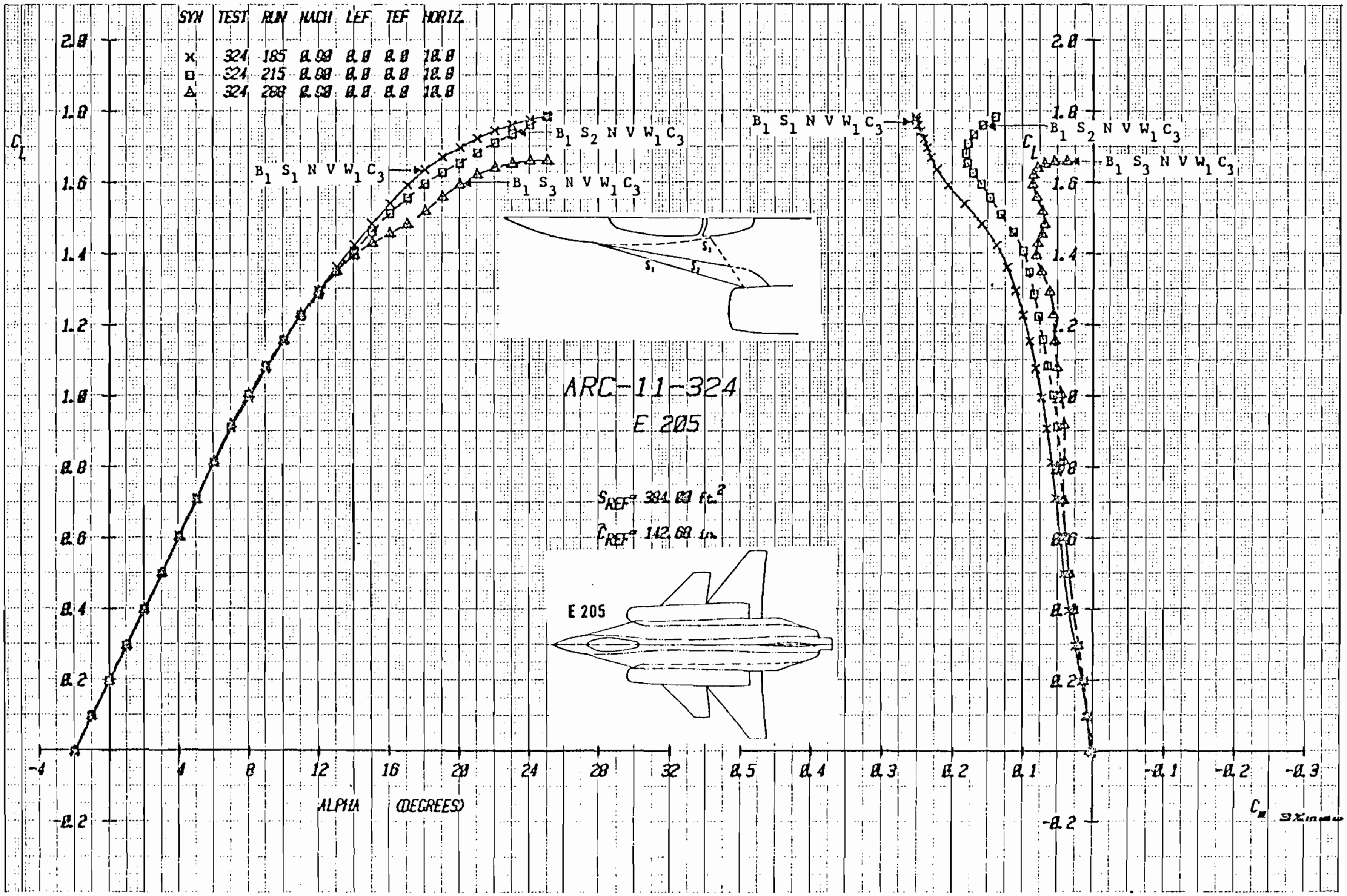

Figure 3-34a Effect of Strake Shape on Lift and Moment with Canard C_3 Deflected +10°, Mach = .9

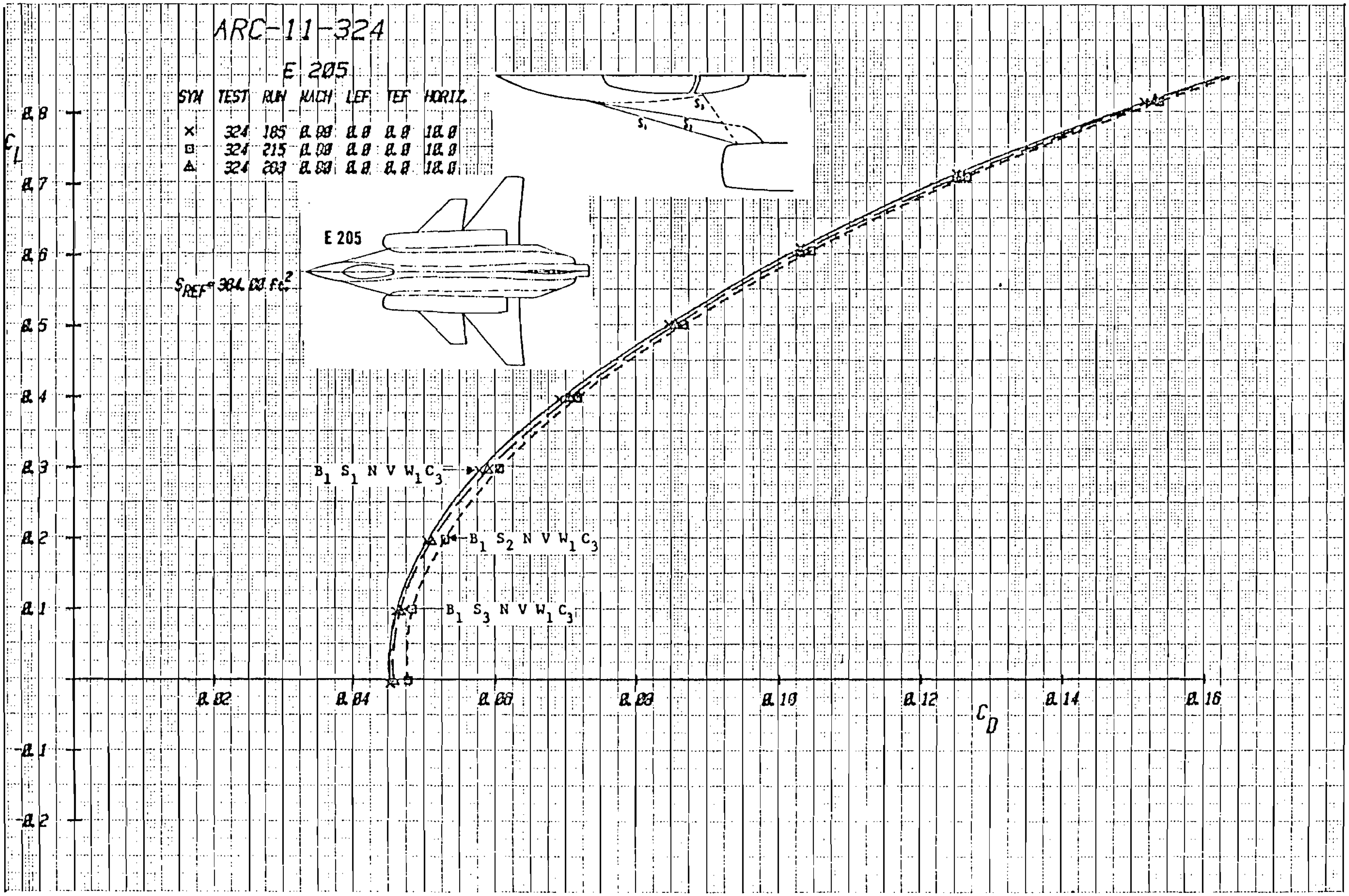

Figure3-34bEffect of Strake Shape on Drag with Canard C_3 Deflected +10°, Mach = .9

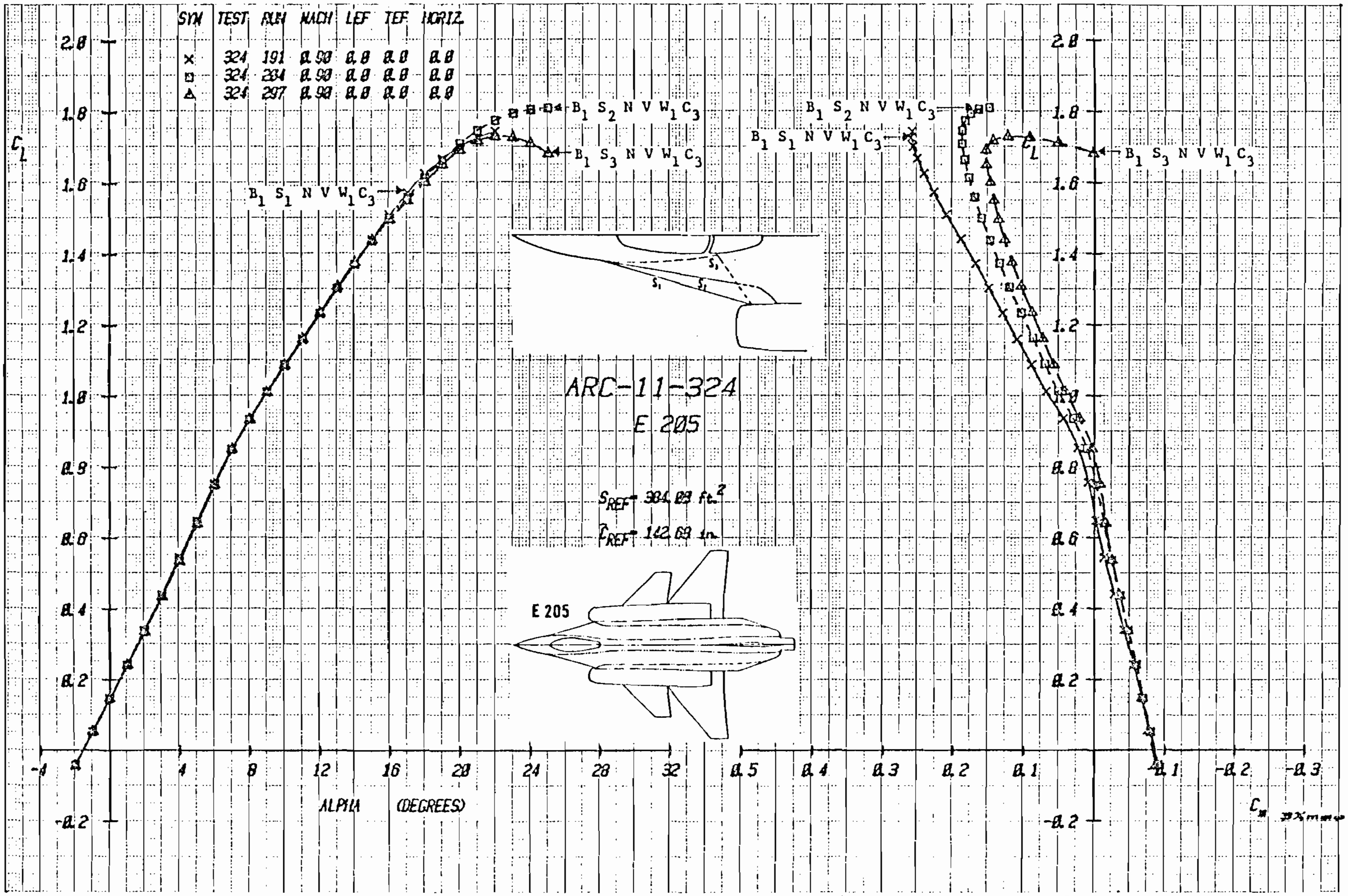

Figure3-35aEffect of Strake Shape on Lift and Moment with Canard C_3 Undeflected, Mach = .9

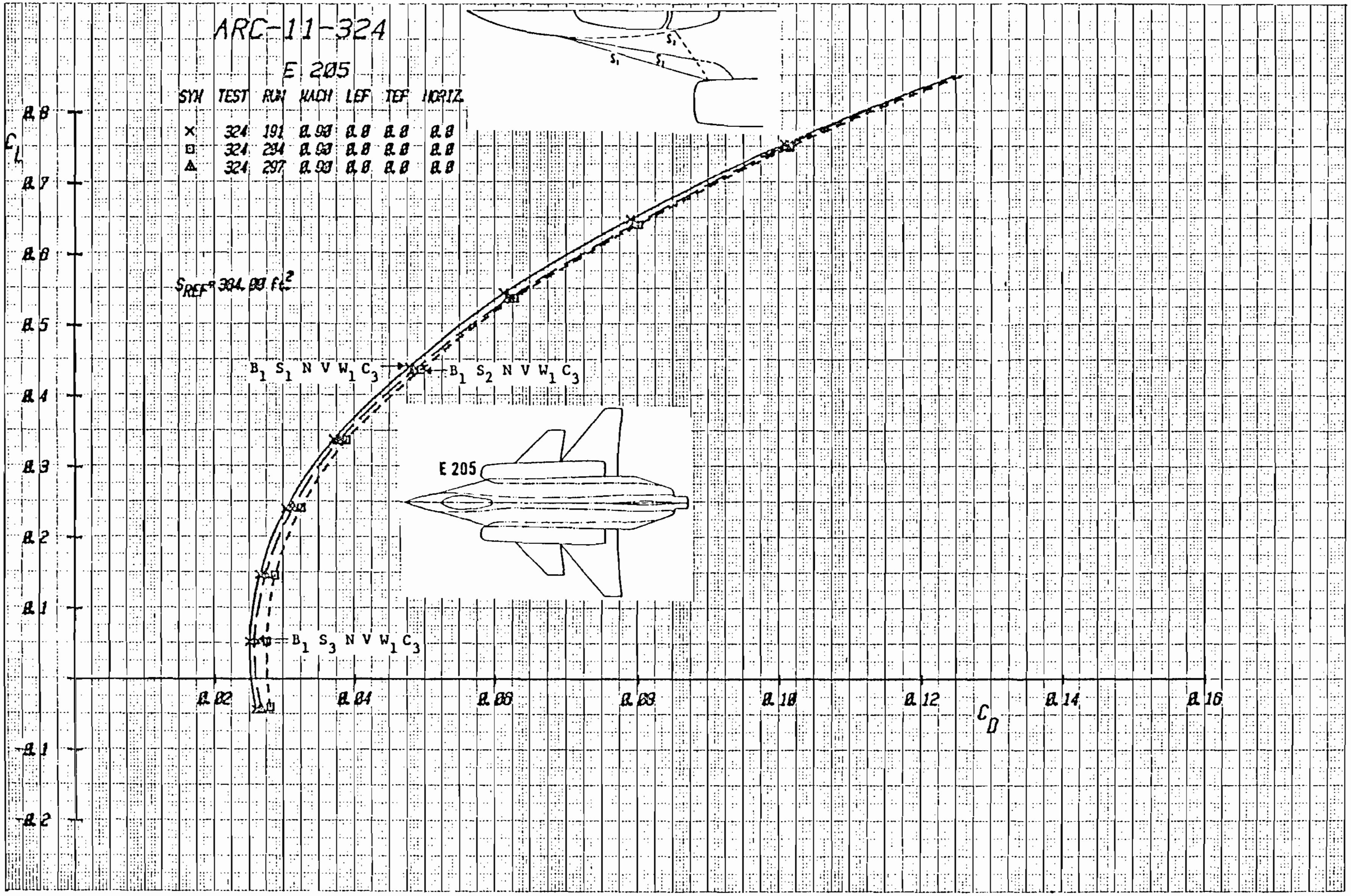

Figure3-35bEffect of Strake Shape on Drag with Canard C_3 Undeflected, Mach = .9

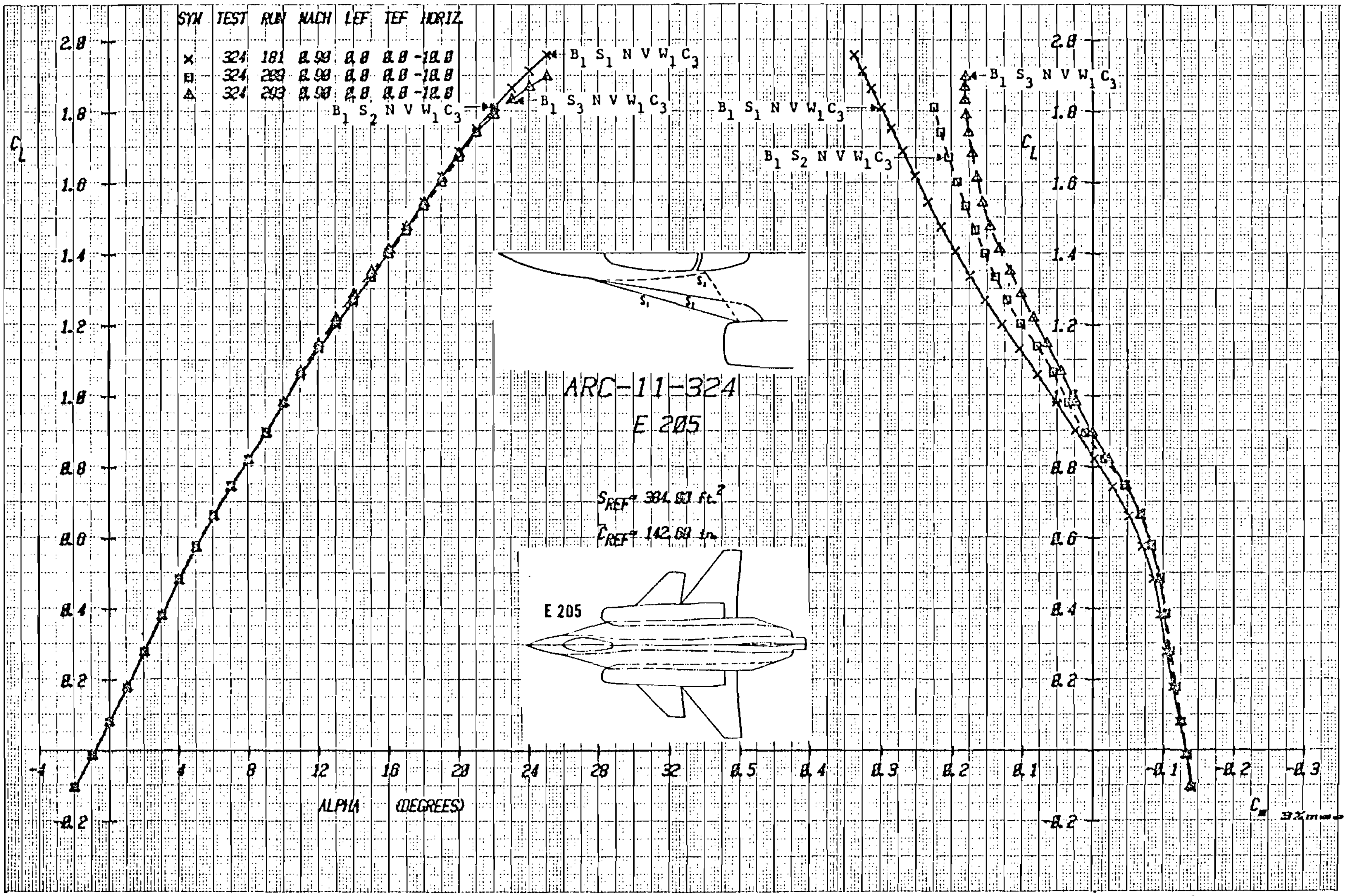

Figure3-36aEffect of Strake Shape on Lift and Moment with Canard C_3 Deflected -10°, Mach = .9

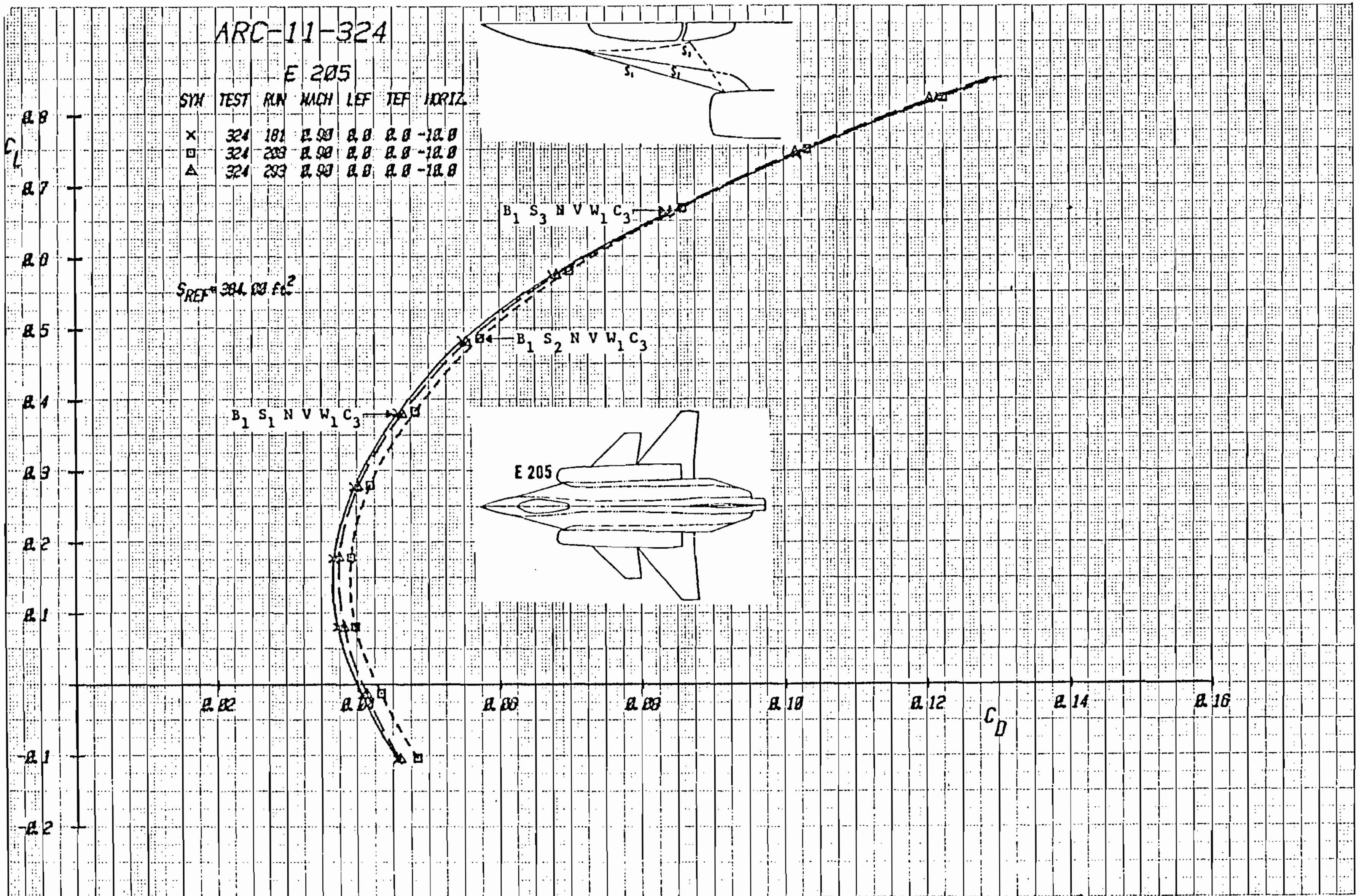

Figure3-36bEffect of Strake Shape on Drag with Canard C_3 Deflected -10°, Mach = .9

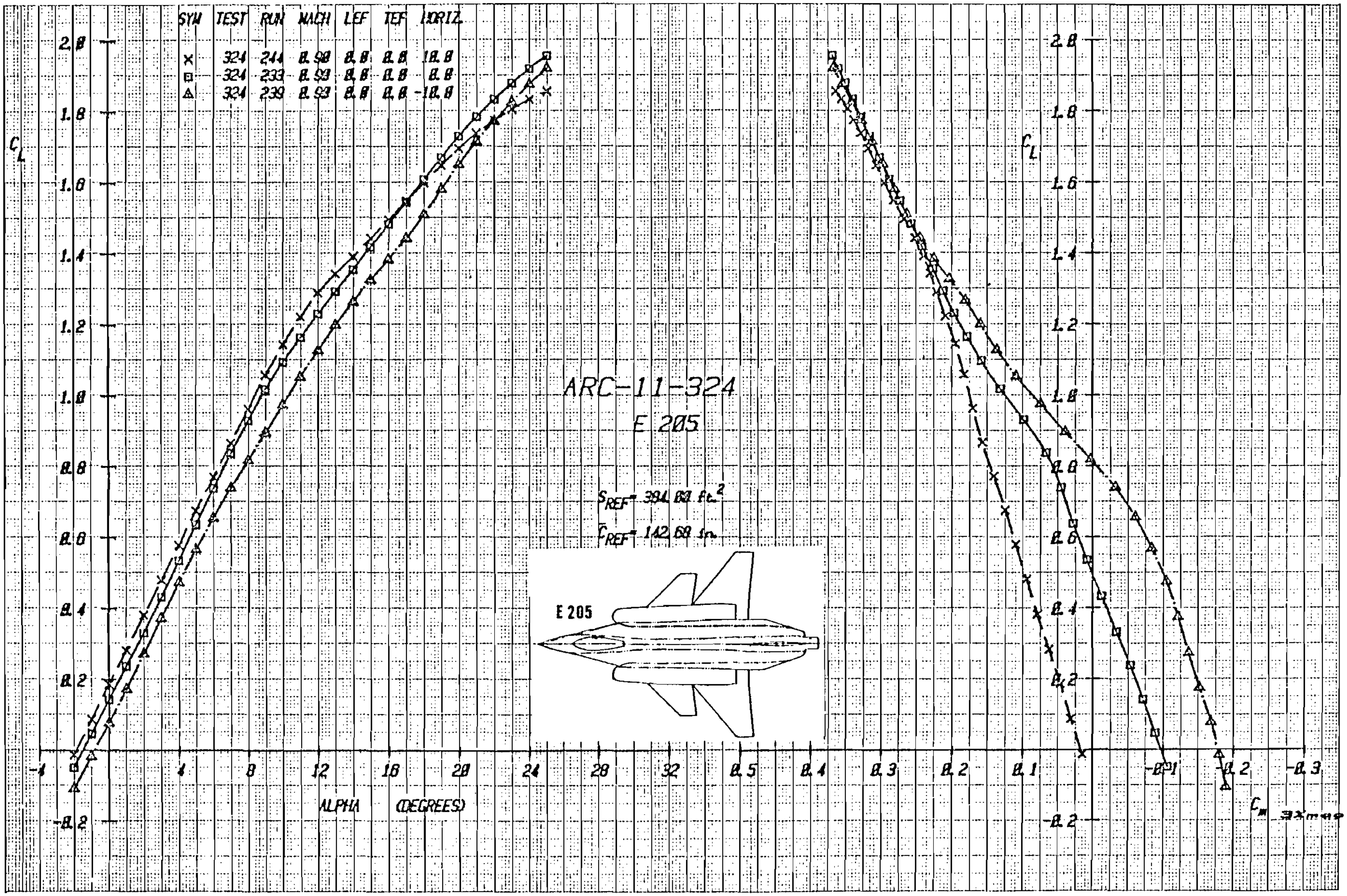

Figure3-37aEffect of Canard Deflection on Lift and Moment With Canard C_1, and Strake S_2, Mach = .9

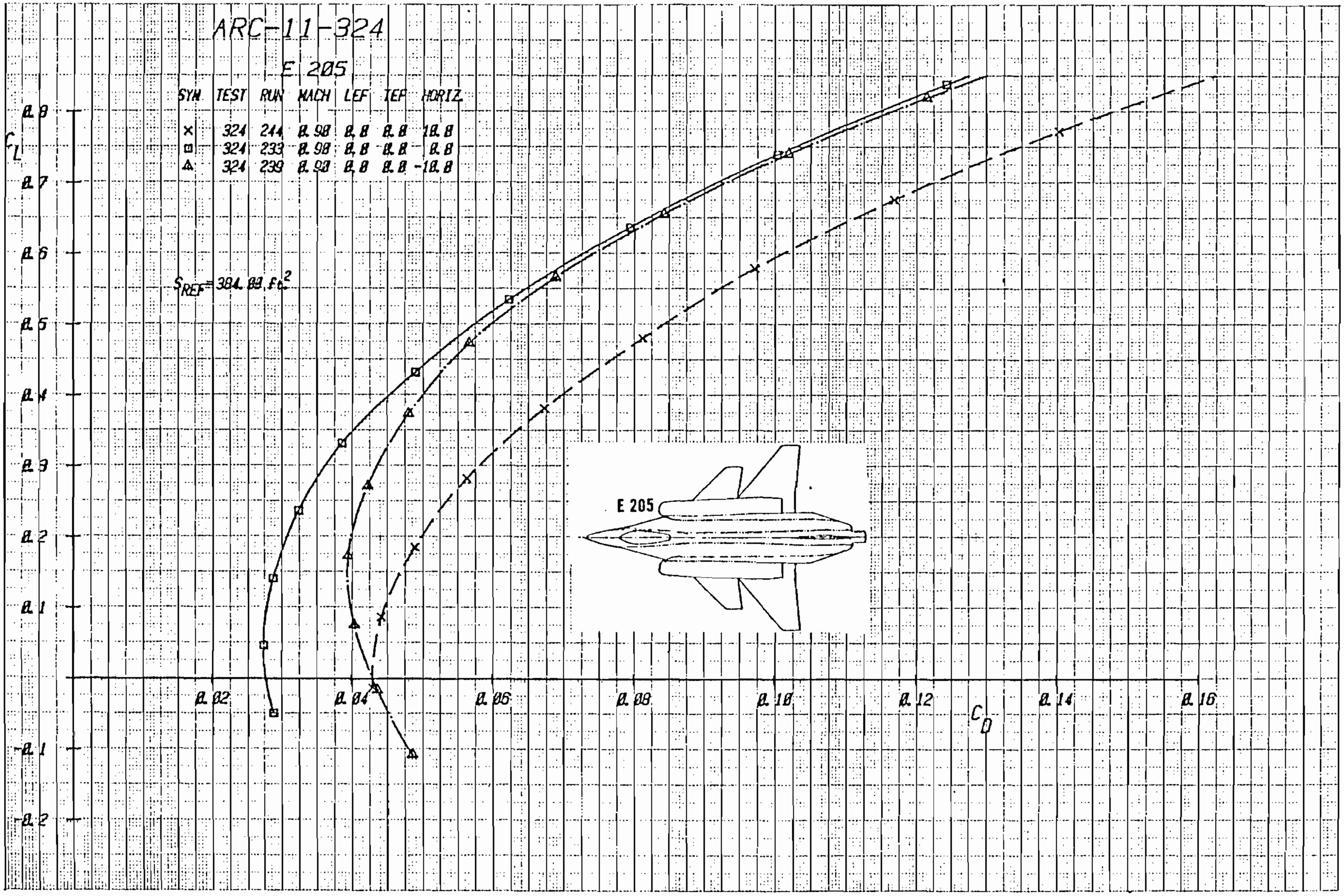

Figure3-37b Effect of Canard Deflection on Drag With Canard C_1, and Strake S_2, Mach = .9

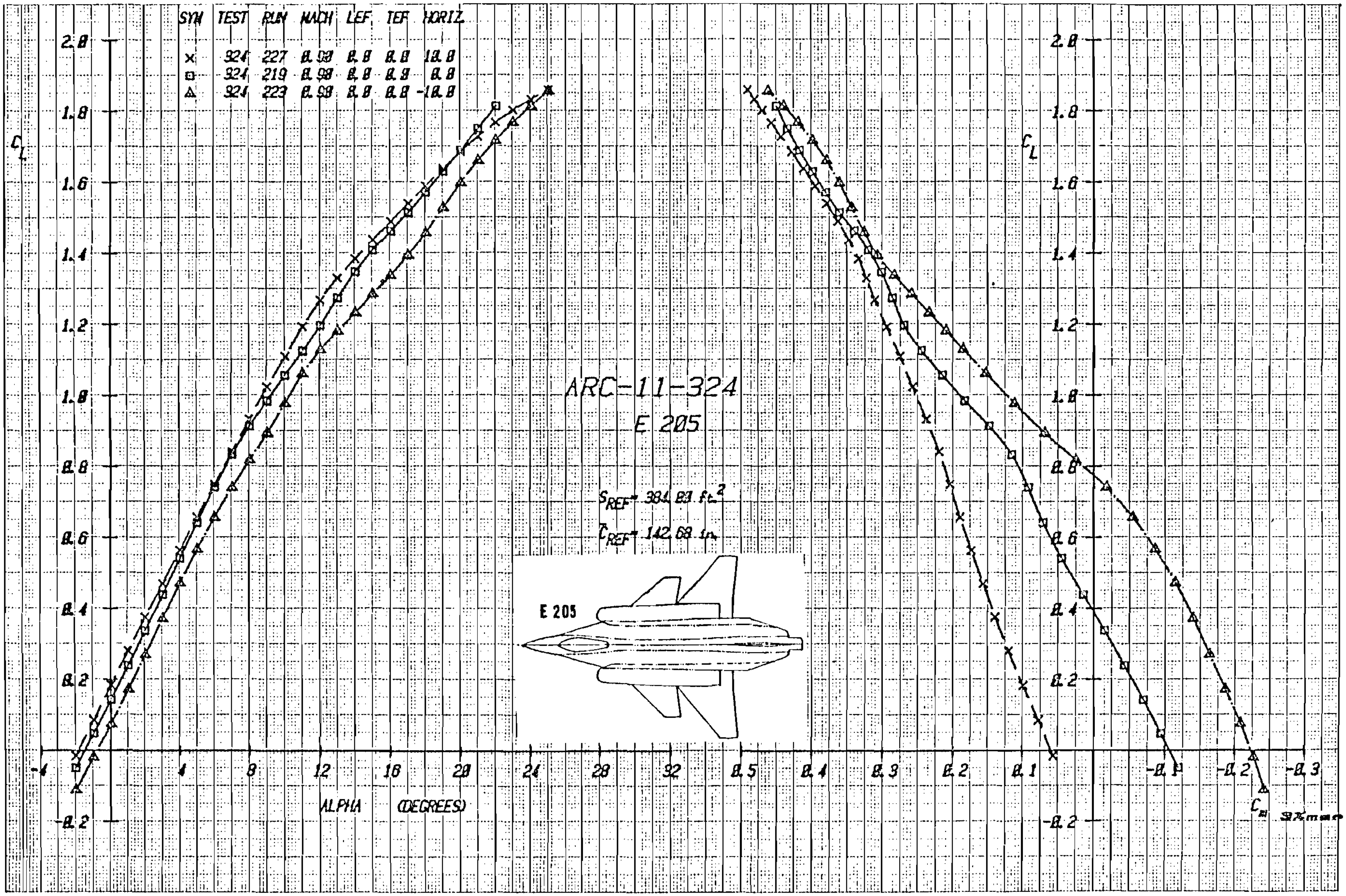

Figure3-38aEffect of Canard Deflection on Lift and Moment With Canard C_2, and Strake S_2, Mach = .9

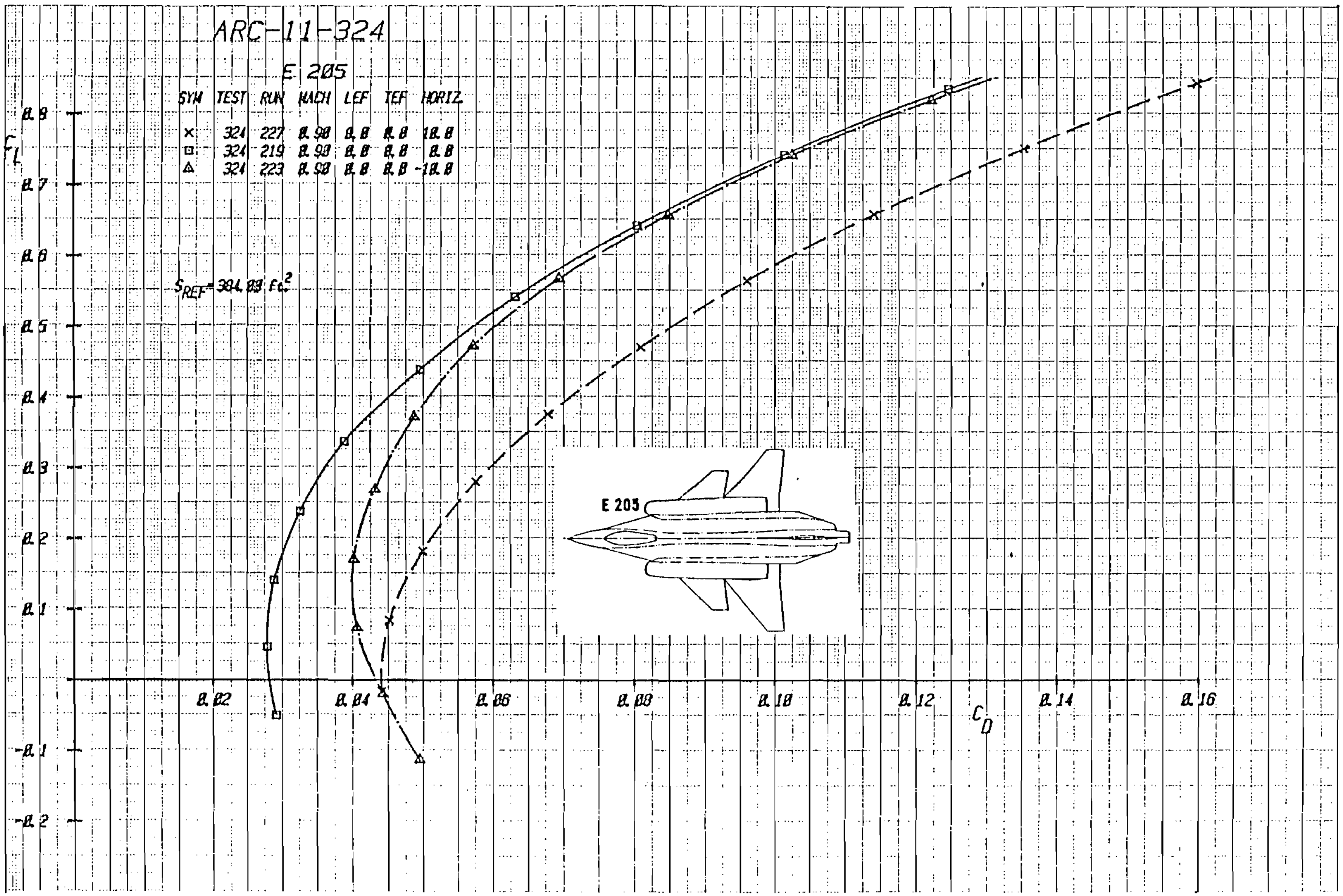

Figure3-38bEffect of Canard Deflection on Drag With Canard C_2, and Strake S_2, Mach = .9

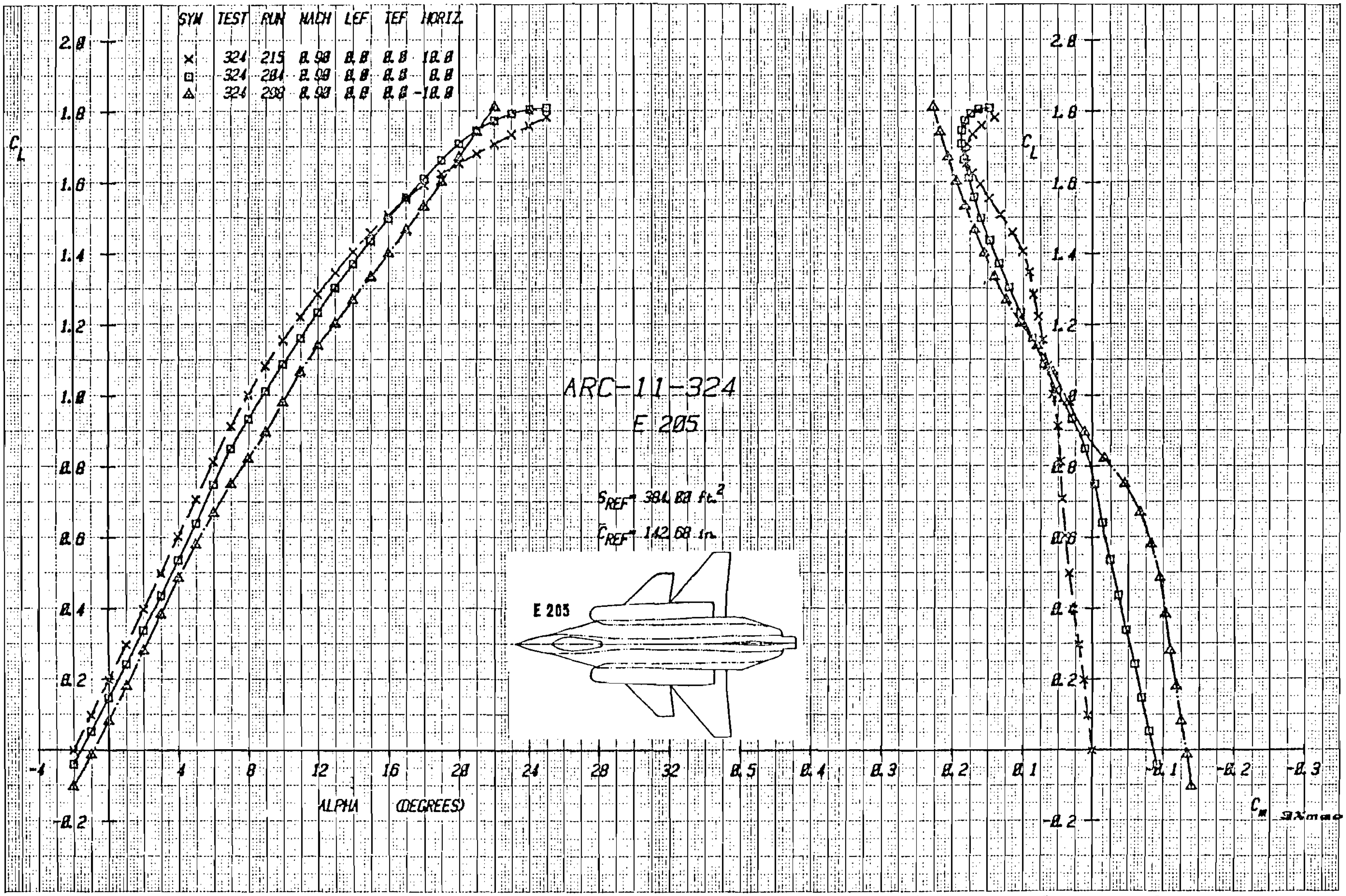

Figure3-39aEffect of Canard Deflection on Lift and Moment With Canard C_3, and Strake S_2, Mach = .9

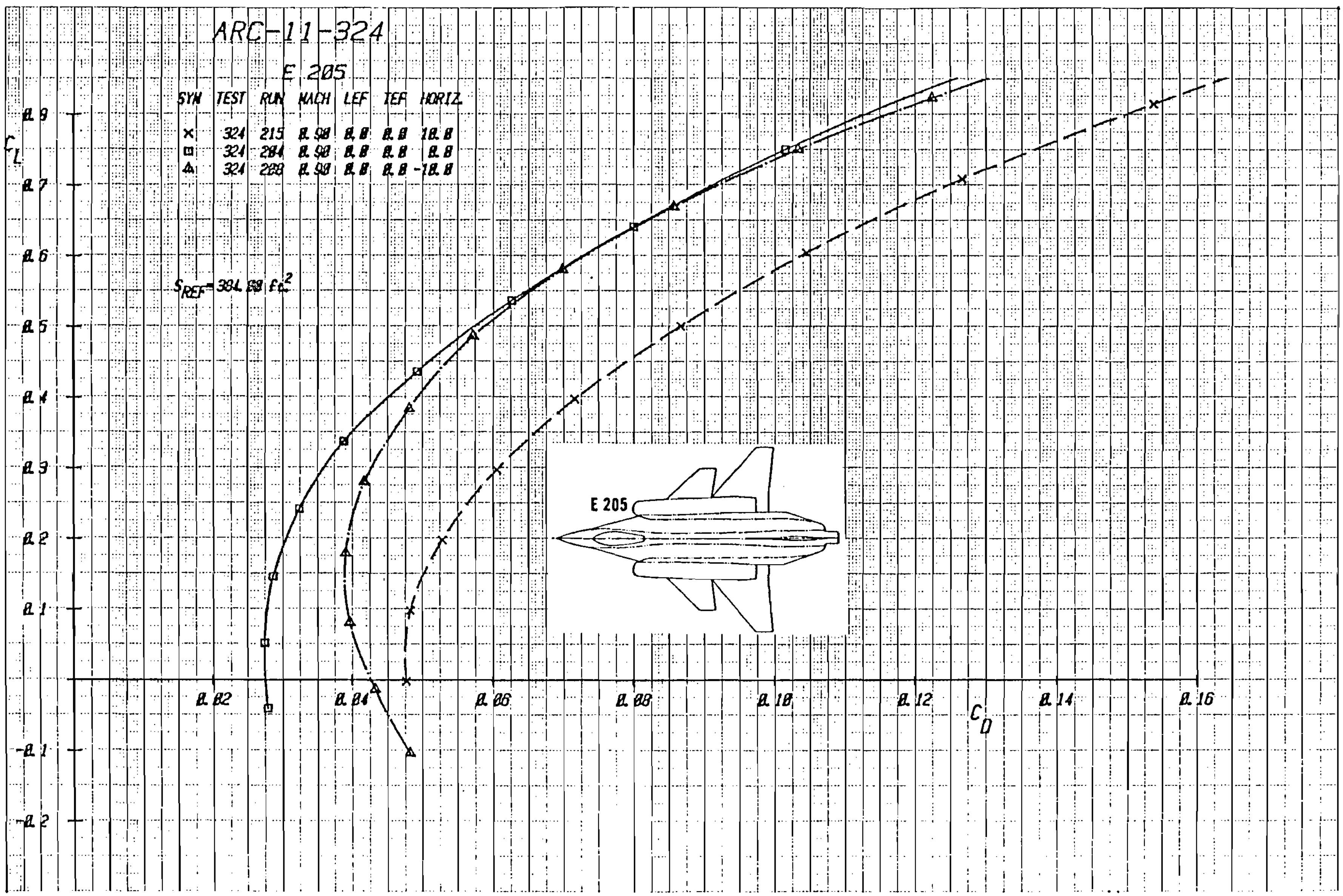

Figure3-39bEffect of Canard Deflection on Drag with Canard C_3, and Strake S_2, Mach = .9

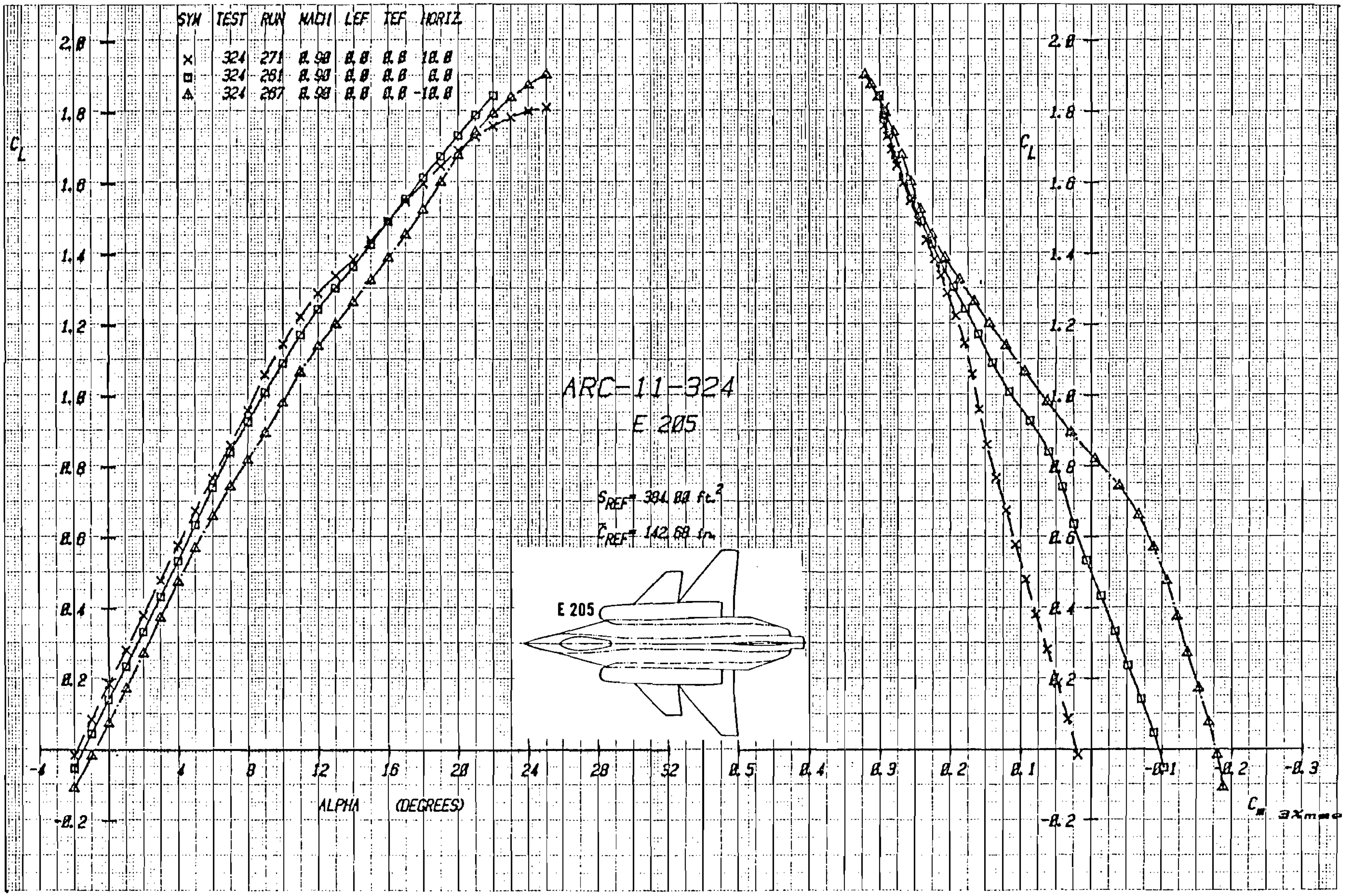

Figure3-40aEffect of Canard Deflection on Lift and Moment with Canard C_1, and Strake S_3, Mach = .9

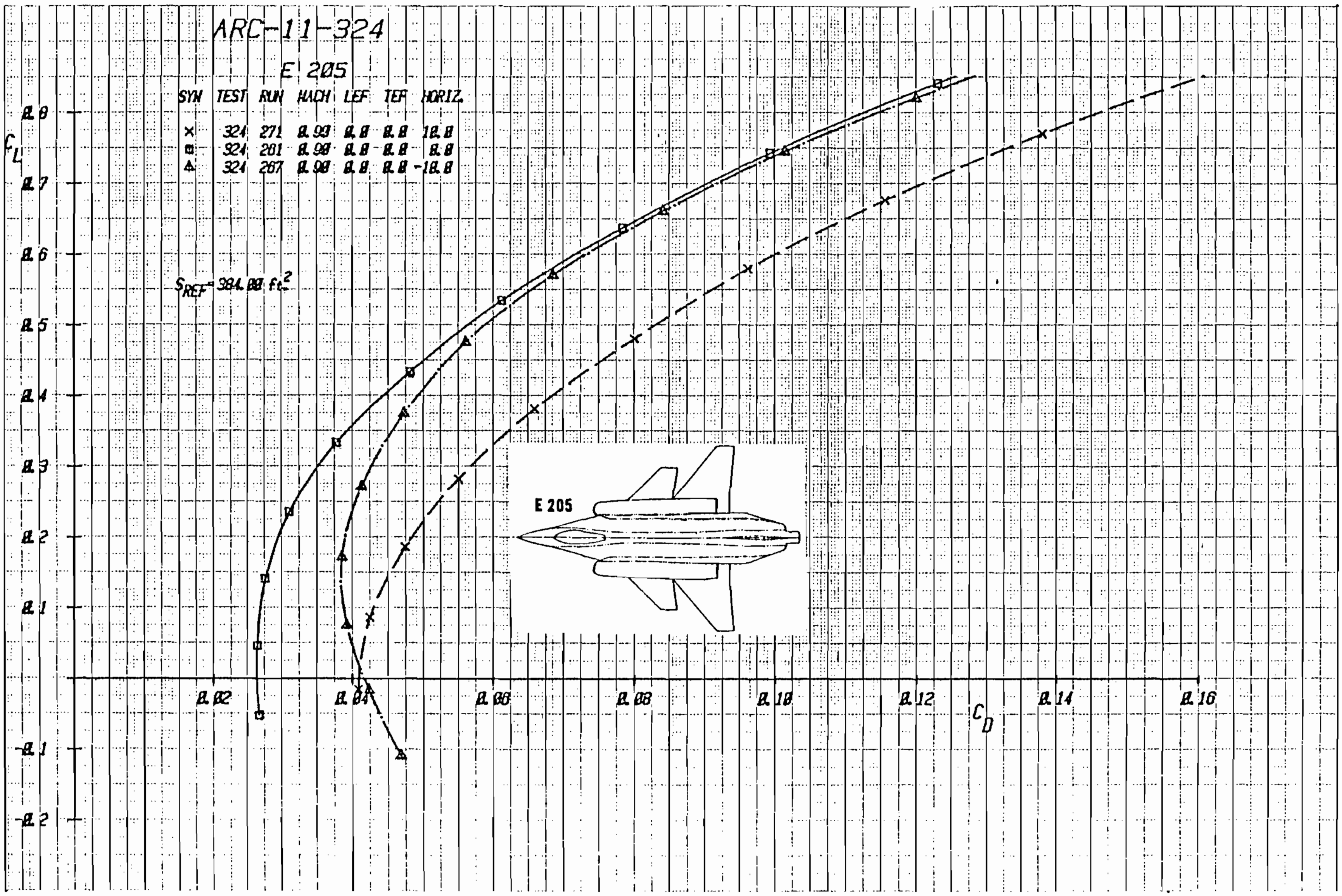

Figure3-40bEffect of Canard Deflection on Drag with Canard C_1, and Strake S_3, Mach = .9

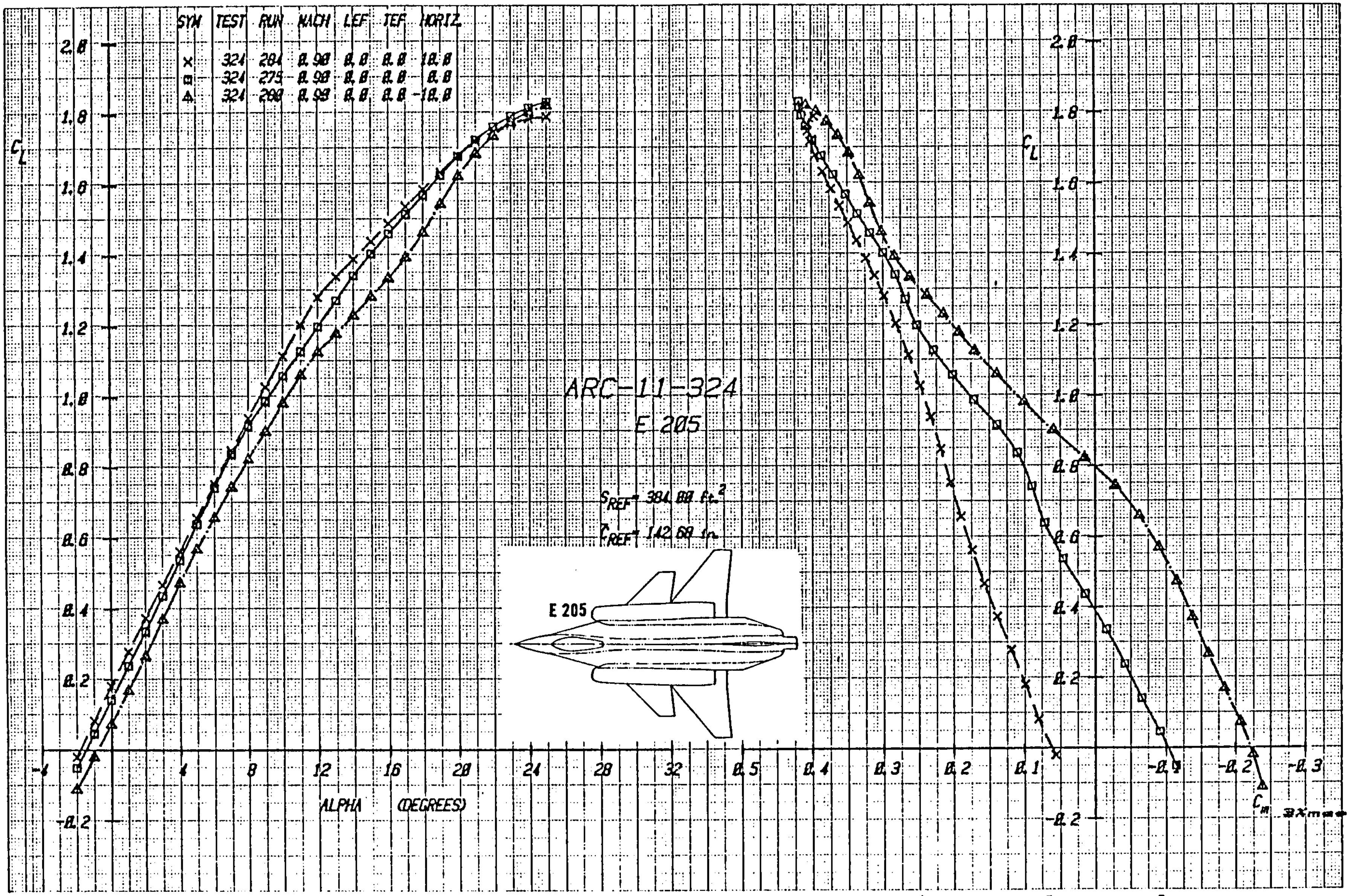

Figure3-41aEffect of Canard Deflection on Lift and Moment with Canard C_2, and Strake S_3, Mach = .9

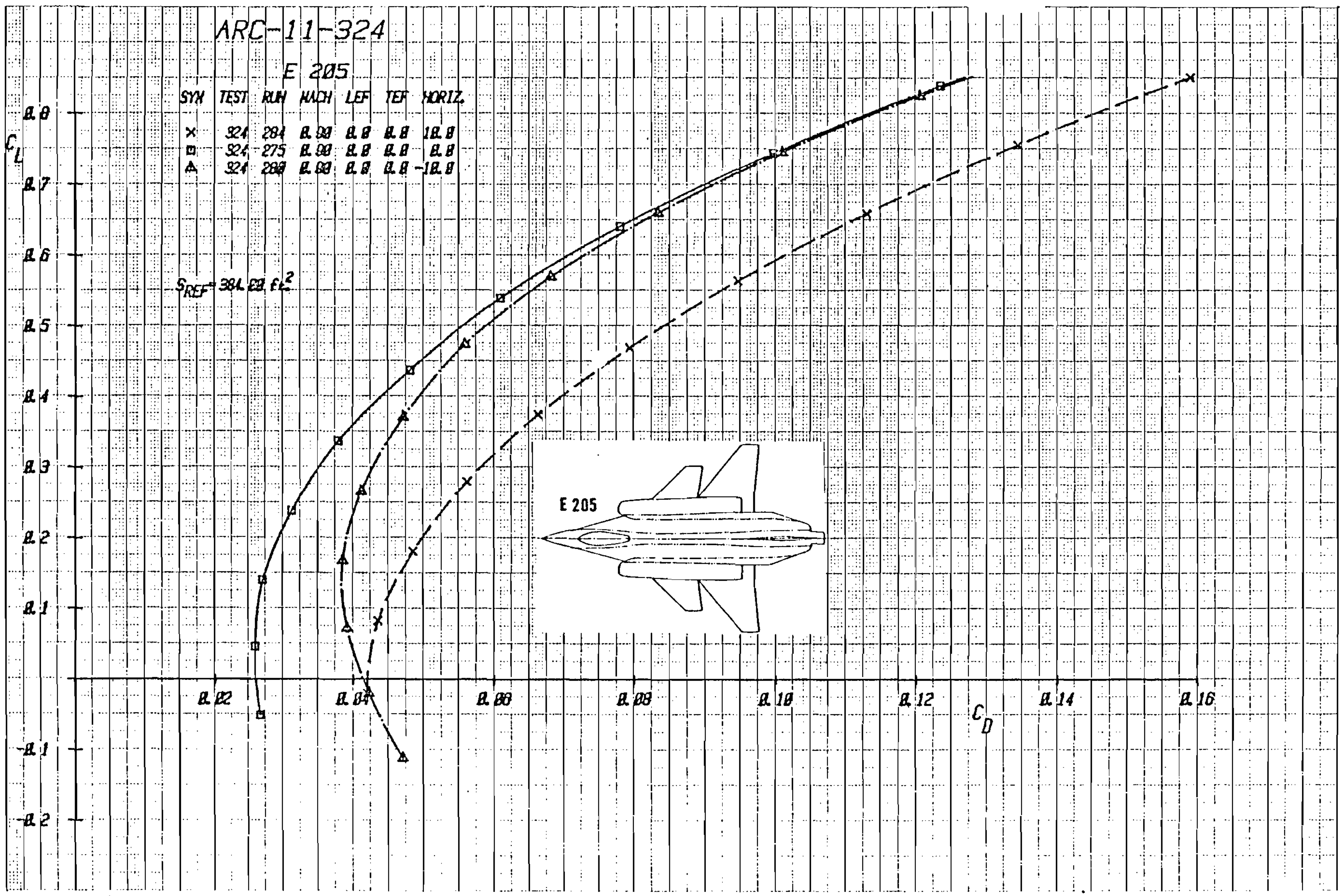

Figure3-41bEffect of Canard Deflection on Drag with Canard C_2, and Strake S_3, Mach = .9

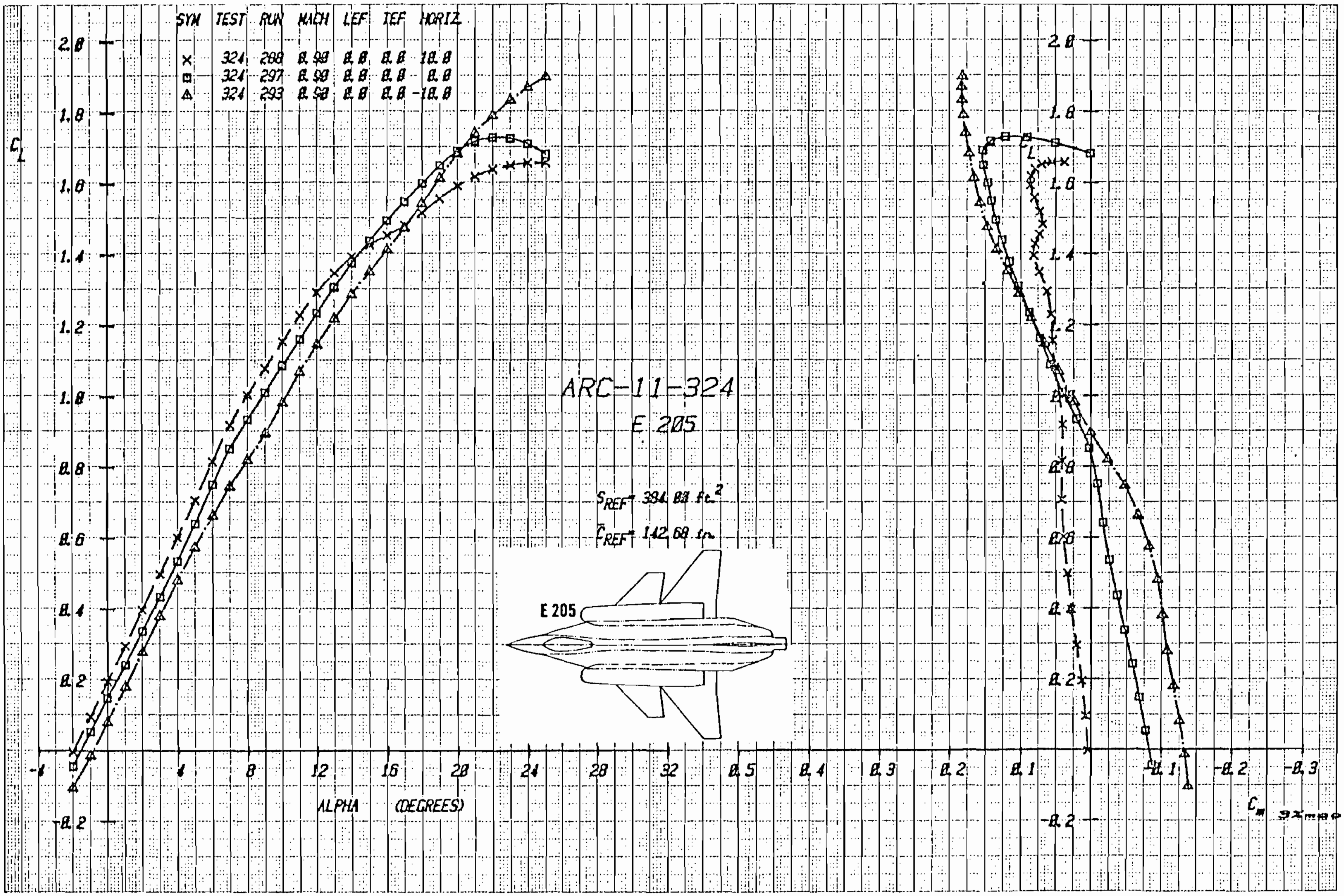

Figure3-42a Effect of Canard Deflection on Lift and Moment with Canard C_3, and Strake S_3, Mach = .9

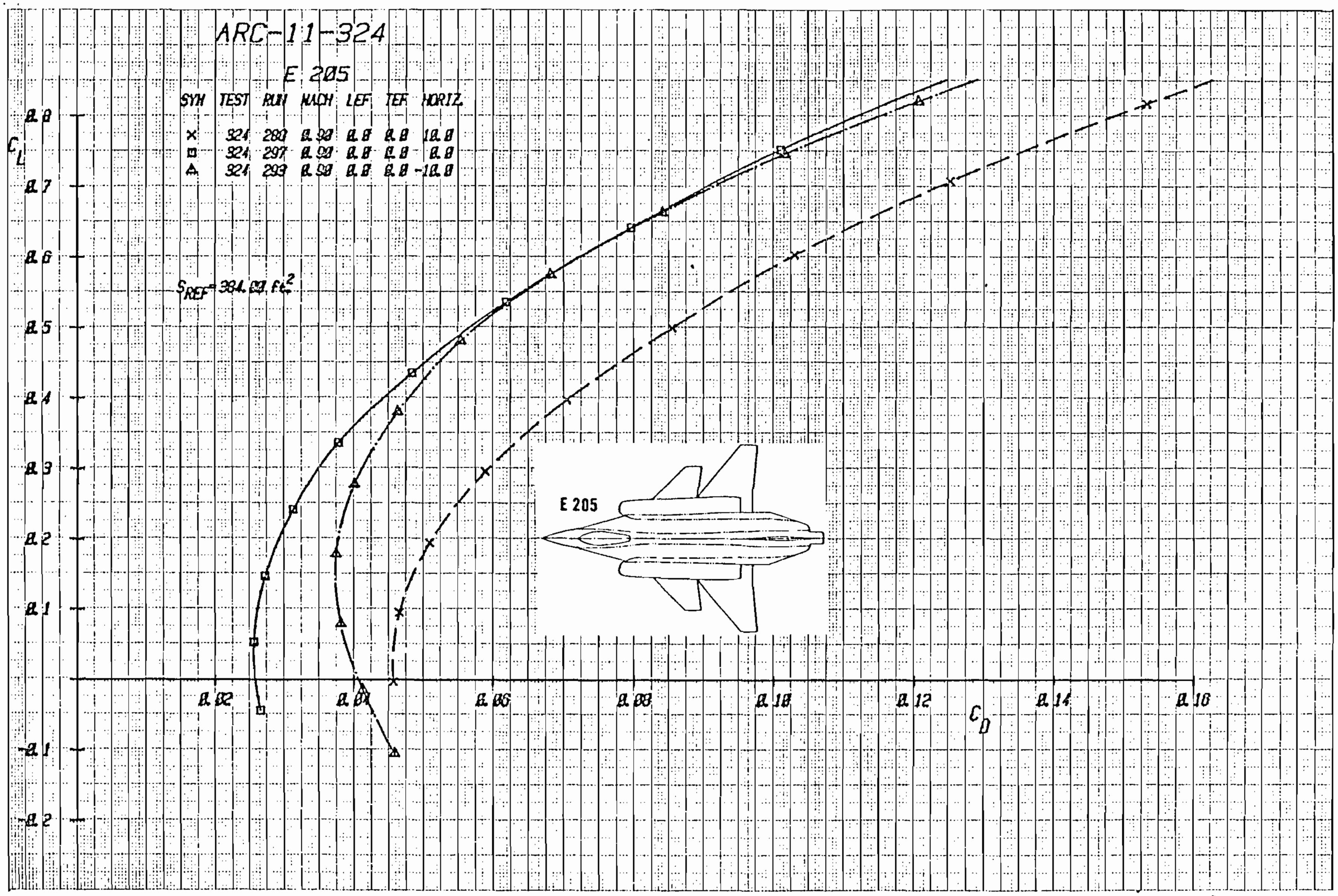

Figure3-42bEffect of Canard Deflection on Drag with Canard C_3, and Strake S_3, Mach = .9

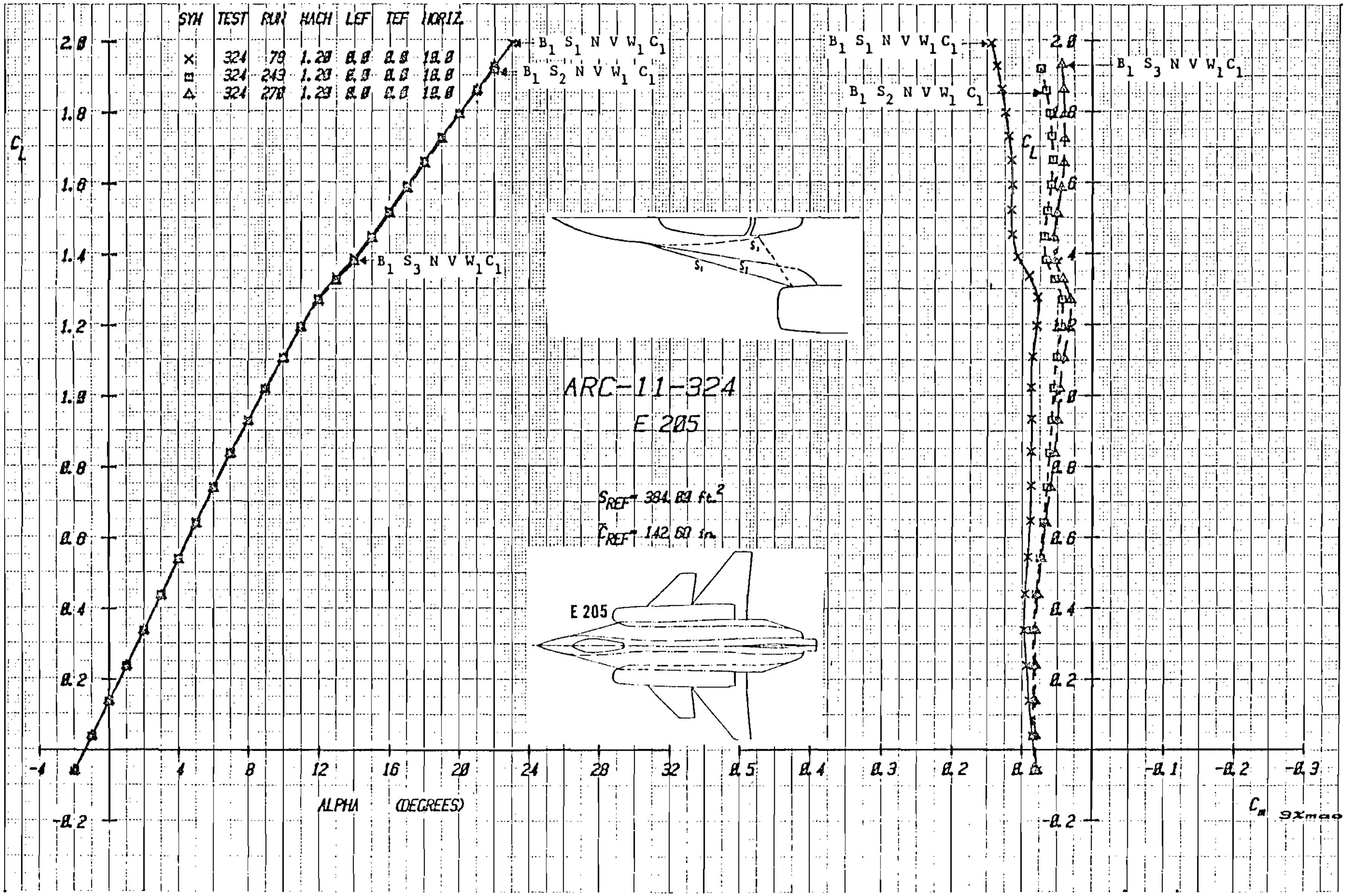

Figure 3-43a Effect of Strake Shape on Lift and Moment with Canard C_1 Deflected +10°, Mach = 1.2

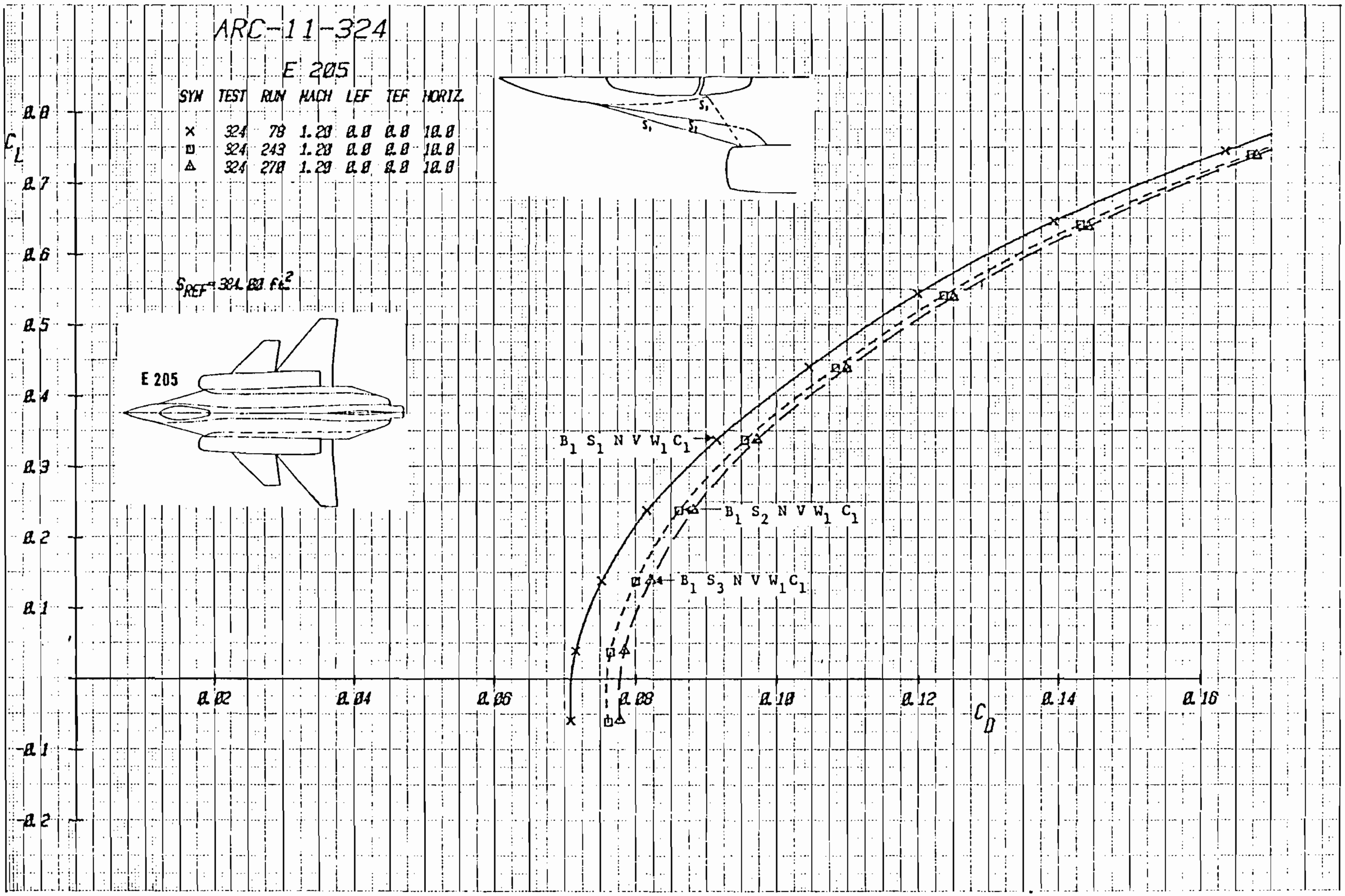

Figure3-43bEffect of Strake Shape on Drag with Canard C_1 Deflected +10°, Mach = 1.2

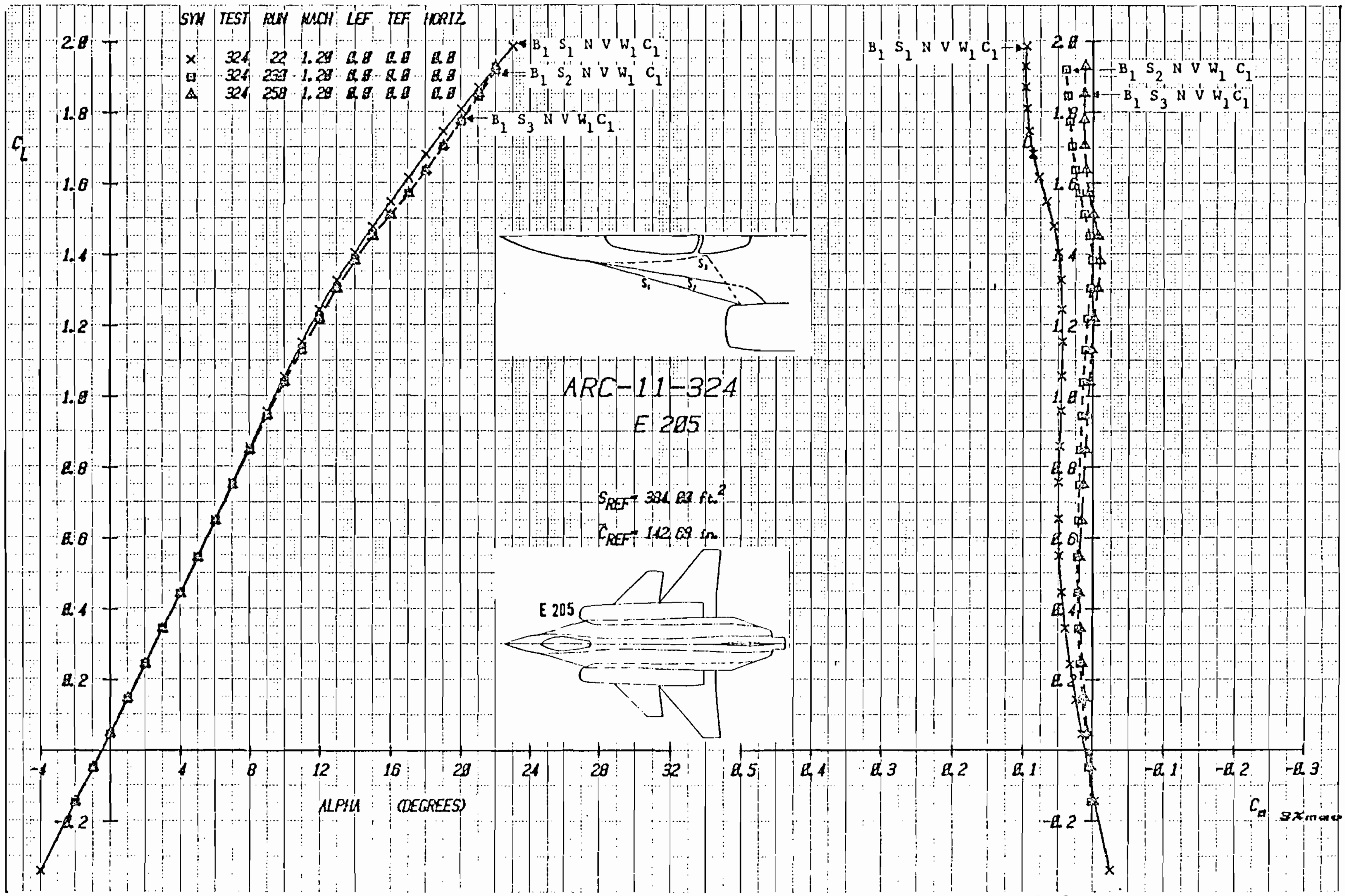

Figure3-44aEffect of Strake Shape on Lift and Moment with Canard C_1 Undeflected, Mach = 1.2

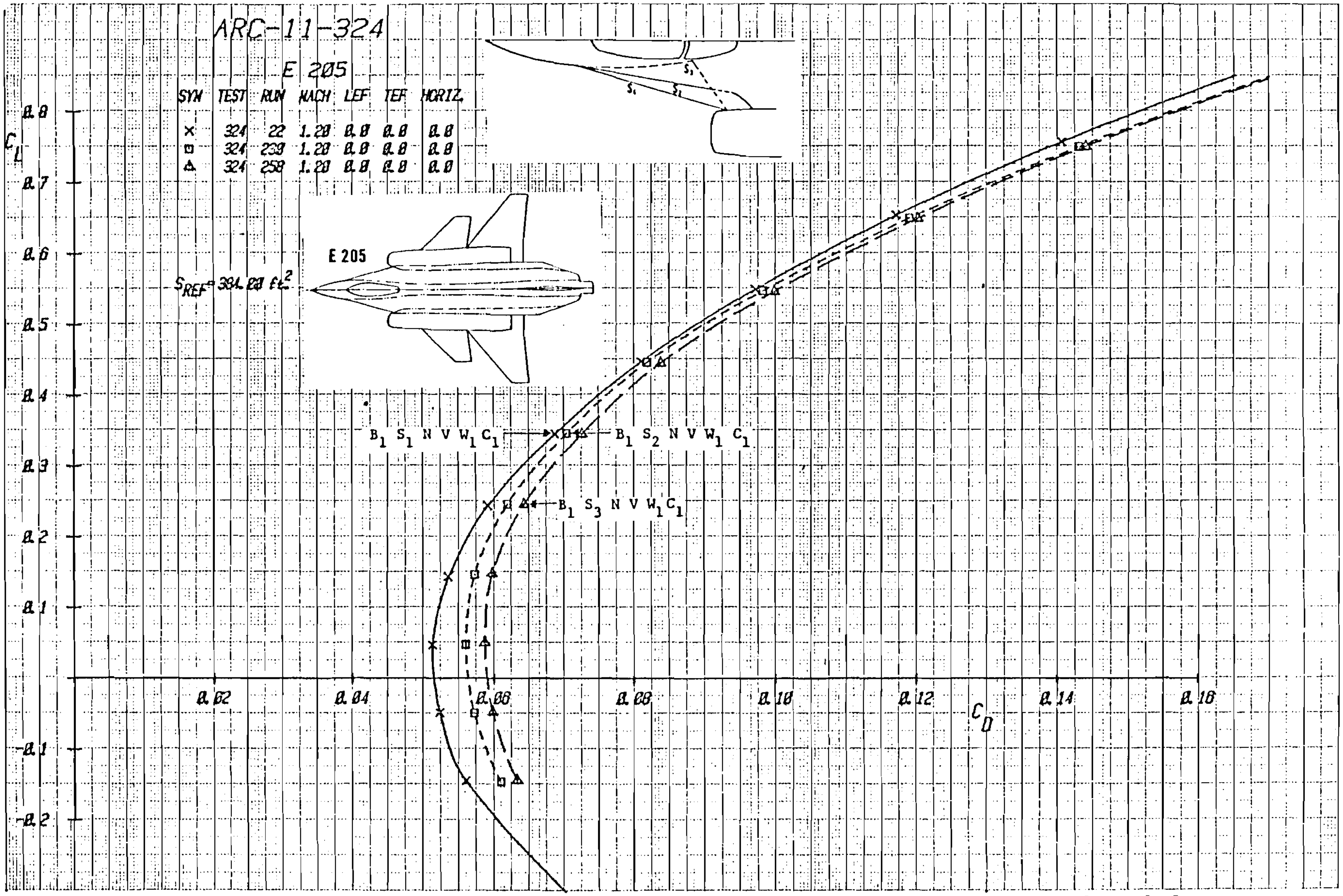

Figure3-44bEffect of Strake Shape on Drag with Canard C_1 Undeflected, Mach = 1.2

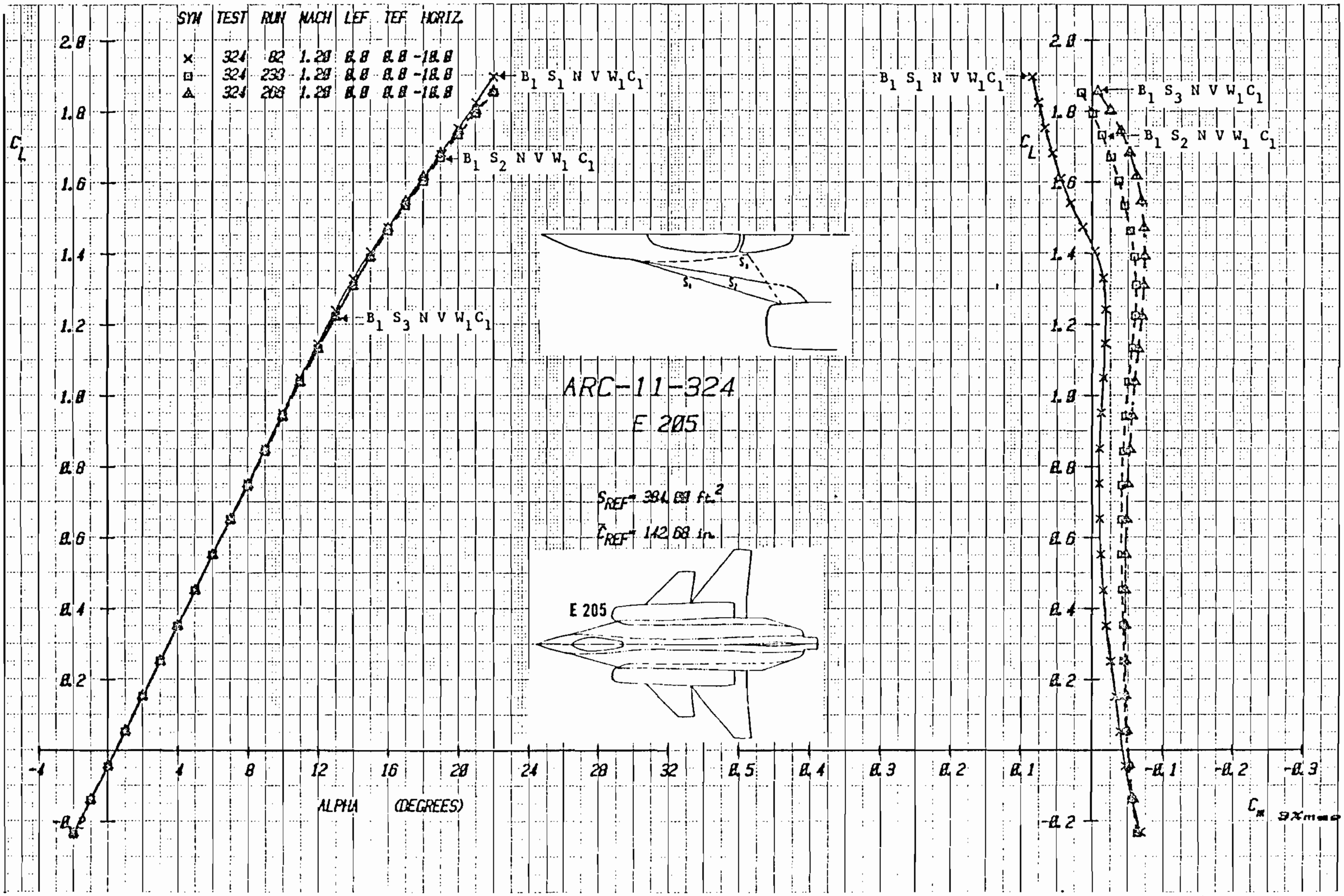

Figure3-45aEffect of Strake Shape on Lift and Moment with Canard C_1 Deflected -10°, Mach = 1.2

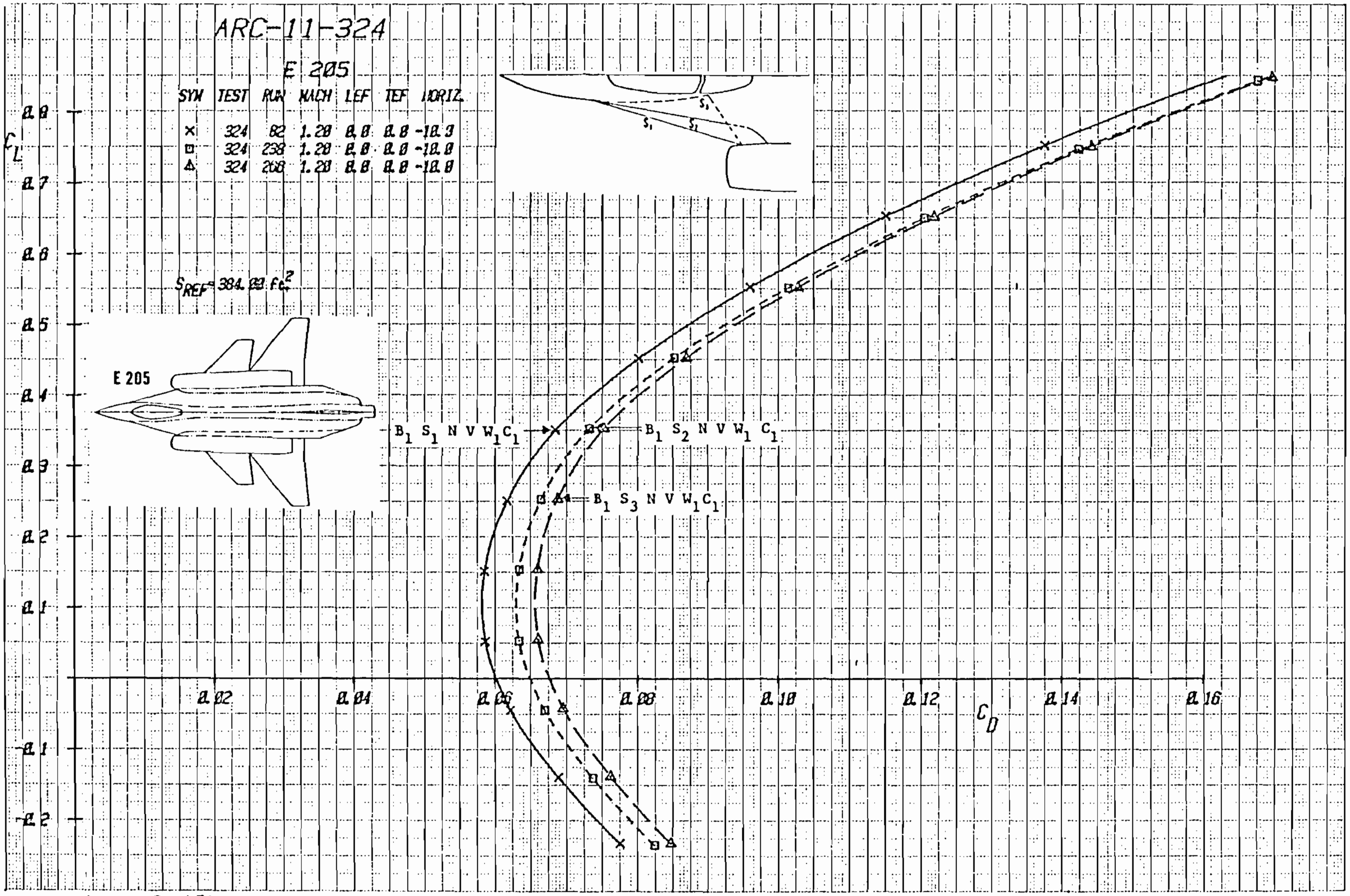

Figure3-45bEffect of Strake Shape on Drag with Canard C_1 Deflected -10°, Mach = 1.2

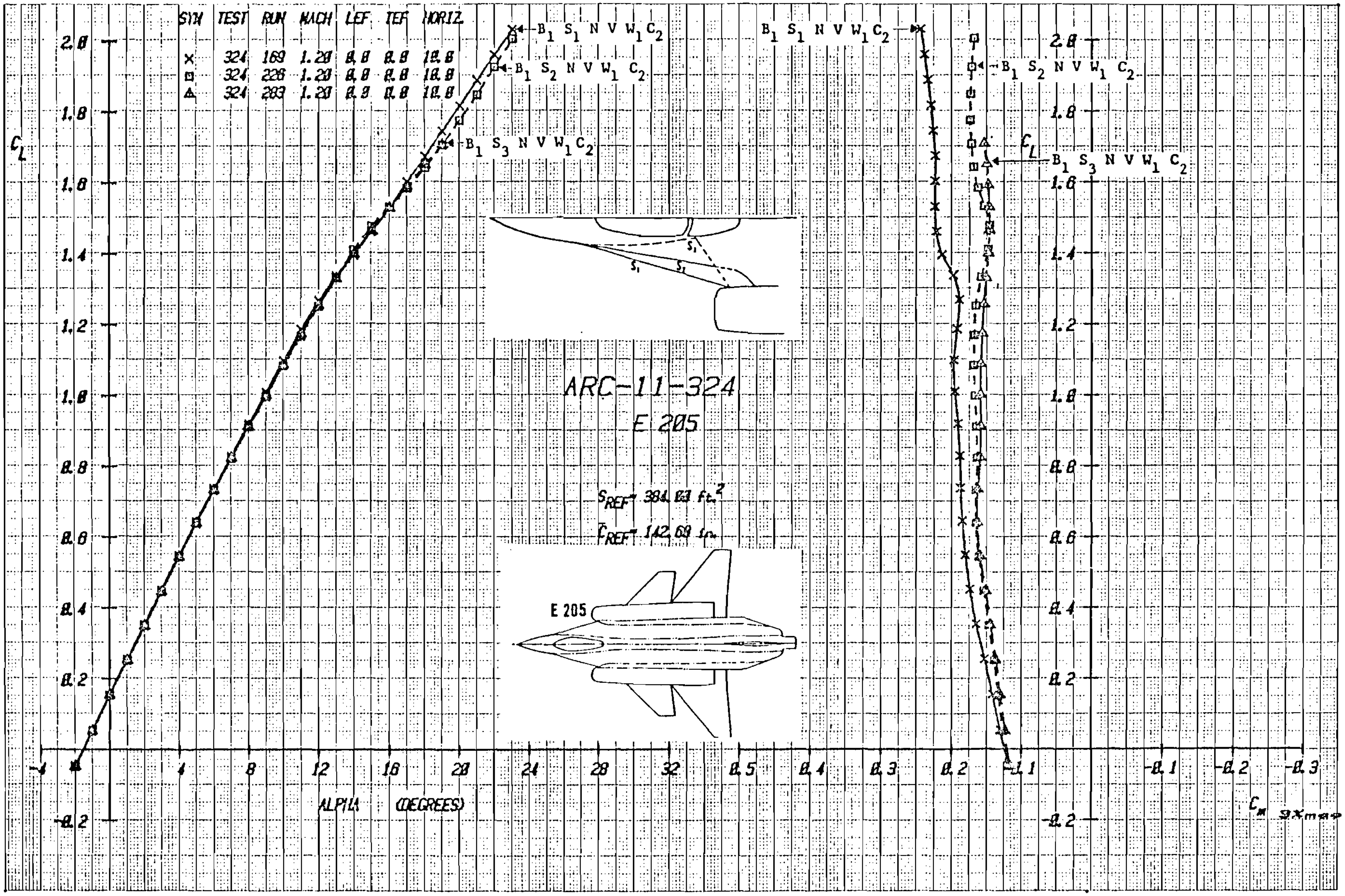

Figure3-46aEffect of Strake Shape on Lift and Moment with Canard C_2 Deflected +10°, Mach = 1.2

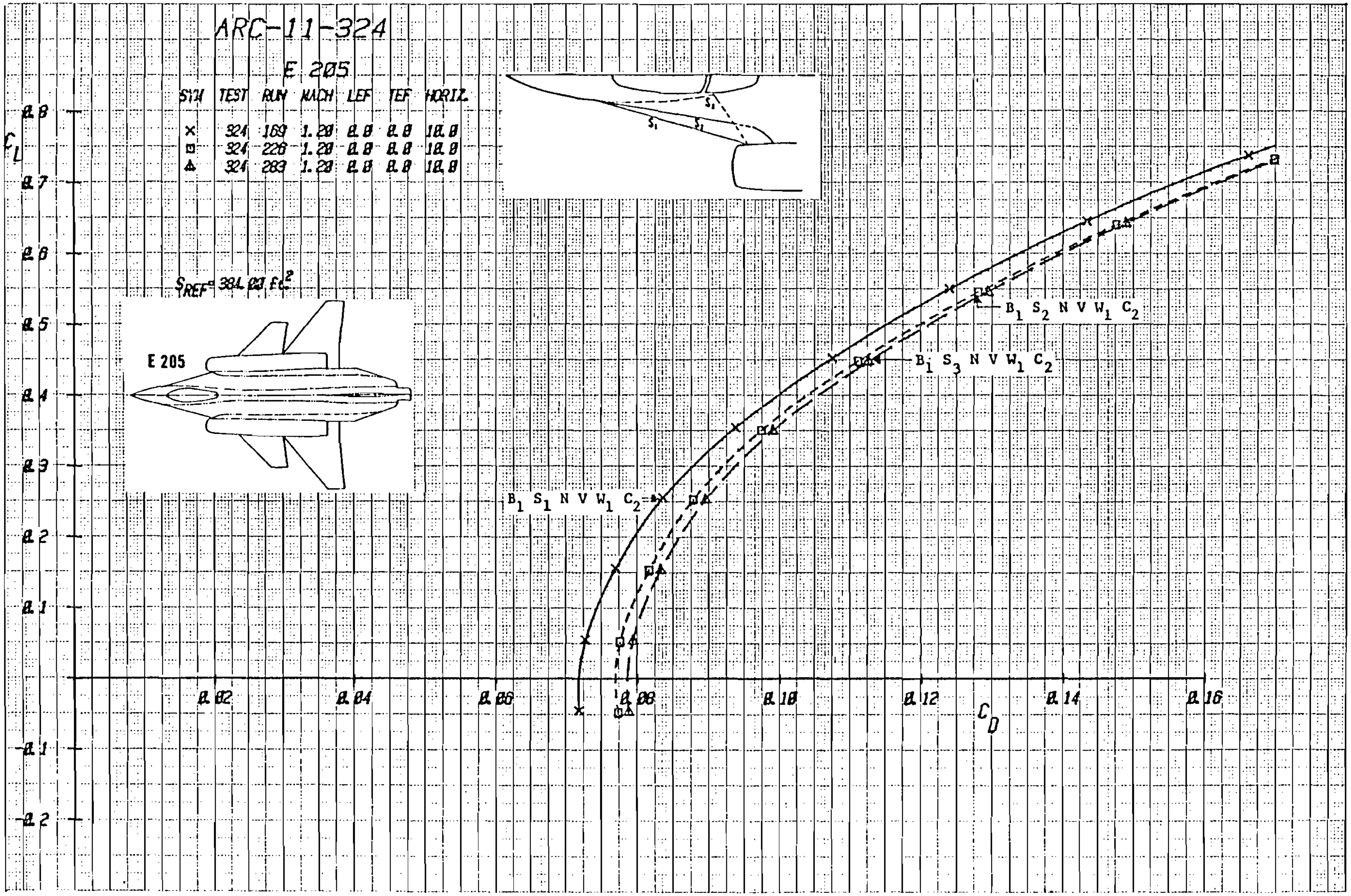

Figure3-46bEffect of Strake Shape on Drag with Canard C_2 Deflected +10°, Mach = 1.2

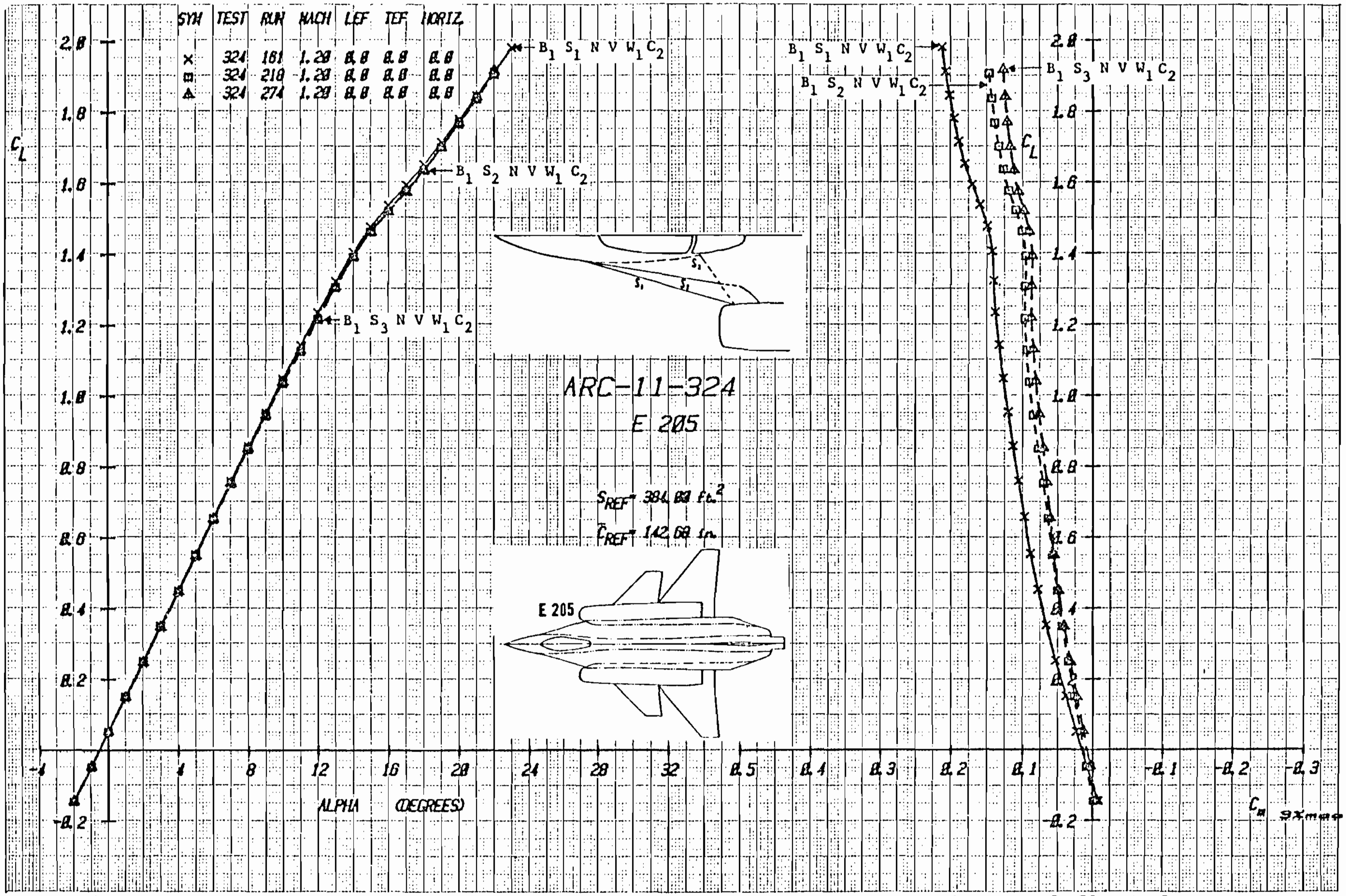

Figure3-47aEffect of Strake Shape on Lift and Moment with Canard C_2 Undeflected, Mach = 1.2

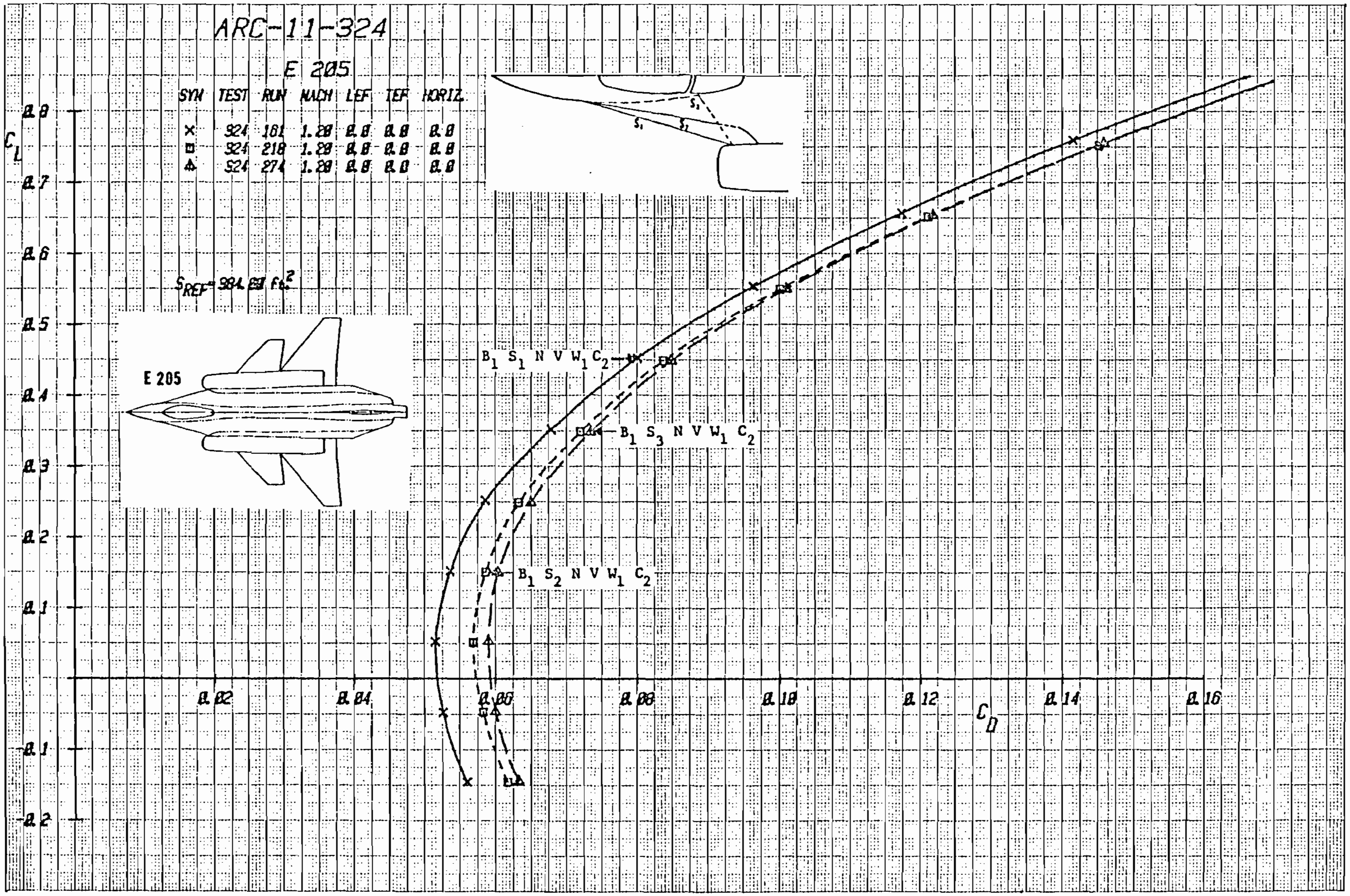

Figure3-47b Effect of Strake Shape on Drag with Canard C_2 Undeflected, Mach = 1.2

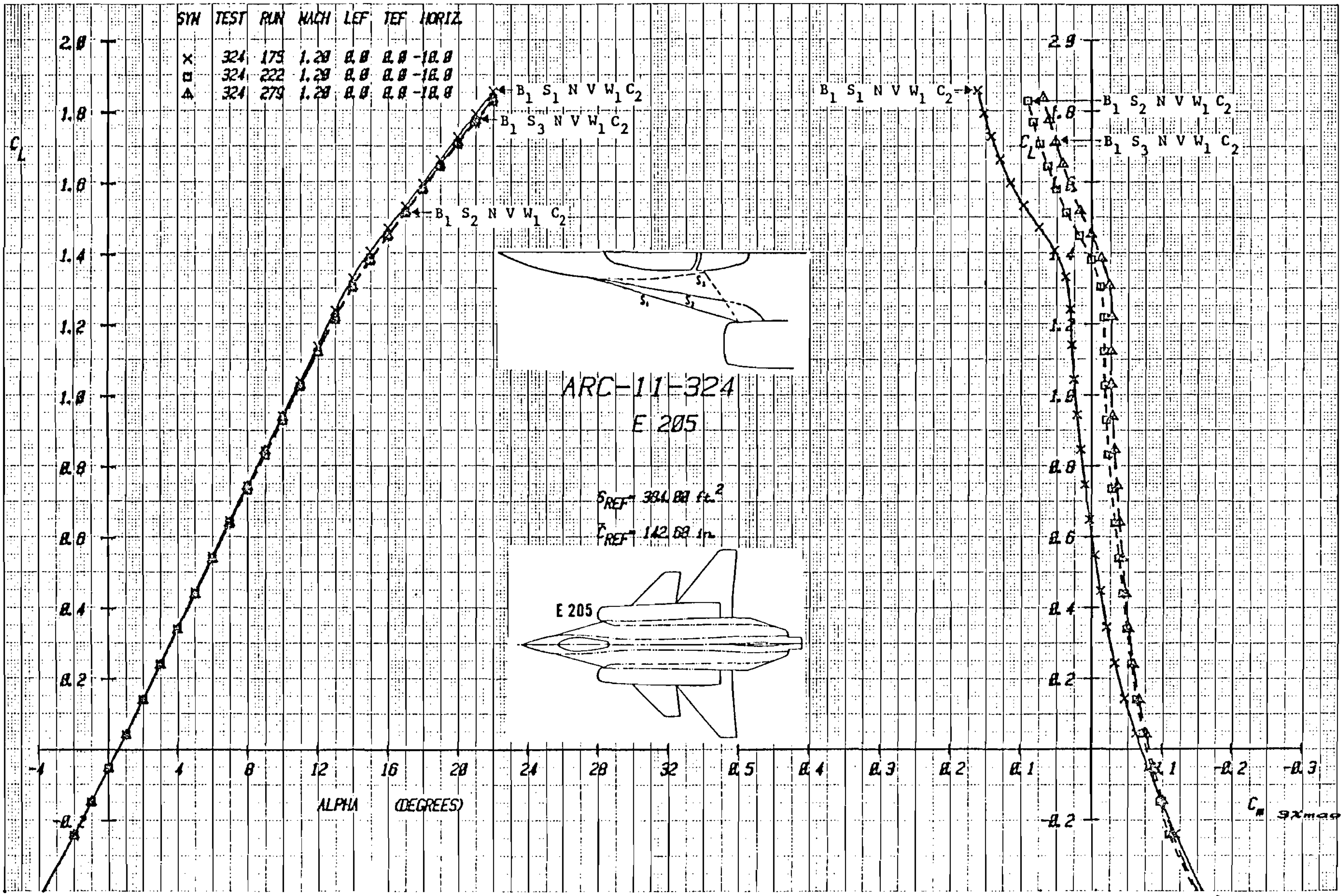

Figure3-48aEffect of Strake Shape on Lift and Moment with Canard C_2 Deflected -10°, Mach = 1.2

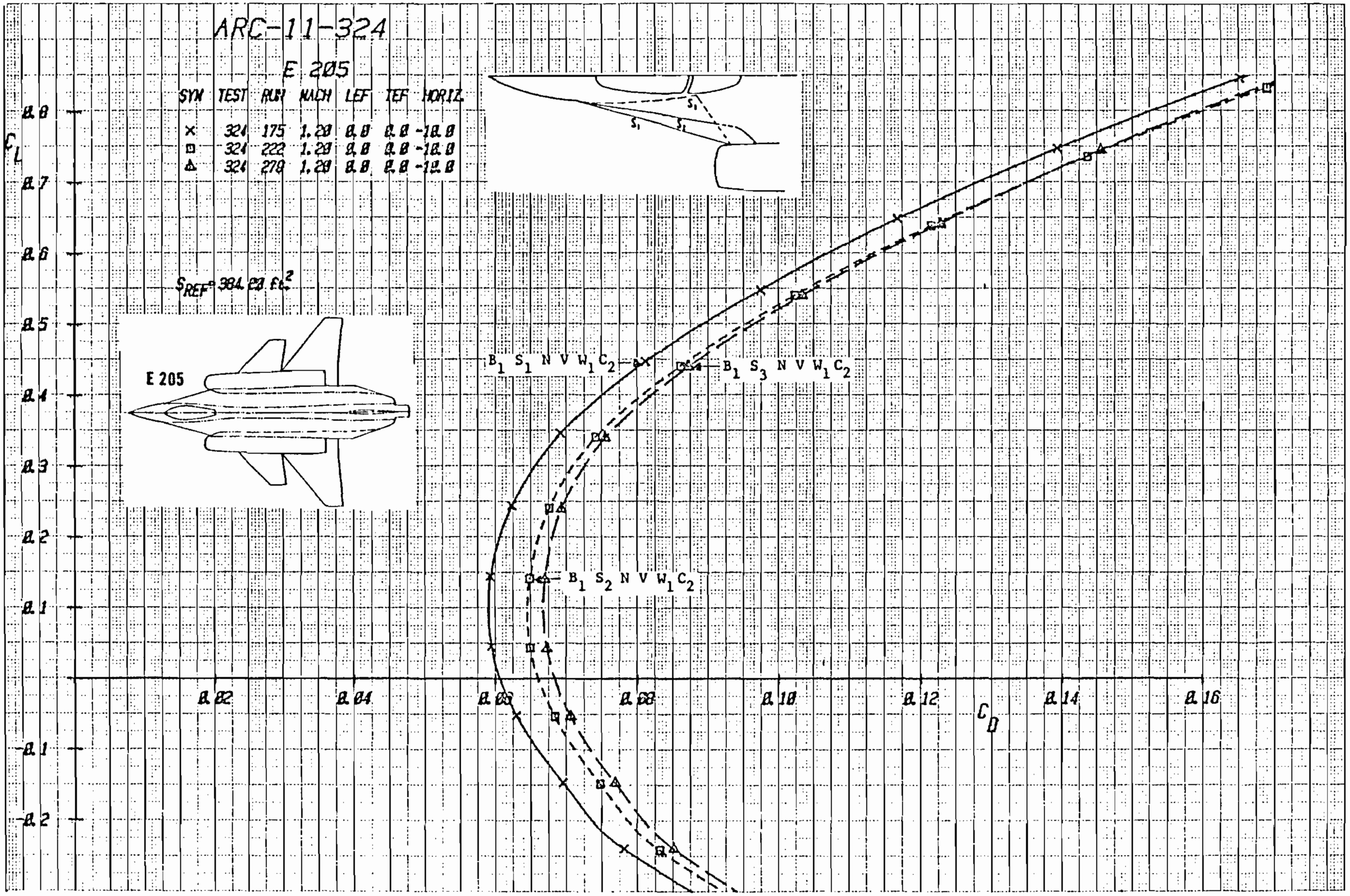

Figure 3-48b Effect of Strake Shape on Drag with Canard C_2 Deflected -10°, Mach = 1.2

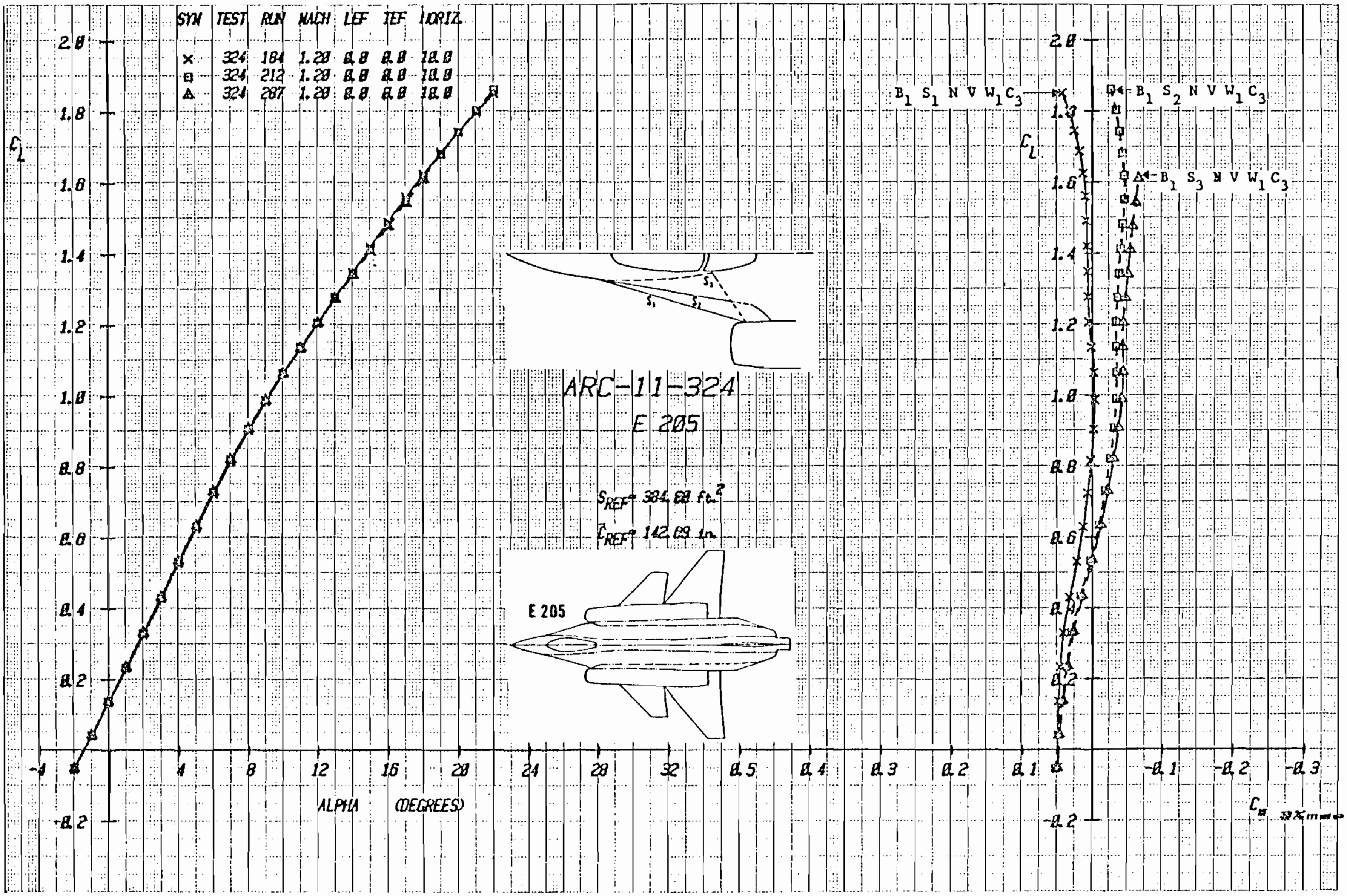

Figure3-49aEffect of Strake Shape on Lift and Moment with Canard C_3 Deflected +10°, Mach = 1.2

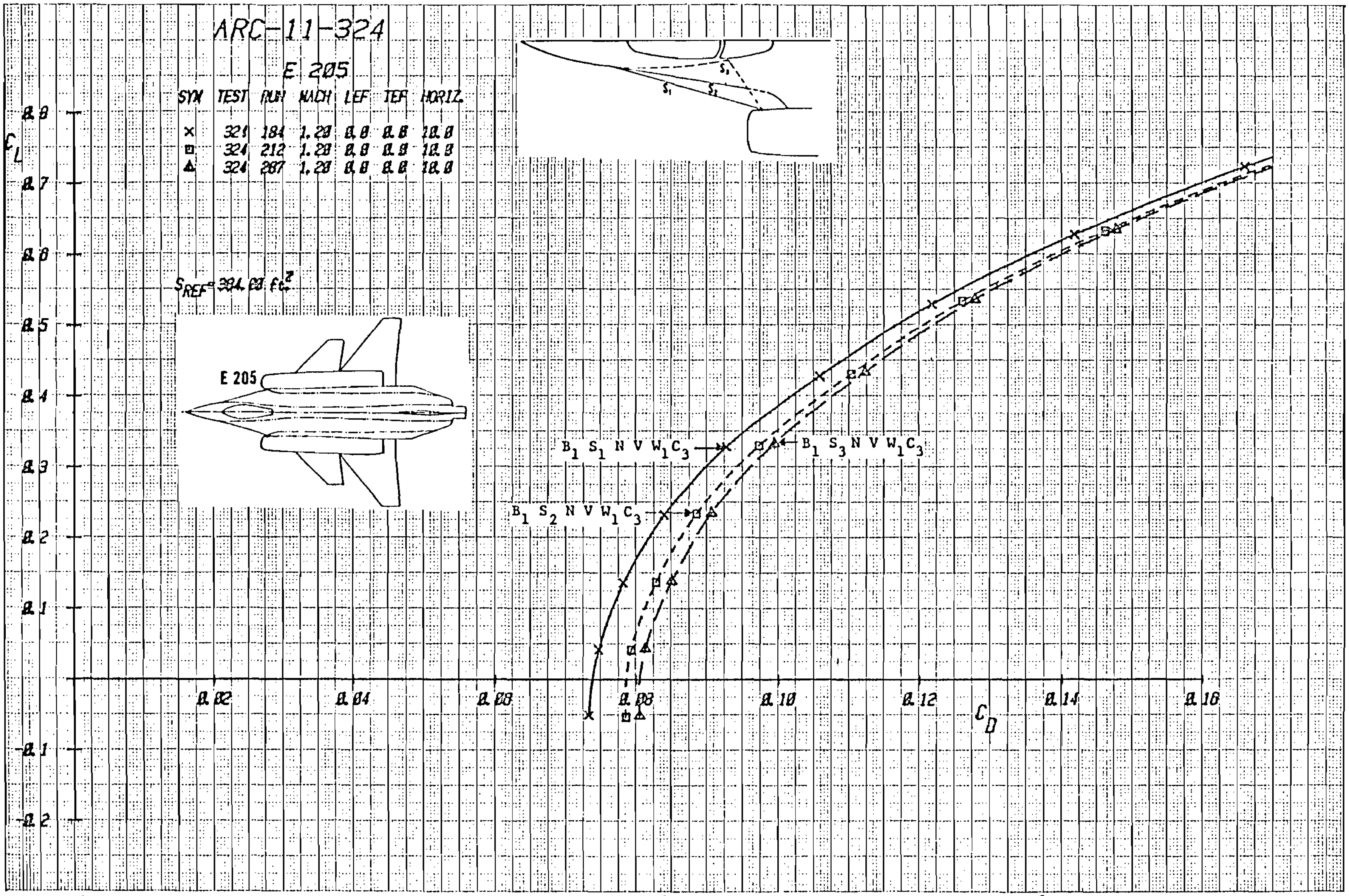

Figure3-49bEffect of Strake Shape on Drag with Canard C_3 Deflected +10°, Mach = 1.2

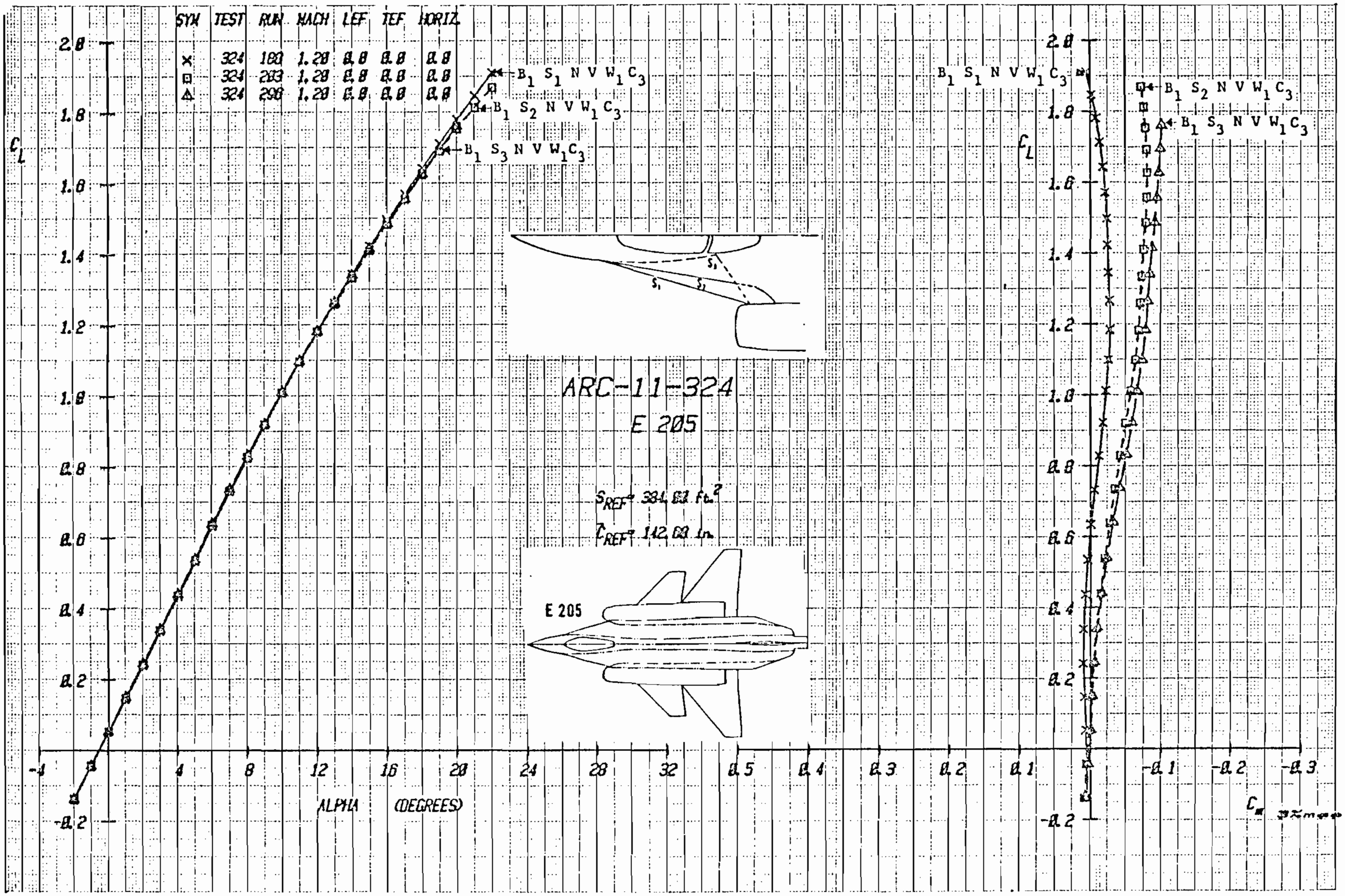

Figure3-50aEffect of Strake Shape on Lift and Moment with Canard C_3 Undeflected, Mach = 1.2

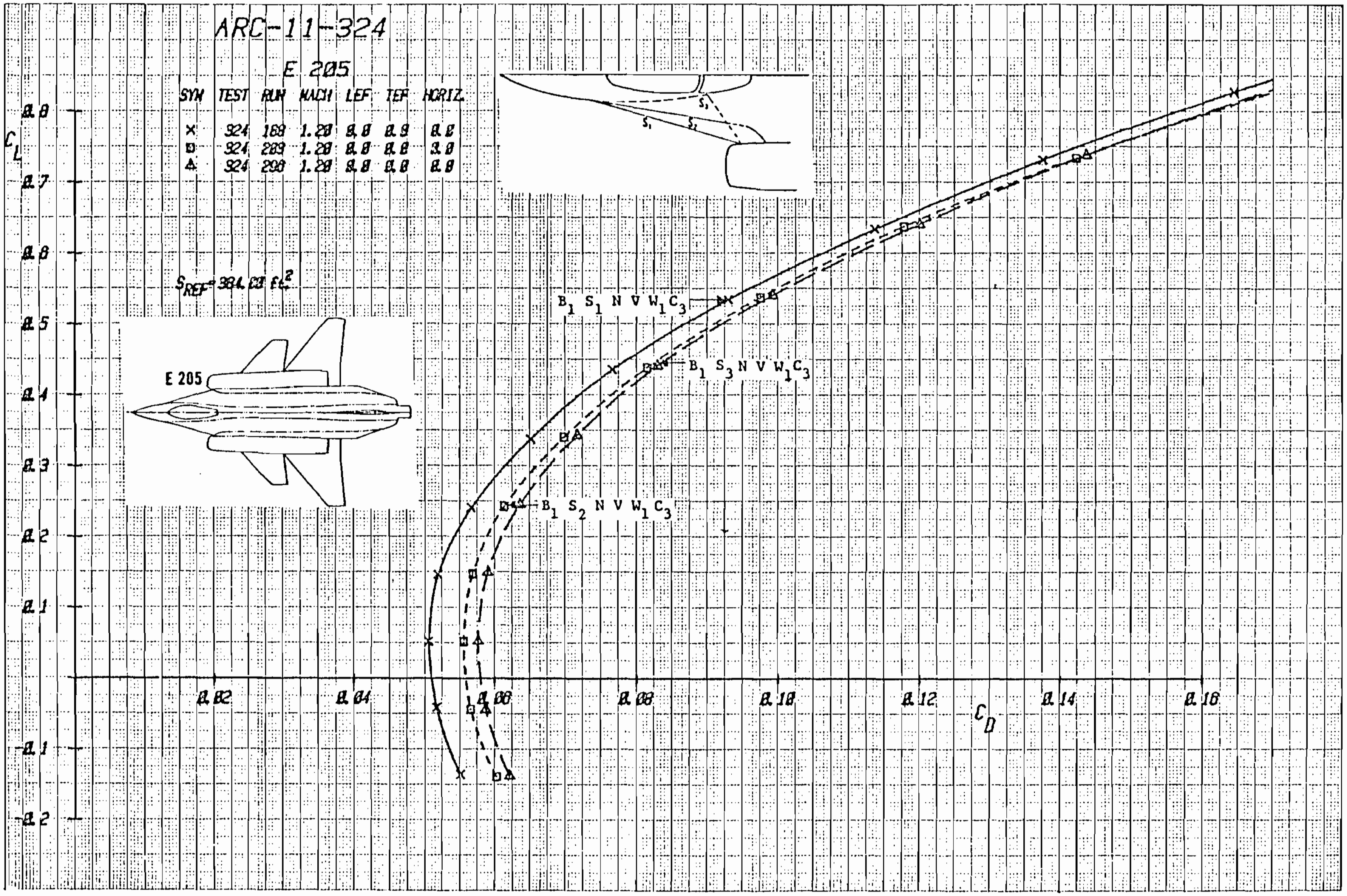

Figure3-50bEffect of Strake Shape on Drag with Canard C_3 Undeflected, Mach = 1.2

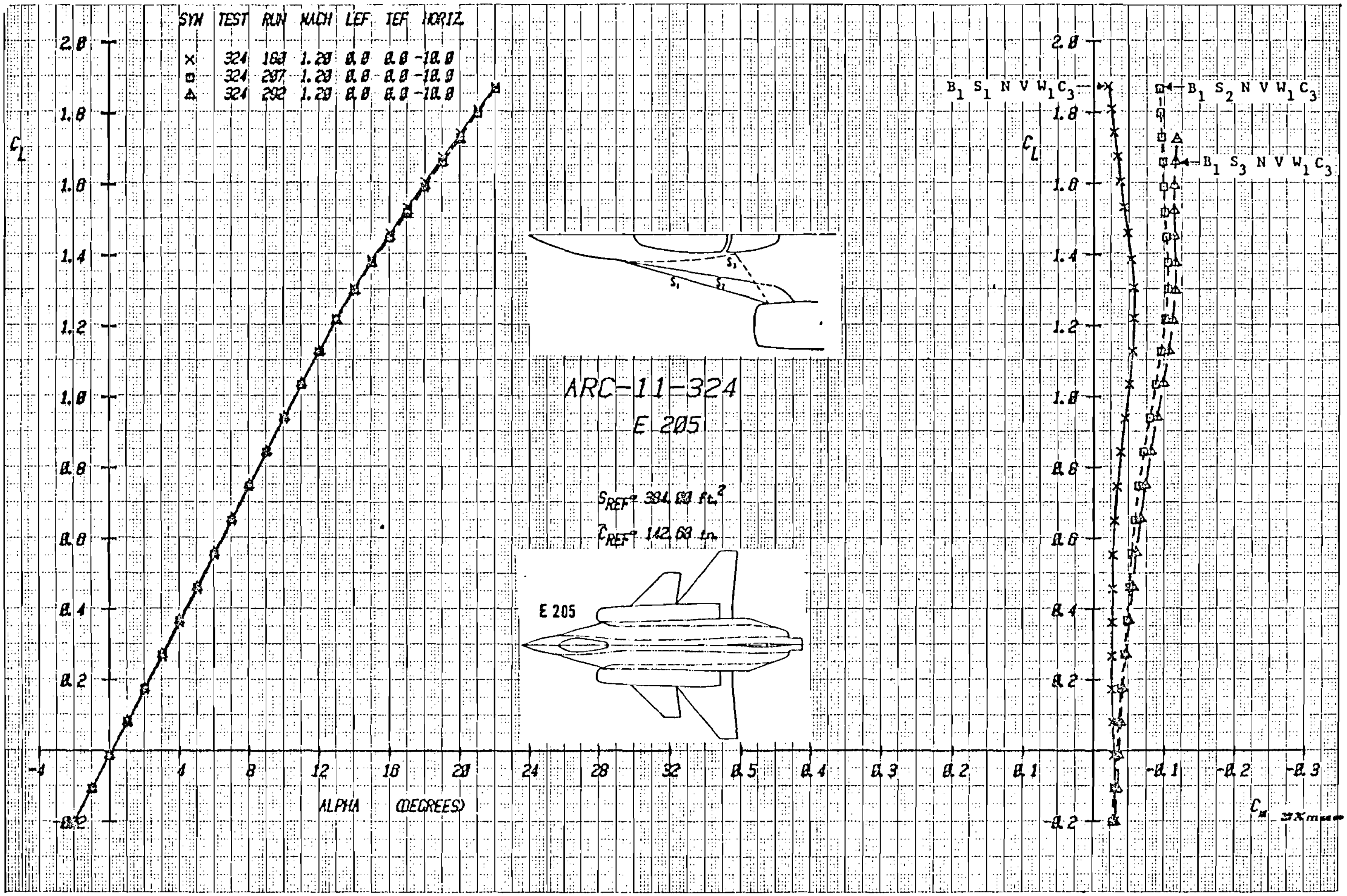

Figure3-51aEffect of Strake Shape on Lift and Moment with Canard C_3 Deflected -10°, Mach = 1.2

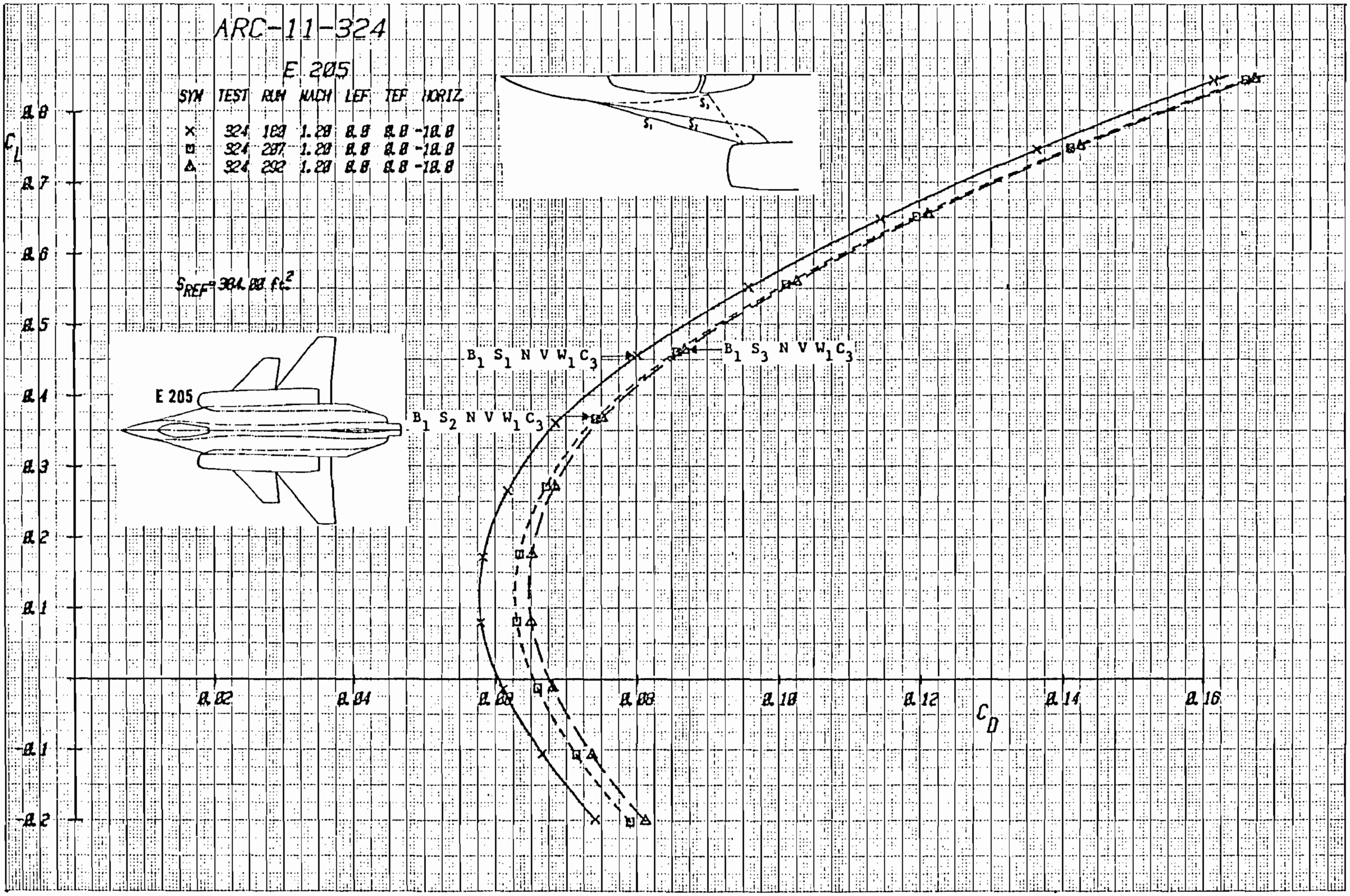

Figure3-51bEffect of Strake Shape on Drag with Canard C_3 Deflected -10°, Mach = 1.2

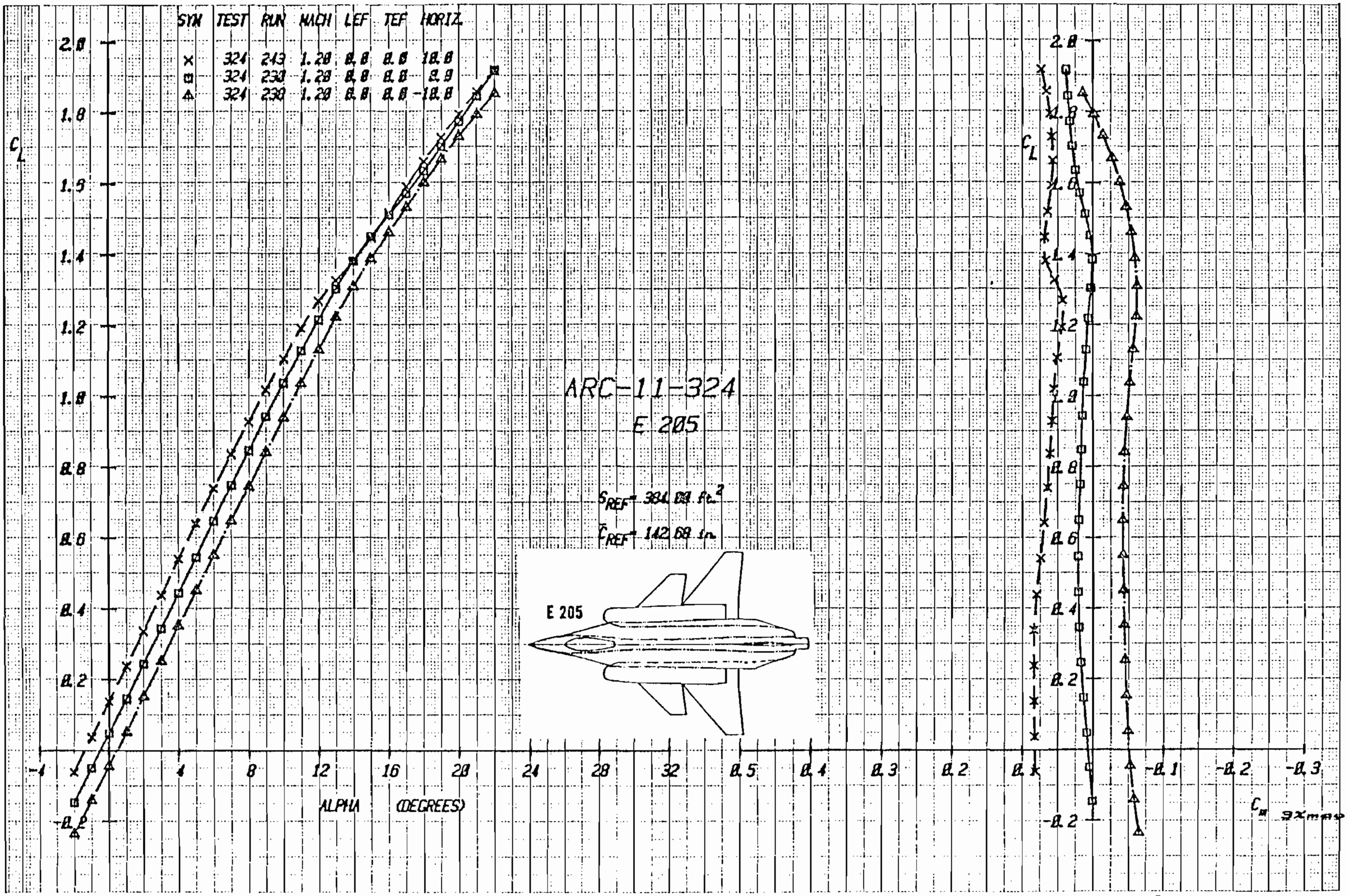

Figure3-52aEffect of Canard Deflection on Lift and Moment With Canard C_1, and Strake S_2, Mach = 1.2

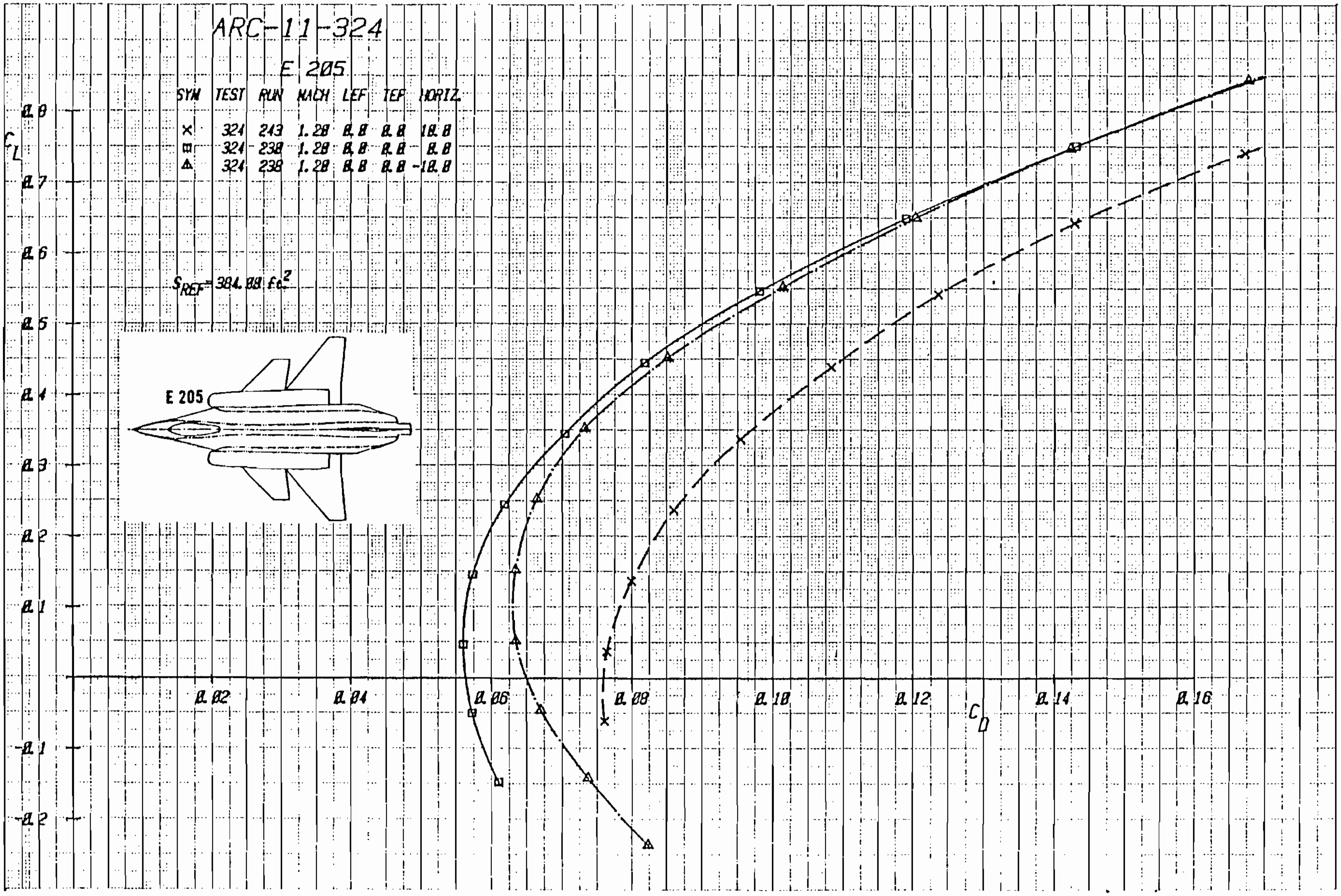

Figure3-52bEffect of Canard Deflection on Drag With Canard C_1, and Strake S_2, Mach = 1.2

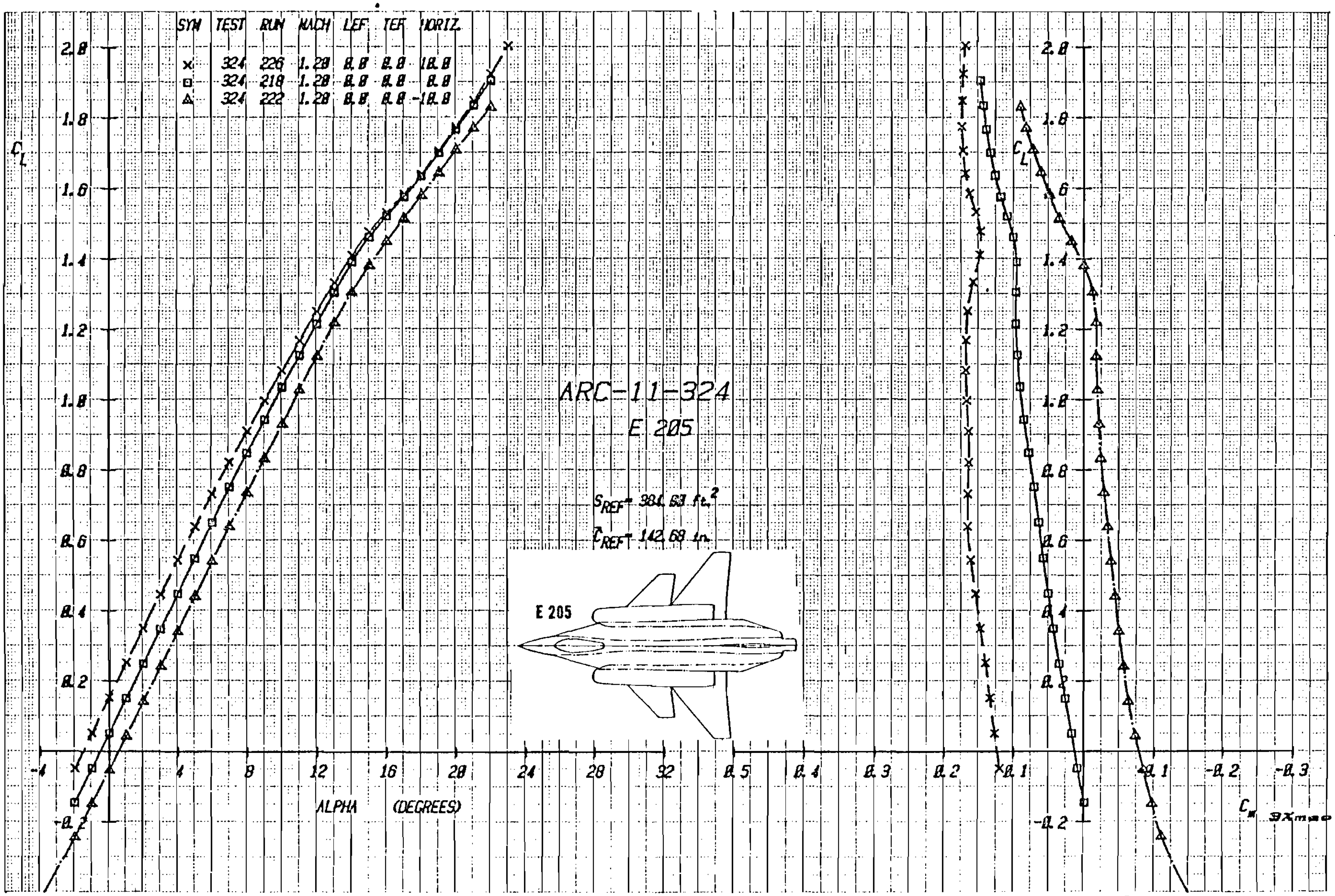

Figure3-53aEffect of Canard Deflection on Lift and Moment With Canard C_2, and Strake S_2, Mach = 1.2

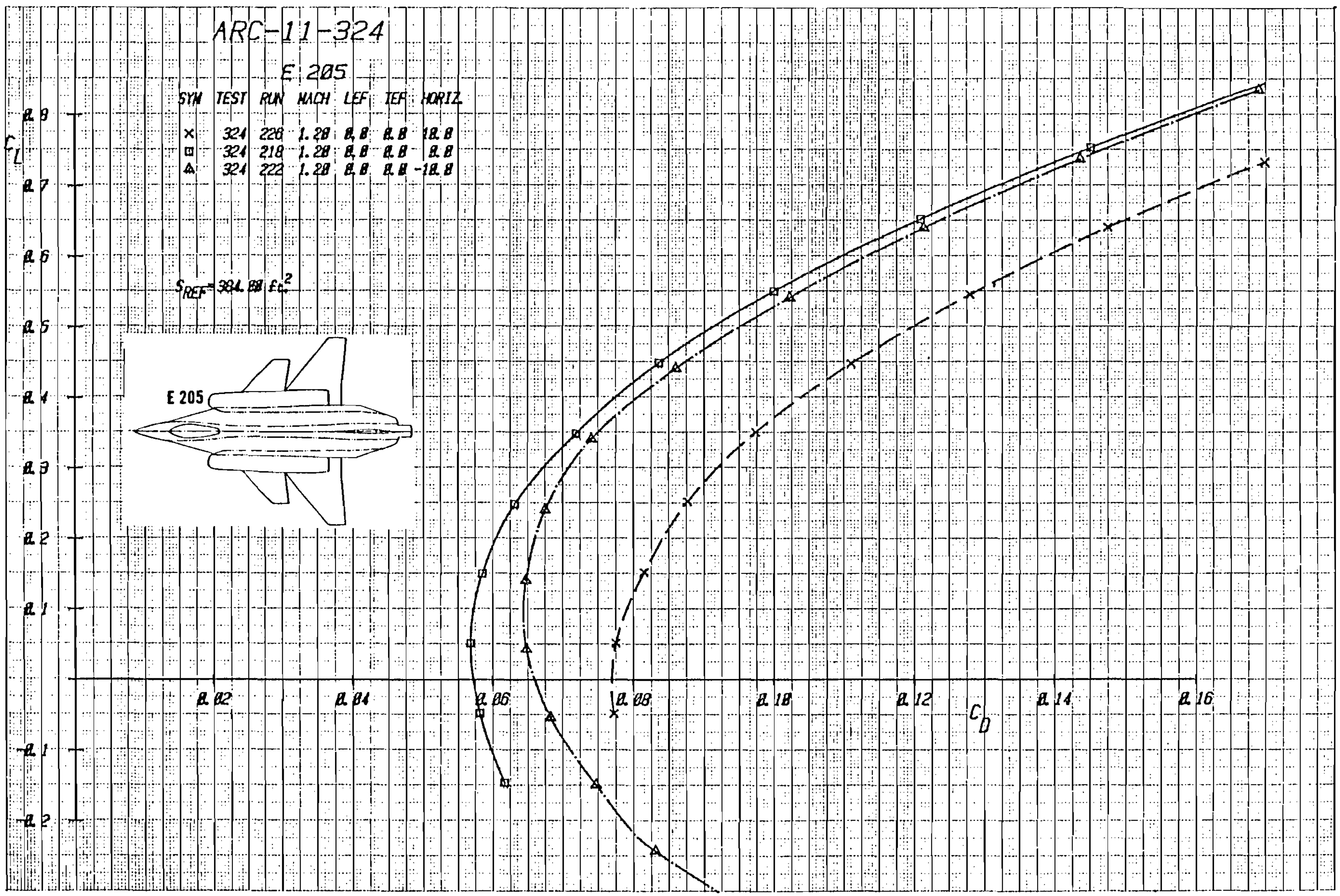

Figure3-53bEffect of Canard Deflection on Drag With Canard C_2, and Strake S_2, Mach = 1.2

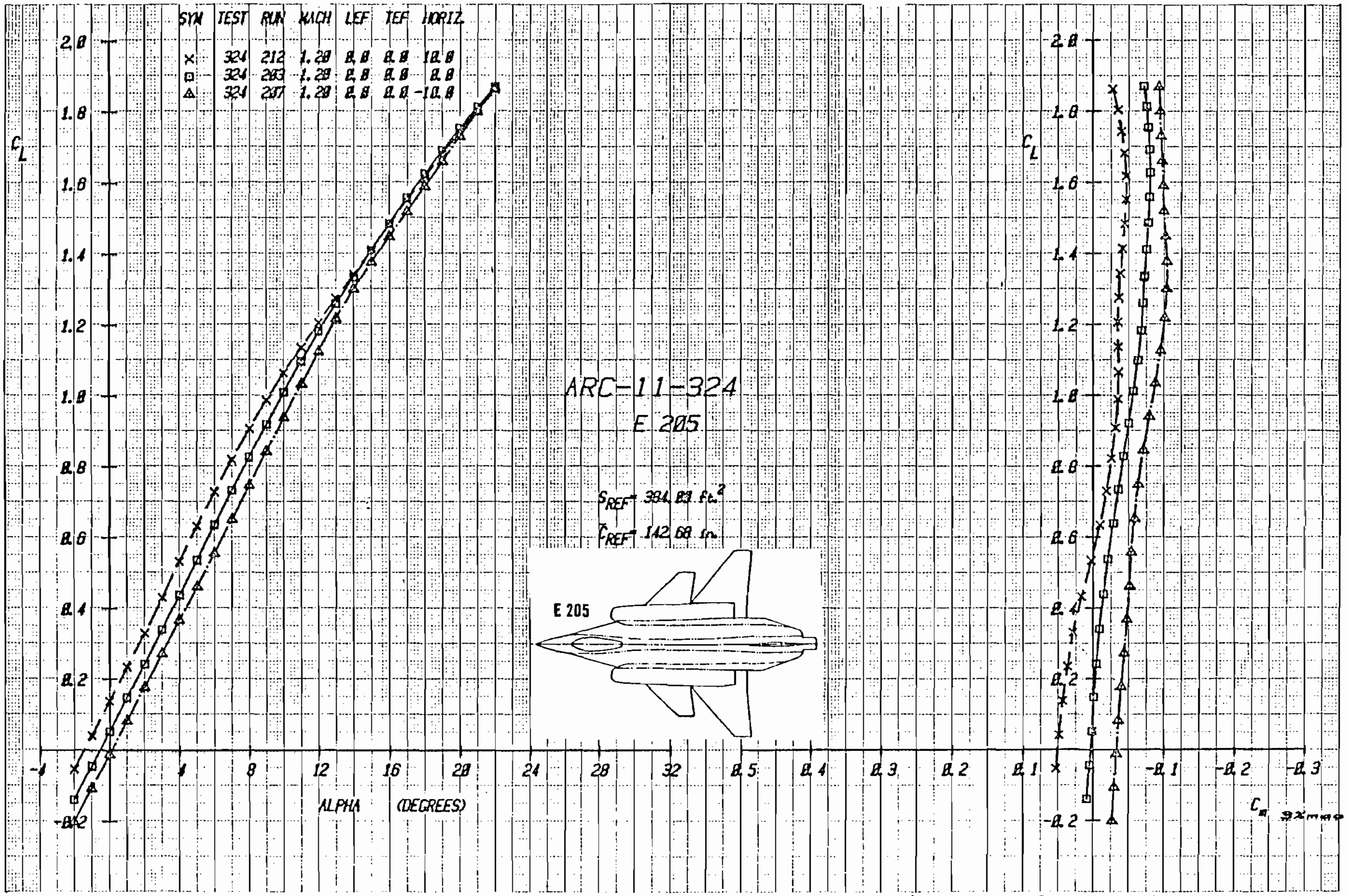

Figure3-54aEffect of Canard Deflection on Lift and Moment with Canard C_3, and Strake S_2, Mach = 1.2

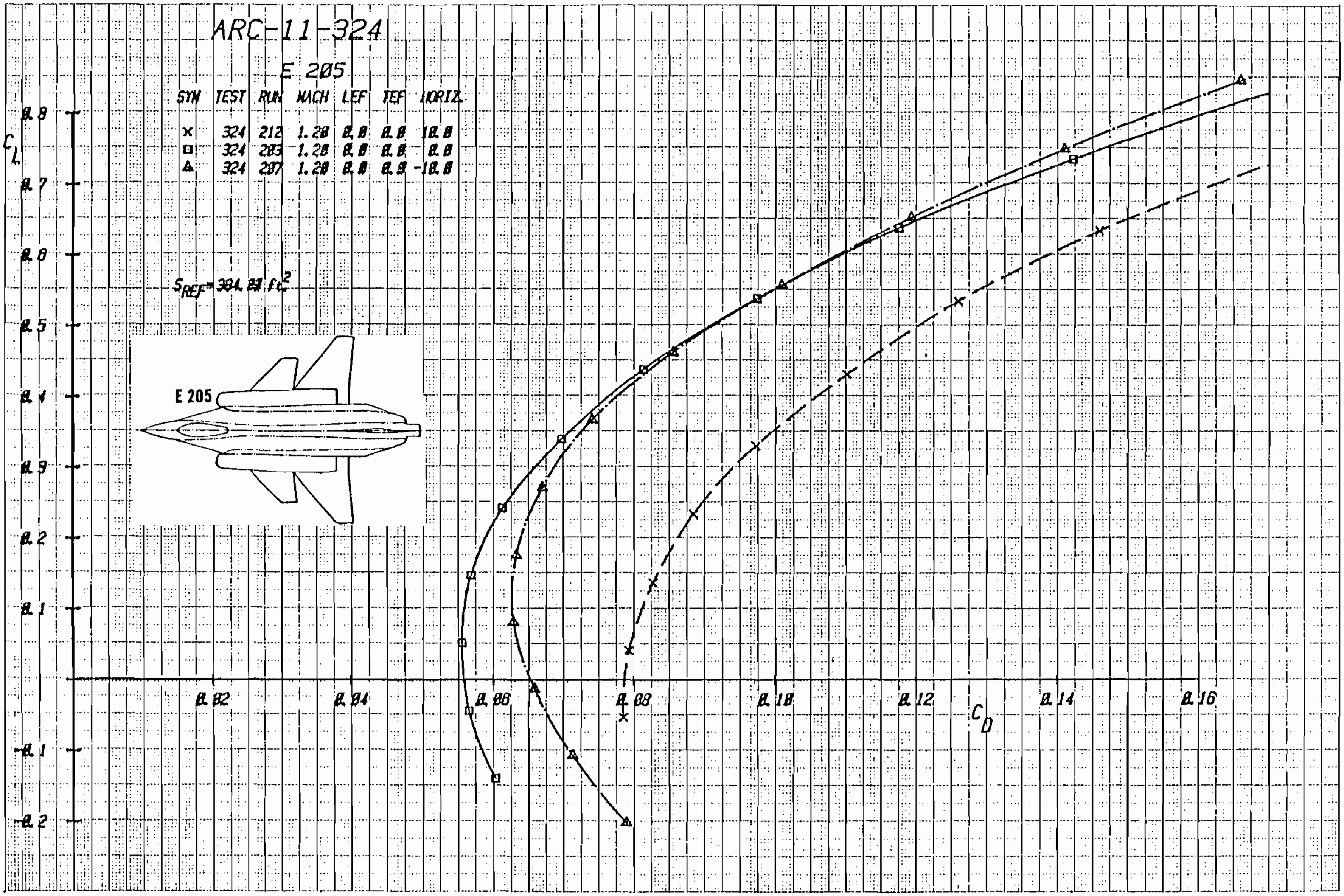

Figure3-54bEffect of Canard Deflection on Drag with Canard C_3, and Strake S_2, Mach = 1.2

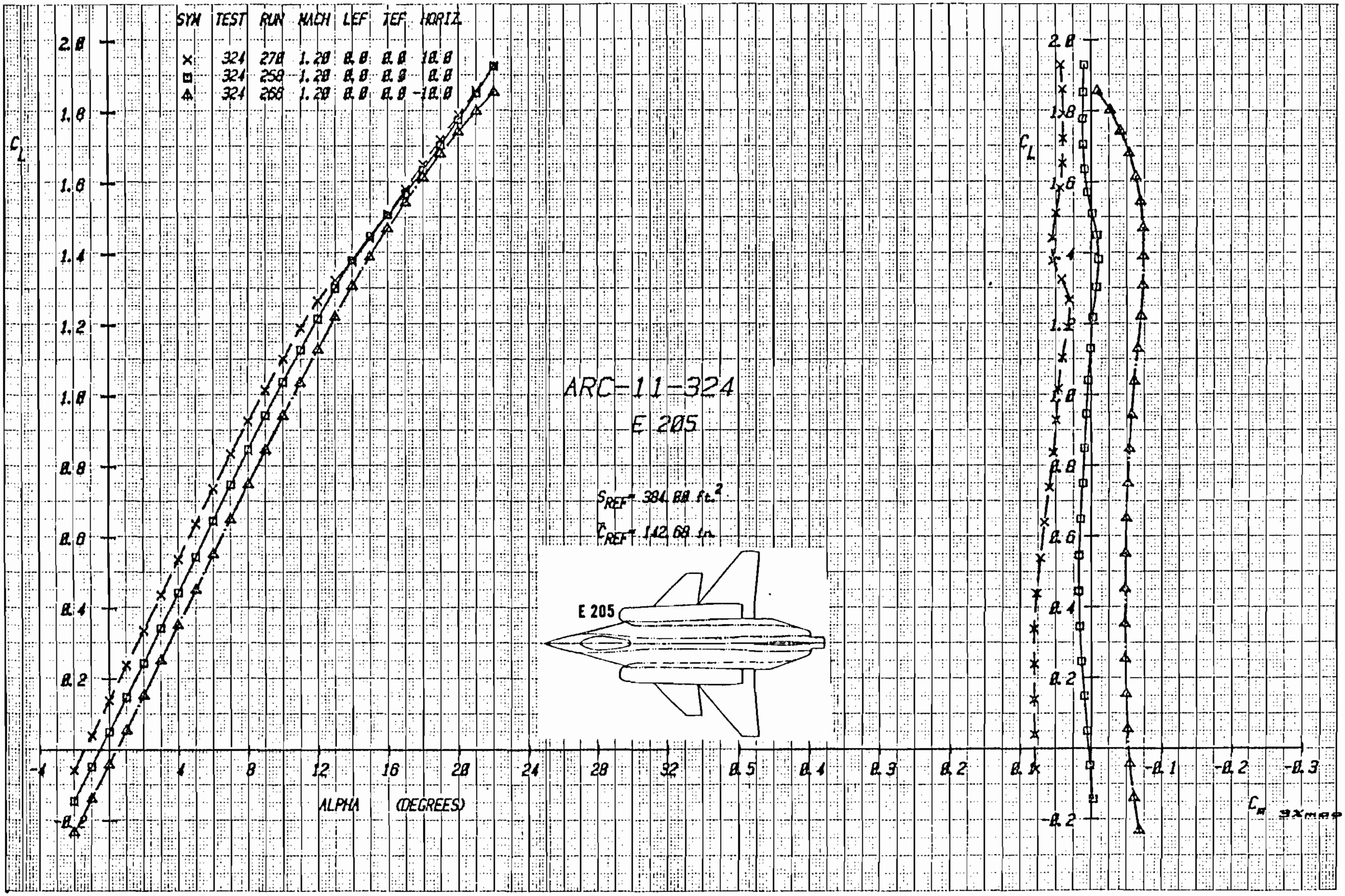

Figure3-55aEffect of Canard Deflection on Lift and Moment with Canard C_1, and Strake S_3, Mach = 1.2

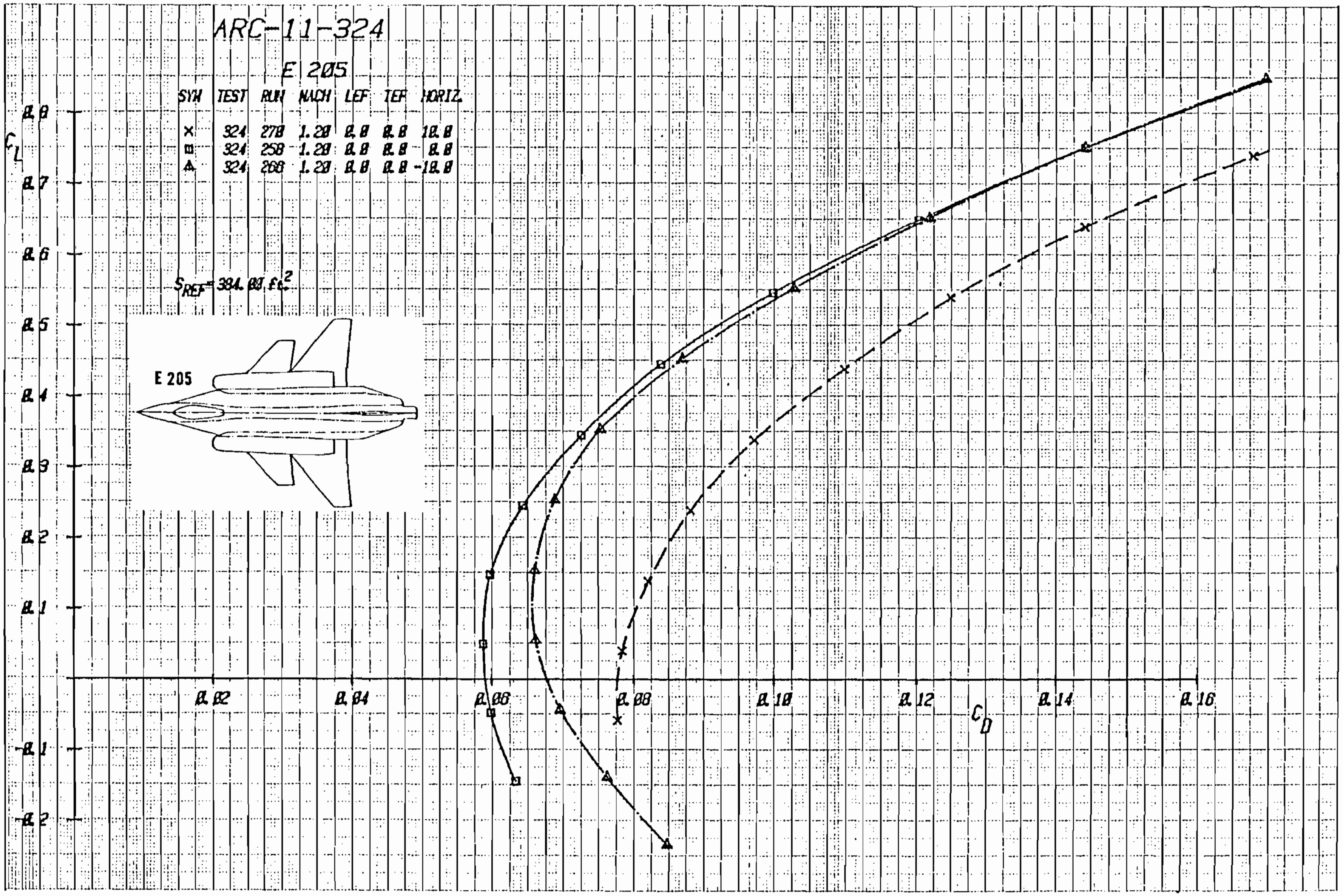

Figure3-55bEffect of Canard Deflection on Drag with Canard C_1, and Strake S_3, Mach = 1.2

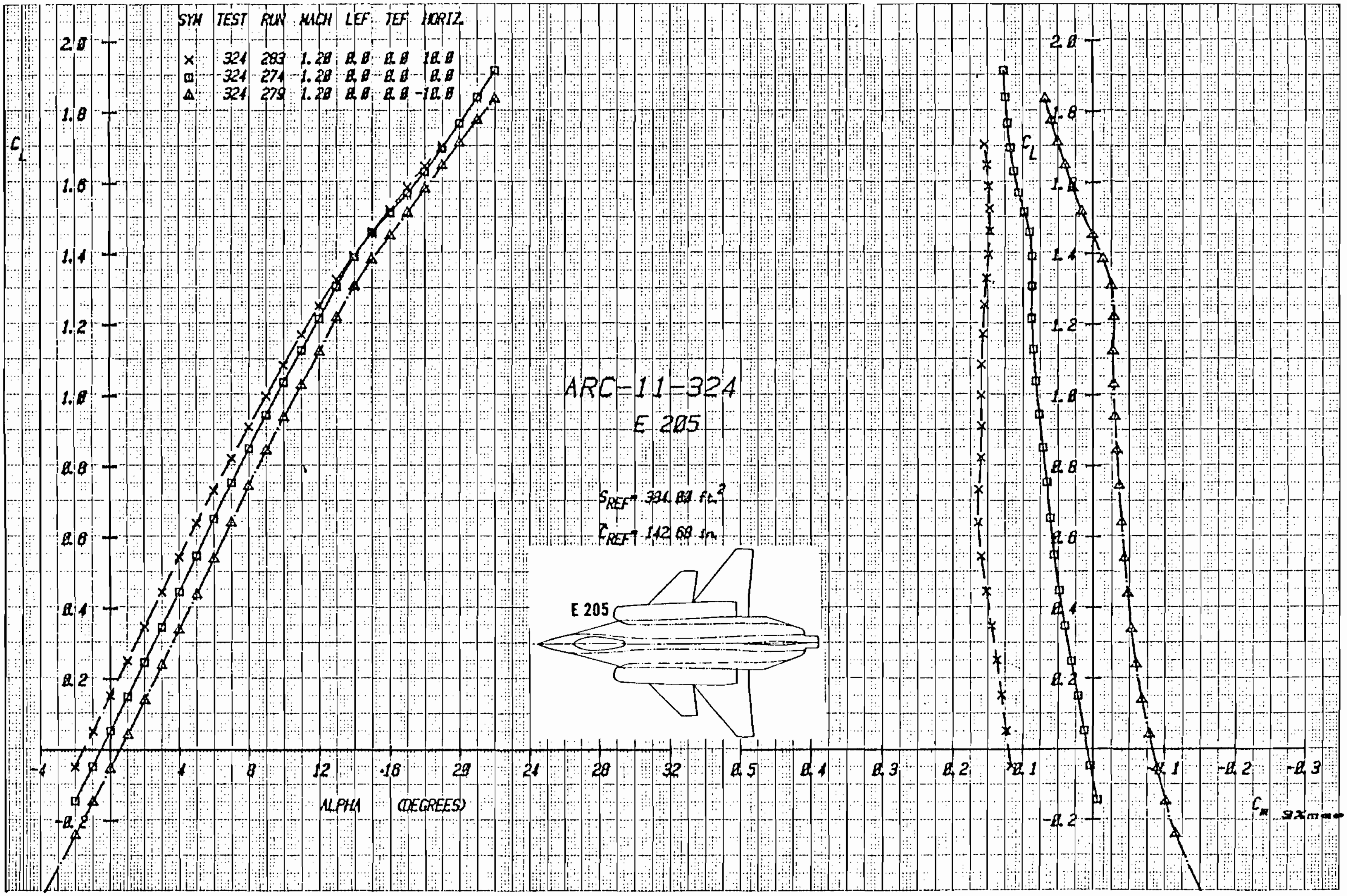

Figure3-56aEffect of Canard Deflection on Lift and Moment with Canard C_2, and Strake S_3, Mach = 1.2

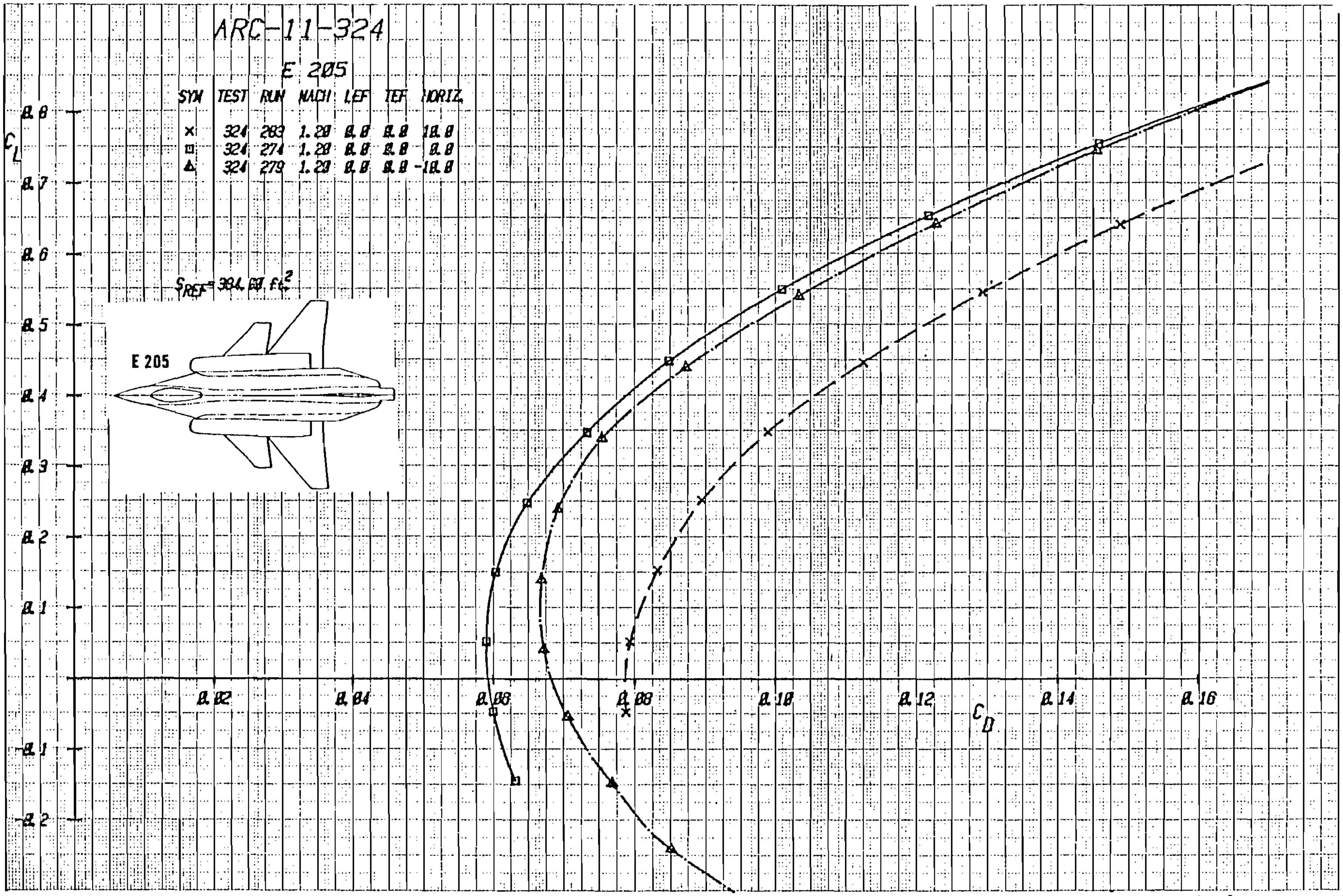

Figure3-56bEffect of Canard Deflection on Drag with Canard C_2, and Strake S_3, Mach = 1.2

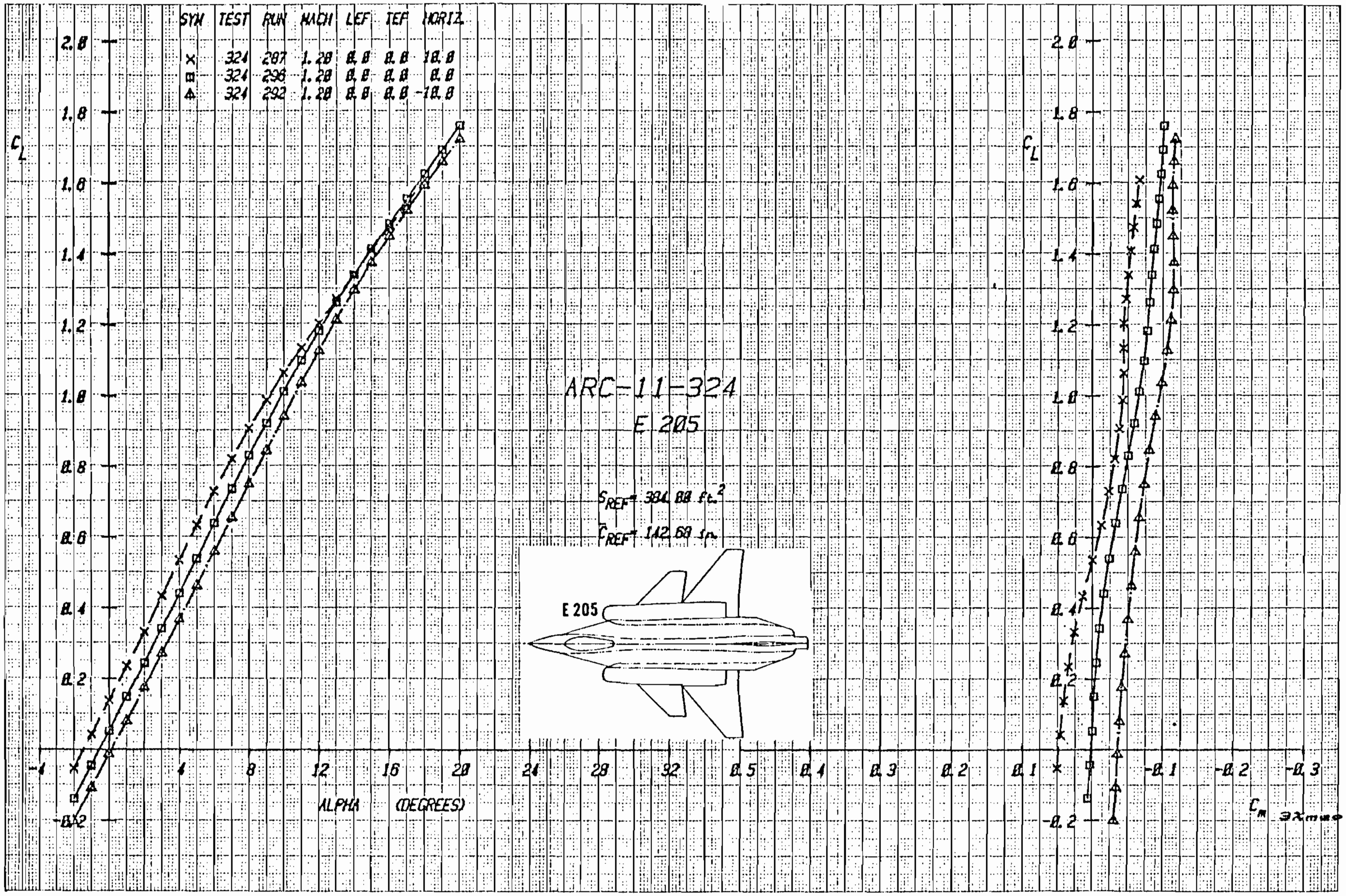

Figure3-57aEffect of Canard Deflection on Lift and Moment with Canard C_3, and Strake S_3, Mach = 1.2

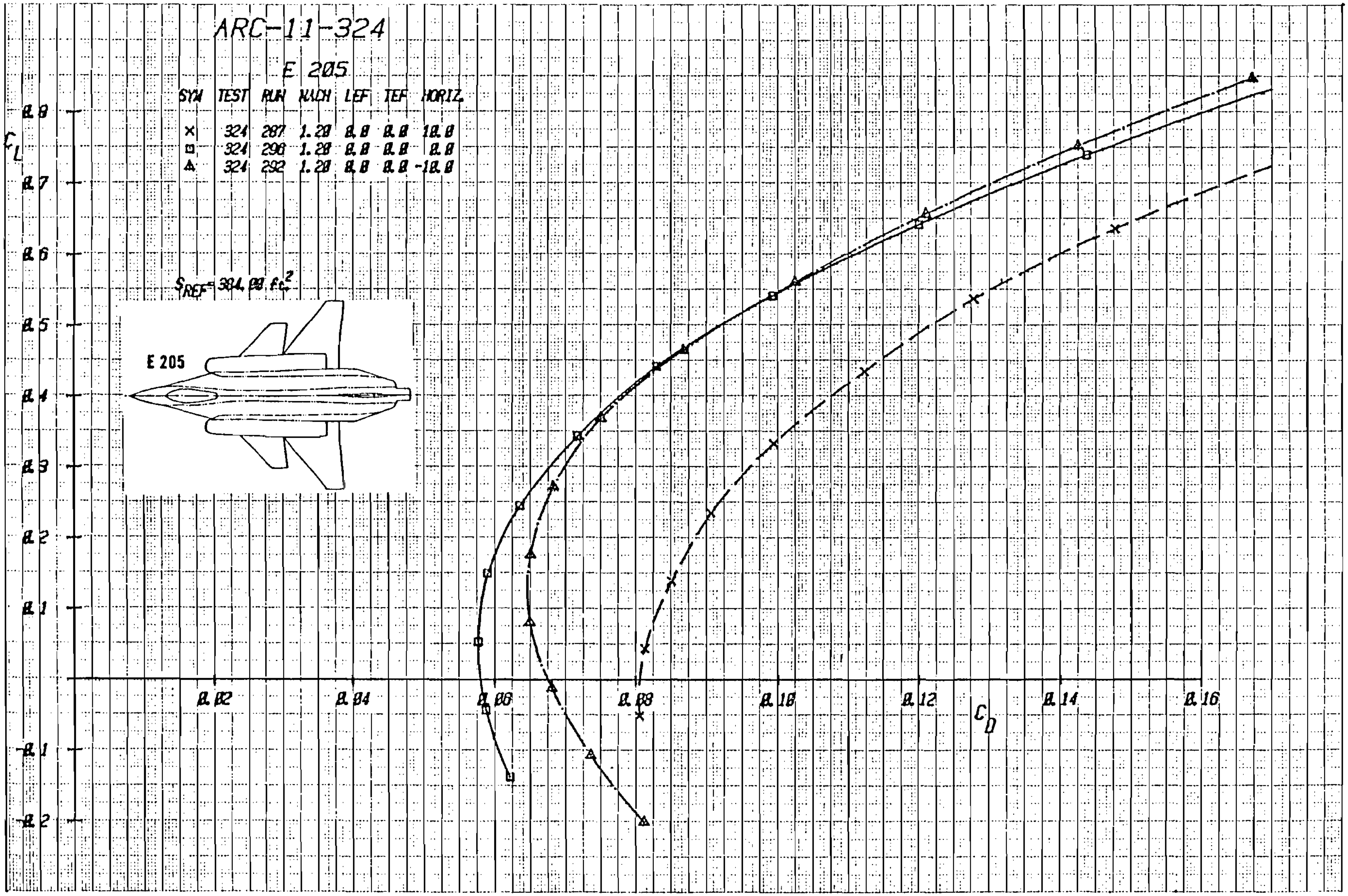

Figure3-57bEffect of Canard Deflection on Drag with Canard C_3, and Strake S_3, Mach = 1.2

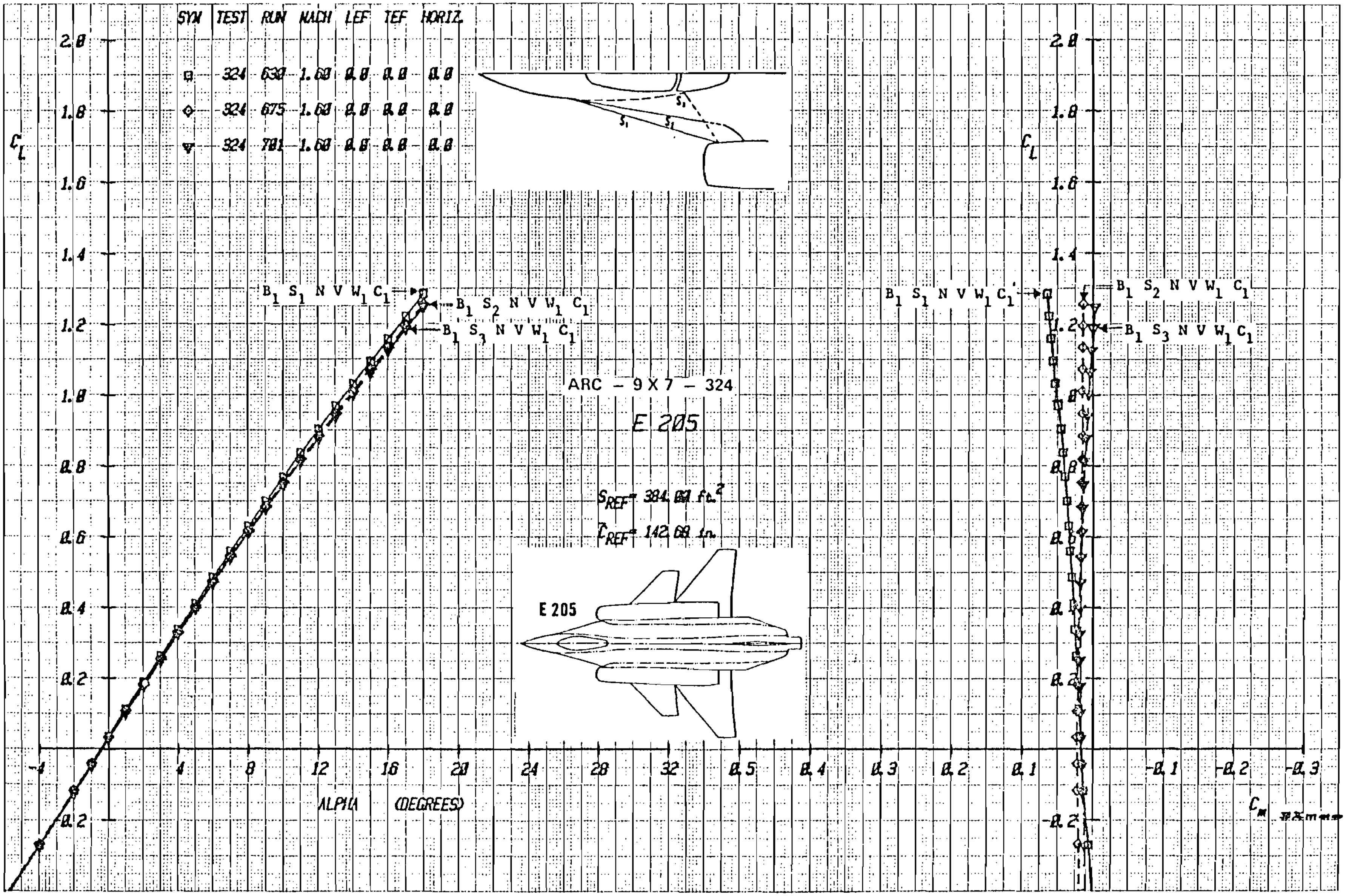

Figure3-58aEffect of Strake Variation on Lift and Moment with Baseline Canard Longitudinal Location, C_1, and $\delta i = 0°$, Mach = 1.6

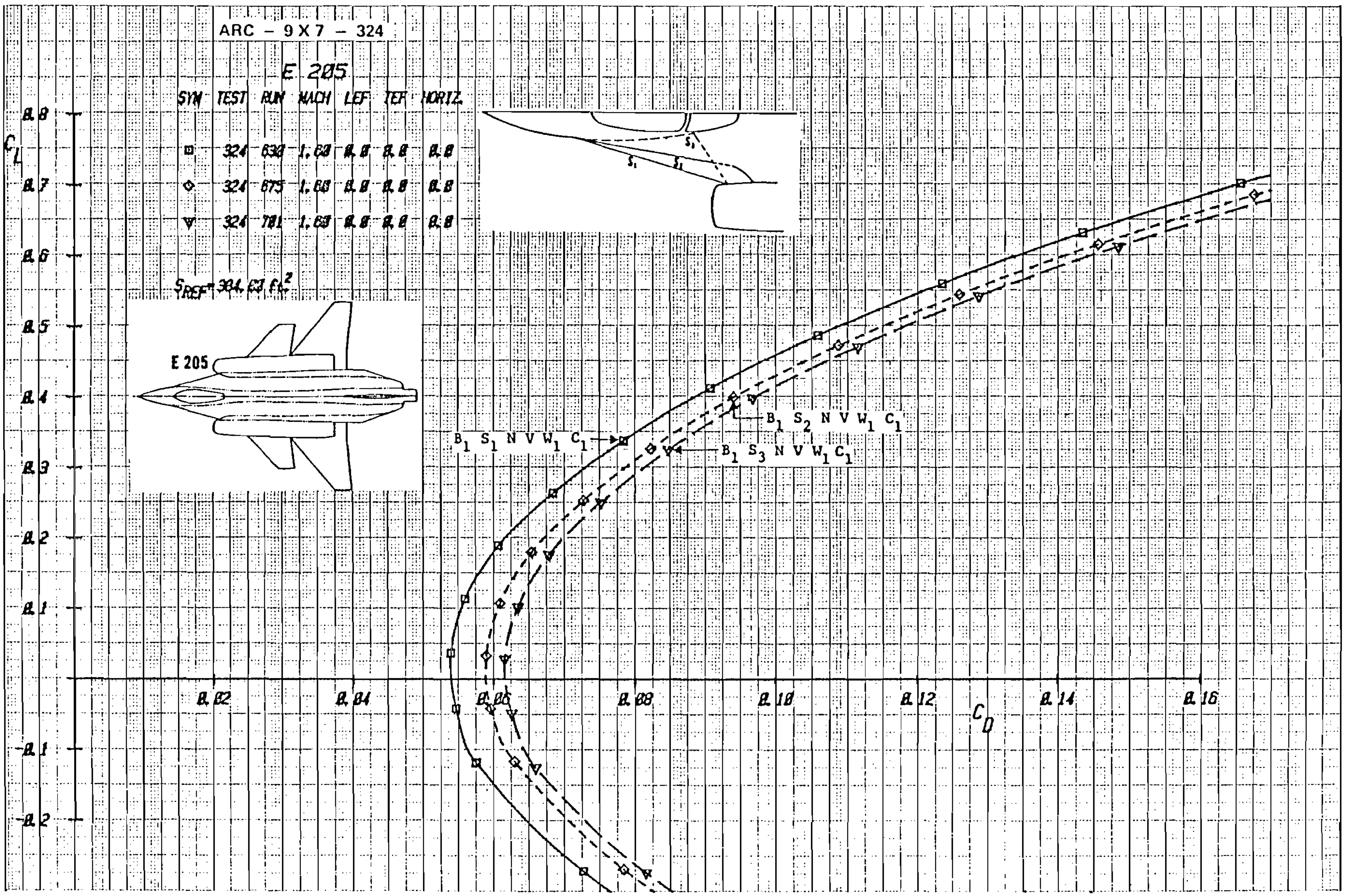

Figure3-58bEffect of Strake Variation on Drag with Baseline Canard Longitudinal Location, C_1, and $\delta i = 0°$, (Expanded Drag Scale), Mach = 1.6

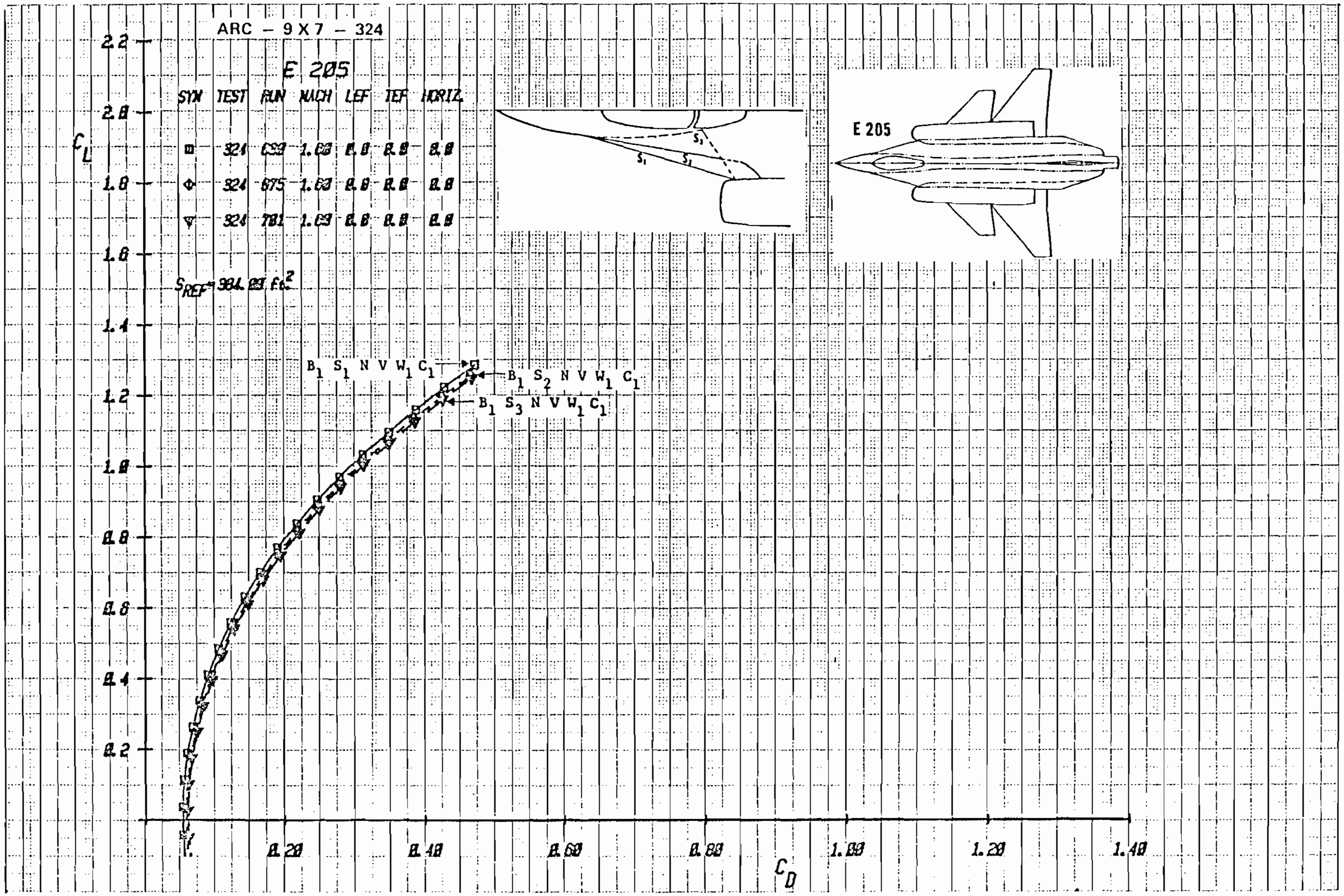

Figure3-58cEffect of Strake Variation on Drag with Baseline Canard Longitudinal Location, C_1, and $\delta i = 0°$, Mach = 1.6.

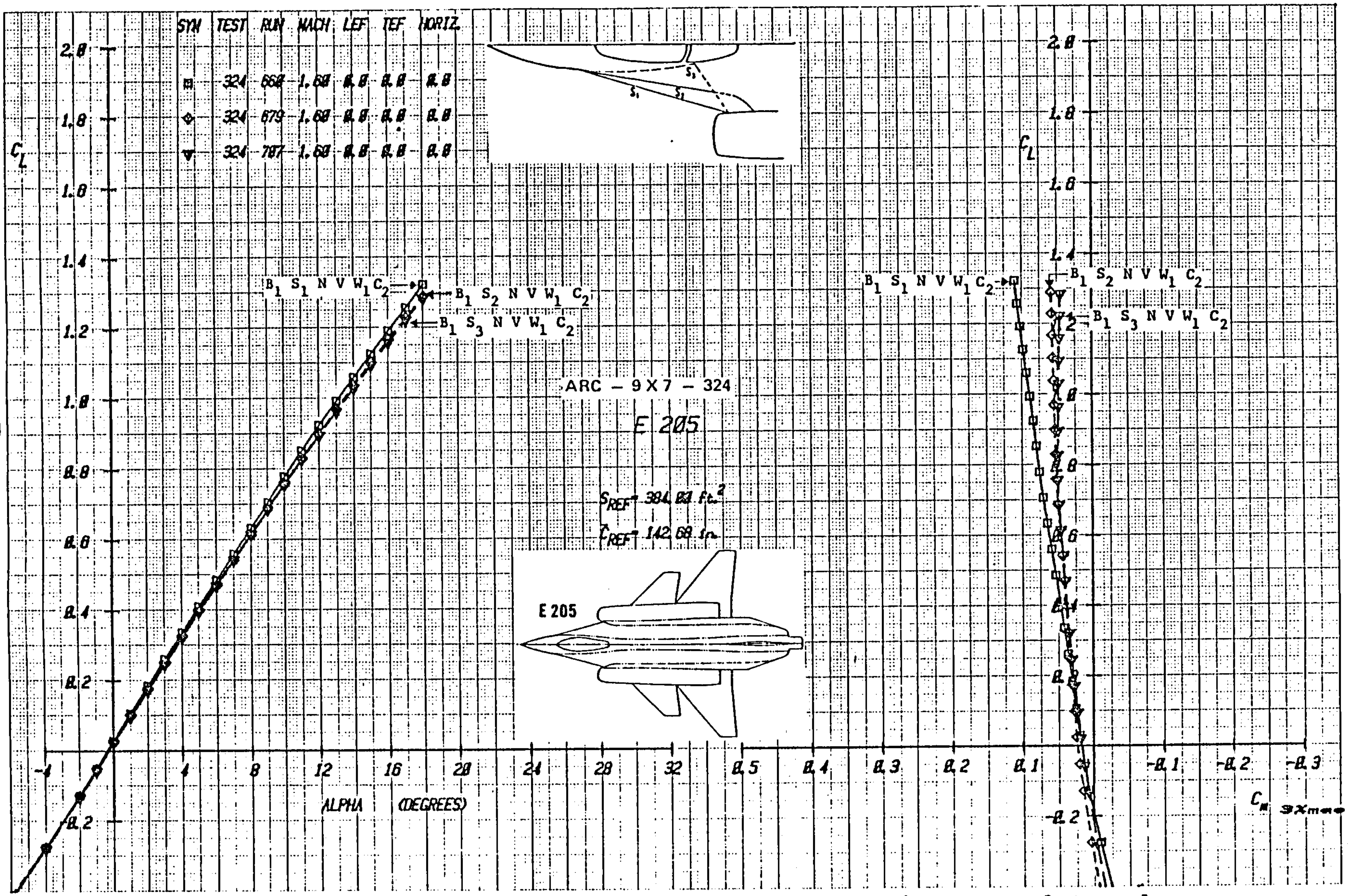

Figure3-59aEffect of Strake Variation on Lift and Moment with Forward Canard Longitudinal Location, C_2, and $\delta i = 0°$, Mach = 1.6.

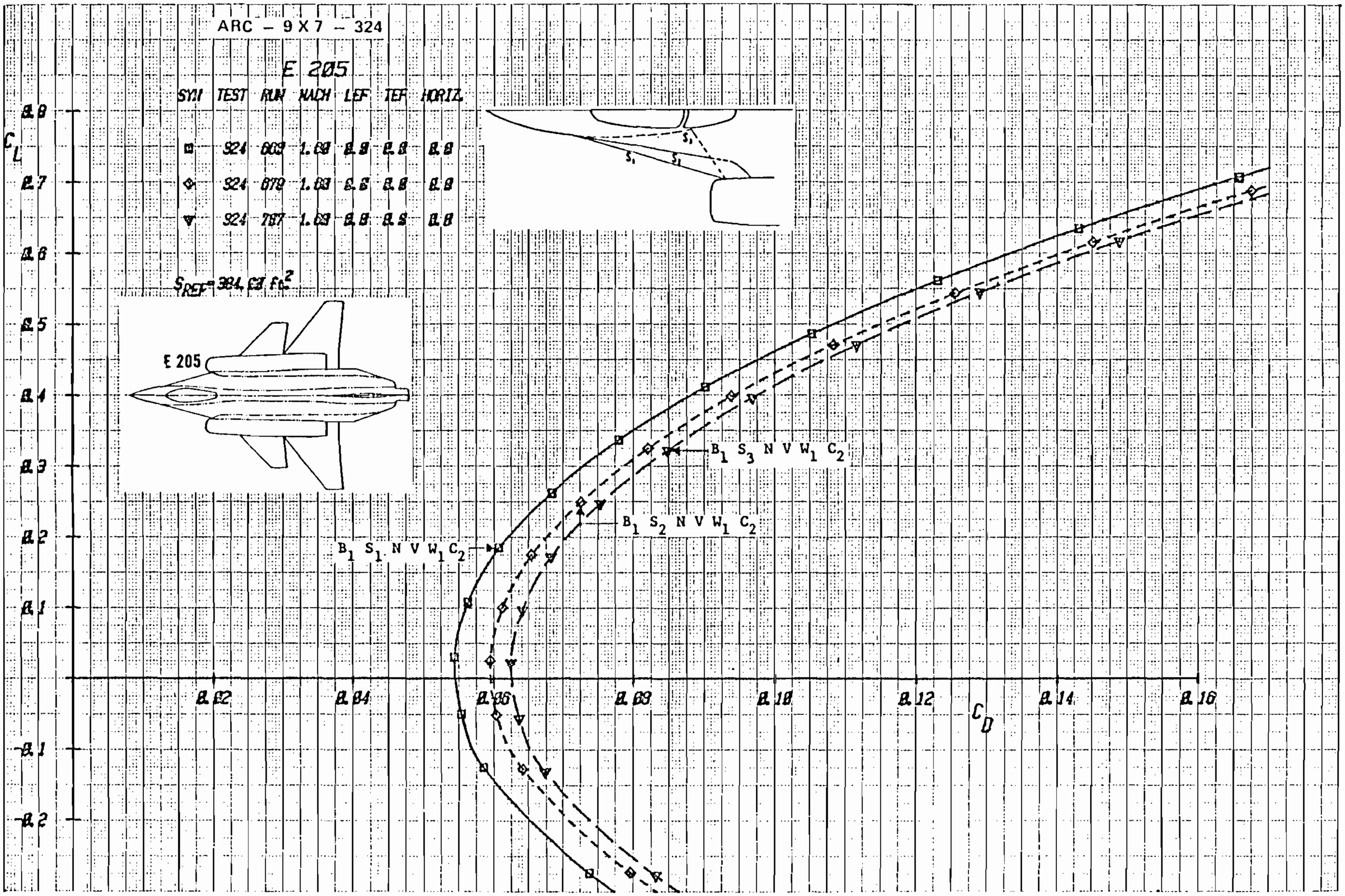

Figure3-59bEffect of Strake Variation on Drag with Forward Canard Longitudinal Location, C_2, and $\delta i = 0°$, (Expanded Drag Scale), Mach = 1.6.

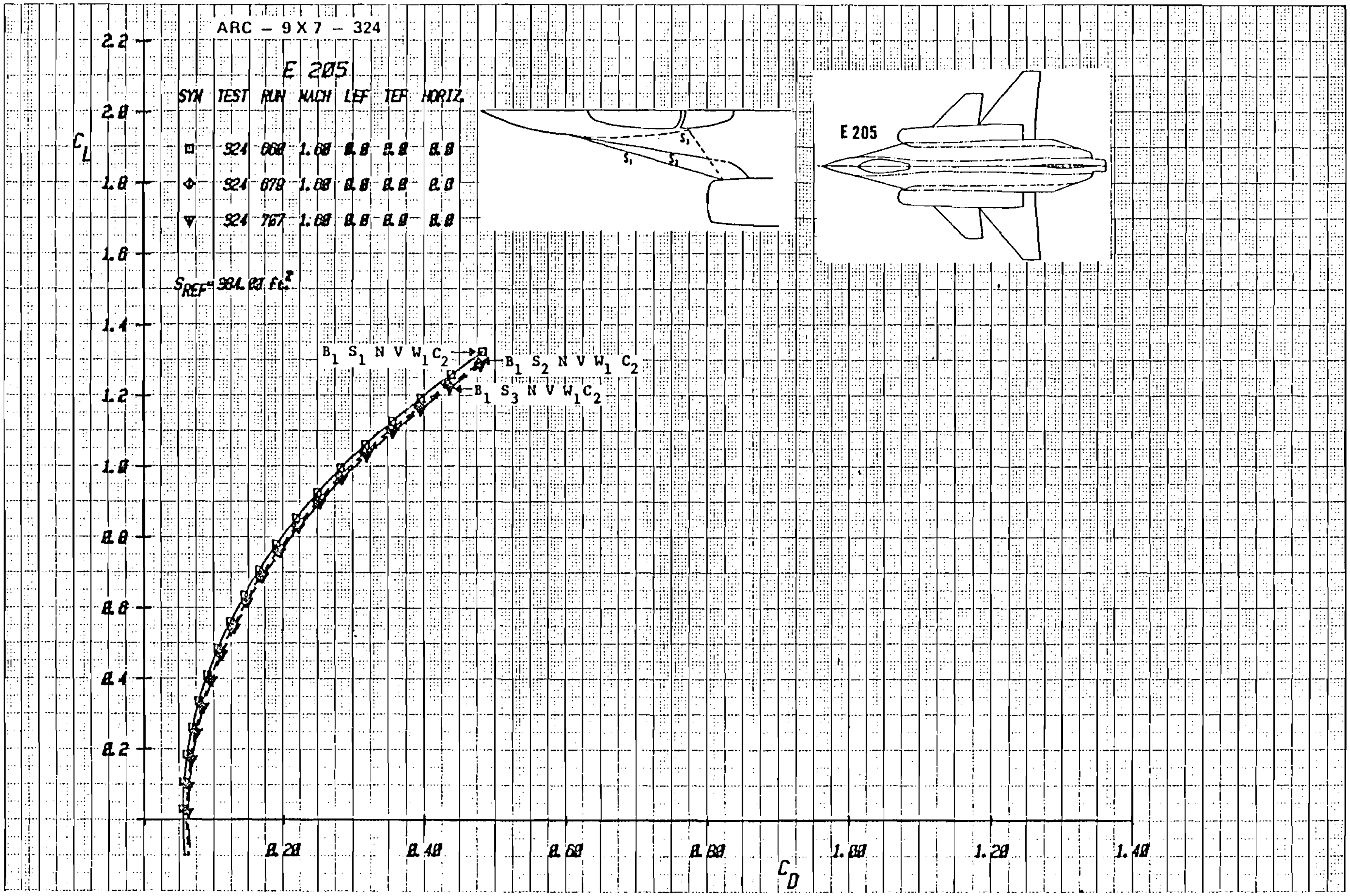

Figure3-59cEffect of Strake Variation on Drag with Forward Canard Longitudinal Location, C_2, and $\delta i = 0°$, Mach = 1.6

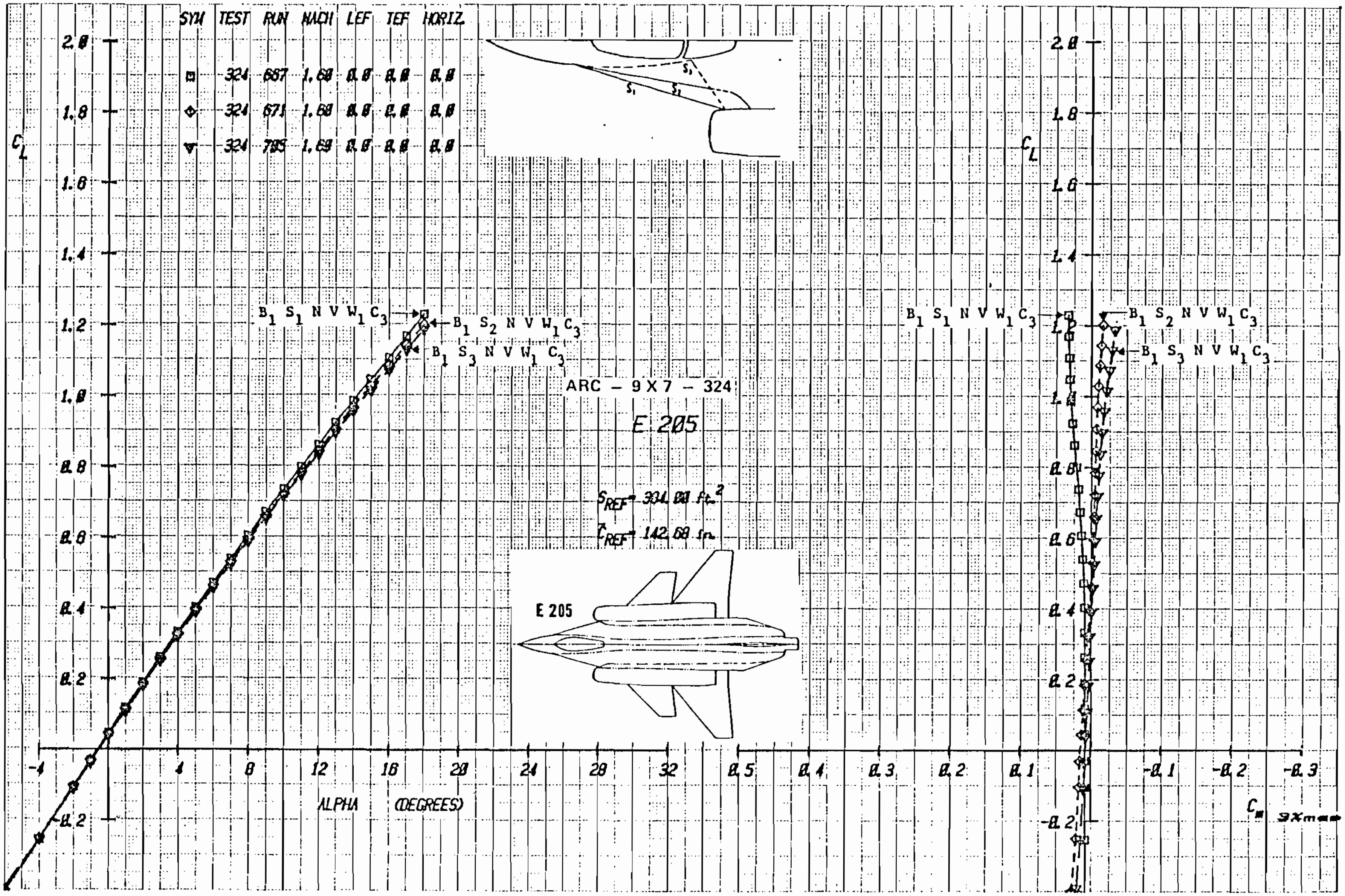

Figure3-60aEffect of Strake Variation on Lift and Moment with Aft Canard Longitudinal Location, C_3, and $\delta i = 0°$, Mach = 1.6

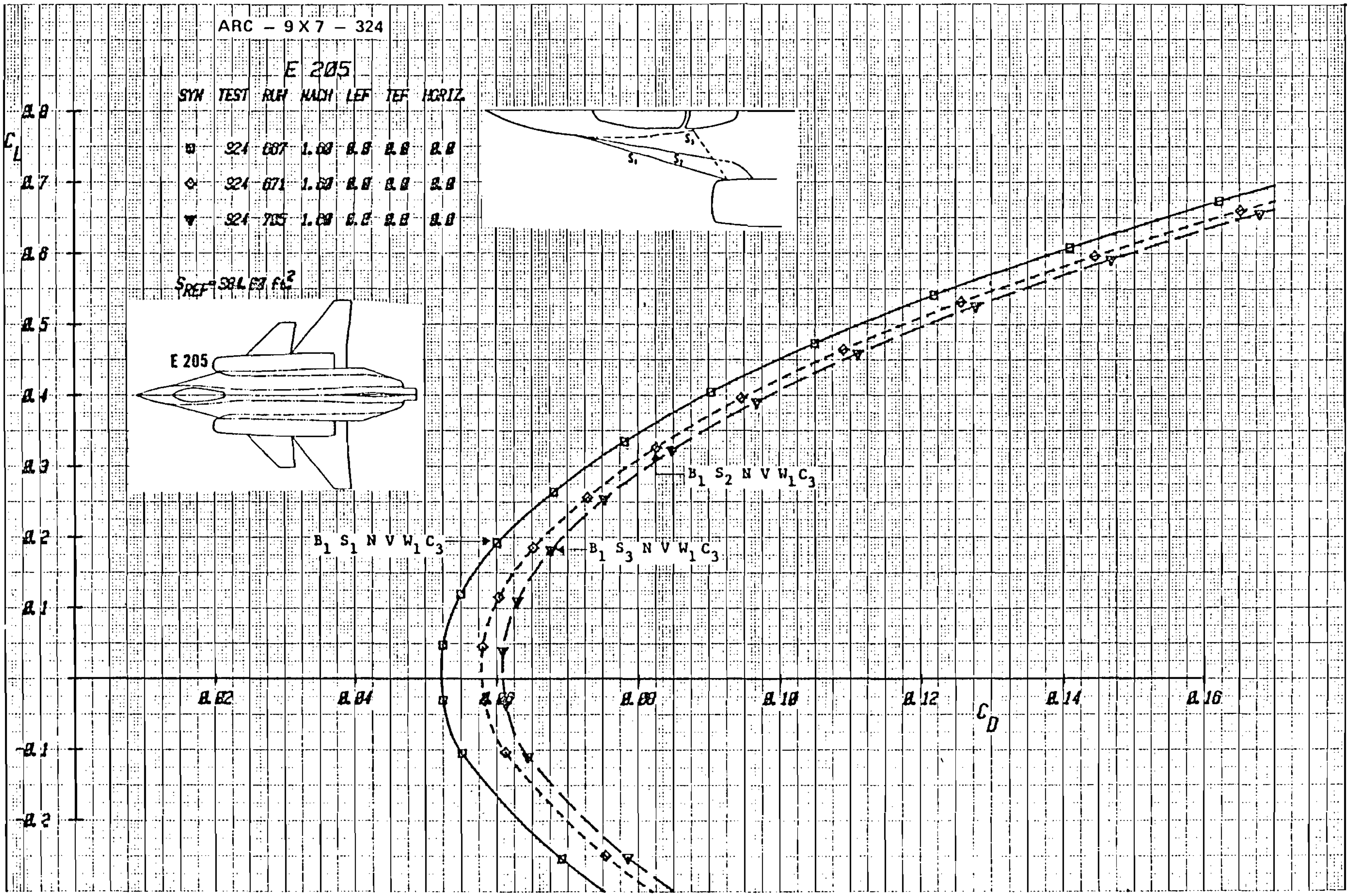

Figure3-60bEffect of Strake Variation on Drag with Aft Canard Longitudinal Location, C_3, and $\delta i = 0°$, (Expanded Drag Scale), Mach = 1.6

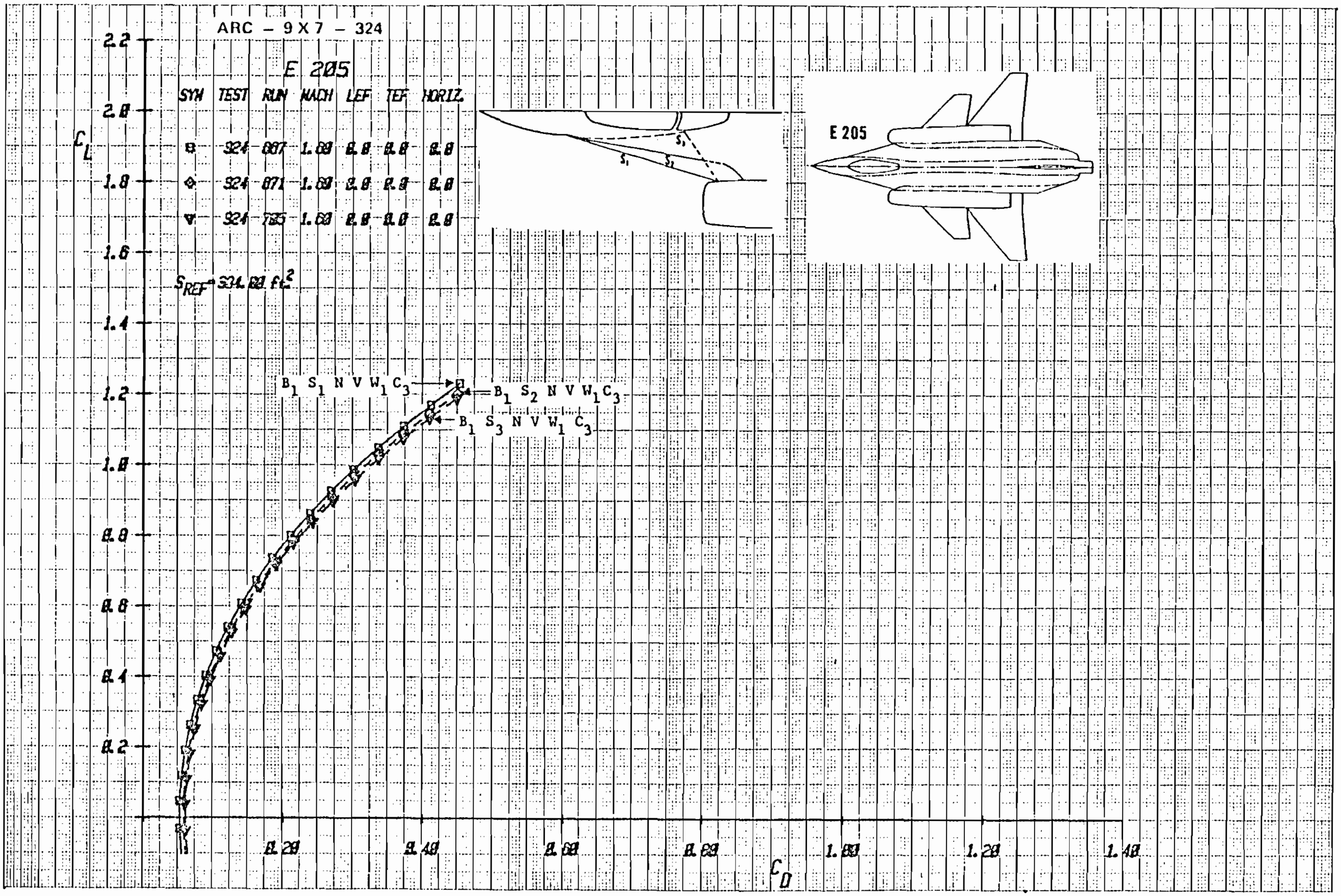

Figure3-60cEffect of Strake Variation on Drag with Aft Canard Longitudinal Location, C_3, and $\delta i = 0°$, Mach = 1.6

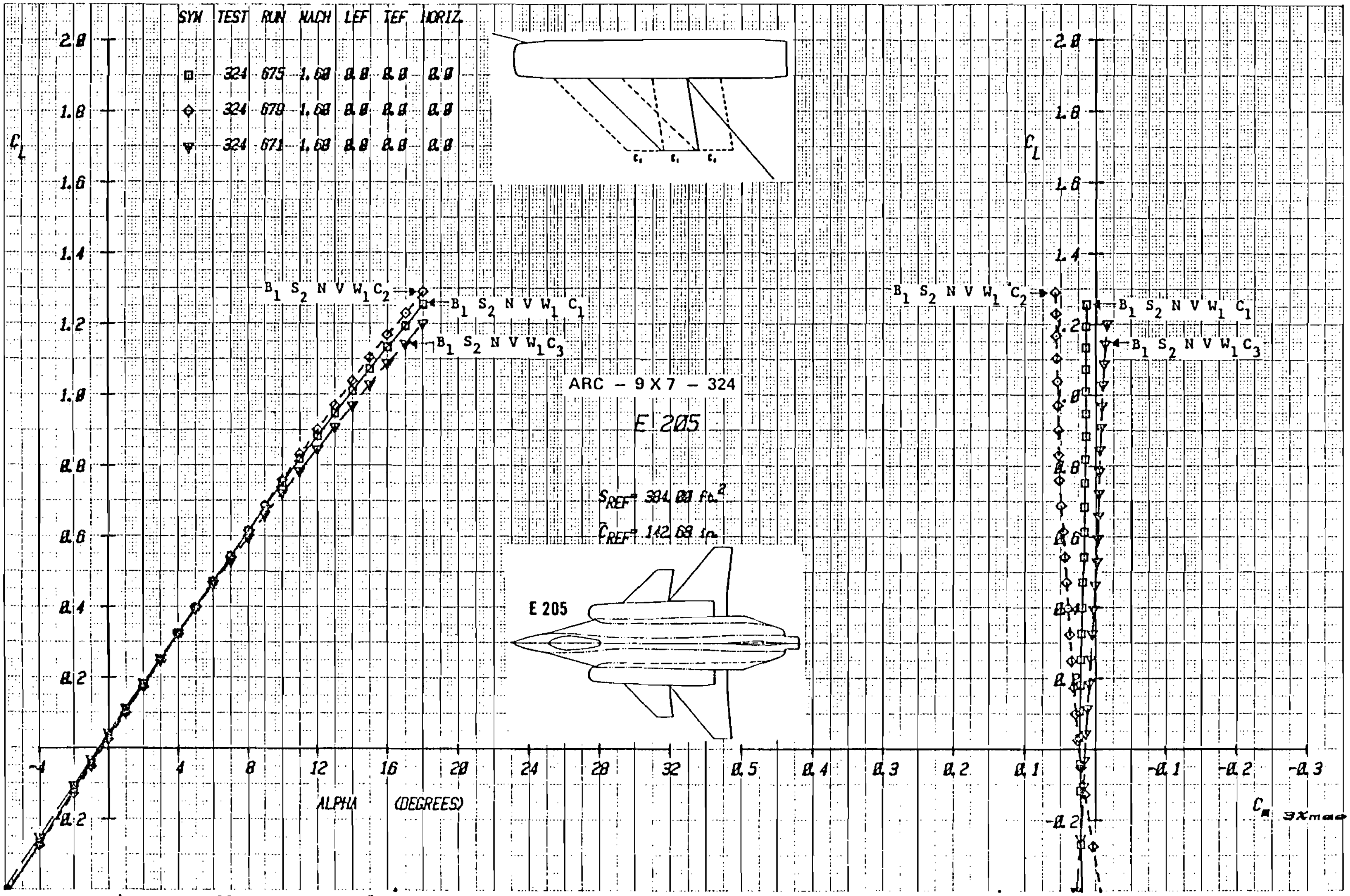

Figure3-61aEffect of Canard Longitudinal Location on Lift and Moment With Strake S_2, Mach = 1.6

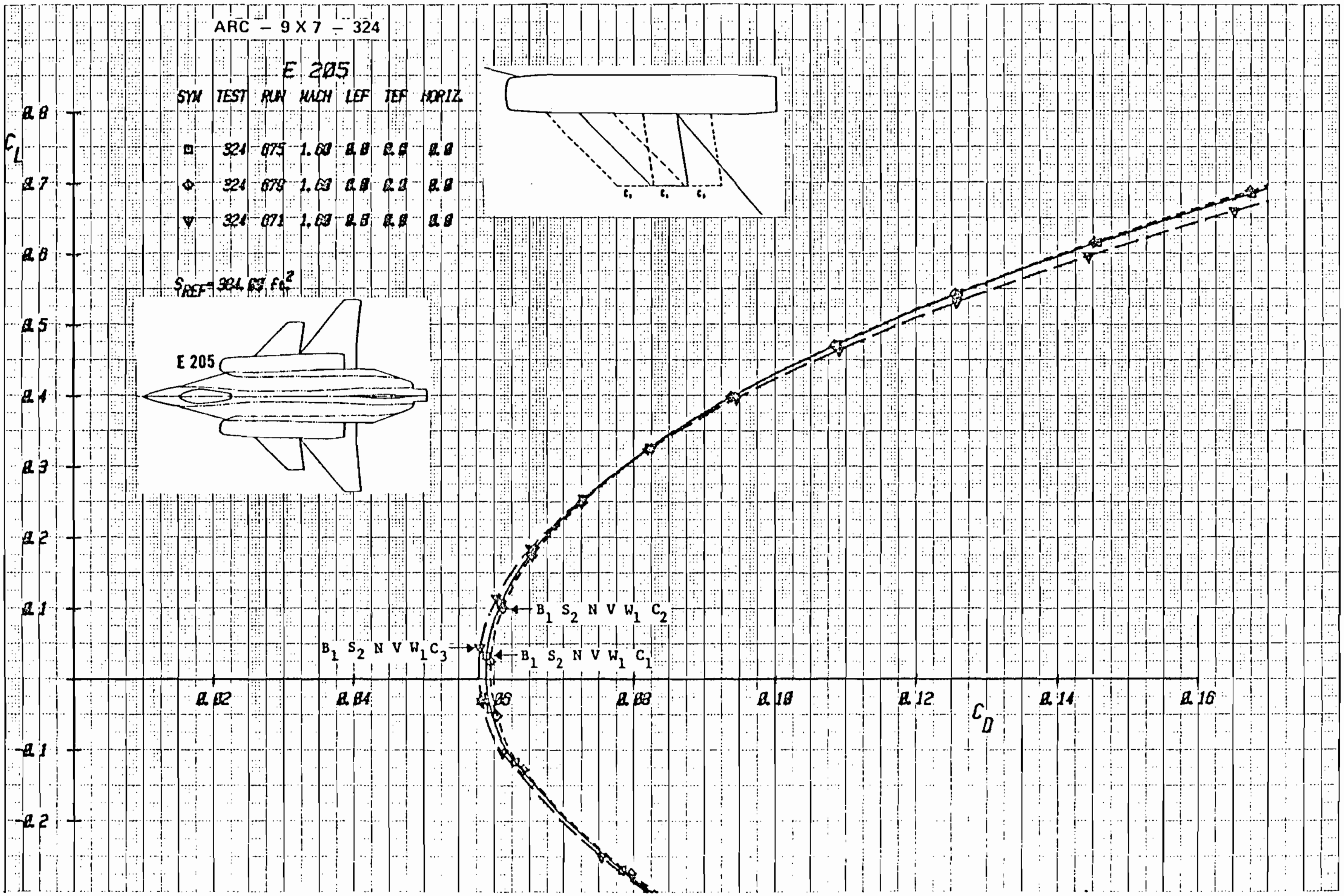

Figure3-61bEffect of Canard Longitudinal Location on Drag With Strake S_2, (Expanded Drag Scale), Mach = 1.6

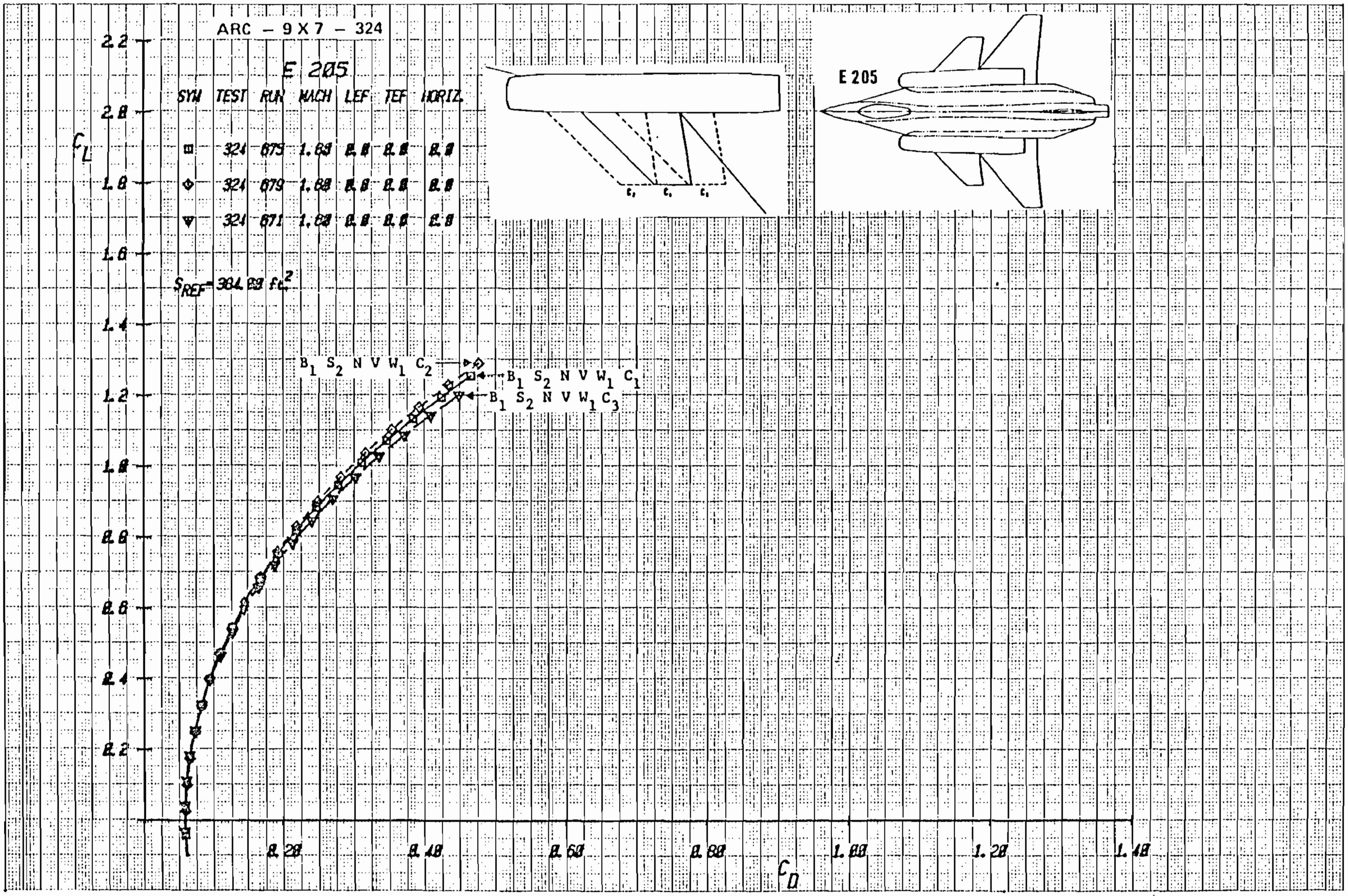

Figure3-61cEffect of Canard Longitudinal Location on Drag With Strake S_2, Mach = 1.6

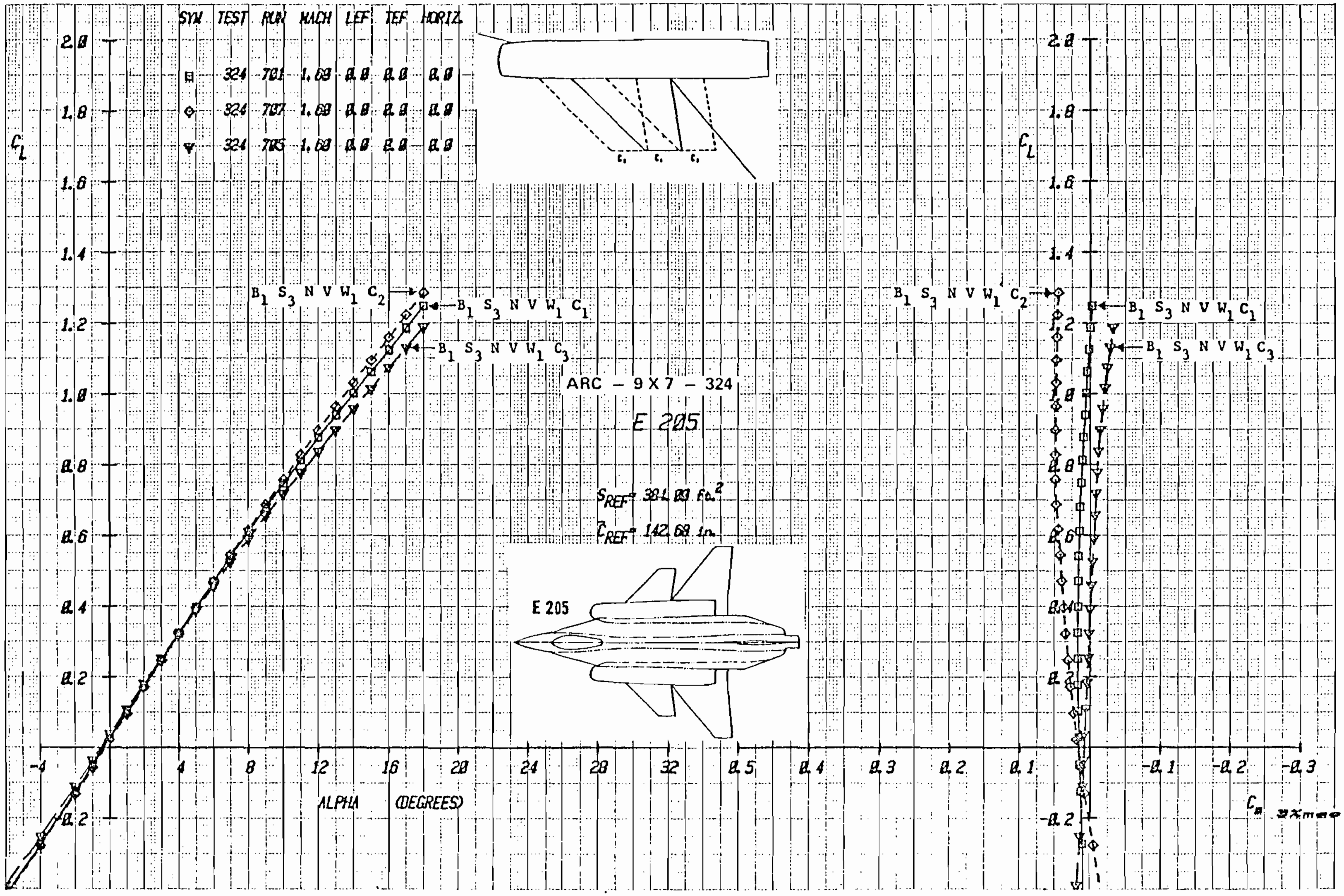

Figure3-62aEffect of Canard Longitudinal Location on Lift and Moment With Strake S_3 , Mach = 1.6

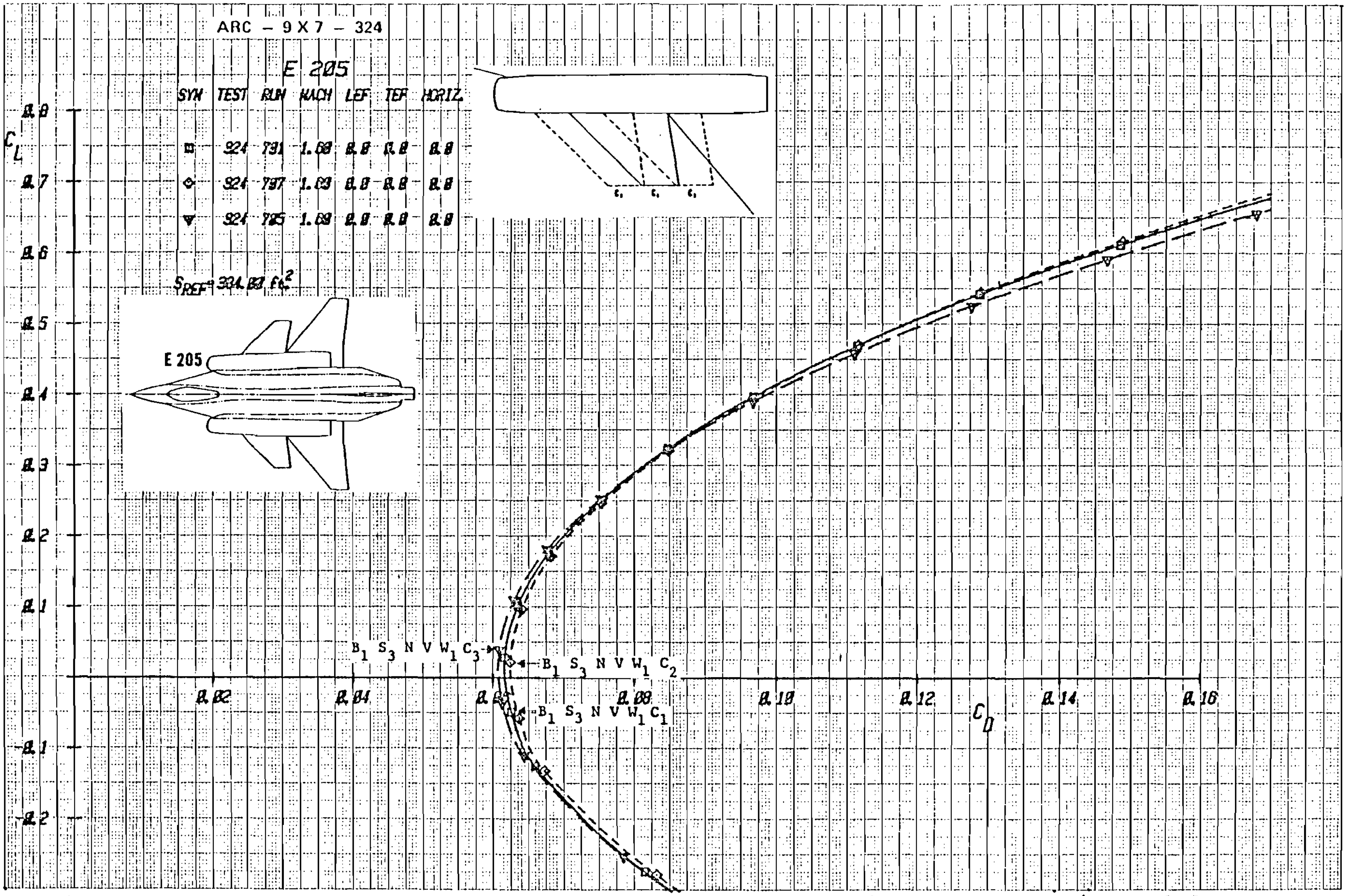

Figure3-62bEffect of Canard Longitudinal Location on Drag With Strake S_3, (Expanded Drag Scale), Mach = 1.6

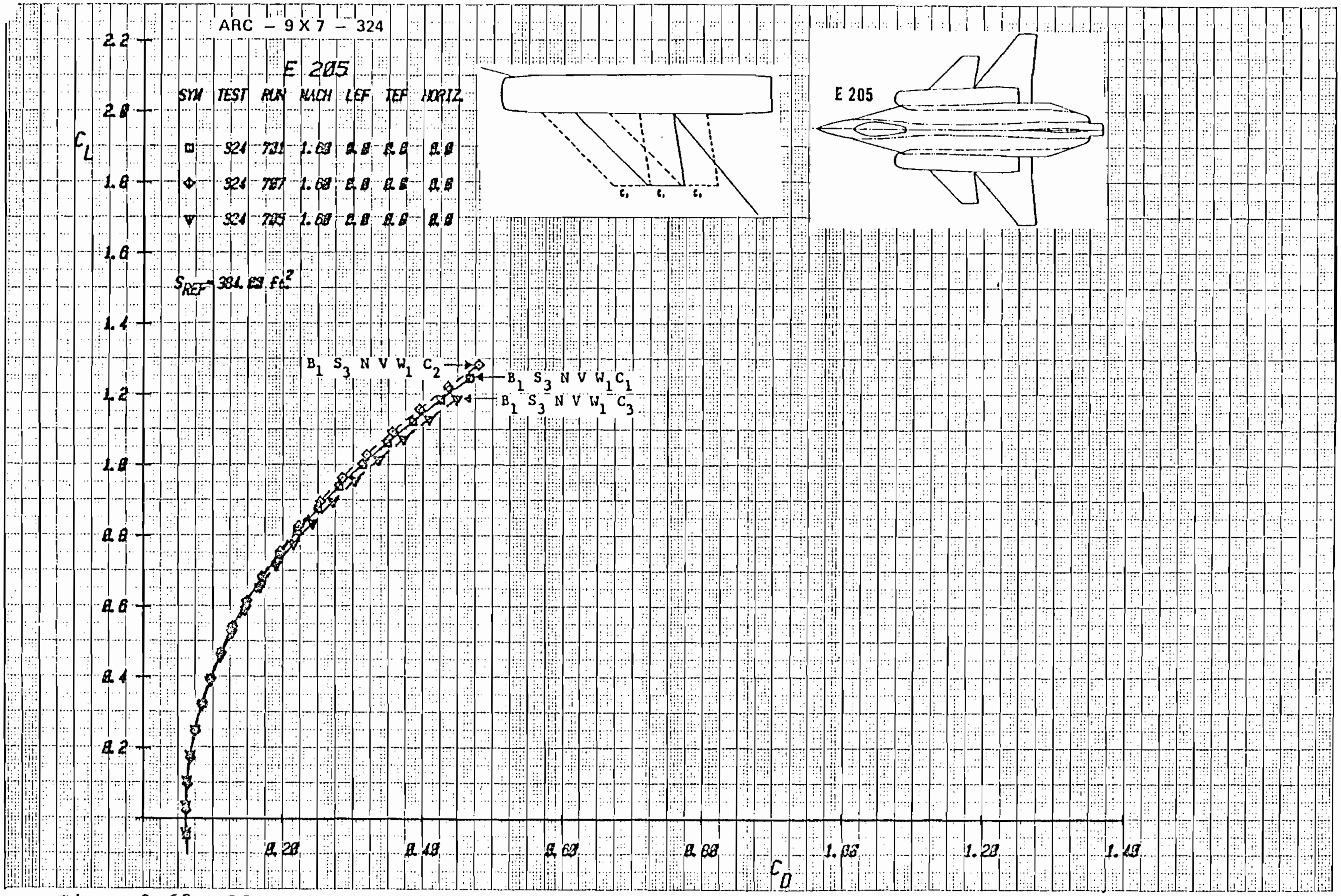

Figure3-62cEffect of Canard Longitudinal Location on Drag With Strake S_3, Mach = 1.6

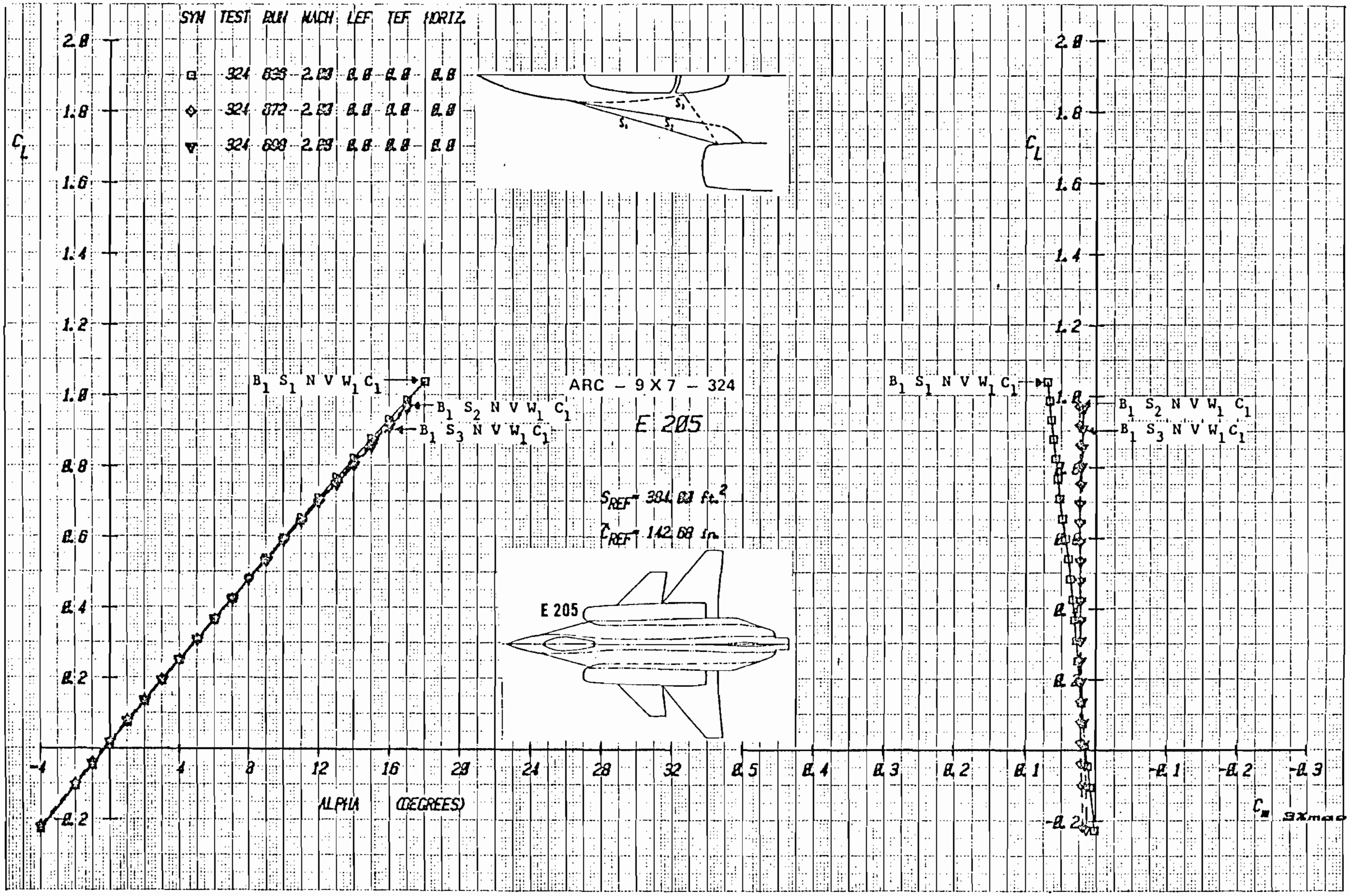

Figure3-63aEffect of Strake Variation on Lift and Moment with Baseline Canard Longitudinal Location, C_1, and δi = 0°, Mach = 2.0

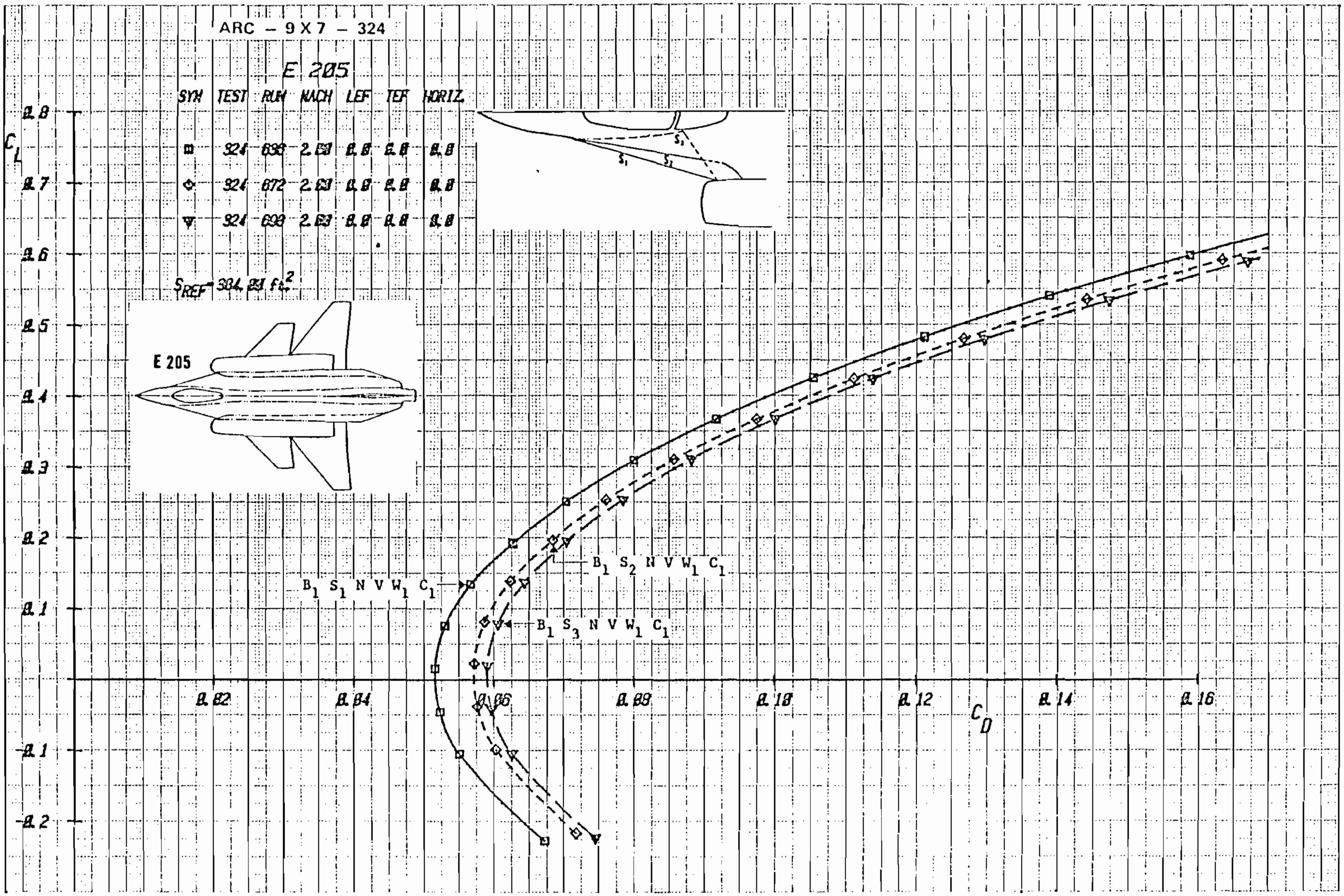

Figure3-63bEffect of Strake Variation on Drag with Baseline Canard Longitudinal Location, C_1, and $\delta i = 0°$, (Expanded Drag Scale), Mach = 2.0.

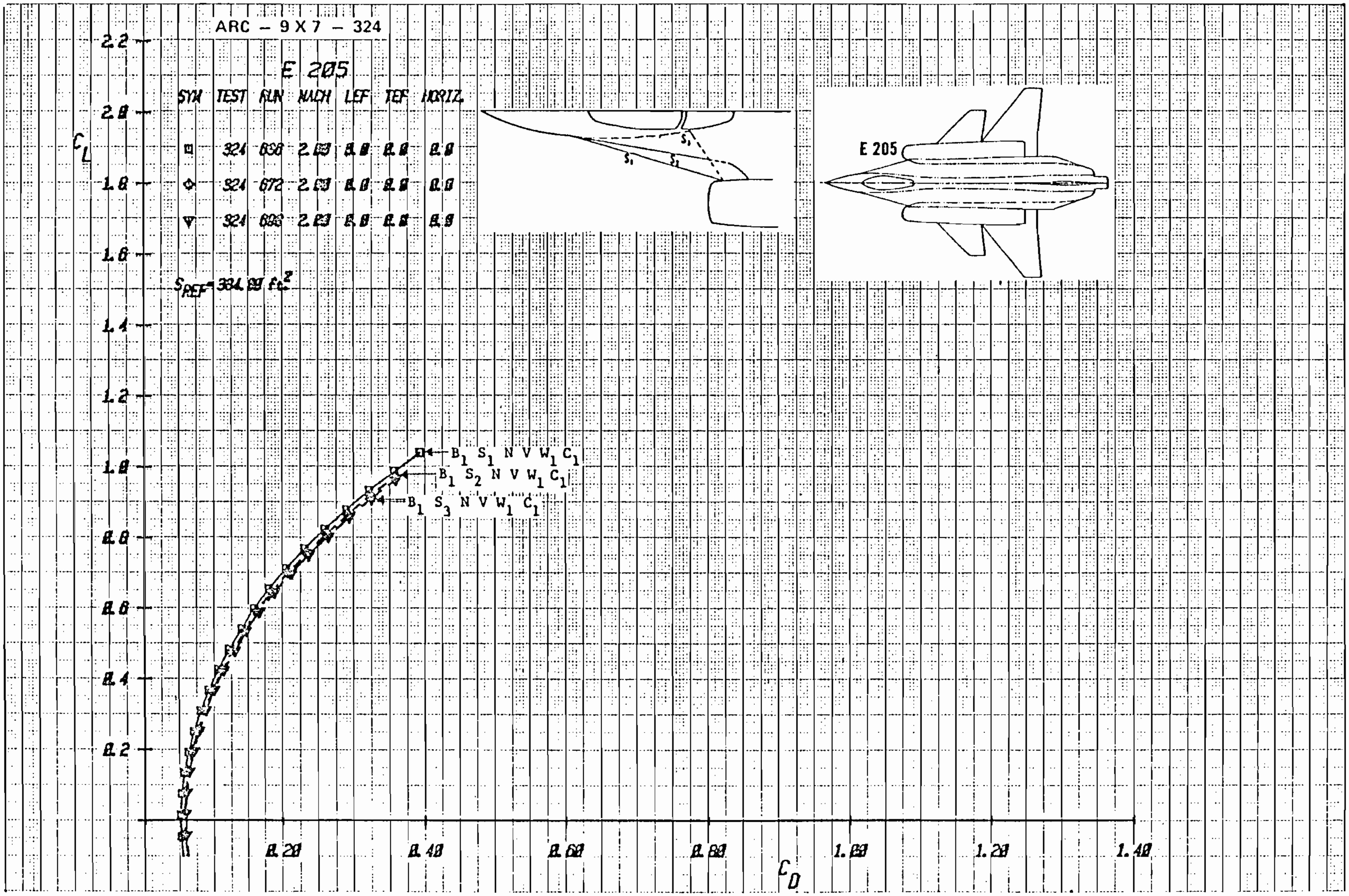

Figure3-63cEffect of Strake Variation on Drag with Baseline Canard Longitudinal Location, C_1, and δi = 0°, Mach = 2.0.

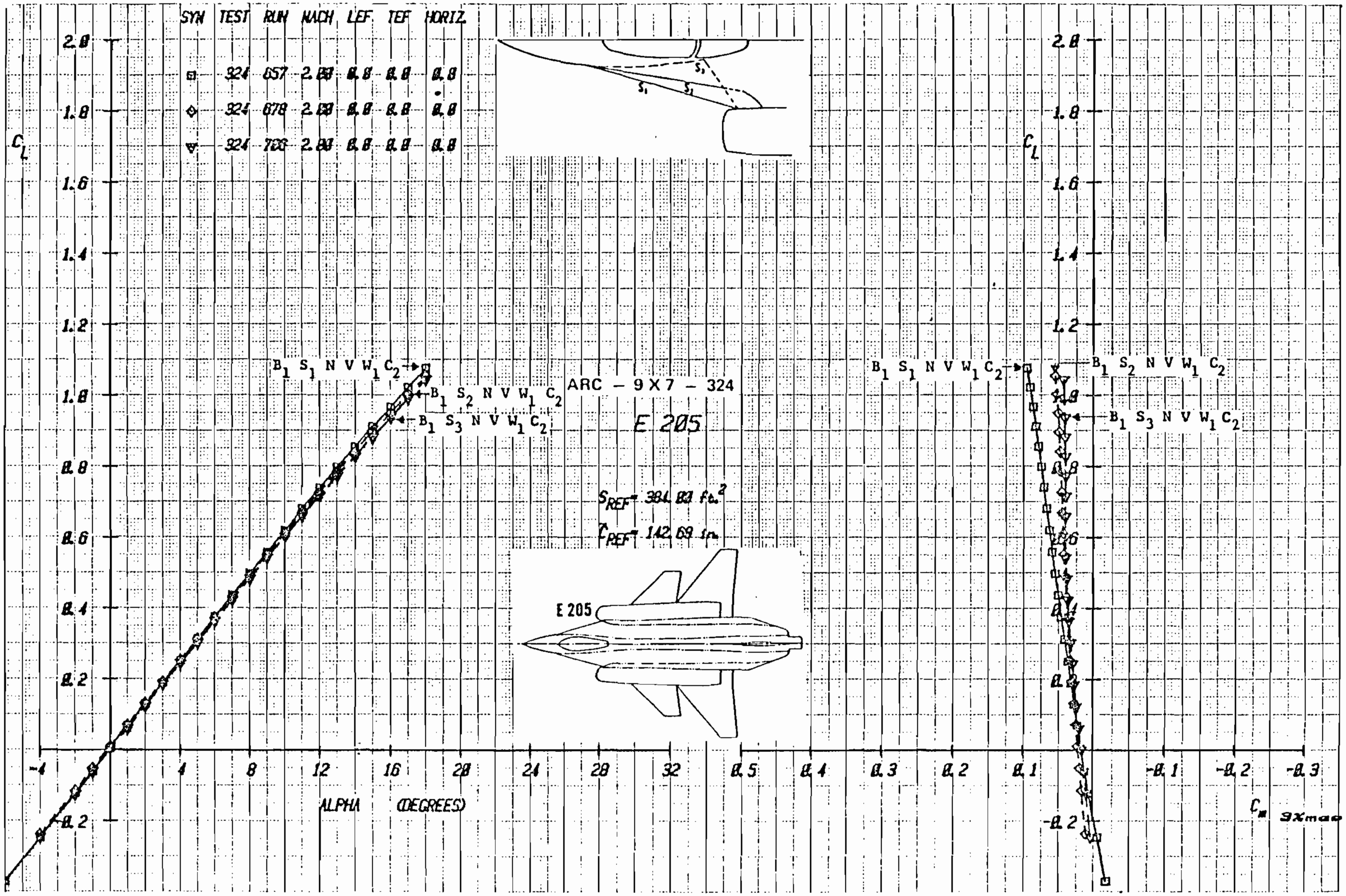

Figure3-64aEffect of Strake Variation on Lift and Moment with Forward Canard Longitudinal Location, C_2, and $\delta i = 0°$, Mach = 2.0

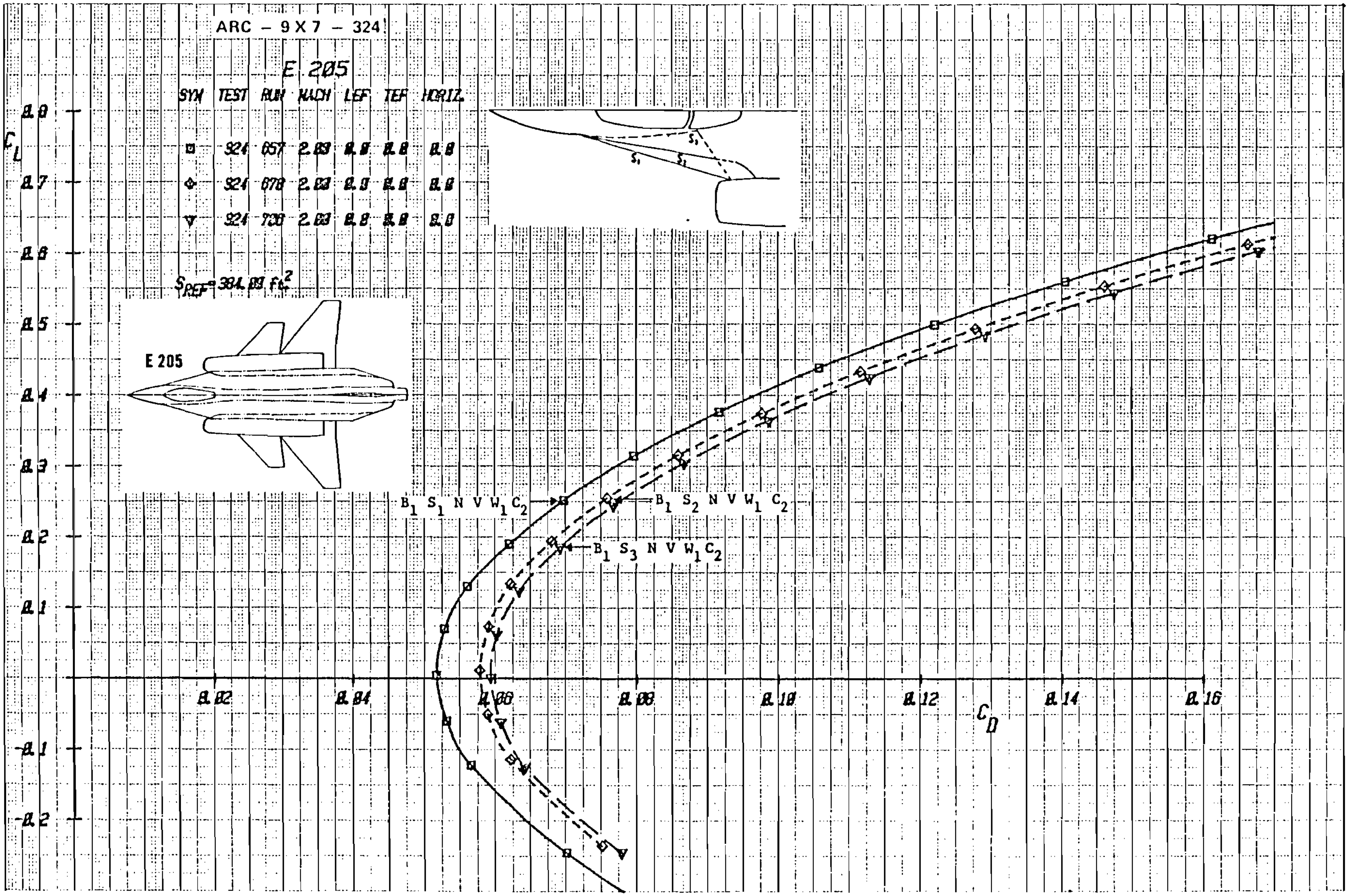

Figure3-64bEffect of Strake Variation on Drag with Forward Canard Longitudinal Location, C_2, and $\delta i = 0°$ (Expanded Drag Scale), Mach = 2.0

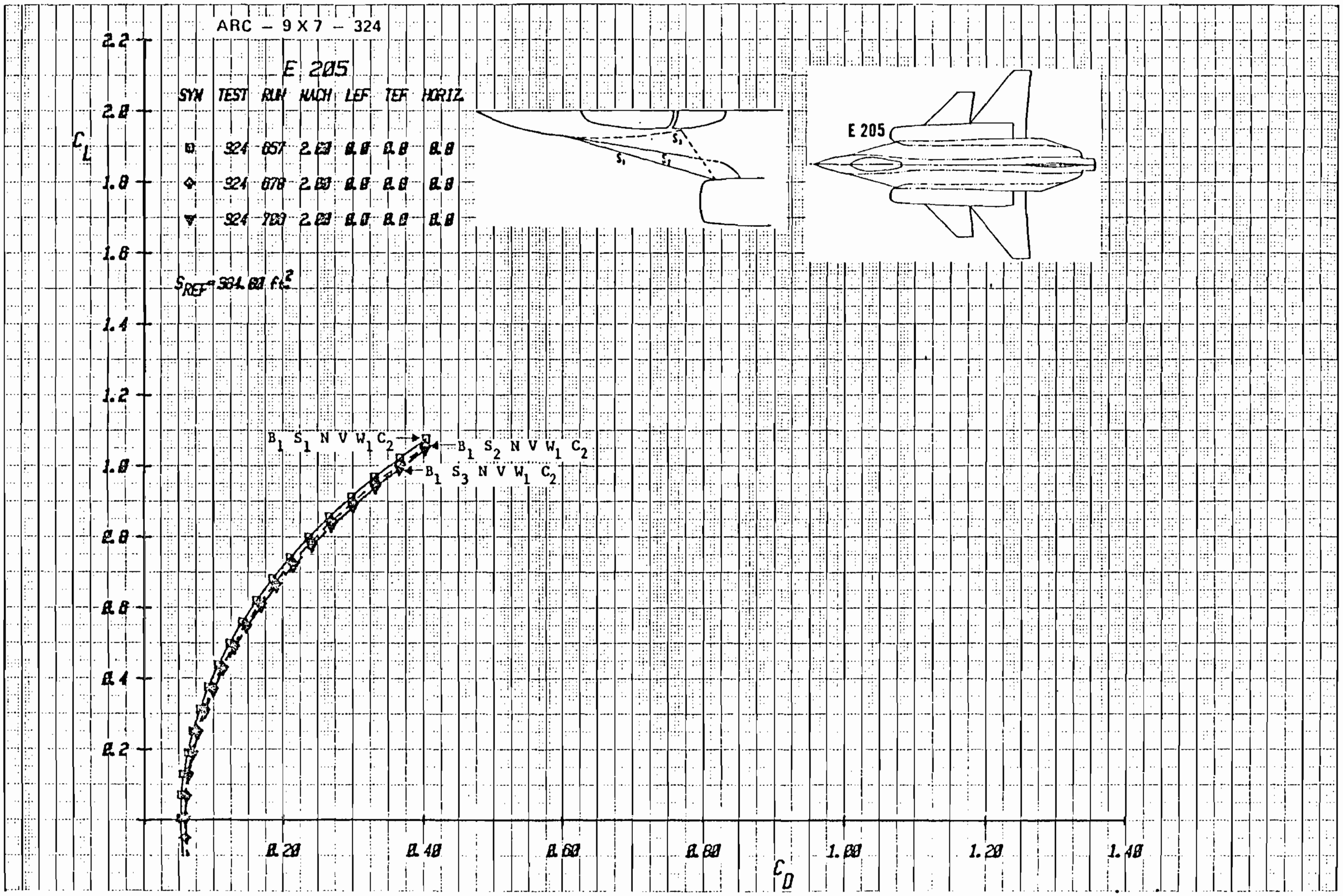

Figure3-64cEffect of Strake Variation on Drag with Forward Canard Longitudinal Location, C_2 and $\delta i = 0°$, Mach = 2.0

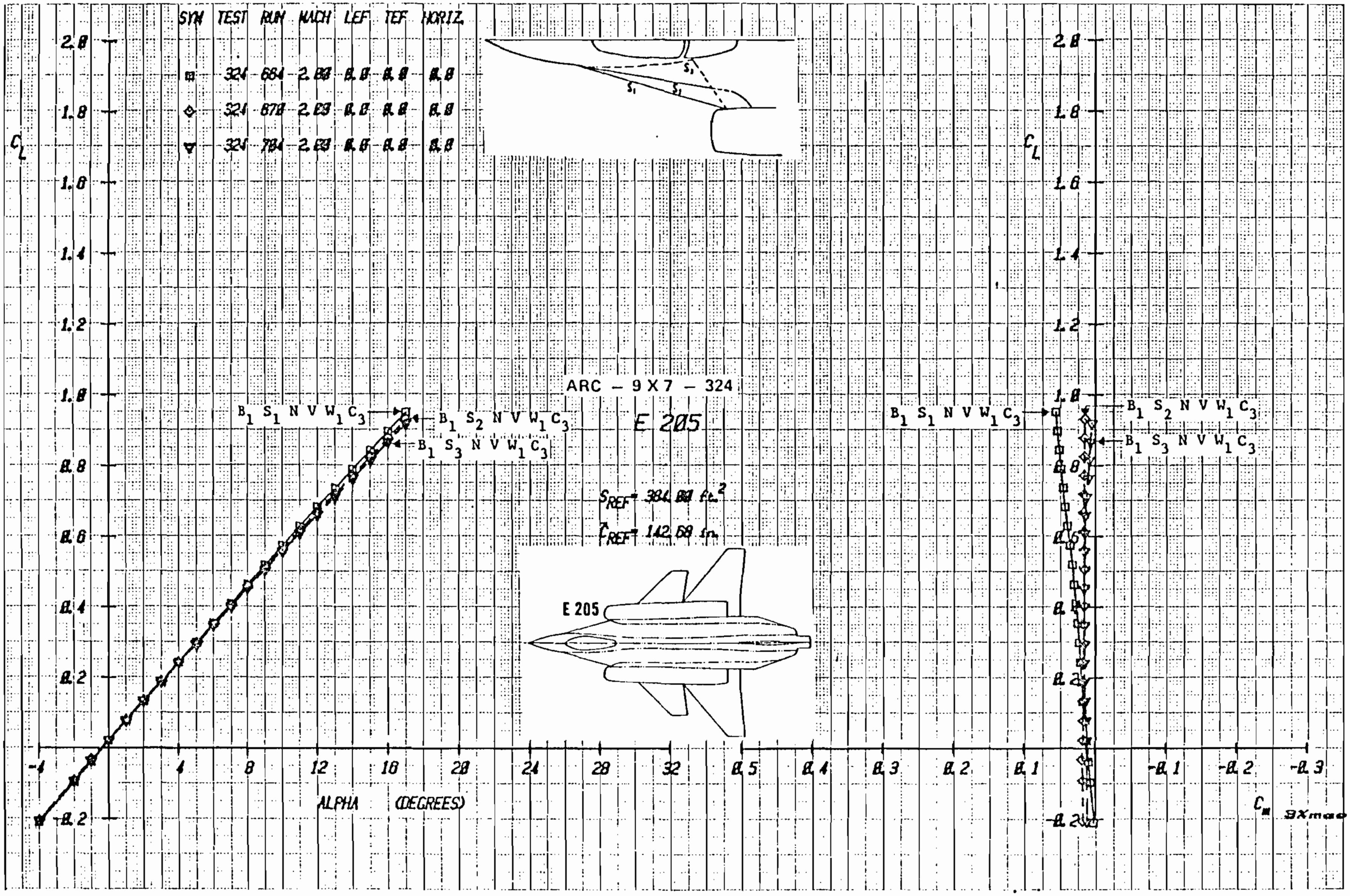

Figure3-65aEffect of Strake Variation on Lift and Moment with Aft Canard Longitudinal Location, C_3, and $\delta i = 0°$, Mach = 2.0

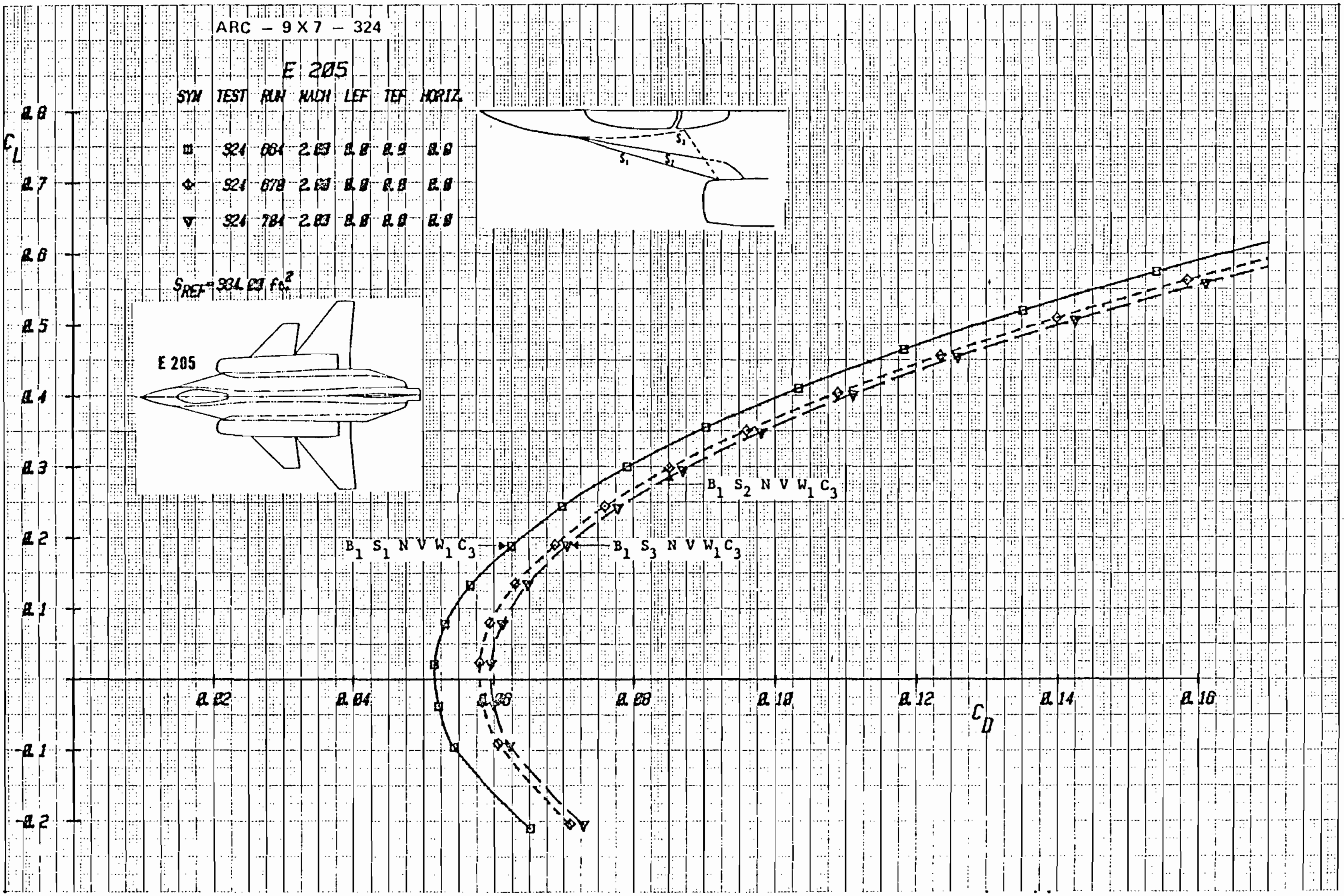

Figure3-65bEffect of Strake Variation on Drag with Aft Canard Longitudinal Location, C_3, and $\delta i = 0°$, (Expanded Drag Scale), Mach = 2.0

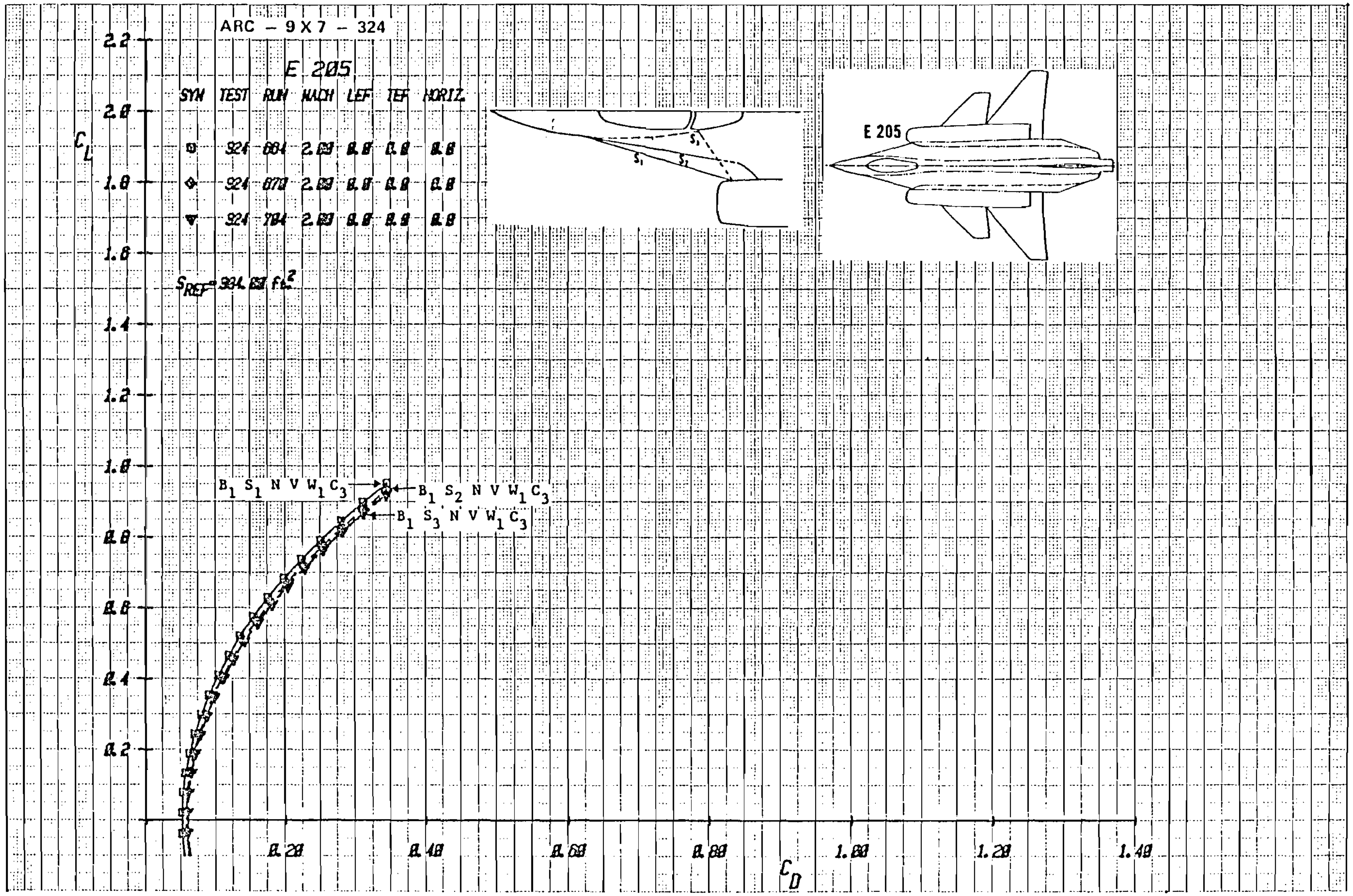

Figure3-65cEffect of Strake Variation on Drag with Aft Canard Longitudinal Location, C_3, and $\delta_i = 0°$, Mach = 2.0

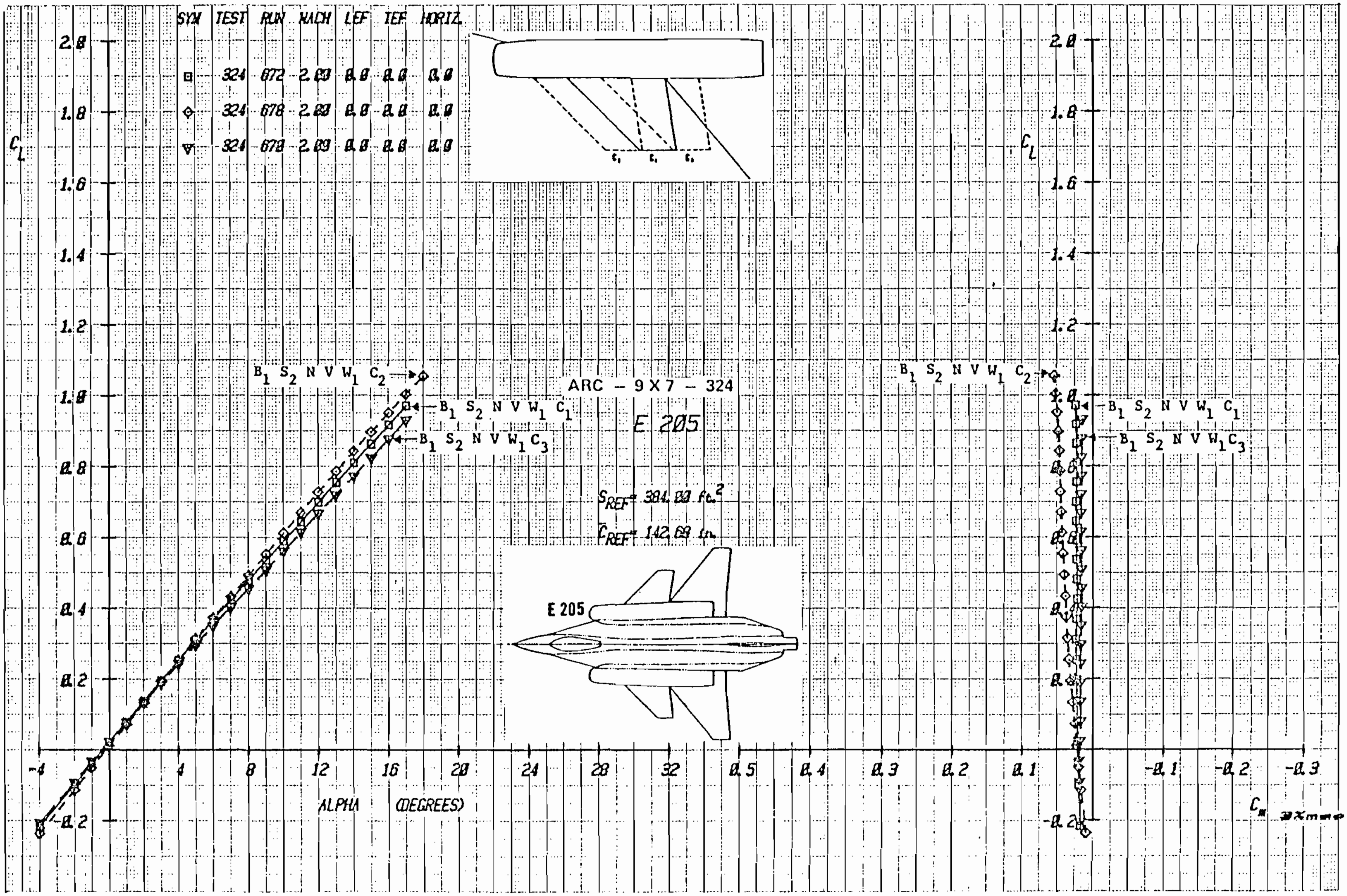

Figure3-66aEffect of Canard Longitudinal Location on Lift and Moment With Strake S_2, Mach = 2.0

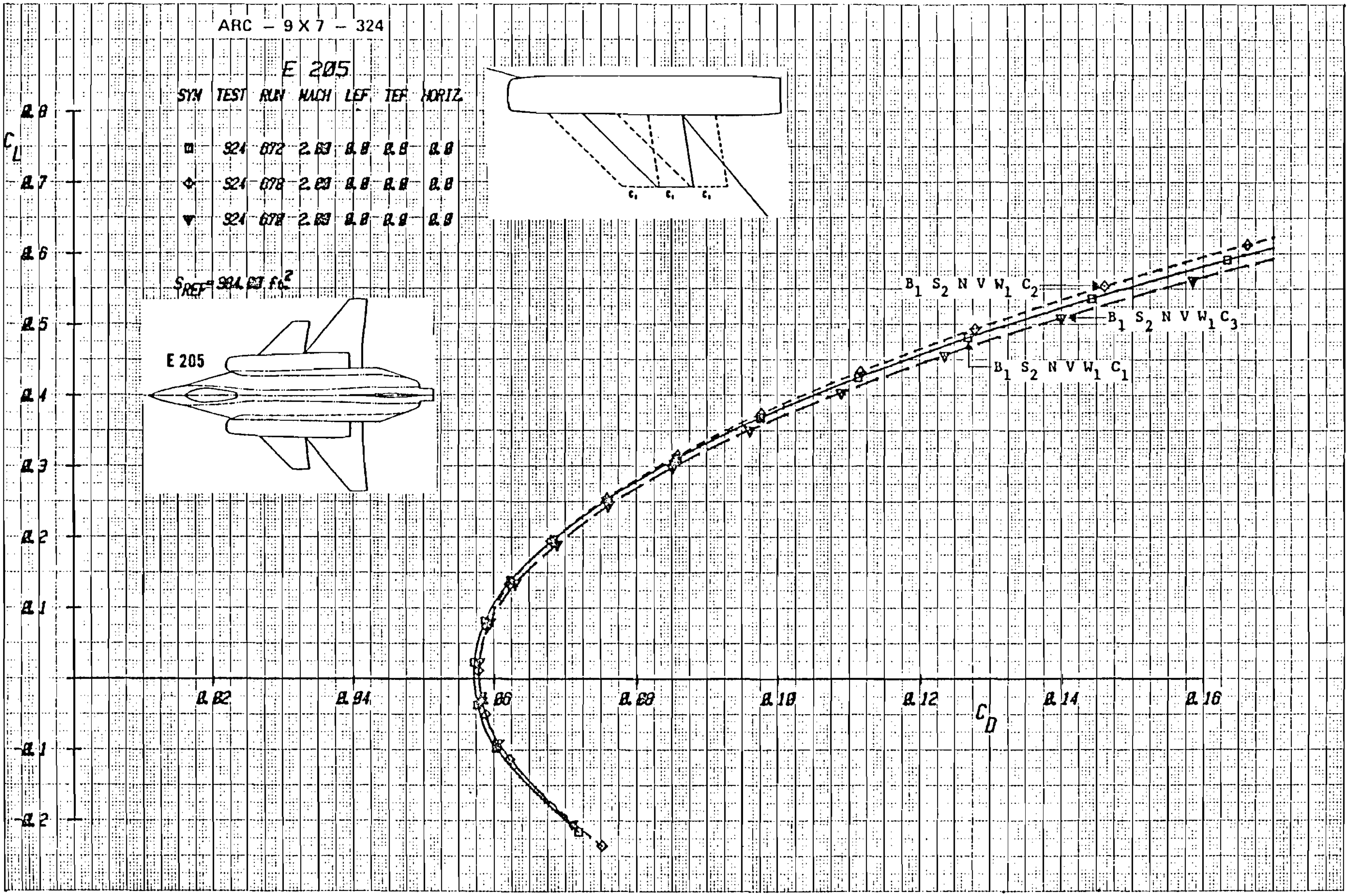

Figure3-66bEffect of Canard Longitudinal Location on Drag With Strake S_2, (Expanded Drag Scale), Mach = 2.0

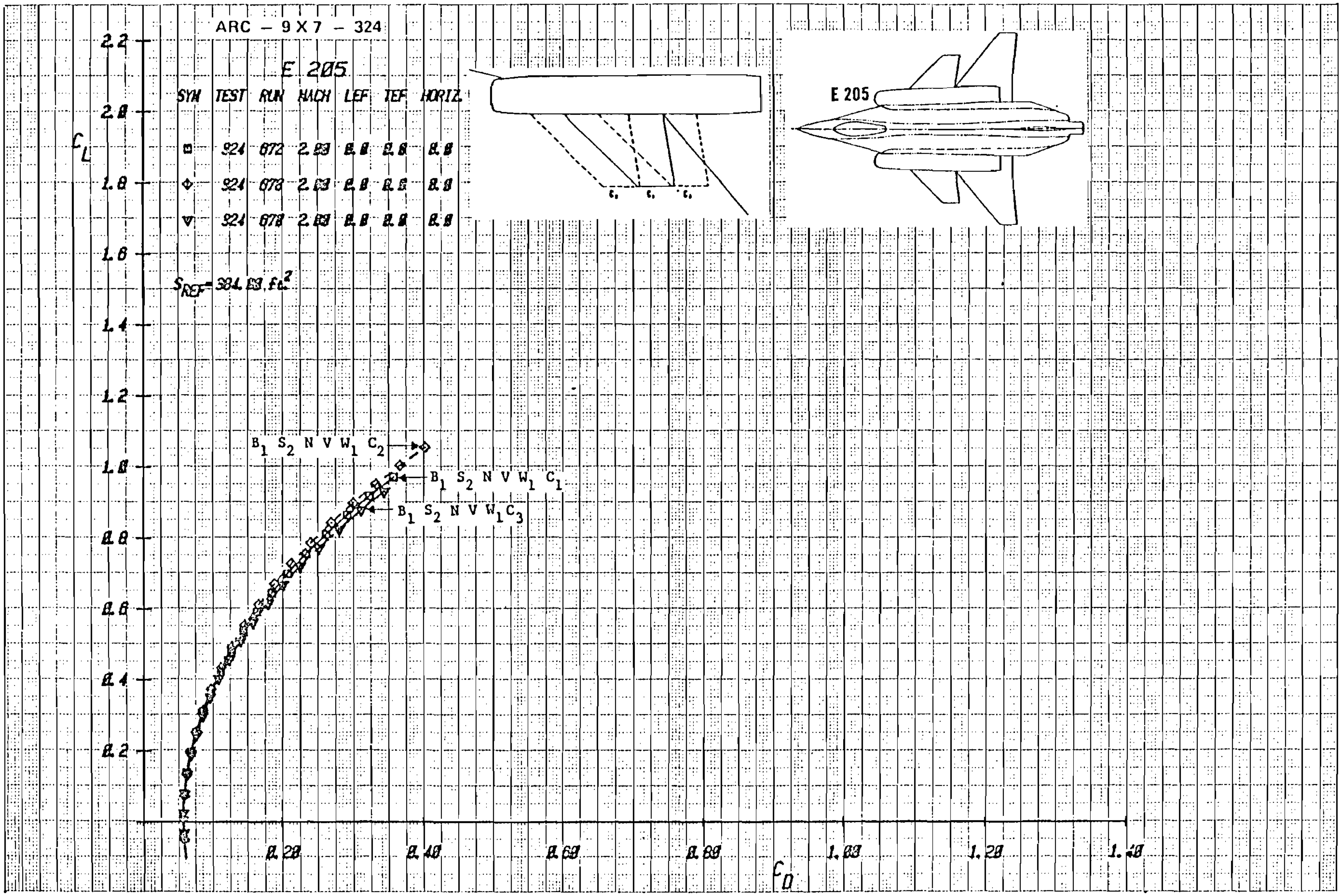

Figure3-66cEffect of Canard Longitudinal Location on Drag With Strake S_2, Mach = 2.0

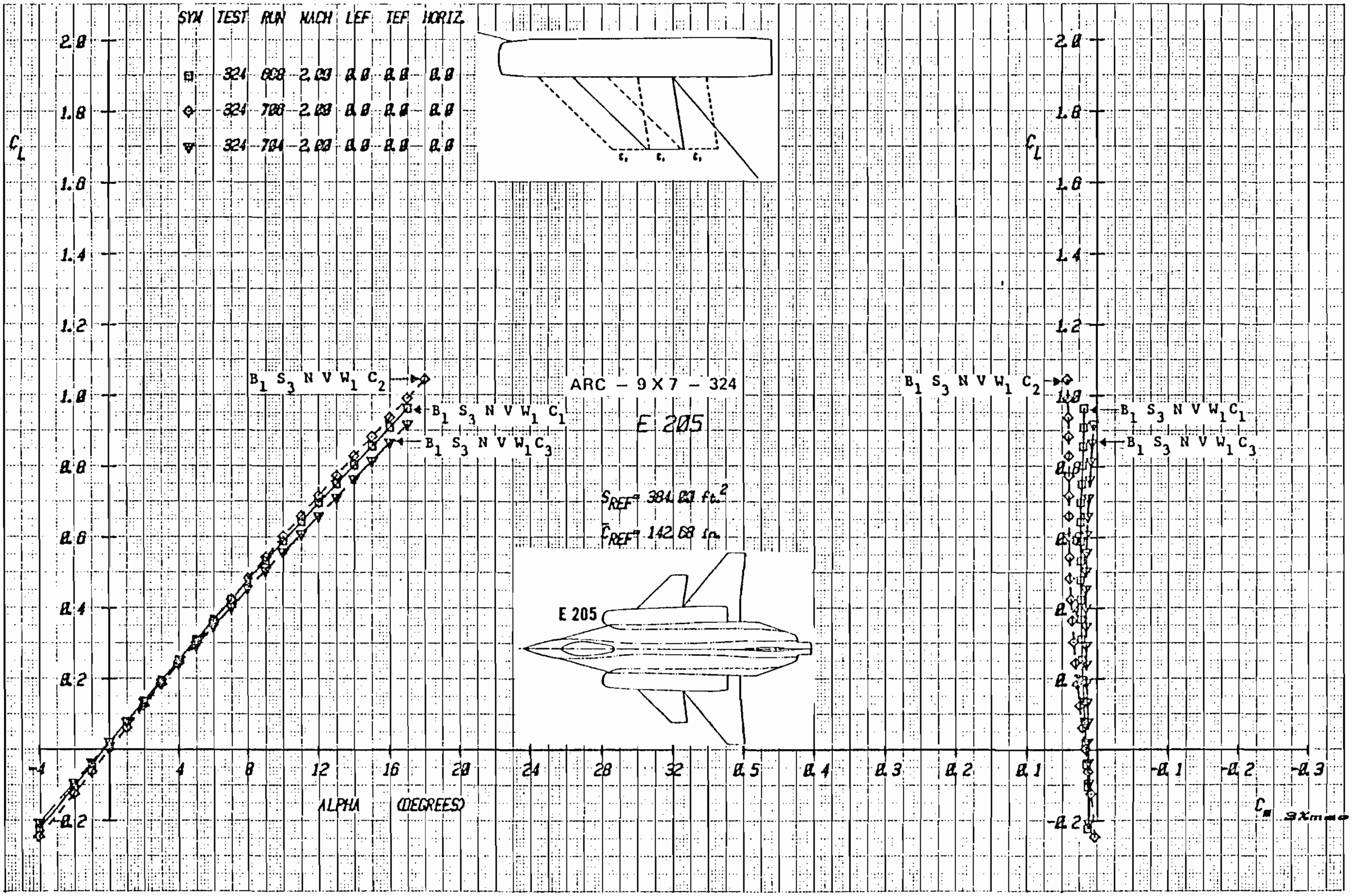

Figure3-67aEffect of Canard Longitudinal Location on Lift and Moment with Strake S_3 , Mach = 2.0

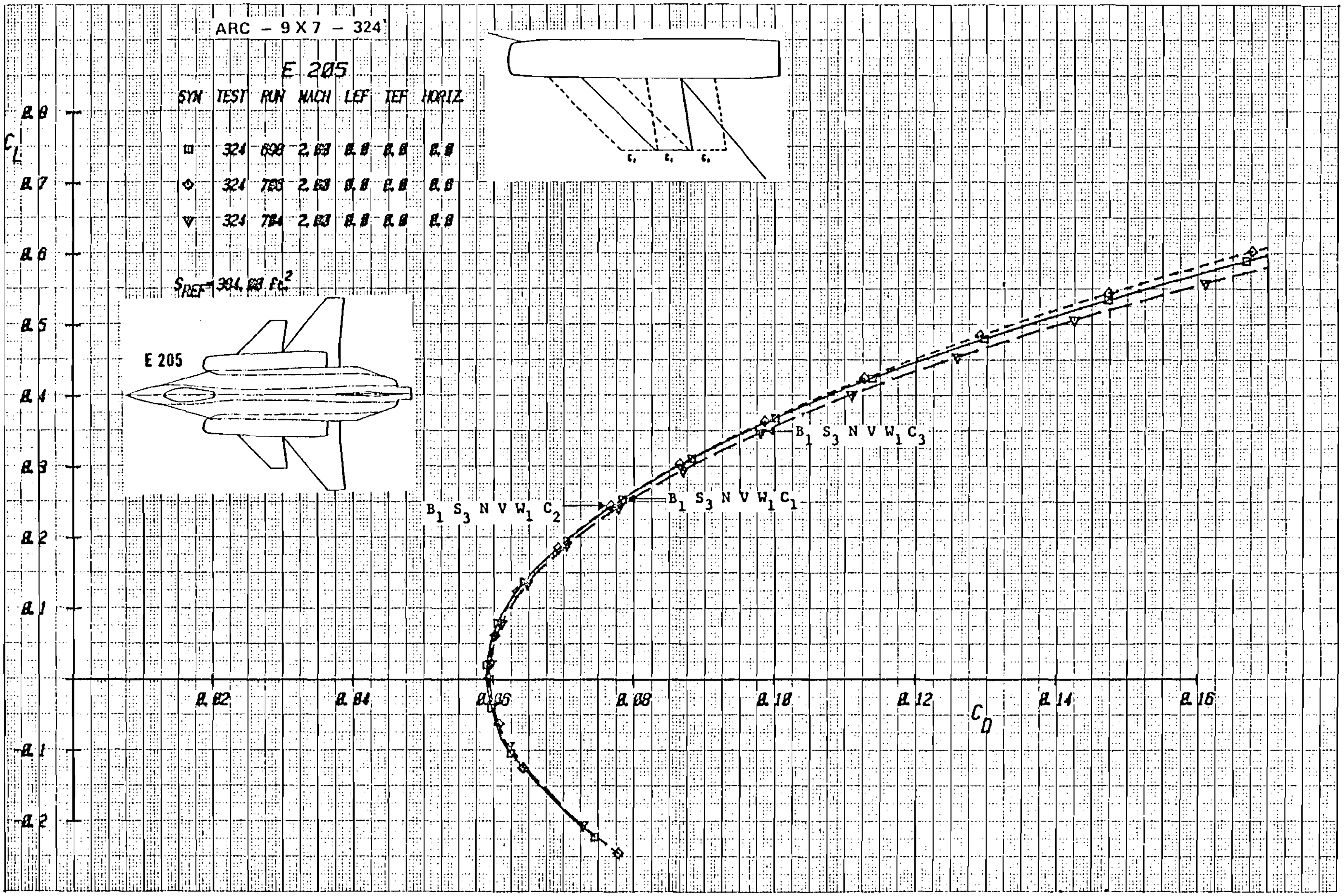

Figure3-67bEffect of Canard Longitudinal Location on Drag with Strake S_3, (Expanded Drag Scale), Mach = 2.0

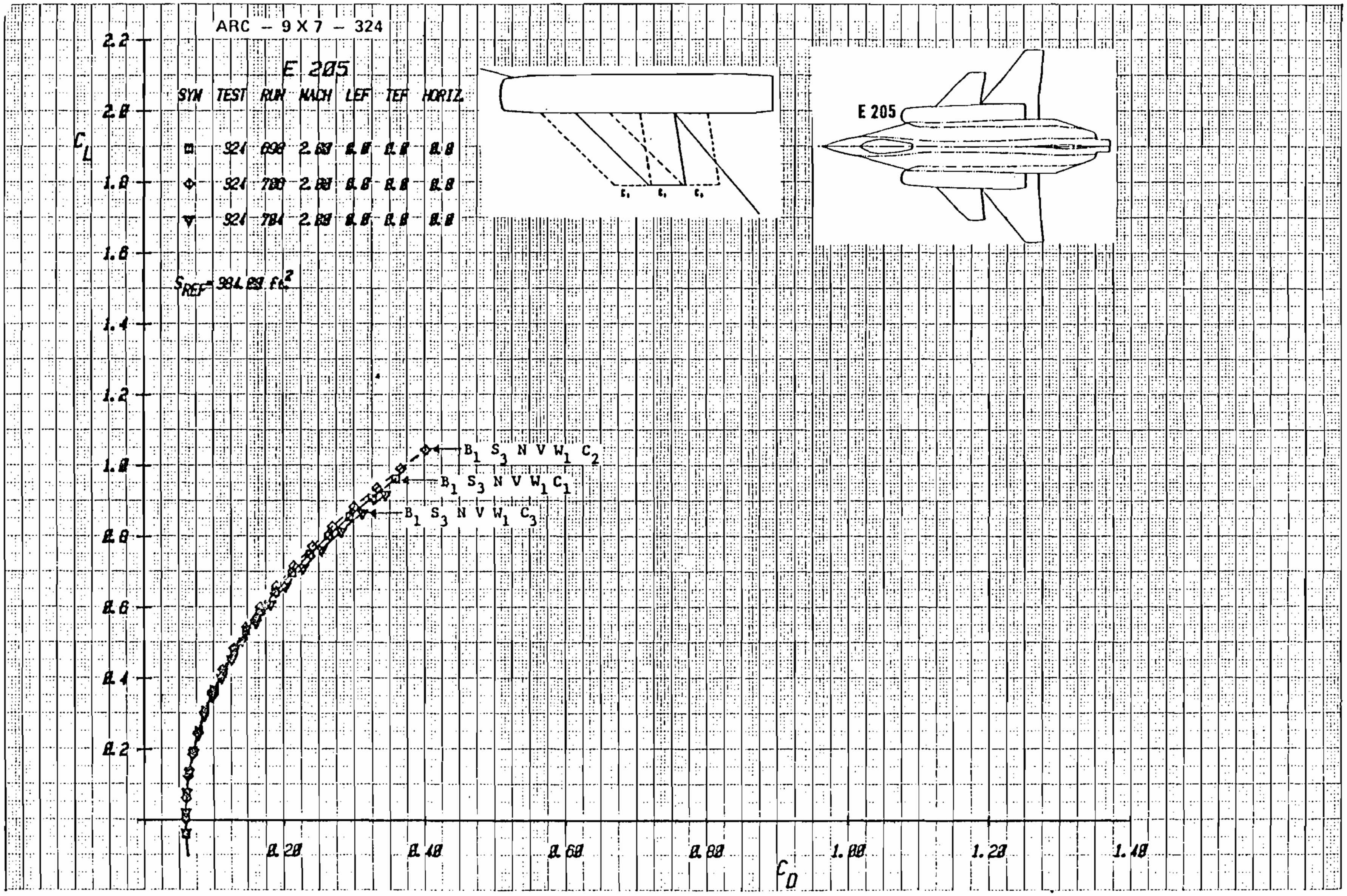

Figure3-67cEffect of Canard Longitudinal Location on Drag with Strake S_3, Mach = 2.0

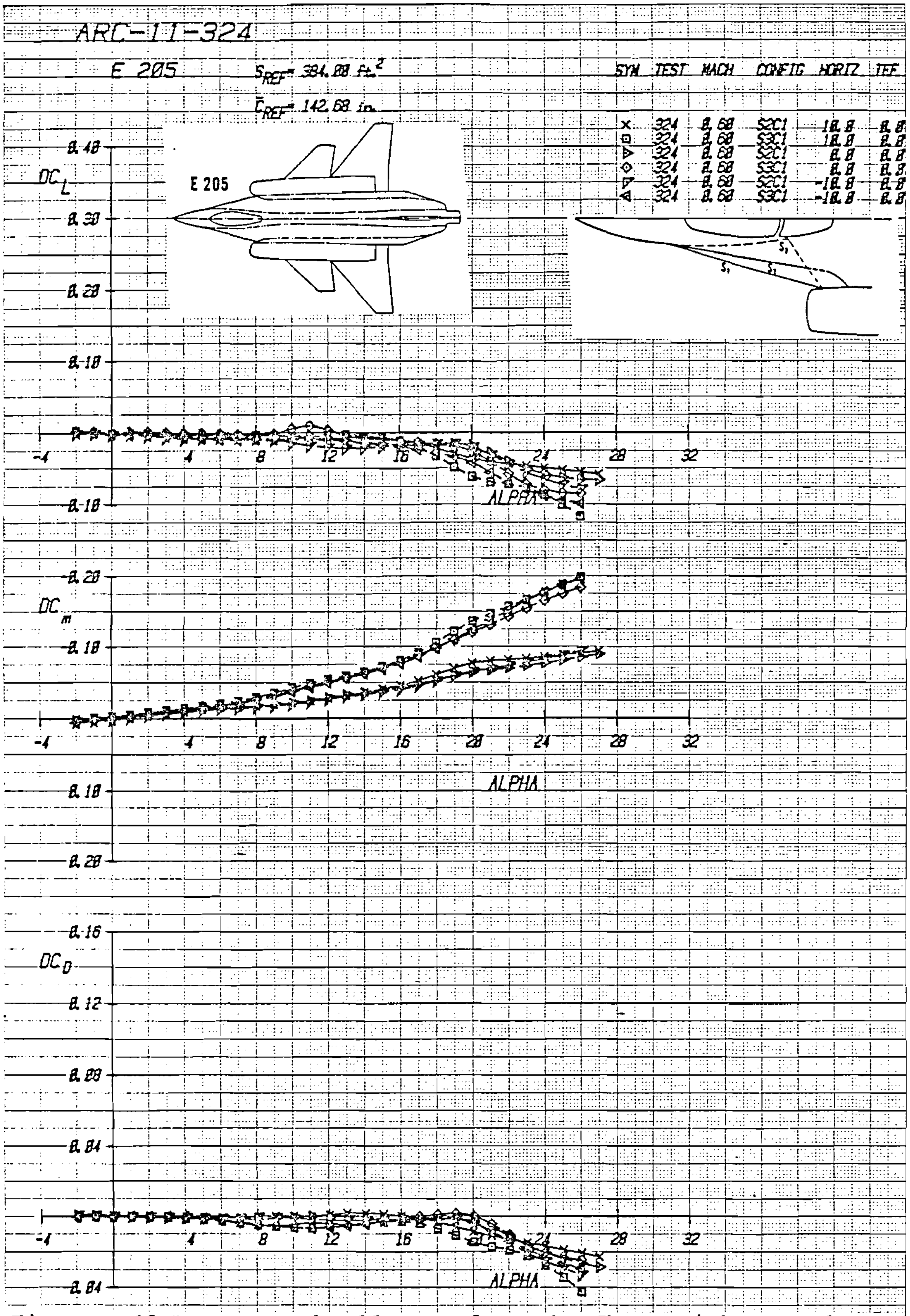

Figure 3-68 Incremental Effects of Strake Shape with Canard C_1 at Various Deflections, Mach = .6

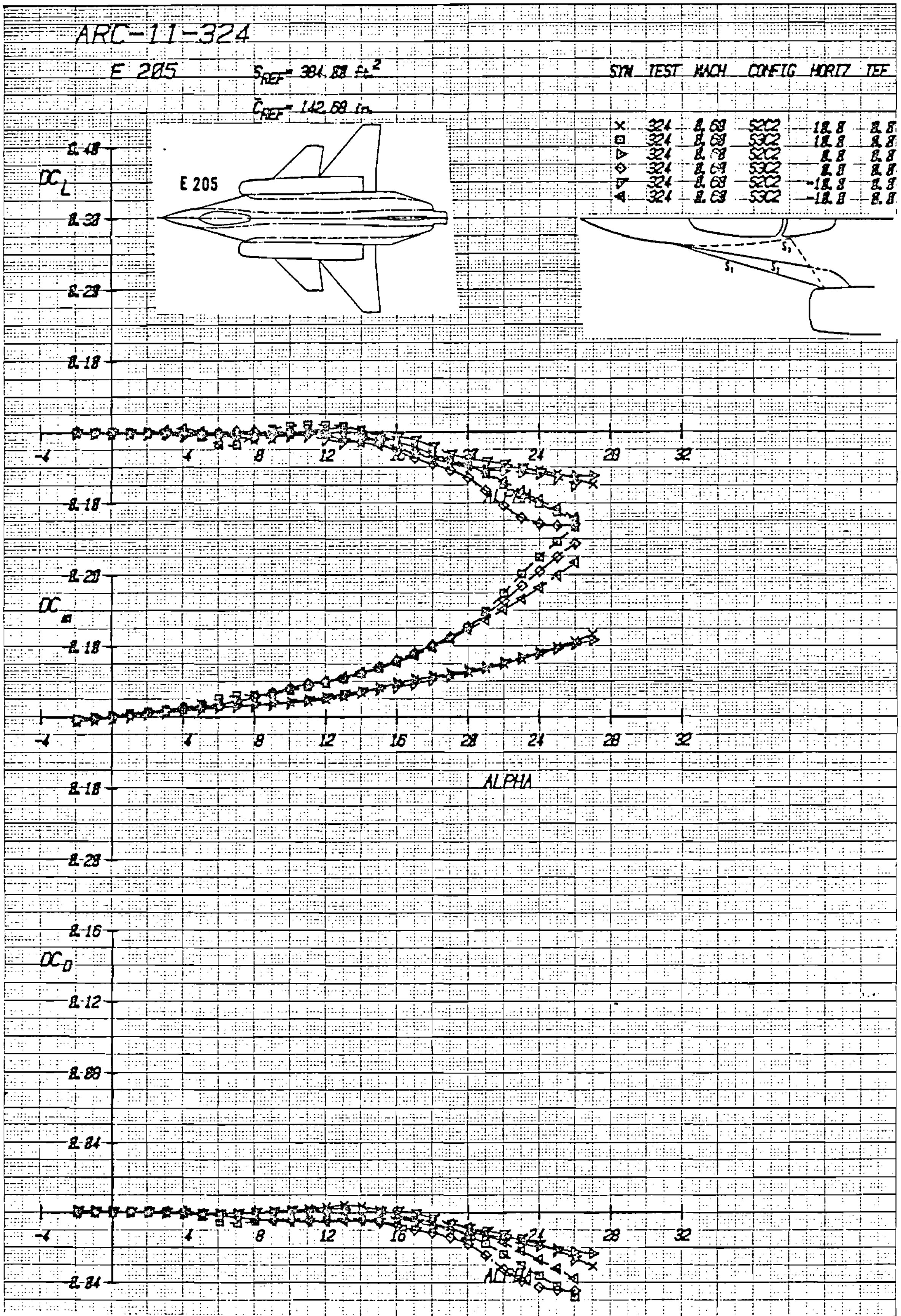

Figure 3-69 Incremental Effects of Strake Shape with Canard C_2 at Various Deflections, Mach = .6

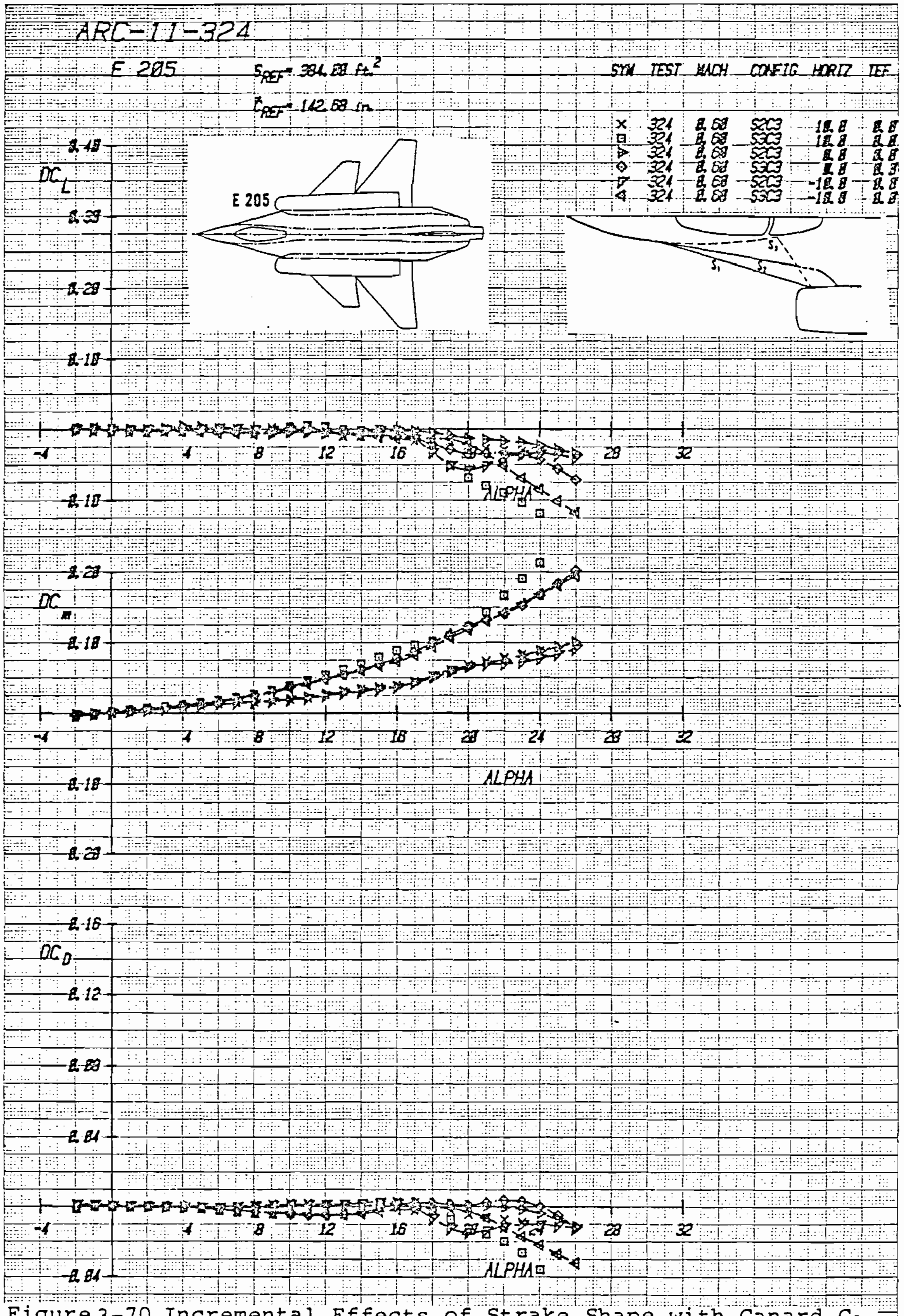

Figure 3-70 Incremental Effects of Strake Shape with Canard C_3 at Various Deflections, Mach = .6

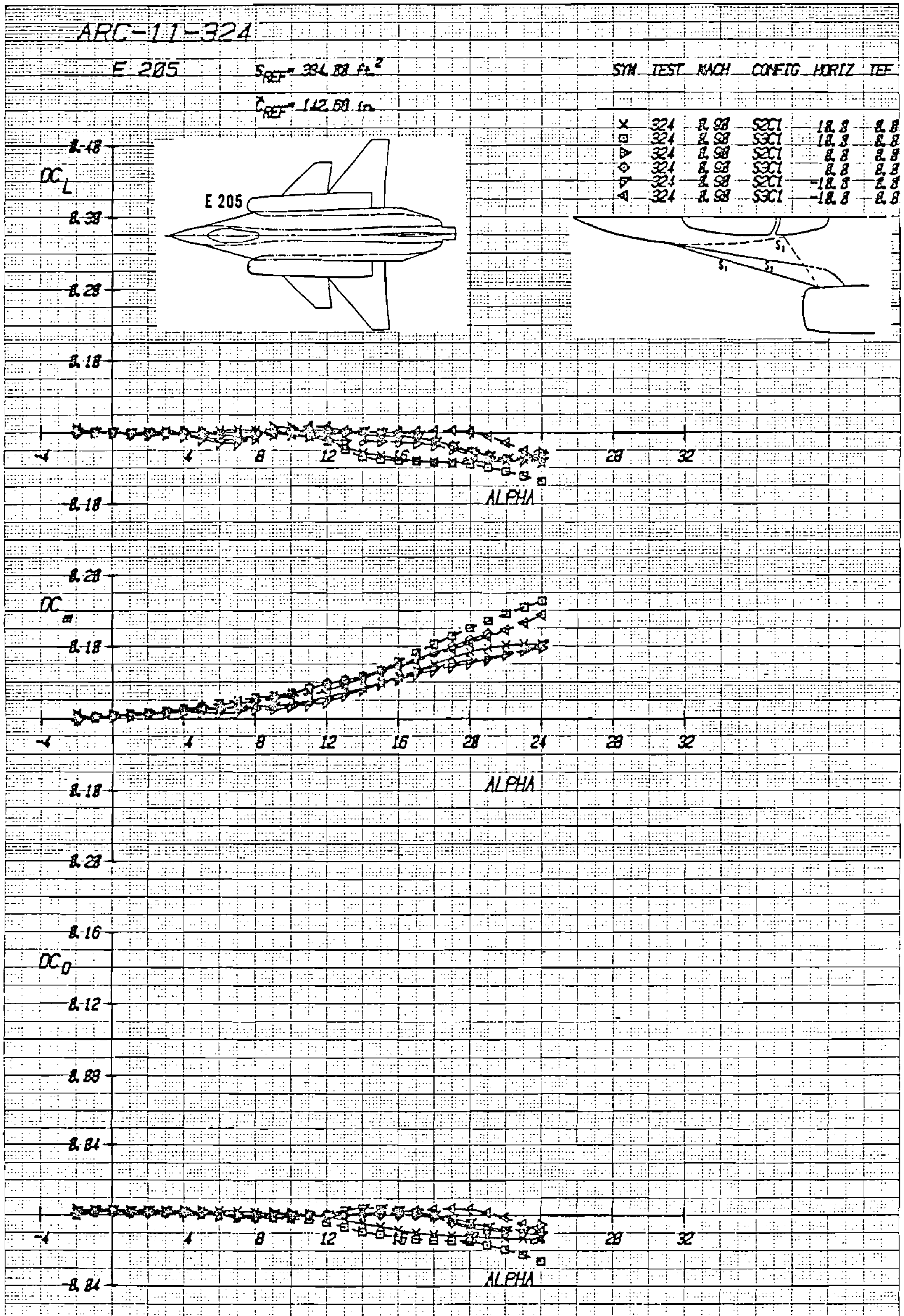

Figure 3-71 Incremental Effects of Strake Shape with Canard C_1 at Various Deflections, Mach = .9

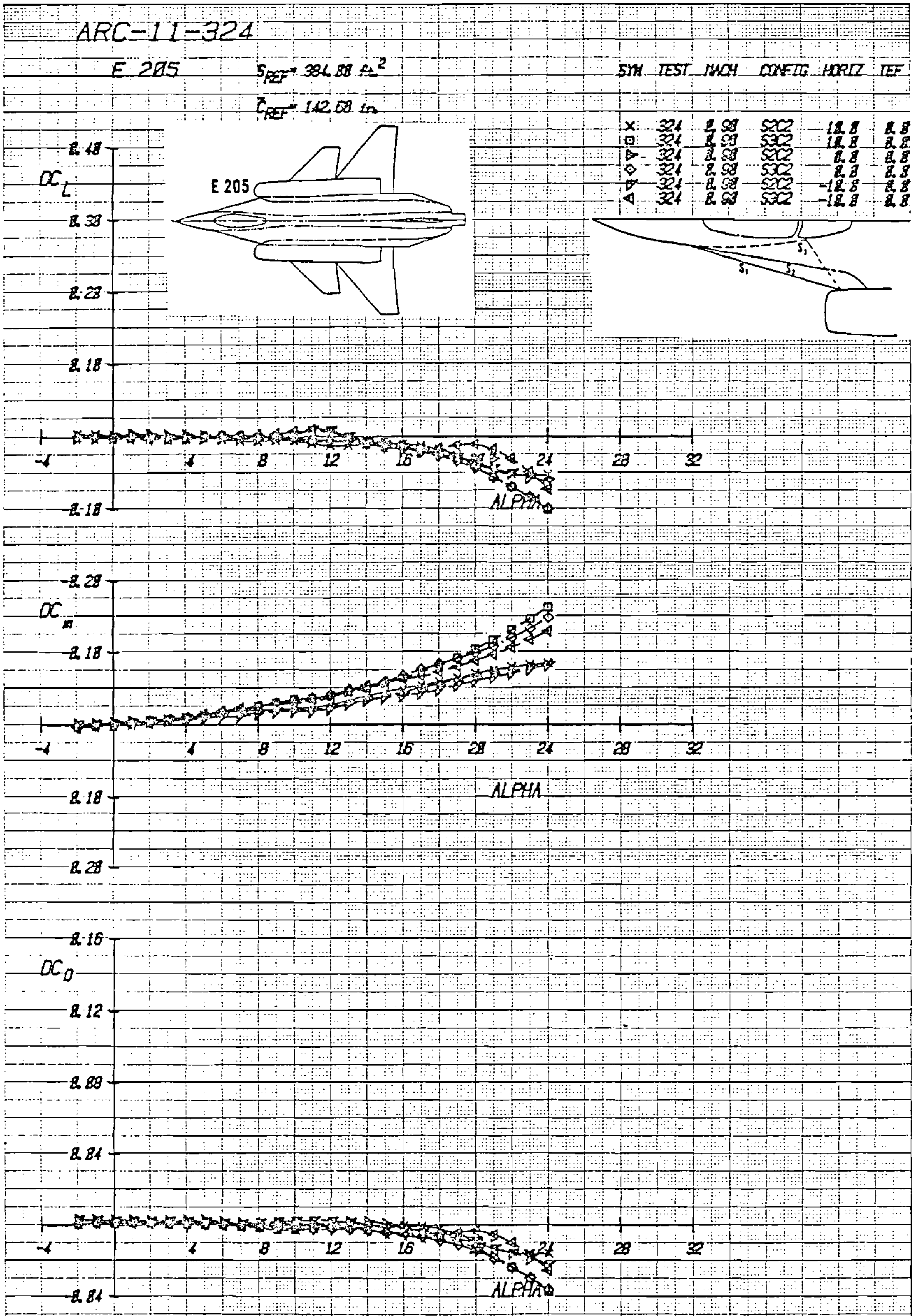

Figure 3-72 Incremental Effects of Strake Shape with Canard C_2 at Various Deflections, Mach = .9

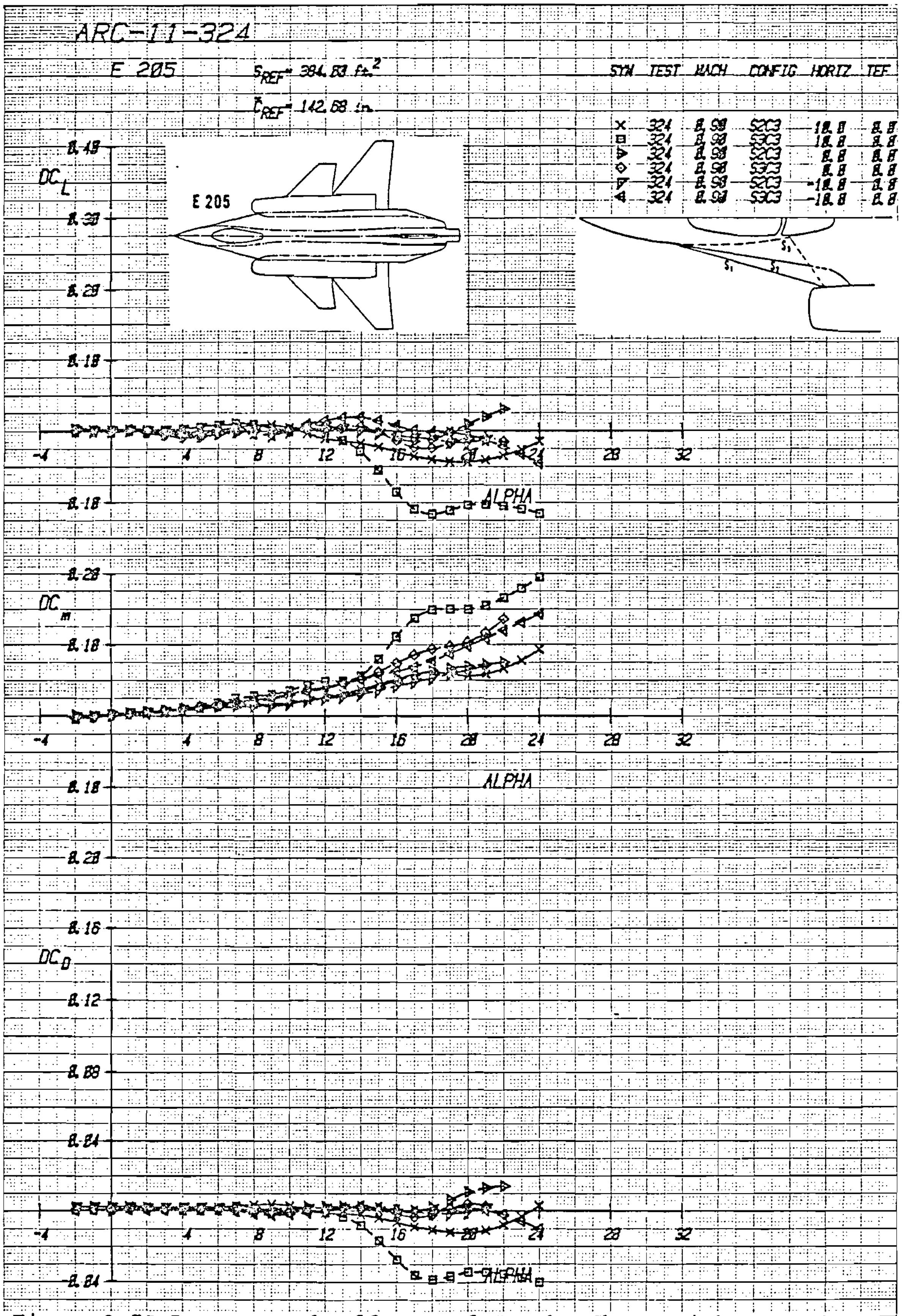

Figure 3-73 Incremental Effects of Strake Shape with Canard C_3 at Various Deflections, Mach = .9

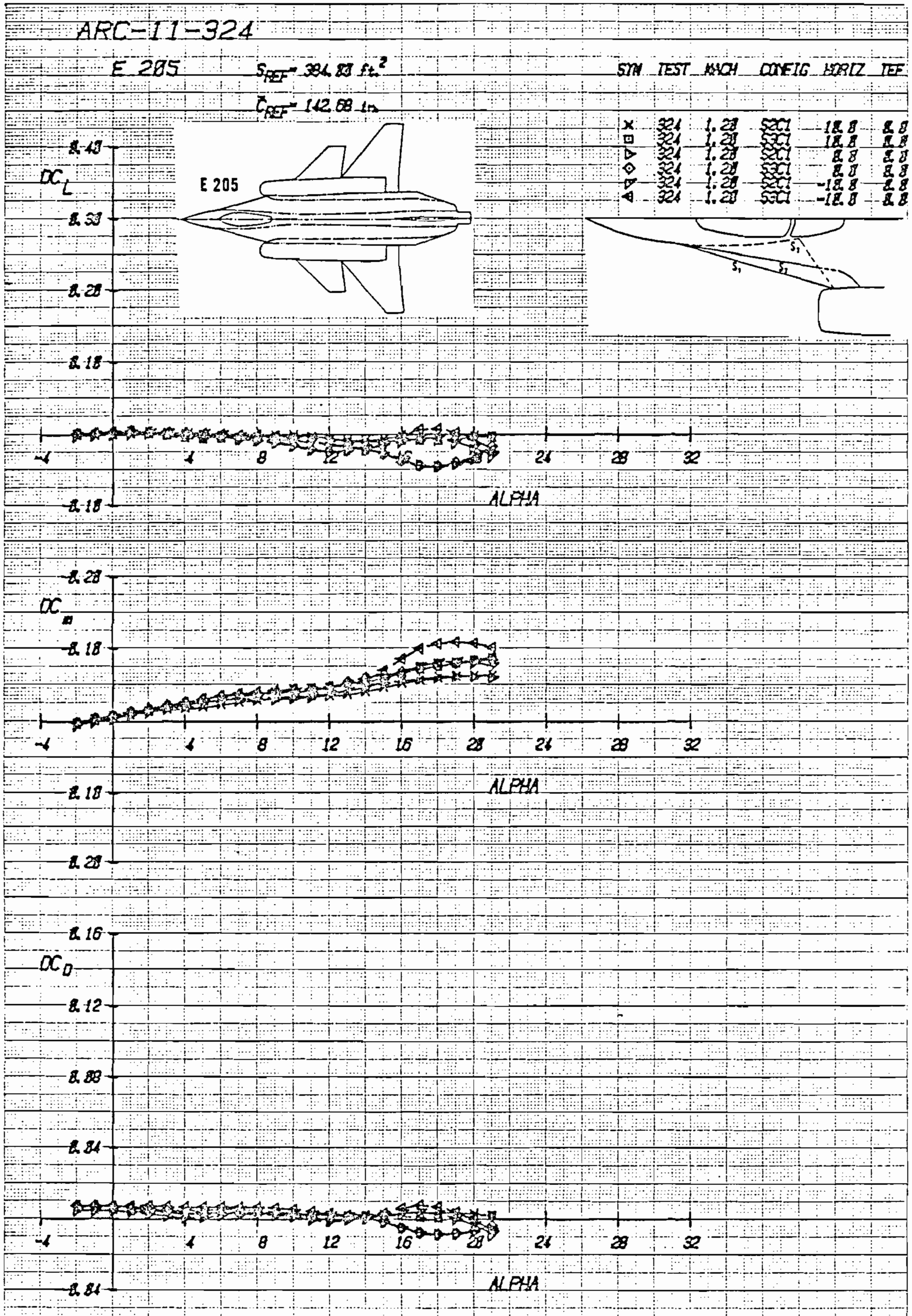

Figure 3-74 Incremental Effects of Strake Shape with Canard C_1 at Various Deflections, Mach = 1.2

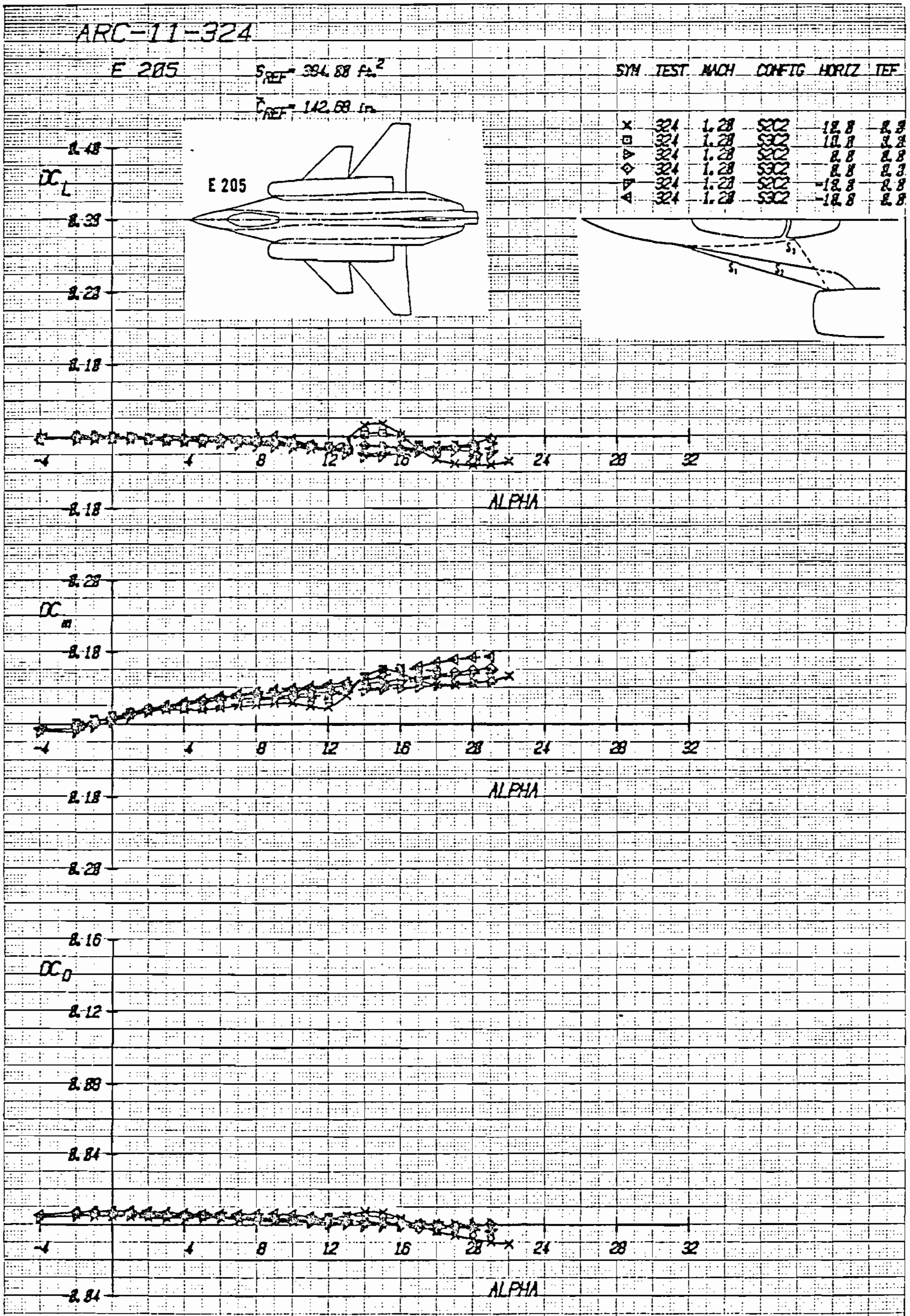

Figure 3-75 Incremental Effects of Strake Shape with Canard C_2 at Various Deflections, Mach = 1.2

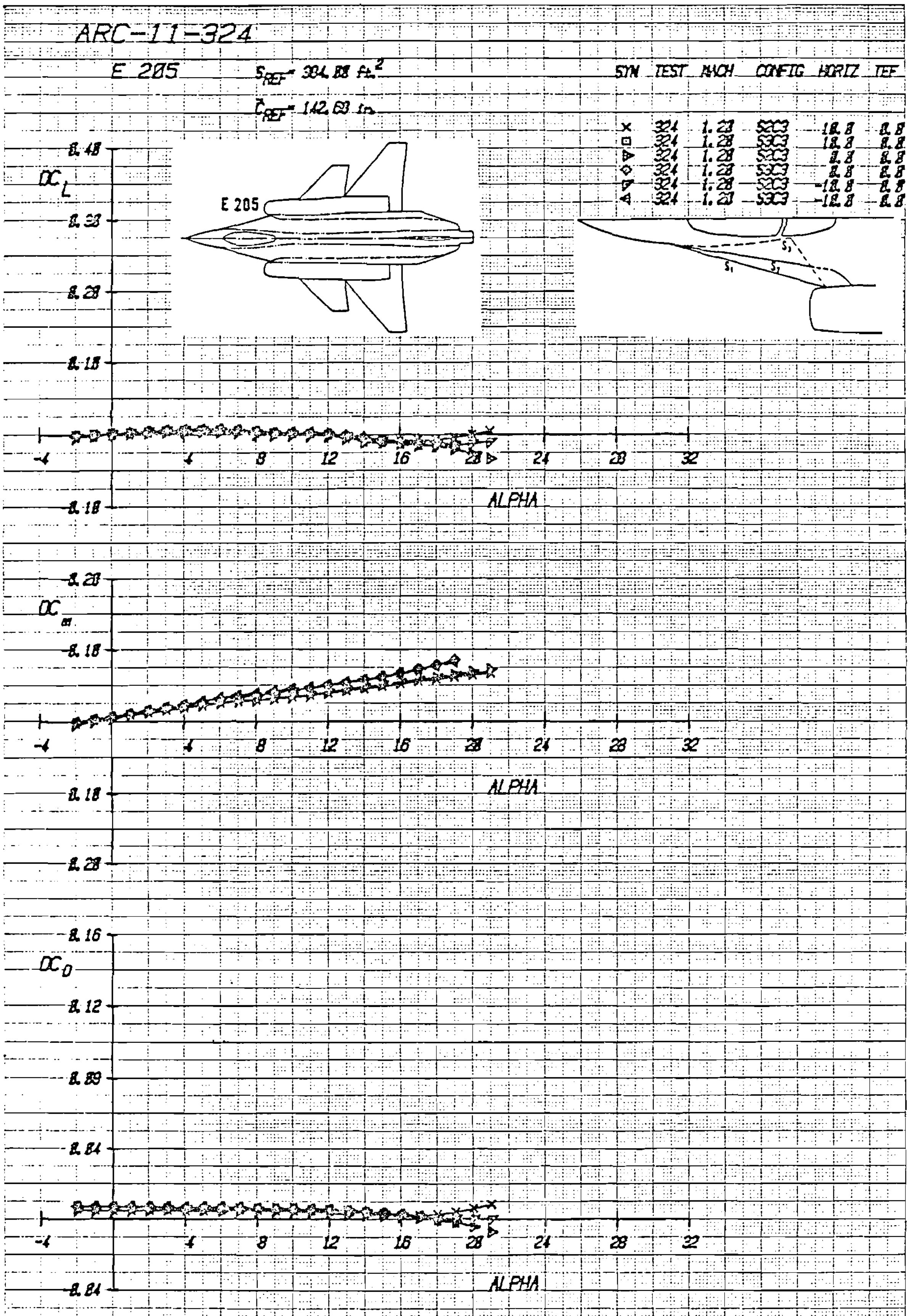

Figure 3-76 Incremental Effects of Strake Shape with Canard C_3 at Various Deflections, Mach = 1.2

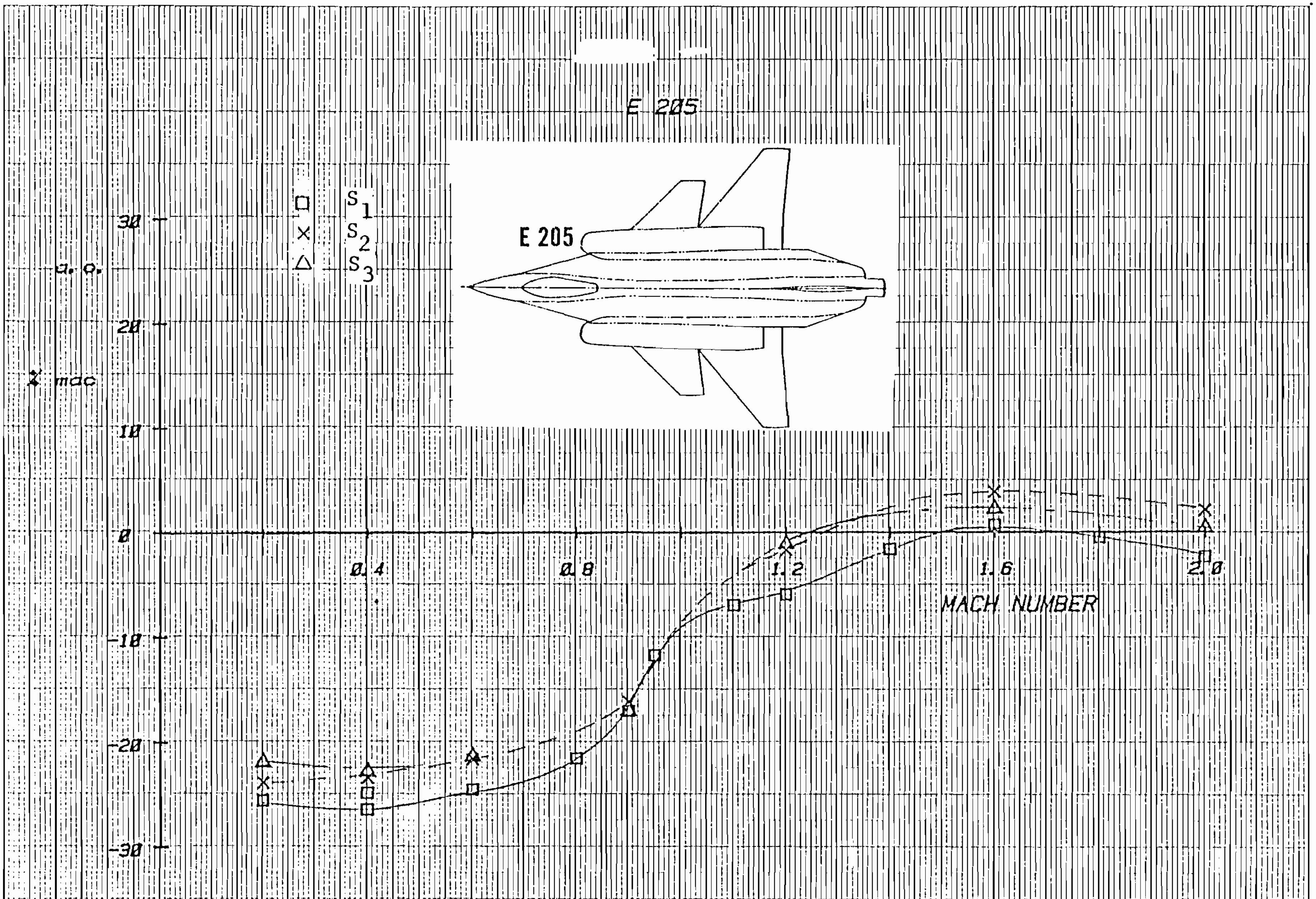

Figure 3-77 Effect of Strake Shape on Aerodynamic Center Variation with Mach Number
(with Baseline Canard Location)

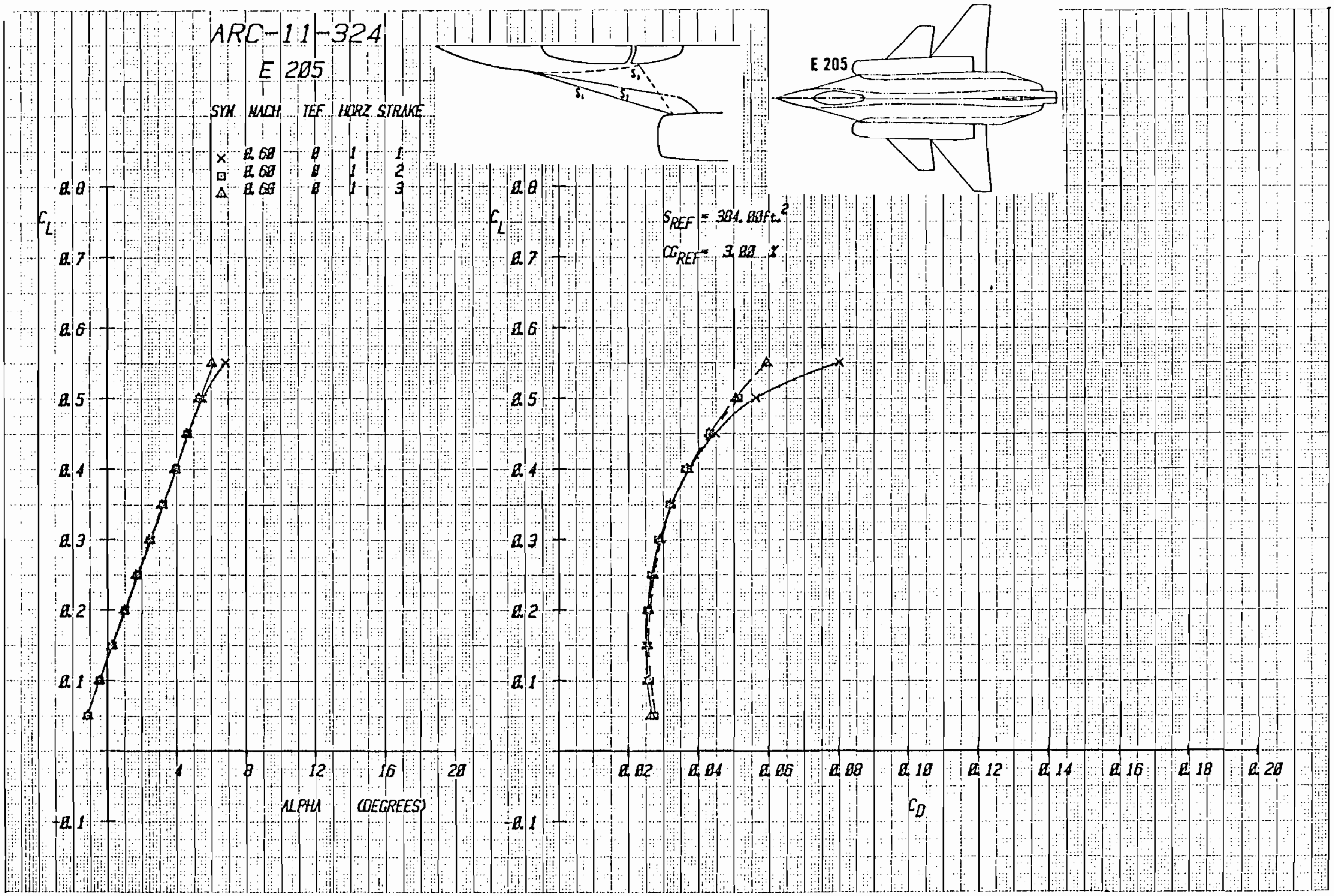

Figure 3-78 Trimmed Lift and Drag With Variations in Strake and Canard C_l, Mach = .6

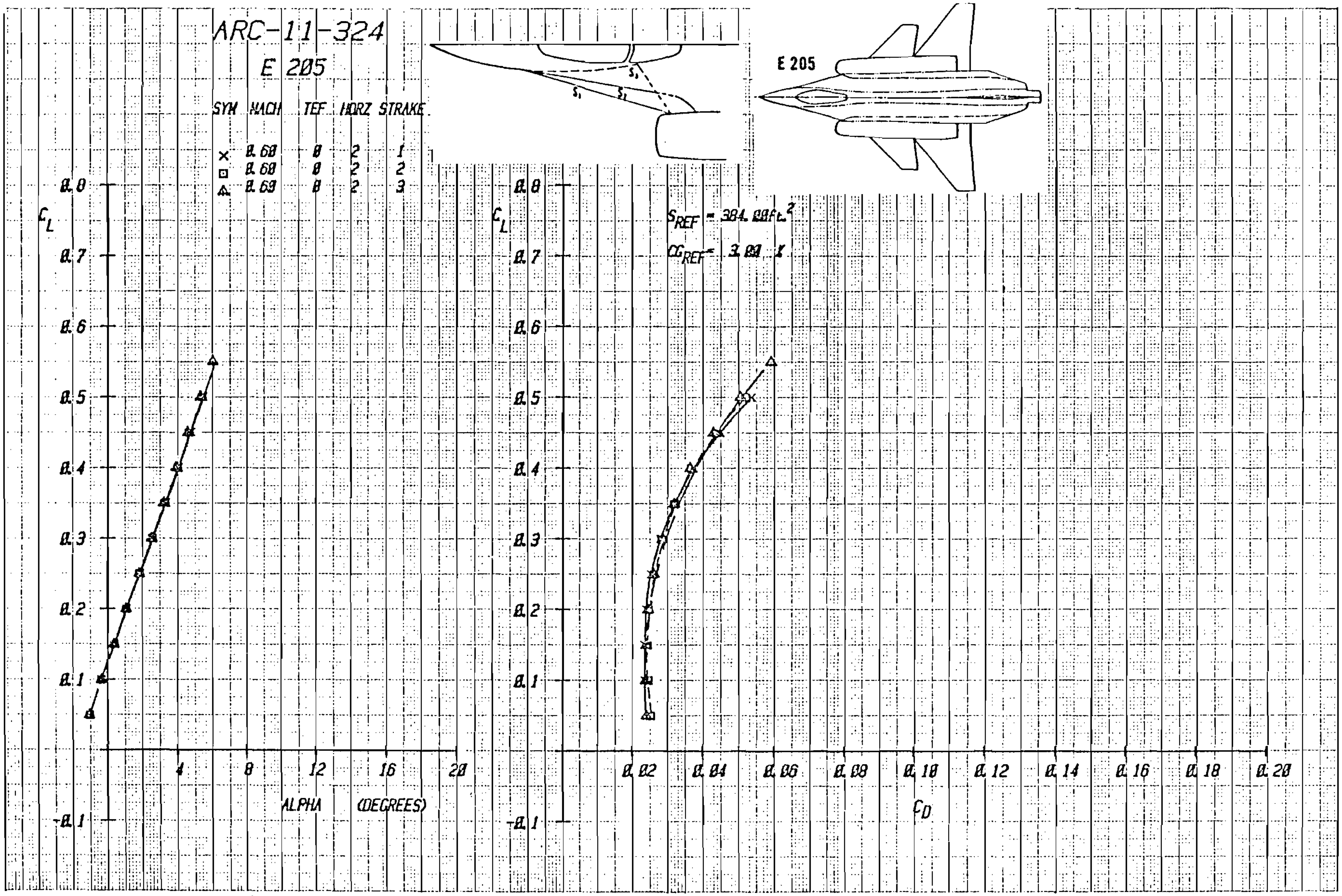

Figure 3-79 Trimmed Lift and Drag With Variations in Strake and Canard C_2, Mach = .6

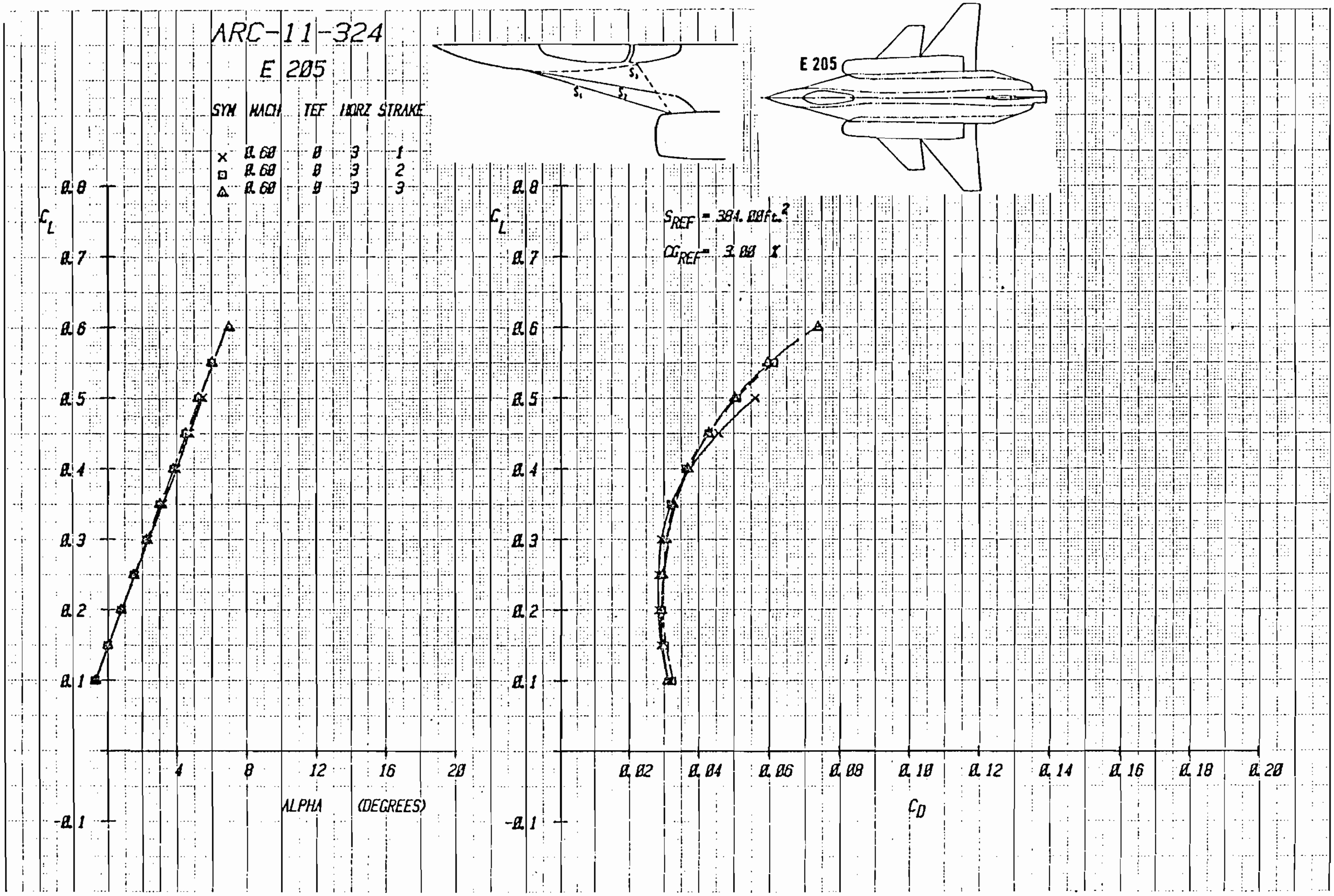

Figure 3-80 Trimmed Lift and Drag With Variations in Strake and Canard C_3, Mach = .6

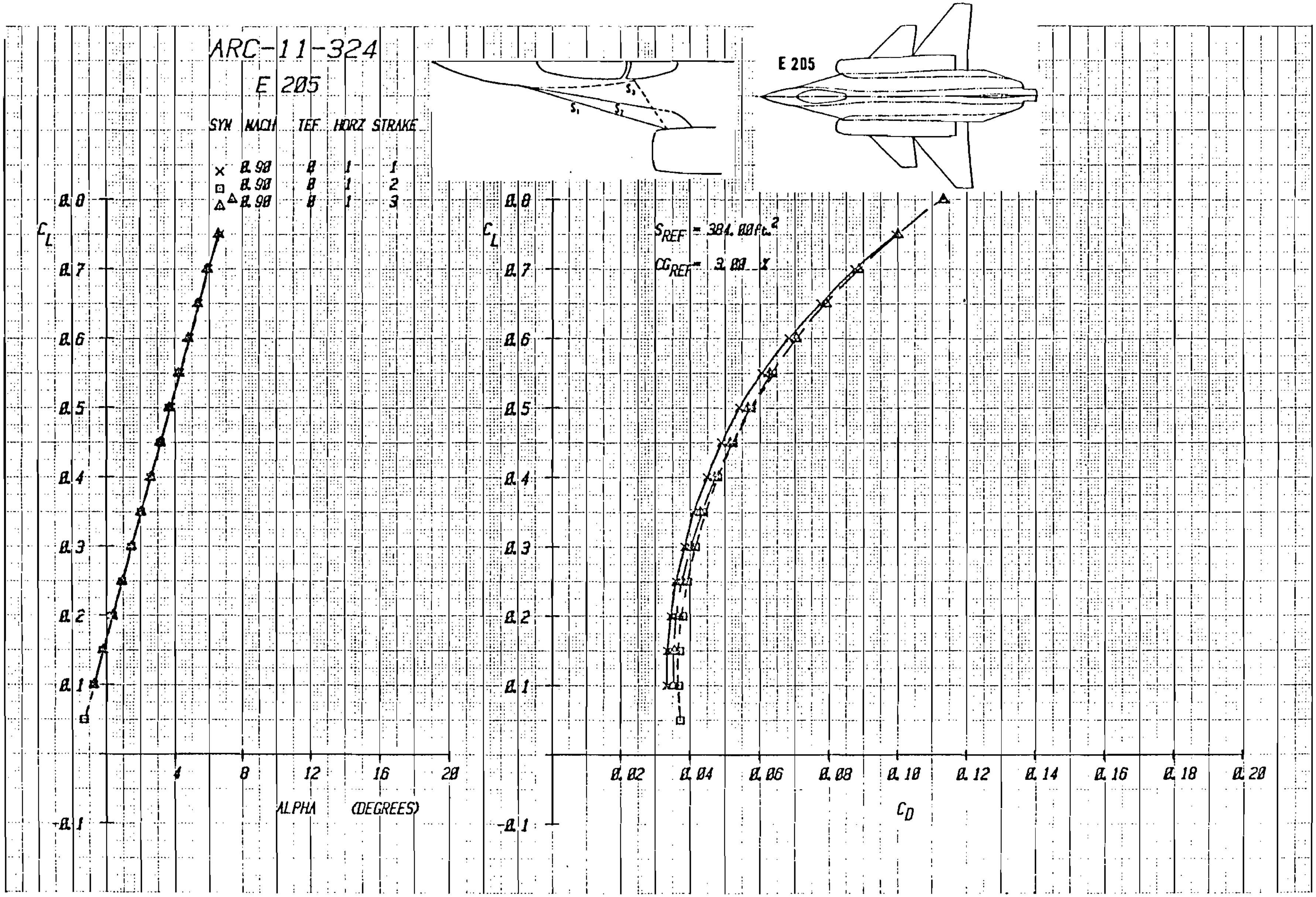

Figure 3-81 Trimmed Lift and Drag With Variations in Strake and Canard C_l, Mach = .9

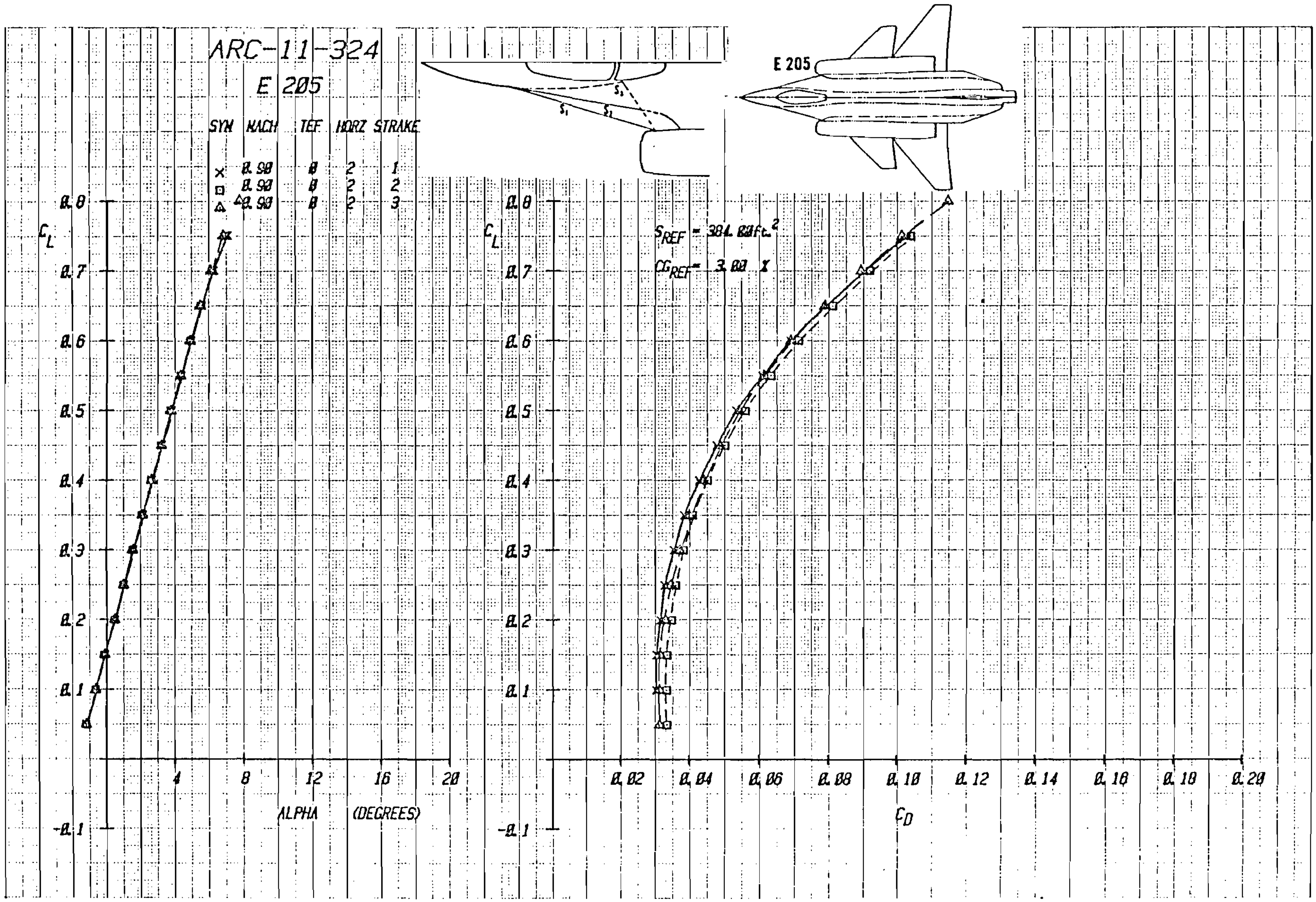

Figure 3-82 Trimmed Lift and Drag With Variations in Strake and Canard C_2, Mach = .9

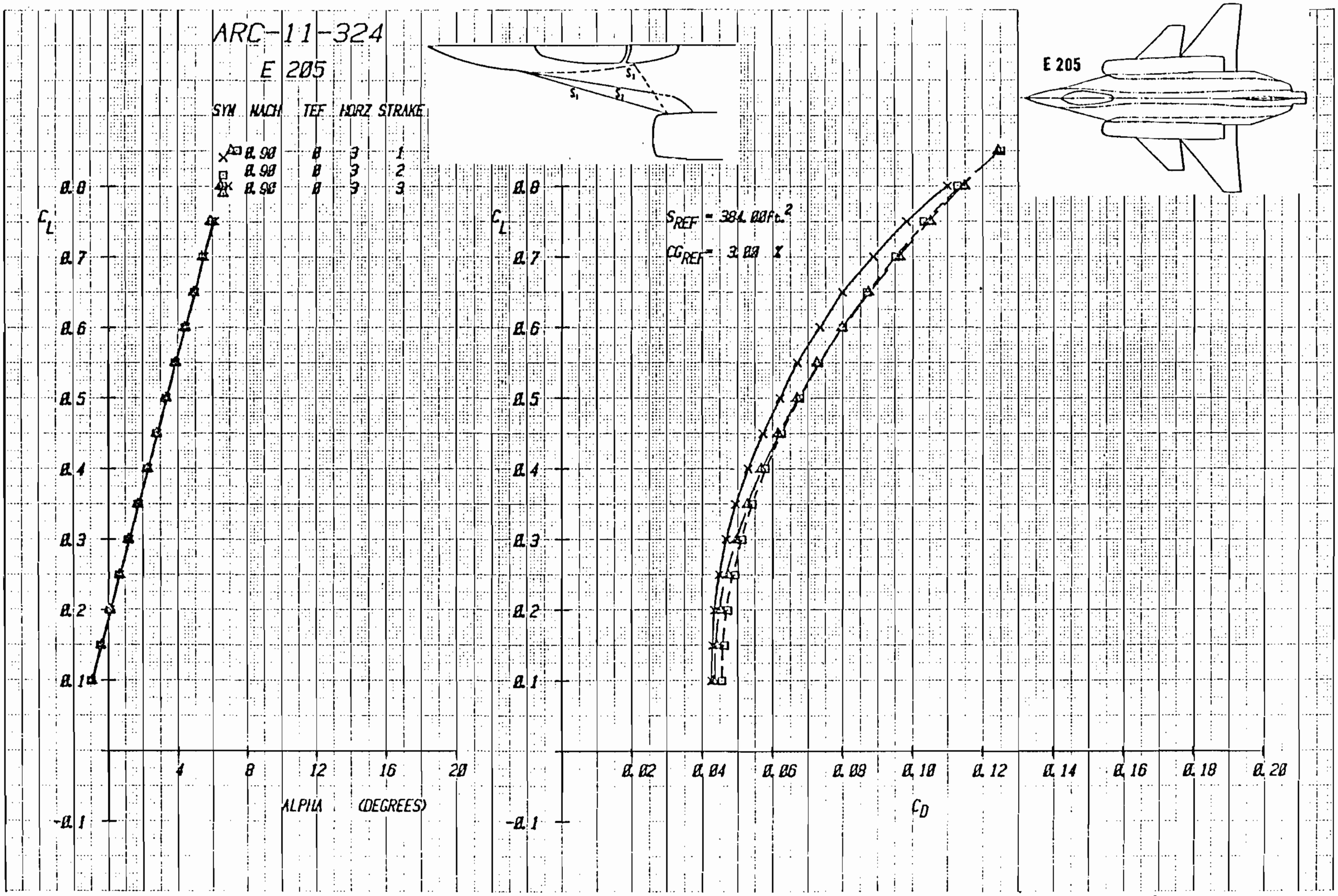

Figure 3-83 Trimmed Lift and Drag With Variations in Strake and Canard C_3, Mach = .9

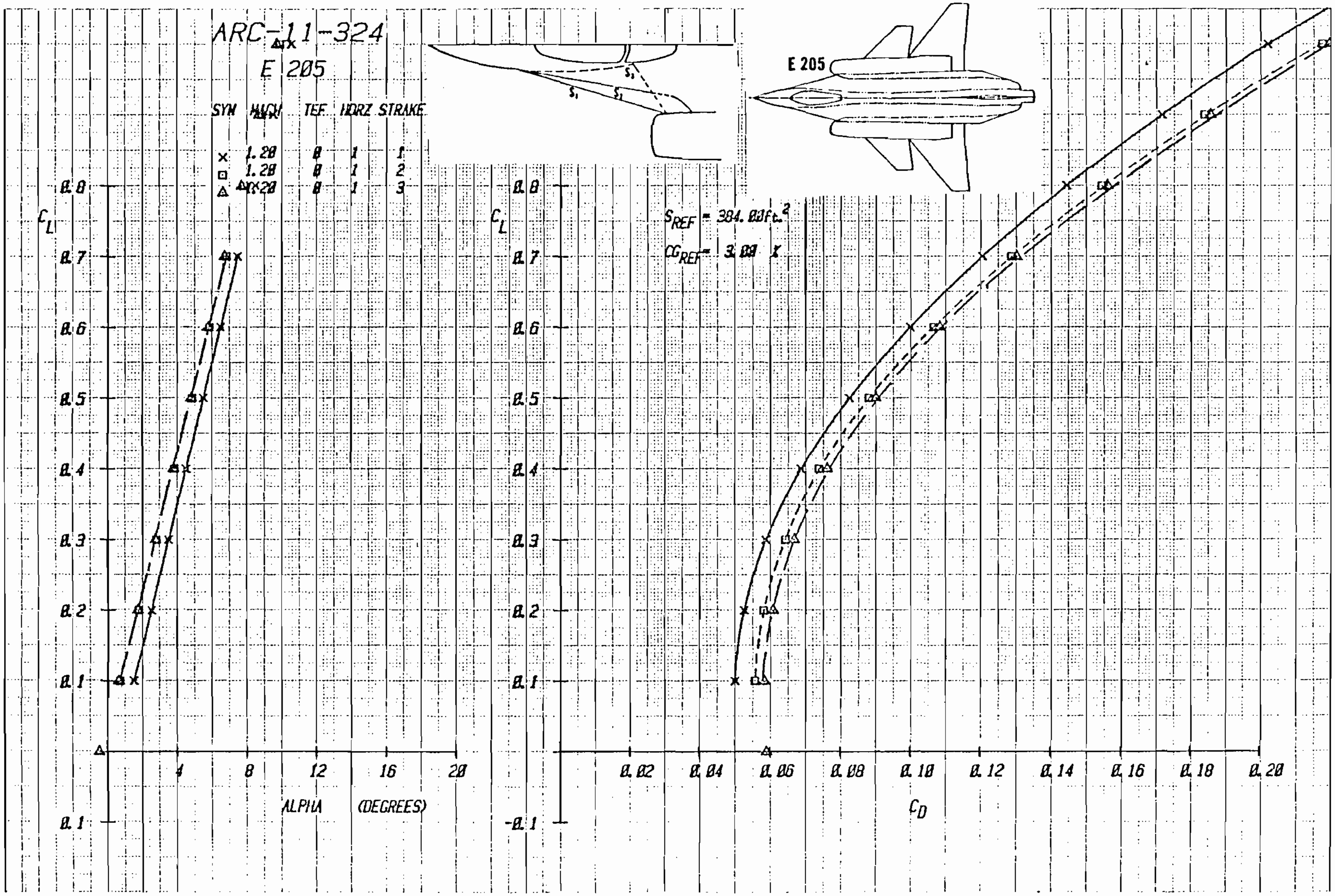

Figure 3-84 Trimmed Lift and Drag With Variations in Strake and Canard C_l, Mach = 1.2

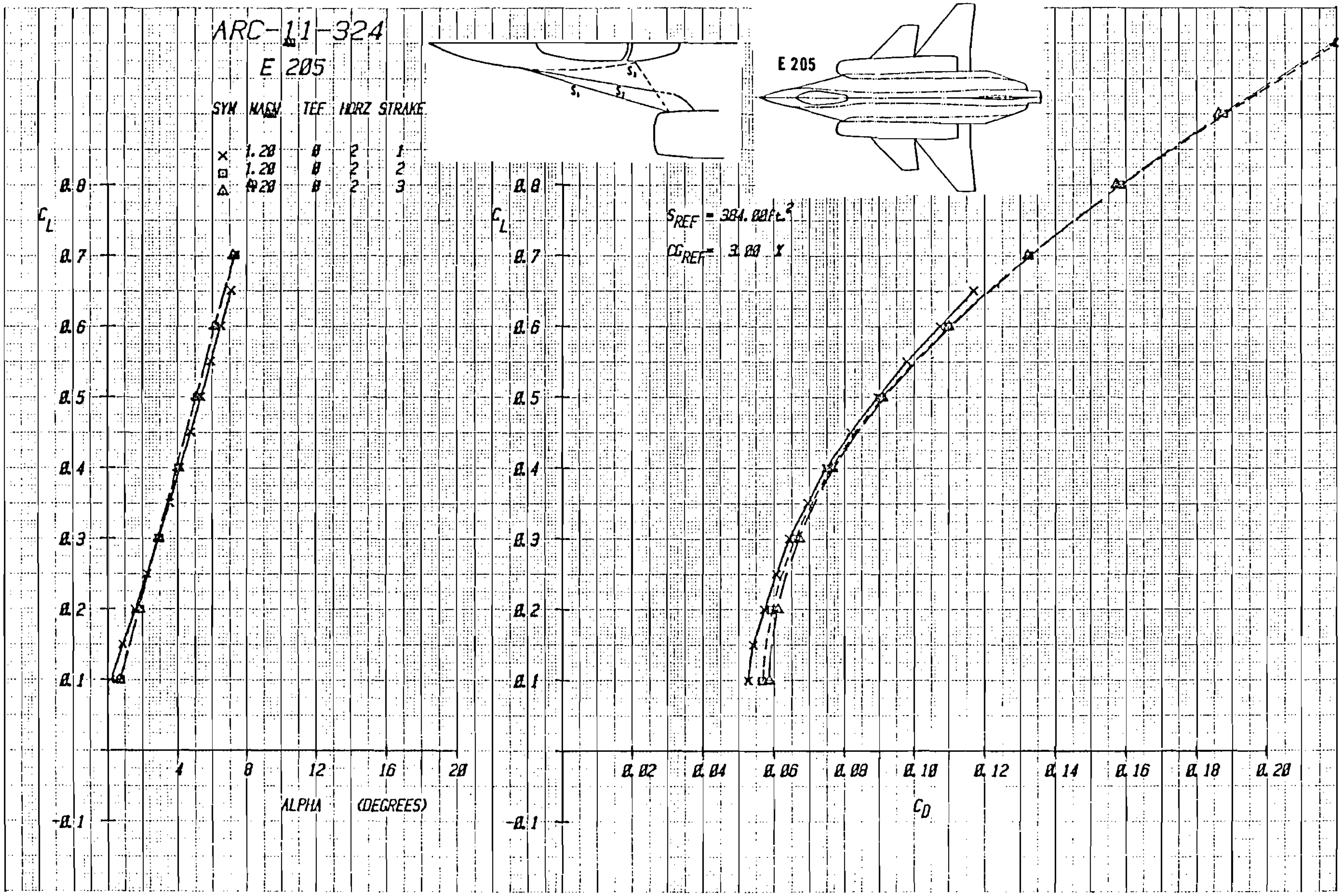

Figure 3-85 Trimmed Lift and Drag With Variations in Strake and Canard C_2, Mach = 1.2

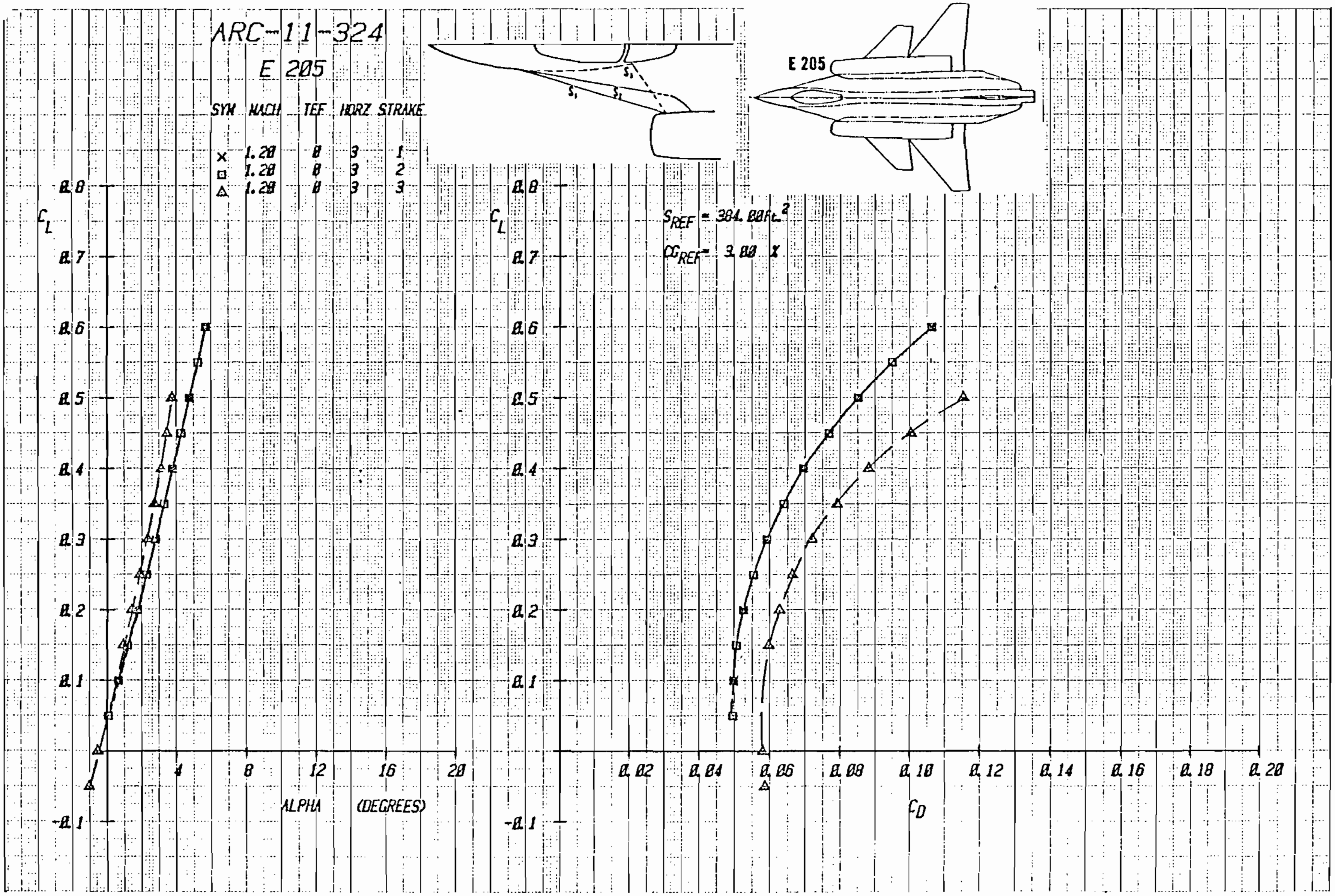

Figure 3-86 Trimmed Lift and Drag With Variations in Strake and Canard C_3, Mach = 1.2

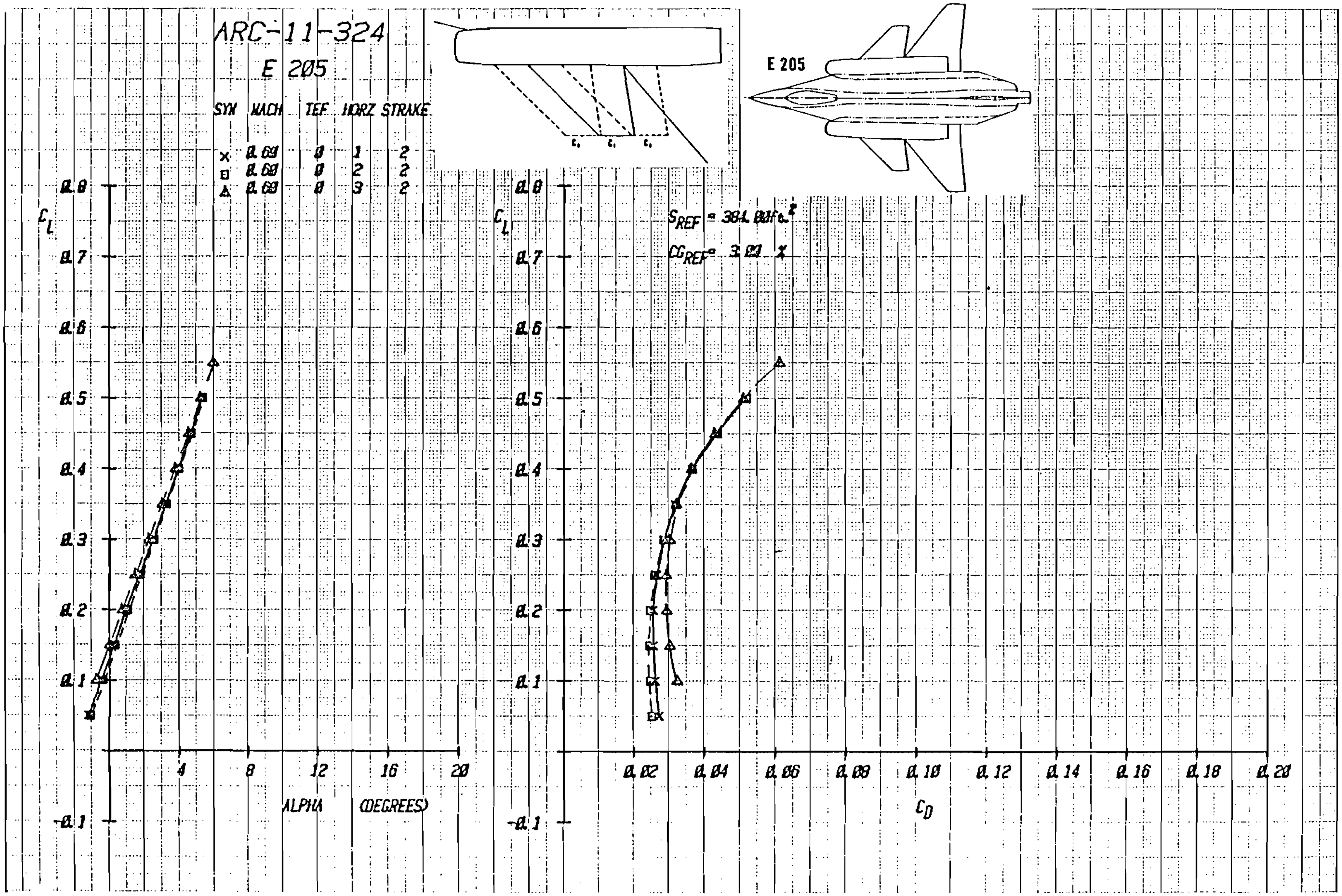

Figure 3-87 Trimmed Lift and Drag With Variations in Canard Longitudinal Location and Strake S_2, Mach = .6

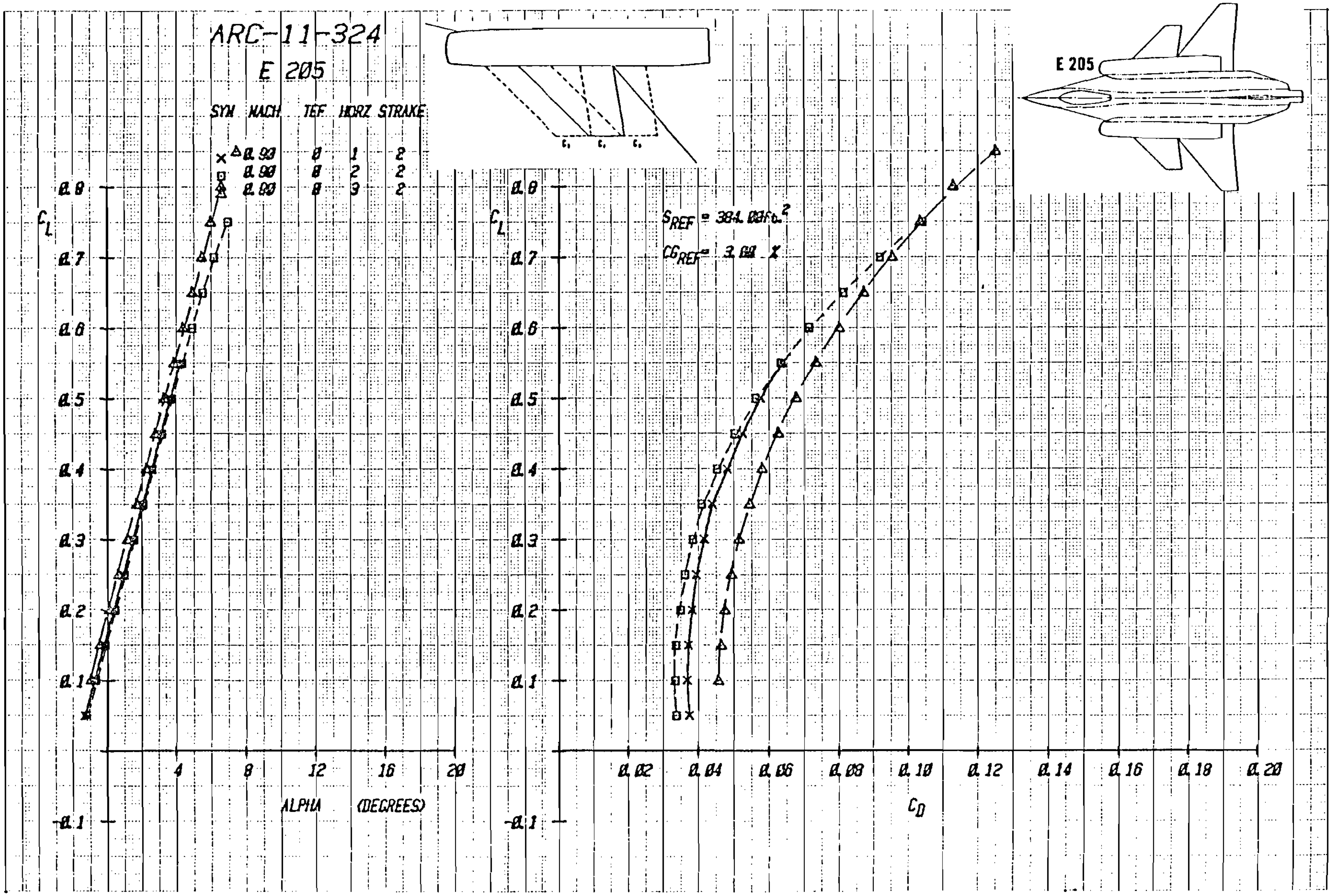

Figure 3-88 Trimmed Lift and Drag With Variations in Canard Longitudinal Location and Strake S_2, Mach = .9

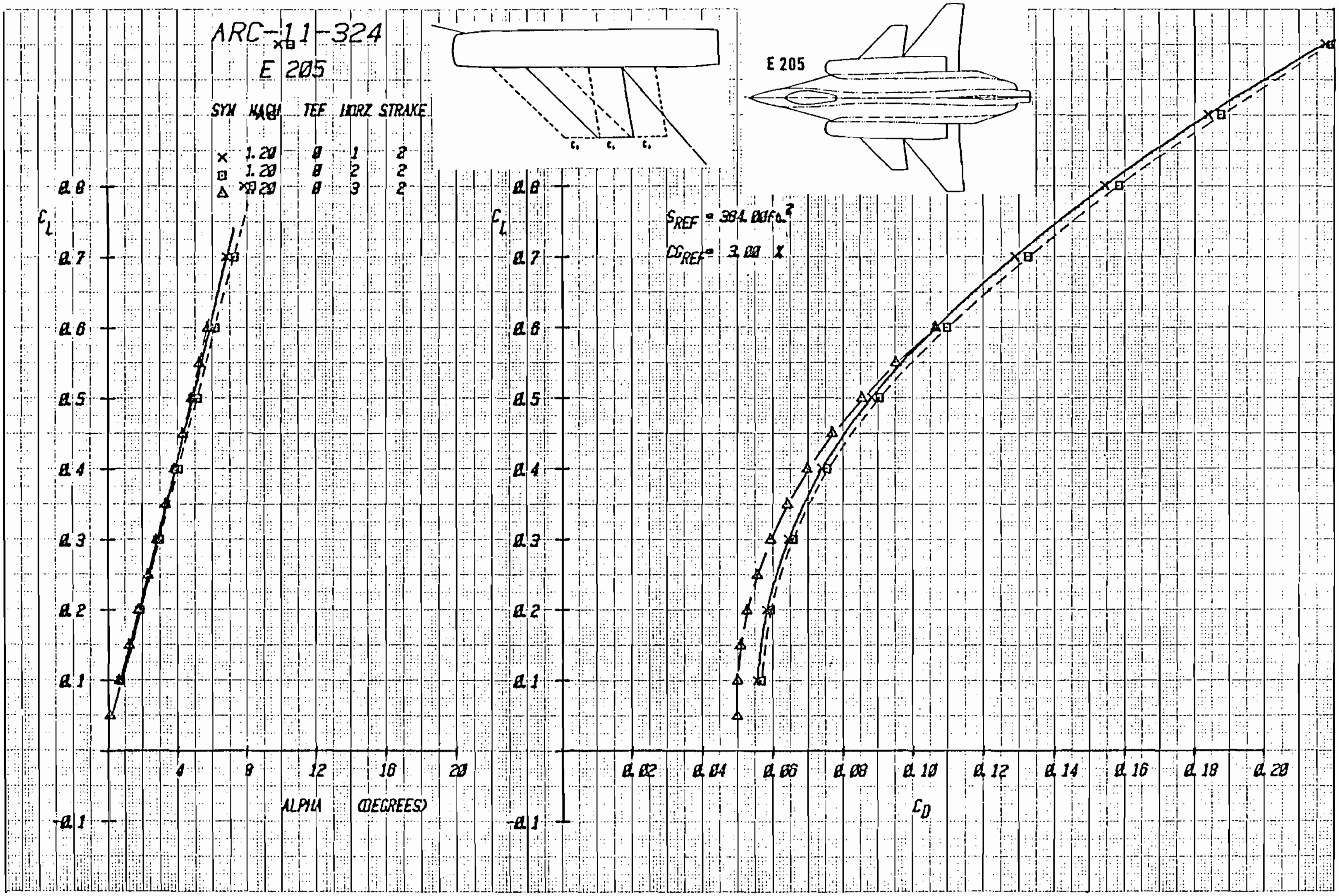

Figure 3-89 Trimmed Lift and Drag With Variations in Canard Longitudinal Location and Strake S_2, Mach = 1.2

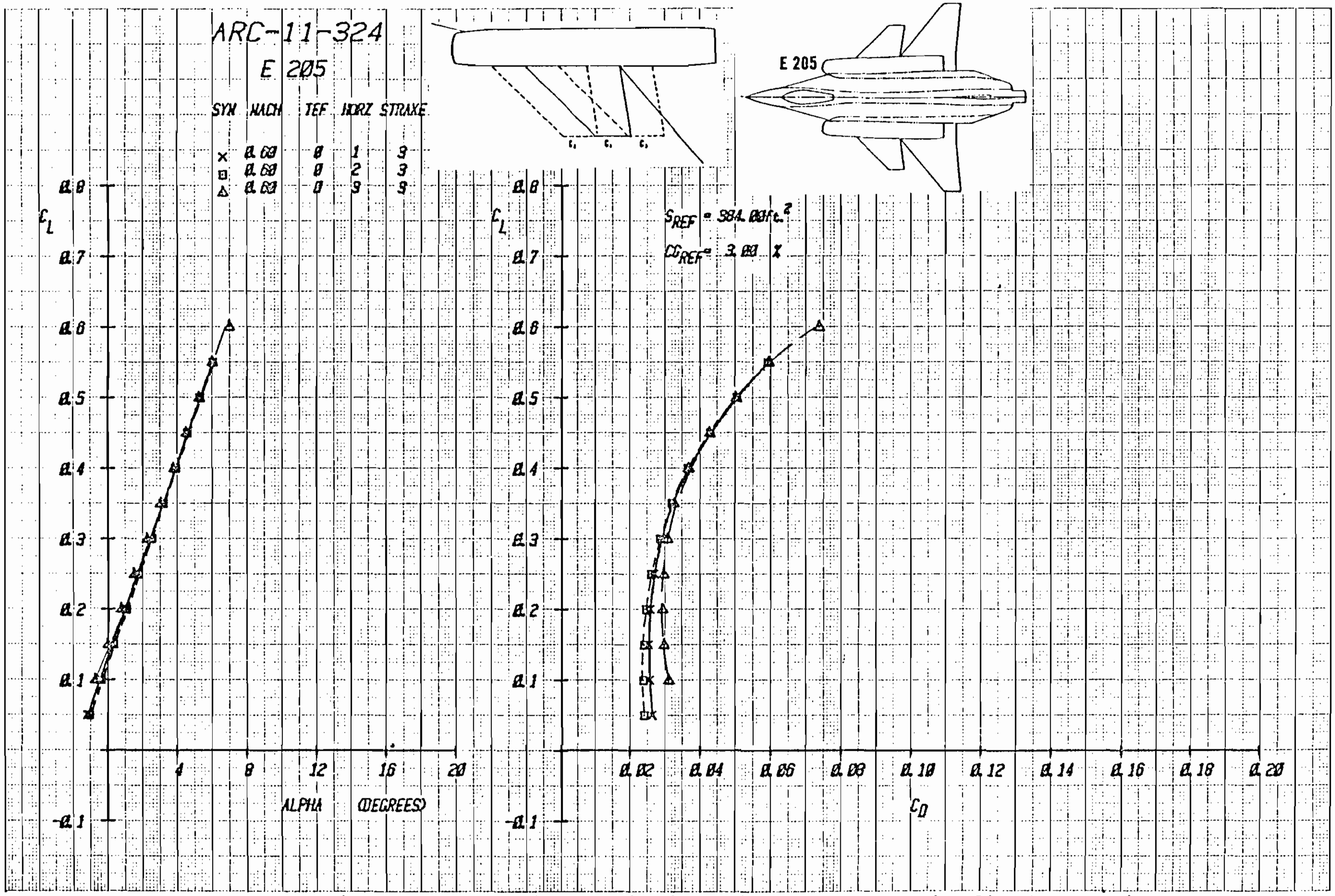

Figure 3-90 Trimmed Lift and Drag With Variations in Canard Longitudinal Location and Strake S_3, Mach = .6

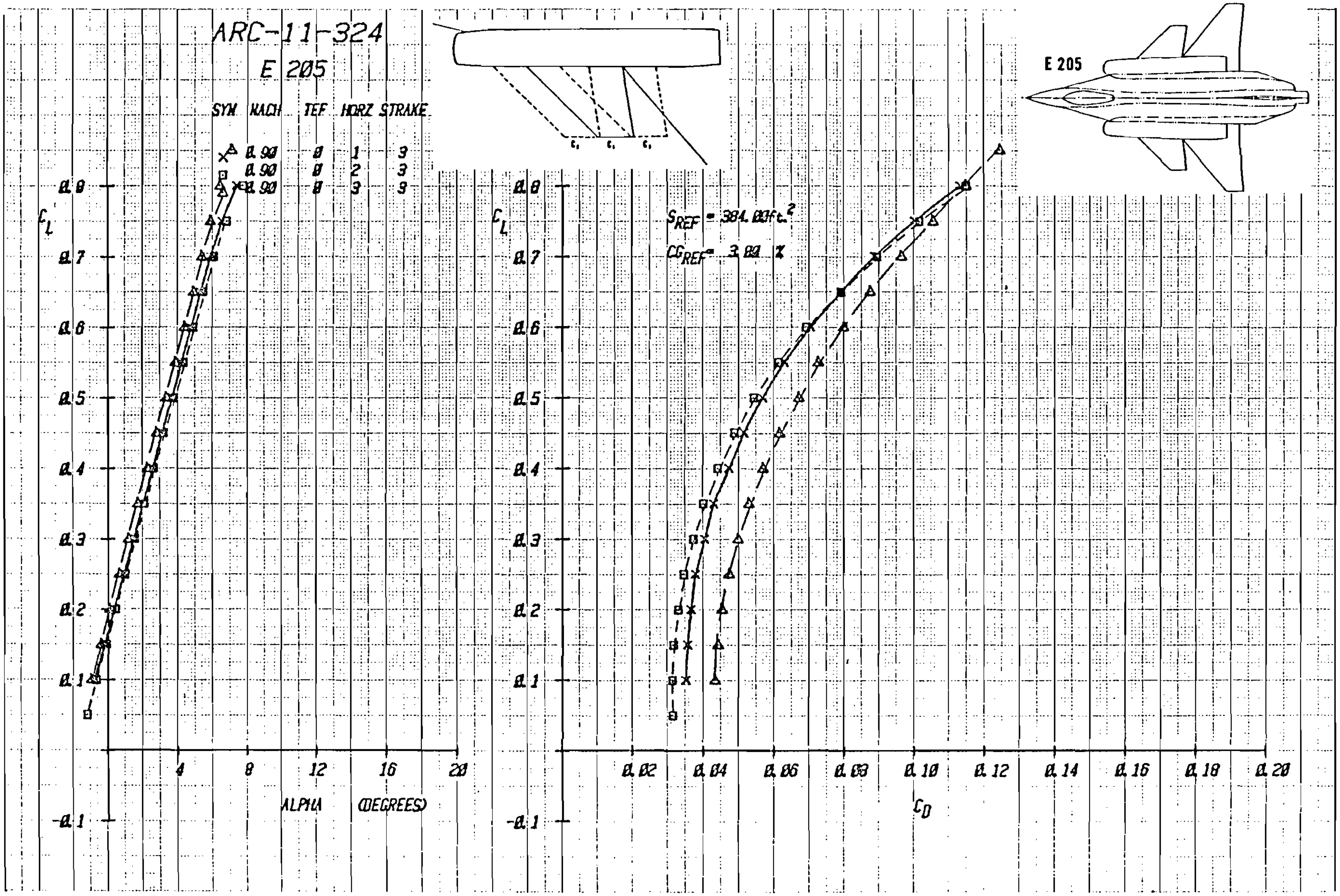

Figure 3-91 Trimmed Lift and Drag With Variations in Canard Longitudinal Location and Strake S_3, Mach = .9

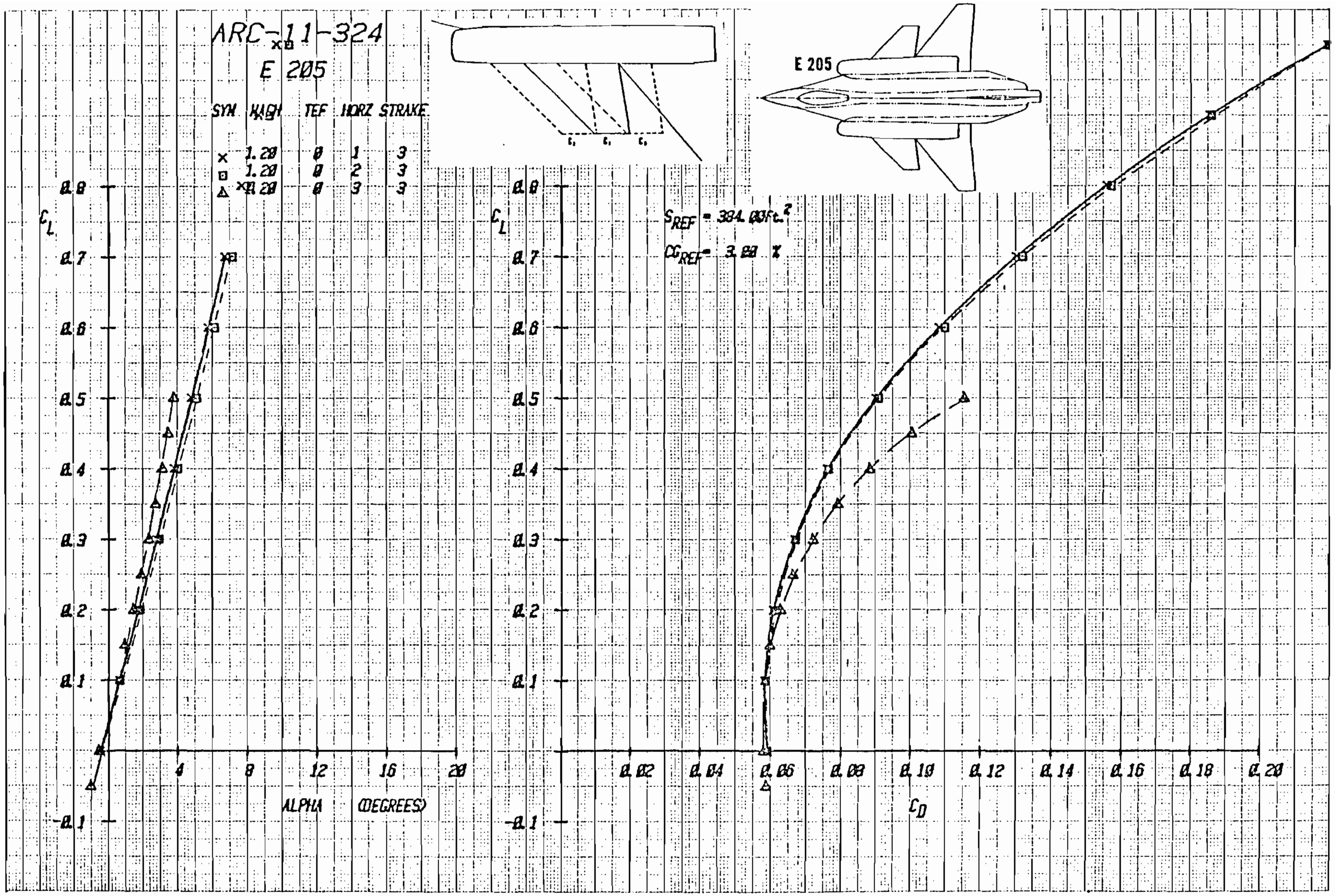

Figure 3-92 Trimmed Lift and Drag With Variations in Canard Longitudinal Location and Strake S_3, Mach = 1.2

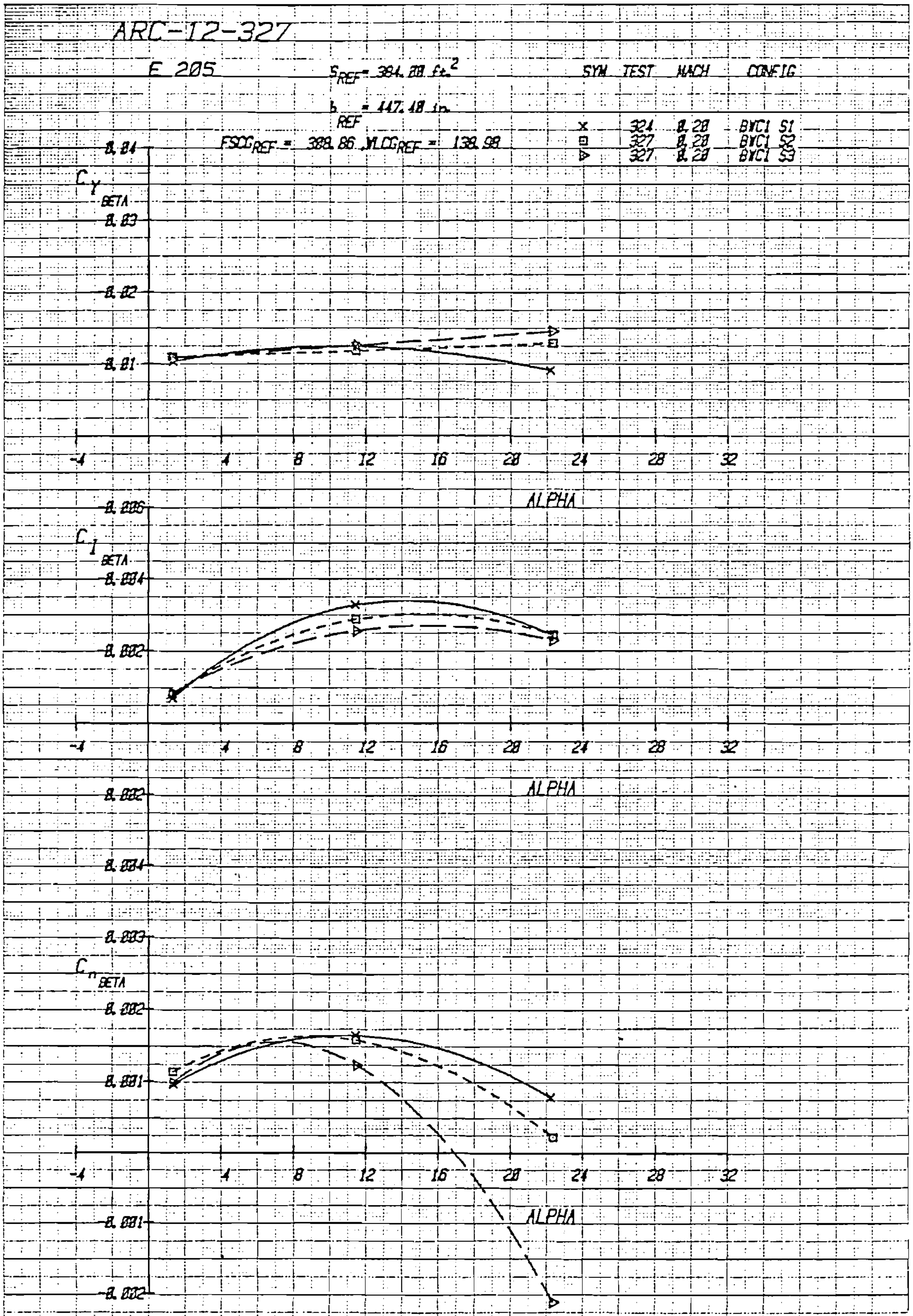

Figure 3-93 Effect of Strake Shape on Lateral-Directional Characteristics with Baseline Canard, Mach = .2

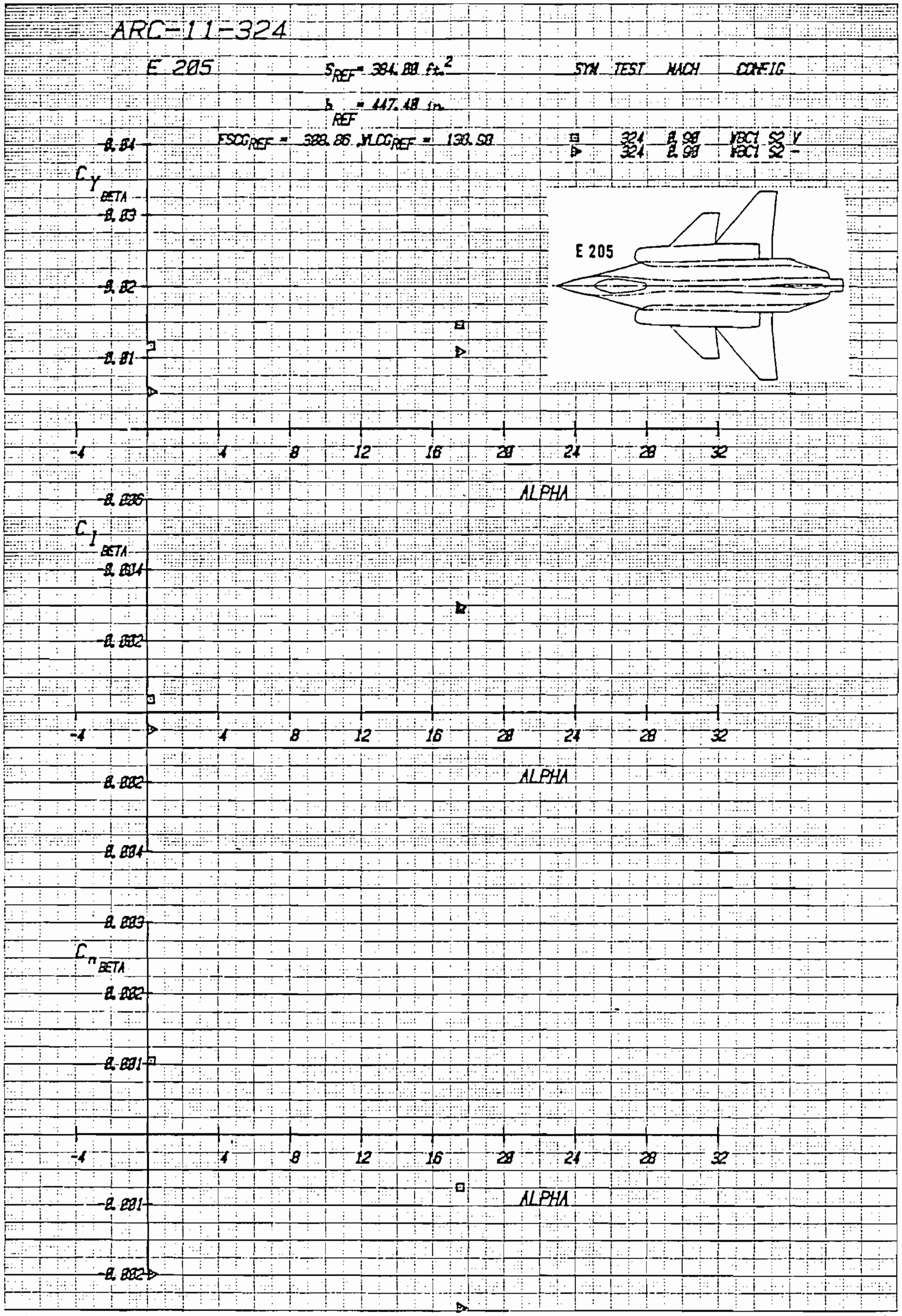

Figure 3-94 Vertical Tail Effectiveness for the E205 Configuration, with Strake S_2, Canard C_1, Mach = .9

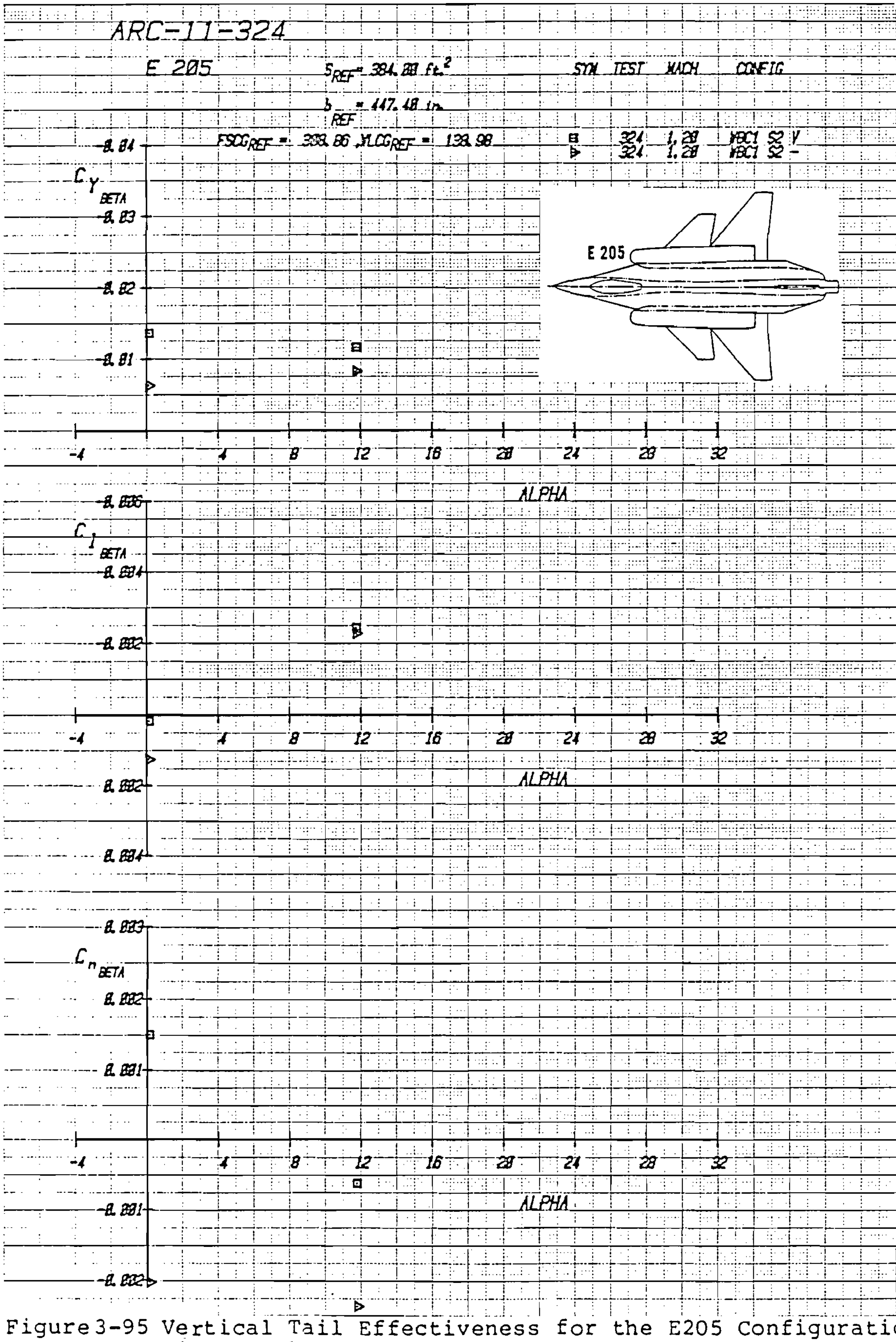

Figure 3-95 Vertical Tail Effectiveness for the E205 Configuration, with Strake S_2, Canard C_1, Mach = 1.2

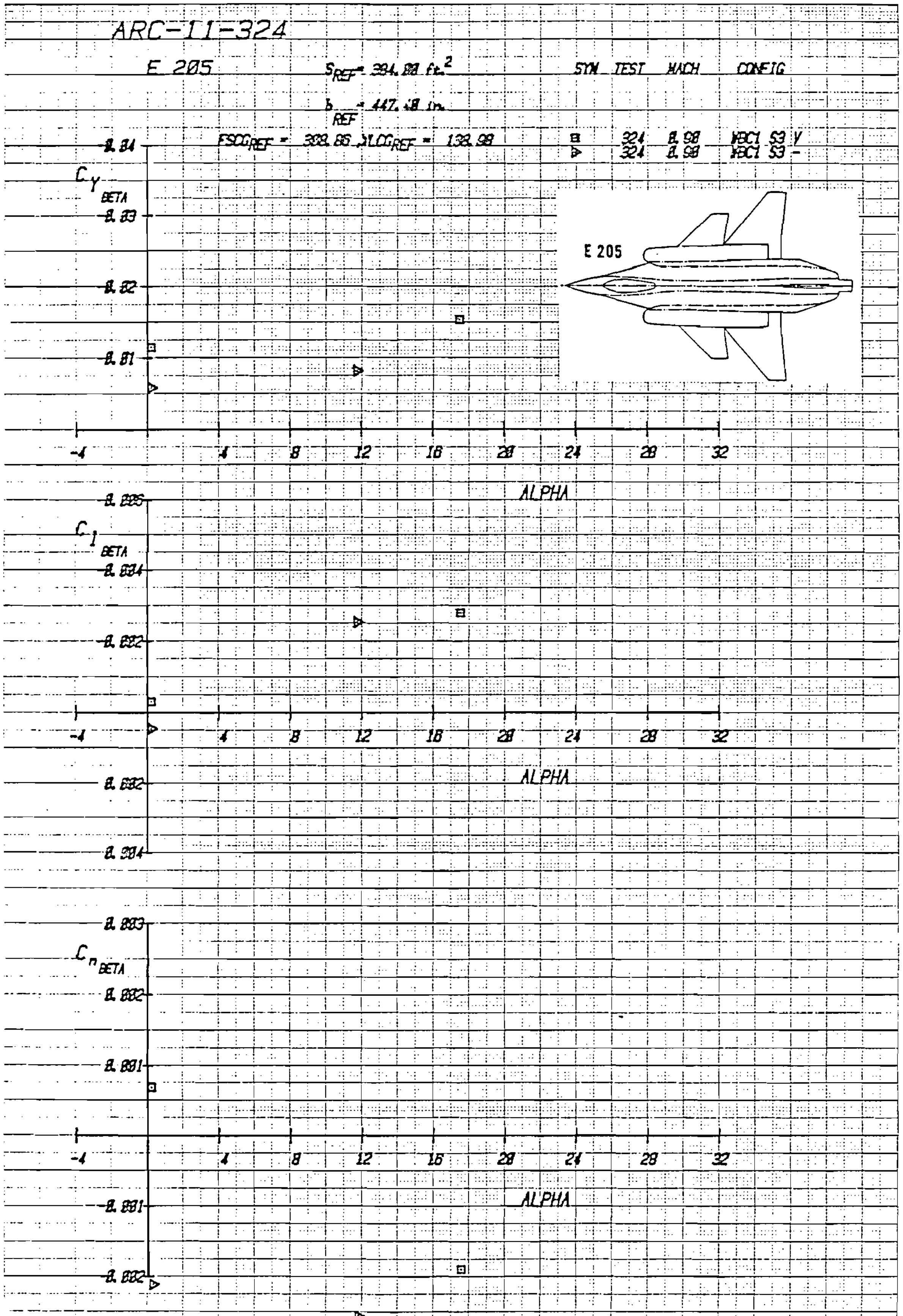

Figure 3-96 Vertical Tail Effectiveness for the E205 Configuration, with Strake S_3, Canard C_1, Mach = .9

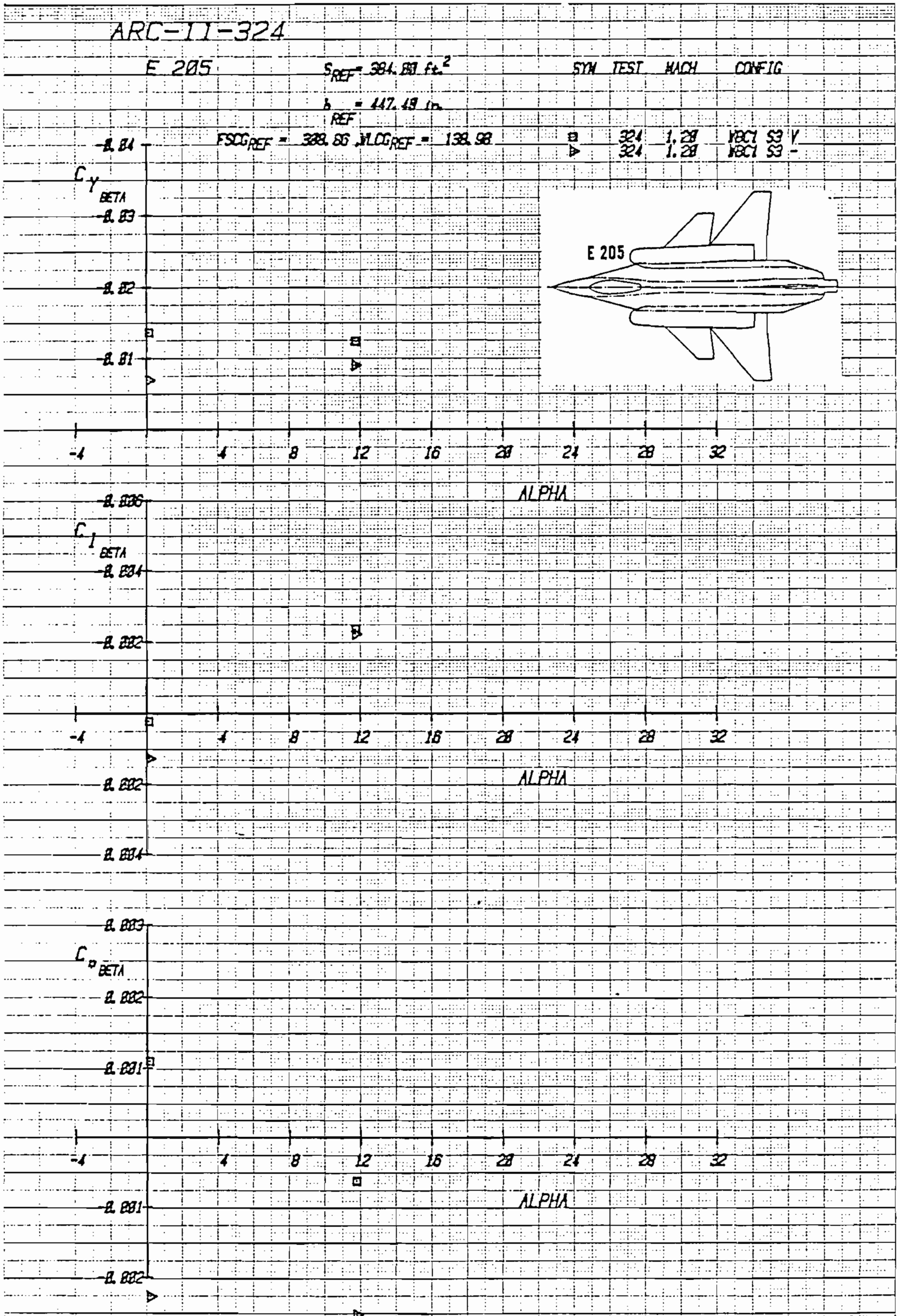

Figure 3-97 Vertical Tail Effectiveness for the E205 Configuration, with Strake S_3, Canard C_1, Mach = 1.2